



**Institute of Geophysics
Polish Academy of Sciences**

**PUBLICATIONS
OF THE INSTITUTE OF GEOPHYSICS
POLISH ACADEMY OF SCIENCES**

Geophysical Data Bases, Processing and Instrumentation

435 (M-33)

**Achievements of the Institute of Geophysics, PAS:
Annual Report 2018**

Warsaw 2021 (Issue 4)

**INSTITUTE OF GEOPHYSICS
POLISH ACADEMY OF SCIENCES**

**PUBLICATIONS
OF THE INSTITUTE OF GEOPHYSICS
POLISH ACADEMY OF SCIENCES**

Geophysical Data Bases, Processing and Instrumentation

435 (M-33)

**Achievements of the Institute of Geophysics, PAS:
Annual Report 2018**

Warsaw 2021

Honorary Editor
Roman TEISSEYRE

Editor-in-Chief
Marek KUBICKI

Advisory Editorial Board

Janusz BORKOWSKI (Institute of Geophysics, PAS)
Tomasz ERNST (Institute of Geophysics, PAS)
Maria JELEŃSKA (Institute of Geophysics, PAS)
Andrzej KIJKO (University of Pretoria, Pretoria, South Africa)
Natalia KLEIMENOVA (Institute of Physics of the Earth, Russian Academy of Sciences, Moscow, Russia)
Zbigniew KŁOS (Space Research Center, Polish Academy of Sciences, Warsaw, Poland)
Jan KOZAK (Geophysical Institute, Prague, Czech Republic)
Antonio MELONI (Istituto Nazionale di Geofisica, Rome, Italy)
Hiroyuki NAGAHAMA (Tohoku University, Sendai, Japan)
Kaja PIETSCH (AGH University of Science and Technology, Cracow, Poland)
Paweł M. ROWIŃSKI (Institute of Geophysics, PAS)
Steve WALLIS (Heriot Watt University, Edinburgh, United Kingdom)
Wacław M. ZUBEREK (University of Silesia, Sosnowiec, Poland)

Associate Editors

Łukasz RUDZIŃSKI (Institute of Geophysics, PAS) – **Solid Earth Sciences**
Jan WISZNIEWSKI (Institute of Geophysics, PAS) – **Seismology**
Jan REDA (Institute of Geophysics, PAS) – **Geomagnetism**
Krzysztof MARKOWICZ (Institute of Geophysics, Warsaw University) – **Atmospheric Sciences**
Mark GOŁKOWSKI (University of Colorado Denver) – **Ionosphere and Magnetosphere**
Andrzej KUŁAK (AGH University of Science and Technology) – **Atmospheric Electricity**
Marzena OSUCH (Institute of Geophysics, PAS) – **Hydrology**
Adam NAWROT (Institute of Geophysics, PAS) – **Polar Sciences**

Managing Editors

Anna DZIEMBOWSKA

Technical Editor

Marzena CZARNECKA

© 2021 The Author(s). Published by the Institute of Geophysics, Polish Academy of Sciences.
This is an open access publication under the CC BY license 4.0

ISBN 978-83-66254-15-2 eISSN-2299-8020
DOI: 10.25171/InstGeoph_PAS_Publs-2021-044

Editorial Office
Instytut Geofizyki Polskiej Akademii Nauk
ul. Księcia Janusza 64, 01-452 Warszawa

C O N T E N T S

Editorial note	4
1. GENERAL	5
1.1 The mission of the Institute of Geophysics, Polish Academy of Sciences.....	5
1.2 Research areas	6
1.2.1 Anthropogenic and natural geohazards	6
1.2.2 Geosystem processes.....	7
1.2.3 Earth structure and georesources.....	7
1.2.4 Climate change and polar research.....	8
1.3 Management	9
1.4 Employment structure	10
1.5 Activity of Scientific Information and Publishers Department	10
1.6 Observatories	12
1.7 Polish Polar Station	13
1.8 Projects, commercial agreements and publications	14
1.9 Professor Adam Dziewoński Medal	16
2. DEPARTMENT OF SEISMOLOGY	17
2.1 About the Department	17
2.2 Personnel	18
2.3 Main research projects	18
2.4 Instruments and facilities	19
2.5 Research activity and results	23
2.6 Seminars and teaching	52
2.7 Visiting scientists	52
2.8 Meetings, workshops, conferences, and symposia.....	52
2.9 Publications	55
3. DEPARTMENT OF ATMOSPHERIC PHYSICS	56
3.1 About the Department	56
3.2 Personnel	56
3.3 Main research projects	57
3.4 Instruments and facilities	57
3.5 Research activity and results	59
3.6 Seminars and teaching	75
3.7 Completed PhD thesis defense	75

3.8 Visiting scientists	76
3.9 Meetings, workshops, conferences, and symposia	76
3.10 Publications	77
4. DEPARTMENT OF LITHOSPHERIC RESEARCH	79
4.1 About the Department	79
4.2 Personnel	79
4.3 Main research projects	80
4.4 Instruments and facilities	80
4.5 Research activity and results	80
4.6 Seminars and teaching	95
4.7 Teaching thesis	95
4.8 Visiting scientists	95
4.9 Meetings, workshops, conferences, and symposia	95
4.10 Publications	96
5. DEPARTMENT OF THEORETICAL GEOPHYSICS	97
5.1 About the Department	97
5.2 Personnel	97
5.3 Main research projects	98
5.4 Research activity and results	98
5.5 Seminars and teaching	108
5.6 Completed PhD thesis defence	108
5.7 Visiting scientists	108
5.8 Meetings, workshops, conferences, and symposia	108
5.9 Publications	110
6. DEPARTMENT OF HYDROLOGY AND HYDRODYNAMICS	111
6.1 About the Department	111
6.2 Personnel	112
6.3 Main research projects	112
6.4 Instruments and facilities	113
6.5 Research activity and results	113
6.6 Seminars and teaching	133
6.7 Completed PhD thesis defence	133
6.8 Visiting scientists	133
6.9 Meetings, workshops, conferences, and symposia	133
6.10 Publications	135

7. DEPARTMENT OF MAGNETISM	138
7.1 About the Department	138
7.2 Personnel	139
7.3 Main research projects	140
7.4 Instruments and facilities	140
7.5 Research activity and results	141
7.6 Seminars and teaching	177
7.7 Teaching thesis	178
7.8 Completed PhD thesis defence	178
7.9 Visiting scientists	178
7.10 Meetings, workshops, conferences, and symposia	179
7.11 Publications	182
8. DEPARTMENT OF GEOPHYSICAL IMAGING	185
8.1 About the Department	185
8.2 Personnel	185
8.3 Main research projects	186
8.4 Instruments and facilities	186
8.5 Research activity and results	187
8.6 Seminars and teaching	205
8.7 Completed PhD thesis defence	206
8.8 Visiting scientists	206
8.9 Meetings, workshops, conferences, and symposia	206
8.10 Publications	208
9. DEPARTMENT OF POLAR AND MARINE RESEARCH	211
9.1 About the Department	211
9.2 Personnel	212
9.3 Main research projects	213
9.4 Instruments and facilities	214
9.5 Research activity and results	215
9.6 Seminars and teaching	231
9.7 Teaching thesis	231
9.8 Completed PhD thesis defence	231
9.9 Visiting scientists	232
9.10 Meetings, workshops, conferences, and symposia	232
9.11 Publications	234

Editorial note

This Monograph, the first one in a series of yearly outlines on the main achievements of the Institute of Geophysics, Polish Academy of Sciences, is a reviewed and edited version of the Annual Report 2018. It provides information about the research done in the seven departments (Seismology, Atmospheric Physics, Lithospheric Research, Theoretical Geophysics, Hydrology and Hydrodynamics, Magnetism, Geophysical Imaging, and Polar and Marine Research), together with the Institute's infrastructure, instrumentation, projects that have been completed or are underway, as well as editorial, educational, and many other activities.

In the year 2018 we celebrated the 65 anniversary of the Institute (originally the Department) of Geophysics, which was established by a resolution of the Presidium of the Polish Academy of Sciences on 18 December 1952.

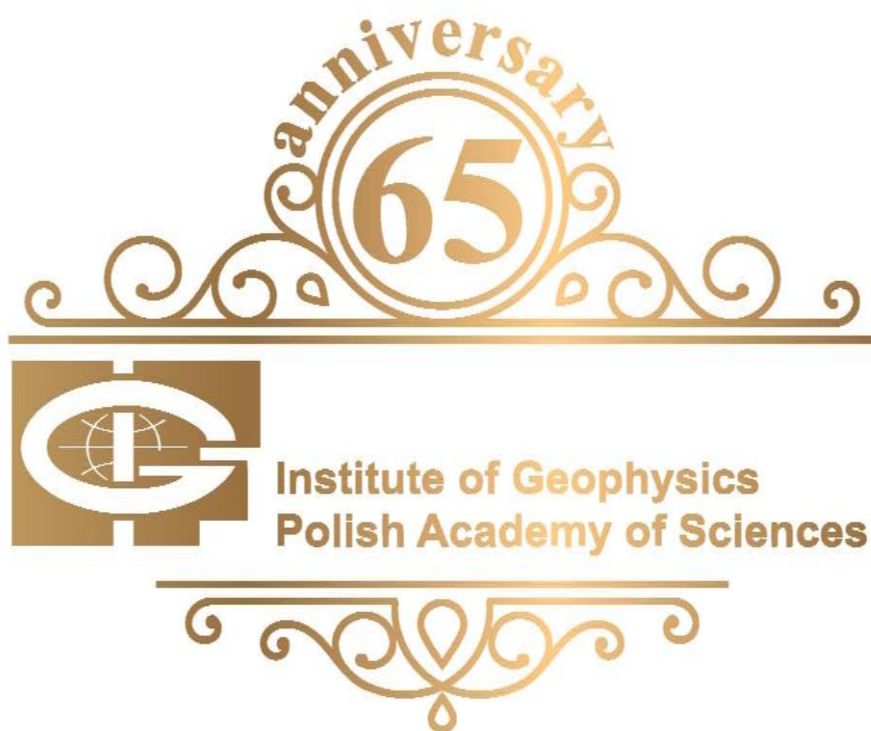
We hope the information contained in this Monograph may be useful for a broader audience, in particular those who may find the presented materials applicable in their work, or perhaps arrange a co-operation with the Institute.

The Editors
of the *Publications of the Institute of Geophysics PAS*

1. GENERAL

Beata Orlecka-Sikora, Mariusz Majdański, Beata Fromelusz, Krzysztof Otto

In the year 2018, the Institute celebrated its 65 anniversary. The Institute of Geophysics of the Polish Academy of Sciences (originally the Department of Geophysics) was established by a resolution of the Presidium of the Polish Academy of Sciences on 18 December 1952. It was based on three geophysical observatories: Magnetic Observatory in Świder, Seismic Station in Warsaw, and Silesian Geophysical Station in Racibórz. The Institute became a natural successor to the glorious tradition of geophysical research in Poland. It is worth mentioning in this context that the pioneer in the field of geophysics in Poland was Prof. Maurycy Pius Rudzki, who in 1898 created the world's first Chair of Geophysics at the Jagiellonian University in Kraków.



1.1 The mission of the Institute of Geophysics, Polish Academy of Sciences

The main statutory tasks of the Institute include scientific research, development, monitoring and educational activities, as well as dissemination of the results of the research and their implementation in the economy.

An important objective of the activity of the Institute of Geophysics, Polish Academy of Sciences, is supporting people beginning their scientific careers and education and development of research workers and specialists with particular skills in the field of geophysical sciences, as well as to anticipate hazards, perform risk assessments and manage critical situations.

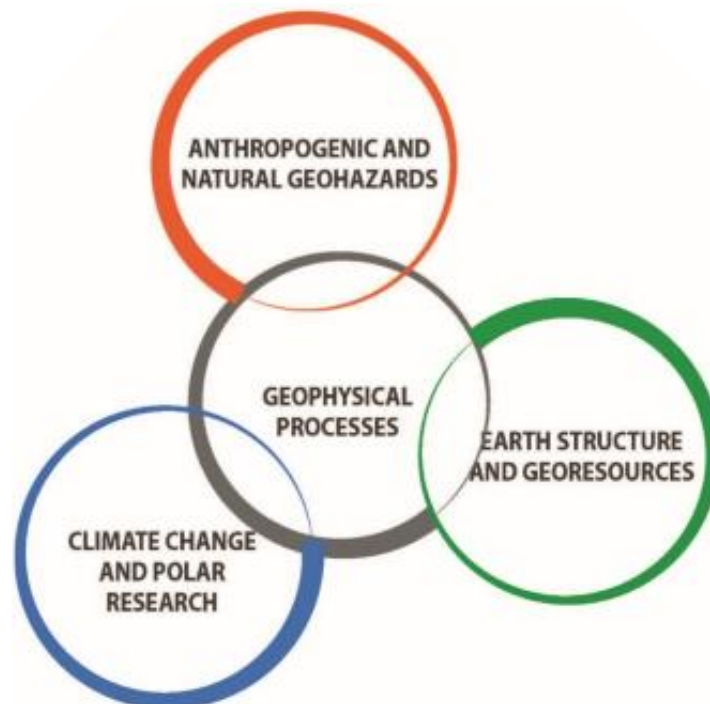
The Institute also conducts extensive cooperation with universities, research institutes and scientific associations, particularly in the field of research and development works. We also ensure the continuous development of international scientific cooperation through creation of research consortia and joint research projects with foreign partners.

The mission of the Institute of Geophysics:

- Studying geophysical processes for a better understanding of the mechanisms controlling the Earth's system and risk management
- Working for the benefit of the society and economic development
- Development and maintenance of strategic research infrastructure
- Geophysical monitoring
- Training future leaders of scientific community

1.2 Research areas

The main research areas and their interrelations, are illustrated below:



Main research areas of the Institute of Geophysics PAS.

1.2.1 Anthropogenic and natural geohazards

The history of mankind and the development of civilizations are full of examples of the subordination and harnessing of nature's forces to serve people. Even though the paradigm of Mankind's mastery over nature has changed somewhat in recent history, being diverted towards sustainable development and living in harmony with the environment, humanity will always struggle with violent and unpredictable natural phenomena. The study of the risks and consequences of sudden and catastrophic processes in the lithosphere, atmosphere, magnetosphere and hydrosphere has for many years been within the scope of scientific research at the Institute of Geophysics, Polish Academy of Sciences (IG PAS). Scientists from the IG PAS are among Poland's and the world's leading specialists in dealing with natural hazards and adverse human impact on the environment. The IG PAS scientific and educational activities in these fields have contributed to finding methods of prediction, analysis and management of geohazards that translate into solutions for better protection against the destructive forces of nature. Through these methods, practical solutions can be developed to mitigate or eliminate humanitarian and economic losses due to both natural and man-made disasters.

Research in the Institute of Geophysics PAS focuses, inter alia, on natural and human-induced geohazards including earthquakes, landslides, floods, torrential rains, local inundations and droughts, water and air pollution, and the negative effects of the UV rays and chemical aerosols on human health. All these natural hazards are thoroughly investigated within the contexts of climate change and evolving societal needs. The use is made of the latest analytical methods, specialized equipment and laboratories within the possession of the IG PAS, including two stations located in both polar regions, as components of leading global geophysical research networks. Methodologies developed by specialists from the IG PAS encompass both basic and applied science, and include mathematical and physical modeling of natural phenomena, magnetic analysis of soil, water and air pollution, seismic monitoring of natural and induced earth-quakes, geophysical imaging of shallow and deep Earth structure, hydrological measurement of seas, rivers and lakes, and investigations of the cryosphere and polar environment in the Arctic and Antarctica.

1.2.2 Geosystem processes

The Earth is a complex system (hereafter called geosystem) in which many components interact across all space and time scales. To address the complex interactions between the atmosphere, hydrosphere, troposphere, ionosphere, and crust, complementary approaches have to be used, combining observational data with theoretical and mathematical models and numerical computing. The quality of such models is intrinsically correlated with the quality and quantity of data available for their calibration and validation. Therefore, structuring adequate monitoring networks is of paramount importance for keeping track of the geosystem dynamics at various spatio-temporal scales.

The study of the present state of the Earth and its environment cannot be done in isolation from its dynamic history. Knowing the past is essential for understanding the present drivers and links between them, as the past is the key to understand the present and to predict the future. Theoretical and numerical modelling helps in capturing the physics of the Planet's evolution from its origin, but monitoring activities are essential in this case.

The last decades revealed how strongly mankind, just a small fraction of the global biota, can effectively disturb the whole ecosystem, paving the way to mass extinction. Before we reach the point of no return, we must learn in detail about how we interfere with nature, and determine the necessary means and actions that have to be undertaken to prevent passing a turning point after which there will be no place for us on the planet. The Geosystem Processes Working Group is a very inclusive group, which combines expertise spanning from atmospheric sciences to lithospheric research, magnetism, and hydrology. Indeed, the complexity of the geosystem dynamics from the deep geological past to the present requires a transdisciplinary approach to be studied. Particular aims of the group for the next few years involve maintenance and further development of the Polish geophysical monitoring system (seismic, magnetic, atmospheric), determination of the influence of ozone layer dynamics on the UV radiation, study of atmospheric electricity and its interactions with aerosols, and investigations of crust structure and dynamics through seismic soundings, including the research into the earthquake source physics and physics of subduction zones.

1.2.3 Earth structure and georesources

The traditional domain of research in this thematic domain was the recognition of the structure of the Earth's crust and upper mantle using various seismic (active, passive, refractive, and reflective) and (electro) magnetic methods, as well as palaeogeographic research and tracking selected tectonic processes on the basis of palaeomagnetic analyzes. The results of these studies were of great cognitive importance and contributed to the development of regional geology,

mainly in Central Europe and the polar regions. The methods developed in the above-mentioned basic research were (and may be in the future) adapted to applied research (recent examples are shale gas exploration, tracing the spread of anthropogenic pollutants, studying structures related to mass movements). While basic research in the field of recognizing the structure and restoring tectonic evolution in various areas will still have a leading share in the research profile of most of IG PAS teams, it is also important to expand the “portfolio” of applied research so that it relates to new civilization challenges.

Earth sciences, including geophysics, are important for various areas of the economy. Sustainable economic growth and social welfare will require, inter alia, access to clean energy sources, minerals and clean water. It is crucial to strengthen our presence in research related to these three aspects. In the case of the energy sector, our methods can be used in projects related to the production of geothermal energy, underground hydrogen storage, capture and underground storage of CO₂, or underground storage of radioactive waste. In the case of searching for mineral resources, including the so-called critical raw materials, it is important to both reduce the cost of exploration and their impact on the natural environment through a greater share of non-invasive geophysical research. In the case of research related to groundwater resources, cooperation with national regulators (e.g. the National Hydrogeological Service) would be of key importance.

Participation in such projects on a national scale is conditioned by the state policy, but it would be desirable to acquire relevant competencies in projects implemented in other EU countries, where, for example, geothermal research is much more developed.

In strictly basic research, their high substantive level should be maintained through the use of the latest methods and the correct selection of research goals. These goals should be clearly defined and relate to possibly large, regional research problems in the field of the structure and evolution of the lithosphere. The results of the research should reach both specialized scientists in this field as well as all others interested in the history of the Earth. Therefore, it is important to popularize the research as much as possible.

1.2.4 Climate change and polar research

The years 2014–2016 were the warmest in the history of meteorological and oceanographic measurements, not only globally, but also in many regions of the world, including Europe. The speed of ongoing changes causes an imbalance in the processes that make up the existing and future state of the climate. Increasing intensity and frequency of extreme phenomena, such as fires, droughts, and floods, indicates a disruption of the balance and increased risk of extinction for many species, including humans.

Modeling the future hydro-climatic conditions at global and local scales is one of the key challenges in earth sciences. Despite the debate over the causes of climate change, the existence of climate change is widely accepted. With the observed changes in the hydro-climatic conditions, the threats to social and economic development increase. Therefore, it becomes particularly important to identify future conditions and develop adaptation to reduce the effects of potential threats.

For example, in the Anthropocene, due to human influence on the functioning of natural processes, drought is no longer just a natural hazard and its management at this stage is not fully effective. Therefore, there is a need to rethink the design of the drought process to account for these interactions. The predicted increase in temperature will affect the hydrologic regime. This is already reflected in the increased frequency and magnitude of droughts, the effects of which are causing increasing losses around the world.

The polar zones are the fastest-changing and most important terrestrial and marine areas for understanding global change, also in relation to other locations, including Poland. This is

particularly important for the assessment of, i.e., climate change scenarios, rising ocean levels, the evolution of the biosphere, and its adaptation to new conditions. Quoting the strategy of Polish polar research, “Important aspects of our involvement in polar research are not only the development of science, but also the possibility of expert support for public administration and the economy, the impact on increasing its innovation, and – in the long term – on sustainable development of our country”.

The melting and disintegration of glaciers and ice sheets of Antarctica and Greenland are responsible for more than half of the currently observed sea-level rise. It is estimated that, with continued high atmospheric greenhouse gas emissions, more than 600 million coastal people may be forced to leave their homes before the end of this century. Current research indicates that the disappearance of glaciers could inhibit the global deep-sea and surface water exchange system, the primary mechanism for heat, salt, and nutrient exchange on Earth. The disappearance of the sea-ice itself, in turn, leads to, among other things, greater absorption of solar energy by the ocean, modification of weather conditions, and an increase in the destructive effects of wave action on Arctic coastlines.

1.3 Management

The Board of Directors:



Prof. Beata Orlecka-Sikora
Director of the IG PAS



Mariusz Majdański
Deputy Director
for Scientific Affairs



Beata Fromelusz
Deputy Director
for Administration and Finance



Krzysztof Otto
Deputy Director
for Technical Issues

1.4 Employment structure

The structure of employment is illustrated by tables and graph below:

The number of employees

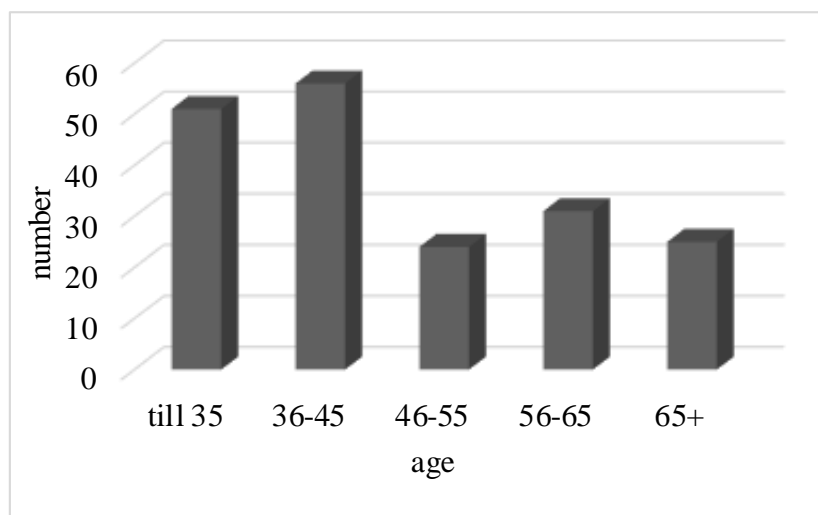
	Total	Researchers	PhD students
2016	175	69	29 (6 KNOW)
2017	178	67	26 (6 KNOW)
2018	187	74	22 (6 KNOW)
Change	+9	+7	-4

The employees by function

Function	Number
Non-research employes	113
Researchers	74
Total	187

⇒

Researchers	Number
Research Assistant	12
Assistant Professor	27
Associate Professor	21
Professor	14



Researchers' age structure.

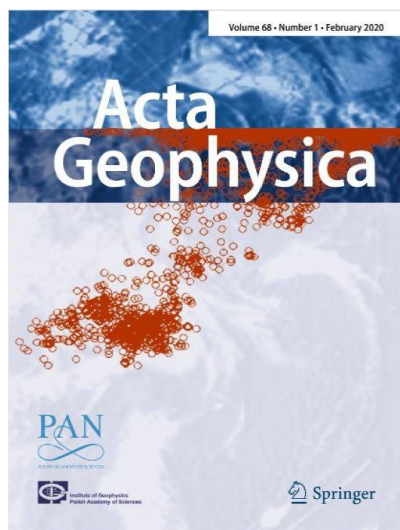
1.5 Activity of Scientific Information and Publishing Department

As in the previous years, in 2018 the activity of the Scientific Information and Publishing Department concentrated on the three titles:

- *Acta Geophysica*,
- *GeoPlanet: Earth and Planetary Sciences Book Series*,
- *Publications of the Institute of Geophysics, Polish Academy of Sciences*.

Acta Geophysica

Acta Geophysica is a leading geophysical journal published by the Institute of Geophysics and Committee of Geophysics, Polish Academy of Sciences. The Editor-in-Chief is Prof. Eleftheria Papadimitriou. In the editing of *Acta Geophysica* she is supported by eminent international experts who hold the position of Associate Editors.



Acta Geophysica is open to all kinds of manuscripts including research and review articles, short communications, comments to published papers, letters to the Editor as well as book reviews. Some of the issues are fully devoted to particular topics; we do encourage proposals for such topical issues. We accept submissions from scientists worldwide, offering high scientific and editorial standards and comprehensive treatment of the discussed topics.

In the year 2018, six issues of *Acta Geophysica* were published. The total number of pages (B5) was 1290, and the number of articles was 114. The impact factor is 1.013. In the upcoming years, a further increase of Impact Factor is expected.

Front cover of *Acta Geophysica*.

GeoPlanet: Earth and Planetary Sciences Book Series

This series is a forum for presenting the state-of-the-art and newest achievements in the Earth and space sciences. Its main objective is a multidisciplinary approach to link scientific activities in various Earth-related fields (geophysics, geology, oceanology) with the Solar System research. Our publications encompass topical monographs and selected conference proceedings, authored or edited by leading experts of international repute as well as by promising young scientists. We believe that the broad scope of problems dealt with by the *GeoPlanet Series* may give a stimulus for new ideas and discoveries. The Editor-in-Chief of *GeoPlanet Series* is Prof. Paweł M. Rowiński.

In the year 2018 four books were published within this series:

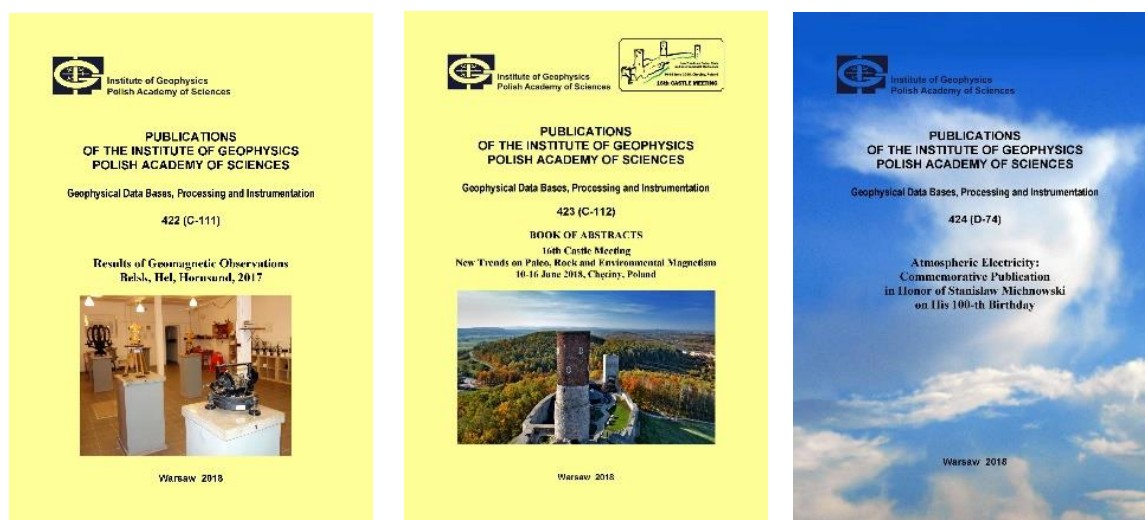


Front covers of *GeoPlanet: Earth and Planetary Sciences* books published in 2018.

Publications of the Institute of Geophysics, Polish Academy of Sciences

It has been published since 1962, initially (until 1970) as *Materialy i Prace Instytutu Geofizyki PAN*. Currently, it is focused on the following subject series: Physics of the Earth's Interior, Seismology, Geomagnetism, Physics of the Atmosphere, Hydrology (formerly Water Resources), Polar Research, and Miscellanea. The materials may be presented as individual publications or collections of papers (monographs, contributed volumes, or special issues).

A subtitle Geophysical Data Bases, Processing and Instrumentation was added in 2017 to underline the fact that the Journal became mainly focused on experimental results from the Institute of Geophysics PAS and other scientific institutions. Nowadays, it appears mainly in the electronic form, although printed issues are also possible. The Editor-in-Chief is Dr. Marek Kubicki, the Honorary Editor is Professor Roman Teisseyre. In the current year, three issues were published.



Front covers of *Publications of the Institute of Geophysics, Polish Academy of Sciences*, published in 2018.

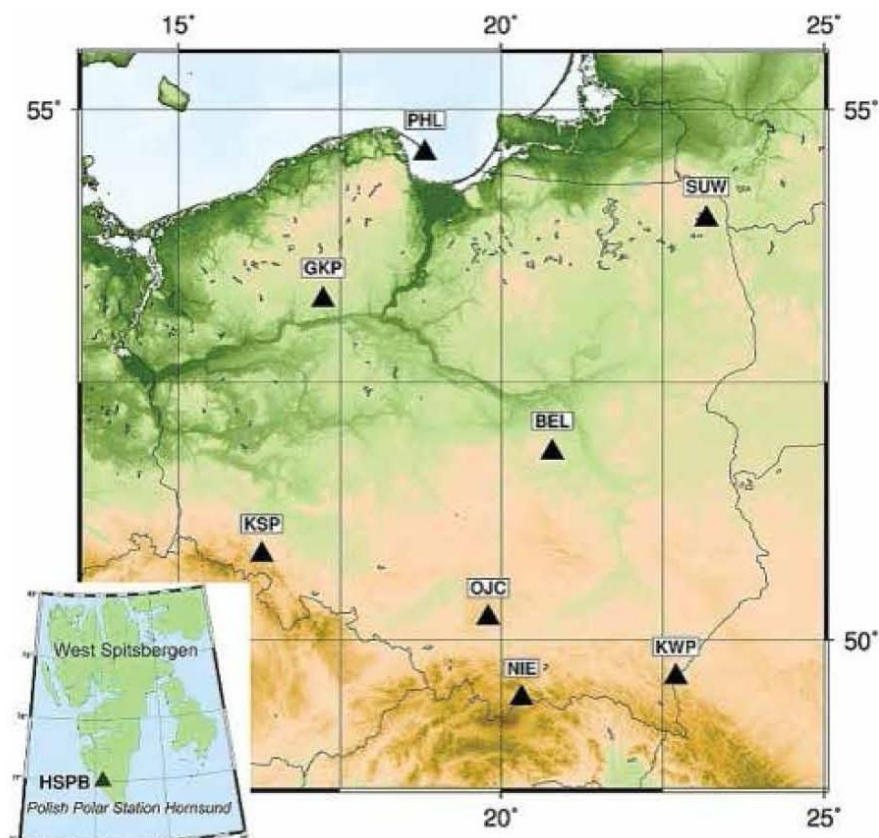
1.6 Observatories

The Institute of Geophysics, Polish Academy of Sciences, is the only institution in Poland that conducts monitoring of global geophysical fields in terms of seismology, geomagnetism and atmospheric physics.

The Institute manages observatories and stations in Poland and the Polish Polar Station Hornsund in the Spitsbergen archipelago. The observatories in Belsk, Świdler, Racibórz, Książ and the Hel Peninsula and the permanent seismic stations in Suwałki, Niedzica, Góra Klasztorna, Ojców, and Kalwaria Paławska register geophysical phenomena, continuously providing data to the World Data Centres.



Observatories at Belsk, Książ, and Racibórz.



Location of geophysical observatories and stations at Belsk (BEL), Książ (KSP), Ojców (OJC), Niedzica (NIE), Hel (PHL), Suwałki (SUW), Kalwaria Paławska (KWP), Górka Klasztorna, and the Polish Polar Station Hornsund (in inset).

1.7 Polish Polar Station

The Polish Polar Station Hornsund, named after Prof. Stanisław Siedlecki, is a modern interdisciplinary research platform located in the southern part of Spitsbergen, the largest island of the Svalbard archipelago. It was established in 1957 and has been in operation year-round since 1978. It is the only year-round Polish research observatory in the Arctic. The main objectives of the monitoring and research programmes carried out at the Station are related to the evolution of the High Arctic environment with respect to Climate Change.



The Polish Polar Station Hornsund


The Station is managed by the Institute of Geophysics, Polish Academy of Sciences (IG PAS) based in Warsaw, Poland. Well-equipped scientific laboratories, satellite communication and high standard accommodation and research facilities are available for over 20 visitors, in addition to the permanent staff of about 10 members of IG PAS Polar Expeditions.



1.8 Projects, commercial agreements, and publications

 NATIONAL SCIENCE CENTRE
POLAND 23 projects

 Ministry of Science
and Higher Education
Republic of Poland 27 projects

 Narodowe Centrum
Badań i Rozwoju 4 project

 THE FRAMEWORK PROGRAMME FOR RESEARCH AND INNOVATION
HORIZON 2020 13 projects

 The Research Council
of Norway 2 projects

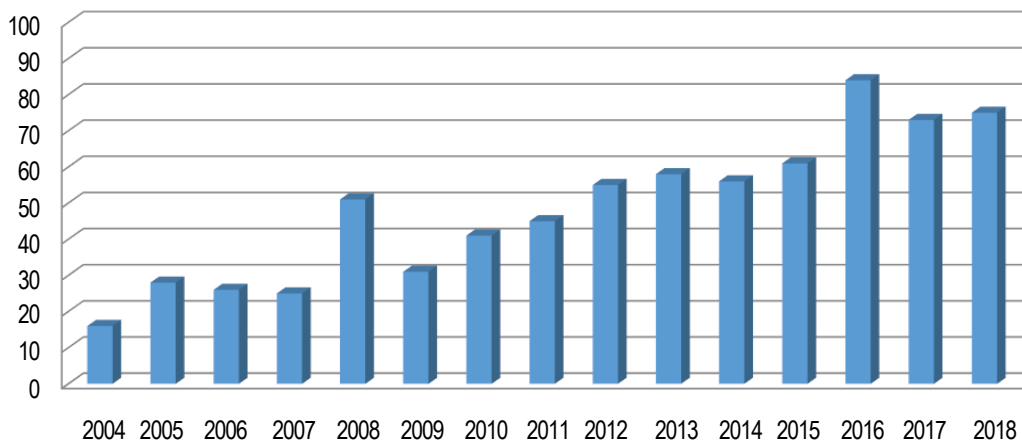
Commercial agreements
GIOŚ, PIG-PIB, WorleyParson, KGHM 19 projects
SA, GeoPro Geophysics, MLU, etc.



Publications statistics

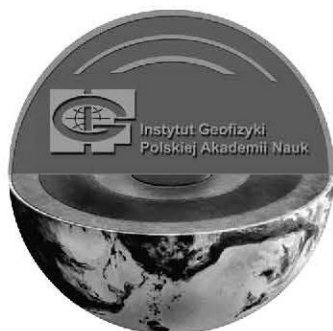
All	Monographs (or chapters)	Academic coursebooks (or chapters)	Publications in reviewed journals			Rest of scientific publications
			Publications 1	Publications 2	Publications 3	
106	5	12	75	0	4	10

JCR papers



1.9 Professor Adam Dziewoński Medal

Professor Adam M. Dziewoński (1936–2016) was an outstanding seismologist and planetary geologist. Having begun his scientific carrier in Poland, he was Professor of Harvard University, Foreign Member of the Polish Academy of Sciences, Member of the American Academy of Arts and Sciences and the National Academy of Sciences, and Doctor Honoris Causa of the AG University of Science and Technology in Cracow. He was the 1998 laureate of the Crafoord Prize (1998), considered to be equivalent to the Nobel Prize, for his research into the structure and processes within the Earth. He created the fundamentals of seismic tomography, and made seminal contributions to our knowledge on the large-scale structure of the Earth's interior and the nature of earthquakes.



The Medal to honour and commemorate the achievements of Professor Adam Dziewoński and his perpetual ties with geophysical research in Poland was instituted in 2017. It is awarded by the Director of the Institute of Geophysics PAS upon recommendation of the Awarding Committee for

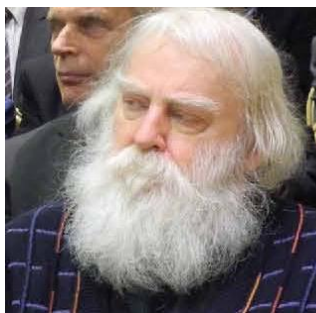
persons of outstanding scientific achievements with special merits to the Institute, in geophysical research (notably, the pioneering international projects), managing scientific work (notably, establishing the working groups and development of scientific staff), and enhancing the international promotion of the results obtained at the Institute. The medal is under the honorary patronage of the Minister of Science and Higher Education, Poland.

The Medal was granted to the first three laureates, Professors Marek A. Grad, Aleksander Guterch, and Roman Teisseyre, during the ceremony commemorating the 65-th Anniversary of the Institute.

Members of the Awarding Committee

- Prof. Barbara Romanowicz, University of California, Berkeley;
- Prof. Krzysztof E. Haman, Faculty of Physics, University of Warsaw;
- Prof. Jacek Jania, University of Silesia in Katowice;
- Prof. Andrzej Kijko, University of Pretoria.

The first Professor Adam Dziewoński Medal Winners



Prof. Marek Andrzej
GRAD
Faculty of Physics
University of Warsaw



Prof. Aleksander
GUTERCH
Institute of Geophysics PAS



Prof. Roman
TEISSEYRE
Institute of Geophysics PAS

2. DEPARTMENT OF SEISMOLOGY

Stanisław Lasocki

2.1 About the Department

Department of Seismology research activity covers a broad range of topics with the main subject of anthropogenic seismicity. All research activities covered by this report can be divided into several general topics: seismicity induced by exploitation of geo-resources, statistical properties of natural and anthropogenic seismic processes, seismicity induced by water reservoirs, engineering seismology, and natural seismicity of Poland. The first topic was the subject of four research projects dealing with hydrofracturing (SHEER, S4CE), carbon dioxide storage and geothermal energy (S4CE), and underground mining of the copper ore (NCN and FNP projects led by A. Caputa and M. Kozłowska). SHEER project findings allowed for a better understanding of fluid path migrations and development of seismic processes related to hydrofracturing. Finally, the project provided guidelines for best practices in environmental monitoring of hydrofracturing operations. The S4CE project covers fundamental studies of fluid transport and reactivity, development of new methods for the detection and quantification of micro-seismic events, and the deployment of the successful detection and quantification technologies in subsurface sites for continuous monitoring of the risks. Projects dealing with underground mining are aimed at aftershock studies and detection as well as the analysis of post-blasting seismic sources aiming at finding some characteristic physical properties of focal mechanisms, which might help in the development of rockburst active prevention. Another research was aimed at tracking possible ground deformation corresponding to a massive collapse in mine after an induced seismic event. The next activity was performed in cooperation with the Luleå University of Technology. The scope was seismic hazards in mines and analysis of seismic patterns and focal mechanisms. Research activity within statistical seismology was mainly focused on seismicity properties evolution in relation to fluid-injection, incompatibility of anthropogenic seismicity with probabilistic models typically used in seismic hazard analysis, and the impact of magnitude uncertainties on seismic catalogue properties. A clear and statistically significant positive correlation between seismicity rates and total injection rates was obtained in the case of the Geysers Geothermal field. It was proved that neither an exponential distribution of magnitude nor a Poisson distribution of event rate can be used to assess the stationary seismic hazard due to the anthropogenic seismicity from Oklahoma. Seismicity induced by water reservoirs was mainly focused on Czorsztyn (Poland) and Lai Chau (Vietnam) reservoirs. The latter is a subject of the NCN research project aimed at an exploration of the natural seismicity, which exists in the area of the dam, and then determining the development of anthropogenic seismic activity associated with the impoundment of water in the reservoir. Natural seismicity of Poland research was focused on monitoring the activity: six tectonic earthquakes were noticed; four in Podhale and two in Krynica region. Other works within tectonic seismicity covered dynamic triggering of shallow slip on forearc faults in Chile. Magnitude–distance relationship of slip triggering was derived. Engineering Seismology branch of our department research was aimed at HVSR methodology application for site effect determination in mining and polar areas. Another part of this activity was SERA project fostering the link between seismology and earthquake engineering. Important work was a prediction of the impact of tremors and surface deformations induced by mining in sections G23 O/ZG Rudna and LU XI O/ZG Lubin on OUOW “Żelazny Most” prepared within the agreement with KGHM Polska Miedź S.A. Hydrotechnical Division, Rudna. Except for significant scientific works Department of Seismology was also involved in the EPOS Programme. In 2018, the EPOS-ERIC was established and Poland joined it. It is one of the main achievements of Department of Seismology within 2018

being a result of several years of involvement in EPOS and a confirmation of the key role of IG PAS in the anthropogenic seismicity research community.

2.2 Personnel

Head of the Department

Stanisław Lasocki
Professor

Associate Professors

Artur Cichowicz
Beata Orlecka-Sikora

Assistant Professors

Maria Kozłowska
Konstantinos Leptokarpoulos
Grzegorz Lizurek
Dorota Olszewska
Łukasz Rudziński
Monika Sobiesiak

Senior Technical Officer

Jan Wiszniowski

Research Assistants

Wojciech Białoń
Alicja Caputa
Szymon Cielesta
Beata Plesiewicz
Monika Staszek
Piotr Sałek
Piotr Tworogowski
Paweł Urban

Technical Assistant

Izabela Dobrzycka
Romualda Koźlakiewicz
Dominika Wenc
Ewa Zarzycka
Kaj Michałowski

Administrative Coordinator

Anna Leśnodorska

PhD Student

Alicja Caputa, Poland; Stanisław Lasocki, Łukasz Rudziński – PhD supervisors

2.3 Main research projects

- SHEER, S. Lasocki, H2020, 2018–2018;
- S4CE: Science for Clean Energy, S. Lasocki, H2020, 2018–2018;

- SERA: Seismology and Earthquake Engineering Research Infrastructure Alliance for Europe, S. Lasocki, H2020, 2017–2020;
- EPOS IP WP14: EPOS Implementation Phase, B. Orlecka-Sikora, H2020, 2015–2019;
- EPOS PL, D. Olszewska, POIT, OPI, 2016–2021;
- Analysis of post-blasting seismic sources recorded after rockburst active prevention, A. Caputa, NCN, 2018–2018;
- Comprehensive analysis of the impact of local production conditions, main shock parameters, and stress transfer on productivity and distribution of aftershocks in induced seismicity – research for improving the safety of natural resources extraction, M. Kozłowska, Fundacja Nauki Polskiej, 2018–2018;
- Initialization and development of anthropogenic seismic processes induced by artificial surface reservoirs, G. Lizurek, NCN, 2018–2018.

2.4 Instruments and facilities

Equipment

Seismic networks:

- LUMINEOS – mining-induced seismicity in Legnica–Głogów Copper District: 17 – broadband (5s) seismometers (VE-53/BB GeoSIG) and 10 strong-motion instruments (AC-73 GeoSIG). Data is used in EPOS IP and NCN projects;
- BOIS – very new network above Lubelski Węgiel “Bogdanka” – 12 broadband (5s) seismometers (VE-53/BB GeoSIG), the network is directly connected with B+R project which is devoted to seismological monitoring of the mine belongs to Lubelski Węgiel “Bogdanka” S.A. Project leader: Department of Seismology IG PAS. Staff involved in the project: Ł. Rudziński, J. Wiszniowski, I. Dobrzycka, D. Wenc, S. Cielesta, P. Urban, P. Sałek. In the middle of 2018, the Department of Seismology started a new collaboration with one of Polish coal mines, the Lubelski Węgiel “Bogdanka” S.A. The main aim of the collaboration is focused on seismological observation of seismic activity induced in the vicinity of the mine. In October 2018, IG PAS installed 12 broadband (5s) seismic stations in the area around the mine. During the last three months of 2018, more than 50 seismic events with magnitude above $M > 1.5$ were detected and localized in the mining region. The collaboration will be continued in 2019;
- SENTINELS – induced seismicity around Czorsztyn–Niedzica artificial water reservoir: 10 broadband (5s) seismometers (VE-53/BB GeoSIG). Data is used in EPOS IP and NCN projects;
- Lai Chau – artificial water reservoir in Vietnam network cooperated with Institute of Geophysics, Vietnamese Academy of Science and Technology: 5 broadband seismometers (VE-53/BB GeoSIG, IG PAS), and 5 broadband seismometers (Guralp CMG-6TC, Samtac 801H, IG VAST). Data is used in EPOS IP and NCN projects;
- Geodynamic monitoring of Poland, 2018. The service is carried out as a part of the project “Geodynamic monitoring of Poland”, contract No. CRZP-240-36/20918 between the Polish Geological Institute – National Research Institute (PGI-NRI) and the Institute of Geophysics, Polish Academy of Sciences (IG PAS). A. Cichowicz, K. Michałowski, B. Plesiewicz, J. Wiszniowski.

The main goal of the project is to monitor the natural seismicity in Poland. The data from 42 seismic stations were used to perform the task. IG PAS provided 23 mobile stations (LE-3D Lite with NDL data loggers, financed within the project) and additionally 7 permanent broadband stations of the Polish Seismological Network – PLSN (financed from statutory activities). The project also has access to seismological data from 12 broadband stations of the

Polish Geological Institute. The software necessary for the analysis of seismic data and the generation of reports and alerts has been fully tested and works correctly. The data collection system is operational, continuous data is stored by the IG PAS Technical Support Department in Warsaw. The completeness of data for stations ranges from 97% to 100%. The Seismology Department of IG PAS generated 37 weekly reports. There was no need to create an alert because there was no natural seismic phenomenon above 3.5 magnitude;

- PGE EJ1 – Leader: Institute of Geophysics PAS. Staff involved in the project (from the Department of Seismology): Ł. Rudziński, B. Plesiewicz, L. Stempowski, K. Michałowski. Department of Seismology in cooperation with Technical Support Department is involved in seismic monitoring of potential nuclear power plant (NPP) site in northern Poland since 2015. During that time, IG has operated 10 seismic stations including broadband and short period devices. The signals are recorded continuously and contain information not only deals with possible local seismic activity but also influences of regional earthquakes. All data recorded in the project will be useful for the future analysis of seismic hazards estimated for the NPP site.

Other infrastructure:

- EPOS IP – WP14 Thematic Core Service Anthropogenic Hazards (TCS AH) – Leader: Institute of Geophysics PAS. Staff involved: B. Orlecka-Sikora, S. Lasocki, K. Leptokarpoulos, S. Cielesta, P. Urban, G. Lizurek, M. Staszek, D. Olszewska, D. Wenc. EPOS IP is the biggest infrastructural project in Europe within the solid earth sciences funded by the European Commission within H2020. The effect of the EPOS Programme will be pan-European scientific infrastructure open to the Member States and associated countries, facilitating the exchange of knowledge and mobility of researchers within the European Research Area and contributing to the dissemination and optimization of scientific results. EPOS programme has been planned until 2040. Currently, from 2015 to 2019, takes its second stage, that is, the Implementation Phase (EPOS IP). In 2008, the project was approved by the European Strategy Forum on Research Infrastructures (ESFRI). It was also placed on the Polish Roadmap for Research Infrastructures in 2011. Under this project, a multi-layered, multidisciplinary and interoperable research infrastructure in the form of measurement networks and database with standardized metadata will be built. The access to the collected and stored data from the distributed measurement networks, developed, standardized, and integrated data products will be provided through the website with relevant applications, analytical and dedicated visualization tools. WP14 Anthropogenic Hazards of EPOS IP is led by B. Orlecka-Sikora (IG PAS). Thematic Core Service Anthropogenic Hazards (TCS AH) is being developed by 14 European research institutions from 9 European countries. In 2018, the EPOS-ERIC was established and Poland joined it. It is one of the main achievements of the Department of Seismology in 2018, being a result of several years of involvement in EPOS and a confirmation of the key role of IG PAS in the anthropogenic seismicity research community. Within WP14, the IS-EPOS web portal has been designed to serve as one of the main pillars of the Thematic Core Service - Anthropogenic Hazards belonging to pan-European multidisciplinary research infrastructure created within the EPOS program. More about TCS AH can be found on the website: <https://www.epos-ip.org/tcs/anthropogenic-hazards>, an access to IS-EPOS platform resources is available via the website: <https://tcs.ah-epos.eu/>;
- EPOS – European Plate Observing System – EPOS-PL – Leader: Institute of Geophysics PAS. Staff involved in the project: Coordinator D. Olszewska, coordinator of task 2 (Induced Seismicity Research Infrastructure Centre – CIBIS) G. Lizurek, K. Michałowski, B. Plesiewicz, P. Urban, J. Wiszniowski. The infrastructure built within the project EPOS-PL is related to the European programme for the development of Research Infrastructure (RI) for Solid Earth Science – EPOS – and

it will be an integral part of it. The research Infrastructure EPOS-PL will integrate both existing and newly built National Research Infrastructures (Theme Center for Research Infrastructures), which, under the premises of the program EPOS, are financed exclusively by the national funds. In addition, the e-science platform will be developed. This would be a new/additional module built within EPOS-IP Thematic Core Services Anthropogenic Hazards (TCS AH).

The first layer of RI is built by the so-called Research Infrastructure Centers (RICs). RIC provides a complete dataset concerning a given research field (e.g. seismic data, geodetic data, geological data). Each national RIC has its own IT support. This solution ensures effective data storage and basic computing resources. Task 2 – Induced Seismicity Research Infrastructure Centre – CIBIS – is the main responsibility of the Department of Seismology within the EPOS PL. It is aimed at the development of a data acquisition system, storage and seismological data analysis from the anthropogenic seismicity hazard areas. Currently, the data acquisition system named CIBIS is operational and allows sharing and accessing the data via the IS-EPOS platform. The second layer of innovative EPOS-PL infrastructure concerns the integration of infrastructure in the scale of Poland. Measurement polygons for the integrated observation of geodynamic processes are going to be built. The first polygons from the group of MUSE – Multidisciplinary Upper Silesian Episode – will be built in mining and post-mining areas of the Upper Silesian Coal Basin (Poland). Collected data and products will be integrated as a Multidisciplinary Upper Silesian Episode and shared through the TCS AH platform (Thematic Core Service Anthropogenic Hazards, <https://tcs.ah-epos.eu>).

The next layer of innovative EPOS-PL structure is related to the Integration of Research Infrastructure at the European level, in the so-called EPOS Thematic Hubs. This will happen through the integration of national RI providing specialized services to communities associated in a number of disciplines in the Earth sciences (e.g. seismology, geodesy, etc.) or interested in particular disciplines. Thematic Hubs create an intermediate layer of the EPOS integration plan. Thematic Core Service of Anthropogenic Hazards (TCS AH) is being built in Poland.

The following institutes are responsible for the implementation of this project: Institute of Geophysics, Polish Academy of Sciences (IG PAS) – Project Coordinator, Academic Computer Centre Cyfronet AGH University of Science and Technology (ACK Cyfronet), Central Mining Institute (GIG), the Institute of Geodesy and Cartography (IGiK), Wrocław University of Environmental and Life Sciences (UPWr), Military University of Technology (WAT). In addition, resources constituting the entrepreneur's own contribution will come from the Coal Company S.A.

- SERA – Seismology and Earthquake Engineering Research Infrastructure Alliance for Europe. Leader: Eidgenössische Technische Hochschule Zürich, Switzerland. Staff involved: M. Sobiesiak, K. Leptokarpoulos, S. Lasocki, P. Sałek.

The major aim of the European Project SERA is to foster the link between seismology and earthquake engineering. The project integrates data, products, infrastructures, and knowledge from both disciplines, like earthquake catalogues, analysis software, experimental set-ups to gain new insights into earthquake processes and their influences on the general infrastructure, both of tectonic as well as induced seismicity. Tasks of IG PAS within the SERA project and contributions in 2018:

- 1) WP22 VA5: Access to data and products of anthropogenic seismicity at IG PAS,
- 2) WP23 JRA1: Physics of the earthquake initiation,
- 3) WP24 JRA2: Characterizing the activity rates of induced and natural earthquakes.

More about scientific outcomes of this project are described in research activity of Engineering Seismology.

Long term service contracts:

Supervising the monitoring of seismic impact due to mining exploitation on the OUOW “Żelazny Most” repository embankment seismic network and the stations monitoring the western foreland of OUOW. Leader: Institute of Geophysics PAS. Staff involved: S. Lasocki, D. Olszewska, S. Cielesta, Ł. Rudziński.

Supervising the monitoring of seismic impact due to mining exploitation on the OUOW “Żelazny Most” repository embankment seismic network and the stations monitoring the western foreland of OUOW has been carried out in line with the contract concluded by and between KGHM Polska Miedź S.A. Hydrotechnical Division, Rudna, and the Institute of Geophysics, Polish Academy of Sciences, in Warsaw. This agreement covers a period of three years, 2017–2019, and is accounted for annual stages. Mentioned supervision is being carried out for the last 16 years. According to the scope of work, the project team supervised ground motion monitoring and maintained and processed ground motion records from the accelerometric stations located at OUOW “Żelazny Most” facilities and the west OUOW foreground. The recorded signals are being uploaded to the SEJS-NET system database by the staff of the Geophysics Station of Rudna Mine. Both the SEJS-NET system and the ground motion database of the OUOW region are maintained on computer facilities of the Institute of Geophysics, Polish Academy of Sciences, in Warsaw. The database is managed by the project team. Upon request of KGHM „Polska Miedź” S.A., Hydrotechnical Division, as the owner of the database, a system administrator grants external users with database access. KGHM “Polska Miedź” S.A. conducts a new SEZAM system to collect and process the data related to induced seismicity in Legnica–Głogów Copper district, caused by underground mine operation. Therefore, there is a need to develop a data exchange of ground motion registrations and seismic catalogues. Access to the data is necessary due to the analysis carried out at the request of KGHM. One of such works is “Supervising the monitoring of seismic impact due to mining exploitation on the

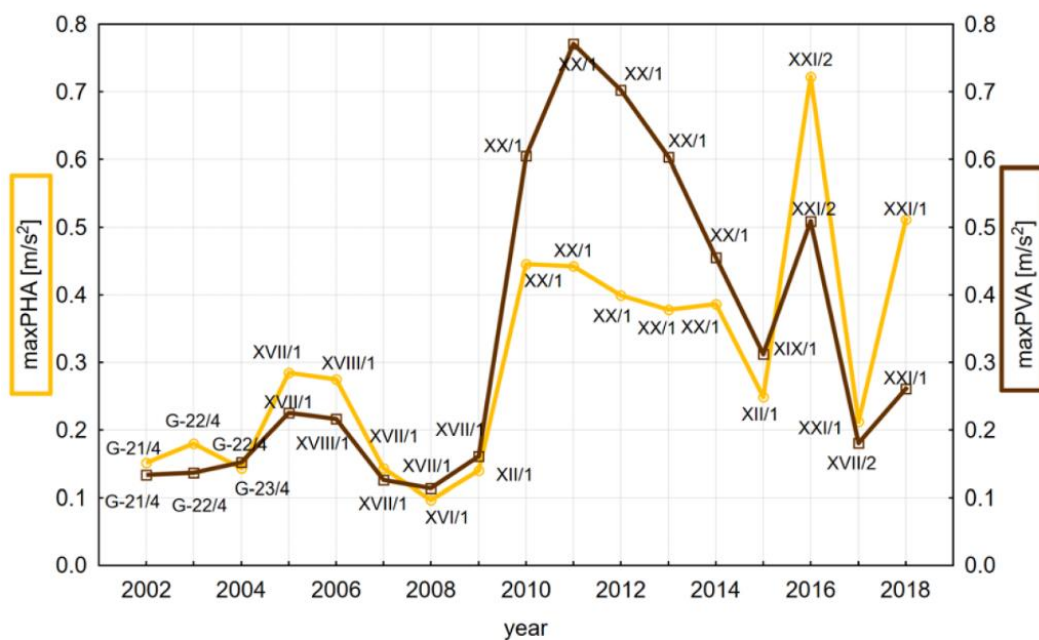


Fig. 1. Annual maxims of PHA10 and PVA10 recorded at the embankment repository. Yellow line – horizontal influence. Brown line – vertical influence. Labels over the marked points present the names of ZG Rudna mine sections, inducing these strongest motions.

OUOW “Żelazny Most” repository embankment seismic network and the stations monitoring the western foreland of OUOW in 2017–2019”. A result of these consultations will be the scope of data, the form of data, and the method of transmission of the data.

Seismometric monitoring consisted of 22 operating measurement stations, with 16 located at the OUOW “Żelazny Most” facilities and 6 located in the west foreground of the OUOW. Every measurement station is equipped with a three-componential accelerometer sensor. The recorded signals, which are caused by mining events, are transmitted to the Geophysical Station of Rudna Mine and then uploaded as text files to the server of SEJS-NET system database. Within the project, a review of the accelerometric records along with the quality assessments of measurements is being prepared. All accelerometric signals from the reporting period are integrated to ground motion velocity records and peak amplitudes of ground acceleration and ground velocity, as well as duration times, were calculated. For records originated by stronger sources, spectral amplitudes are being computed. Within every report, the description of seismic sources of the recorded ground motion is done along with a presentation of the seismic activities of ZG Rudna, ZG Lubin, and ZG Polkowice-Sieroszowice mines. Reports include also seismic events impacts in reporting period with respect to the hazard to the “Żelazny Most” repository, which they evoke. Figure 1 presents annual maximal horizontal and vertical impacts, expressed in peak ground acceleration components, recorded by the monitoring stations at the OUOW embankment from 2002 to 2018. Peak values of the horizontal and vertical components of the ground motion acceleration in the frequency range up to 10 Hz, recorded at the “Żelazny Most” repository facilities, are also being compared with respective estimates calculated by means of the recent ground motion prediction equations.

Laboratory

Department of Seismology is equipped with 78 modern seismic stations: 62 broadband and 6 very broadband seismometers as well as 10 strong-motion devices. 44 stations are already installed in seismically active areas: two mining regions in Poland and two regions with seismicity induced by water reservoirs in Poland and Vietnam. The data recorded by the stations are (or will be soon) available on the IS-EPOS Platform (<http://tcs.ah-epos.eu/>). The e-platform devotes to hazards related to anthropogenic activities. IS-EPOS platform is a gateway for the data and research applications related to anthropogenic hazards. One of the main storages, called e-Node, is managed by the Department of Seismology, second storage is located and managed by EOST in Strasbourg. Currently, 27 out of 28 datasets called episodes are available on IS-EPOS platform and are stored in Polish e-Node. Both e-Nodes and IS-EPOS platform are developed within EPOS IP project within WP14 Anthropogenic Hazards.

2.5 Research activity and results

Brief description/abstracts/summaries of some of the achievements of the Department’s staff:

SHALE GAS EXPLORATION AND EXPLOITATION INDUCED RISKS (SHEER)

S. Lasocki, B. Orlecka-Sikora, D. Olszewska, G. Lizurek, M. Staszek, S. Cielesta, K. Leptokaropoulos, M. Kozłowska, P. Urban

The Shale gas Exploration and Exploitation induced Risks (SHEER) project has taken up the very current problem of competent assessment of the possible impact of shale gas production on the environment. It was implemented as part of an international consortium of seven scientific institutions from Italy, Poland, Germany, Netherlands, UK, and USA. Polish scientists from the Institute of Geophysics, Polish Academy of Sciences (IG PAS), led three out of eight work packages (WP2, WP3, WP6), responsible for running a multidisciplinary database and integrating it with e-Platform IS-EPOS, environmental monitoring, and assessment of the impact of hydrofracturing on air pollution. Their contribution to the implementation of the other

packages and the whole project was also significant: prof. Stanisław Lasocki, the leader of the Polish group, was part of the three-man Project Management Team.

For the first time in Europe, multidisciplinary environmental monitoring was carried out before, during, and after hydrofracturing. In the area around the exploration well of PGNiG S.A., in the village of Wysin in Pomerania, Poland, equipment for measuring seismicity, groundwater quality and air quality has been deployed (see Fig. 1). The hydrofracturing in Wysin was carried out in two horizontal, ~ 1.7 km long holes (Wysin-2H and Wysin-3H), located at a depth of 4 km, in two ten-day cycles, successively in June and July 2016.

The seismic monitoring of seismicity induced by technological works in the Wysin wells lasted from November 2015 to January 2017 with the use of 31 surface seismometers and three installed in 50 m deep boreholes. Two shallow seismic events, with magnitude $M_w = 1.0$ and $M_w = 0.5$, recorded a few days after hydrofracturing, were located in the close vicinity of the well. Small distances between the well and epicenters and the temporal correlation between technological operations and occurring seismicity suggest a possible relationship between hydrofracturing and the two mentioned seismic events. Four wells reaching the groundwater table were used to monitor the water quality. Parameters – such as water levels, absolute pressure, temperature, or electrical conductivity – were recorded at 15-minute intervals, in situ, from December 2015 to February 2018. Additionally, every 4–6 week's water samples were collected for laboratory analysis. In the mentioned period, no impact of hydrofracturing on groundwater parameters, whether the water level or the chemical composition of groundwater was recorded, both in the short- and medium-term scale. Air pollution was monitored continuously using an automatic measuring station located ~ 1000 m east of the drilling platform. Concentration levels of various pollutants, including NO , NO_2 , NO_x , CO , PM_{10} , O_3 , CO_2 , CH_4 , NMHC, and Radon, were analyzed. Air quality measurements covered the period from July 2015 to July 2017. During the entire monitoring period, levels of air pollution near the drilling rig remained low in relation to generally accepted standards. Only three short, 1–2 hour periods of increased methane levels were detected on July 30, September 1 and 2, 2016. During this time, the wells previously used for fracturing were shut down. Detailed monitoring did not show any significant impact of technological work in Wysin on the condition of the environment. The collected data together with data from other world locations for the use of underground water injection in order to obtain energy and energy resources became part of the SHEER project database, managed and maintained at the IG PAS.

The interdisciplinary nature of the data collected as part of the project and the amount itself required the creation of a “smart” database, integrating seven independent episodes. The SHEER project database has been made available on the IS-EPOS e-Platform for Anthropogenic Hazards located in Poland. From the beginning of May 2018, the data collected in the project is open to all registered users of the free scientific platform available at <https://tcs.ah-epos.eu/>. The SHEER project database has been used in research conducted by consortium members. Project members developed, among others, a statistical description of induced seismicity processes and an assessment of seismic dependence with operational/technological parameters. Researchers developed methods for tracking and modelling the development of fractures in the rock mass and the permeability changes caused by water injection. As part of the SHEER project, a statistical method for assessing the environmental impact and risks in the entire shale gas exploitation cycle was created. This method integrates many causes of risks and many of the hazards implied by these risks. After testing on the SHEER database, the method was recommended to the European Commission as a way to comprehensively evaluate the possible effects of shale gas exploitation. More information about the project, its results, publications, reports, and reports on individual work packages, bulletins, and materials promoting the project are available on the project website: <http://www.>

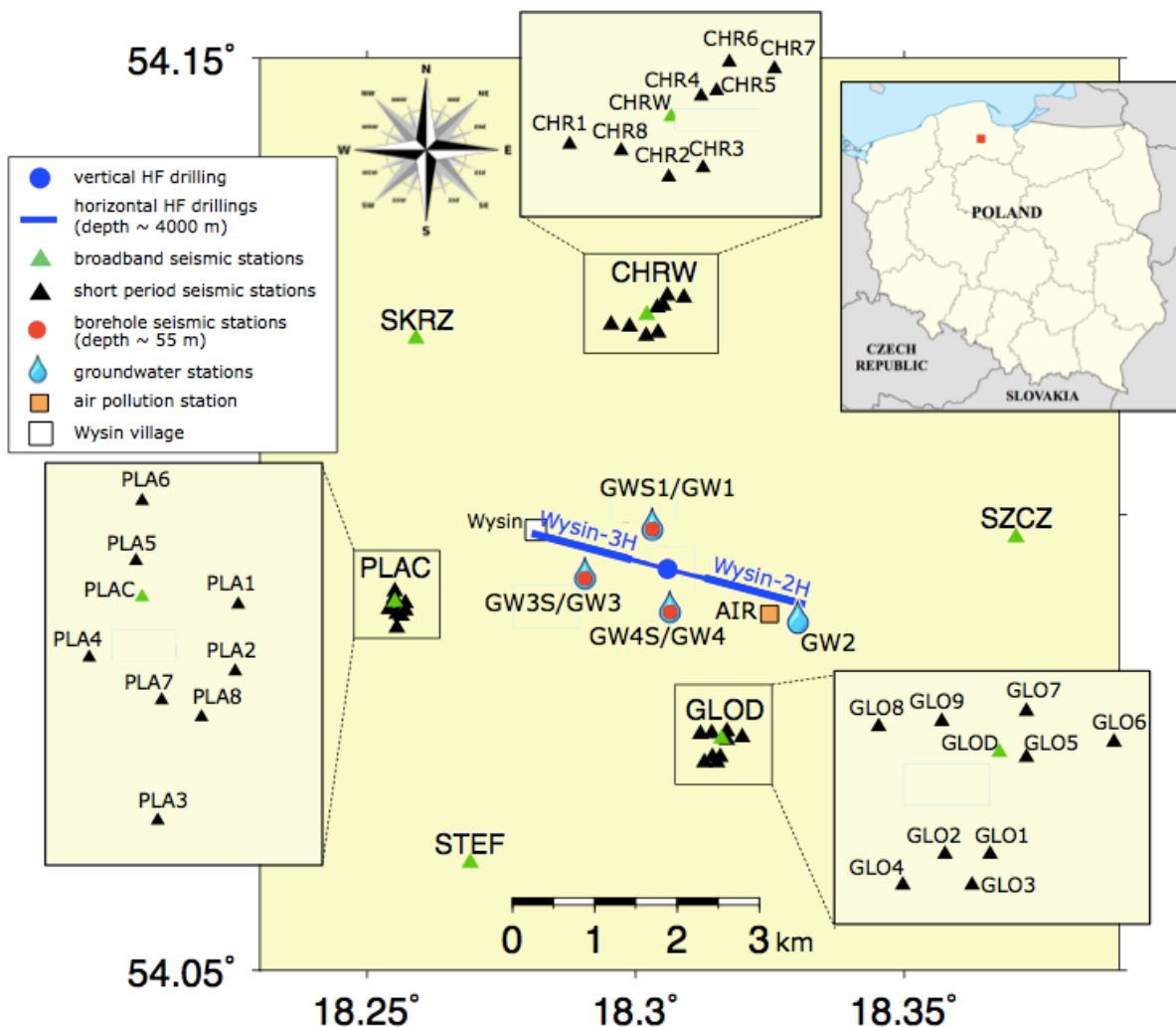


Fig. 1. Map of seismic, air, and groundwater monitoring at the Wysin site (Poland). The seismic monitoring includes broad-band stations (green triangles), small-scale arrays (inset boxes) composed by 8–9 short-period stations each (black triangles), and borehole stations (red circles). The air pollution station (orange square) is located at Stary Wiec village. Groundwater borehole monitoring stations are denoted by water drop symbols; some of them are located next to the borehole seismic stations. Wellhead (blue dot) and horizontal boreholes (blue lines) are shown. The inset map shows the hydraulic fracturing area (red square) in Poland (after López-Comino et al. 2018).

sheerproject.eu/. The main achievements of the project were published in several publications and a special issue of *Acta Geophysica* dedicated to SHEER.

TRACKING THE DEVELOPMENT OF SEISMIC FRACTURE NETWORK FROM THE GEYSERS GEOTHERMAL FIELD

B. Orlecka-Sikora, S. Cielesta, S. Lasocki

The problem of tracking the fracture growth as a possible way for fluid migration in the rock mass is of scientific-wide concern in studies dealing with the exploitation of geo-resources. Most of the possible environmental impacts and risks are linked to undesired evolution of the fracturing process and enhancement of permeability. Understanding how far this enhanced permeability pattern can develop in space and time can be approached by the description of the possible fracture network growth and fracture network connectivity.

In the framework of the SHEER project, the problem of development of fracture networks towards the potential for forming the pathways for fluid migration was studied using the equivalent dimensions approach. In this research activity, an example of this way of fracture system identification was applied to the injection-induced seismicity data from the north-western part of The Geysers (TG) geothermal field in California, USA. Seismicity of The Geysers results from thermoelastic and proelastic effects that change the local stress field in the reservoir. The seismic activity in TG highly correlates with the injection operations. The analysed north-western seismicity was isolated from the rest of seismic activity in the broader area of the TG field. The seismic catalogue for this specific seismicity cluster in addition to occurrence time, location and magnitude contains seismic moment tensors and spectral parameters. Thanks to that and the application of equivalent dimension transforms, criteria for possible linking of fractures in a prescribed direction were formulated, based on (i) fault plane orientations of fractures, (ii) locations of hypocenters with respect to the injection well, (iii) sources radii, and (iv) angles between the fault planes of fracture segments. To identify fracture arrays, the hierarchical clustering was used. The potential of an array to link fractures into longer crevices is quantified by the number of fractures' intersections. Considering hydraulically induced fracturing, the information about the fracture segment location and fracture plane orientation is necessary to map a build-up of the fracture network. In this connection, three parameters of the earthquake were selected. The first parameter was the distance between the open hole of Prati-9 well and the event hypocenter, r . This parameter allowed to track the reaction of the rock mass to driving stresses of fracturing, which are assumed to propagate from the well out. The fracture growth depends also on principal stress orientation. This second factor can result in an elongation of the fracture network. Usually, an observed shape of the anthropogenic seismicity clusters is consistent with the regional stress field. Following up, for proper identification of activation of fracture networks potentially comprising linked fractures, which were probably preferentially aligned parallel to the stress field orientation, a deflection parameter was introduced. The deflection, def , was the angle between the position vector of hypocenter of a seismic event and SH_{max} direction. The third parameter was a 3D rotation, rot . Based on P and T axes' orientations, the rotations of DC sources of events to the fault plane strike/dip/rake: 26/45/-45, were calculated. The assumed fault plane compromises the prevailing orientations of fault planes in the study area. The rotations were expected to be in general consistent with the stresses promoting failures. Similar rot values indicated the similarity of fault plane orientations. To identify fracture structures within the data, hierarchical clustering with the agglomerative approach was used. The distance between events was the indicator of the fracture network development—the smaller distance between events the stronger link between them. The linkage method of Ward was used for the above quantification. Characteristics of each identified cluster were analysed towards a possibility of fracture linking. Each seismic event was attributed with the section of strike line of length equal to two times source radius and centered at the event epicenter. As a proxy of the number of connections among fractures, the number of intersections among these sections was used. These intersections were called nodes. The connectivity coefficient C was calculated. This is the ratio between the actually observed number of nodes in a cluster and the number of possible nodes within the cluster. To get an insight into a relation between connectivity within fracture networks and injection rate, those events, which had occurred during two injection cycles, were extracted (Fig. 1). The value of connectivity parameter, C , in the families distinctly changes between stages of injection in which the events in the family occurred.

The test indicates that the connectivity values in the stages before and after the peak injection are significantly greater than the connectivity in the peak injection stage. The differences between C values in the stages before and after the peak injection have not been

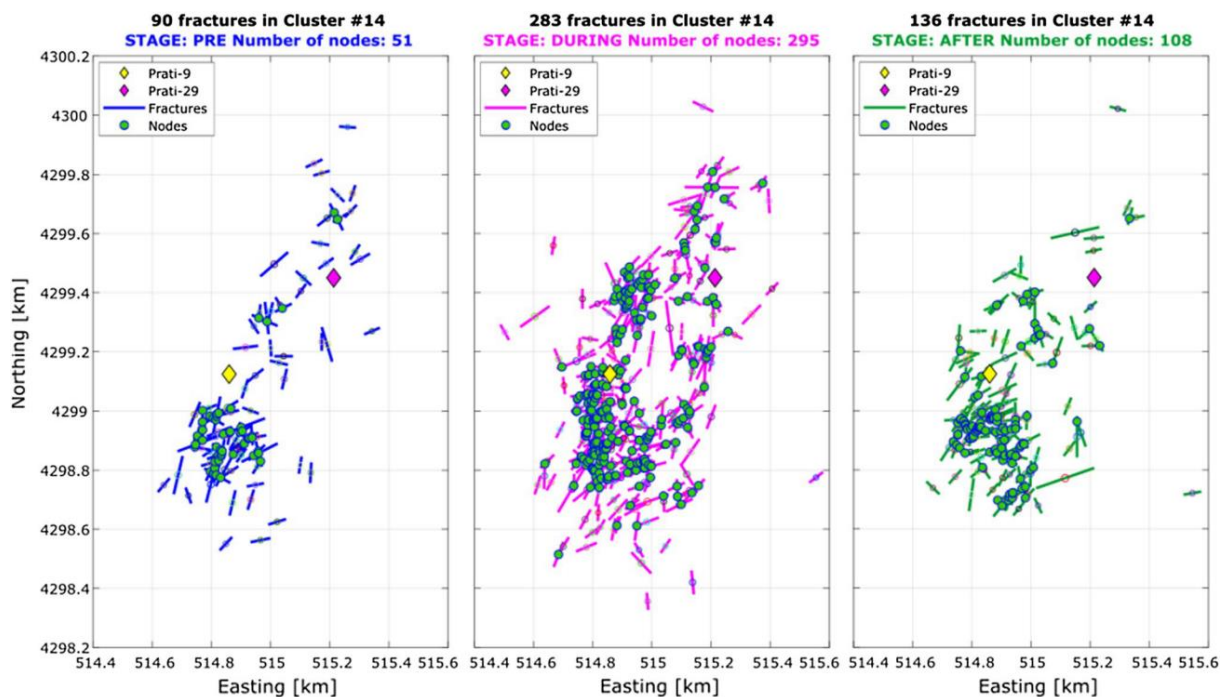


Fig. 1. Connections among fractures from the extracted 13 clusters in the three stages of injection. Fractures occurred during the stages before, during and after the peak injection are plotted in blue, pink, and green, respectively. Intersections (nodes) are marked with green dots. Open holes of Prati-9 and Prati-29 injection wells are shown as yellow and pink diamonds, respectively (after Orlecka-Sikora et al. 2019).

found significant. The test results suggest that lower injection rates favour linking fractures, whereas higher injection rates inhibit such linking tendency.

References

Orlecka-Sikora, B., S. Cielesta, and S. Lasocki (2019), Tracking the development of seismic fracture network from The Geysers geothermal field, *Acta Geophys.* **67**, 341–350, DOI: 10.1007/s11600-018-0202-6.

EPOS IP. IS-EPOS THEMATIC CORE SERVICE ANTHROPOGENIC HAZARDS – IS-EPOS PLATFORM DEVELOPMENT

B. Orlecka-Sikora, S. Lasocki, K. Leptokaropoulos, S. Cielesta, P. Urban, G. Lizurek, M. Staszek, D. Olszewska

WP14 Anthropogenic Hazards of EPOS IP project is led by B. Orlecka-Sikora (IG PAS). EPOS IP is the biggest infrastructural project in Europe within the solid earth sciences funded by the European Commission within H2020. Thematic Core Service Anthropogenic Hazards (TCS AH) is being developed by 14 European research institutions from 9 European countries. In 2018, the EPOS-ERIC was established and Poland joined it. It is one of the main achievements of Department of Seismology in 2018, being a result of several years of involvement in EPOS and a confirmation of the key role of IG PAS in anthropogenic seismicity (AS) research community. IS-EPOS web portal, whose scheme is shown in Fig. 1, has been designed to serve as one of the main pillars of the Thematic Core Service – Anthropogenic Hazards belonging to the pan-European multidisciplinary research infrastructure created within the EPOS program. IS-

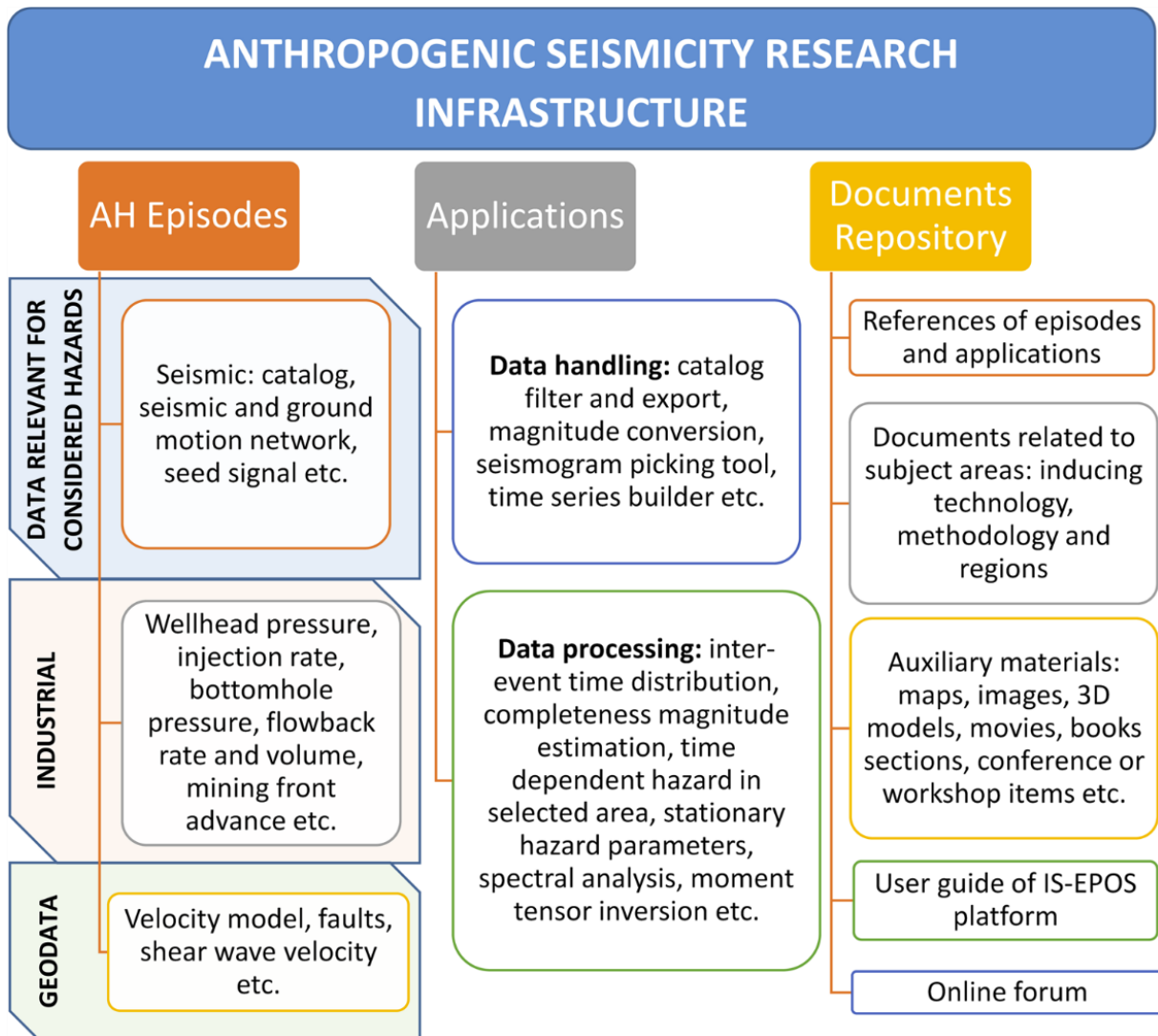


Fig. 1. Scheme of research infrastructure integrated within IS-EPOS e-platform (after Leptokaropoulos et al. 2019).

EPOS platform is open for the research community and general public according to its rules of access, receiving an open-access tool for the experimentation and training of students and young scientists, who want to perform AS research. Several successful workshops and demonstrations for undergraduate as well as postgraduate students on AS and hazard have been carried out in Germany, Poland, Greece, Sweden, Finland, and USA. Collaboration abilities are scheduled to be integrated into the upcoming platform version, enabling team generation and sharing common projects, data, applications, and results among the users. Currently, 28 datasets called episodes from 11 countries from Asia, Europe, and North America are available on the IS-EPOS platform. Episodes are stored in two e-Nodes: Polish e-Node hosted by IG PAS and French hosted by EOST Strasbourg. IS-EPOS promotes new opportunities to study and understand the dynamic and complex solid earth system response to human activities by integrating the use of data, data products, analysis models, and online facilities. IS-EPOS has been already used to facilitate scientific research in recently published papers connected with anthropogenic as well as natural seismicity by utilizing data, applications and/or the interface and facilities of the platform. The above-mentioned research abilities are supported by over 30 web-based research applications available for the users. At the end of 2018, the IS-EPOS platform had 877 users

from 127 institutions located in 27 countries. The main achievement of this activity is the dissemination and a summary of the features and impact of the IS-EPOS platform on the IS community so far. More about EPOS WP14 can be found on the website: <https://www.epos-ip.org/tcs/anthropogenic-hazards>; the access to IS-EPOS platform resources is available via the website: <https://tcs.ah-epos.eu/>.

References

Leptokaropoulos, K., S. Cielesta, M. Staszek, D. Olszewska, G. Lizurek, J. Kocot, S. Lasocki, B. Orlecka-Sikora, M. Sterzel, and T. Szepieniec (2019), IS-EPOS: a platform for anthropogenic seismicity research, *Acta Geophys.* **67**, 299–310, DOI: 10.1007/s11600-018-0209-z.

SCIENCE FOR CLEAN ENERGY – S4CE

S. Lasocki, K. Leptokaropoulos, P. Urban

Science4CleanEnergy, S4CE, is a multi-disciplinary consortium, of world-leading academics, research laboratories, SMEs and industries. S4CE will develop a project that includes fundamental studies of fluid transport and reactivity, development of new instruments and methods for the detection and quantification of emissions, micro-seismic events, etc., lab and field testing of such new technologies, and the deployment of successful detection and quantification technologies in sub-surface sites for continuous monitoring of the risks identified by the European Commission. S4CE leverages approximately 500M EUR in existing investments on 4 scientific field sites. S4CE will utilize monitoring data acquired during the project in these field sites on which: (a) it will be possible to quantify the environmental impact of sub-surface geo-energy applications; (b) new technologies will be demonstrated; (c) data will be collected during the duration of the project, and potentially after the end of the project. Using reliable data, innovative analytical models and software, S4CE will quantify the likelihood of environmental risks ranging from fugitive emissions, water contamination, induced micro-seismicity, and local impacts. Such quantifications will have enormous positive societal consequences because environmental risks will be prevented and mitigated. S4CE set up a probabilistic methodology to assess and mitigate both the short and long term environmental risks connected to the exploration and exploitation of sub-surface geo-energy. S4CE will maintain a transparent dialogue with all stakeholders, including the public at large, the next generation of scientists, academics and industrial operators, including training of young post-graduate students and post-doctoral researchers. S4CE will deliver the independent assessment of the environmental footprint related to geo-energy sub-surface operations, having as primary impact the assistance to policy making.

The S4CE consortium consists of 22 parties. Activities of the Institute of Geophysics, Polish Academy of Sciences in S4CE are carried out by the Department of Seismology. The Department is involved in five out of nine work packages, namely:

- WP3 – Instruments and Tools: Development and Deployment,
- WP5 – Data Gathering and Model Implementation,
- WP6 – Implementation of Novel Technologies,
- WP8 – International Cooperation and Policy Recommendations,
- WP9 – Dissemination, Exploitation and Innovation.

In WP6 the Department leads Task 6.5 “Assessing rapid fluid transport probability and tracking fluid pathways in the rockmass”. The assessments of the probability of rapid fluid coupling will be based on the methodologies developed for the volcanic environment to the fluid-solid coupling of two phases fluid (gas and water) in the unconventional hydrocarbon

reservoirs. Tracking fluid pathways within the rockmass will be based on the transformation to equivalent dimensions of microearthquake parameters. Event clusters will be identified in the multi-parameter equivalent dimension spaces. The identification of these families of events will be achieved by defining prescribed conditions of crack parameters, such as directions, dimensions and mutual distances. The probability of generation of a given length fissure, resulting from the linkage among smaller cracks of the same cluster will be subsequently determined.

In WP9 the Department of Seismology leads Task 9.7 “S4CE Database on IS-Epos platform”. The IS-EPOS, which is the main technical pillar of the Thematic Core Service Anthropogenic Hazards (TCS AH), belonging to European Plate Observing System (EPOS) platform, is to be used in S4CE as storage of newly acquired data.

COMPREHENSIVE ANALYSIS OF THE IMPACT OF LOCAL PRODUCTION CONDITIONS, MAIN SHOCK PARAMETERS, AND STRESS TRANSFER ON PRODUCTIVITY AND DISTRIBUTION OF AFTERSHOCKS IN INDUCED SEISMICITY – RESEARCH FOR IMPROVING THE SAFETY OF NATURAL RESOURCES EXTRACTION

M. Kozłowska

The goal of the project is to understand the geological, seismological and/or technological factors influencing the productivity of aftershocks in induced seismicity. Since the beginning of the project the analysis of the aftershock activity in Kiruna mine, Sweden, was performed. That research was performed in cooperation with the foreign partner of the project – prof. Savka Dineva from Luleå University of Technology (LTU) and included 3-weeks training at the LTU. The scientific paper has been written regarding this study and it’s now under review. Two relatively strong mining seismic events in Kiruna mine occurring in two seismically active blocks were investigated. Focal mechanisms and source parameters of the two strong events were studied to model the resulting static stress changes. The level and distribution of seismicity occurring before the strong events were evaluated and then used in the modelling of the aftershocks with the rate-and-state model. The model worked well for one of the events – it predicted both the number and area of aftershocks. In the case of the second event, the model performed worse underestimating the number of aftershocks (Figs. 1 and 2). Perhaps, in that case, some additional processes, not included in the model, took place and influenced the seismic activity, e.g. dynamic triggering.

Under the project, the cooperation with a master’s student from AGH University in Kraków has started. The scope of this cooperation is studying the seismic activity of Rudna mine,

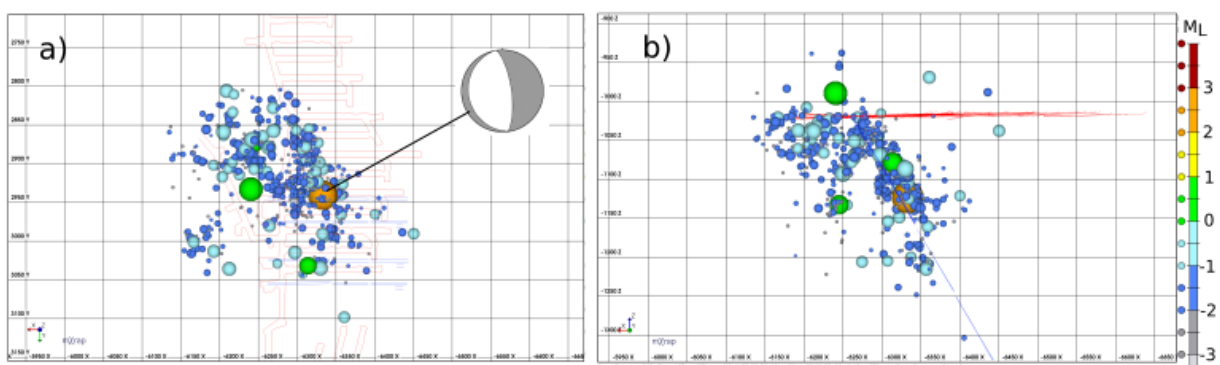


Fig. 1. The horizontal (a) and vertical (b) distribution of aftershock following one of the studied strong seismic events in Kiruna mine, Sweden (after Kozłowska et al. 2021).

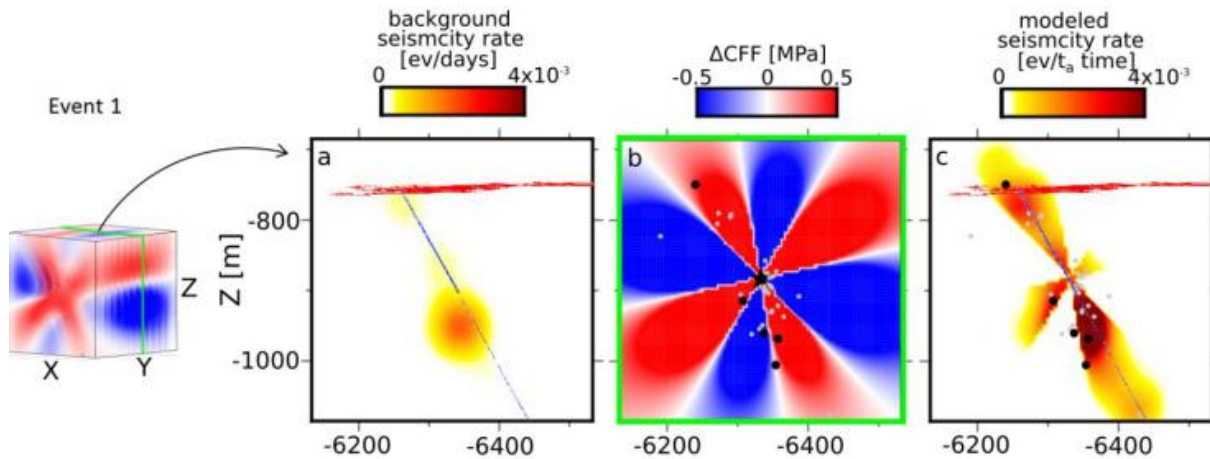


Fig. 2. Input parameters (a) and (b) and results (c) of a rate-and-state based modelling for the second studied event (after Kozłowska et al. 2021).

Poland. We seek to find the physical difference between strong events producing a series of aftershocks and strong events producing no aftershocks. This topic is also the topic of a master thesis of a student.

References

Kozłowska, M., B. Orlecka-Sikora, S. Dineva, Ł. Rudziński, and M. Boskovic (2021), What governs the spatial and temporal distribution of aftershocks in mining-induced seismicity: insight into the influence of coseismic static stress changes on seismicity in Kiruna Mine, Sweden, *Bull. Seismol. Soc. Am.* **111**, 1, 409–423, DOI: 10.1785/0120200111.

STUDYING OF POSSIBLE GROUND DEFORMATION CORRESPONDING TO A MINING-INDUCED SEISMIC EVENT FOLLOWED BY A MASSIVE COLLAPSE IN MINES

Ł. Rudziński

The scientific activity is dealt with ground deformations and its possible connection with seismic activity in mining regions. In 2018 research works were focused on a tragic seismic event occurred in Upper Silesian Coal Basin in 2015. On April 17, 2015, the Wujek/Śląsk underground coal mine in Poland was struck by a strong induced tremor of magnitude $M4.0$. The event was followed by a massive rockburst and a collapse of tunnels in the vicinity of the hypocentre. The earthquake was widely felt in the densely populated surrounding area. Using two different methods based on SAR and seismological observations a possible connection between seismological parameters was described. Special attention was focused on such parameters as the seismic source location and the focal mechanism. Next seismological results with the ground deformation just above the collapsed tunnels, which arose in a very short time after the event occurred, was performed (Fig. 1). It was shown that joint seismological and satellite observation can be very valuable and important tools not only to improve the knowledge concerning mining rockbursts and tunnel collapses but also to find their influences on the ground effects observed on the surface.

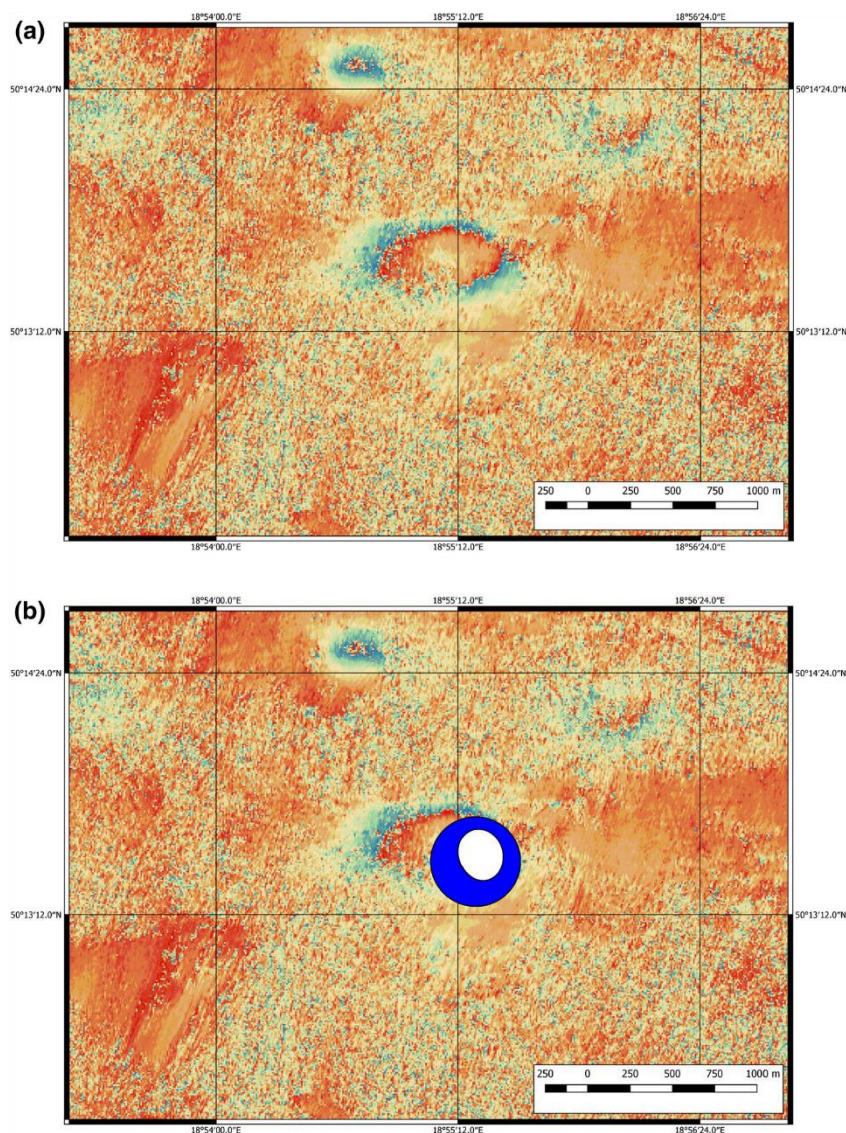


Fig. 1: (a) Interferograms of the Wujek/Śląsk mining area between 12 April and 24 April 2015; (b) The same interferograms together with the source mechanism corresponding to the final MT. The location of the focal sphere in the image corresponds to the epicentre, while the size of the beach ball corresponds to the location errors (after Rudziński et al. 2019).

References

Rudziński, Ł., K. Mirek, and J. Mirek (2019), Rapid ground deformation corresponding to a mining-induced seismic event followed by a massive collapse, *Nat. Hazards* **96**, 461–471, DOI: 10.1007/s11069-018-3552-0.

ANALYSIS OF POST-BLASTING SEISMIC SOURCES RECORDED AFTER ROCKBURST ACTIVE PREVENTION

A. Caputa, Ł. Rudziński

The main aim of the research within the project is focused on the study of mining-induced seismic tremors, which occurred during or a short time after the rockburst prevention inside the tunnels of Rudna mine, Poland. The project started on January 30, 2018, and is going to last till the end of 2019. Research within the project is related to high seismic activity and rockburst hazard associated with exploitation of copper ore deposits in Legnica–Głogów Copper District (LGCD), Poland. During twenty years (1990–2010) more than 11 200 strong mining tremors (magnitude $M > 2$) were recorded in LGCD and 323 events were associated with rockbursts.

This project is focused on induced seismicity provoked by blasting works, which are performed within excavation of copper ore and active rockburst prevention. Blasting is considered as an effective way to destress rockmass in the vicinity of the mining faces. It is noticed that about 30% of all mining events in LGCD were provoked by active prevention. Currently, the only way to quantify the effectiveness of the stress reduction during active prevention is based on cumulative energy released during the established waiting time, the time which is set up after detonations. However, the physical processes responsible for stress reduction during or after blasting are still not clear. The project aims at the analysis of the seismic sources induced by mining, occurred on Rudna mine. The most important question to solve is whether any features which are common for events in the waiting time and if they exist can be found. Another important issue is how they are related to physical parameters estimated for other, unexpected (common) seismic tremors. In 2018, the research activity was focused on tests with synthetic data for both networks. In the tests, all synthetic waveforms were generated for a selected “ideal” point source models: shear (Fig. 1) and non-double couple models. Sources were located in different locations within Rudna mine panels. It is expected, that these tests will be useful to define specific problems and limitations of the seismic networks and will be essential for the next steps of the project.

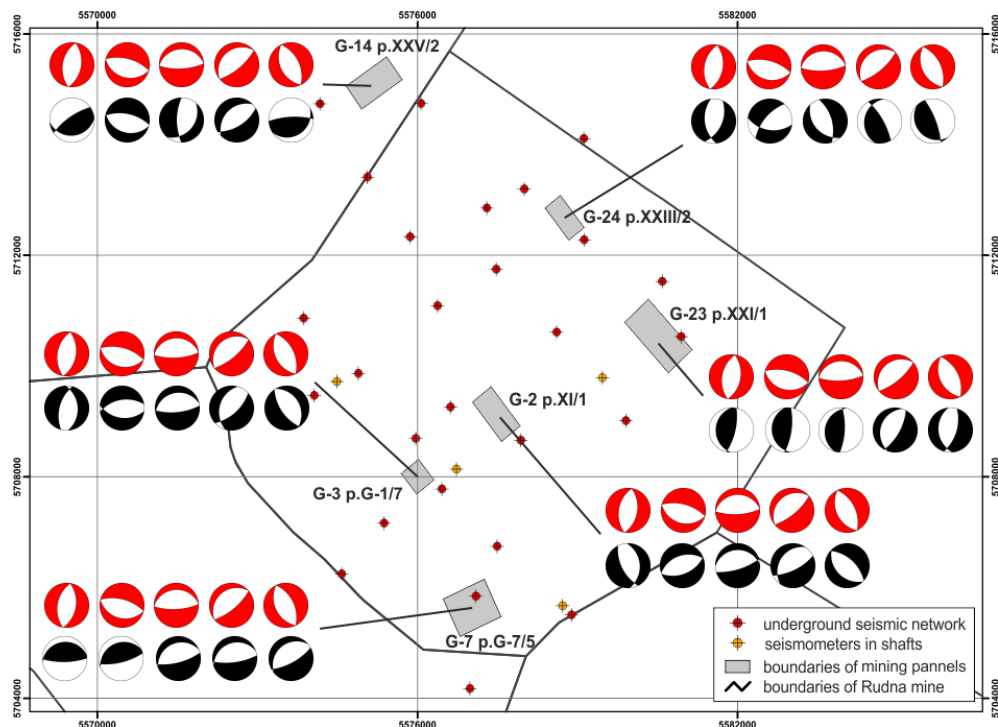


Fig. 1. Comparison between synthetic (red) and inverted (black) source mechanisms (double-couple) for different locations within Rudna mine panels.

VINNOVA SIP STRIM – SWEDISH PROJECT GRANTED BY LKAB A.B LEADER: LULEÅ UNIVERSITY OF TECHNOLOGY, LULEÅ, SWEDEN. DEPARTMENT OF SEISMOLOGY IG PAS IS A NON-PROFIT PARTNER IN THE PROJECT

S. Lasocki, B. Orlecka-Sikora, Ł. Rudziński, M. Kozłowska, K. Leptokarpoulos

The main aim of the project is focused on the development of specific criteria due to seismic risk for temporary closing/re-opening of seismically active mines. The issue is a common problem in all seismically active mining regions and is under debate also in Polish copper and coal mines. IG PAS was invited as a partner to consult the scientific and technical ideas, which can

improve the current knowledge concerning possible criteria. Two main seismological issues which can help with the project were considered and consulted during the last year: seismic hazards in mines (Prof. Dr. S. Lasocki, Dr. Ing. B. Orlecka-Sikora, Dr. K. Leptokaropoulos) as well as analysis of seismic patterns and focal mechanisms (Dr. Ł. Rudziński, Dr. Ing. M. Kozłowska).

During the last year, the characteristics of Kiruna mine Block 34 seismicity were analysed in space-time-size domain, together with its relation to blasting activities. The analysis conducted indicated some interesting results, however, it revealed potential problems in the data used. Therefore, revised data are needed before proceeding to (and partially re-performing) the analysis. Based on data recorded on the regional broadband network, the study focused on source mechanisms analysis has started. Next, the results were used to investigate a seismicity pattern, especially aftershock sequences for selected mining tremors that occurred in Kiruna mine, northern Sweden (Fig. 1).

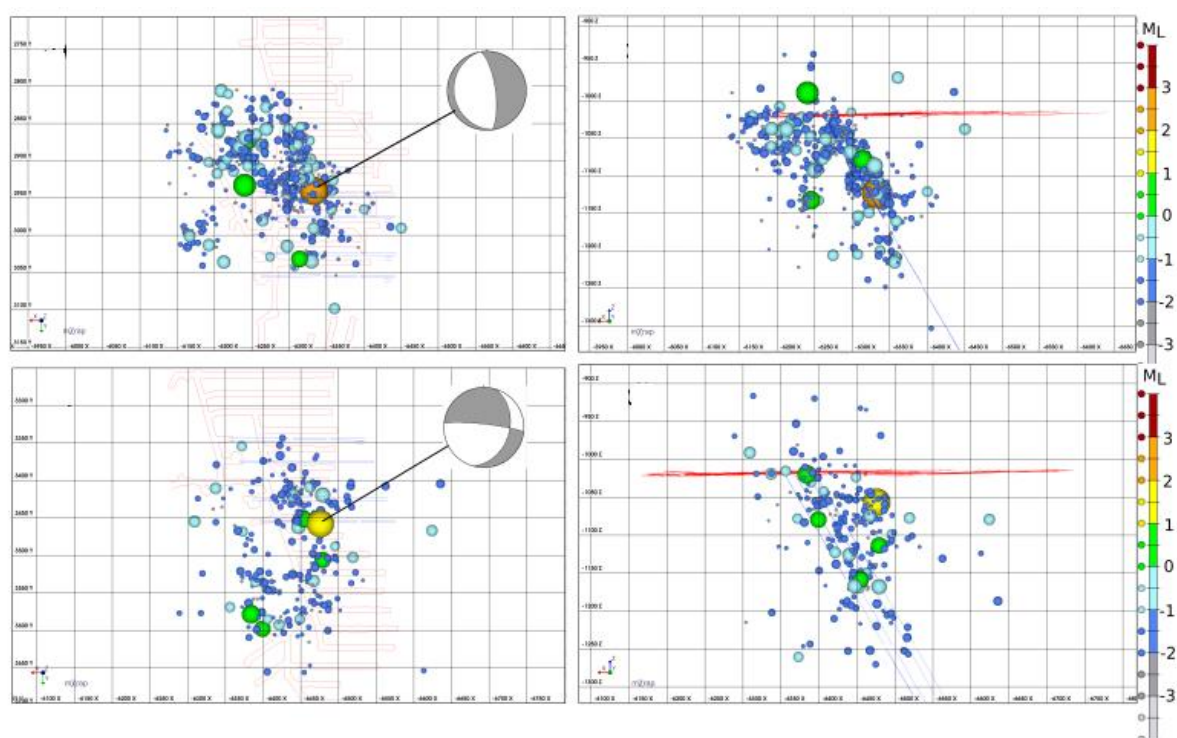


Fig. 1. Examples of two different seismic sequences recorded on Kiruna mine, Sweden (after Kozłowska et al. 2021).

References

Kozłowska, M., B. Orlecka-Sikora, S. Dineva, Ł. Rudziński, and M. Boskovic (2021), What governs the spatial and temporal distribution of aftershocks in mining-induced seismicity: insight into the influence of coseismic static stress changes on seismicity in Kiruna Mine, Sweden, *Bull. Seismol. Soc. Am.* **111**, 1, 409–423, DOI: 10.1785/0120200111.

SEISMICITY PROPERTIES EVOLUTION IN RELATION TO FLUID-INJECTION IN THE GEYSERS GEOTHERMAL FIELD

K. Leptokaropoulos, M. Staszek, S. Lasocki, B. Orlecka-Sikora, S. Cielesta

Within this research activity, a detailed correlation analysis between seismicity properties and operational parameters was carried out. The analysis was performed in an isolated cluster from

the North-Western The Geysers geothermal field, for which a high-quality seismic catalogue is available. Firstly, the correlation between spatio-temporal seismicity evolution and variation of the injection data was performed by investigation of original and smoothed time-series through diverse statistical tools (cross-correlation function, binomial test for investigating significant rate changes, magnitude distribution analysis). To do so, seismicity and operational data associated with two injection wells (Prati-9 and Prati-29) which cover a time period of approximately 7 years (from November 2007 to August 2014) were used (see Fig. 1). A clear and statistically significant positive correlation between seismicity rates and total injection rates was obtained. This correlation statistically differs from zero at 0.05 significance level. The maximum correlation occurs with a seismic response delay of ~ 2 weeks, following injection operations, whereas a range between 0–85 days is statistically significant at 0.01 level. This time lag is preserved even after considering hypocentre uncertainties, i.e. when the seismicity cloud is shifted at a shallower location as far as 300 m from its original hypocentre. The analysis also indicated time variations of b -value, which exhibits a significant positive correlation with injection rates as can be seen in Fig. 2.

Next, a detailed investigation of the variation of injection rates on microseismicity magnitude distribution was performed. A direct comparison between injection rate changes and the b -value response was attempted after the appropriate selection of data subsets. Due to the relatively small sample (1121 events, corresponding to an average rate of ~ 0.45 events/day), seismic activity in two families corresponding to increasing and decreasing injection rates was aggregated, respectively. The b -values were calculated as a function of time lag related to the

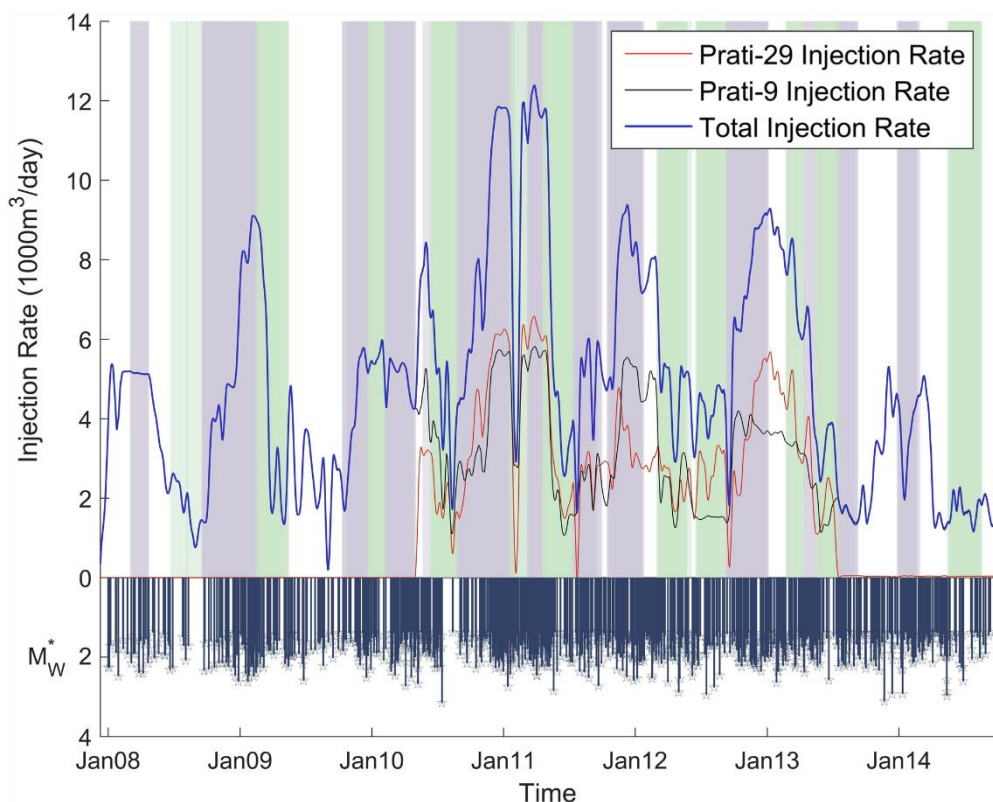


Fig. 1. Daily total injection rates (blue curve) in relation to the occurrence of earthquakes (stem plot). The daily rates of fluid injected individually into wells Prati-9 and Prati-29 are indicated by black and red curves, respectively. The vertical bars indicate time periods of 50 days which have significantly increased (grey bars) or decreased (green bars) seismicity rates, in comparison with the preceding 50 days window. The time step applied in the analysis is 2 days, so the time windows are overlapping with each other (after Leptokaropoulos et al. 2018a).

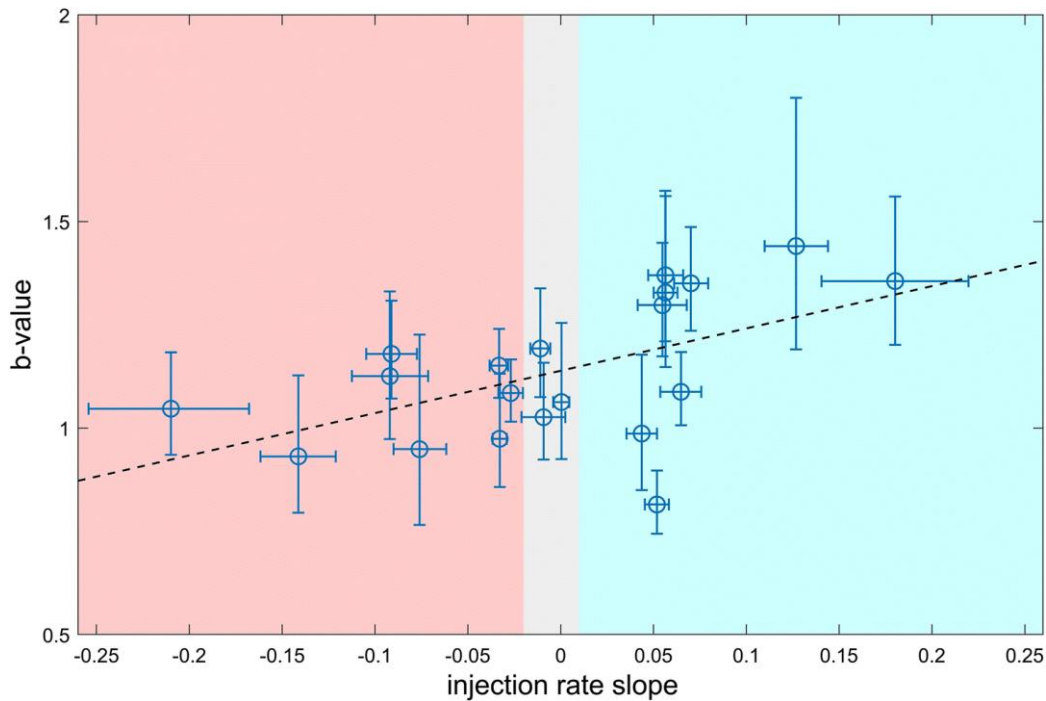


Fig. 2. Estimation of b value for the 20 datasets described in Leptokaropoulos and Staszek (2019). Blue-shaded area corresponds to periods of increasing injection rate, red-shaded area corresponds to periods of decreasing injection rate, and grey-shaded area corresponds to periods of almost stable injection rate. The horizontal and vertical error bars indicate one bootstrap standard deviation (σ) of the injection rates' slopes and b values, respectively. The slope of the least-square linear regression curve, denoted by the dashed line, is ~ 1 .

injection activity. In agreement with previous studies, a statistically significant direct relation between b -values and injection rate changes, which occurred at a zero or very short time lag (from 0 to ~ 15 days) was found. However, the b -value changes are related to the slope (i.e., the second derivative of injection volume), instead of the absolute values of injection rates. The increasing injection rates correspond to $b = 1.18 \pm 0.06$, whereas the decreasing injection rates correspond to $b = 1.10 \pm 0.05$. The corresponding values estimated by the repeated medians technique are $b = 1.97 \pm 0.20$ and $b = 1.50 \pm 0.13$. Both differences are significant at 0.05 level. Furthermore, Prati-9 injection well, which is located in the close vicinity of the seismicity cloud, was found to contribute mainly, but not exclusively to the b -value fluctuation. Finally, no significant influence of static stress drops, vertical distribution of microseismicity and absolute injection rates on b -values was detected under the performed analysis.

References

Leptokaropoulos, K., and M. Staszek (2019), Temporal response of magnitude distribution to fluid injection rates in The Geysers geothermal field, *Acta Geophys.* **67**, 327–339, DOI: 10.1007/s11600-018-0215-1.

IMPACT OF MAGNITUDE UNCERTAINTIES ON SEISMIC CATALOGUE PROPERTIES

K. Leptokaropoulos

Magnitude distribution properties in noise-contaminated synthetic data comprising a complete and an incomplete part, when this distribution is controlled by the Gutenberg–Richter law were

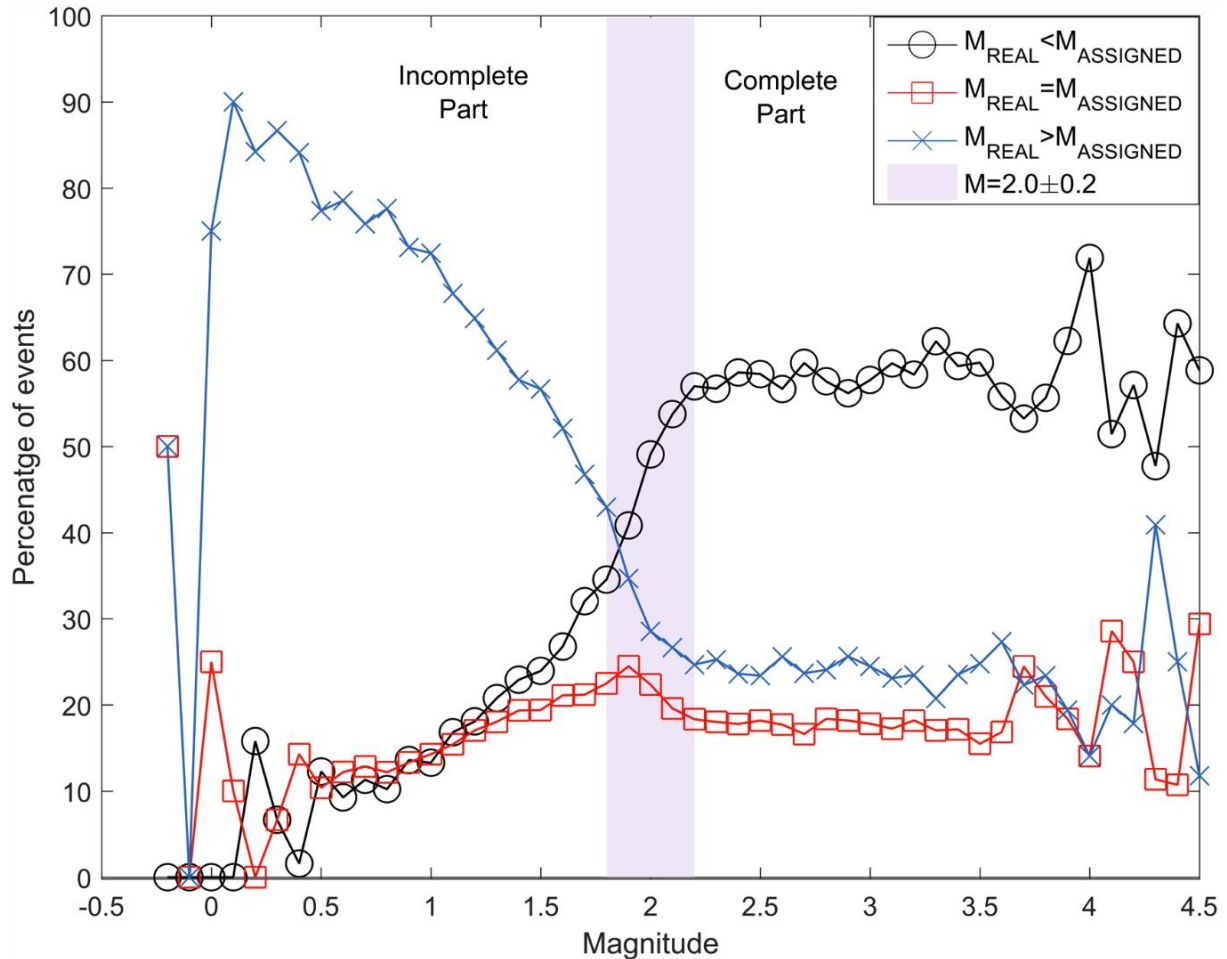


Fig. 1. Percentage of events in the synthetic catalog A which have underestimated (blue crosses), overestimated (black circles) or correctly estimated (red squares) magnitudes when Gaussian noise ($\mu M = 0$ and $\sigma M = 0.2$) is added, plotted against true (synthetic) magnitude. The shaded area indicates 0.2 units on both sides of $M = 2.0$. Note the shift towards larger magnitudes (after Leptokaropoulos et al. 2018b).

studied. The efficiency of the maximum likelihood estimator introduced by Aki (1965) was estimated using synthetic datasets exhibiting diverse but well-defined properties. The completeness magnitude, M_C , was also estimated by means of several different techniques (maximum curvature, the goodness of fit test, b -value stability and modified goodness of fit test). The deviation of the b -value estimation from its real value is quantified by Monte Carlo simulations as a function of catalogue features and data properties such as sample size, magnitude uncertainties distribution, round-off interval of reported magnitude values and magnitude range. Analysis showed that the noise introduced to the data generally leads to a systematic overestimation of magnitudes close to and above M_C . This fact causes an increase in the average number of events above M_C , which in turn leads to an apparent decrease of the b -value (see Fig. 1). To summarize, the analysis performed shows that under the assumed conditions the following conclusions are drawn:

- (1) The b -values tend to be underestimated when the noise of the character we have investigated is introduced to magnitude values. The degree of underestimation is proportional to the noise standard deviation (for Gaussian noise);

- (2) Different methods for MC estimation lead to different results (MC and b -value), which are strongly influenced by sample size, noise properties, magnitude range and b -value itself;
- (3) b -value analysis, especially for small datasets should be carried out together with ΔM analysis. Relevant nomograms should be constructed and used;
- (4) Even above a well-defined MC , a catalog is unlikely to be complete because of a bidirectional flow of data below and above MC . For $M_{\min} \gg MC$, the actual number of events is overestimated by a factor depending primarily on the noise standard deviation (especially for $N > \sim 800$).

References

Aki, K. (1965), Maximum likelihood estimate of b in the formula $\log N = a - bM$ and its confidence limits, *Bull. Earthq. Res. Inst. Univ. Tokyo* **43**, 237–239.

INCOMPATIBILITY OF ANTHROPOGENIC SEISMICITY WITH PROBABILISTIC MODELS TYPICALLY USED IN SEISMIC HAZARD ANALYSIS: THE CASE OF OKLAHOMA EARTHQUAKES

S. Lasocki, P. Urban

The exponential distribution model for magnitude arises from the Gutenberg–Richter magnitude–frequency relationship and the exponential model for interevent time is valid if the earthquake occurrences are governed by a homogeneous Poisson process. The Gutenberg–Richter rule for magnitudes and the Poisson process for earthquake occurrences are typically assumed in stationary earthquake hazard estimation although there are reports showing significant violations of these assumptions in both tectonic as well as anthropogenic seismicity cases. Anderson–Darling test was used to investigate the validity of these assumptions for injection-induced earthquake data from Oklahoma (Oklahoma Geological Survey, www.ou.edu/content/ogs/research/earthquakes/catalogs.html). The epicentres of analysed events form two distinct spatial clusters, the one, A, in a north-western part of the study area and the second one, B, in a south-eastern part. The hypothesis that the magnitudes follow exponential distribution is rejected for the whole dataset and for cluster B. The hypothesis that the interevent times follow exponential distribution is rejected for the whole dataset and both spatial clusters. The side hypothesis that the occurrence process is an inhomogeneous Poisson process where interevent times follow a Weibull distribution, is also rejected for all three datasets. Neither an exponential distribution of magnitude nor a Poisson distribution of event rate can be used to assess the stationary seismic hazard due to the anthropogenic seismicity from Oklahoma. For the seismicity cases like in Oklahoma, therefore, a new method to approximate event rate distribution, based on the estimation of interevent time distribution and computer simulation of event occurrences from this distribution estimate, is proposed. Regarding magnitude, it is proposed to replace the Gutenberg–Richter relation-led model with nonparametric estimates of the distribution functions. This approach is fully data-driven, hence it reproduces correctly the distributions that underlay data. The differences between hazard estimates obtained with the use of the inappropriate probabilistic distributions: exponential for magnitude and Poisson for event rate, and attained from the proposed approach are significant. Results indicate that in anthropogenic seismicity cases hazard assessments should be preceded by tests of conformity of the distribution models, which are to be used, with observations. When the tests turn down any of these models, the approach introduced here should be applied.

MONITORING OF SEISMICITY IN POLAND

A. Cichowicz, I. Dobrzycka, K. Michałowski, B. Pleśiewicz, M. Sobiesiak, J. Wiszniowski

The research on natural seismicity of Poland was focused on monitoring the activity. After analysing 38,440 hours of continuous recordings and rejection of induced phenomena, six tectonic earthquakes were noticed; four in Podhale and two in the Krynica region. The largest earthquake was M_L 3.1. Location of events confirms the Podhale, Pieniny, and Krynica region as main tectonic seismicity zones in Poland. A list of events with their occurrence time, location and magnitude is given in Table 1. Figure 1 shows the location of six tectonic earthquakes and location of 10 short-term mobile stations in Podhale and Krynica regions.

Table 1
List of events with their occurrence time, location, and magnitude

Region	Date and time	Latitude	Longitude	Magnitude
Podhale	2018/04/22 03:15:02.38	49.3186	19.9621	0.5
Podhale	2018/04/23 10:12:02.84	49.6245	20.1322	1.7
Podhale	2018/04/27 16:11:30.87	49.3806	20.3559	3.1
Podhale	2018/05/11 22:36:01.16	49.4488	20.0383	1.0
Krynica	2018/07/15 21:19:44.74	49.3321	21.0260	2.9
Krynica	2018/07/16 01:54:05.67	49.3967	20.9862	2.7

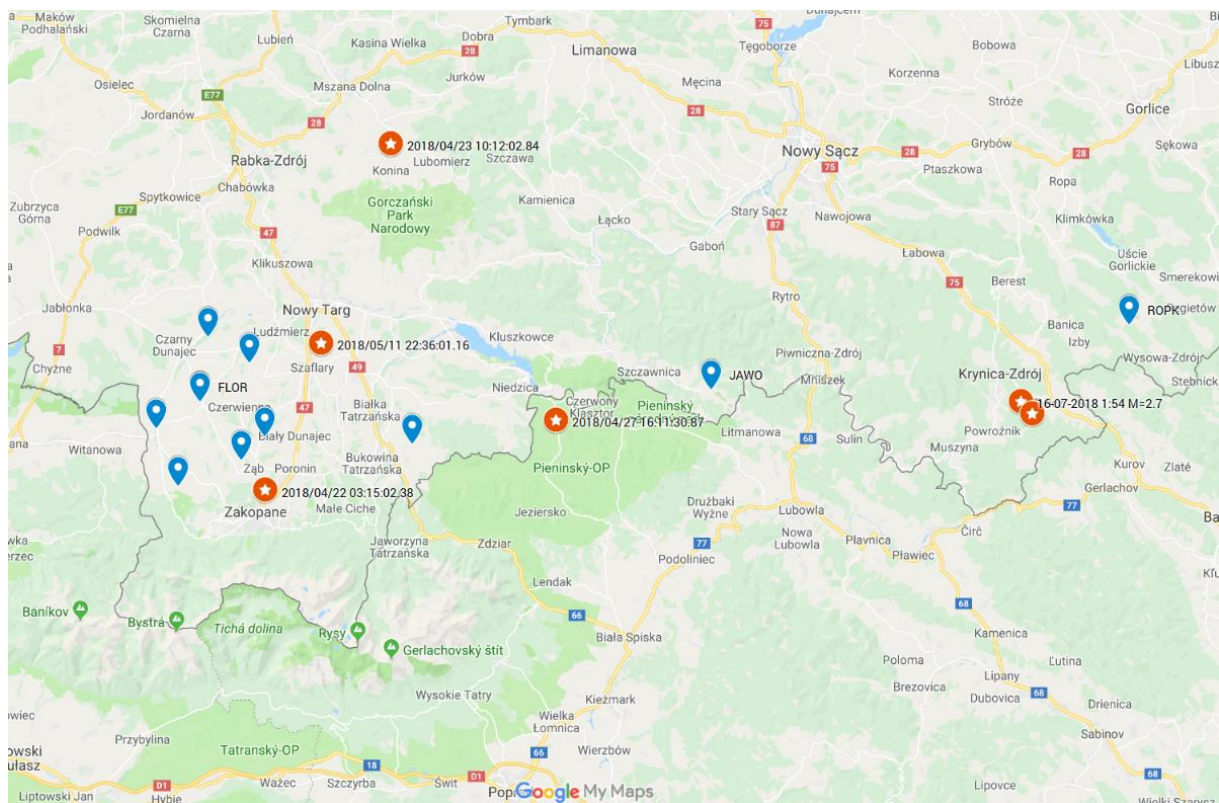


Fig. 1. Location of six tectonic earthquakes (orange) with the location of 10 stations (blue) in the Podhale and Krynica regions.

DYNAMIC TRIGGERING OF SHALLOW SLIP ON FOREARC FAULTS

M. Sobiesiak

It is a long-standing discussion whether tectonic faults can be triggered to move by earthquakes in the local, regional or global distance range. In the above-listed publication, crustal faults in the forearc of the Northern Chilean convergent plate margin using different instrumental components of the IPOC (Integrated Plate Boundary Observatory in N-Chile) were studied. The observations document dynamic triggering on the surveyed faults which can be attributed to triggering by the passage of surface waves from far-field earthquakes and by the passage of body waves from seismic events in the near field. With these observations, a magnitude–distance relationship of slip triggering was derived. This observed surface displacement does not occur by continuous creep but through discrete displacement events.

THE IQUIQUE LOCAL NETWORK AND PICARRAY

M. Sobiesiak

The Iquique Local Network (ILN) consisted of 14 broad-band and 6 additional short period seismological stations around the city of Iquique in Northern Chile. As one instrumental component of the IPOC (Integrated Plate Boundary Observatory in N-Chile), its purpose was to enhance the regional permanent IPOC network to aim at a better resolution for small magnitude events on the crustal faults of the subduction zone forearc as well as on the interface between the downgoing Nazca Plate and the overriding South American Plate. It was installed in this region according to the identification of possible seismogenic structures through gravity field surveys. At a later stage, several stations were newly installed to form an array around the village of Pica in order to monitor seismic events on a deeper part of the subduction interface for studying the interactions between seismogenic zone and the deeper subduction seismicity.

INITIALIZATION AND DEVELOPMENT OF ANTHROPOGENIC SEISMIC PROCESSES INDUCED BY ARTIFICIAL SURFACE RESERVOIRS

G. Lizurek, J. Wiszniowski, B. Plesiewicz, K. Leptokarpoulos

The aim of the project is to study the anthropogenic seismicity induced by the filling of water reservoirs (Lai Chau and Song Tranh2) and the assessment of the risks related to this activity.

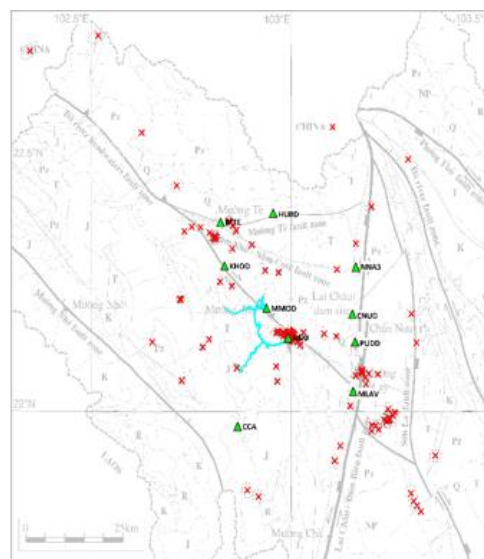


Fig. 1. River Da whose waters are backed up with Lai Chau dam (left, photo: G. Lizurek). Location of tectonic events (red crosses) recorded in the Lai Chau region in the period from October 2014 to June 2015 (right).

Within the framework of the project, close cooperation with the Institute of Geophysics, Vietnamese Academy of Science and Technology (IGP VAST) is foreseen. In Vietnam, seismological measurements had started before the reservoir in Lai Chau was filled up. It allows exploration of the natural seismicity, which exists in the area of the future dam, and then determination the development of anthropogenic seismic activity associated with the impoundment of water in the reservoir. Measurements are conducted by a dense seismic network consisting of 10 seismic stations located within 20 km from the reservoir. This area is characterized by tectonic seismic activity; therefore, there is a high probability to collect appropriate material to study the anthropogenic seismic activity. In 2018 it allowed exploration of the natural seismicity, which exists in the area of the future dam. Location of seismic events several months prior to the reservoir impoundment was calculated with the use of the existing seismic network, which finally reached 10 stations in the reservoir vicinity. Events were mainly located near the dam along the Da river headwaters fault (Fig. 1). However, only 4 stations were available for

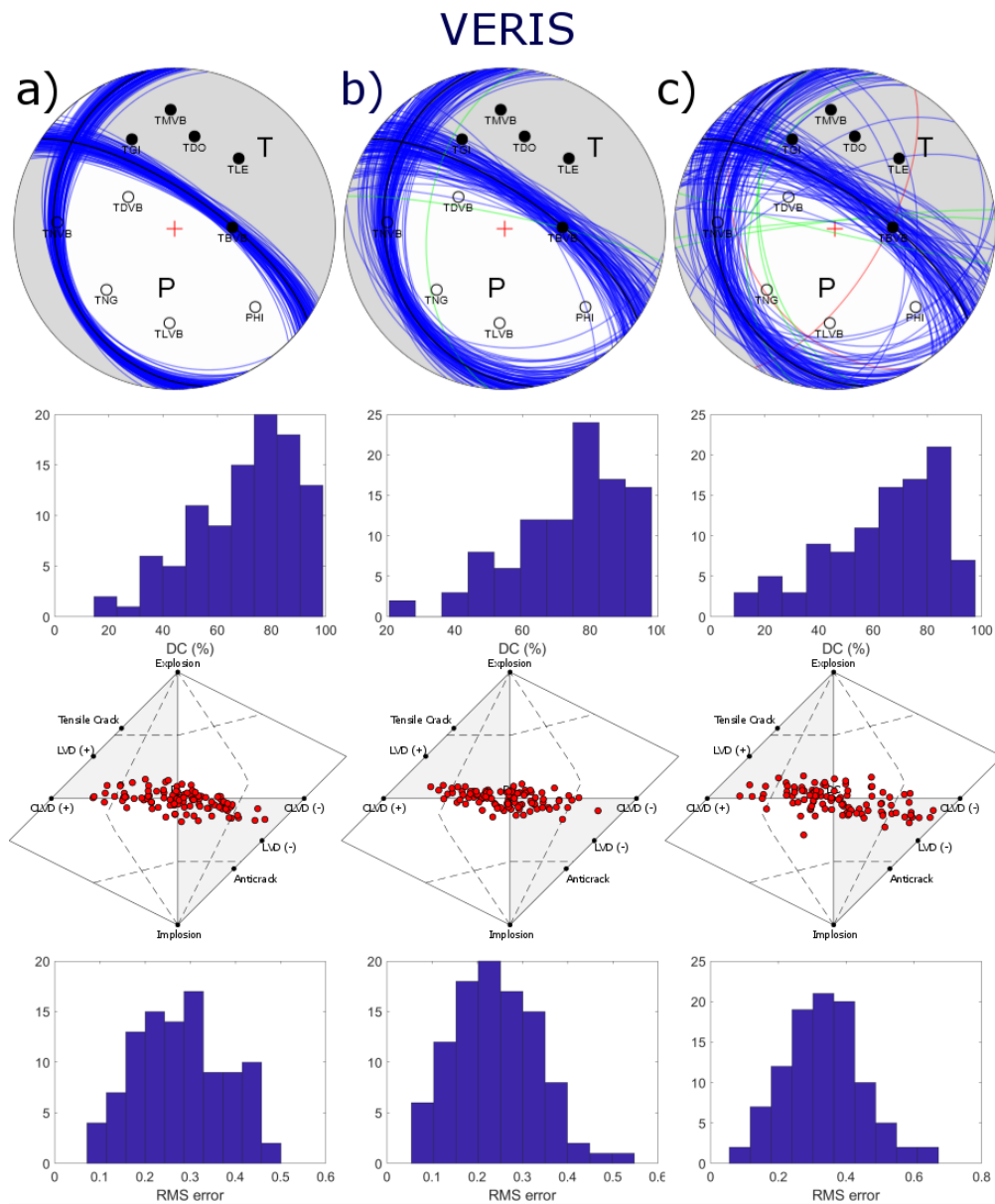


Fig. 2. Full MT solutions obtained in resampling bootstrap test for VERIS: (a) up to 20%, (b) up to 40%, and(c) up to 60% noise contamination (after Lizurek et al. 2021).

all the period before impoundment. Despite the network limitations, completeness of seismic catalogue b -value and its temporal behaviour were determined and can be used as a baseline for further analysis of seismicity in this area. The capability of the local network for moment tensor inversion was also determined with the use of synthetic data tests. Test results provided the requirements for the station number according to azimuthal coverage of the network to obtain the reliable full moment tensor (MT) solution. Further measurements are continued in the region of Song Tranh 2, where joint Vietnamese-Polish seismic network recorded more than 5000 seismic events. The improving of the location of events and more accurate determination of the focal mechanisms are the main goals for this region research. Analysis of the magnitude distribution was performed. They covered the multimodality and bump tests for the clusters of seismicity recognized earlier as well as for the whole seismic catalogue available for Song Tranh2. The results show that for all analysed datasets, the magnitude distribution follows an exponential distribution. However, two main clusters are characterised by the low probability of unimodal distribution.

Another part of this research was aimed at testing the influence of noise on moment tensor inversion results. The sensitivity of the amplitude of P-wave first-motion moment tensor inversion method on noise and focal coverage setups was tested. Three different fault types: normal, thrust and strike-slip geometries of pure shear faulting were used to generate synthetic amplitudes. Then the amplitudes were contaminated with various amounts of noise and inversion was performed for eight different focal coverage setups. Test results showed the noise being the main factor of the spurious non-DC components in MT solutions and the nodal planes determination. The best and the worst performing focal coverage setups were identified. Finally, the case study of a seismic network designed for monitoring of seismicity related to Song Tranh2 reservoir seismicity in Central Vietnam was performed. The investigated network performed well in the noise influence tests proving its robustness in MT inversion when the noise level is not higher than 40% of the initial displacement amplitude (Fig. 2).

References

- Lizurek, G., K. Leptokaropoulos, J. Wiszniowski, N.V. Giang, I. Nowaczyńska, B. Plesiewicz, D.Q. Van, and A. Tymińska (2021), Seasonal trends and relation to water level of reservoir-triggered seismicity in Song Tranh 2 reservoir, Vietnam, *Tectonophysics* **820**, 229121, DOI: 10.1016/j.tecto.2021.229121.

PHYSICAL PROPERTIES OF SEISMIC SOURCES IN CONNECTION WITH REGIONAL TECTONICS

W. Białoń, G. Lizurek

Within this part of research related to reservoir triggered seismicity works upon Czorsztyn lake seismic activity was performed. Czorsztyn lake is located in extremely complex geo-technical conditions, between the border zone of Inner and Outer Carpathians separated by the Pieniny Klippen Belt. Before the Czorsztyn 2D seismic survey, knowledge of tectonic boundaries and velocities was very limited. The seismic survey confirmed assumptions of flower type faults system and provided the first 3D velocity model for this area. Location and moment tensor are crucial in the investigation of the origins of seismogenic process related to industrial operations. Therefore, the relocation of the events and validation of the moment tensor solutions for the SENTINELS network were conducted with the use of 3D velocity model (Fig. 1).

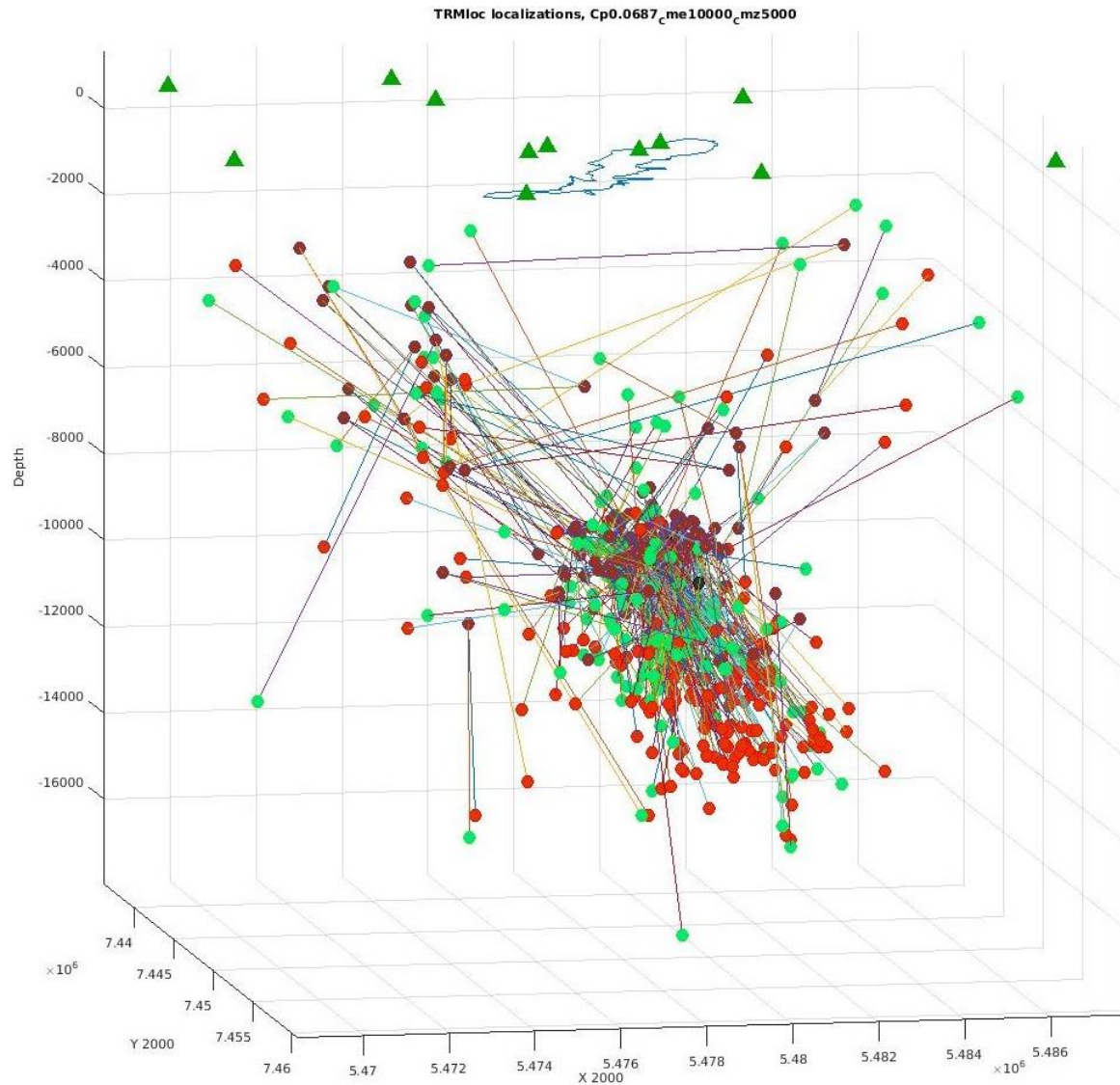


Fig. 1. North-South cross-section of Czorsztyn lake area with relocated events. Violet dots mark the location from LocSat, green ones TRMloc Rml, and red ones TRMloc Rav, dark green triangles show station locations. The lines between violet-green and violet-red dots are marking a change in location. Location in XY2000 coordinates system.

The validation of the mechanism was conducted with the use of the synthetic tests based on the 1D velocity model derived from the 3D velocity model, taking into account its lateral velocity anisotropy. It was based on the synthetic amplitudes generated with assumed normal and strike-slip faulting similar to the obtained solutions. The validation proved that the focal mechanisms are reliable even in a sparse focal coverage and noise not exceeding 40% of the P-wave amplitude. Most of the events are normal or strike-slip with nodal planes striking NW-SE or NE-SW (Fig. 2).

References

Białoń, W., G. Lizurek, J. Dec, K. Cichostępski, and K. Pietsch (2019), Relocation of seismic events and validation of moment tensor inversion for SENTINELS local seismic network, *Pure Appl. Geophys.* **176**, 11, 4701–4728, DOI: 10.1007/s00024-019-02249-6.

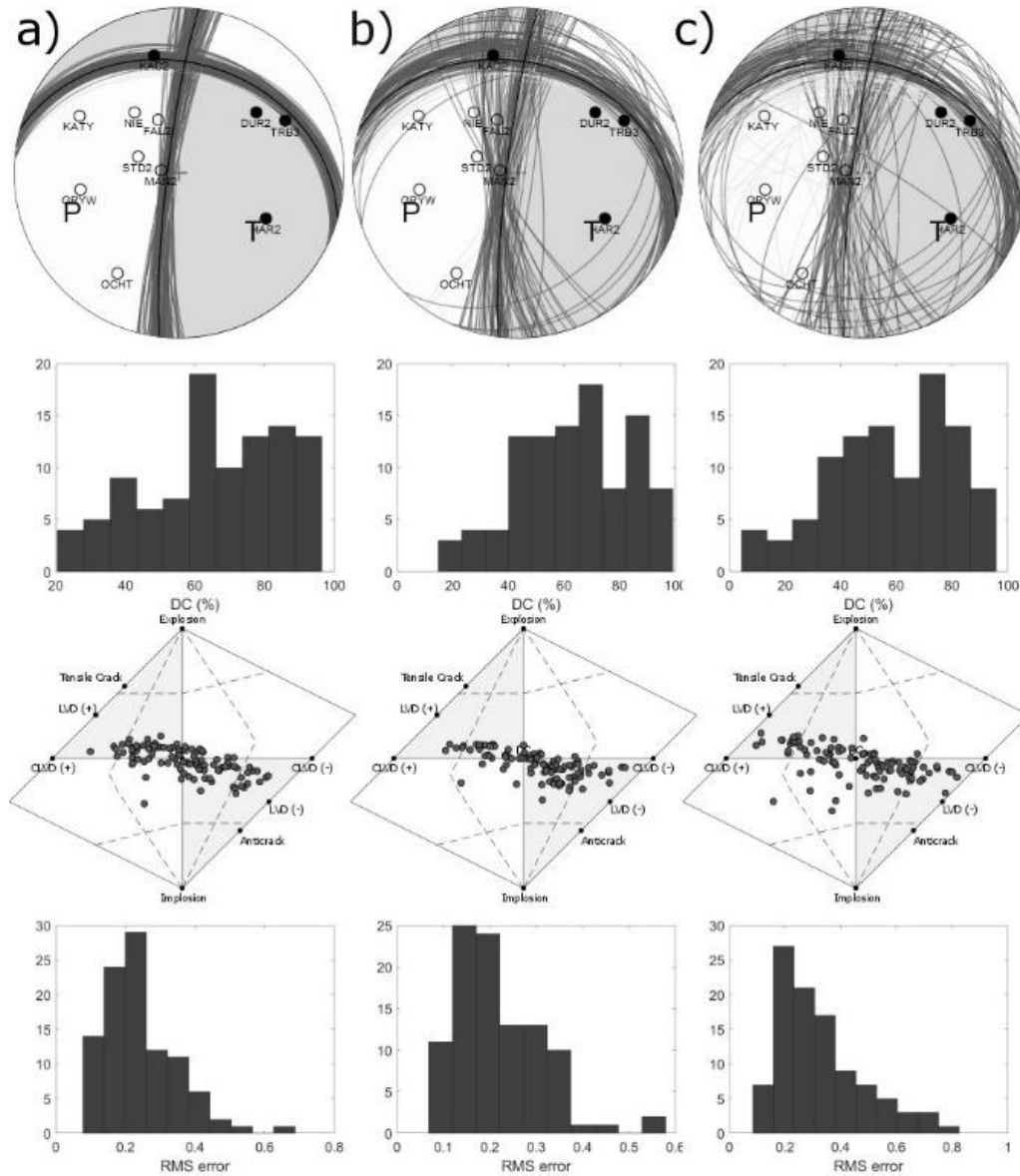


Fig. 2. Results of the bootstrap noise influence tests of strike-slip fault solutions. From the left: noise contamination up to 20, 40, and 60% (after Białoń et al. 2019).

SERA

M. Sobiesiak, K. Leptokaropoulos, S. Lasocki, P. Salek

Research activity within the framework of SERA was conducted within the following tasks:

- WP23 JRA1: Physics of the earthquake initiation.

Observations about the development of seismicity in space and time are crucial in terms of understanding the process of earthquake initiation. One possibility to gain such information is the application of statistical methods to seismicity catalogues to study, i.e., the seismicity rate changes or the complexity of the magnitude-frequency relation over space and time. The contribution of IG PAS to this issue comprises two toolboxes for the investigation of statistical parameters of seismic catalogues to apply to induced as well as tectonic seismicity. Namely, these are Toolbox for clustering – transformation to equivalent dimensions, Toolbox for magnitude complexity (including the Anderson–Darling test of exponentiation and test for multimodality). At the moment the implementation of the toolboxes on the IS-EPOS Platform for

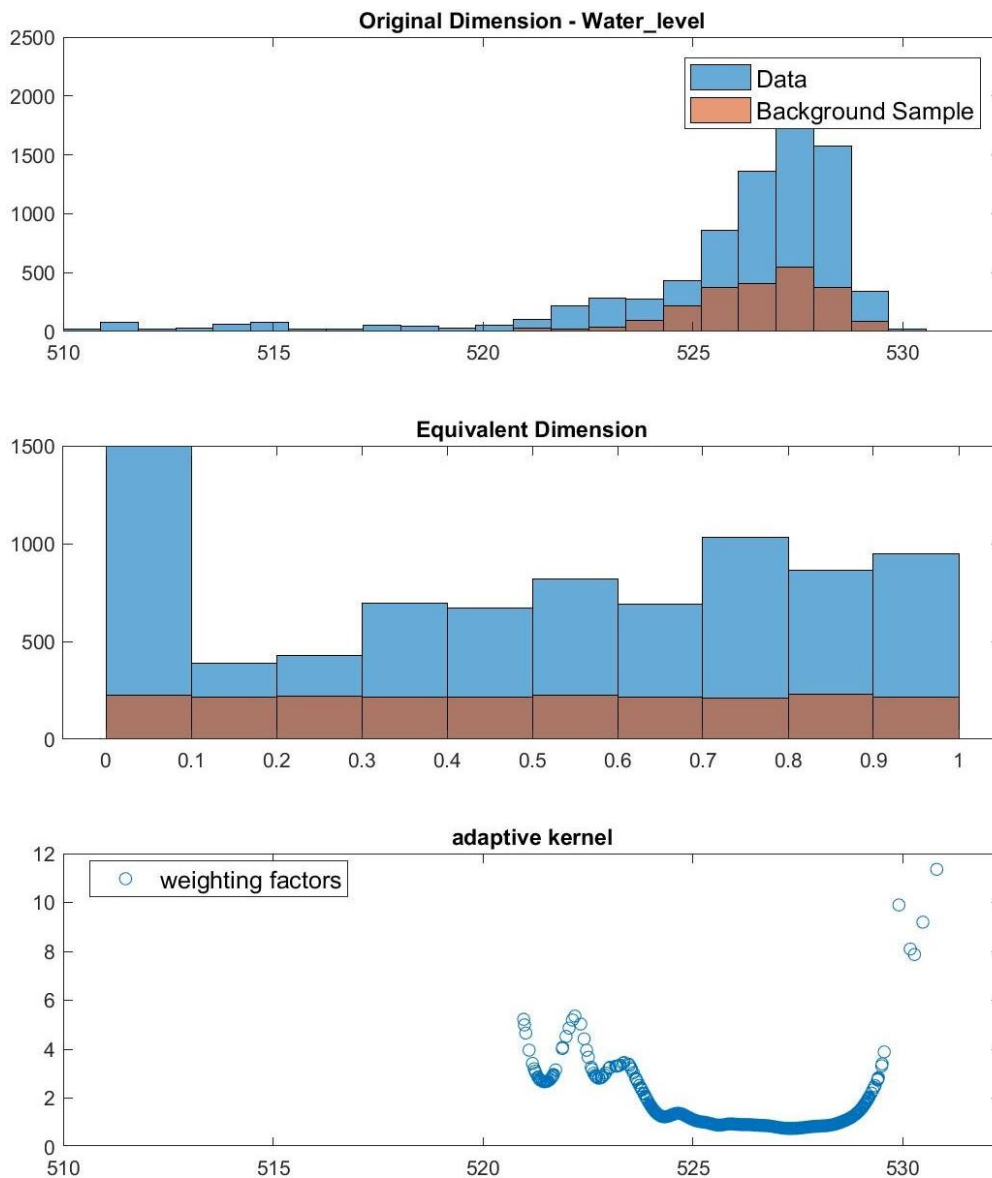


Fig. 1. Water level changes of the Czorsztyn water reservoir. Top frame: Water level (m) histograms for the entire sample (blue, 1996–2018) and for the selected background sample (brown, 1998–2004). Middle frame: The respective entire and background sample after transformation to equivalent dimensions (ranging within $[0,1]$). Bottom frame. The corresponding weighting factors of the adaptive kernel.

Anthropogenic Hazard is prepared and is foreseen to be completed in 2019. Figure 1 shows an example of the transformation to equivalent dimensions of water-level variation in Czorsztyn water reservoir. This image has been realized with Toolbox 1 (clustering and transformation to equivalent dimensions). As seismic catalogues are essential for the above-mentioned studies, the completeness in magnitude ranges and timely availability are important aspects of the quality of any results. Therefore, we are testing the possibility of automated phase detection and location of seismic events for induced seismicity. As a first testing environment, the data sets of Rudna Copper Mine have been chosen to test the performance of the BTBB program (Back-Track BB) which is executing multi-frequency array detection and location of seismic sources. One important feature of this program is the characteristic function (CF) to do the detection of seismic wave first arrivals and which can be defined by the user depending on i.e. frequency content and signal to noise ratio of the wavefield. Three disastrous earthquakes concerning

Rudna Mine have been chosen to build a 4-weeks data set around the main shock event, respectively, in order to account for potential fore- and aftershocks: M_L 4.2, 19 March 2013, M_w 3.4, 29 November 2016, and M_w 3.7, 15 September 2018. Figure 2 shows the calculation of the location of the M_w 3.7, 15 September 2018 event with the probabilistic approach of BTBB software.

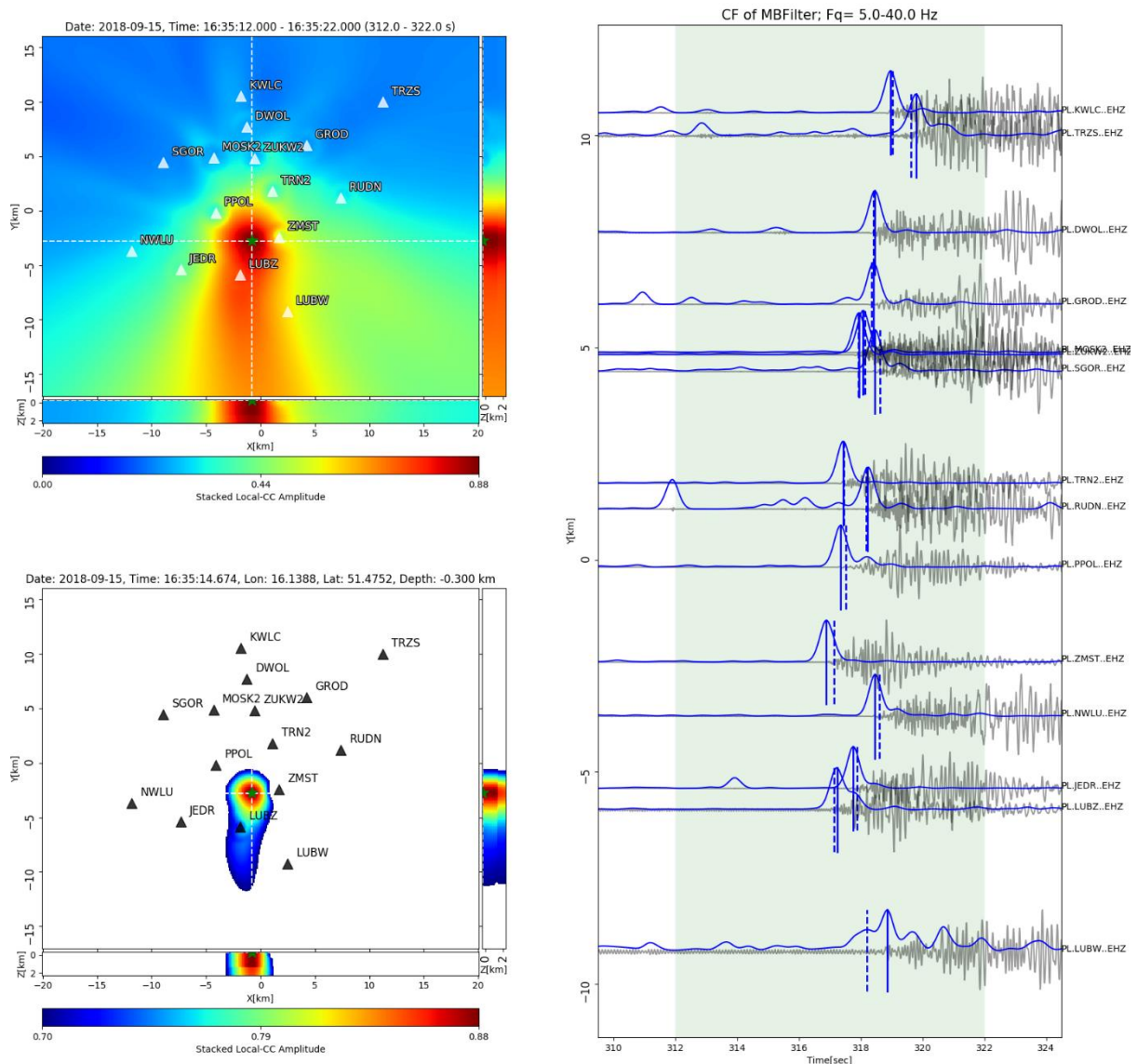


Fig. 2. P-wave phase detection and location procedure for the M_w 3.7 earthquake of 15 September 2018 in Rudna Mine. The color coding is due to the probabilistic approach of the locating procedure showing the distribution of the stacked seismogram amplitudes. On the right side, the seismograms at the different stations are shown in grey color. The blue graphs represent the characteristic function for each respective trace (after Sobiesiak et al. 2019).

- WP24 JRA2: Characterizing the activity rates of induced and natural earthquakes

According to the increasing amount of high-quality seismological data and catalogues, the work package aims at an equivalent modernizing of tools for hazard assessment. In addition, evidence of complex magnitude distribution leads to the non-parametric kernel estimation of magnitude probability distribution functions. IG PAS is contributing to this aim with the third toolbox for hazard assessment in induced seismicity environments incorporating time dependency of the

hazard process resulting from the temporal variation in production parameters, as well as a variety of parametric and non-parametric magnitude distribution models. This toolbox is already implemented on the IS-EPOS Platform for Anthropogenic Hazard and thus is available to the SERA community. The tool consists of several components which are: Estimation of source parameters in time-varying production parameters geometry, Time-dependent hazard in mining front surroundings, and Time-dependent hazard in the selected area.

References

Sobiesiak, M.M., N. Poiata, P. Bernard, Ł. Rudziński, and S. Lasocki (2019), Automated detection and location of mining induced seismicity from Rudna Copper Mine, SW Poland. **In:** *American Geophysical Union Fall Meeting Abstracts 2019*, S11F-0385, San Francisco, USA.

PREDICTION OF IMPACT OF TREMORS AND SURFACE DEFORMATIONS INDUCED BY MINING IN SECTIONS G23 O/ZG RUDNA AND LU XI O/ZG LUBIN ON OUOW “ŻELAZNY MOST” CONSIDERING ITS EXTENSION

S. Lasocki, B. Orlecka-Sikora

This project was carried out in the years 2017–2018 as part of the scientific research work of the Institute of Geophysics PAS in the framework of contract No. KGHM-ZH-U-0162-2017 between KGHM Polska Miedź S.A. Hydrotechnical Division, Rudna. The project consisted of two stages. Stage 1 “Continuous Deformations” was produced by a subcontracted team composed of the AGH University of Science and Technology under the activity of the Stanisław Staszic Scientific Association in Kraków. It concerned a prognosis of surface deformations caused by the mining exploitation of a copper ore deposit performed and planned by the Rudna mine and Lubin mine within the range of impact of this exploitation on the Żelazny Most tailings storage facility (TSF) and its planned development—i.e. on the Southern Extension. It was shown that the expected values of deformation rates caused by mining exploitation by the Rudna mine in the area of the western dam of the Żelazny Most TSF should not exceed the permissible values. Similarly, the exploitation in Lubin mine will not cause any significant surface deformations exceeding the permissible values for the dam which will be surrounding the Southern Extension. The second project stage, “Dynamic Impacts” was worked out by the team from the Department of Seismology, Institute of Geophysics PAS, with a help of an expert on rock mechanics from the Faculty of Geoengineering, Mining, and Geology, Wrocław University of Technology. In this stage, limiting values of the horizontal and vertical components of dynamic impacts on OUOW “Żelazny Most”, resulting from the exploitation plans within section G-23 O/ZG Rudna and LU-XI O/ZG Lubin, were predicted. The prediction was carried out by means of the probabilistic seismic hazard analysis in mines on an intermediate scale. Both the geological and mining conditions of the planned exploitation panels, as well as the works’ programs in particular parts of these panels, were taken into account. Results of the analysis are shown in Fig. 1. The strongest impact on the current OUOW earth dams is expected to be due to the future exploitation within section G-23 O/ZG Rudna. The largest limiting values estimates reached 1 m/s^2 for the horizontal component of ground acceleration in the frequency band up to 10 Hz and 0.5 m/s^2 for the vertical component. The strongest impact on the embankment of the Southern Extension is expected to be due to the exploitation within sections G-8 and G-6 O/ZG Lubin. Depending on which of the two possible ways the seismic process will proceed, it may be expected either up to 1.2 m/s^2 for the horizontal component and 0.9 m/s^2 for the vertical component or up to 1.95 m/s^2 for the horizontal component and 1.4 m/s^2 for the vertical component.

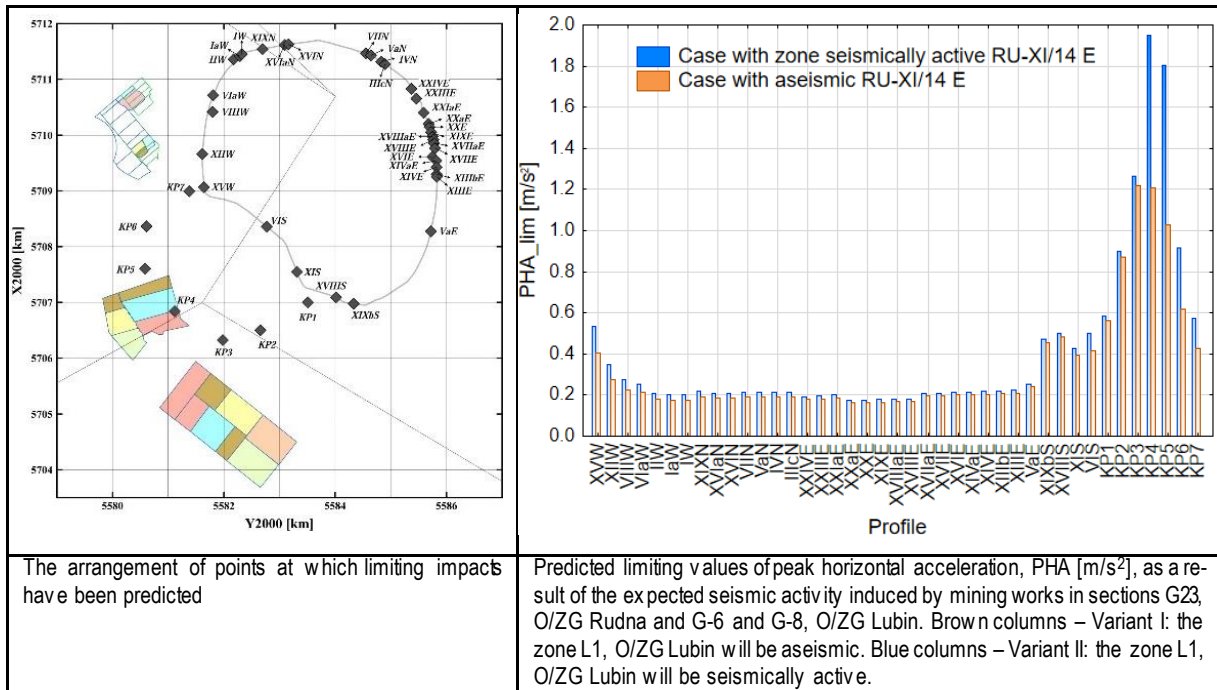


Fig. 1. Results of the PHA analysis.

HORIZONTAL-TO-VERTICAL SPECTRAL RATIO VARIABILITY IN THE PRESENCE OF PERMAFROST

D. Olszewska

This work is an example of using the HVSR method. This method is one of the most well-known techniques used in engineering seismology for the recognition of site effect. The permafrost and its active layer exhibit characteristics and morphological features common to the polar areas. The low population density of these regions does not detract from the importance of permafrost studies, as they are relevant to permafrost engineering and to environmental research, such as studies on increased methane emissions. Due to the high resistivity contrast between frozen and thawed geological media, direct current (DC) resistivity methods are frequently used in permafrost studies, and the employment of Electrical Resistivity Tomography (ERT) is currently standard practice. Also common in permafrost geophysics is the use of seismic methods, which are suitable for studying the permafrost table, as shown by a high contrast in shear wave velocity (V_s). Of these methods, the horizontal-to-vertical spectral ratio (HVSR) was chosen for the purpose of this study. This project applies a methodology that uses seismic noise to calculate horizontal-to-vertical ratio curves (H/V curves). Seismic noise is a complex phenomenon as it is a combination of both natural and artificial signals. However, the statistical features of seismic noise are essentially time-independent. Furthermore, HVSR is also nearly time-independent in terms of both the frequency and amplitude of H/V peaks. This study aims to investigate the reliability of the HVSR method in the presence of permafrost. In addition, it assesses whether the HVSR method can be used to estimate the thickness of the active layer of the permafrost. For the purposes of the H/V ratio investigation, the use was made of a data set compiled at the seismic station near the Polish Polar Station, Hornsund (station code: HSPB). The results of the analysis are presented with reference to air and ground temperatures and in comparison with electrical resistivity tomography measurements conducted nearby.

The analysis was done using the seismic measurement from 2012 to 2015. The example of the result is shown in Fig. 1. The bottom panel of Fig. 1 shows the variability in HVSR curves in the course of 2012. Data samples were taken daily from 09:00 to 15:00. The whole year

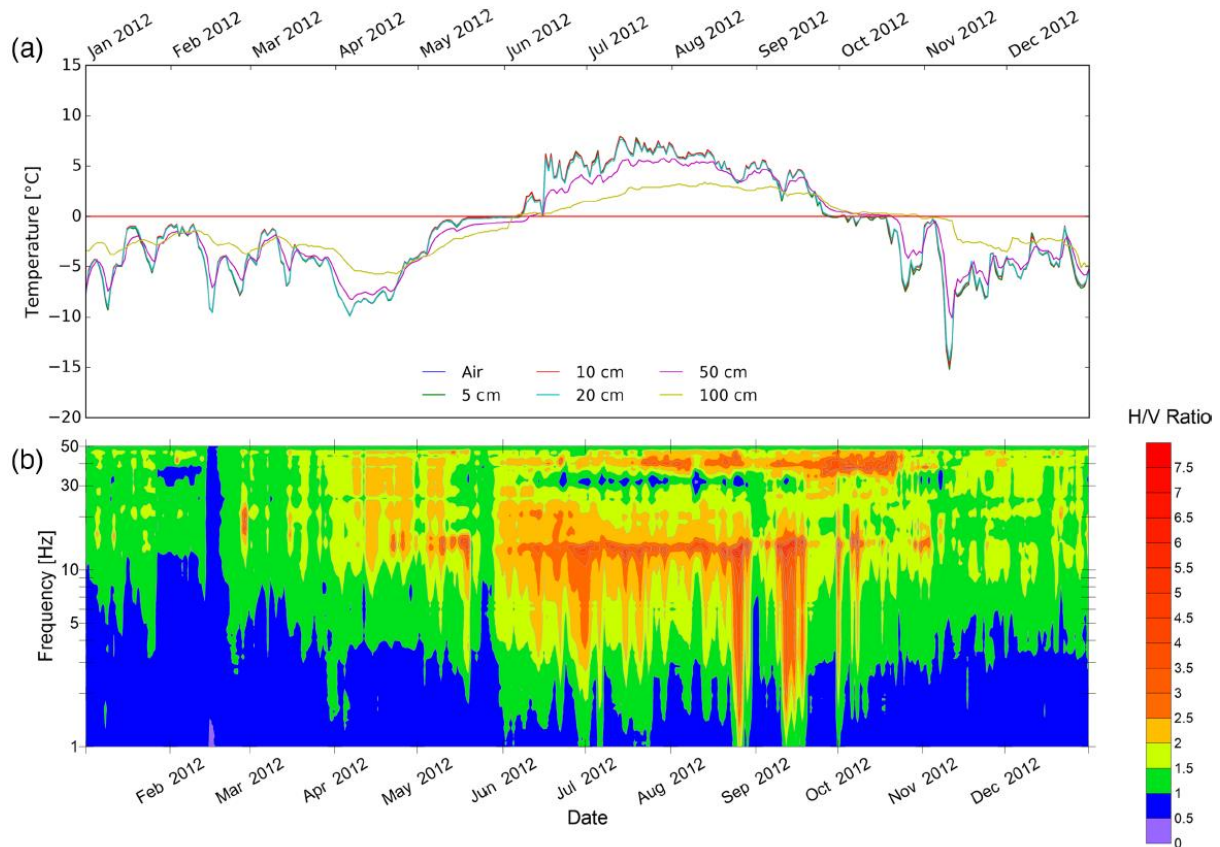


Fig. 1. Mean daily temperatures of air and ground measured at 5, 10, 20, 50, 100 cm: (a) versus variability of H/V value, (b) in 2012 (after Kula et al. 2018).

can be divided into three parts. The first part lasts from the beginning of the year until mid-May. In this period, the value of the H/V curve barely exceeds 2, the only exceptions being a few narrow peaks around 15 Hz. From June to November, an area of H/V curve values is visibly higher than the corresponding values observed at the beginning and the end of the year. There is a clearly visible local maximum at approximately 13 Hz, extending to lower frequencies. A significant drop in the H/V values at approximately 30–35 Hz appears in late June, fading out in September. Moreover, one more local maximum is evident at frequencies of approximately 40 Hz between late July and mid-October. The period from November until the end of the year is similar in terms of values to the beginning of the year. As a result, the variability in the HVSR curve can also be divided into winter and summer seasons. The H/V ratio fluctuations correlate well with the observed air and ground temperatures (Fig. 1). A visible minimum can be observed at a frequency of approximately 30–35 Hz at the start of the thawing process. A maximum at an even higher frequency (40 Hz) becomes visible in mid-July. The fadeout of this maximum correlates well with a temperature drop to below 0 °C. The overall increase of the H/V value during the summer season may be connected to the above-mentioned temporary increase in human activity that occurs at this time. The results of this study showed fluctuations in the H/V ratio at the Arctic site in the course of a year. These variations correlate well with the increases in ground temperatures (above 0 °C). The first peak, observed at approximately 12 Hz on the H/V curves obtained, is more likely to have been caused by a deeper impedance contrast than by the depth of the permafrost table. This maximum is continuous throughout the summer season. During the rest of the year, it is non-continuous and its occurrence correlates with increased average wind velocity in the area. The second maximum occurs at around 35–45 Hz and is thought to be linked to an impedance contrast at the permafrost table.

It is worth noting that this frequency range is beyond the range that geoscientists and engineers generally consider when using the HVSR method. This second peak is not always present in data from previous years. The sampling frequency of the seismometer is 100 Hz, which gives a Nyquist frequency equal to 50 Hz. Furthermore, the frequency range of the seismometer is between 120 s and 50 Hz. All these features mean that the second peak is on the edge of a spectrum that can be recovered with hardware used at the HSPB seismic station. The HVSR curve inversion provided useful and expected results. No peaks are present in the curves during the winter season, which enables a wide range of velocity models to fit the curve. On the other hand, two peaks were obvious in the curves obtained during the summer season, and consequently, the inversion provides a velocity model where the range of possible combinations narrows near the surface and widens with depth. The depth at which a velocity increase occurs fits the depth of the boundary between the low and high-resistivity layers (inferred from the ERT results). The first increase in shear wave velocity is visible at 1.5–2 m. This depth correlates well with ERT results, which shows a low-resistivity layer 1.5–2 m thick. The low V_s and low resistivity that characterize the first layer correspond closely to in situ observations. They also reflect the geophysical characteristics of the permafrost active layer. The HVSR method is claimed to be stable over time. However, this study shows that under specific circumstances, such as in the presence of permafrost and in its active layer, the H/V ratio does change over time, and the changes correlate with the thawing of the ground. Due to the lower power of high frequencies during the winter, it was impossible to identify other features such as deeper impedance contrasts that may be present throughout the year.

A STUDY OF SITE EFFECT USING SURFACE-DOWNHOLE SEISMIC DATA IN A MINING AREA

D. Olszewska

The aim of this study is to examine the phenomenon of site effect using surface-downhole seismic data caused by mining tremors in the Upper Silesia Coal Basin (USCB). The USCB is located in southern Poland and as a consequence of underground mining operations about 1000 mining tremors occur annually with a local magnitude of $M_L \geq 1.5$. The strongest event which occurred on 9 February 2010 reached $M_L = 4.2$ and the peak ground acceleration (PGA) observed was approximately 2 m/s^2 . Induced events which can be treated as minor shallow earthquakes also have an impact on the surface. Thus, monitoring of ground motion is carried out and provided by the Central Mining Institute in this area – the Upper Silesian Seismological Network USSN (data are available as “episode USCB” on the IS-EPOS platform at <https://tcs.ah-epos.eu/>). The network for ground motion monitoring is equipped with 7 free-field surface triaxial accelerometers GeoSIG AC-63 and 2 downhole accelerometers GeoSIG AC-63DH located in 30 m deep boreholes. Thanks to that, 2 sites with surface and downhole ground motion measurements (Imielin and Miechowice) are available. The accelerations caused by seismic events during the period from January 2014 up to June 2017 were used in the analysis. The magnitude of the registered events varies from 2.3 up 4.1. The PGAs registered by surface stations were up to 0.37 m/s^2 . A mean shear velocity up to 30 m is equal to 423 m/s at the Imielin site and 352 m/s at the Miechowice site. These give the ground types B at the Imielin site and C at the Miechowice site – according to the European Standard “Eurocode 8: Design of structures for earthquake resistance (Part 1)” (Eurocode:8). The amplification factors in the time domain were calculated as a ratio of the surface and downhole PGA at Imielin and Miechowice stations. That factors were obtained for NS, EW, and merged horizontal components and for the vertical one. The greatest amplification factor was obtained for the Miechowice site for the NS horizontal component (6.7). The Imielin amplification factors were around

2.1–2.4, only the value for the EW component was slightly greater (2.68). The greatest amplification factor was obtained for the Miechowice site for the NS horizontal component (6.7). In the next step of the analysis, the surface-downhole spectral ratios (SR) were calculated using data from Imielin and Miechowice stations. That is, the transfer function (TF) between a depth of 30 m and the surface, which shows how components are amplified by this layer in the frequency domain. Calculations were done for NS, EW, and the merged horizontal component and the vertical one; likewise, a calculation of amplification factors was done. The shape of TF curves for Imielin and Miechowice differ in the number of local maximum and its frequencies. That result shows also the differences for NE-SW orientation. Therefore more detailed analysis should be performed in the future to check whether this effect is caused by anisotropy or other phenomena. The SR variability for the Imielin site is less than for the Miechowice site. That could be the effect of site characteristic or the number of analysed data (no of events registered by the Imielin site is 273 and the Miechowice only 57). Therefore this analysis should be repeated in the future when more useful data from the Miechowice site will be available. HVSR was used for estimating the amplification for the Miechowice and Imielin sites. This method is based on surface measurements only. Thus, records from surface stations are used in this part of the analysis. Figure 1 compares the TF obtained from the above analysis and the HVSR curves. The merged horizontal components (surface and downhole) were used for this comparison – HHSR (Horizontal to Horizontal Spectral Ratio). As can be seen from that figure, there is satisfactory compatibility between the graphs for the Imielin site, compared to Miechowice site. The Imielin HVSR curve has also three main local maximums found in the same frequency as the HHSR curve. The amplitudes of the HVSR peaks is almost two times smaller than the HHSR peaks. Taking into account the Miechowice site, the HVSR and HHSR curves vary in the numbers of local maximums and their frequencies. From the graph in Fig. 1 we can see that more comparable to the HVSR curve is the HHSR curve calculated for an epicentral distance above 10 km (dark blue line in Fig. 1).

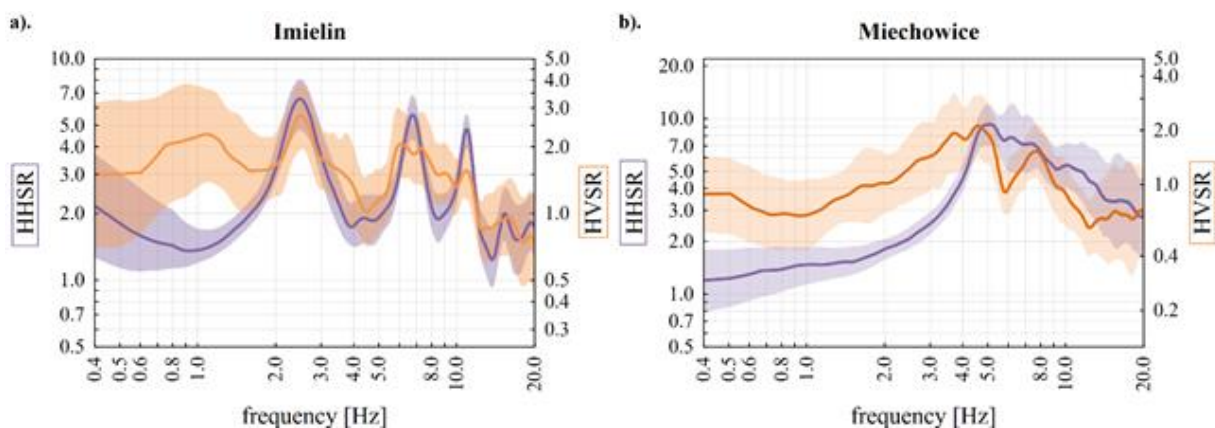


Fig. 1. A HHSR and HVSR at Imielin (a) and Miechowice (b) stations.

In this work, the amplification factors were calculated for the Imielin and Miechowice sites. Thanks to a comparison of the obtained results and profiles of shear waves up to 30 m, the characteristics of both sites were examined. The obtained result shows that the surface layer can play an important role in the amplification of ground motion. The geological structure and therefore a shear mean velocity up to 30 m are correlated with the amplification factor. Transfer functions of both components were calculated using surface and downhole data. Amplification behaviour of surface waves by the surface layer may differ from the corresponding body wave amplification. In the case of induced seismicity, the body waves are mostly recorded – the epicentral distances are too small to facilitate the observation of surface waves. However,

surface waves could also be observed in the case of events with greater magnitudes, at a depth of up to 1 km and an epicentral distance to the stations greater than 3 km. The obtained result shows that the distance between the event and the station is important in the case of induced events. The amplification factor is significantly different for shorter distances than for longer ones. Additionally, the characteristics of transfer function calculated for registration caused for short distances differ from those that are longer. Nevertheless, additional study is needed to confirm that the main reason for such a situation is the fact that for such short distances, surface waves are not registered. These phenomena could be also caused by an incidence angle or back-azimuth. The HVSR curves were calculated and the results were compared with suitable transfer functions. These results show that the HVSR method could be used for estimating site effect in the case of induced seismicity.

2.6 Seminars and teaching

Seminars and lectures outside of the IG PAS:

- Ł. Rudziński, Complex mechanism of rockbursts observed on Polish Copper Mines, Oulu University, Oulu, Finland, Invited lecture;
- G. Lizurek, Introduction to EPOS AH Platform, Oulu University, Oulu, Finland, Invited lecture;
- K. Leptokarpoulos, Properties of induced seismicity and its connection to fluid injection: The NW The Geysers geothermal field case study, Aristotle University of Thessaloniki, Thessaloniki, Greece, Seminar.

2.7 Visiting scientists

- S. Dineva, Luleå University of Technology, Luleå, Sweden, 16–18.04 and 20–23.08.2018;
- T. Ishida, Kyoto University, Kyoto, Japan,
- J. Martinsson, LKAB, Malmberget, Sweden, 16–18.04.2018;
- V. Tornman, LKAB/Luleå University of Technology, Kiruna/Luleå, Sweden, 16–18.04.2018.

2.8 Meetings, workshops, conferences, and symposia

Presentations of the Department's members:

European Seismological Commission, Valetta, Malta

- Sz. Cielesta, B. Orlecka-Sikora, Seismic response and fracture growth due to fluid injection, Oral;
- G. Lizurek, J. Wiszniowski, Giang N.V., B. Plesiewicz, and Dinh Quoc Van, Moment tensor and stress inversion derived from anthropogenic seismicity in the Song Trahn 2 Reservoir, Vietnam, Oral;
- D. Olszewska, G. Lizurek, G. Mutke, J. Kryński, W. Rohm, A. Araszkievicz, A. Barański, Multidisciplinary Upper Silesian Episode as a new holistic approach in building research infrastructure, Poster;
- A. Blanke, G. Lizurek, G. Kwiatek, P. Urban, B. Orlecka-Sikora, S. Lasocki, J.-R. Grasso, A. Karimov, M. Schaming, A. Fremand, J. Schmittbuhl, P. Bigarre, J.-L. Kinscher, A. Garcia, G. Saccorotti, P. Roselli, J. Nevalainen, E. Kozłovskaya, S. Toon, J. Pringle, J. Kocot, M. Sterzel, T. Szepieniec, Integration of anthropogenic seismicity data within the EPOS Implementation Phase (EPOS-IP) to encourage interdisciplinary research and collaboration, Poster;

- F. Haslinger, D. Bailo, C. Cippoloni, L. Danciu, D. Aurelien, K. Elger, S. Grellet, R. Häner, R. Heaven, T. Hoffmann, O. Lange, M.P. Litwin, G. Lizurek, M. Locati, H. Lorenz, What are you talking about? Towards harmonizing and formalizing vocabularies within seismology and beyond, Oral;
- P. Paradisopoulou, C. Gkarlaoui, G. Spyrou, A. Panou, A. Adamaki, K. Leptokarpoulos, Impact of friction coefficient and fault parameters variation on Coulomb stress change analysis, Poster.

European Geosciences Union, Wien, Austria

- M. Sobiesiak, S. Lasocki, B. Orlecka-Sikora, K. Leptokarpoulos, J. Kocot, P. Urban, Developments on the IS-EPOS platform for analyzing anthropogenic hazard, Oral;
- M. Sobiesiak, K. Leptokarpoulos, IS-EPOS: development, current status and future challenges, demonstration of the IS-EPOS platform at the EPOS booth, Oral;
- P. Victor, O. Oncken, M. Sobiesiak, M. Kemter, Remote triggering of forearc faulting – surface displacement along the Atacama fault system monitored with the ipoc creepmeter array (N-Chile), Poster;
- S. Lasocki, P. Urban, Incompatibility of anthropogenic seismicity with probabilistic models typically used in seismic hazard analysis: the case of Oklahoma earthquakes, Oral;
- A. Adamaki, K. Leptokarpoulos, C. Gkarlaoui, P. Paradisopoulou, The impact of magnitude errors on basic catalogue properties investigated numerically with synthetic magnitude catalogues, Poster;
- B. Orlecka-Sikora, S. Lasocki, Seismic response and fracture growth due to fluid injection, Oral.

Seminar of the Institute of Mine Seismology, Johannesburg, South Africa

- S. Dineva, Ł. Rudziński, D. Mihaylov, B. Lund, Source parameters of seismic events in underground mines from regional data and in-mine seismic systems: Examples from Swedish and Polish mines, Oral.

SHEER Final Meeting, Kraków, Poland

- Sz. Cielesta, WP3 – Monitoring of environmental effects of shale gas operations - lessons learned from Wysin study, Oral;
- G. Lizurek, B. Orlecka-Sikora, SHEER dataase, SHEER Final meeting, Oral;
- K. Leptokarpoulos, S. Lasocki, B. Orlecka-Sikora, Some advances in the assessments of hazards related to injection-induced seismicity, obtained in SHEER project, Oral.

7th EAGE Workshop on Passive Seismic, Kraków, Poland

- S. Cielesta, S. Lasocki, K. Leptokarpoulos, S. Cesca, The SHEER approach to shale gas exploration and exploitation associated risks, Poster;
- K. Leptokarpoulos, A. Adamaki, Uncertainty of b-value estimation in connection with magnitude distribution properties of small data sets, Oral;
- B. Orlecka-Sikora, Step-change in tackling grand challenges of seismic hazard associated with exploitation of geo-resources, Oral.

65th IG-PAS Anniversary, Warszawa, Poland

- K. Leptokarpoulos et al., Leadership of the design, development and management of integration of research and infrastructures of anthropogenic seismicity in Europe and beyond, Oral.

COST Action TIDES Workshop on: "Induced Seismicity: from the Monitoring of Non-stationary Processes to the Definition of Performance-based Mitigation Strategies", Bologna, Italy

- B. Orlecka-Sikora, M. Staszek, S. Lasocki, K. Leptokarpoulos, G. Kwiatek, and S. Cielesta, Static stress drop of induced earthquakes in seismic hazard assessment, Induced Seismicity: from monitoring of non-stationary processes to definition of performance-based mitigation strategies, Oral;
- K. Leptokarpoulos, and the IS-EPOS and EPOS-IP teams, IS-EPOS: Development, current status and future challenges, Induced Seismicity: from monitoring of non-stationary processes to definition of performance-based mitigation strategies, Oral;
- S. Lasocki, Seismicity and its relation with industrial factors, studied with the use of equivalent dimension approach. Assessments of fluid migration pathways buildup, Oral.

SERA JRA1/JR2 Joint Workshop, Kraków, Poland

- K. Leptokarpoulos, M. Sobiesiak, and S. Lasocki, Introduction to clustering toolbox and magnitude complexity toolbox, Oral;
- K. Leptokarpoulos, Hands on clustering toolbox and complexity toolbox – on-line demonstration, Oral;
- S. Lasocki, Influence of injection rate on ordering of induced seismic sources, Oral.

Workshop "Development of Criteria for Temporary Closing/re-opening of Seismically Active Mines Due to Seismic Risk", Luleå, Sweden

- K. Leptokarpoulos, S. Lasocki and S. Dineva, Characteristics of Kiruna mine seismicity (Block 34) in space-time-size domain and its relation to blasting activities, Oral;
- M. Kozłowska, Model for estimating the spatio-temporal behavior of seismic activity after strong seismic events (Kiruna mine), Oral.

I Konferencja Projektu EPOS-PL „EPOS-System Obserwacji Płyty Europejskiej”, Jachranka, Poland

- G. Lizurek, Od integracji infrastruktury badawczej i danych pomiarowych do publikacji artykułu naukowego na przykładzie badań sejsmiczności wywoływanej eksploatacją zbiornika wodnego Song Tranh w Wietnamie, Oral;
- B. Orlecka-Sikora, Step-change in tackling grand challenges of seismic hazard associated with exploitation of geo-resources – thematic core service anthropogenic hazards, Oral.

GIS w Nauce, Warszawa, Poland

- P. Tymków, Ł. Guźniczak, M. Karpina, J. Kocot, T. Szepieniec, M. Sterzel, P. Urban, K. Kura, Prezentacja wybranych danych przestrzennych i produktów projektu EPOS – System Obserwacji Płyty Europejskiej w środowisku GIS 3D, Oral.

Science 4 Clean Energy, 1st Annual Consortium Meeting, Reykjavik, Iceland

- S. Lasocki, Studies of influence of injection rate on ordering of induced seismic sources, WP6 Implementation of novel technologies, Task 6.5 Assessing rapid fluid transport probability and tracking fluid pathways in the rockmass, Oral;
- S. Lasocki, S4CE Database on IS-EPOS platform, WP9 Dissemination, exploitation and innovation, Task 9.7 S4CE Database on IS-EPOS platform, Oral.

SHEER, Final Review Meeting, Brussels, Belgium

- S. Lasocki, WP3 On-site monitoring, Oral.

2.9 Publications

ARTICLES

- López-Comino, J.A., J. Jarosławski, **S. Lasocki**, et al. (2018), Induced seismicity response of hydraulic fracturing: results of a multidisciplinary monitoring at the Wysin site, Poland, *Sci. Rep.* **8**, 8653, DOI: 10.1038/s41598-018-26970-9.
- Leptokaropoulos, K., M. Staszek, S. Lasocki**, et al. (2018a), Evolution of seismicity in relation to fluid injection in North-Western part of The Geysers geothermal field, *Geophys. J. Int.* **212**, 2, 1157–1166, DOI: 10.1093/gji/ggx481.
- Leptokaropoulos, K.**, et al. (2018b), Impact of magnitude uncertainties on seismic catalogue properties, *Geophys. J. Int.* **213**, 2, 940–951, DOI: 10.1093/gji/ggy023.
- Leptokaropoulos, K.**, and **M. Staszek** (2019), Temporal response of magnitude distribution to fluid injection rates in The Geysers geothermal field, *Acta Geophys.* **67**, 327–339, DOI: 10.1007/s11600-018-0215-1.
- Kula, D., **D. Olszewska**, et al. (2018), Horizontal-to-vertical spectral ratio variability in the presence of permafrost, *Geophys. J. Int.* **214**, 1, 219–231, DOI: 10.1093/gji/ggy118.
- Rudziński, Ł.**, et al. (2019), Rapid ground deformation corresponding to a mining-induced seismic event followed by a massive collapse, *Nat. Hazards* **96**, 461–471, DOI: 10.1007/s11069-018-3552-0.
- Victor, P., **M. Sobiesiak**, et al. (2018), Dynamic triggering of shallow slip on forearc faults constrained by monitoring surface displacement with the IPOC Creepmeter Array, *Earth Planet. Sci. Lett.* **502**, 57–73, DOI: 10.1016/j.epsl.2018.08.046.

3. DEPARTMENT OF ATMOSPHERIC PHYSICS

Janusz Krzyściński

3.1 About the Department

The Department's activities focus on the long-term monitoring of various atmospheric parameters in the atmosphere (including surface layer, the troposphere, and the stratosphere), short-term campaigns within national and international grants, and modelling changes in geophysical fields and dynamical/chemical processes in different time scales from hours up to decades. The observations are routinely carried out at IG PAS observatories in Poland (Belsk, Racibórz, and Świdler) and in Svalbard (Polish Polar Station, Hornsund). The field experiments in 2018 include observations in the Beskid Mountains (with the use of the Szyndzielnia Mountain cable car) and Ny-Alesund (Svalbard). Modeling using both statistical and dynamical (solving time-dependent equations in 3-D spatial configuration) approach is developed to find sources of the atmosphere variability and directions of changes of environmental variables affecting human life (e.g. surface and column amount of ozone, intensity of UV radiation at the ground level, electrical field, aerosols concentrations, and surface trace gases concentration). Atmospheric processes in various spatial scales are examined in 2018, including: the local scale (contamination of the atmosphere in vicinity of the shale gas wells in Wysin and valleys in the Beskid range near the Szyndzielnia Mountain, thunderstorms in Warsaw and its suburban areas, and UV intensity over Warsaw and Łódź), regional scale (UV index forecast over the territory of Poland, surface warm layers in the Bay of Bengal during Indian monsoon, and trans-boundary aerosol transport between Poland and neighboring countries), and global scale (global electrical circuit, impact of aviation emissions on chemical composition of the atmosphere and global circulation, and health exposure optimal index to control safe sunbathing over any place).

3.2 Personnel

Head of the Department

Janusz Krzyściński
Professor

Professor

Janusz Borkowski

Associate Professors

Janusz Jarosławski
Jacek Kamiński
Aleksander Pietruczuk

Assistant Professors

Agnieszka Czerwińska
Magdalena Kossakowska
Marek Kubicki
Anna Odzimek
Michał Posyński
Artur Szkop

Post-Doctoral Researchers

Dariusz Baranowski
Jakub Guzikowski

Izabela Pawlak
Piotr Sobolewski

Research Assistants

Piotr Barański
Sabina Kucięba
Beata Latos
Jakub Wink

Observers

Anna Głowacka
Dorota Sawicka
Wiesława Zawisza

PhD Students

Alnilam Fernandez, India; Aleksander Pietruczuk – PhD supervisor
Maria Kłeczek, Poland; Jacek Kamiński – PhD supervisor
Beata Latos, Poland; Aleksander Pietruczuk – PhD supervisor
Anahita Sattari, Iran; Jacek Kamiński – PhD supervisor

3.3 Main research projects

- Aerosols, clouds, and trace gases research infra structure, A. Pietruczuk, H2020, 2015–2019;
- Global coordination of Atmospheric Electricity Measurements (GloCAEM), M. Kubicki, NERC, 2016–2018;
- Atmospheric electricity network: coupling with the Earth system, climate and biological systems, A. Odzimek, COST, 2016–2018;
- Shale gas exploration and exploration induced Risk, J. Jarosławski, H2020, 2015–2018;
- Monitoring of total ozone amount in the atmosphere and UV-B radiation at Belsk Observatory in 2017–2020, J. Jarosławski, Chief Inspectorate of Environment Protection, 2017–2020;
- Impact of absorbing aerosols on the planetary boundary layer height, M. Posyniak, NCN, Poland, 2017–2020.
- UV Intercomparison and Integration in a High Arctic Environment (UV-ICARE), P. Sobolewski, NILU, 2017–2018;
- Multi-scale interactions over the Maritime Continent and their role in weather extremes over Central and Eastern Europe, D. Baranowski, FNP, 2018–2020;
- Parameterization of solar radiation attenuation by clouds in UV index forecast for Poland, J. Guzikowski, NCN, 2016–2018;
- Genetic and environmental factors affecting the therapy outcome of psoriasis in the Polish population, J. Krzyściński, NCN, 2015–2018.

3.4 Instruments and facilities

Equipment

LLDN – Local Lightning Detection Network consisting of four lightning detection stations (2 in Warsaw, 1 in Świder, and 1 in Milanówek – the Warsaw suburban zone) to monitor vertical structure of the lightning in the vicinity of Warsaw.

System for monitoring aerosol properties in experiments with use cable car on the Szyndzielnia Mountain. It includes:

- particle counters OPC-N2 (6 psc.), PMS 7003 (6 psc.),
- sun photometer CIMEL, CE-318-1 Standard Model with 1020-870-675-440-936-500-340-380 nm filters (routinely operated at the Racibórz station),
- black carbon monitor AE51,
- meteo station Gill Met Pac (2 psc.).

Standard automatic system for monitoring air-quality at Belsk and Świder (measurements of the surface concentration of the following trace gases: ozone, NO, NO₂, NO_x, SO₂, CO, PM₁₀) plus monitoring of important green-house gases including CO₂ and methane (only at Belsk).

Laboratory

Equipment at Świder:

- Electric field (potential gradient) by radioactive collector,
- Electric field (potential gradient) by rotating-dipole field mill,
- Air-Earth current density by Wilson antenna,
- Air conductivity (positive and negative) – Gerdien counter,
- Aerosol measurements – condensation counter: model TSI 3025, 3 nm – 3 μm, portable counter: model TSI 8525, 20 nm – 1 μm, and model TSI 3007, 10 nm – 1 μm,
- Air radioactivity – concentration of radionuclides at ASS-500 station: ⁷Be, ¹³⁷Cs, ²¹⁰Pb, ⁴⁰K.

Equipment in Hornsund:

- Sunshine duration sensor CSD3,
- CMP21 pyranometer,
- CNR4 net radiometer,
- UVS-E-T UV radiometer,
- TSI 3330 optical particle sizer,
- TSI 3910 particle size spectrometers,
- CHM 15k ceilometer.

Equipment at Belsk:

- Dobson spectrophotometer no. 084 (total ozone and vertical ozone profile measurements),
- Brewer spectrophotometer mark II no. 064 (total ozone, vertical ozone profile measurements, and UV spectra 290–325 nm),
- Sun photometer CIMEL, CE-318-1 standard model with 1020-870-675-440-936-500-340-380 nm filters,
- Gaseous pollutants analyzers (CO, NO, NO₂, NO_x, O₃, SO₂, PM₁₀, CO₂, CH₄),
- CM21 pyranometer (total solar radiation and spectral range: 280–3000 nm),
- UVS-AE-T UV radiometer Kipp&Zonen (biological active solar radiation and spectral range: 280–400 nm),
- Sunshine duration sensor CSD3 (3 photo-diodes with specially designed diffusers to make an analogue calculation when it is sunny),

- Campbell-Stokes heliograph (the glass sphere –4 inches in diameter to focus the rays from the sun onto a card mounted at the back),
- Zonntag actinometer (direct Sun radiation measurements),
- Weather station Vaisala-MILOS 520 (temperature, humidity, wind speed and direction, and pressure),
- Lidar (constructed at Belsk) to monitor tropospheric and stratospheric aerosols characteristics.

Equipment in Warsaw (roof of the IG PAS main building in Warsaw):

- Brewer spectrophotometer mark III no. 207 – double monochromator (total ozone, vertical ozone profile measurements, and UV spectra 290–363 nm),
- Davis meteo-station (temperature, humidity, wind speed and direction, pressure, rainfall, solar total irradiation, and UV index),
- Hand-held UV biometers (UV index and vitamin D3 production in IU/per minute).

Equipment in Racibórz:

- Ceilometer CHM-15K Nimbus LUFT,
- Broad band biometer (Kipp&Zonen UVS-E-T),
- Cimel sunphotometer CE-318-1 standard model with 1020-870-675-440-936-500-340-380 nm filters used to monitor the vertical structure of aerosols in the atmospheric boundary layer (part of global aerosols network – AERONET).

3.5 Research activity and results

Brief description/abstracts/summaries of some of the achievements of the Department's staff:

MODELLING AND OBSERVATIONS OF SOLAR RADIATION FOR THE PURPOSE OF PUBLIC HEALTH

J. Krzyścin, J. Guzikowski

The beneficial (e.g. vitamin D3 synthesis) and harmful (e.g. skin cancers) effects of solar radiation are well recognized. Recently, many efforts have been made in the Department of the Physics of the Atmosphere to provide outdoor activity scenarios allowing people to balance between these effects. To inform people about actual ultra violet index (UVI) distribution over the territory of Poland we provide 24-hour UVI forecast for every hour between 8 am and 5 pm. It was available (April–October 2018) on the Institute web page for cloudless and for all-sky conditions based on forecasted total ozone and cloudiness level.

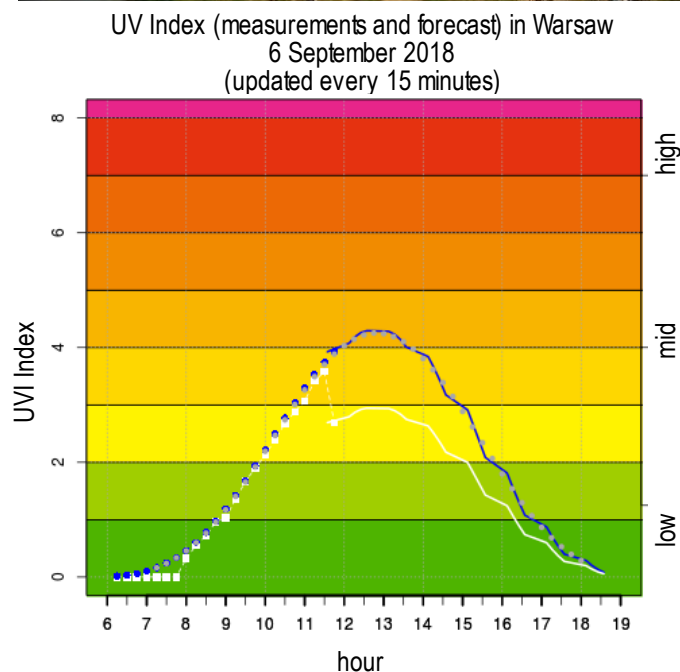
Cloud forecast is still a serious problem in the weather prediction because the micro-physical processes governing the cloud cover and their transparency require high resolution calculation grid impossible to be implemented in routine weather forecasts. Sometimes the prediction is no-clouds but a heavy cloud appears and vice-versa. Thus, we propose a new methodology that is able to resolve cloud attenuation of solar radiation. It is based on UV nowcasting (near-real time measurements of UV radiation) and short term UVI prediction (next 15 minute). The new model and its validation using UVI observations in Warsaw and Łódź are shown in our recent paper by Krzyścin et al. 2018 (Perspectives of UV nowcasting to monitor personal pro-health outdoor activities, *J. Phot. Photoch. Photobio B* **184**, 27–33). Reliable forecast of duration of safe sunbathing (without erythema risk) could be provided by a smartphone application for sites located in the distance less than 10 km from the UVI observing stations. The station in Warsaw is located on the roof of IG PAS building. It serves as the UV source for the short-term forecasts that are valid for sand beaches located on the right bank of

the Vistula river. Famous beach – Poniatówka (Fig. 1a), one of the most popular among Warsaw’s residents, is near the Prince Poniatowski Bridge. An example of the UVI measurements (white circles), hypothetical clear-sky representatives (blue circles), and UVI forecast since 11.15 pm (white curve) for 19th May are shown in Fig. 1b.

Skin synthesis of vitamin D3 is a basic source of vitamin D in the European population. However, in periods when the UV intensity is high ($UVI > 2$) and thus proper for vitamin D production, people should limit outdoor activities and/or apply several steps to reduce solar exposure. A typical diet could provide less than 10% of the required daily production of vitamin D. Thus, a question appears on how to make a balance between beneficial (vitamin D3 skin synthesis) and harmful (erythema, skin cancer, skin aging) UV effects. To solve this problem, we introduce a dimensionless index, i.e. health-optimum exposure index to get the target amount of vitamin D3 dose (HOEI, Guzikowski et al. 2018, Adequate vitamin D3 skin synthesis versus erythema risk in the Northern Hemisphere midlatitudes, *J. Photoch. Photobio B* **179**, 54–65). It gives the number of daily target vitamin D3 doses (e.g. recently recommended 2000 IU per day) produced during the maximum possible duration of safe (without skin erythema) exposure. HOEI larger than 1 means proper conditions for healthy sunbathing. We find an



a)



b)

Fig. 1. Poniatówka Beach (a) and UVI forecast for Warsaw on 19 May 2018 (b). Photo by T. Rudzki, Poniatówka Beach (https://commons.wikimedia.org/wiki/File:POL_Warszawa_plaza_18.JPG).

approximate formula, which is valid in midlatitudes sites in spring and summer during near noon hours regardless of human skin color. It gives that a young person (age~20 yr.) should expose at least 20% of his/her body to get 2000 IU of vitamin D without the erythema risk. Older people (age over 60 yr.) need to expose more than 40% of the whole body which is only possible during warm days. Optimal sunbathing near local noon to get 2000 IU vitamin D3 in central Poland in summer lasts between ~15–20 minutes (for cloudless days) up to 1–1.5 hrs. (for heavy cloudiness) for a young person exposing 25% of the whole skin.

A new subject of the research in 2018 is modelling of melatonin reduction in humans due to natural (solar) light. Melatonin is a hormone that plays a role in sleep. It is also powerful antioxidant slowing down harmful chemical reactions damaging cells thus helps to protect nerve and brain cells from damage. The production and release of melatonin in the brain increase in darkness, usually during sleep hours, and decrease when it's light. A number of studies have reported benefits of supplemental melatonin. There are also suggestions that melatonin helps with multiple sclerosis (MS) symptoms. Various factors might contribute to the MS risks including genetics and geographical factors. A risk for MS increases with a distance from the equator. It leads us to calculate the geographical (latitudinal) distribution of

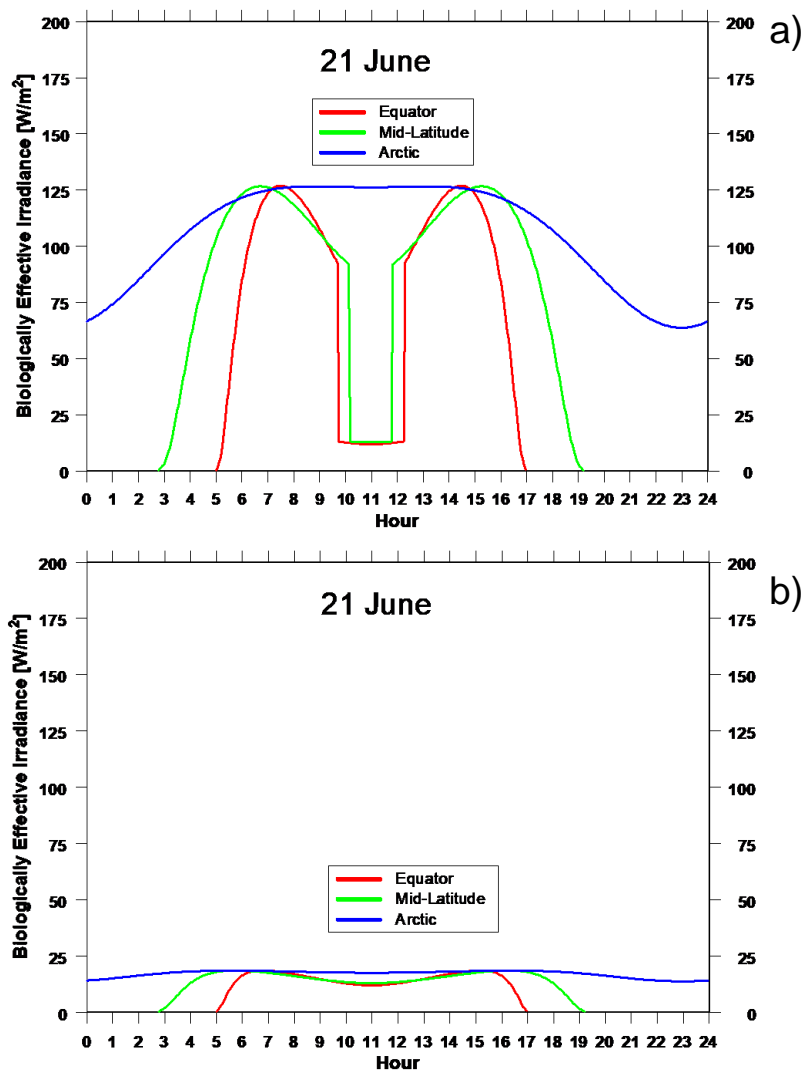


Fig. 2. The daily course (21 June 2018) of radiation effective for melatonin suppression received by a standing person: face towards the Sun (a), and face opposite to the Sun (b).

the radiation effective for melatonin suppression. Radiation in the UV and in the visible blue range are essential for the melatonin suppression.

Figure 2 shows the daily course of radiation dose effective for melatonin suppression for three regions: the equator (20°E), the mid-latitudes (Belsk), and the Arctic (Hornsund) on 21 June 2018 derived from the radiative model simulations. The model takes into account the field of view of typical eye of a standing person. Two cases are considered: face towards or opposite to the direction of the Sun. It means that radiation is due to superposed direct Sun and sky radiation or only due to sky radiation, respectively. A working hypothesis to lower MS risks is reducing solar exposure since 3–4 pm GMT (e.g. by wearing glasses with blue/UV cut off filter) and stop using blue light at home during night.

STATISTICAL TRAJECTORY TECHNIQUE FOR DETERMINING AIR-POLLUTION SOURCE REGIONS IN POLAND

A. Pietruczuk, A. Szkop

Atmospheric aerosols are one of the least recognized climate-shaping factors. They influence climate both directly, by interacting with solar radiation passing through the atmosphere, and indirectly, by modifying cloud evolution. Moreover, aerosols influence the health and wellbeing of the human population by causing illnesses and premature deaths, as well as by modifying the amount of UV radiation reaching the Earth's surface they change the probability of skin carcinogenesis and modify the rate of D3 vitamin synthesis. This makes improving the aerosol pollution forecasts a very important issue. This requires the detailed knowledge of statistics of aerosol types over a given territory, recognition of trends in their changes and identification of regions from which the aerosols were emitted.

The main scientific goal of research is to develop an analytic scheme that allows for the determination of aerosol source regions and the identification of aerosol types based on remote sensing techniques and data from atmospheric models. We investigated the multi-year trends in aerosol pollution over Poland. We show that, while the local sources might have dominated in the past decades, there are statistically insignificant trends in the last twenty years which it difficult to unambiguously determine the types and sources of the currently observed aerosols. We proposed an innovative method for the determination of dominant source regions from which the identified aerosol types originated based on a statistical analysis of air-mass backward trajectories. The method was then expanded with an additional analysis focused on the study of changes in the aerosol optical parameters observed during transport that allows for the determination of additional source regions.

Aerosol classification based on two chosen optical parameters is usually found in the literature. The introduction of a third, absorption based, parameter into the analysis makes a differentiation between industrial, biomass-burning and desert type aerosols possible. The proposed method for backward trajectory analysis allows for associating an air-mass source with an aerosol source. Moreover, the utilization of the novel normalization scheme for trajectory densities inhibits the main problems in the usually used methods, namely the anomalously high densities in the vicinity of the receptor and the overrepresentation of regions associated with extreme concentrations of aerosols.

The developed novel method of data analysis allows for obtaining a significant amount of information on atmospheric aerosols and their sources based on a limited number of measurements performed by a sparsely distributed network of remote optical sensors in Poland. This should result in the better verifiability of atmospheric pollution forecasts and consequently mitigate the adverse influence of aerosols on the human population. Moreover, the research may prove useful for national policymakers as well as local authorities. The identification of source regions of individual aerosol types makes it easier to intensify the efforts on emissions reduction in regions where it stands to provide a maximal advantage.

ELECTRICAL SIGNATURES OF NIMBOSTRATUS AND STRATUS CLOUDS IN GROUND-LEVEL VERTICAL ATMOSPHERIC ELECTRIC FIELD AND CURRENT DENSITY AT MID-LATITUDE STATION ŚWIDER, POLAND

A. Odzimek, P. Barański, M. Kubicki, D. Jasinkiewicz

We analyze the occurrences of low-level stratiform clouds such as Nimbostratus and Stratus, in Świder, Poland (51.15 N, 21.23 E) in the years 2005–2015. There have been on average 44 days with Nimbostratus a year between 2005 and 2015 at Świder and 51 days with Stratus over this period. Atmospheric electric field, current density and air conductivity available for the rec-

orded cloud cases from the years 2012–2015 have been analyzed and their average values obtained for all cases and separately for the cloud cases with their main types of precipitation: rain and snow for Nimbostratus, drizzle and granular snow for Stratus. The analysis of atmospheric electricity parameters confirms previous results indicating differences in the electrical behavior of raining and snowing clouds. The atmospheric electric field and conduction current are more likely downward under Stratus cloud as is its precipitation-convection current. This type of cloud mostly behaves like a passive element of the global circuit. The electric field under Nimbostratus during rain at the ground is upward and upward precipitation current occurs during heavier rain. Such raining mid-latitude Nimbostratus can potentially be an electric cloud generator which charges the Earth's global atmospheric circuit, the contribution of which needs to be investigated in more detail (see sketch the scenarios in Fig. 1).

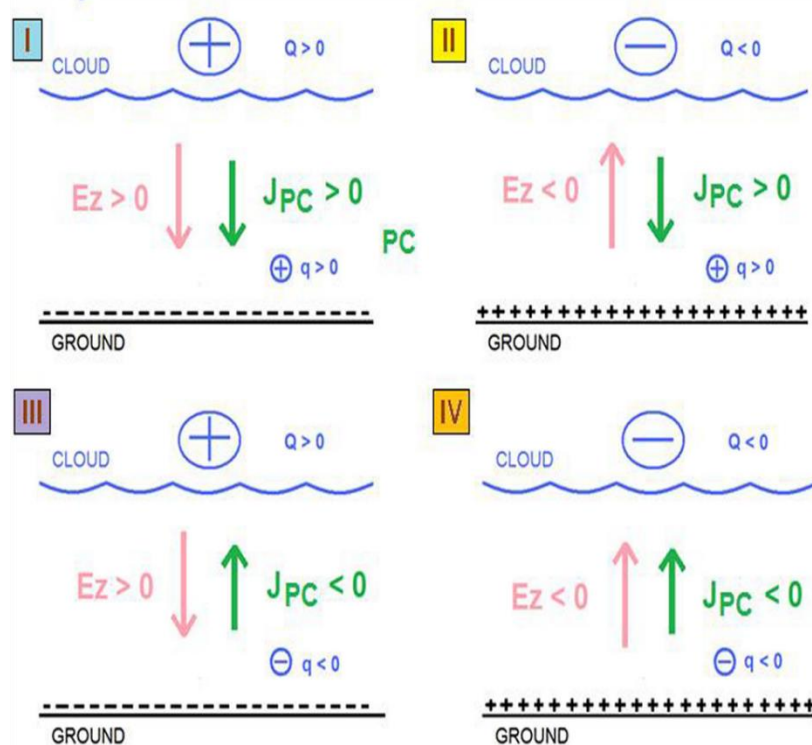


Fig. 1. Four possible different scenarios illustrating directions of the electric field and precipitation-convection (J_{PC}) current. Atmospheric ions or precipitation particles of charge q flow between the ground and the cloud layer of dominant charge Q , in relation to different directions of the vertical electric field (E_z) at ground level. The effect of the cloud precipitation (and/or convection) current may be the charging process of the ground electrode (overall globally negative), or conditions similar to “fair-weather” – discharging process of the ground electrode. Small blue circle with “+” or “-” near the ground denotes a precipitation particle and its resultant electric charge acquired after leaving the cloud base. The sign of E_z and J_{PC} is taken as positive when positive charge flows to the ground, according to the atmospheric electricity sign convention (after Odzimek et al. 2018b).

POTENTIAL IMPACT OF AVIATION EMISSIONS ON THE ATMOSPHERE IN THE ARCTIC

J.W. Kamiński, M. Kossakowska

The following summary pertains to a multi-year and multi-agency research project that was finalized in December 2018. The project was carried out at York University, WxPrime Corporation, Warsaw University of Technology, and the Institute of Geophysics. The project was funded by Transport Canada, Federal Aviation Administration of the US Department of Transportation. PhD student Dr. Magdalena Kossakowska received a grant (Preludium) from the

Polish National Science Centre to participate in the project. The overall objectives were to assist Transport Canada and FAA in the assessment of aviation emission impact on the Arctic environment.

Summary

In the course of the project, a research methodology was developed, and an integrated modelling framework was applied to study the potential effect of aviation emissions on atmospheric chemistry and dynamics in the upper troposphere and lower stratosphere (UTLS) in the current (2000–2010) and future (2045–2055) climates.

Introduction of pollutants from aviation emissions results in changes in the chemical composition of the atmosphere triggering highly non-linear chemical processes that lead to perturbation in atmospheric heating rates and consequently changes in large-scale transport processes.

In order to carry out the research objectives, a number of model scenario simulations were done using the Global Environmental Multiscale Atmospheric Chemistry model (GEM-AC). GEM-AC is an on-line interactive tropospheric and stratospheric chemistry model that provides a consistent framework between the meteorological and chemistry aspects of the atmospheric system.

For evaluation purposes, the GEM-AC model was run for 10 years in current climate conditions. Model results were compared with long-term satellite observations. It was determined that the model could accurately simulate atmospheric dynamical and physical processes in the current climate. The distribution of the temperature and zonal wind fields were consistent with observed climatology. The maximum zonal average mixing ratio of ozone had a value of ~10 ppm at the altitude of ~30 km for October, as calculated from a long-term average. The predicted ozone mixing ratio field was consistent with satellite and ozonesonde observations. Also, the distribution of other minor species compared quite well with satellite observations.

In order to assess the impact of aviation emissions on the atmosphere, GEM-AC was run for 10 years for scenarios without and with aviation emissions that were prepared using the Aviation Environment Design Tool (AEDT 2006). Atmospheric response to aviation emissions was assessed using model results from these scenarios. Specifically, changes in the distribution of water vapour, temperature, ozone, halogens, reactive nitrogen species, and aerosols were evaluated from differences between model simulations for scenarios with and without aviation emissions.

The largest differences in water mixing ratio between emission scenarios were in the spring for the current climate and the fall for the future climate. The GEM-AC model simulations indicate an increase of temperatures in the UTLS in high latitudes in the regions of high aviation emissions for current and future climate model simulations. The biggest changes in the temperature in the Arctic UTLS region were predicted during the spring. The GEM-AC model simulation showed a large increase of ozone mixing ratios in the winter for the current climate and in the spring in future climate. A similar pattern was present in the distribution of BrO_x family mixing ratio in the Arctic UTLS region. An increase of ClO_x mixing ratio was predicted in the summer for the current climate and in the spring in the future climate.

The GEM-AC model simulation showed that aviation emissions do impact the composition, radiative properties and dynamics of the Arctic atmosphere. Since the atmospheric response to the chemical perturbation is highly non-linear additional research and aviation emissions scenario runs are needed.

Challenges

There are on-going research and development activities in the fields of climate modelling and atmospheric chemistry, mainly in the EU and USA. The major challenge is to keep the GEM-

AC model current. This would involve porting the chemical and aerosol modules to the latest version of the host meteorological model. Also, the chemical and aerosol modules would have to be updated and the model lid raised to 85 km or higher. Raising the model lid is a major challenge, as additional physical and radiative transfer processes would have to be introduced in the host GEM model. However, this would put GEM-AC on par with American (NCAR, Stanford) and European (ECMWF, UK Met Office) models. Should there be any plans and commercial viability of supersonic transport at altitudes of 65 000 ft. (20 km), only models with high lids could be used for modelling and environmental impact assessments.

The way forward

The developed modelling framework could be used for environmental impact assessment of proposed new technologies such as propulsion and alternative fuels, where the impact of higher cruising altitudes and chemistry associated with nitrate aerosols would have to be carefully evaluated. Also, emissions from rockets that deliver satellites to Earth's orbit should be taken into account in any new scenario runs. Model evaluation should be a routine and continuous activity using all available satellite and in situ observations.

ELECTRIC STRUCTURE OF MULTIPLE CG FLASHES OBTAINED FROM THE LLDN RECORDINGS DURING THUNDERSTORMS IN THE WARSAW REGION IN MAY–SEPTEMBER 2018

P. Barański, M. Kubicki

In the present work we analyze the E-field signatures of multiple flashes obtained from the Local Lightning Detection Network (LLDN) shown in Fig. 1.

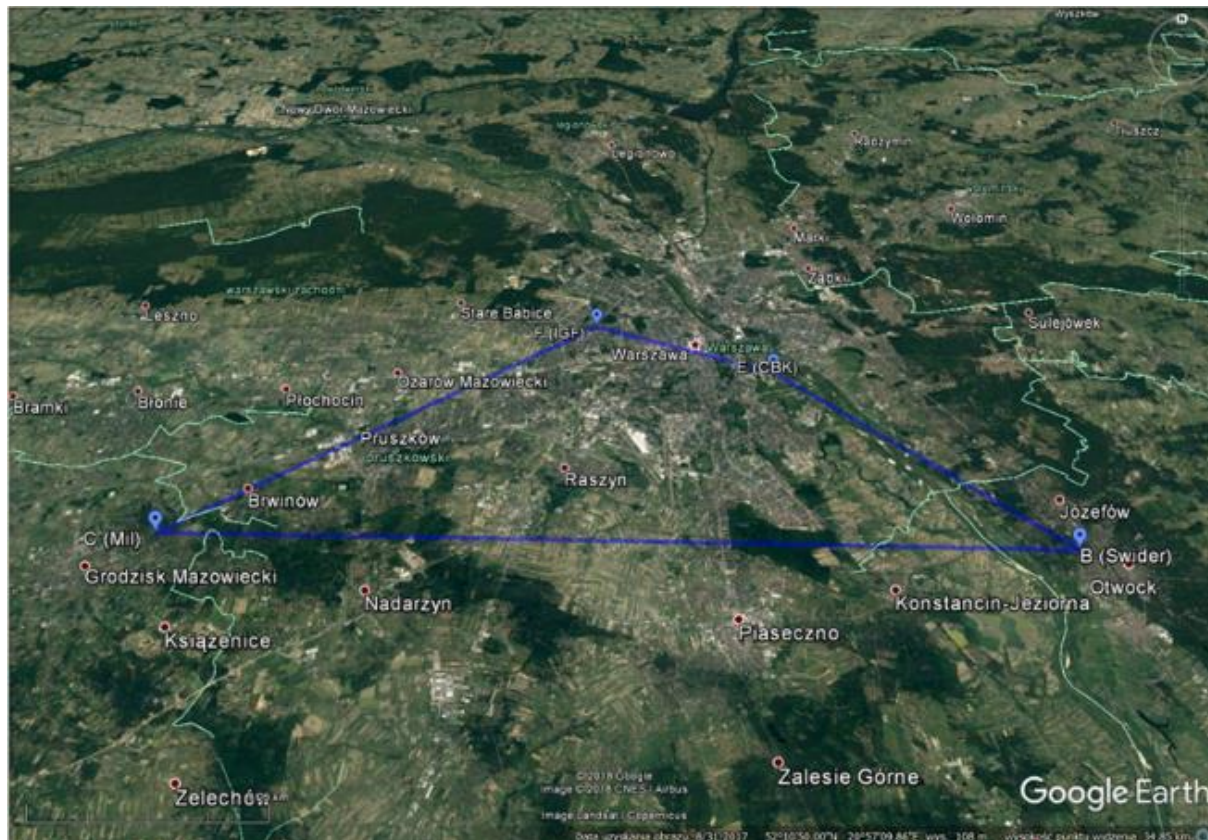


Fig. 1. The LLDN configuration during the field measurement campaign in 2018. The distances between particular LLDN stations are: LLDN-C(Milanówek)-LLDN-F(IGF) – 23 km, LLDN-F(IGF)-LLDN-E(CBK) – 9.4 km, LLDN-E(CBK)-LLDN-B(Świder) – 16 km, LLDN-C(Milanówek)-LLDN-B(Świder) – 39.1 km.

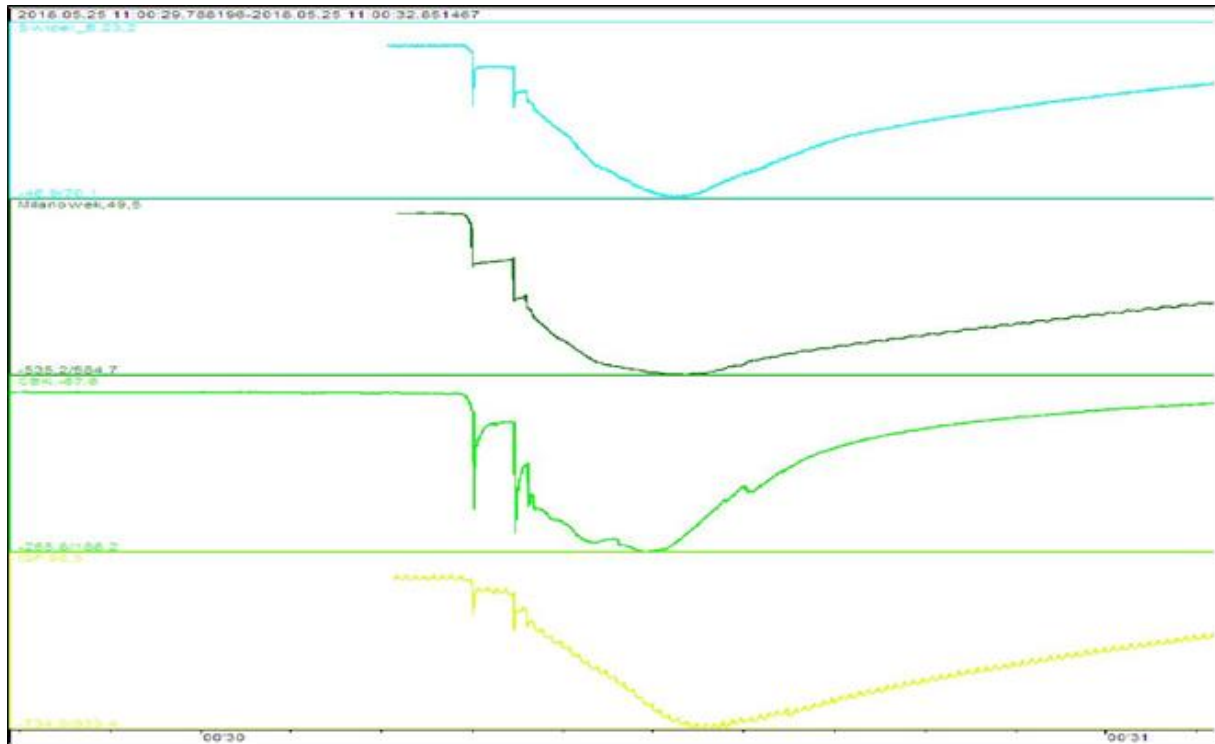


Fig. 2. E-field signatures of multiple negative CG (cloud-ground) flash simultaneously recorded by four LLDN stations. The multiple CG flash was recorded at 11:00:30 UT, consisted of three return strokes, and ended with continuing current stage; this flash lasted 0.21 s.

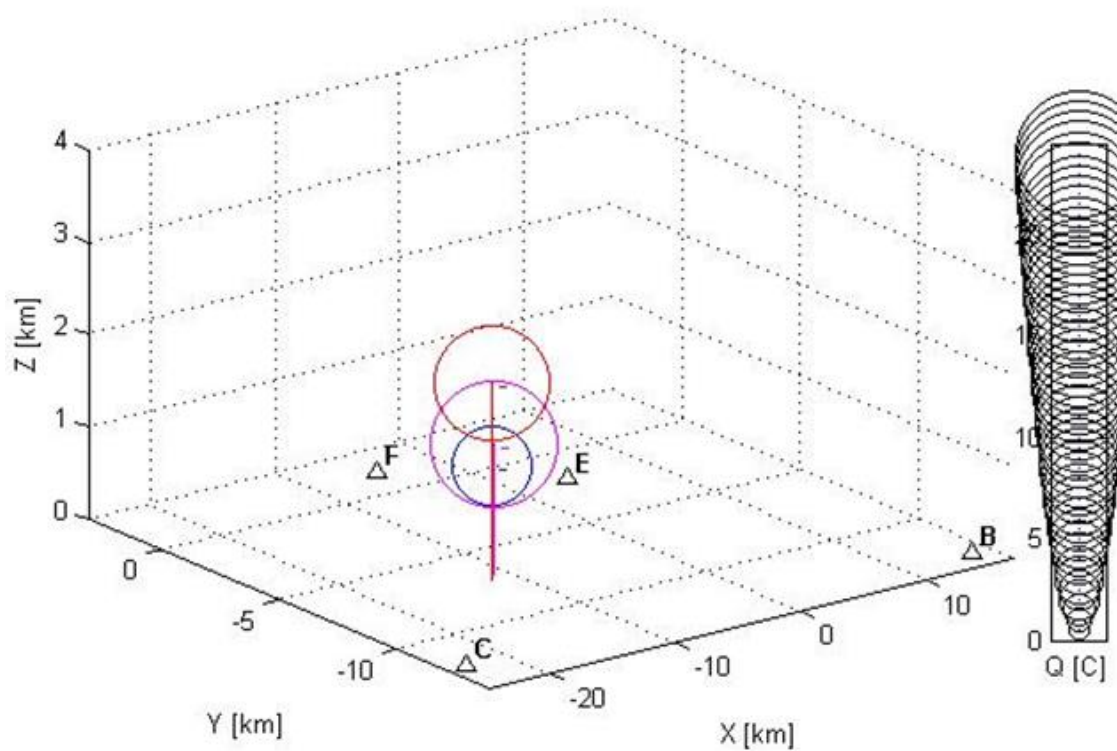


Fig. 3. The (x, y, z, Q) parameters for 3 return strokes involved in multiple CG (cloud-ground) flash recorded at 11:00:30 UT; the first stroke is marked by red color, the second by magenta color, and the third one by blue color. These strokes discharged a total electric charge equal to -51.5 C in a thundercloud.

The lightning data delivered by the LLDN can be used in the post-time processing for reliable evaluation of the electric structure of multiple CG flashes by giving their important stroke parameters, i.e., the exact time occurrence up to 1 μ s (Fig. 2), 3D location (Fig. 3), and the amount of electric charge discharged by the particular stroke. On the other hand, the E-field signatures of such flashes that are recorded in the radio VLF range and are archived in the recorder memory buffer and are covering the all-time development of the considered cloud-ground (CG) lightning discharges, i.e., from the early preliminary breakdown, the stepped leader stage and the return stroke sequence with ending continuing current phase. Such comprehensive presentation and documentation of these CG lightning events cannot be obtained from any lightning location systems routinely operated on a large scale in Poland, e.g., Polish PERUN or German LINET. It is worth noting that the LLDN lightning data superimposed at the same time on the PCAPPI and VCUT radar maps can indicate these thundercloud regions that are favorable for the initiation of multiple CG flashes. Any kind of supplementary lightning data connected with initiation of multiple CG flashes is very desired to ensure relevant lightning protection of the urban high-rise buildings, especially in the Warsaw region.

SHALE GAS EXPLORATION AND EXPLOITATION INDUCED RISKS

J. Jarosławski, I. Pawlak, J. Guzikowski

Measurements results of the concentration of selected air pollutants in the vicinity of the shale gas wells area near Wysin site, Pomerania (Fig. 1) collected during the realization of the SHEER project were analyzed in order to detect and estimate the impact of processes related to the exploration and exploitation of shale gas deposits on ambient air quality. The measurements were carried out before, during, and after the key stages of exploration: preparation for hydro-fracturing, hydro-fracturing and final works related to closing the wells and cleaning up the area. Continuous monitoring was made of the concentration of a number of pollutants important from the point of view of various aspects of the potential impact of exploration/exploitation activities related to shale gas: primary and secondary communication pollutants (nitrogen oxides, carbon monoxide, carbon dioxide, particulate matter PM₁₀, ozone) and pollutants that could be directly emitted from the wells (methane, non-methane hydrocarbons, radon). The measurements were carried out using a mobile air pollution monitoring station with the standard equipment used in air pollution monitoring networks. The station was placed approximately 1000 m from the boreholes, taking into account the prevailing wind direction, in the nearest village.



Fig. 1. Shale gas exploration site in Wysin, Poland, with a visible gas flare. Photo by J. Jarosławski (after Jarosławski et al. 2022).

Analysis of the obtained measurement results leads to the conclusion that the presence of individual shale gas wells does not have a significant impact on the ambient air quality in close proximity (at distances of the order of 1000 m). Concentrations of all types of pollutants measured during the experiment remained at background levels for a significant majority of measurement time. Air quality criteria have been met for all investigated pollutants, except particulate matter and surface ozone. The few episodes when limit values have been exceeded (in the case of particulate matter and ozone) were associated with larger-scale air pollution events. Slight increases in concentration of the communication type of pollutants were observed during periods of increased activity on the well, especially during hydro-fracturing. No elevated methane concentrations were observed except for several short-term episodes of methane and non-methane hydrocarbons concentrations associated with the outflow of methane from wells during the performance of operating procedures just after the hydrofracturing phase.

References

Jarosławski, J., I. Pawlak, J. Guzikowski, and A. Pietruczuk (2022), Impact of shale gas exploration and exploitation activities on the quality of ambient air—the case study of Wysin, Poland, *Atmosphere* **13**, 8, 1228, DOI: 10.3390/atmos13081228.

MEASUREMENTS OF AEROSOL PROPERTIES DURING CAMPAIGNS IN POLAND AND SVALBARD

M. Posyniak

The planetary boundary layer is the lowest part of the atmosphere that is directly influenced by its contact with the Earth's surface. Atmospheric aerosols are minute particles suspended in the atmosphere, which are created both naturally and as a result of human activity.

In the beginning of 2018 we made a field experiment on the Szyndzielnia Mountain in Bielsko-Biała (Fig. 1). The aim of field measurements was the examination of the development of the planetary boundary layer and absorbing aerosols optical and microphysical properties. We are using devices collecting samples of the air and instruments performing remote measurements (using scattered laser light). Within the framework of this project it is proposed to develop vertical profiling of atmospheric aerosols properties by placing measuring set on a cable car. Figure 2 shows an example of collected data. Higher concentrations of PM₁₀ and BC

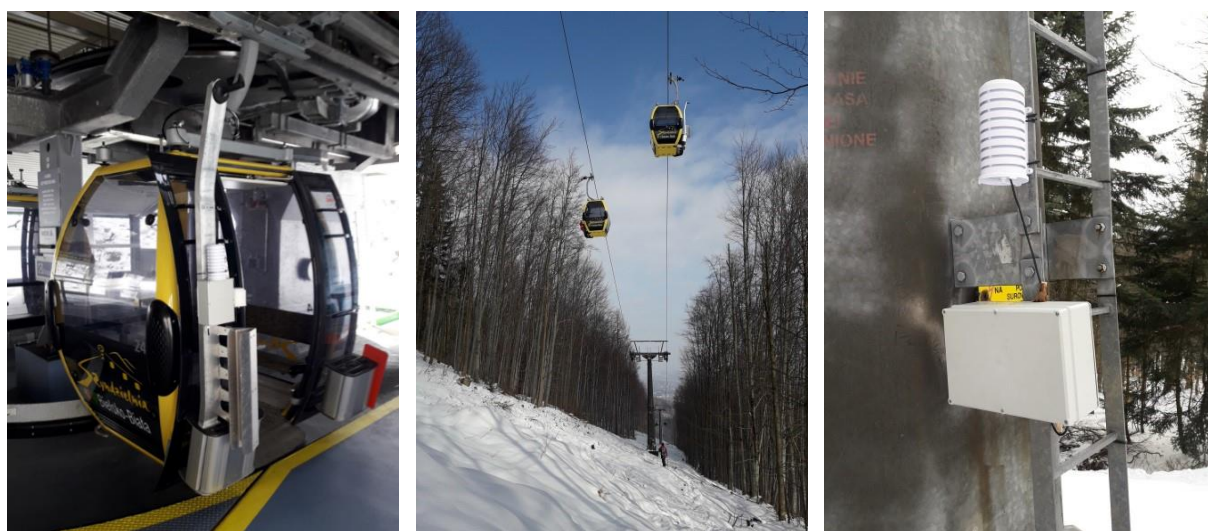


Fig. 1. Equipment on the Szyndzielnia cable car (left, center) and pillars (right). Photos by M. Posyniak.

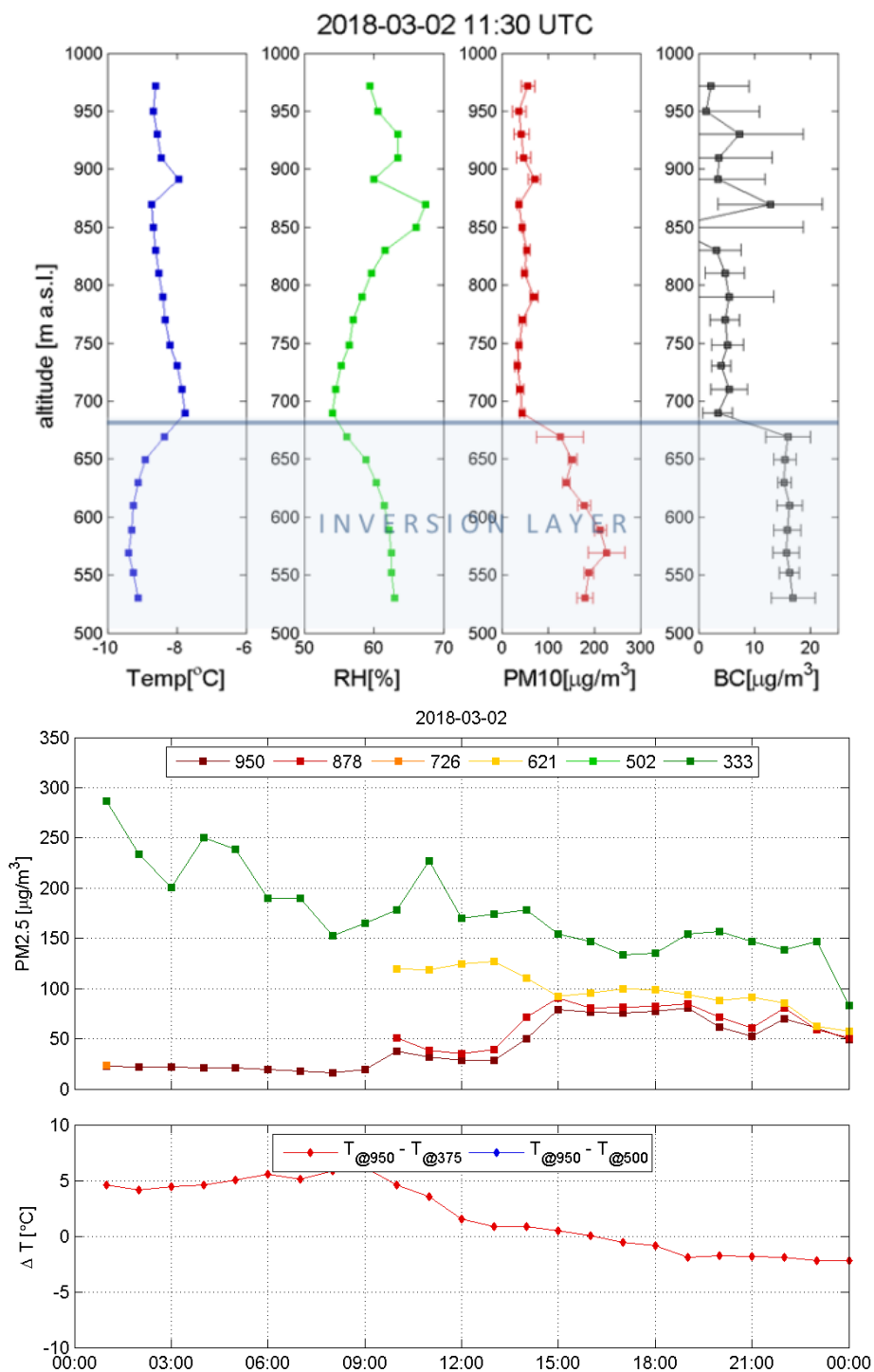


Fig. 2. Results from cable car measurements on 2 March 2018.

are observed below 700 m a.s.l. on 2 March 2018. This is related to temperature inversion. Numerical models, used for carrying out computer simulations of physical processes in the atmosphere, will also be applied.

The fieldwork was done in Hornsund from 30 August to 16 September 2018 to enrich the ongoing monitoring of aerosol properties. The set of aerosol particle counters (TSI 3330 and 3910) was installed in “environmental laboratory” in the vicinity of the Polish Polar Station Hornsund (Fig. 3). Additional service works among currently operating equipment were also made.



Fig. 3. Environmental laboratory in Hornsund: visible air inlet on the roof (left) and equipment inside (right). Photos by M. Posyniak.

INTERCOMPARISON OF UV METERS IN NY-ALESUND IN APRIL 2018

P. Sobolewski

There are a few sites in Svalbard where surface UV radiation has been regularly observed. The length of the UV data sets taken at Ny-Ålesund and Hornsund exceeds 20 years. This led to the idea of uniting the efforts of different research teams in the UV irradiance studies and integration of the existing Svalbard stations in a network that would be able to provide more compre-



Fig. 1. UV meters participating in the UV-ICARE inter-comparison campaign. Instruments, from left to right: UV-RAD, GUV, UVS-E-T of IG-PAS, UVS-E-T of USB (top panel). Comparison of the dark current effect by covering the meters with hats (bottom panel) (after Petkov et al. 2019).

hensive information for scientists working on climatic and biological issues in the Arctic and for validation of satellite data.

The UV Intercomparison and Integration in a High Arctic Environment (UV-ICARE) project (RIS 10871, <https://www.researchinsvalbard.no/project/8626>) was aimed to make the first step toward the creation of such a network starting with an intercomparison of the instruments carried out from 17 to 23 April (Fig. 1). Considering the Brewer spectrophotometer as a reference instrument it was found that the values of erythemal weighted solar UV irradiances provided by different devices agree with each other within 3% for solar zenith angles (SZA) less than 75° , 5% for $75^\circ < \text{SZA} < 80^\circ$, and 7–10% for $\text{SZA} > 80^\circ$. As regard the ozone column measurements the GUV, UV-RAD and Brewer radiometers showed less than 3% differences to each other.

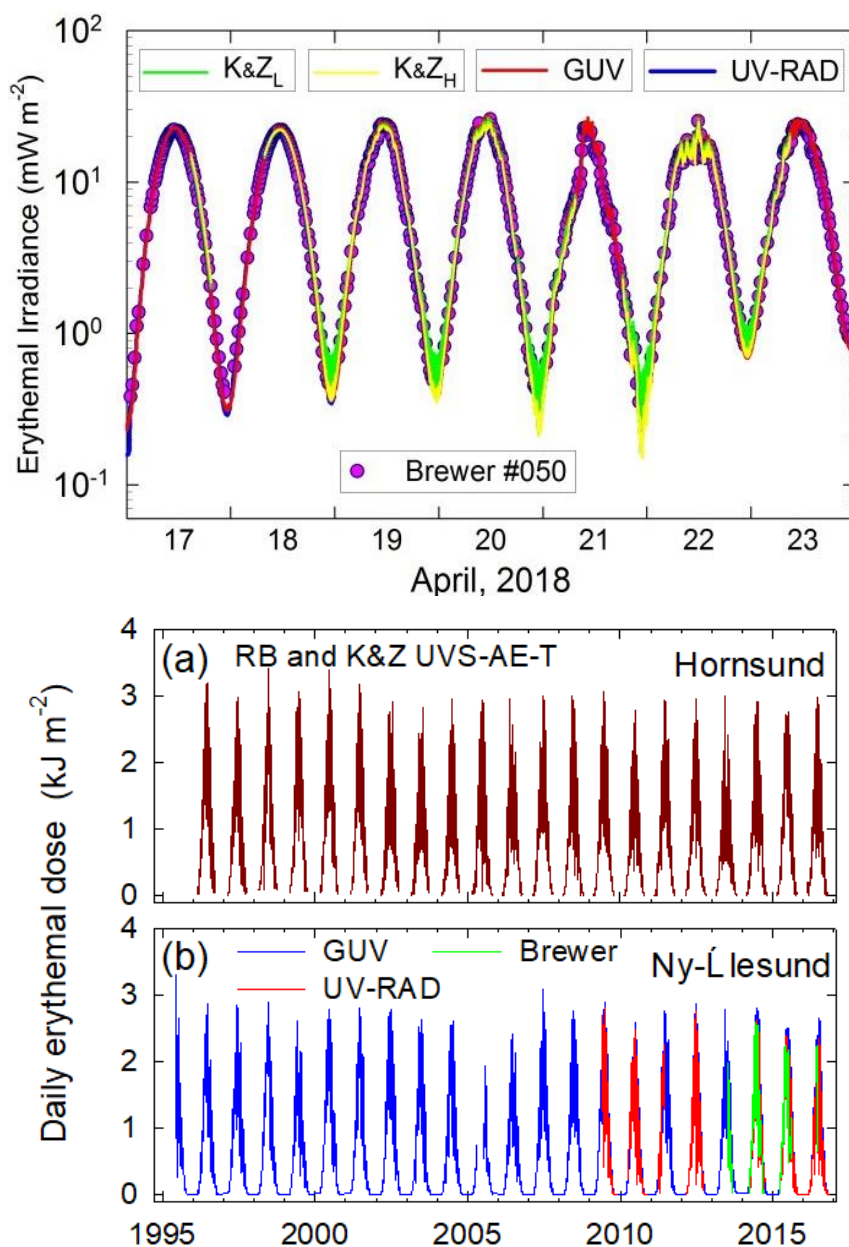


Fig. 2. Results of the comparison of all four instruments (top panel), and long period UV data sets (1996–2018) for the Polish Polar Station Hornsund and Ny-Ålesund (bottom panel) (after Petkov et al. 2019).

Such results were considered to demonstrate a good consent among the different devices bearing in mind that they are characterised with quite different spectral selection technique and electronic equipment.

Intercomparison started on 17 April, at 14:58 UT. The UVS-E-T instruments were stored in the same data logger and had to be read out regularly to be stored on a PC. The correction factor for the instrument of IG PAS has been calculated, and after applying it, we achieved very good agreement between all the UV meters (Fig. 2).

References

Petkov, B.H., V. Vitale, G.H. Hansen, T.M. Svendby, P.S. Sobolewski, K. Laska, J. Elster, A. Viola, M. Mazzola, and A. Lupi (2019), Observations of the solar UV irradiance and ozone column at Svalbard. **In:** *SESS Report 2018, The State of Environmental Science in Svalbard – An Annual Report*, Ch. 8, Svalbard Integrated Arctic Earth Observing System, Longyearbyen, 170–183.

MONITORING OF TOTAL OZONE AMOUNT IN THE ATMOSPHERE AND UV-B RADIATION AT CENTRAL GEOPHYSICAL LABORATORY IG PAS IN 2018

I. Pawlak, P. Sobolewski, J. Wink, J. Borkowski, J. Krzyścin, J. Jarosławski, A. Pietruczuk
Monitoring of total ozone content and its vertical profile in the atmosphere (by the Dobson and the Brewer spectrophotometers), and UV-B radiation (UV spectra by the Brewer spectrophotometer, erythemally weighted irradiance by various broad-band biometers) at the Belsk Observatory have been carried for many years: ozone since March 1963, UV since May 1975 (Fig. 1). The staff of the observatory put many efforts to have the data calibrated and homogenized, thus proper for the long-term analyses. The same is also applied to the data collected in 2018.

The monthly mean values of total ozone in 2018 were slightly lower than the long-term average (1963–2017) for several months April–September with a maximum decline of 7% in April. The values above the norm were found in winter and autumn. Sunny conditions appeared frequently in spring and summer in 2018 moving the monthly mean erythemal doses high above the norm for that period. The highest increase, of about 30%, was found in April and about 10–20% in August and September. The yearly dose was also ~4% above the 2000–2017 norm. For 28 days in 2018, the maximum daily intensity of UV radiation could be classified as very high according to World Health Organization (WHO) classification. For such days, people should follow special scenarios of outdoor activities to limit UV overexposure. In 2018, IG PAS released forecast of the daily course of UV index (between April and October) to inform the public of excessive UV radiation.



Fig. 1. Measuring equipment at the Belsk Observatory. From the left: Dobson spectrophotometer, Brewer spectrophotometer, UV-S-AE-T, Kipp & Zonen meter. Photos by P. Sobolewski.

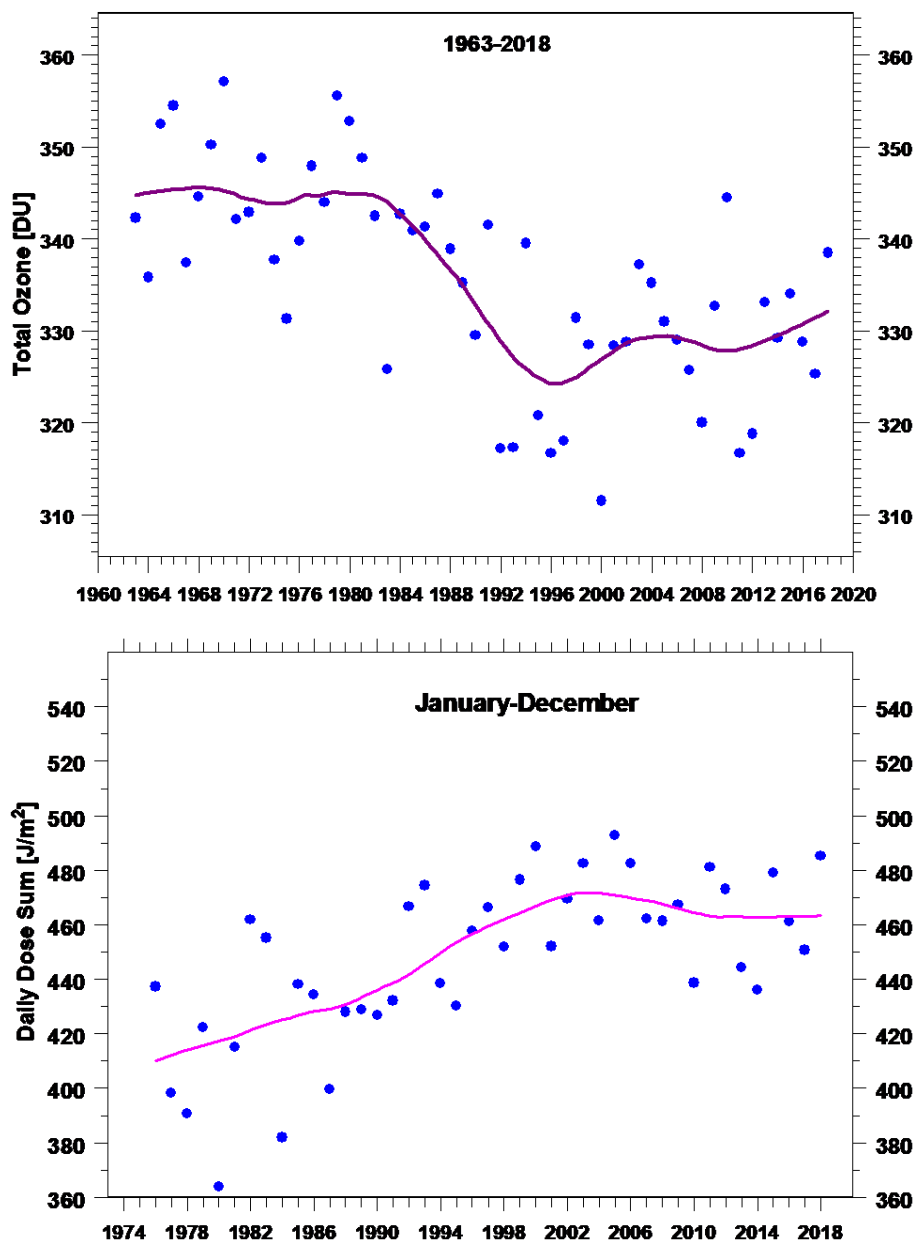


Fig. 2. Yearly means (in Dobson units) of total ozone at Belsk for the period 1963–2018 (top panel) and yearly dose of erythemal irradiance (in kJ/m^2) for the period 1976–2018 (bottom panel). Continuous curves show the smoothed pattern.

Time series of UV and ozone measurements at Belsk are among the longest series in the world; thus, they are appropriate for analyses of the long-term trends somewhat related to climate changes. Figure 2 illustrates the yearly pattern of the total ozone and erythemal dose. The declining tendency in total ozone for the period 1980–1996 and the corresponding increase in the UV radiation are apparent. A slight increase of total ozone is seen in the XXI century. This is called the ozone recovery due to less contamination of the stratosphere by ozone destructive chemicals that was forced by an international agreement – the Montreal Protocol signed by UN countries in 1987. The UV level seems to be stabilized in the XXI century as a superposition of the cloud/aerosols/ozone effects. More detailed analyses of the stratospheric ozone and the surface UV variability at Belsk in a global perspective are the subject of other activities of the Department of the Atmosphere Physics.

OCEANIC WARM LAYER VARIABILITY IN THE BAY OF BENGAL DURING INDIAN MONSOON.

D. Baranowski

Interactions between the atmosphere and the ocean play an important role in the development and evolution of the summer monsoon in the Bay of Bengal (BoB). Convective cloud systems that form over the BoB's warm waters bring rainfall to the Indian subcontinent during the summer monsoon season. The amount of energy available for the development of the convective systems is highly dependent on the sea surface temperature (SST).

Surface warm layers in the ocean are relatively thin (~5 m) and short-lived (~8 h), and often develop at the ocean surface during the daytime through solar heating and increased SST. Persistent neglect of this layer in weather forecast models results in underestimation of the net energy flux from the ocean to the atmosphere, which may lead to biases in monsoon precipitation patterns. Although it plays an important role throughout many stages of convective development, diurnal warm layers are rarely directly measured and their spatial and temporal variability and dependence on the environmental conditions is poorly understood. The existence of warm layers is challenging for numerical weather and climate predictions, especially on subseasonal to seasonal time scales. The numerical framework not only must consist of coupled atmosphere-ocean models, the oceanic component needs sufficient vertical resolution in the upper ocean (~1 m) and coupling needs to be performed frequently (timescale of less than 1 h). All those requirements tremendously increase the costs of simulations.



Fig. 1. Kongsberg seaglider onboard R/V Sindhu Sathana BoBBLE cruise (2016) during self-tests prior to launch. Photo by D. Baranowski.

During the Bay of Bengal Boundary Layer Experiment (BoBBLE) 5 gliders (Fig. 1) were deployed to measure upper ocean properties at high resolution across the BoB in July 2016. This dataset provides a unique insight into warm layer development, evolution and decay as well as its spatial and temporal variability and dependence on varying environmental conditions. Time series from the 5 individual platforms show clear variability of warm layer characteristics. In this presentation, dependence on atmospheric (surface wind speed, solar insolation and precipitation) and oceanic (stratification and currents) conditions on warm layer evolution will be addressed based on observations from those platforms. Further insight into warm layer occurrence and its spatial and temporal variability has been gained by high resolution simulations with KPP ocean model set up to represent conditions during the BoBBLE experiment. Our results indicate that although warm layer formation is primarily forced by atmospheric conditions, its characteristics (e.g. amplitude of SST anomaly) depend on states of both atmosphere (wind speed and insolation) and ocean (stratification and currents).

DYNAMICAL PRECURSORS OF FLOODS IN SUMATRA – METEOROLOGY AND SOCIAL MEDIA

D. Baranowski, B. Latos

The Maritime Continent is an archipelago within Indo-Pacific warm pool characterized by the largest precipitation amount, globally. Such environmental conditions combined with complex topography make it favorable for extreme precipitation events and its adverse effects such as floods and mudslides.

Extreme precipitation events not only disrupt affected communities but also enhance communications related to those events. These communications include television coverage and journal articles but also social media. Given the popularity of Twitter in Indonesia, extreme weather events cause spikes in communication done using this platform as well. Such spikes in a number of Twitter posts related to flooding are analyzed and attributed to individual events over Sumatra, an equatorial island in the western part of the archipelago. These data are combined with satellite remote sensing data about precipitation (GPM satellite) and outgoing longwave radiation, which is a measure of the strength of atmospheric convection (Meteosat 7 and Himawari 8 geostationary satellites). Therefore, crowd-sourced, local measures of how an event was disruptive for a local community can be analyzed in the context of local atmospheric forcing – precipitation over an affected region, as well as larger-scale atmospheric circulation.

We present an analysis of Twitter-based flooding events in relation to seasonal, intra-seasonal and synoptic-scale variability in the atmospheric circulation. Seasonal circulation is due to monsoon, intraseasonal (30–90 days periodicity) is related to the Madden-Julian Oscillations (MJO) and synoptic-scale variability is represented by the activity of equatorial waves, primarily convectively coupled Kelvin waves (CCKW). Because both MJO and CCKWs propagate eastward from the Indian Ocean towards Indonesia, it makes Sumatra an ideal candidate for such a study.

The results show that all major flooding events are preceded by extreme 5-day precipitation accumulation. Such accumulation often occurs during prolonged periods of above normal precipitation over the island, typical for active monsoon or MJO conditions. However, many flooding events are actually triggered by synoptic-scale CCWs embedded in those large-scale circulations. In some cases, even CCKW events can trigger flooding by themselves. Since CCKWs affecting Sumatra are often initiated over the central Indian Ocean, there is potentially extended range predictability of such events, which may enable early warning for to-be-affected communities by various channels, including social media.

Further investigation will be conducted during ELO field campaign in 2019. Two Seagliders will be deployed in the ocean to measure diurnal variation in temperature and salinity during 4-months long deployment. Atmospheric measurements near Padang (western Sumatra) will be conducted using enhanced upper soundings and surface radars.

3.6 Seminars and teaching

Seminars and lecture outside of the IG PAS:

- D. Baranowski, Atmospheric convectively coupled Kelvin waves over Indian Ocean and Maritime Continent Past, Present and Future, University of East Anglia, Norwich, UK, Seminar.

3.7 Completed PhD thesis defense

- J. Guzikowski, Modelling solar UV exposure for purpose of public health, Supervisor: J. Krzyściński;
- A. Szkop, Identification of aerosols source regions based on measured aerosols physical characteristics and backward air mass trajectories, Supervisor: A. Pietruczuk;

- M. Kossakowska, Modelling the impact of the aircraft on dynamic processes in the upper troposphere and the lower stratosphere, Supervisor: J. Kamiński.

3.8 Visiting scientists

- Prof. Earle R. Williams, Massachusetts Institute of Technology Cambridge, Cambridge, USA, 12–13.11.2018.
- Prof. Richard Menard, Environment and Climate Change, Montreal, Canada, October 2018.

3.9 Meetings, workshops, conferences, and symposia

Presentations of the Department's members:

ICAE 2018, Nara City, Nara, Japan, 17–22 June 2018

- P. Barański, J. Guzikowski, M. Kubicki, M. Morawski, A. Skrzyński, Dynamic and electric charge structure of thunderclouds obtained from the WRF_ELEC model and related to electric field signatures of lightning strokes recorded by the Local Lightning Detection Network in the Warsaw region during thunderstorm season in 2017, Poster;
- G. Karnas, G. Masłowski, P. Barański, Designation of the M-component characteristics in time and time-frequency domain on the basis of cloud-to-ground flash electric field signatures recorded by the new autonomous detection station in Rzeszów, Poster;
- M. Kubicki, M. Gołkowski, On the number of lightning discharges from the GLD 360 network and the atmospheric electric field E_z in polar and middle latitude regions, Poster.

34th International Conference on Lightning Protection (ICLP), Rzeszów, Poland, 2–7 September 2018

- G. Karnas, G. Masłowski, P. Barański, Automated discrimination of lightning stepped leader stage from the power spectrum density of the related electric field recordings, Poster.

Polar Symposium, Poznań, Poland, 7-10 June 2018

- M. Kubicki, A. Odzimek, Preliminary analysis of measurements taken in Polish Polar Station in Hornsund (Spitsbergen), Poster.

Seminar on Polar Climatology and Meteorology, Sosnowiec, Poland, 11–12 May 2018

- A. Odzimek, Polar regions in the Earth's global atmospheric electric circuit, Poster.

EGU General Assembly, Vienna, Austria, 7–13 April 2018

- D. Baranowski, Equatorial Line Observations (ELO): a comprehensive study of coupled atmospheric and oceanic processes within the Maritime Continent, Oral;
- J.A. Lopez et al. including J. Jarosławski, Induced seismicity response of hydraulic fracturing: results of a multidisciplinary monitoring at the Wysin site, Poland, Oral;
- J. Jarosławski, I. Pawlak, Analysis of impact of the shale gas exploration and exploitation activities on the quality of ambient air – case study of Wysin, Poland, Oral;
- J. Kamiński, M. Kossakowska, Potential impact of aviation emissions on chemical composition of the UTLS and global circulation – GEM-AC model simulations, Poster;
- J. Kamiński, Impact of electromobility development on air quality in Poland; Poster.

1st International Conference on Tropical Meteorology and Atmospheric Sciences, Bandung, Indonesia, 18–20 September 2018

- B. Latos, D. Baranowski, Equatorial Line Observations: predicting floods in Sumatra using crowdsourcing, tweeter, newspapers and meteorology, Oral.

Ny-Ålesund Atmosphere Flagship open workshop, Potsdam, Germany, 15–19 October 2018

- P. Sobolewski, J. Krzyściń, M. Posyniak, UV Observations at the Polish Polar Station Hornsund in 2018, Oral.

Workshop on Changes of the Polar Ecosystem 19. výroční zasedání Polární sekce České geografické společnosti, Malá Skála, Czech Republic, 7–9 November 2018

- P. Sobolewski, J. Krzyściń, M. Posyniak, Comparison of UV meters in Ny-Alesund and Observations at Hornsund in 2018, Oral;
- J. Krzyściń, Recovery of column amount of ozone based on multi-sensor reanalysis data for the period 1979-2017, Oral.

Jubileusz 65-lecia Instytutu Geofizyki PAN, Warsaw, Poland, 29 May 2018

- J. Krzyściń, Foto-dermatologia-ostatnie osiągnięcia ZFA, Oral.

Complex Atmospheric Monitoring and Research, Tatranska Lomnica, Slovakia, 11–13 June 2018

- J. Krzyściń, Total ozone trends from 1979 to 2017 over Central Europe derived from satellite data, Oral.

II Conference “Hot” Topics Dermatology, Toruń, Poland, 12–14 April 2018

- P. Sobolewski, Physics in dermatology, Oral;
- J. Krzyściń, The “morning after pill” in dermatology, Oral.

78th Annual DGG meeting, Leoben, Austria, 12–15 February 2018

- S. Cesca et al. including J. Jarosławski, Results of a multidisciplinary monitoring of hydraulic fracturing stimulation in Poland, Oral.

European Conference on Solar UV Measurements, Vienna, Austria, 12–14 September 2018

- J. Krzyściń, Modelling and measurements of ground-based UV radiation at the Institute Geophysics PAS, Oral.

4th ACTRIS-2 General Meeting 2018, Nafplio, Greece, 17–19 April 2018

- A. Pietruczuk, A. Szkop, Synergy of ceilometer and photometer, GRASP retrievals at Racibórz, Poland, Oral.

3.10 Publications

ARTICLES

Guzikowski, J., J. Krzyściń, A. Czerwińska, and W. Raszewska (2018), Adequate vitamin D3 skin synthesis versus erythema risk in the Northern Hemisphere midlatitudes, *J. Photochem. Photobiol. B* **179**, 54–65, DOI: 10.1016/j.jphotobiol.2018.01.004.

López-Comino, J.A., et al., **J. Jarosławski,** S. Lasocki (2018), Induced seismicity response of hydraulic fracturing: results of a multidisciplinary monitoring at the Wysin site, Poland, *Sci. Rep.* **8**, 8653, DOI: 10.1038/s41598-018-26970-9.

- Lisok, J., et al., **J.W. Kamiński** (2018), Radiative impact of an extreme Arctic biomass-burning event, *Atmos. Chem. Phys.* **18**, 12, 8829–8848, DOI: 10.5194/acp-18-8829-2018.
- Vandaele, A.C., et al., **J. Kamiński** (2018), NOMAD, an integrated suite of three spectrometers for the ExoMars Trace Gas Mission: technical description, science objectives and expected performance, *Space Sci. Rev.* **214**, 80, DOI: 10.1007/s11214-018-0517-2.
- Krzyścin, J.W.**, et al., **P. Sobolewski, J. Guzikowski** (2018), Perspectives of UV nowcasting to monitor personal pro-health outdoor activities, *J. Photochem. Photobiol. B* **184**, 27–33, DOI: 10.1016/j.jphotobiol.2018.05.012.
- Krzyścin, J.W.**, and **P.S. Sobolewski** (2018), Trends in erythemal doses at the Polish Polar Station, Hornsund, Svalbard based on the homogenized measurements (1996–2016) and reconstructed data (1983–1995), *Atmos. Chem. Phys.* **18**, 1, 1–11, DOI: 10.5194/acp-18-1-2018.
- Chiliński, M.T., K.M. Markowicz, and **M. Kubicki** (2018), UAS as a support for atmospheric aerosols research: case study, *Pure Appl. Geophys.* **175**, 3325–3342, DOI: 10.1007/s00024-018-1767-3.
- Odzimek, A., P. Barański**, and A. Dziembowska (eds.) (2018a), Atmospheric electricity: commemorative publication in honor of Stanisław Michnowski on his 100-th birthday, *Publs. Inst. Geoph. PAS* **424 (D-74)**, 272 pp., DOI: 10.25171/InstGeoph_PAS_Publs-2018-085.
- Odzimek, A., P. Barański, M. Kubicki**, and **D. Jasinkiewicz** (2018b), Electrical signatures of Nimbostratus and Stratus clouds in ground-level vertical atmospheric electric field and current density at mid-latitude station Swider, Poland, *Atmos. Res.* **209**, 188–203, DOI: 10.1016/j.atmosres.2018.03.018.
- Kleimenova, N.G., **A. Odzimek, S. Michnowski**, and **M. Kubicki** (2018), Geomagnetic storms and substorms as space weather influence on atmospheric electric field variations, *Sun Geosph.* **13**, 1, 101–107, DOI: 10.31401/SunGeo.2018.01.14.
- Stachlewska, I.S., et al., **A. Pietruczuk, A. Szkop** (2018), Modification of local urban aerosol properties by long-range transport of biomass burning aerosol, *Remote Sens.* **10**, 3, 412, DOI: 10.3390/rs10030412.
- Petkov, B.H., et al., **P.S. Sobolewski** (2018), Altitude-temporal behaviour of atmospheric ozone, temperature and wind velocity observed at Svalbard, *Atmos. Res.* **207**, 100–110, DOI: 10.1016/j.atmosres.2018.03.005.

CHAPTERS

- Barański, P., J. Guzikowski, M. Kubicki**, M. Morawski, and **A. Skrzyński** (2018), Dynamic and electric charge structure of thunderclouds obtained from the WRF_ELEC model and related to electric field signatures of lightning strokes recorded by the local Lightning Detection Network in Warsaw region during thunderstorm season in 2017. **In:** *Proc. 16th Int. Conf. on Atmospheric Electricity ICAE 2018, Nara City, Nara, Japan, 17–22 June 2018.*

4. DEPARTMENT OF LITHOSPHERIC RESEARCH

Tomasz Janik and Working Group¹

4.1 About the Department

In the year 2018, works in the Department of the Lithospheric Research were continued in two general scientific tasks: "Structure and evolution of Central Europe's lithosphere with particular emphasis on the area of Poland" (NSL1) and "Structure and evolution of the northern Atlantic lithosphere in the contact zone of the Eurasian and North American plate in the Arctic and selected areas of Antarctica" (NSL2).

In the frame of the first task, the team was working on different stages of the projects: GEORIFT 2013 (Belarus–Ukraine), RomUkrSeis (Romania-Ukraine), TTZ-South (Poland–Ukraine), LUMP (Poland), and Sudetes (SW Poland). In the second task, the passive/active project KNIPAS (Knipovich Ridge) was implemented. A new active seismic project KNIPSEIS (Knipovich Ridge and Barents Sea) was started. Some projects were finalized by publication, others were in the process of preparing seismic sections, interpretation, modelling or preparing the publication. For others, field measurements were carried out. They are described in more detail later in the report. Apart from the above-mentioned projects, which we devoted the most attention to, we also dealt with other projects: KOKKY and ESO (Finland), BalTec (Baltic Sea), BASIC (Sweden), VRANCEA 2001 (Romania), and modelling of 3-D structure and anisotropy of the Earth crust in SE Poland. Materials from these projects will be subject to elaboration in subsequent years. Most of the projects are carried out in international or national cooperation. Final results of our projects consist of the geological/tectonic interpretation of experimental data collected in active and passive seismic experiments.

4.2 Personnel

Head of the Department

Tomasz Janik
Associate Professor

Professor

Aleksander Guterch

Associate Professor

Piotr Środa

Assistant Professors

Wojciech Czuba
Monika Bociarska

Research Assistants

Dariusz Wójcik

Technician

Edward Gaczyński
Jarosław Grzyb

¹ Working Group of the Department of Lithospheric Research: Monika Bociarska, Wojciech Czuba, Tomasz Janik, Julia Rewers, Piotr Środa, Dariusz Wójcik.

PhD Students

Julia Rewers, Poland; Piotr Środa – PhD supervisor

4.3 Main research projects

- Profile of deep seismic soundings TTZ-South, T. Janik, National Science Centre, 2017–2020;
- Determination of the seismic anisotropy of the lithosphere in the Lower Silesia area, P. Środa, National Science Centre, 2017–2020;
- Structure of the Knipovich Ridge on the basis of seismic surveys – KNIPSEIS, W. Czuba, National Science Centre, 2018–2021.

4.4 Instruments and facilities

Equipment

- 90 × TEXAN portable seismic recorders with 1C 4.5 Hz geophones,
- 60 × DATA-CUBE portable seismic recorders with 1C (60 pcs) and 3C (20 pcs) 4.5 Hz geophones,
- 10 × Güralp CMG-DM24S3EAM broadband seismic stations with CMG-6T 30 s seismometers,
- 4 × Ocean Bottom Seismometers, semi-broadband (Güralp),
- 20 × L-4C-3D 1 Hz seismometers,
- 6 × timing system devices (for shot time recording).

4.5 Research activity and results

Brief description/abstracts/summaries of some of the achievements of the Department's staff:

LITHOSPHERIC STRUCTURE ALONG WIDE-ANGLE SEISMIC PROFILE GEORIFT 2013 IN PRIPYAT–DNIEPER–DONETS BASIN (BELARUS AND UKRAINE)

GEORIFT 2013 Project

The GEORIFT 2013 (GR'13) WARR (wide-angle reflection and refraction) experiment was carried out in 2013 on the territory of Belarus and Ukraine in broad international cooperation. The aim of the work is to study the basin architecture and deep structure of the Pripyat-Dnieper-Donets Basin (PDDB), which is the deepest and best-studied Palaeozoic rift basin in Europe. The PDDB is located in the southern part of the East European Craton (EEC) and crosses Sarmatia—one of the three segments of the EEC. The PDDB was formed by Late Devonian rifting associated with domal basement uplift and magmatism.

The GR'13 extends in NW-SE direction along the PDDB strike and crosses the Pripyat Trough (PT) and Dnieper Graben (DG) separated by the Bragin Uplift (BU) of the basement. The field acquisition along the GR'13 (of 670 km total length) involved 14 shots and recorders deployed every ~2.2 km for several shot points (Fig. 1). The good quality of the data, with first arrivals visible up to 670 km for several shot points, allowed for construction of a velocity model extending to 80 km depth using ray-tracing modelling (Fig. 2). The thickness of the sediments ($V_p < 6.0 \text{ km s}^{-1}$) varies from 1–4 km in the PT, to ~5 km in the NW part of the DG, to 10–13 km in the SE part of the profile. Below the DG, at ~330–530 km distance, we observed an upwarping of the lower crust (with V_p of ~7.1 km s^{-1}) to ~25 km depth that represents a rift pillow or mantle underplate. The Moho shallows southeastwards from ~47 km in the PT to 40–38 km in the DG with mantle velocities of 8.35 and ~8.25 km s^{-1} in the PT and DG, respectively. A near-horizontal mantle discontinuity was found beneath BU (a transition zone

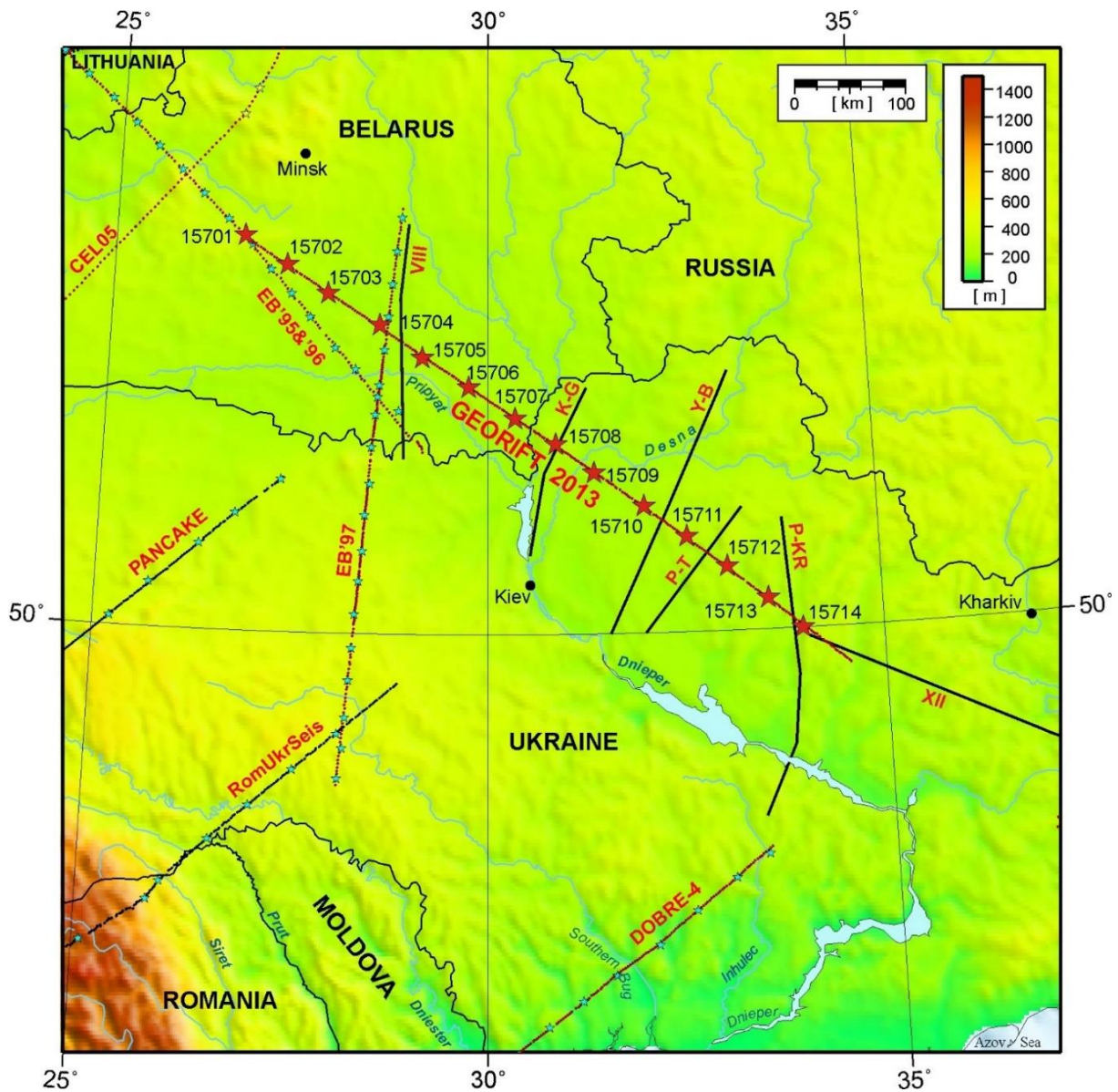


Fig. 1. Location of the composite GEORIFT 2013 profile and previous refraction seismic profiles in the study area. Stars represent shot points, dots – recording stations. Abbreviations of profiles: K-G – Kiev–Gomel, Y-B – Yagotyn–Baturin, P-T – Piryatyn–Talalaivka, P-KR – Putyvl–Kryviy Rig, XII – geotraverse XII (Poltava–Sverdlovsk), VIII – deep CDP line – all these lines represent main parts of the profiles.

from the PT to the DG) at the depth of 50–47 km. It dips to the depth of ~60 km at distances of 360–405 km, similar to the intersecting EUROBRIDGE'97 profile.

The crust and upper mantle structure on the GR'13 may reflect the varying intensity of rifting in the PDDB from a passive stage in the PT to active rifting in the DG. The absence of Moho uplift and relatively thick crystalline crust under the PT is explained by its tectonic position as a closing unit of the PDDB, with a gradual attenuation of rifting from the southeast to the northwest. The most active stage of rifting is evidenced in the DG by a shallower Moho and a presence of a rift pillow caused by mafic and ultramafic intrusions during the active phase. The junction of the PT and the DG (the BU) is located just at its intersection with the NS regional tectonic zone Odessa–Gomel. Most likely, the “blocking” effect of this zone did not allow for further propagation of active rifting to the NW.

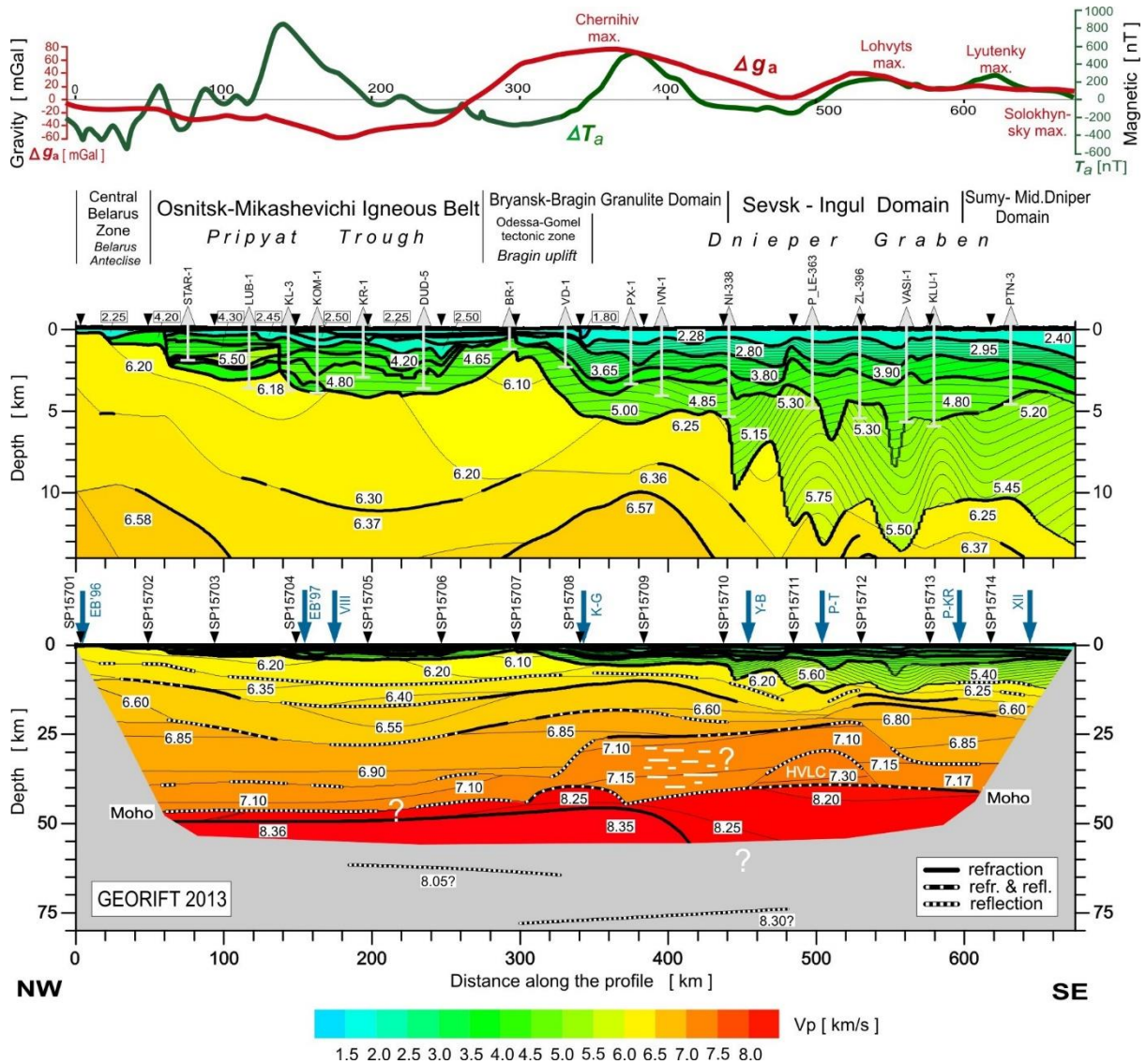


Fig. 2. Two-dimensional model of seismic P -wave velocity in the crust and upper mantle derived by forward ray-tracing modelling using the SEIS83 package (Červený and Pšenčík 1984) along the GEORIFT 2013 profile. Thick, black solid and dashed lines represent major velocity discontinuities (interfaces). Colours represent velocity isolines with values in km s^{-1} shown in white boxes. The position of tectonic units is indicated. Arrows show positions of shotpoints. Blue arrows show intersections with other profiles. Vertical exaggerations are $\sim 11:1$ for upper part of the model, and $\sim 2.4:1$ for the whole model. Bouguer gravity and total magnetic field anomalies along the profile are shown on top diagrams (Starostenko et al. 1986, Pashkevich et al. 2014).

Follow the final publication:

Starostenko, V., T. Janik, T. Yegorova, W. Czuba, P. Środa, D. Lysynchuk, R. Aizberg, R. Garetsky, G. Karataev, Y. Gribik, L. Farfuliak, K. Kolomiyets, V. Omelchenko, K. Komminaho, T. Tiira, D. Gryn, A. Guterch, O. Legostaeva, H. Thybo, and A. Tolkunov (2018), Lithospheric structure along wide-angle seismic profile GEORIFT 2013 in Pripyat-Dnieper-Donets Basin (Belarus and Ukraine), *Geophys. J. Int.* **212**, 3, 1932–1962, DOI: 10.1093/gji/ggx509.

References

- Červený, V., and I. Pšenčík (1984), SEIS83 – numerical modeling of seismic wave fields in 2-D laterally varying layered structures by the ray method. **In:** E.R. Engdahl (ed.), *Documentation of Earthquake Algorithms*, World Data Center A, Vol. 35, 36–40.
- Starostenko, V.I., V.G. Kozlenko, S.M. Oganessian, E.L. Shen, M.G. Oganessian, T.P. Yegorova, and G.V. Dyadura (1986), 3-D distribution of the density in the crust of the Dnieper Graben, *Geophys. J.* **8**, 3–19 (in Russian).
- Pashkevich, I.K., M.I. Orlyuk, and T.V. Lebed' (2014), Magnetic data, fault tectonics of consolidated earth crust and oil-and-gas content of the Dnieper-Donets avlakogen, *Geophys. J.* **36**, 1, 64–80, DOI: 10.24028/gzh.0203-3100.v36i1.2014.116150 (in Russian).

SEISMIC MODEL OF THE CRUST AND UPPER MANTLE ACROSS THE EASTERN CARPATHIANS – FROM THE APUSENI MOUNTAINS TO THE UKRAINIAN SHIELD RomUkrSeis Project

The RomUkrSeis profile is a controlled source wide-angle reflection and refraction (WARR) profile acquired in August 2014. It is 675 km long (Fig. 1), running roughly SW-NE from the Apuseni Mountains in Romania and the Transylvanian Basin behind the arc of the Eastern Carpathian orogen, crossing this and terminating in the East European Craton (EEC) in SW

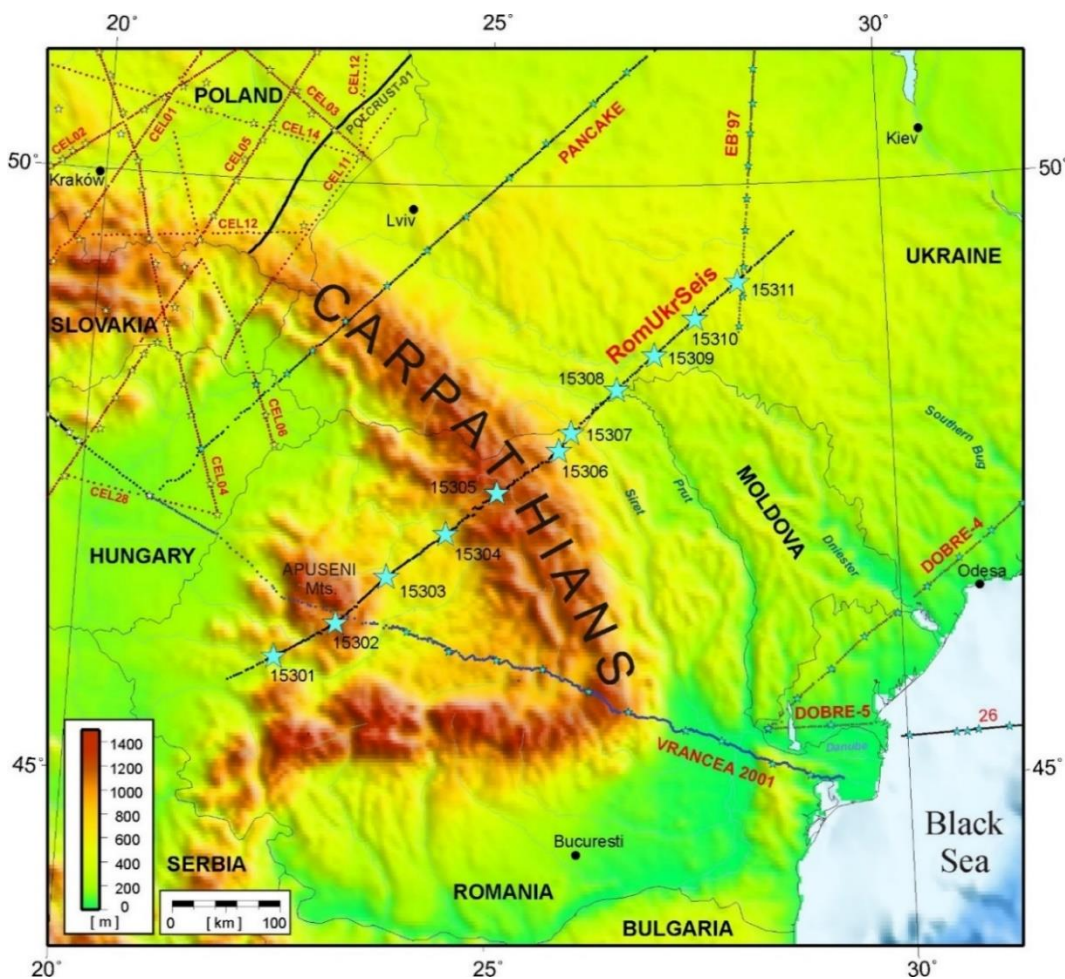


Fig. 1. Location of the composite of the RomUkrSeis profile and previous refraction seismic profiles in the study area. Stars represent shot points, dots – recording stations.

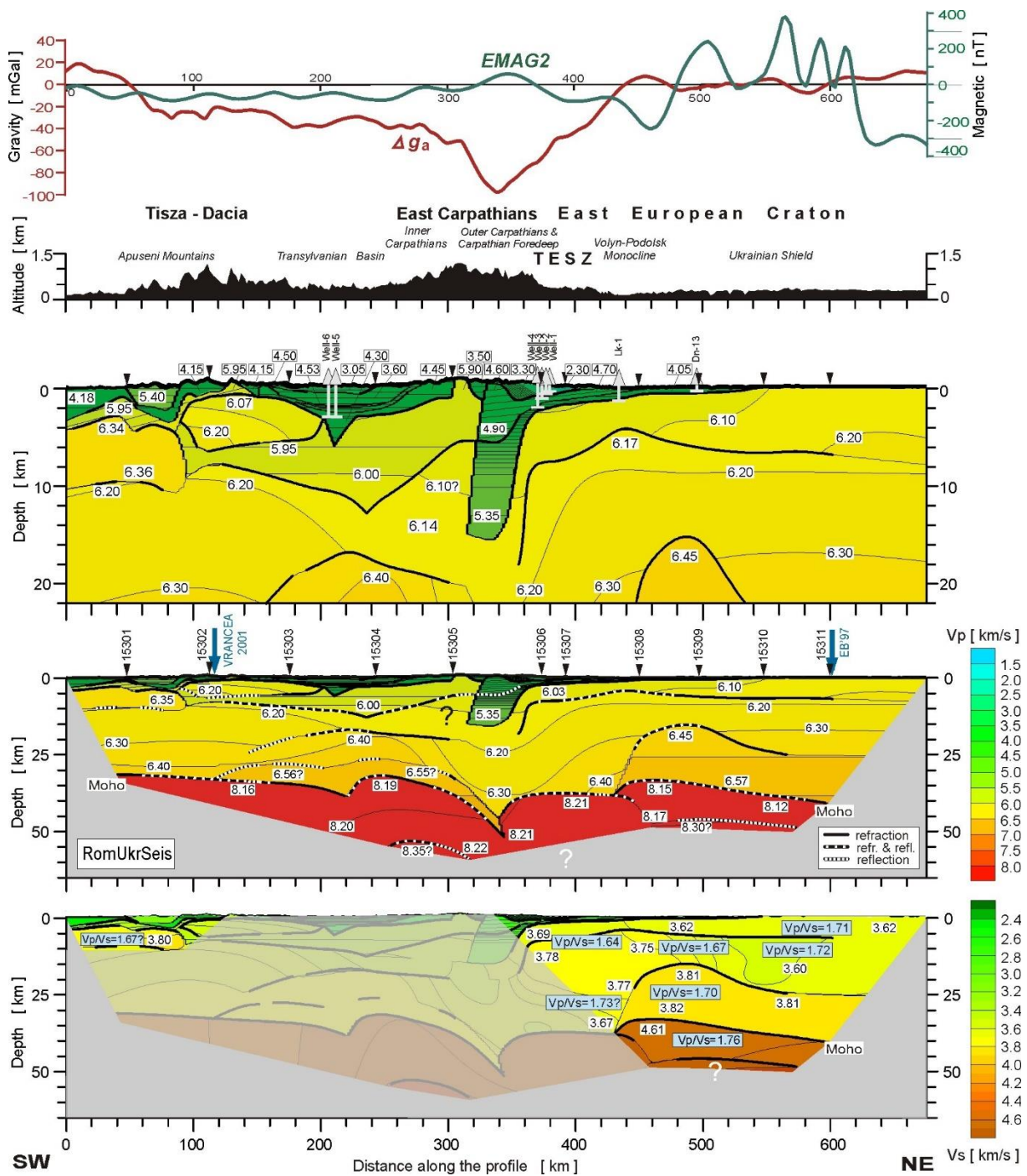


Fig. 2. Two-dimensional models of seismic P- and S-wave velocity in the crust and upper mantle derived by forward ray-tracing modelling using the SEIS83 package (Červený and Pšenčík 1984) along the RomUkrSeis profile. Thick, black solid and dashed lines represent major velocity discontinuities (interfaces). Only those parts of the discontinuities that have been constrained by reflected or refracted arrivals of P-waves are shown. Thin lines represent velocity isolines with values in km s^{-1} shown in white boxes. The position of tectonic units is indicated. Arrows show positions of shot points. Blue arrows show intersections with the other profiles. Abbreviations as on Fig. 1. Vertical exaggerations are $\sim 11:1$ for upper part of the model, and $\sim 2.4:1$ for the whole model. Bouguer gravity and total magnetic field anomalies along the profile are shown on top diagrams (Starostenko et al. 1986; Pashkevich et al. 2014). For the EEC, model of V_p/V_s ratio distribution is shown.

Ukraine. A well-constrained velocity model has been constructed along the RomUkrSeis profile from 350 single component seismic recorders and eleven shotpoints in a single deployment. The Eastern Carpathian arc and the complex tectonic processes that formed it in the Cenozoic have obscured the pre-existing Trans-European Suture Zone, which is the transition zone between the EEC and terranes accreted to its southwest in pre-Cenozoic (especially Palaeozoic) times.

The good quality of the data, with first arrivals visible up to 675 km for several shot points, allowed for construction of a velocity model extending to 50 km depth using ray-tracing modelling (Fig. 2). Relatively low velocities are determined throughout the whole crust along the RomUkrSeis profile. The velocities in the southwestern part of the model (beneath the Apuseni Mts. and the Transylvanian Basin) are comparable with those of the Pannonian Basin ($V_p < 6.6$ km/s) observed elsewhere while the crustal thickness is higher (>30 km). A high velocity body ($V_p \sim 6.36$ km/s) appears at depths of 3–12 km, its location corresponding to the surface expression of ophiolites in the Apuseni Mts. Immediately below this body, lower velocities are found. In the central part of the model, there is a large sedimentary wedge that comprises the Cenozoic Carpathian foreland itself as well as older sedimentary units. The wedge consists of two thick layers characterized by $V_p \sim 4.7$ and 5.35 km/s of ~ 30 km width, asymmetrically dipping to the SW and reaching a depth of ~ 15 km. Below it, up to a depth of 45 km, V_p value of ~ 6.3 km/s is determined. On the EEC side of the model, the velocities near the crustal base (to depths of 33–43 km) reach values $V_p \sim 6.6$ km/s. Strongly differentiated Moho depths are observed along the profile as a whole. Four segments can be identified from the southwest to the northeast, with depth variations from 32 to 50 km. Velocities below the Moho boundary are: 8.15–8.2 km/s and ~ 8.3 –8.35 km/s below a sub-Moho discontinuity in the uppermost mantle (at depths ~ 52 km in the central part of the profile and ~ 47 km in its northeastern part).

A comparative study of the RomUkrSeis profile and two other WARR profiles that cross the Eastern Carpathians, PANCAKE to the northwest and VRANCEA-2001 to the southeast, will illuminate important aspects of the relationship between the emplacement of the Carpathian arc and the earlier crustal architecture of this fundamental tectonic transition zone.

Follow the final publication:

Starostenko, V., T. Janik, V. Mocanu, R. Stephenson, T. Yegorova, T. Amashukeli, W. Czuba, P. Šroda, A. Murovskaya, K. Kolomiyets, D. Lysynchuk, J. Okoń, A. Dragut, V. Omelchenko, O. Legostaieva, D. Gryn, J. Mechie, and A. Tolkunov (2020), RomUkrSeis: Seismic model of the crust and upper mantle across the Eastern Carpathians – From the Apuseni Mountains to the Ukrainian Shield, *Tectonophysics* **794**, 228620, <https://doi.org/10.1016/j.tecto.2020.228620>.

References

- Červený, V., and I. Pšenčík (1984), SEIS83 – numerical modeling of seismic wave fields in 2-D laterally varying layered structures by the ray method. **In:** E.R. Engdahl (ed.), *Documentation of Earthquake Algorithms*, World Data Center A, Vol. 35, 36–40.
- Starostenko, V.I., V.G. Kozlenko, S.M. Oganessian, E.L. Shen, M.G. Oganessian, T.P. Yegorova, and G.V. Dyadura (1986), 3-D distribution of the density in the crust of the Dnieper Graben, *Geophys. J.* **8**, 3–19 (in Russian).
- Pashkevich, I.K., M.I. Orlyuk, and T.V. Lebed' (2014), Magnetic data, fault tectonics of consolidated earth crust and oil-and-gas content of the Dnieper-Donets avlakogen, *Geophys. J.* **36**, 1, 64–80, DOI: 10.24028/gzh.0203-3100.v36i1.2014.116150 (in Russian).

DEEP SEISMIC SOUNDINGS PROFILE TTZ-SOUTH

TTZ-South Project

In the period 7–14 September 2018, after over one year of logistical preparation, measurements of deep seismic soundings along the TTZ-South profile were carried out, extending the transect TTZ-CEL03 located along the Teisseyre–Tornquist Zone (TTZ). This profile is ~ 545 km long and runs in Poland (~240 km), partially overlapping the CEL03 profile, and in Western Ukraine (~ 300 km), to the border with Moldova (Fig. 1). The experiment was carried out by the teams of the Department of Seismic Research of the Lithosphere of the Institute of Geophysics PAS and the Institute of Geophysics of the National Academy of Sciences of Ukraine in cooperation with Geofizyka Toruń Sp. z o.o. and Ukrgeofizika, using also 150 seismic receivers from the GeoForschungsZentrum (GFZ) Potsdam equipment pool. Seismic energy was generated in

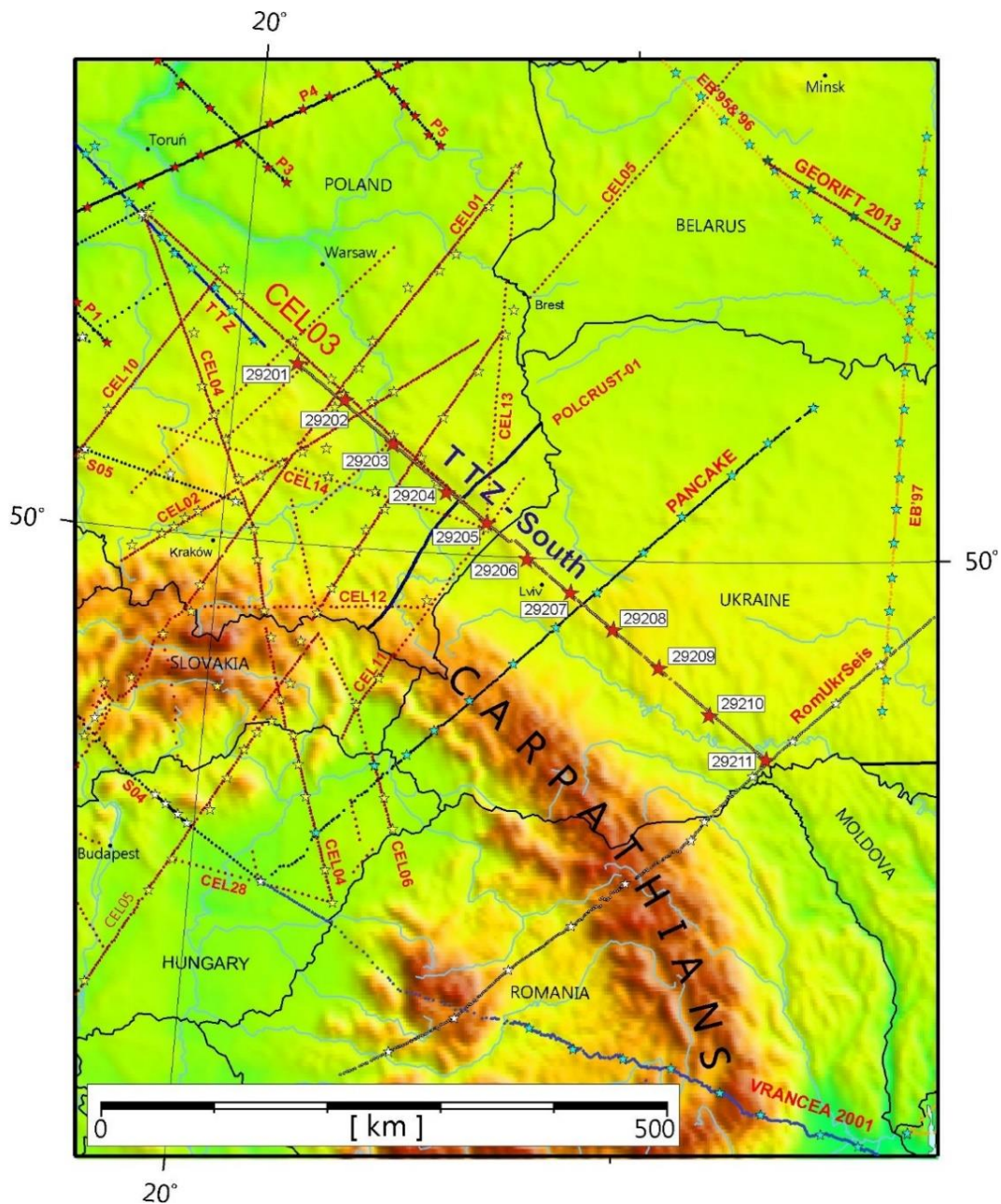


Fig. 1. Location of the composite of the TTZ-South profile and previous refraction seismic profiles in the study area. Stars represent shot points, dots – recording stations (after Janik et al. 2022).

eleven shot points using explosives (600–1000 kg TNT) placed in 20–30 m deep holes, deployed every 45–60 km along the profile. Seismic registrations were conducted by ~300 field seismic stations deployed along the profile every 2.5–3.5 km. The analysis of the experimental data obtained, carried out with the proven, modern interpretation methods (2D modelling), will be the basis for studies of the structure of the Earth's crust and the upper mantle.

The TTZ-South experiment aims at the determination of the structure along a seismic profile located in the region of southeastern Poland and western Ukraine, along the Teisseyre–Tornquist Zone (TTZ). Studies of the tectonic structure of this area are extremely important for the understanding of geodynamical processes which shaped the present structure of the lithosphere

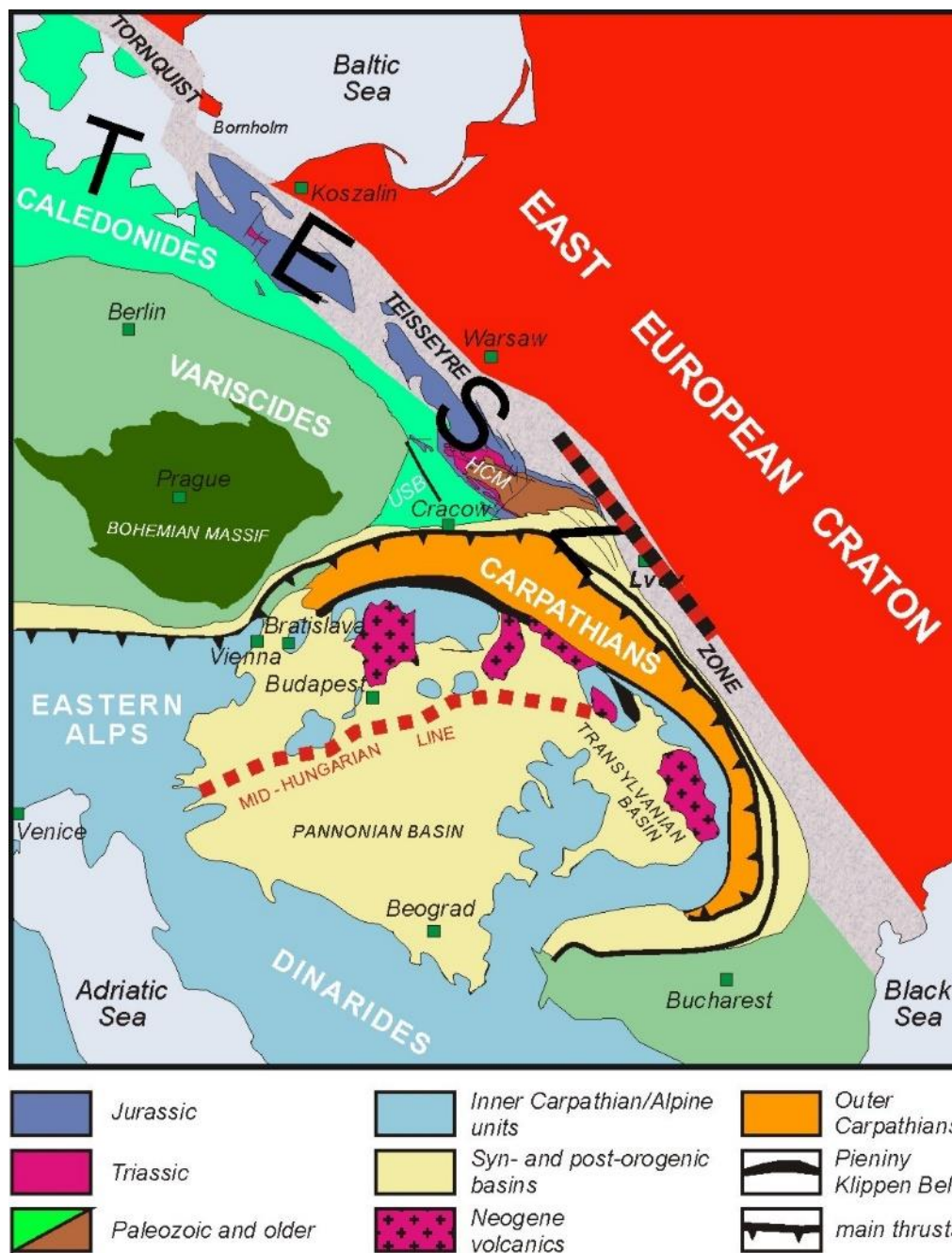


Fig. 2. Location of the profile on the background of tectonic map of Central Europe. USB – upper Silesian block, HCM – Holly Cross Mountains, TESZ – Trans-European Suture Zone. Stars represent shot points, dots – recording stations (after Guterch et al. 2001).

in this region of Central Europe. The oldest tectonic unit in this area is the East European Craton, of the age of over 1 Ga (Fig. 2). The southwestern part of Poland consists of younger (about 300–400 Ma), thinner, warmer, and more mobile lithosphere of the Palaeozoic Platform of Central and Western Europe. In the south, it is bordered by young alpine orogen, represented in Poland by the Carpathian Mountains. The contact of these three large tectonic systems is represented by a broad transition zone (TESZ – Trans-European Suture Zone), extending from North Sea to Black Sea (Berthelsen 1992). The northeastern edge of the TESZ, located near the EEC margin, is called the Teisseyre–Tornquist Zone (Winchester et al. 2002).

Previously, the seismic investigations were performed along the Polish part of the TTZ (transect TTZ-CEL03, Janik et al. 2005). Due to the nature of the deep seismic profiling method, the structure near both ends of the transect (ca. 100 km at each end) is relatively poorly documented. In this method, seismic rays used for imaging the deep structure do not probe the crust vertically, but at certain angle. Therefore, a particularly important from tectonic point of view part of the transect – located in the southeastern Poland – was not illuminated by rays. It is an unique area of contact of these three large geological systems of Europe. Moreover, it is crossed by the boundary between two main units of the EEC – Fennoscandia and Sarmatia. The proposed deep seismic profile runs across this important tectonic node of the European continent. Results of previous seismic investigations performed on the Polish side (conducted within CELEBRATION 2000 project) and in Ukraine (conducted within PANCAKE and RomUkrSeis projects) revealed zones of substantial gradients of the crustal thickness (depth of the Moho discontinuity) perpendicularly to the TTZ. This suggests segmentation of the Precambrian crust to the SE from the Fennoscandia-Sarmatia suture, and possibly parallel to this suture. Planned investigations could help to solve this question, which is of great importance for the determination of the structure of the EEC, as well as for studies of Phanerozoic tectonic evolution of the Carpathian fragment of TTZ and TESZ.

References

- Berthelsen, A. (1992), From Precambrian to Variscan Europe. **In:** D. Blundell, R. Freeman, and S. Mueller (eds.), *A Continent Revealed – the European Geotraverse*, Cambridge University Press, New York, 153–164.
- Guterch, A., M. Grad, G.R. Keller, and CELEBRATION 2000 Organizing Committee (2001), Seismologists celebrate the New Millenium with an experiment in Central Europe, *EOS* **82**, 45, 529, 534–535, DOI: 10.1029/01EO00313.
- Janik, T., M. Grad, A. Guterch, R. Dadlez, J. Yliniemi, T. Tiira, G.R. Keller, E. Gaczyński, and CELEBRATION 2000 Working Group (2005), Lithospheric structure of the Trans-European Suture Zone along the TTZ-CEL03 seismic transect (from NW to SE Poland), *Tectonophysics* **411**, 1–4, 129–156, DOI: 10.1016/j.tecto.2005.09.005.
- Janik, T., V. Starostenko, P. Aleksandrowski, T. Yegorova, W. Czuba, P. Środa, A. Murovskaya, K. Zayats, J. Mechie, K. Kolomiyets, D. Lysynchuk, D. Wójcik, V. Omelchenko, O. Legostaieva, A. Głuszyński, A. Tolkunov, T. Amashukeli, D. Gryn', and S. Chulkov (2022), Lithospheric structure of the East European Craton at the transition from Sarmatia to Fennoscandia interpreted from the TTZ-South Seismic Profile (SE Poland to Ukraine), *Minerals* **12**, 2, 112, DOI: 10.3390/min12020112.
- Winchester, J.A., and The PACE TMR Network Team (2002), Palaeozoic amalgamation of Central Europe: new results from recent geological and geophysical investigations, *Tectonophysics* **360**, 1–4, 5–21, DOI: 10.1016/S0040-1951(02)00344-X.

VERIFICATION OF THE SEISMIC P WAVE VELOCITIES UNDER MOHO BOUNDARY: CENTRAL POLAND CASE STUDY, LUMP PROFILE

LUMP Project

Published: Dec, M., M. Polkowski, T. Janik, K. Stec, and M. Grad (2019), *Acta Geophys.* **67**, 41–57, DOI: 10.1007/s11600-018-0236-9.

The tectonic settings investigated by several seismic projects in previous research targeting the structure in Central Poland mainly focused on the Earth's crust. We present P -wave velocity verification in the uppermost mantle beneath the LUMP profile towards SSE-NNW (Figs. 1–3). Using recordings of 36 DATA-CUBE recorders from ca. 300–490 km far earthquake in the coal mine “Janina” in southern Poland, we calculated travel times to verify P -wave velocity below the Moho boundary from previous studies. It shows that a significantly lower mean velocity value should be used for the upper mantle while counting these offsets of travel times in the SSE-NNW direction than that used on previous profiles. We present two possible models: first (Fig. 2), the most simple one that fits the observed first arrivals, and the second (Fig. 3) with a low-velocity layer beneath the Moho boundary. In both cases, we used a priori crustal model focusing only on P -wave velocity in the uppermost mantle. Both of them significantly improved the adjustment of travel times to the observed data. To evaluate the tendency of adopt-

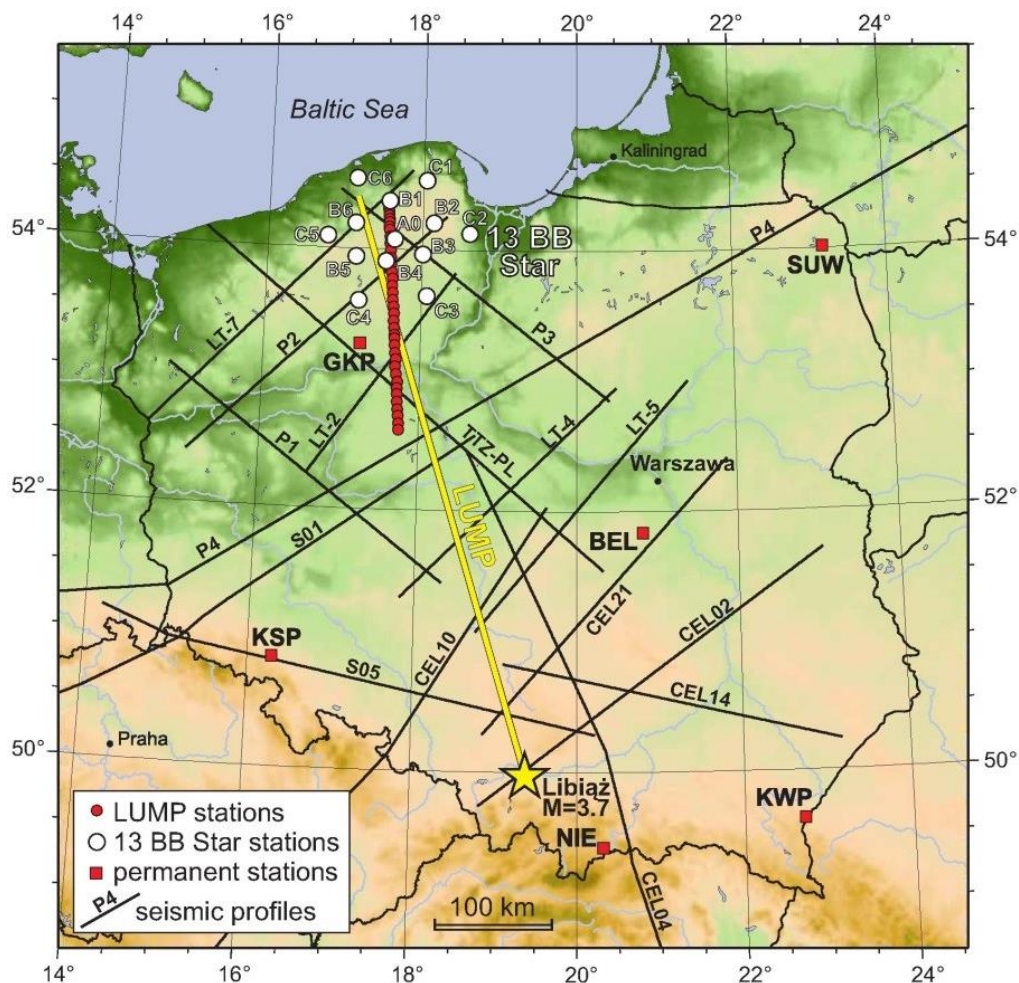


Fig. 1. The net of selected profiles from the region neighboring the LUMP profile on the background of the topographic map. Yellow star shows location of Libiąż earthquake which was recorded at LUMP seismic stations (red dots). “13 BB Star” array of broadband stations is denoted with white dots and permanent seismic stations with red squares, respectively. Yellow line shows the LUMP profile. Thin black lines are profiles used for construction of the Model Z.

ing too high velocities beneath the Moho, we used also 11 broadband stations, Reftek 151-121 “Observer”, from “13 BB Star” passive experiment and 6 STS-2 seismometers from permanent stations of the Polish Seismological Network (PLSN).

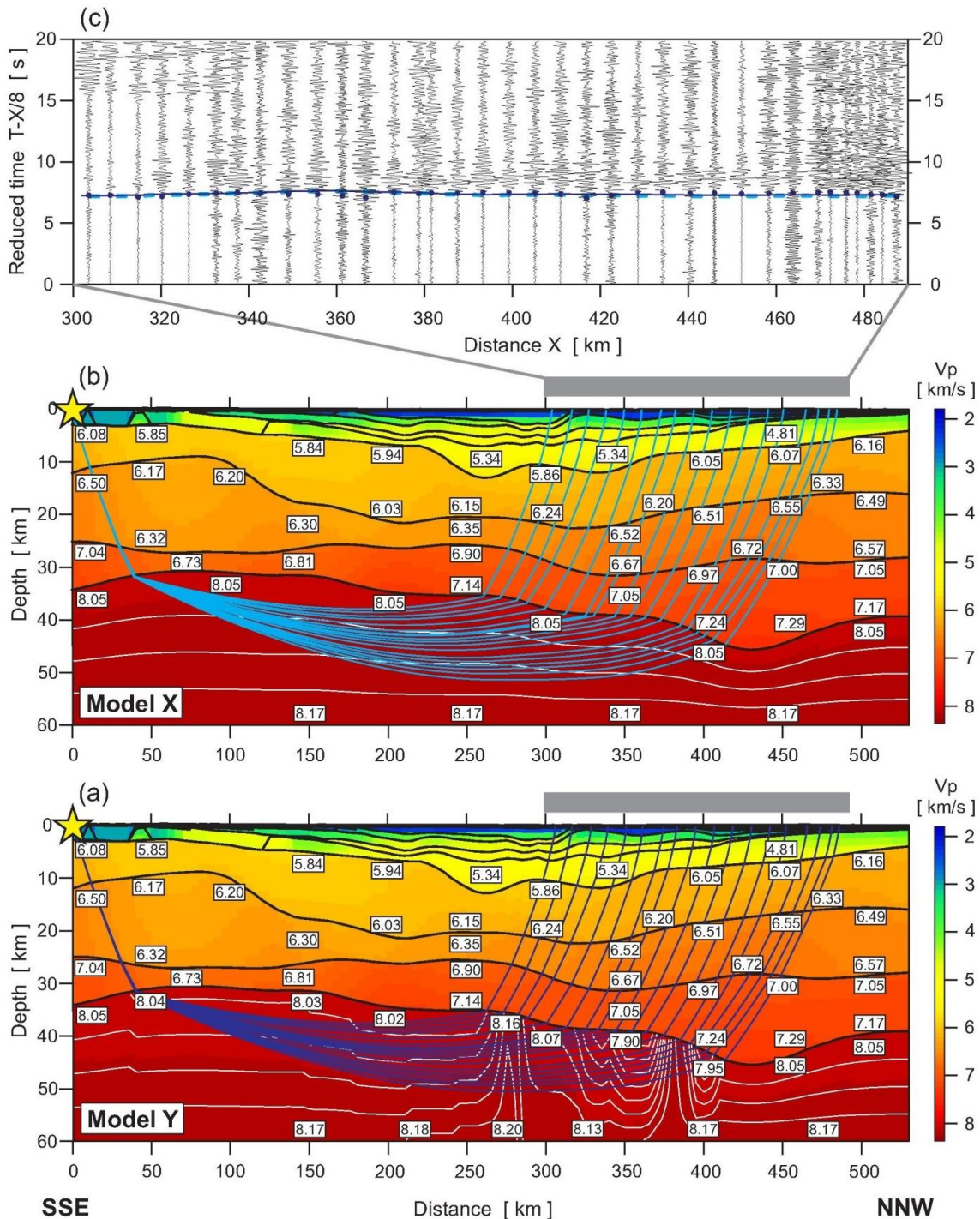


Fig. 2: (a) The Model Y of the LUMP profile obtained by seismic inversion (Model Y). Thick, black lines represent velocity discontinuities (interfaces). Velocity values in km/s are shown in white boxes. Thin, white lines represent velocity contour lines (each 0.03 km/s). Blue lines correspond to ray paths; (b) The Model X – vertical cross-section obtained from 3D model of P-wave velocity in Poland between event location and middle point of the LUMP profile with Model X below the Moho discontinuity; (c) Seismic section with calculated travel times: navy blue line – for the new model presented in (a); light blue dashed line – for model (b), and first arrivals (navy blue dots), filtration 1.5–6.0 Hz.

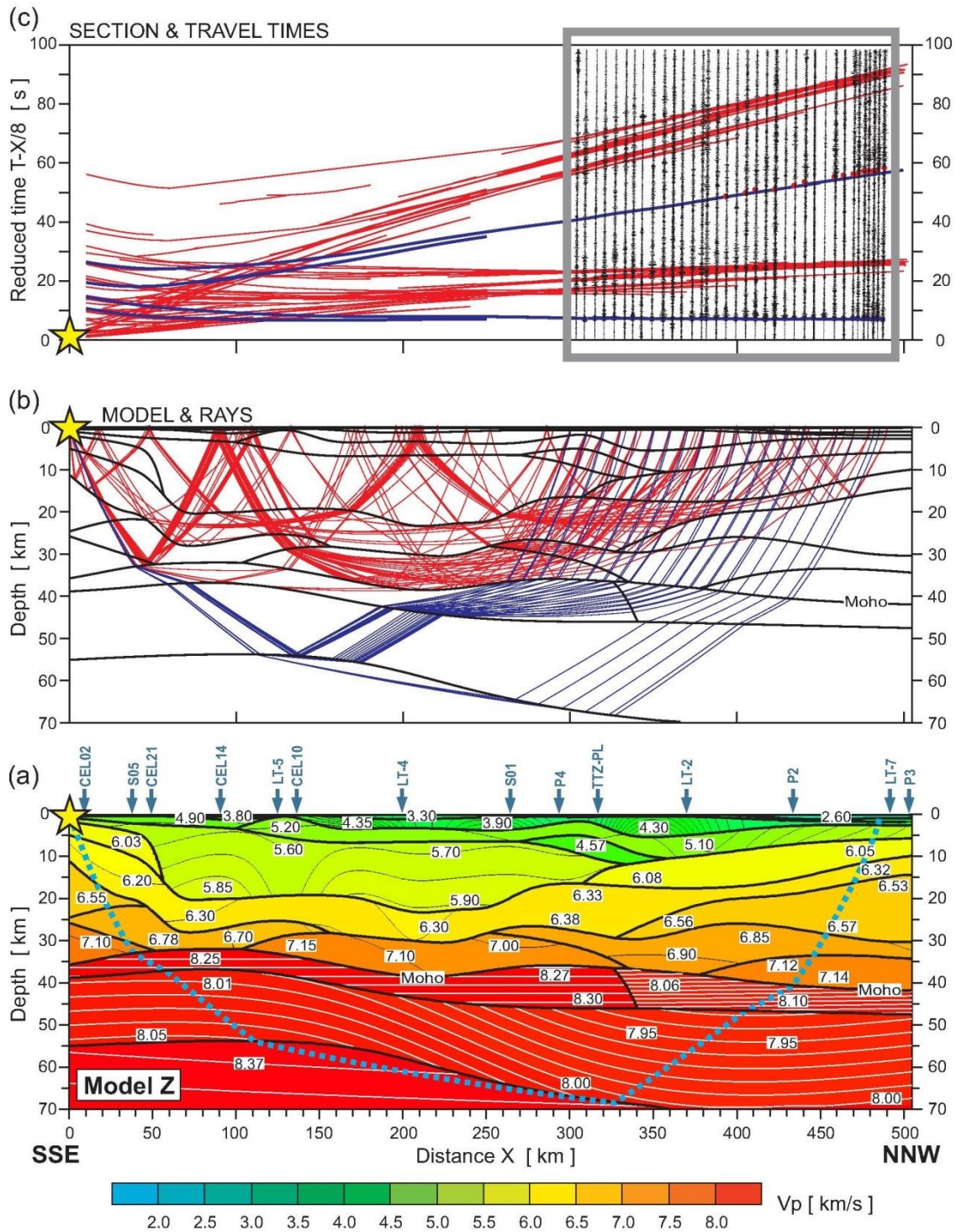


Fig. 3: (a) The Model Z – 2D raytracing P-wave velocity model for the LUMP profile. Please note that the crustal part of the model is constructed from previously carried out models, which cross the LUMP profile. Only velocities in the uppermost mantle were modelled. Thick, black lines represent velocity discontinuities (interfaces). Thin black lines represent velocity contour lines in the crust (each 0.1 km/s). Thin white lines represent velocity contour lines under Moho (each 0.01 km/s). Blue lines correspond to ray paths. Blue dashed line corresponds to range of rays propagation. Velocity values in km/s are shown in white boxes; (b) The ray paths refracted and reflected at crustal uppermost mantle discontinuities with multiples; (c) Seismic section with travel times calculated for the model presented in (a). Red rays on (b) and travel times on (c) diagrams represent selected crustal multiples which can explain high amplitudes after first arrivals. They are not included in modelling.

DETERMINATION OF SEISMIC ANISOTROPY OF THE UPPER MANTLE BENEATH THE SUDETES – A PASSIVE SEISMIC EXPERIMENT

Sudetes Project

In 2017, a passive seismic experiment was launched, involving 23 broadband and 6 short-period seismic stations deployed in the area of Sudetes and Fore-Sudetic block, between Elbe Fault in SW and Odra Fault in NE. The measurements cover a $\sim 200 \times 100$ km large area, with spacing between stations of ~ 30 km (Fig. 1). The stations, deployed for a period of 18 months, will provide broadband recordings of local, regional and teleseismic events. Obtained data will be supplemented with the data from five permanent seismic stations, operating in this area in Poland and Czech Republic. The aim of the experiment is to study the structure, seismic velocity variations including anisotropy distribution, and to map the upper mantle seismic discontinuities (Moho, lithosphere-asthenosphere boundary, mantle transition zone). An example of seismic data recorded by stations working in the experiment is presented in Fig. 2.

The area of the Sudetes, located at the margin of the Bohemian Massif, represents the NE part of the Variscan internides. The region consists of a collage of several units. It has complex tectonic history ranging from the upper Proterozoic till the Quaternary. The crustal structure of this region is relatively well studied, e.g. by seismic wide-angle experiment SUDETES 2003. However, unlike for other parts of the Bohemian Massif where numerous seismic passive (teleseismic and regional) studies have been carried out, in Polish Sudetes only scarce data about the upper mantle properties were collected.

The results of the seismic experiment will provide new information on the mantle structure of the region and will be compared with recent results of petrological studies of crystal preferred orientation in upper mantle xenoliths found in Tertiary volcanics in Lower Silesia. Based on obtained results, we will attempt to enhance the understanding of the evolution and deformations of the Sudetic lithosphere, including the impact of the Alpine orogeny on the present architecture of Sudetes.

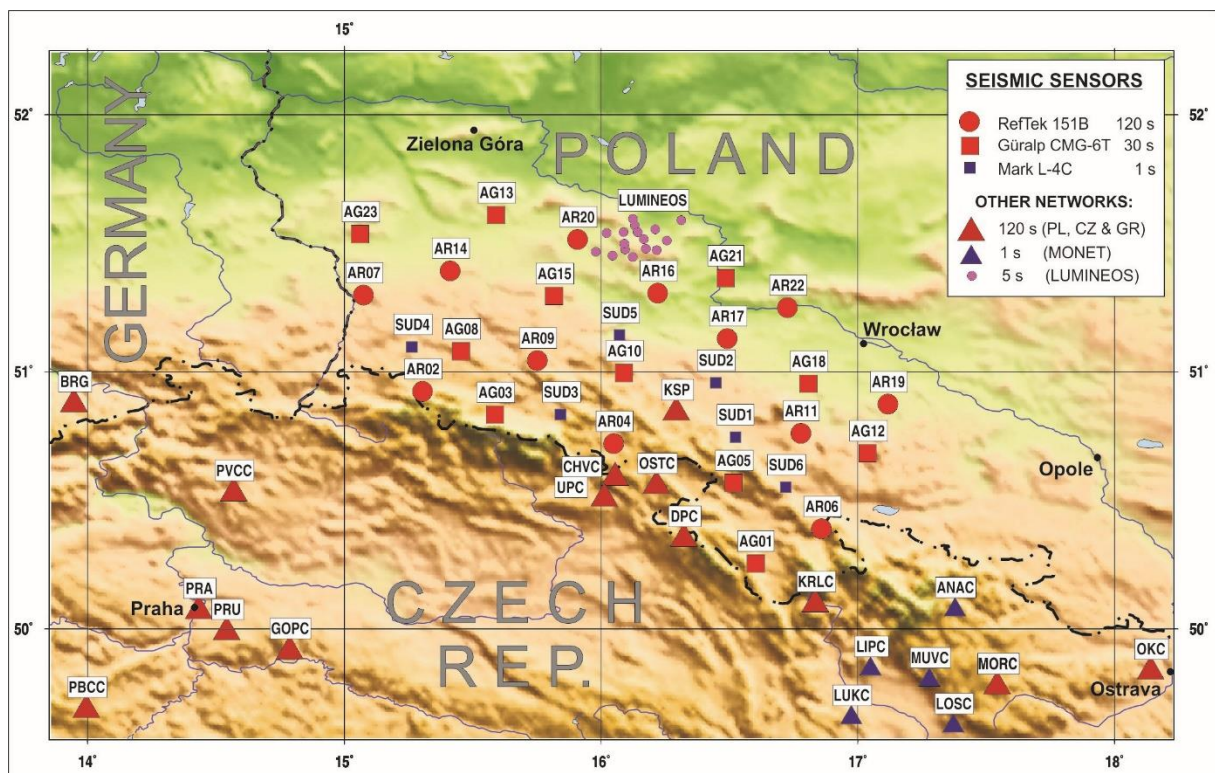


Fig. 1. Location of seismic stations operating during the experiment.

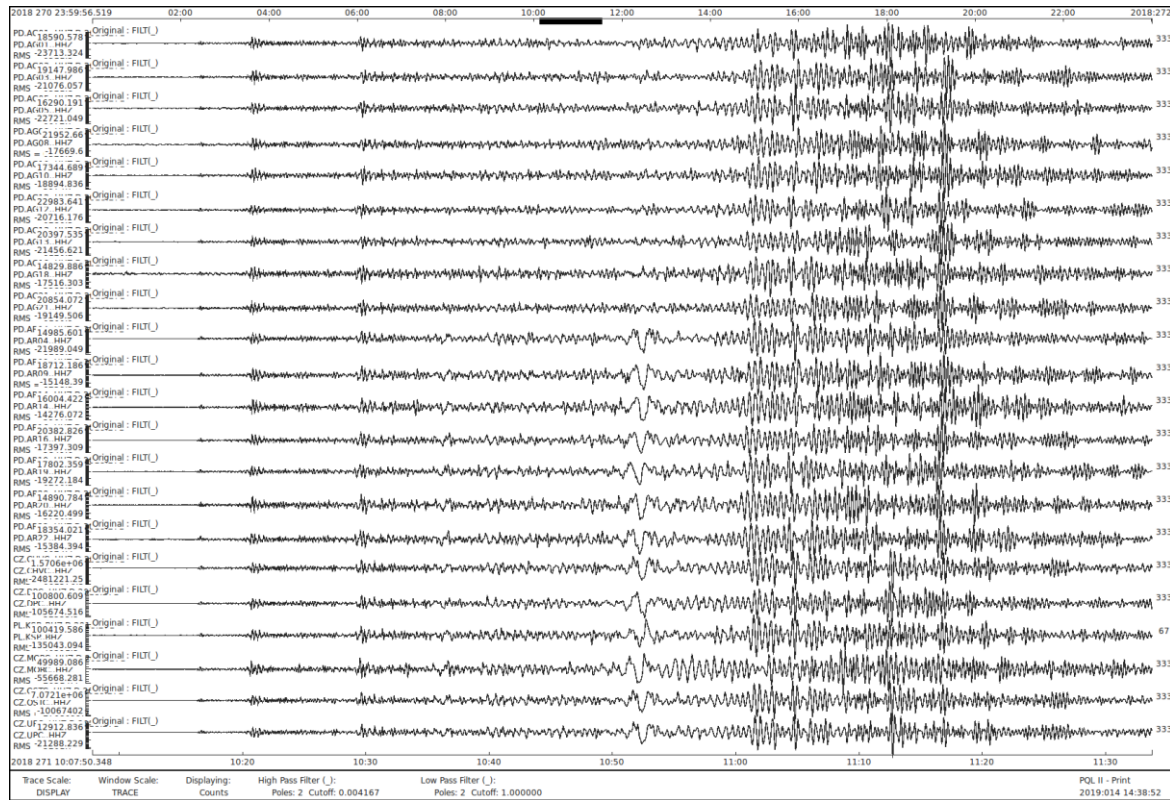


Fig. 2. Example of seismic recording – event of 28 September 2018, M7.5, Indonesia, Z-component.

SEISMIC MODELING OF THE LITHOSPHERE STRUCTURE NEAR THE LOGACHEV SEA MOUNT IN THE REGION OF KNIPOVICH RIDGE

KNIPAS Project

To better understand the lithospheric structure beneath the ultraslow-spreading ridges, the active seismic survey within the Knipovich Ridge Passive Seismic Experiment (KNIPAS) was carried out. The aim of this work was to provide a segment-scale image of lithosphere structure, velocity field and its boundaries beneath the Logachev Seamount on the Knipovich Ridge. The whole work has been done in cooperation with Germans, including scientists from the Alfred Wegener Institute for Polar and Marine Research.

Active seismic profiles were acquired during cruise no. MSM67 in September 2017. On the ocean floor at depths from 2.3 to 3.3 km seismic energy was recorded by 8 ocean bottom seismometers (OBS). In total, 320 km of seismic data were collected along 6 profiles with lengths varying from 30 to approximately 60 km covering the area of around 2200 km². The profiles are crossing each other over the centre of the Logachev Seamount (Fig. 1). High-resolution bathymetric data acquired during the cruise combined with previous bathymetry data sets were utilized as an ocean bottom layer within the seismic model. Our intention underlying this work is to provide evidence of crustal thickness variation beneath the Logachev Seamount and therefore substantially contribute to an understanding of this type of ridges. For the 2D modelling process, only data from OBSs near the profiles were used (Fig. 2). Seismic model was prepared for each seismic line by iterative trial-and-error ray tracing.

After preparation and initial processing of the acquired data, picking of visible first breaks on all seismic sections has been done. Layers of the model were added to assume the best fit between calculated travel times and picks. Five lithospheric layers for the longest profiles were separated with substantial velocity contrasts at the boundaries. Besides first arrivals, later

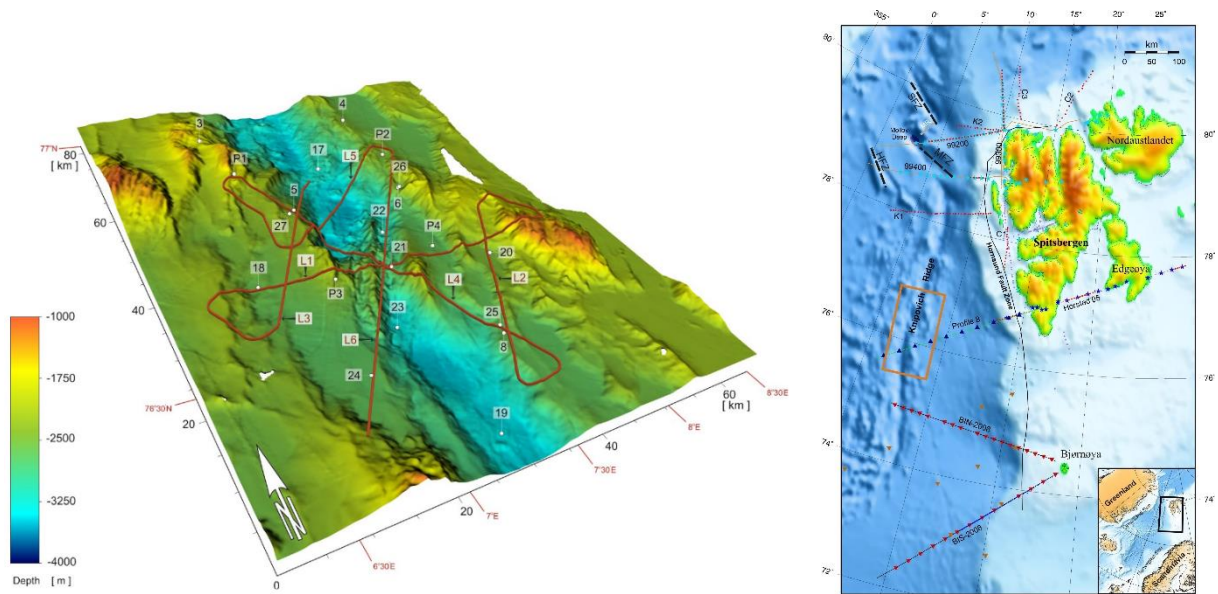


Fig. 1. Bathymetry of the study area with seismic lines with OBSs and location of the study area (red rectangle).

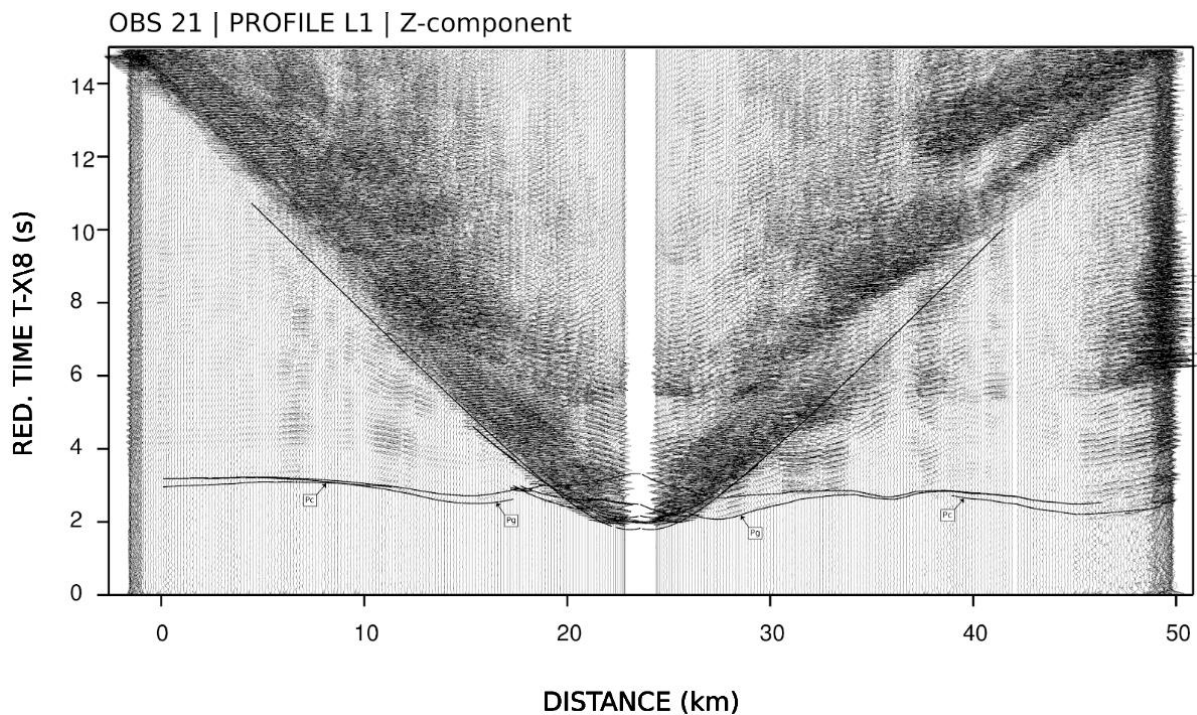


Fig. 2. Example of seismic record section (receiver gather) from OBS 21 on the profile L1 with calculated traveltimes.

phases and multiples were used. Water wave and its multiples allowed estimation of the velocity in the sea water. Available non-linear information from all profiles will be used for further 3D tomography modelling.

By combining the available observables from all seismic profiles we draw the following conclusions. The resulting 2D lithosphere models show relatively high-velocity gradients, especially for the middle oceanic crust. High velocities, of 5.3–5.8 km/s, are observed just below the surface over the seamount centre. We found ca. 1.5 km uplift of the lower oceanic

crust layer to the East of the Logachev Seamount. For the longest profile layer with a velocity above 8 km/s was distinguished at depth of approximately 10 km which can suggest the presence of the Moho discontinuity.

Preliminary results of the seismic modelling were presented during the SEISMIX 2018 Symposium by Dariusz Wójcik.

4.6 Seminars and teaching

Seminars and lecture outside of the IG PAS:

- W. Czuba, Lithospheric Research Infrastructure Centre (CIBSBL) in the EPOS-PL project, Institute of Geophysics, Warsaw University, Warsaw, Poland, Seminar.

4.7 Teaching thesis

- J. Rewers, Modeling of seismic anisotropy of the Earth's crust and the upper mantle in the region of fore-Sudetic Monocline and Bohemian Massif, Supervisor: P. Środa.

4.8 Visiting scientists

- Vitaly Starostenko, Viktor Omelchenko, Dima Lysynchuk, Olga Legostaeva, Sergey Czulkov, Institute of Geophysics, National Academy of Sciences of Ukraine, Kiev, Ukraine, 23–26.10.2018,
- G. Randy Keller, University of Oklahoma, Norman, OK, USA, 29.05–5.06.2018,
- Ewald Brueckl, Vienna University of Technology, Vienna, Austria, 30.05–2.06.2018.

4.9 Meetings, workshops, conferences, and symposia

Presentations of the Department's members:

EGU General Assembly, Vienna, Austria, 7–13 April 2018

- S. Mazur, M. Mikołajczak, P. Krzywiec, M. Malinowski, M. Lewandowski, and P. Środa; Fossil margin of Baltica in SE Poland – an analogue to present continental margins?, Poster;
- V. Schlindwein, F. Krüger, F. Schmid, W. Czuba, T. Janik, KNIPAS – exploring active sea-floor spreading processes at segment-scale, Poster.

SEISMIX 2018, Cracow, Poland, 18-22 June 2018

- D. Wójcik, W. Czuba, T. Janik, V. Schlindwein, F. Schmid, Preliminary results of the Logachev Seamount seismic modelling, Poster/oral;
- D. Wójcik, T. Janik, BASIC: A high-density crustal-scale refraction seismic profile across the Bergslagen ore district, Sweden, Poster;
- P. Środa, M. Bociarska, Passive seismic experiment in Sudetes, SW Poland, Poster;
- RomUkrSeis Working Group: T. Amashukeli, W. Czuba, A. Dragut, D. Gryn, T. Janik, K. Kolomiyets, O. Legostaeva, D. Lysynchuk, J. Mechie, V. Mocanu, J. Okoń, V. Omelchenko, T. Skrzynik, V. Starostenko, R. Stephenson, P. Środa, and T. Yegorova, RomUkrSeis: the deep structure of the TESZ where it is obscured by the Eastern Carpathians, Poster;
- V. Schlindwein, F. Krüger, F. Schmid, W. Czuba, T. Janik, KNIPAS – exploring active sea-floor spreading processes at segment-scale, Poster;
- P. Hrubcová and P. Środa, Anomalous upper-mantle phases in the Western Carpathians: Indication of the ALCAPA and the European Plate contact, Poster.

AGU General Assembly 2018, Washington, USA, 10–14 December 2018

- S. Mazur, M. Mikołajczak, P. Krzywiec, M. Malinowski, M. Lewandowski, and P. Środa, Crustal-scale high density body at the fossil rifted margin of Baltica in Poland – an analogue to Atlantic continental margins?, Poster.

1st Scientific and Technical Conference dedicated to the EPOS-PL project, Jachranka, Poland, 19–21 November 2018

- D. Wójcik, Database construction, metadata structure, formats and standards of CIBSBL, Oral;
- W. Czuba, Task 7: Lithospheric Research Infrastructure Centre (CIBSBL): Data and measurement facilities held, Oral.

4.10 Publications

ARTICLES

- Majdański, M., **J. Grzyb**, B. Owoc, et al. (2018), Near-surface structure of the Carpathian Fore-deep marginal zone in the Roztocze Hills area, *Acta Geophys.* **66**, 179–189, DOI: 10.1007/s11600-018-0131-4
- Pashkevich, I., et al., **T. Janik** (2018), Lithospheric structure based on integrated analysis of geological-geophysical data along the DOBREfraction'99/DOBRE-2 profile (the East European Platform —the East Black Sea Basin), *Geophys. J.* **40**, 5, 98–136, DOI: 10.24028/gzh.0203-3100.v40i5.2018.147476.
- Starostenko, V., **T. Janik**, et al., **W. Czuba**, **P. Środa**, **A. Guterch** (2018), Lithospheric structure along wide-angle seismic profile GEORIFT 2013 in Pripyat–Dnieper–Donets Basin (Belarus and Ukraine), *Geophys. J. Int.* **212**, 3, 1932–1962, DOI: 10.1093/gji/ggx509.

5. DEPARTMENT OF THEORETICAL GEOPHYSICS

Zbigniew Czechowski

5.1 About the Department

Scientific activity of the Department of Theoretical Geophysics is concentrated on the following issues: seismic source, fracture mechanics, fluid flows, stochastic models, time series modeling, and monitoring of rotational effects.

Regarding the theoretical investigation of seismicity and seismic source, two approaches were applied:

- The asperity fault model was proposed to find the relations of megathrust fault physical features with their seismicity patterns, such as fast and slow slip interplay and spatial and temporal variations of the b -value in the Gutenberg–Richter frequency-magnitude law. The model is based on the slip-dependent friction law with the stress-dependent healing;
- For estimating the source time function from seismograms, the time reversal technique was applied. The method can become competitive with regard to the full waveform inversion techniques or the Empirical Green Function method.

Fracture mechanics is associated with many geophysical and geological processes. Our research activity within this topic is concentrated around an analysis of various aspects of breaking brittle materials by the Discrete Element Method – the modern numerical simulation method which allows a detailed description of solid body fragmentation.

An important problem of hydrology is the flow in channels with obstacles at the bottom or at walls of the channel. Two problems were solved by analytical methods – the problem of gravity-driven flow over the sinusoidal bottom and the problem of steady flow through a tube with a wavy wall, have been studied by using the methods of asymptotic analysis.

The time series monitored by geophysical instruments reflects the complexity of phenomena under consideration. For modeling of p -order persistent time series, the modified Langevin equation was proposed. In the analysis of data, the technique of transforming time series into graphs and the concept of HVG irreversibility with the Kullback–Leibler Divergence were used.

Monitoring of rotational effects in the ground was conducted in the Lower Silesian Geophysical Observatory at Książ by different types of rotational seismometers. In 2018, the rock shooting works were done in immediate vicinity to the Observatory. This gave a unique occasion to study small shocks at a close distance and testing the possibility of different devices.

5.2 Personnel

Head of the Department

Zbigniew Czechowski

Professor

Professors

Wojciech Dębski

Roman Teisseyre

Associate Professors

Włodzimierz Bielski

Piotr Senatorski

Specialist

Krzysztof Teisseyre

PhD Students

Piotr Klejment, Poland; Wojciech Dębski – PhD supervisor

Alicja Kosmala, Poland; Wojciech Dębski – PhD supervisor

5.3 Main research projects

- Development and adaptation of the Time Reversal Mirroring technique to the analysis of full seismic waveforms, W. Dębski, National Science Centre (NCN), 2016–2018;
- A network for Gravitational Waves, Geophysics and Machine Learning, W. Dębski, COST-EU, 2018–2020;
- Introducing the stochastic Langevin-type model and procedures of its reconstruction from persistent of order p geophysical time series, Z. Czechowski, National Science Centre (NCN), 2017–2020;
- Complex network studies on natural and induced seismicity, Z. Czechowski, CONICYT Chile, 2018–2020;
- A network for Gravitational Waves, Geophysics and Machine Learning, Z. Czechowski, COST-EU, 2018–2020;
- Investigation of dynamical features of earthquake's temporal distribution based on the analysis of field, laboratory and simulated interevent data, Z. Czechowski, SRNSF Georgia, 2018–2020.

5.4 Research activity and results

Brief description/abstracts/summaries of some of the achievements of the Department's staff:

MODELING SEISMICITY OF SUBDUCTION ZONES: SEISMICITY PATTERNS AND FAULT PARAMETERS

P. Senatorski

The main purpose was an attempt to relate megathrust fault physical (material, structural) features with their seismicity patterns, such as fast and slow slip interplay and spatial and temporal variations of the b -value in the Gutenberg–Richter frequency-magnitude law. This has been done within the asperity fault model context. The asperity mechanical model has been based on the slip-dependent friction law with the stress dependent healing. The friction law depends on two independent parameters: strength and slip-weakening distance. The first parameter enables us to define asperities as regions with high strength value. The second one enables us to distinguish among different asperity types. Both parameters can be related to physical fault characteristics: topographic or structural heterogeneities, such as subducted seamounts, sediments, and released fluids. The healing has been interpreted within a subduction channel context as related to underplating or erosion processes at the channel roof.

Strong, coupled interface patches (asperities) and their weaker surroundings are modeled as respective distributions of frictional peak stresses and slip-weakening distances. Such an approach, which is an alternative for the commonly used rate and state friction law approach, has been justified by available observational and laboratory results.

The proposed model has been used to explain some debated observations concerning seismic and aseismic slips that occur at the same sites, hierarchical nature of the megathrust dynamics, and different roles played by subducted seamounts: whether they restrain or promote huge megathrust earthquakes. Two related effects, the changing fault stiffness and different slip-weakening distance values, provide the key to understand those findings.

The main results can be summarized as follows (Senatorski 2019):

- Complex processes within a subduction channel can be modeled by using the slip-dependent friction law with strength and slip-weakening distance as two model parameters;
- Slow or fast slip is more than the friction law problem only; it depends also on the changing system stiffness, which is related to the rupture area size;
- Relatively large slip-weakening distance value leads to a variety slip patterns with both small and large earthquakes possible.

The next problem to be explained in terms of the proposed asperity model and plate interface characteristics concerns observed earthquake statistics, such as variations of the Gutenberg–Richter law’s b -value. To this end, several related concepts or ideas have been applied: the hierarchical asperity model, the slip budget and earthquake recurrence time, the stable and unstable slip conditions, and the MEP approach to the G-R law (Senatorski 2017).

Two theoretical results are essential for solving the problem. First is relation between the b -value and the exponent in the rupture area versus slip scaling (Senatorski 2017). It enables us to relate changing b -value with earthquake rupture dynamics and physical fault characteristics, so the link between earthquake statistics and physics is established. Second is the relation between system stiffness and its critical value. It enables us to explain the interplay between seismic and aseismic slips during the earthquake cycle. Explanations of the following observations have been suggested by using these two results in the hierarchical asperity model perspective (Senatorski 2018a,b, 2020):

- large b -value for the largest global earthquakes,
- decrease of the b -value before the largest earthquake,
- increase of the b -value after the largest earthquake,
- increase of b -value increase related to aseismic slip.

In general, the b -value increases when the asperities become more isolated, whereas it decreases when the asperities become more interconnected. These conditions change during an earthquake cycle, so the b -value variations can be used to recognize the processes leading to huge earthquakes and, in this way, to the largest megathrust earthquakes forecasting task.

The significance of the obtained results is to contribute to the asperity megathrust model, which is the key to understand the subduction zone seismicity and the largest earthquakes forecasting.

References

- Senatorski, P. (2017), Effect of slip-area scaling on the earthquake frequency-magnitude relationship, *Phys. Earth Planet. In.* **267**, 41–52, DOI: 10.1016/j.pepi.2017.04.004.
- Senatorski, P. (2018a), Megathrust large earthquakes: asperities and b -values. **In:** *Proc. Conf. 20th EGU General Assembly, 8–13 April 2018, Vienna, Austria* (poster).
- Senatorski, P. (2018b), Gutenberg–Richter’s b -value and earthquake asperity models. **In:** *Proc. Conf. Best Practices in Physics-based Fault Rupture Models for Seismic Hazard Assessment of Nuclear Installations: Issues and Challenges Towards Full Seismic Risk Analysis, 14–16 May 2018, Cadarache-Chateau, France* (poster).
- Senatorski, P. (2019), Effect of slip-weakening distance on seismic-aseismic slip patterns, *Pure Appl. Geophys.* **176**, 3975–3992, DOI: 10.1007/s00024-019-02094-7.
- Senatorski, P. (2020), Gutenberg-Richter’s b -value and earthquake asperity models, *Pure Appl. Geophys.* **177**, 1891–1905, DOI: 10.1007/s00024-019-02385-z.

SOURCE TIME FUNCTION INVERSION BY THE TRM METHOD

W. Dębski, K. Waśkiewicz

The classical analysis of seismic data for seismic source characterization includes hypocenter location, moment tensor inversion and spectral analysis which lead to estimation of seismic scalar movement, source radius, static stress drop and apparent stress to name the most important parameters. Additional important source parameters like, for example, source duration, source directivity, rupture speed, and even a dynamic stress drop, can be inferred from seismic data provided a source time function – the function describing a seismic moment release from the source is known. Estimating the source time function is, however, a challenging task which new-days is accomplished either by using the full waveform inversion techniques or an approximate technique called the Empirical Green Function method. While the first approach is numerically demanding and requires high-quality data, the latter one has limited accuracy. In this paper, we propose yet another approach to estimating source time function. It is based on the principle of time reversal symmetry of a governing wave equation. The method is based on observation that when the far-field seismograms are back propagated to the source foci according to the time-reversal technique then a retrieved signal at the source location approximates the thought source time function. Thus, the source time function can efficiently be retrieved with only a few forward modeling needed by the time-reversal techniques without any complex inversion or deconvolution. In this paper, we explain basic mathematical and physical elements of the time-reversal technique and show how it can be applied for the inversion of the seismic source time function. The proposed method is a cornerstone of the TRSTI algorithm and is illustrated with 2D numerical examples. In Fig. 1 there are shown source-receiver configurations used in the experiment.

We have considered homogeneous media with three different receiver arrangements and perfectly reflecting boundary conditions. The simulated waves were recorded, inverted in time and resent to medium from virtual sources located at receiver positions. The resend waves positively interfere at the true source position. The location and time of the maximum amplitude of this interference very accurately estimate the source position and its activation time. This is a very well-known fact. However, we have also demonstrated another feature of the back projected signal, namely that the temporal variation of the collimated signals very well approximates the original STF. This is a new and very important aspect of the TRM method, unknown until now. The retrieved STF functions are shown in Fig. 2.

The obtained result opens a new way of an efficient retrieving source time functions for the real seismic events being the alternative to the classical full waveform inversion (accurate but

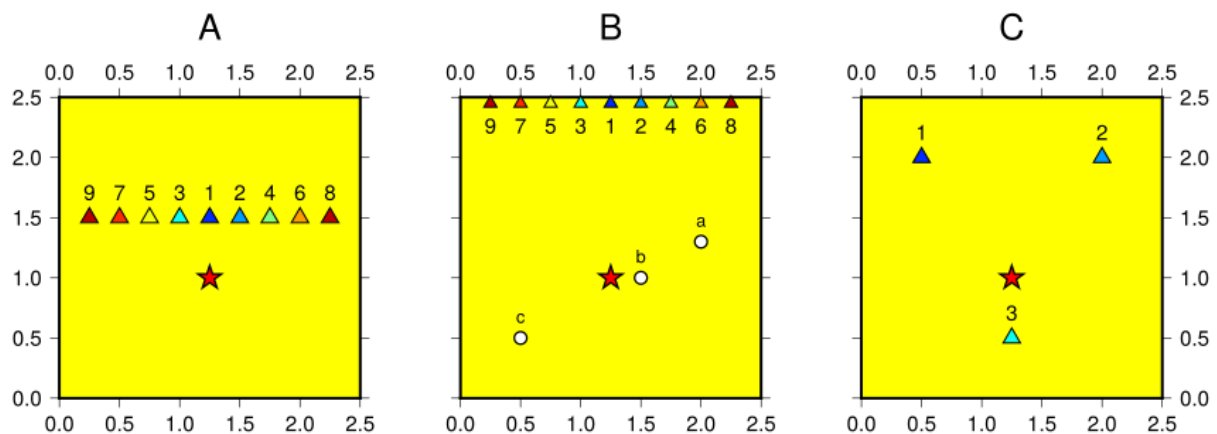


Fig. 1. Three different configurations of receivers used in the acoustic TRM numerical experiment (after Waśkiewicz 2018).

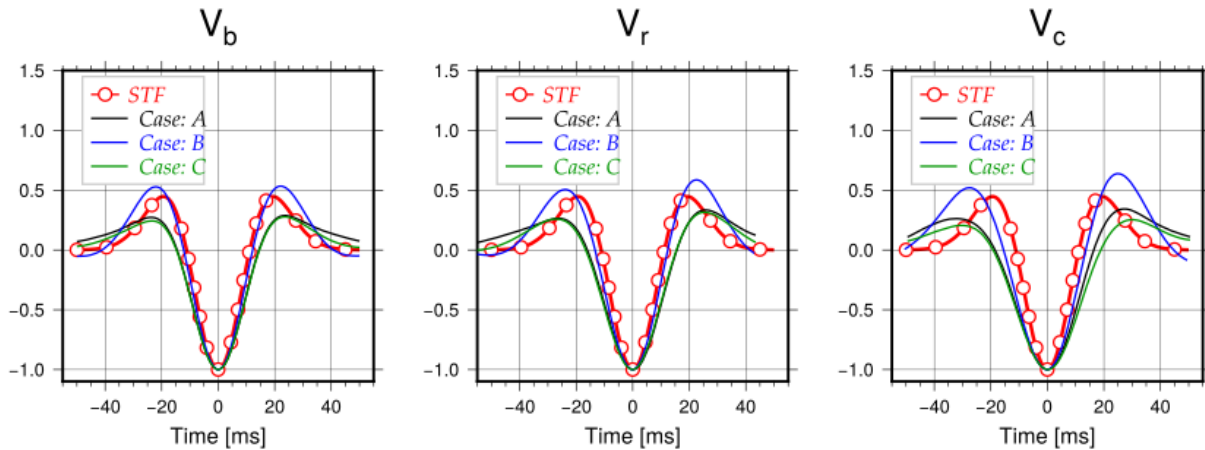


Fig. 2. The original STF function (red) used for generating synthetic data (acoustic waves) which were subsequently used by the TRSTI algorithm. The retrieved STF functions were obtained using 3 different velocity models: the same as for synthetics generation (left panel), the velocity model with random (white noise) perturbations (middle panel), and the model with coherent noise (right panel). In both cases amplitude of disturbing noise was 10% of background velocity. The inferred functions very well approximate the original STF (after Waśkiewicz 2018).

extremely slow from computational point of view) and fast, but inaccurate approach based on the Empirical Green's Function approach. The achieved results become a part of the PhD thesis by K. Waśkiewicz, former PhD student at IG PAS defended in 2018.

References

Waśkiewicz, K. (2018), Zastosowanie, techniki skał czasowych do modelowania i inwersji akustycznego pola falowego, PhD Thesis, Institute of Geophysics, Polish Academy of Sciences, Warsaw (in Polish).

DISCRETE ELEMENT SIMULATION OF BRITTLE MATERIAL FAILURE

W. Dębski, P. Klejment, A. Kosmala

The research activity within this topic concentrated around the analysis of various aspects of breaking brittle materials by the Discrete Element Method – the modern numerical simulation method which allows a detailed description of fragmentation solid bodies. Three issues were analyzed:

1. Brazilian test. The tensile strength of solid materials is one of the most important parameters describing the behavior of the material under external mechanical loading and thus its knowledge is of great practical importance. However, the direct measurement of tensile strength, especially for brittle materials, is quite difficult and only limited results are available. To cope with this situation, various methods of indirect measurements have been proposed, including the so-called Brazilian test which is the most popular. The method relies on diametrically loading of disc-like sample of the brittle material until it splits apart due to a induced tensile stress. In this paper, we report our effort to describing the fracturing process during the Brazilian test from the “microscopic” point of view. For this purpose, we use an advanced implementation of the Discrete Element Method – the ESyS-Particle software. We represent a rock specimen as a set of interacting spherical particles which mimic grains of real rock material. We have observed that the maximum loading force that the sample can withstand almost

linearly scales up with a ratio of maximum-to-minimum particle diameters. This is shown in Fig. 1 where maximum load, accumulated potential energy and deformation at which sample breaks are shown as a function of grain size.

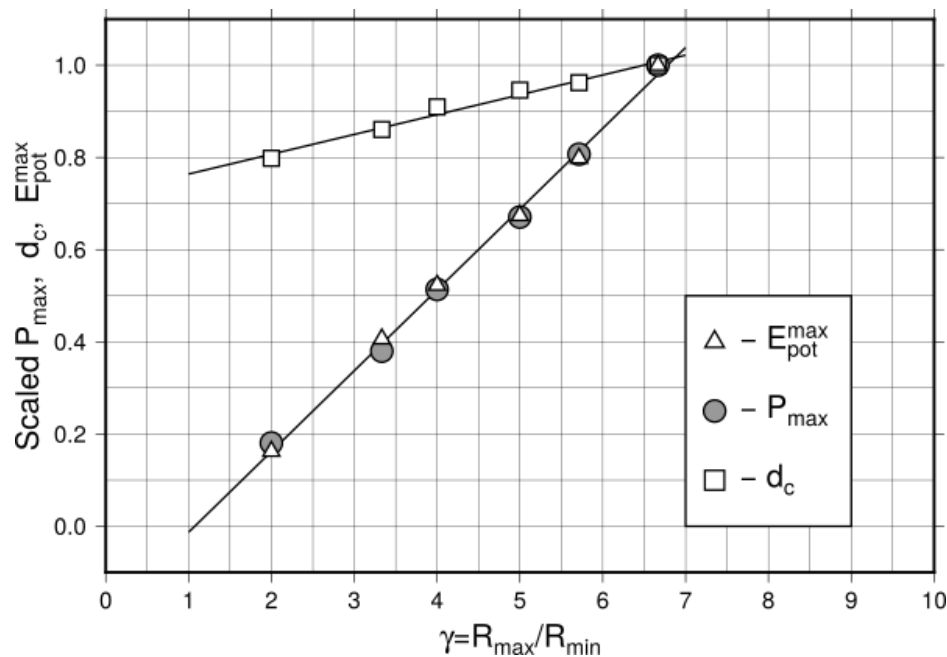


Fig. 1. The maximum critical load, critical strain d_c , and potential energy at d_c strain as the function of radii ratio $\gamma = R_{max}/r_{min}$. (after Klejment and Dębski 2017).

2. Crack nucleation in the tensional regime. Cracking of materials is an extremely complicated process that includes processes in scales from atomic (breaking intermolecular bonds) up to a scale of thousands of kilometers in the event of catastrophic earthquakes (in the energy scale from individual eV to 10^{24} J) (Teisseyre 1995). Such a large span of the scale raises a lot of questions, in particular about the scalability of cracking processes, the existence of factors determining the final size of the fracture area (on a macroscopic scale), course of the preceding and occurring processes during material destruction, etc. (Christensen 2013). The aim of this research was to try to look at the cracking processes on a scale typical for engineering and seismology (millimeters to meters) using micro-physics methods. The proposed research methodology was based on large-scale simulations using the Discrete Element technique. We mainly focused on cracking hypothetical three-dimensional materials subjected to uniaxial stretching with constant velocity and sample deformation. The above assumptions underlying the simulations may seem quite unrealistic. In fact, however, they quite well allow to describe the behavior of cracking structures, such as thin films (e.g. biological structures), metal coverings (e.g. aircraft fuselages), tailoring materials, and crack propagation (Christensen 2013). The well-known fact is that cracking solid bodies are determined by the structure of a given material, its atomic and micro-structural structure, but also by the way of applying external forces leading eventually to its destruction and fragmentation (Jaeger et al. 2007). Usually, the rupture source is described by a single crack or dislocation, following the pioneering vision of Griffith (1921). The dynamic crack propagation causes relaxation of stresses and energy release, leading in the consequence to material failure. It was shown experimentally that the micro-destruction leads to macro-destruction. Correct analysis of complexity of the fracture process or/and interactions of micro-cracks at big concentrations typical for pre-fracture state is possible only in terms of statistical models. The kinetic model of evolution of crack population was introduced by

Czechowski (1991) and developed in Czechowski (1993) and Newman et al. (1994). It lies at a level intermediate between the purely statistical approach and the fully microscopic treatment. The elementary objects are micro-cracks which can nucleate, propagate, and coalesce. The problem of crack interaction and fusion is faced in its simplest aspects (binary interaction) but avoids its most delicate features by introducing extra mechanical probabilistic assumptions. The kinetic approach operates on the crack size distribution function that evolution is governed by the modified coagulation equation (mesoscopic level). Relations with the macroscopic picture, concerning the stress field evolution and the relationship between the time to fracture and the applied stress, were derived. Both panels of Fig. 2 demonstrate two observed fracture modes.

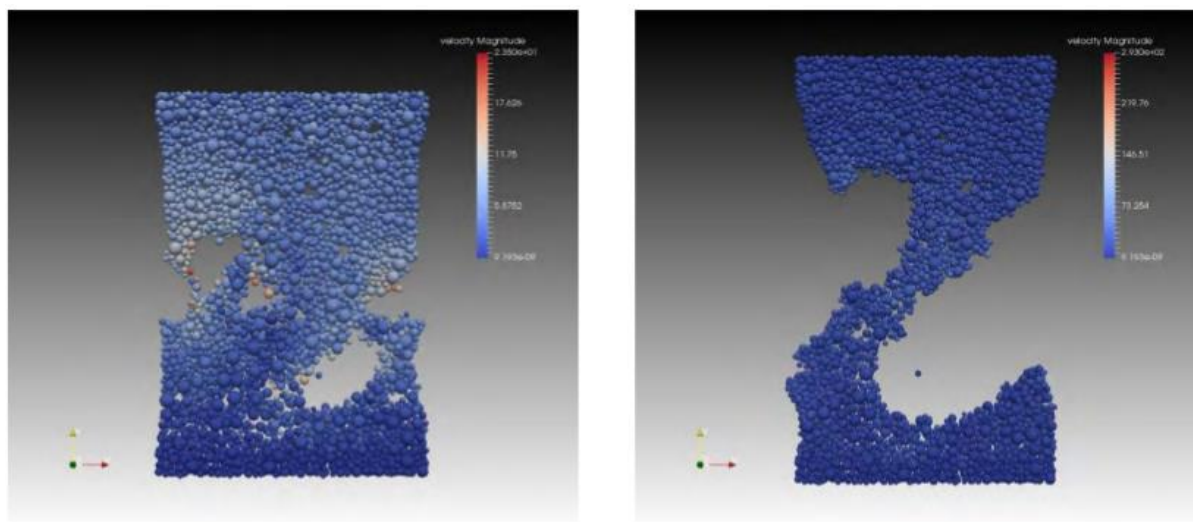


Fig. 2. Cracks propagation under different uniaxial stretching regime (after Klejment and Dębski 2018).

References

- Christensen, R.M. (2013), *The Theory of Materials Failure*, Oxford University Press, Oxford.
- Czechowski, Z. (1991), A kinetic model of crack fusion, *Geophys. J. Int.* **104**, 2, 419–422, DOI: 10.1111/j.1365-246X.1991.tb02521.x.
- Czechowski, Z. (1993), A kinetic model of nucleation, propagation and fusion of cracks, *J. Phys. Earth* **41**, 3, 127–137, DOI: 10.4294/jpe1952.41.127.
- Griffith, A.A. (1921), The phenomena of rupture and flow in solids, *Philos. Trans. Roy. Soc. A* **221**, 163–198, DOI: 10.1098/rsta.1921.0006.
- Jaeger, J.C, N.G. Cook, and R. Zimmerman (2007), *Fundamentals of Rock Mechanics*, Wiley-Blackwell, Malden, MA, 488 pp.
- Klejment, P., and W. Dębski (2017), Brazilian test – a microscopic point of view on tensile fracture generation. **In:** *Proc. V Int. Conf. on Particle-based Methods – Fundamentals and Application, Particles 2017*, 78–89.
- Newman, W.I., A. Gabrielov, T.A. Durand, S.L. Phoenix, and D.L. Turcotte (1994), An exact renormalization model for earthquakes and material failure statics and dynamics, *Physica D* **77**, 1–3, 200–216, DOI: 10.1016/0167-2789(94)90134-1.
- Teisseyre, R. (ed.) (1995), *Theory of Earthquake Premonitory and Fracture Processes*, PWN, Warszawa.

FLOWS OF VISCOUS FLUIDS IN NON-TYPICAL OPEN AND CLOSED CHANNELS. THEORETICAL MODELING AND PERSPECTIVES

W. Bielski

An important problem of hydrology or geohydrology is flow in channels with obstacles at the bottom or at walls of the channel. The bottom may be uneven, rough, sloped, wave, with vegetables, plants and so on. Then the velocity field is drastically changed in comparison with the flow over plane bottom. The problem of resistance is one of the important issues in hydrology. Particularly, corrugated tubes are an example of such problems and have an application to the technical and medical sciences. Similarly, phenomena of such kind occur in the propagation of gravity (or density) currents.

In our research activity, we have solved some problems of the flows by analytical methods, which stand as a start point to further study and obtaining numerical results to compare the compatibility of the experiment with the results of theoretical modeling.

First, the problem of gravity-driven flow over the sinusoidal bottom, see Fig. 1, is studied by using the methods of asymptotic analysis including expansions in the Taylor and Fourier series, accordingly to the sinusoidal shape of the channel bottom, which leads to a cascade system of equations to be solved (Wojnar and Bielski 2018).

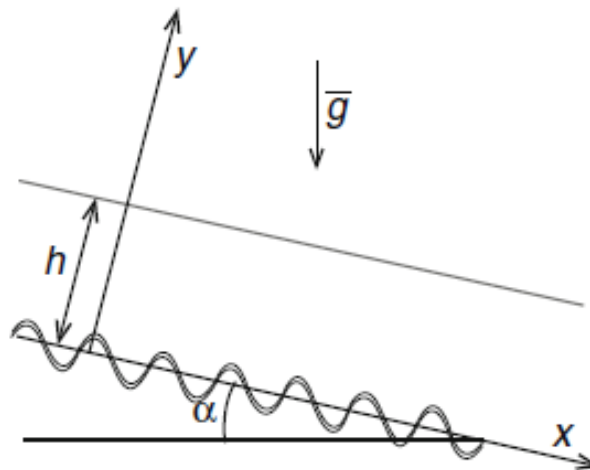


Fig. 1. The gravity-driven flow past a wavy bottom with the mean slope α to the horizontal plane. The vector g denotes the gravity acceleration. The depth of the stream in subsequent calculations is taken as $h = 1$. The proportions of the bottom waviness are exaggerated (after Bielski and Wojnar 2018).

The second problem concerns the steady flow through a tube with a wavy wall. This is related to geophysical problems of stream flows past the channels with rough walls in Karst phenomena (appearing as a result of the dissolution of soluble rocks such as limestone, dolomite). To account for this phenomenon, the effect of small amplitude wall waviness on the steady flow in a tube is examined. We consider a Stokesian pressure-driven flow in a tube with a wavy wall as the axially-symmetric problem. Thus, we are dealing with two-dimensional steady problem described by two position co-ordinates, r and z .

The problem is solved again by means of analytical methods involving the asymptotical analysis. We assume that the radius R of the pipe cross-section is a periodic function of the z variable, which means that the wall shape is described by a surface periodic along the z -axis, $R = R_0 + \varepsilon a \cos(Kz)$. Here R_0 is the mean value of the pipe radius, ε is a dimensionless small parameter, a is the amplitude of the wall wave, and $K = 2\pi/\lambda$, where λ denotes the length of the wall wave, see Fig. 2.

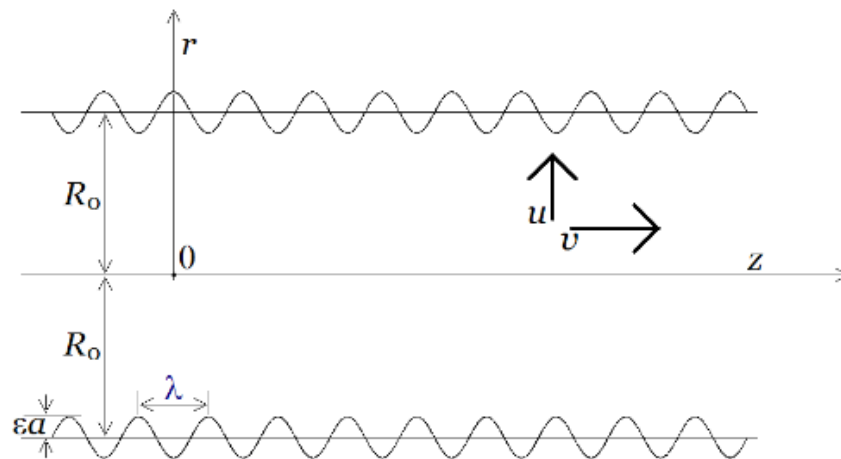


Fig. 2. Cross-section of the considered axially-symmetric tube. Here R_0 is the mean value of the pipe radius, ε is a dimensionless smallness parameter, a is the amplitude of the wall waveness, and λ denotes the length of the wall waviness (after Wojnar and Bielski 2018).

The solution was obtained by expanding the stream function in a Fourier series and expanding the boundary surfaces in Taylor's series. Even in the first-order approximation $O(\varepsilon)$, new results are obtained (Bielski and Wojnar 2018).

The obtained solution for the velocity v belongs to the class of periodic functions with period λ in z . Thus, a study of Stokesian flow is performed on the basis of the asymptotic analysis and a correction to Hagen-Poiseuille's type flow is found.

The methods of asymptotic expansion and averaging (homogenization) are fruitful tools for solving many physical problems.

The results obtained currently will be verified by a numerical method, and next will be applied to the description of gravity currents propagating in channels with rough bottom, which is to be a subsequent step in our activity.

References

- Bielski, W., and R. Wojnar (2018), Stokes flow through a tube with wavy wall. **In:** J. Awrejcewicz (ed.), *Dynamical Systems in Theoretical Perspective*, Springer, Cham, 379–390.
- Wojnar, R., and W. Bielski (2018), Gravity driven flow past the bottom with small waviness. **In:** P. Drygaś and S. Rogosin (eds.), *Modern Problems in Applied Analysis*, Birkhauser, Cham, 181–202, DOI: 10.1007/978-3-319-72640-3_13.

TIME SERIES ANALYSIS AND MODELING

Z. Czechowski

The time series monitored by geophysical instruments reflects the complexity of phenomena under consideration and its important features; nonlinearity, multifractality, and non-Markovian properties. A typical non-regularity of geophysical data induces us to accept the assumption about stochastic basis of geophysical time series.

Therefore, for the modeling, nonlinear models of the Langevin-type were taken into account. In our approach, the standard Langevin equation had to be modified to describe some non-Markov processes – persistent of order p (Czechowski 2018). For this goal, the additional random factor was introduced to the diffusion term, i.e., a function c , which determines a sign

of the term and is dependent on signs of p previous jumps. The main task of modeling, besides choosing the proper mathematical model, is to propose a reconstruction procedure of the model from data. However, for the modified Langevin equation, typical reconstruction procedures fail. Therefore, the novel procedure was introduced and tested on synthetic data. The results showed good efficiency of the procedure.

Recently, scientists have shown a growing interest in the process of transforming time series into graphs (and vice versa). This creates a very attractive relation that enables to use simultaneously well-developed methods of time-series and graphs (complex networks) theories to the examination and discrimination of data sets. Basing on this idea, a spatiotemporal analysis of the dynamical system of the seismic area was performed (Pastén et al. 2018). The complex network for earthquakes is built according to the location of hypocenters and the network nodes are marked by their final connectivity given by the time sequence of the seismic events. Then, the procedure of transforming the graph into connectivity time series follows the time sequence of the occurrence of seismic events. Therefore, some features of both, the constructed complex network and the appropriate connectivity time series, can be examined. The procedure was applied to four data sets in Chile with different levels of seismic activity. It was shown that the multifractal properties of connectivity time series are different – the multifractality is diminishing with the occurrence of large earthquakes. It is reflecting the spatiotemporal organization of these seismic systems.

Unlike typical deterministic systems, stochastic differential equations have a built-in direction of time flow. This directly leads to the problem of reversibility/irreversibility of time series that can be treated as a realization of a stochastic process. Our next task corresponded to finding a direct relation between time irreversibility and memory (namely, a persistence) of time series (Telesca and Czechowski 2018). To this aim, HVG irreversibility with the Kullback–Leibler Divergence as a tool for estimating the level of time irreversibility of persistent/antipersistent time series was applied. The HVG irreversibility concept is based on the Visibility Graph method of transforming time series into graphs. The modified Langevin equation was utilized as a generator of time series with different levels of time persistence. A non-trivial relationship, characterized by a non-symmetric shape, between the degree of irreversibility and the level of persistence was found – time irreversibility increases with the level of persistence or antipersistence.

References

- Czechowski, Z. (2018), Modelling of persistent time series by the nonlinear Langevin equation. **In:** T. Chelidze, F. Vallianatos, and L. Telesca (eds.), *Complexity of Seismic Time Series. Measurements and Application*, Elsevier, 141–160, DOI: 10.1016/B978-0-12-813138-1.00005-5.
- Pastén, D., Z. Czechowski, and B. Toledo (2018), Time series analysis in earthquake complex networks, *Chaos* **28**, 8, 083128, DOI: 10.1063/1.5023923.
- Telesca, L., and Z. Czechowski (2018), Relation between HVG-irreversibility and persistence in the modified Langevin equation, *Chaos* **28**, 7, 073107, DOI: 10.1063/1.5030680.

MONITORING OF ROTATIONAL EFFECTS

Krzysztof Teisseyre

Rotational effects in the ground are monitored in the Lower Silesian Geophysical Observatory at Książ by the following types of seismometers: fiber optic Sagnac gyroscopes (FOGs, manufactured and maintained by the Military University of Technology WAT in Warsaw); a set of

two TAPSES – Twin Pendulum Antiparallel Seismometers (manufactured in our Institute), and two rotational sensors of lower sensitivity (prototypes, made in the Czech Academy of Sciences).

There are two reasons to record rotation with various sensors collocated. First, each equipment has its own shortages; therefore, comparing the results allows for better data understanding and cleaning; second – different families of seismic sensors are under development, which is facilitated by practical testing.

Studies on seismic rotations and strains are relevant to seismology, the technologies of architecture, and care of the buildings' safety. The technological aspect of rotational seismology is nowadays especially important because some experiments show that rotational motions can be dangerous to man-made constructions, but tests for these motions are not comprised in the routine.

In 2018, rock shooting works were done in the immediate vicinity of the Observatory – two new entrances to the huge Książ undergrounds were cleaved. This gave seismologists a unique occasion to study small shocks at a close distance – about 80 m in the case of the above-mentioned sensors; various distances to the temporary network of seismometers. Unfortunately, the broadband seismometer was blocked in the time of these works, for its safety. The blasts differed in strength and details of location; each blast embraced several explosions in adjacent

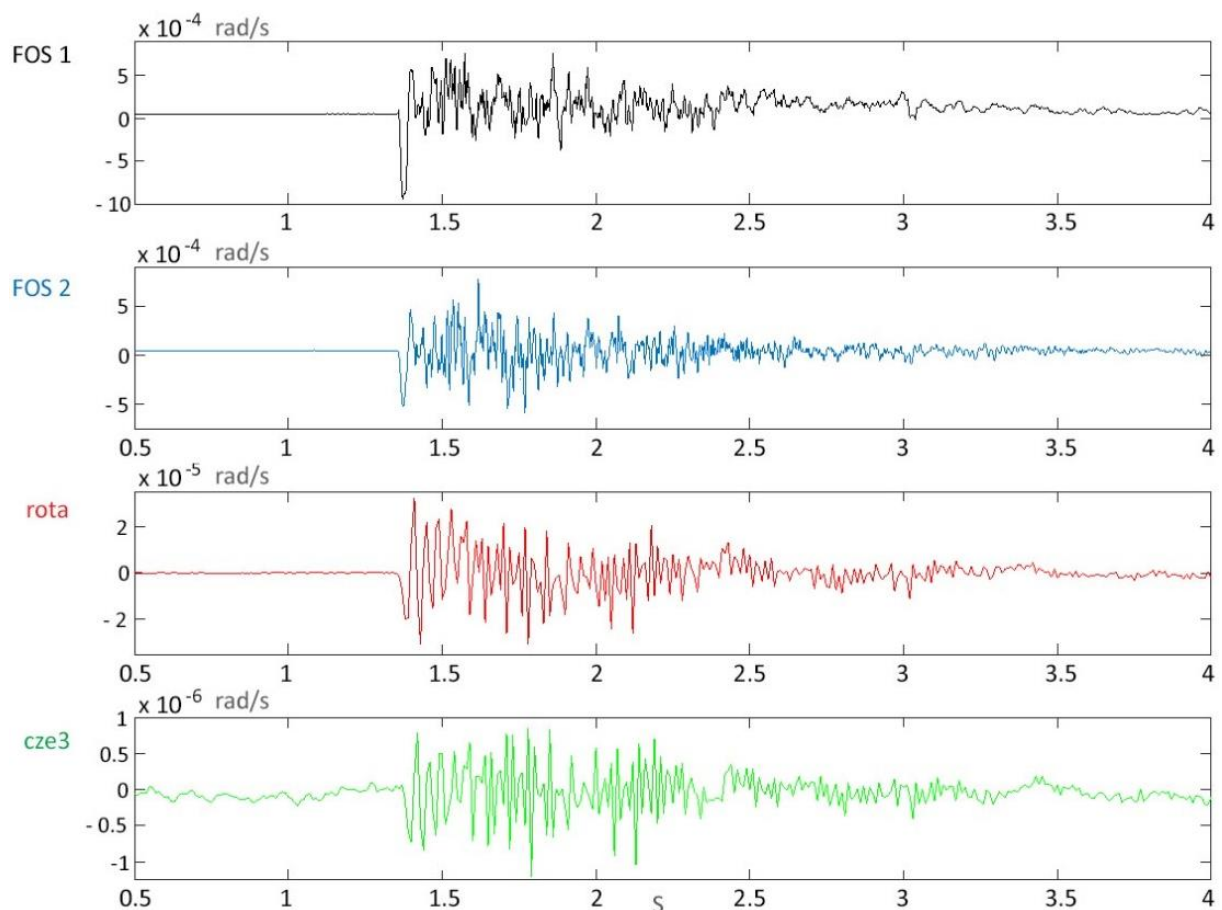


Fig. 1. Example of simultaneous recording of the ground rotation, excited by the mining (engineering) blast at Książ. From the top: FOS 1 – recording from the fiber optic gyroscope “FOS1”; FOS 2 – recording from the fiber optic gyroscope “FOS2”; rota – rotation calculated from the set of two TAPSES; cze3 – recording from the liquid-filled rotational seismometer of Czech production (“3” is the number of channel).

places and controlled, very small retardation. First data processing concentrated on comparing simultaneous recordings from the six mentioned rotational seismometers; the next step will include comparison with the results from the temporary network.

Figure 1 presents an example of simultaneous blast recordings, showing signals from two FOGs (FOS1 and FOS2), rotation obtained from the set of TAPSeS (rota), and the signal recorded by liquid-filled Czech sensor (cze3). The other Czech sensor exhibited too low sensitivity for this study. General conformity of results is seen, but differences caused by the characteristics of instruments are visible too.

References

- Donner, S., H. Igel, C. Hadziioannou, and the Romy Group (2018), Retrieval of the seismic moment tensor from joint measurements of translational and rotational ground motions: sparse networks and single stations. **In:** S. D’Amico (ed.), *Moment Tensor Solutions*, Springer, Cham, 263–280, DOI: 10.1007/978-3-319-77359-9_12.
- Jaroszewicz, L.R., A. Kurzych, Z. Krajewski, P. Marć, J.K. Kowalski, P. Bobra, Z. Zembaty, B. Sakowicz, and R. Jankowski (2016), Review of the usefulness of various rotational seismometers with laboratory results of fibre-optic ones tested for engineering applications, *Sensors* **16**, 12, 2161, DOI: 10.3390/s16122161.
- Jaroszewicz, L.R., A. Kurzych, K.P. Teisseyre, and Z. Krajewski (2018), Measurement of rotational events in regions prone to seismicity: A review. **In:** A. Okiwelu (ed.), *Geophysics*, IntechOpen, London, 19–39, DOI: 10.5772/intechopen.72169.

5.5 Seminars and teaching

Seminars and lecture outside of the IG PAS:

- Z. Czechowski, Reconstruction of the modified Langevin equation from p-order persistent time series, University of Chile, Department of Physics, Santiago, Chile, Lecture;
- K. Teisseyre, Henryk Arctowski i Epoka Odkryć – Henryk Arctowski and The Discoveries Epoch, Polish Academy of Sciences, Warsaw, Poland, Invited lecture.

5.6 Completed PhD thesis defence

- K. Waškiewicz, Zastosowanie techniki skał czasowych do modelowania i inwersji akustycznego pola falowego, Supervisor: W. Dębski,
- P. Klejment, The microscopic insight into fracturing of brittle materials with the Discrete Element Method, Supervisor: W. Dębski.

5.7 Visiting scientists

- T. Matcharashvili, M. Nodia Institute of Geophysics of Ivane Javakhishvili Tbilisi State University, Tbilisi, Georgia, 4–11.08.2018,
- S. Pradhan, Porolab Excellence Center, Physics Department, NTNU, Trondheim, Norway, 10–22.07.2018.

5.8 Meetings, workshops, conferences, and symposia

Presentations of the Department’s members:

EGU General Assembly, Vienna, Austria, 8–13 April 2018

- P. Senatorski, Megathrust large earthquakes: asperities and b-values, Poster;

- P. Klejment, The microscopic insight into calving process in grounding tidewater glaciers – the Discrete Element Method numerical approach, Poster;
- A. Kosmala, Investigation of fracturing fluid penetration with the Discrete Element Method, Poster;
- P. Klejment, W. Dębski, Application of the Discrete Element Method for analysis of fundamental particle interactions during rupturing seismic sources, Poster;
- W. Dębski, K. Waśkiewicz, Estimating source time function by Time Reversal Method, Poster;
- P. Klejment, A. Kosmala, W. Dębski, High-performance computing in geophysics: Application of the Discrete Element Method to materials failure problem, Poster.

Best Practices in Physics-based Fault Rupture Models for Seismic Hazard Assessment of Nuclear Installations: issues and challenges towards full Seismic Risk Analysis, Cadarache-Chateau, France, 14–16 May 2018

- P. Senatorski, Gutenberg-Richter's b -value and earthquake asperity models, Poster.

ISCPS2018 International Summer Conference on Probability and Statistics, Pomorie, Bulgaria, 25–30 June 2018

- Z. Czechowski, Reconstruction of the modified Langevin equation from p -order persistent time series, Oral.

ICCS 2018 The Ninth International Conference on Complex Systems, Cambridge, MA, USA, 22–27 July 2018

- Z. Czechowski, A. Budek, M. Białecki, Bi-SOC-states in one-dimensional random cellular automaton, Oral.

The 7th International Conference on Complex Networks and Their Applications COMPLEX NETWORKS 2018, Cambridge, United Kingdom, 11–13 December 2018

- D. Pastén, Z. Czechowski, B. Toledo, Time series analysis in earthquake complex networks, Oral.

Conference on Complex Systems 2018, Thessaloniki, Greece, 23–28 September 2018

- M. Petelczyc, Z. Czechowski, Time irreversibility of persistent time series generated by discrete Ito equation, Oral.

2nd Workshop on Porous Media, UWM, Olsztyn, Poland, 28–30 June 2018

- W. Bielski, R. Wojnar, Plane flow through the porous medium with chessboard-like distribution of permeability, Oral.

Solmech 2018, Warsaw, Poland, 27–31 August 2018

- W. Bielski, P. Kowalczyk, R. Wojnar, Two temperature heat transfer and thermal stresses, Oral.

Fatigue-2018, Poitiers, France, 27 May – 1 June 2018

- P. Klejment, W. Dębski, Crack nucleation in solid materials under external load – simulations with the Discrete Element Method, Poster.

Supercomputing Frontiers 2018, Warsaw, Poland, 12–15 March 2018

- P. Klejment, A. Kosmala, W. Dębski, Application of the Discrete Element Method for analysis of fundamental particle interactions during rupturing seismic sources, Oral.

1st International Conference on Theoretical, Applied and Experimental Mechanics, Paphos, Cyprus, 17–20 June 2018

- P. Klejment, W. Dębski, A. Kosmala, Particle-based DEM model for simulating brittle cracks extension in rock-like materials during the hydraulic fracturing process, Oral.

36th General Assembly of the European Seismological Commission, Valletta, Malta, 2–7 September 2018

- L. Jaroszewicz, A. Kurzych, Z. Krajewski, K. Teisseyre, J. Kowalski, M. Dudek, Recordings of rotational motions resulting from artificial detonations by set of fiber-optic rotational seismometers, Oral.

5.9 Publications

ARTICLES

Telesca, L., and **Z. Czechowski** (2018), Relation between HVG-irreversibility and persistence in the modified Langevin equation, *Chaos* **28**, 7, 073107, DOI: 10.1063/1.5030680.

Pastén, D., **Z. Czechowski**, and B. Toledo (2018), Time series analysis in earthquake complex networks, *Chaos* **28**, 8, 083128, DOI: 10.1063/1.5023923.

Dębski, W. (2018), Dynamic stress drop for selected seismic events at Rudna copper mine, Poland, *Pure Appl. Geophys.* **175**, 4165–4181, DOI: 10.1007/s00024-018-1926-6.

CHAPTERS

Bielski, W., and R. Wojnar (2018), Stokes flow through a tube with wavy wall. **In:** J. Awrejcewicz (ed.), *Dynamical Systems in Theoretical Perspective*, Springer, Cham, 379–390.

Wojnar, R., and **W. Bielski** (2018), Gravity driven flow past the bottom with small waviness. **In:** P. Drygaś and S. Rogosin (eds.), *Modern Problems in Applied Analysis*, Birkhauser, Cham, 181–202, DOI: 10.1007/978-3-319-72640-3_13.

Czechowski, Z. (2018), Modelling of persistent time series by the nonlinear Langevin equation. **In:** T. Chelidze, F. Vallianatos, and L. Telesca (eds.), *Complexity of Seismic Time Series. Measurements and Application*, Elsevier, 141–160, DOI: 10.1016/B978-0-12-813138-1.00005-5.

Klejment, P., and **W. Dębski** (2018), Crack nucleation in solid materials under external load – simulations with the Discrete Element Method. **In:** *12th Int. Fatigue Congress (FATIGUE 2018), MATEC Web Conf.* **165**, 22019, DOI: 10.1051/mateconf/201816522019.

Klejment, P., N. Foltyn, A. Kosmala, and **W. Dębski** (2018), Discrete Element Method as the numerical tool for the hydraulic fracturing modelling. **In:** T. Zieliński, I. Sagan, and W. Surosz (eds.), *Interdisciplinary Approaches for Sustainable Development Goals*, GeoPlanet: Earth and Planetary Sciences, Springer, Cham, 217–235, DOI: 10.1007/978-3-319-71788-3_15.

Klejment, P., **W. Dębski**, and A. Kosmala (2018), Particle-based DEM model for simulating brittle cracks evolution in rock-like materials during the tensional fracturing process. **In:** E. Gdoutos (ed.), *Proc. First Int. Conf. on Theoretical, Applied and Experimental Mechanics. ICTAEM 2018*, Ser. Structural Integrity, Vol. 5, Springer, Cham, DOI: 10.1007/978-3-319-91989-8_47.

Jaroszewicz, L.R., A. Kurzych, **K.P. Teisseyre**, and Z. Krajewski (2018), Measurement of rotational events in regions prone to seismicity: A review. **In:** A. Okiwelu (ed.), *Geophysics*, IntechOpen, London, 19–39, DOI: 10.5772/intechopen.72169.

6. DEPARTMENT OF HYDROLOGY AND HYDRODYNAMICS

Jarosław Napiórkowski

6.1 About the Department

Under the framework of NHH02, the following objectives have been achieved.

- **Flood Risk Assessment Methods. The aim of this objective is to investigate:**
 - a) Hydrological projections and reconstruction of past hydrological conditions. Two methods of aggregating statistical models for estimation of flood quantiles are compared, i.e. averaging the magnitudes of quantiles of the same order from candidate distributions and averaging over the probabilities of non-exceedance of the fixed flow value from the individual models;
 - b) Closed-form expressions for asymptotic standard error of design quantiles in complex flood frequency models. Standard errors have been developed for: seasonal approach to annual maxima quantiles, two methods of model aggregation, and two-stage non-stationary flood frequency analysis;
 - c) The methods and errors of the flood estimation when there is no systematic observations and only historical floods are known, inference based on type II left side censored samples.
- **Uncertainty related to the derivation of flood inundation extent including observations based on tele-detection:**

The main goal of the studies undertaken is the development of a methodology for the derivation of future projections of flood inundation extent. The idea of an emulator of a flow routing model is applied to shorten the computation costs. The research is further extended towards an application of remote sensing based on unmanned aerial vehicles (UAV) for the development, calibration and validation of distributed flow routing models. The application of low-cost, well georeferenced UAV images of river shorelines is an unprecedented source of distributed observations.

- **Modelling of transport processes. The aim of this objective is to investigate:**
 - a) Water-vegetation interface in open channel flow. The results indicate that seasonality significantly affects the shear layer dynamics in vegetated channels, with implications on lateral transport of mass and momentum. We demonstrate how vegetation can be incorporated into channel designs, to improve resilience to flooding, control the transport of substances, and how the vegetation encroaches on fluvial sandbars. As far as the interactions between turbulent flow and representative flexible submerged vegetation are concerned, results showed that both morphological and biomechanical traits may cause certain flow disturbances, where water velocity and turbulence were diminished;
 - b) Effect of water-air heat transfer and impact of initial conditions on the prediction of the spread of thermal pollution in a river;
 - c) Experimental studies on gravity currents and sedimentation of particles in complex ambient conditions. A methodology for experimental study of gravity currents and measurement methodology using image analysis methods have been developed and tested.
- **Modelling of hydrological processes. The aim of this objective is to investigate:**
 - a) Innovative metaheuristics and their application to the calibration of hydrological models. A detailed review and intercomparison of metaheuristics that belong to the very successful JADA and SHADE family of methods has been given. Based on this experience, an important innovation has been added to four recent L-SHADE variants. It was shown that the modified versions outperform former algorithms on a large number of optimization problems;

- b) Relationship between calibration time and final performance of conceptual rainfall-runoff models. Two models were tested (HBV and GR4J), each applied with or without error correction procedure, and with three calibration procedures (GLPSO, MDE_pBX, and SPS-LSHADE-EIG) at five catchments Biała Tarnowska and Supraśl, Poland, Cedar River, Fanno Creek, and Irondequoit Creek, USA located in temperate climatic conditions;
- c) Performance of the air2stream model that relates air and stream water temperatures. In the study 12 optimization algorithms were tested for the calibration of the air2stream model with eight parameters, for hydro-meteorological daily data from six streams located in USA, Poland, and Switzerland. It was shown that the performance of the air2stream model largely depends on the selected calibration procedure;
- d) The hydrology of a small Arctic permafrost catchment. The overall aim of the study was to examine the relationships between temporal changes of active layer depth and hydrological model parameters, together with variation in the catchment response. The analysis was carried out for the small unglaciated catchment Fuglebekken, located in the vicinity of the Polish Polar Station Hornsund on Spitsbergen.

6.2 Personnel

Head of the Department

Jarosław Napiórkowski
Professor

Professors

Renata Romanowicz
Paweł Rowiński

Associate Professors

Krzysztof Kochanek
Marzena Osuch
Adam Piotrowski

Assistant

Ewa Bogdanowicz
Monika Kalinowska
Emilia Karamuz
Iwona Kuptel-Markiewicz
Anna Łoboda
Magdalena Mrokowska
Michael Nones

Research Assistant

Joanna Doroszkiewicz

PhD Students

Łukasz Przyborowski, Poland; Robert Bialik – PhD supervisor

6.3 Main research projects

- Impact of expected climate change on water temperatures of selected Polish rivers, A. Piotrowski, National Science Center Poland, 2017–2020;
- Hindcasting and projections of hydro-climatic conditions of Southern Spitsbergen, M. Osuch, National Science Center Poland, 2018–2021;

- Hydrological research using unmanned aerial vehicles (UAV), J. Doroszkiewicz, E. Karamuz, MN, 2017–2018;
- Comprehensive hydrological research of the Świder basin using modern measurement techniques, E. Karamuz, M. Osuch, A. Łoboda, MN, 2018–2019;
- Seaweed reaction to mechanical stresses – a lesson of biomechanics of marine plants, A. Łoboda, MN, 2018–2019;
- Experimental studies on the impact of density gradient in a liquid column on settling dynamics of non-spherical particles, M. Mrokowska, MN, 2018–2020;
- Relationship of permafrost with geomorphology, geology and cryospheric components based on geophysical research of the Hans glacier forefield and its surroundings. Hornsund, Spitsbergen, M. Osuch, National Science Center Poland, 2017–2019;
- Field experimental investigation of hydrodynamics of water flow-vegetation-sediment interactions at the scale of individual aquatic plant, A. Łoboda, Ł. Przyborowski, National Science Center Poland, 2015–2019.

6.4 Instruments and facilities

Equipment

- Model 801 Electromagnetic Open Channel Flow Meter
- Model 10 Field Fluorometer au-005-ce (sn. 6857)
- Fluorometer: (sn. 800606)
- YSI Professional Plus handheld multiparameter meter
- GPS LEICA gx1230gg (sn. 467006)
- ProODO Optical Dissolved Oxygen Instrument
- A wireless weather station Pro2™ Plus including UV and Solar Radiation Sensors
- ADCP – acoustic Doppler current profiler model RiverSurveyor S5 (SonTek)
- Bench Top Testing Machine 5ST (Tinius Olsen)
- ADV – acoustic Doppler velocimeter (Sontek)
- ADV – acoustic Doppler velocimeter (Nortek) (×2)
- Cameras: GoPRO HERO 3 (×1), GoPRO HERO 3+ Silver (×2), GoPRO HERO 3+ Black (×2)
- Microscope model Delta optical Genetic Pro Trino (Delta Optical)

Laboratory

Main equipment in Hydrodynamic Models Laboratory:

- Sony video camera
- high-resolution macro image acquisition system
- refractometer
- two hydraulic channels

6.5 Research activity and results

Brief description/abstracts/summaries of some of the achievements of the Department's staff:

FLOOD RISK ASSESSMENT METHODS

The parametric instability of hydrological models was analysed to develop hydrological projections as well as reconstruction of past hydrological conditions. We compared the two methods of aggregating statistical models for estimation of flood quantiles, i.e., averaging the magnitudes of quantiles of the same order from candidate distributions, and averaging over the

probabilities of non-exceedance of the fixed flow value from the individual models. The formulas for the asymptotic standard error of design quantiles were developed for both averaging procedures. A Monte Carlo simulation was used to illustrate the coverage probability that the confidence interval contains the true value of interest. The case study of two distributions with almost equal weights is presented in Fig. 1. The work resulted in developing methods of estimating flood quantiles using a multi-model approach, which gives more accurate and robust estimates of quantiles with long return periods. This method is currently being improved and developed.

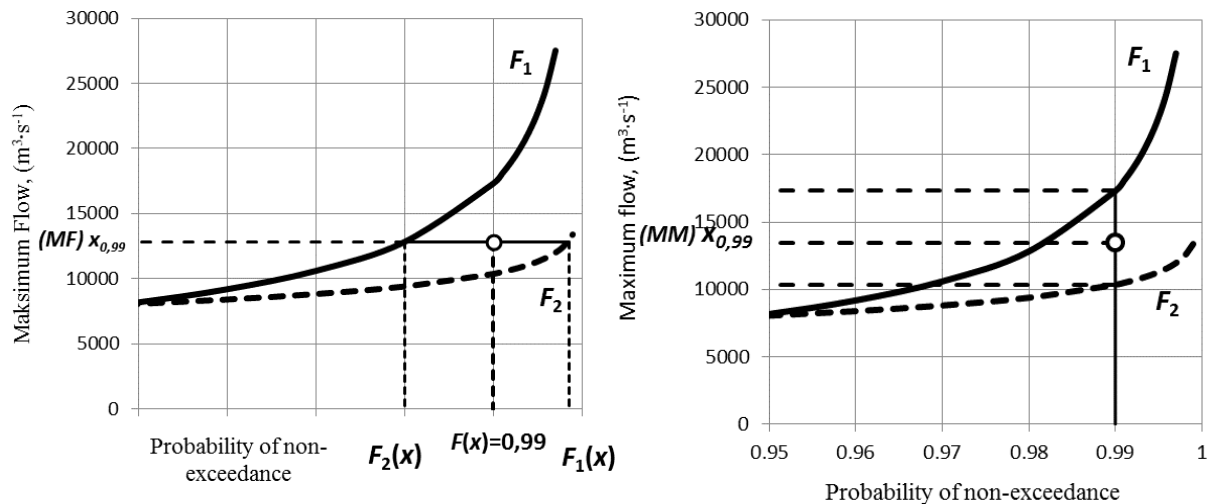


Fig. 1. Two ways of aggregating/averaging distributions: (a) aggregation according to magnitudes of quantiles (MM), and (b) aggregation according to the probability of non-exceedance (MF) (after Markiewicz et al. 2018).

In areas where floods occur in two distinct seasons in a year, a seasonal approach to estimation of annual maxima (AM) quantiles is required. The problem can be identified as an estimation of AM quantiles based on two-component distribution and assessment of accuracy/uncertainty of AM quantiles obtained in such a way. The seasonal maxima distributions are estimated for each season separately using any estimation method. It is assumed that in each year the seasonal maximum flow is regarded as a flood in the Flood Frequency Analysis (FFA), so its distribution is a continuous one, and, moreover, that seasonal maxima flood flows are mutually independent. The main subject is a derivation of a closed-form expression for accuracy of AM quantile estimated from two-component distribution. In practice, seasonal statistical models can differ not only in respect of distribution types and parameters but also in estimation methods used. The formula has been developed for asymptotic standard error of AM flow quantile estimate applicable for any pair of seasonal distributions commonly used in the FFA and any parameter estimation method with known variances of quantiles of the component distributions. It is the function of PDFs, CDFs, and the quantile variances of both seasonal distributions. The version for dependent seasonal maxima has also been developed in the case of the Archimedian copula function and Inference Functions for Margins (IFM) method of estimation of copula parameter. As an example, probabilities p_1 and p_2 for the hydrological station Sarzyna, showing the domination of winter or summer floods within the range of annual maximum flow, are shown in Fig. 2.

Additionally, as part of work on the analysis of the risk of flood occurrence, analytical formulae were derived to determine the confidence intervals of design quantiles for the methods used in the non-stationary analysis of the frequency of floods. In addition, software was devel-

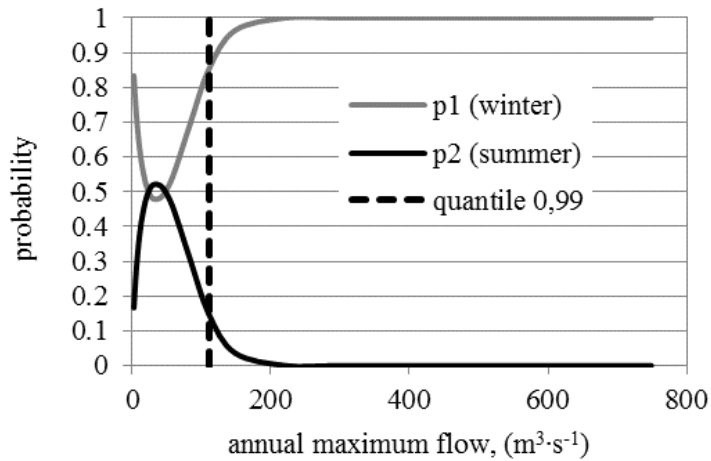


Fig. 2. Probabilities showing the domination of winter or summer floods within the range of annual maximum flow (after Strupczewski et al. 2018).

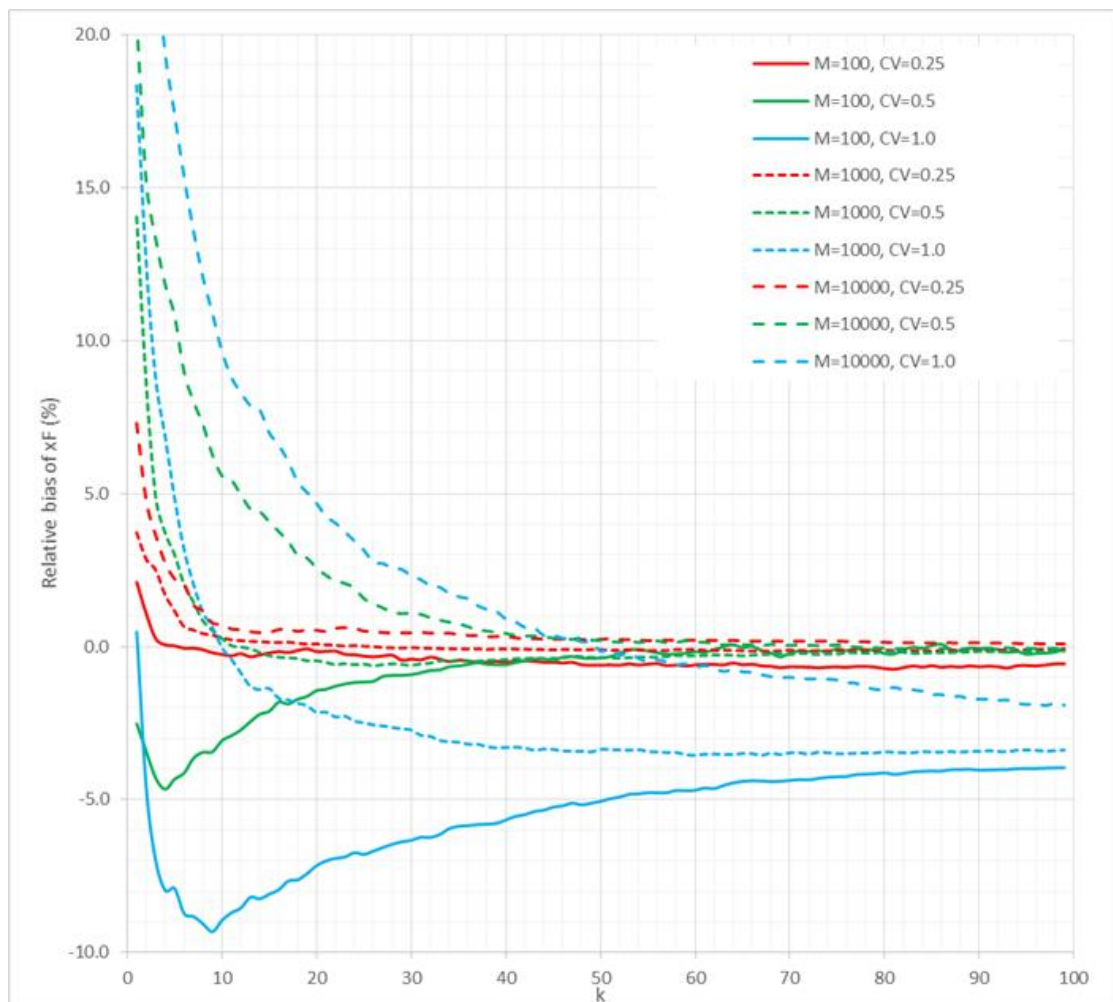


Fig. 3. Bias of the upper quantile estimate by means of heavily censored dataset of historical information.

oped to calculate the limits of confidence intervals by derived analytical formula. The results were compared with those obtained by Monte Carlo techniques. It is worth noting that the above-mentioned analytical elaboration of standard errors of flood quantiles is an original achievement of our team. Derived patterns were announced at the Third Congress of Polish

Hydrologists; however, they are still the subject of research and testing and will soon be published in a major international journal.

As part of the flood frequency task, research on the quality of flood estimation was also continued when only historical or prehistoric historical information about old floods is known. Such datasets are called heavily censored ones. The historical information is often incomplete, i.e., limited to the biggest floods, and culmination discharge is roughly estimated by means of high flood marks and historical logs. It is assumed that both data sets, complete and incomplete (heavily censored) historical series represent the same population. Therefore, these two sets can be combined into one sample modelled by the statistical model whose parameters and quantiles are estimated. It turns out that using only historical information and appropriate statistical techniques, one can get a relatively accurate estimation of quantiles with a long return period – the quantiles bias is much smaller than expected. Preliminary results of the study were announced at the Congress of Polish Hydrologists. As an example, we present the diagrams (Fig. 3) showing the errors of estimation of quantile $x_T = 100$ years for heavy censored datasets when k elements of the historical peak flows are known within M -long historical period for various coefficients of variation (CV). The historical data were generated by means of the Gumbel distribution function, and then the quantiles are estimated by the same model (true assumption of the distribution function). Contrary to our expectations and theoretical features of the maximum likelihood method, the bias of quantile for heavily-censored sample does not disappear even for large k and M .

UNCERTAINTY RELATED TO THE DERIVATION OF FLOOD INUNDATION EXTENT INCLUDING OBSERVATIONS BASED ON TELE DETECTION

The main result of studies undertaken is the development of a methodology for the derivation of future projections of flood inundation extent until the end of the 21st century. The idea of the emulator of a flow routing model was applied to shorten the computation costs of flow routing model. This idea is further explored and the review of analytical solutions to flow routing was presented and the relevance with the emulator-based flow routing model was shown. The research on flow routing in open channels was further extended towards the analysis of changes of river flow and its causes.

Figure 1 presents the comparison of two maximum inundation contours at the Tuchow meander. The first contour is derived using the distributed MIKE11 model (blue line), the second (green line) presents the same maximum inundation area obtained using the MIKE11 model emulator. The results show that the differences between both contours are very small.

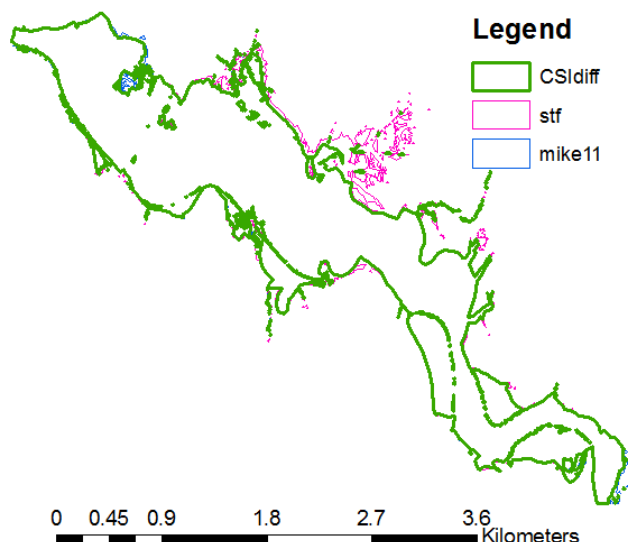


Fig. 1. Maximum inundation extent of MIKE11 (blue), emulator of MIKE11 (magenta) for the year 1997 for a part of the Tuchow meander, and the CSI based difference (green) (after Doroszkiewicz et al. 2018).

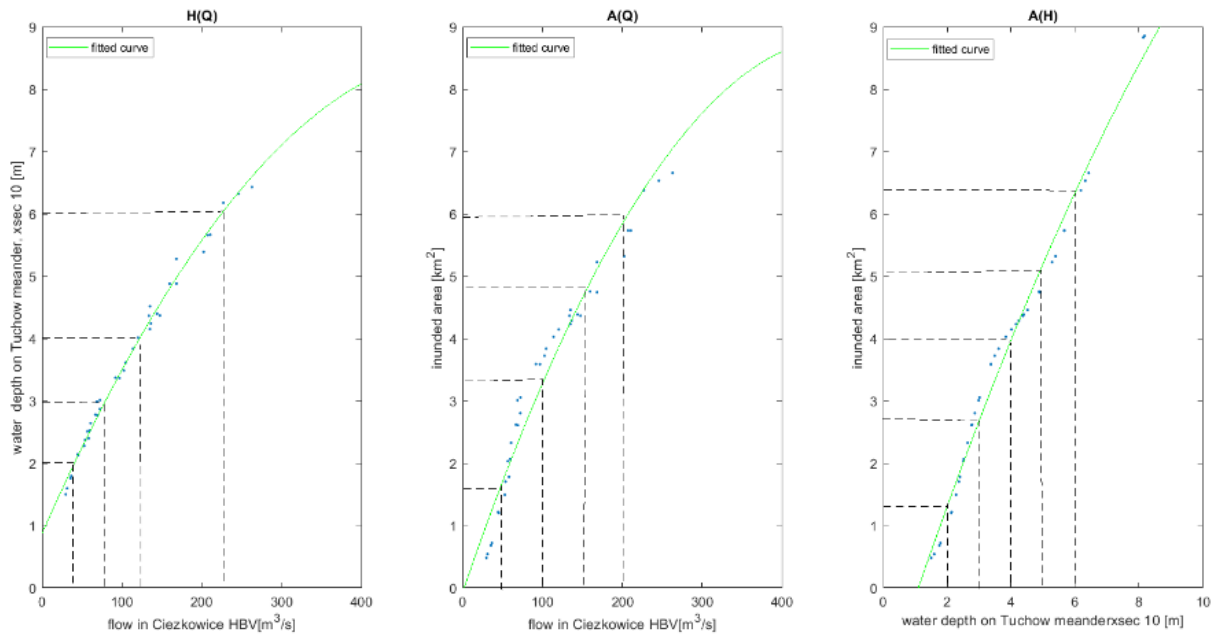


Fig. 2. Dependence of hydrological input (annual maxima) and routing model predictions for Tuchow meander for the reference period 1971–2010: (a) water depth values on 10th cross-section of meander versus maximum annual flow, (b) inundation areas of Tuchow meander versus maximum annual flow, and (c) inundation area versus maximum annual water depth at 10th cross-section of Tuchow meander; blue dots denote the data, green lines denote the fitted curve to square polynomial (after Doroszkiewicz et al. 2018).

Figure 2 presents the projected relationships between the water depth at Tuchow meander cross-section and flow in the Cieżkowice upstream (left-hand panel), relation of maximum inundation area and annual maximum flow in Cieżkowice (middle panel), and inundated area extent versus water depth at Tuchow meander (right-hand panel).

Those results may be used to derive the sensitivity of inundation area extent to changes of flow upstream related to climate changes.

In order to provide an uncertainty assessment of the projections, apart from the uncertainty related to the MIKE11 emulator, also the uncertainty of MIKE11 distributed predictions is required. With this aim in mind, a series of experiments were planned using the unmanned aerial vehicles (UAV).

Figure 3 presents a report from the UGCS photogrammetry processing tool obtained on the Tuchow meander subreach of the Biała Tarnowska. The aim of the experiment was providing the observations of shorelines at the meander studied in the paper of Doroszkiewicz et al. (2018) to help in the validation of a distributed model and its emulator and to derive the uncertainty bands of the predictions of inundation extent. The experiment is the first of the series planned for the future. Its results were used to improve the methods of obtaining the distributed images from the UAV.

Remote sensing based on unmanned aerial vehicles (UAV) is a novel approach and it is becoming popular due to its flexibility and fast decreasing costs. One of its most advantageous features is the possibility of acquisition of field data independently of weather conditions and a possibility of straightforward analysis of georeferenced results nested in Geographic Information System. In particular, UAV can provide precise information about the location of river shorelines. This information is particularly useful for the development, calibration and validation of distributed flow routing models. The application of low-cost, well georeferenced UAV images of river shorelines is an unprecedented source of distributed observations.

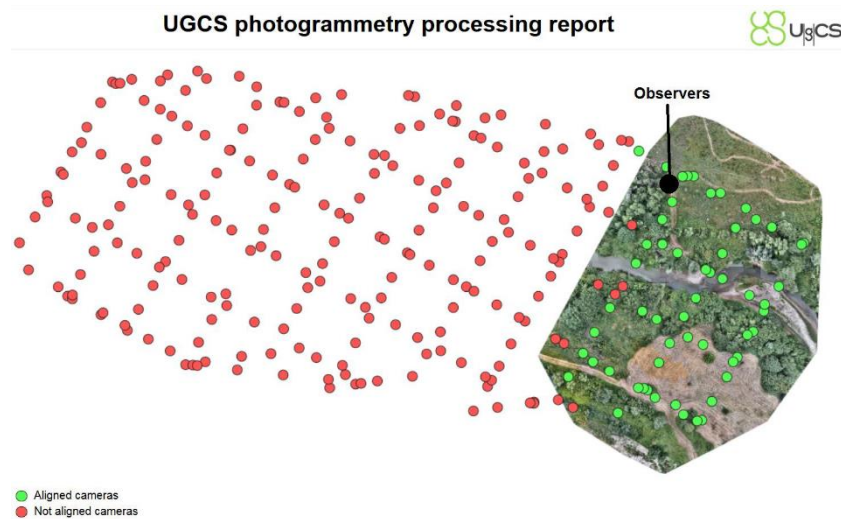


Fig. 3. Report from the UGCS photogrammetry processing tool with flight pathways (red and green points).

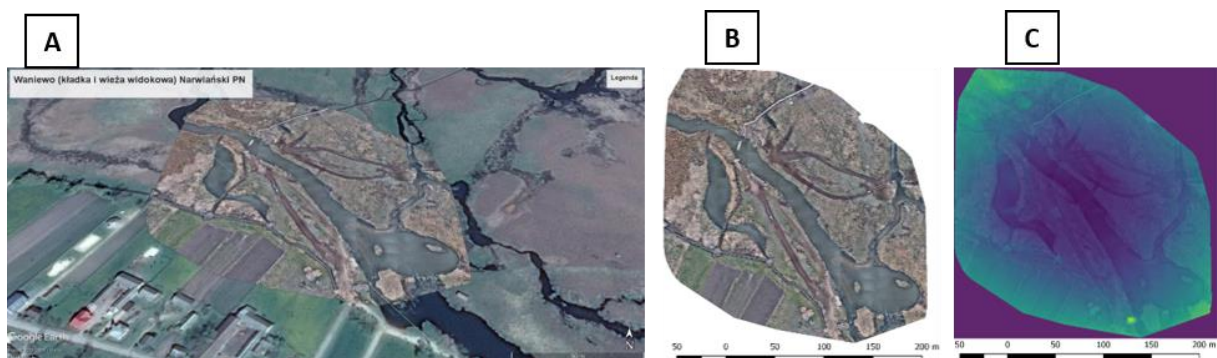


Fig. 4. Orthophotomap (A, B) and DSM (C) from the UAV aerial photograph (Waniewo – Narew National Park).

Further work aimed at exploring the potential for this approach to provide valuable information about the river shorelines at varying flow velocities. The River Świder, southeast of Warsaw and the Upper Narew River (Fig. 4) are used as case studies. We applied DJI PHANTOM 4 unmanned quadcopter which provides sequences of pictures. After the geoprocessing, they serve as a source of spatial digital data. UgCS software is used for campaign planning and post-processing of collected data. The HEC RAS 1-2-D distributed model will be used for flow routing. The calibration and validation of its roughness coefficients will be performed using vector-fitting criteria based on the comparison of modelled and observed river shorelines.

Figure 4 presents orthophotomap and Digital Surface Model (DSM) of the side in the neighborhood of Waniewo in Narew National Park. The upper panel shows the general location of the area studied; the lower left panel presents detailed UAV photograph of the river reach and the right lower panel shows the DSM coverage. These images are used as a documentation of the present state of the Narew case study area.

MODELLING OF TRANSPORT PROCESSES

Turbulence at water-vegetation interface in open channel flow

Riparian vegetation generally presents a complex and seasonally variable morphology that, together with its reconfiguration behaviour, deeply affects the flow in channel-vegetated bank

systems. The aim of this research was to investigate the influence of foliation and flexibility-induced reconfiguration on velocity statistics, onset and coherence of turbulent structures, and turbulence anisotropy across the shear layer formed at the horizontal interface between vegetation and open water. The investigations were conducted in a laboratory flume that was partly vegetated to mimic emergent woody plants with underlying grassy understory. The natural-like vegetation exhibited a realistic reconfiguration behaviour with density and morphological characteristics comparable to those of woody riparian species. Seasonality effects were investigated using the same emergent woody vegetation under foliated and leafless conditions (see Fig. 1).

The mean and turbulent flow structure was determined with acoustic Doppler velocimetry, and dynamic plant motions were derived from video footage. The presence of morphologically complex plants, their reconfiguration behaviour and seasonal variability profoundly affected the overall characteristics of the flow. Foliation induced stronger cross section-scale mixing effects, whereas for the leafless vegetation the local effects induced by the stems were predominant. The interface coherent structures were found to be two-dimensional with a characteristic frequency consistent with the canonical mixing layer theory.

Reconfiguration and dynamic plant motions affected the onset and coherence of interfacial large-scale turbulent structures by altering the vegetative drag and the drag discontinuity at the interface. Our results indicated that reconfiguration and seasonality significantly affect the shear layer dynamics in natural partly vegetated channels, with implications on lateral transport of mass and momentum through the cross-section.

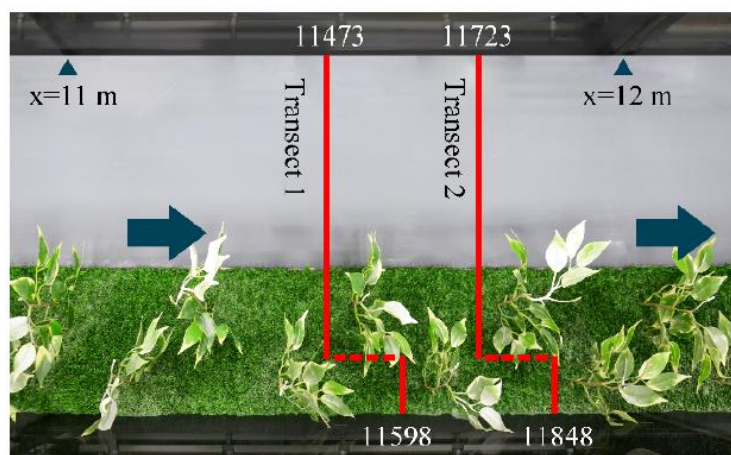


Fig. 1. Plan view of the investigated transects for the foliated case (after Caroppi et al. 2019).

References

- Caroppi, G., K. Västilä, J. Järvelä, P.M. Rowiński, and M. Giugni (2019), Turbulence at water-vegetation interface in open channel flow: Experiments with natural-like plants, *Adv. Water Resour.* **127**, 180–191, DOI: 10.1016/j.advwatres.2019.03.013.

MODELLING OF TRANSPORT PROCESSES

Flow structure through a fluvial pool-riffle sequence

Pools and riffles in gravel-bed rivers have a major effect on the variables of the flow equations. Obtaining measurements of these variables requires comprehensive research conducted in rivers. Detailed measurements were taken from one reach of the Kaj River, Iran (Fig. 1). The subsequent results showed a phase shift for: X-component of velocity, near-bed velocity in X and Z directions, and bed shear stress versus bed elevation profiles. In the riffle section, vectors of



Fig. 1. Local map of the selected reach of Kaj River (after Najafabadi et al. 2018).

the vertical velocity component were oriented towards the bed. However, in the pool section, vectors were oriented downward close to the bed, and upward at higher levels. Quadrant analysis for the pool illustrated the dominance of ejection and sweep interactions near the bed and near the water surface, respectively. However, in the riffle, outward interactions were dominant near the bed, and sweep interactions were dominant near the water surface. The spectral analysis revealed that flow over pool-riffle does not follow the scaling regime of Kolmogorov, used to illustrate the slope of $-5/3$ in the inertial sub-range.

MODELLING OF TRANSPORT PROCESSES

Vegetation as a tool for nature-based solutions (NBS) in river management

New sustainable, cost-effective solutions are urgently needed for river management since conventional practices have posed serious ecological threats on streams, rivers, and the surrounding riparian areas. Besides addressing the societal needs, e.g. for flood management, river management should increasingly address the ecosystem requirements for improved water quality and biodiversity. We argue that it is not feasible to solve existing and future river management

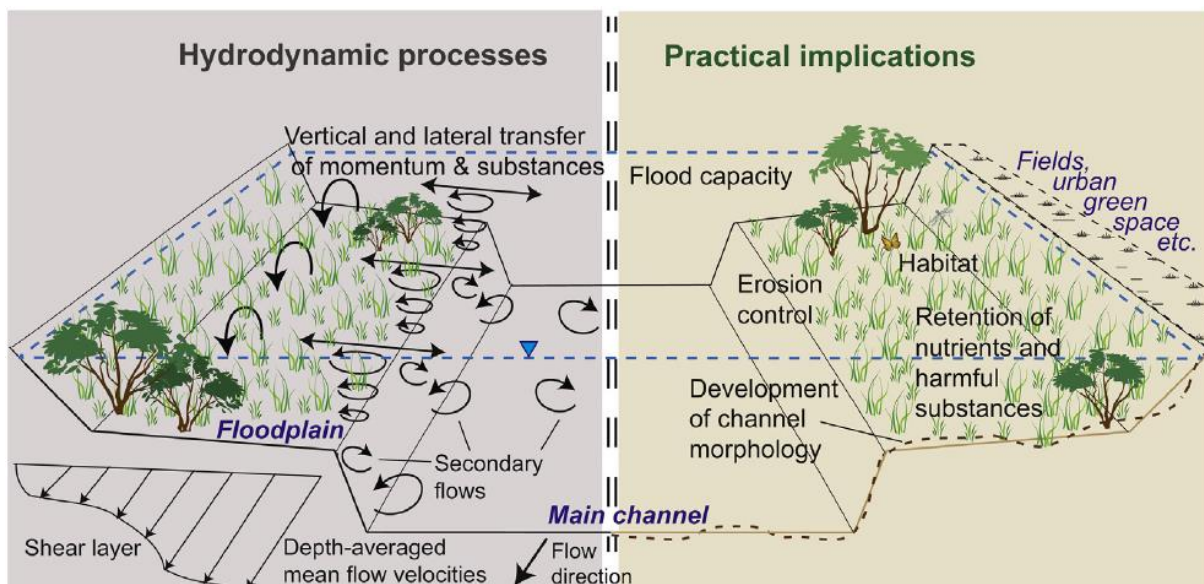


Fig. 1. Two-stage channel design offers flood capacity while the floodplain vegetation controls the sediment deposition and nutrient retention (after Rowiński et al. 2018).

challenges with intensive restoration projects. Instead, we believe that less resource-intensive solutions using natural channel processes and features, including vegetation, should be investigated. Besides directly supporting biota, aquatic and riparian vegetation traps, takes up and helps to process nutrients and harmful substances, and thus this paper emphasizes vegetation as a tool for NBS in river management. It has been shown that the fate of substances in channel systems is largely controlled by abiotic and biotic processes facilitated and modified by vegetation, including flow hydrodynamics, channel morphology, and sediment transport. Subsequently, we demonstrate how vegetation can be incorporated into channel designs, focusing on a two-stage (compound) design to improve resilience to flooding, control the transport of substances, and enhance the ecological status (Fig. 1). As a conclusion, clever use and maintenance of vegetation present an unused potential to obtain large-scale positive environmental impacts in rivers and streams experiencing anthropogenic pressures.

MODELLING OF TRANSPORT PROCESSES

The vegetation encroachment on fluvial sandbars

Starting from the case study of a reach of the Po River (Italy), monitored during the last two years in collaboration with the University of Bologna, we are studying the vegetation encroachment on fluvial sandbars by means of satellite imagery, evaluating the changes of the Normalized Difference Vegetation Index (NDVI). This index can be validated against field information retrieved from a fixed video camera that operated in 2017–2018, after rectifying the images based on ground control points. The study will provide additional insights into the ongoing discussion about the oversimplification of this river because of a decrease of water/sediment discharge due to the anthropogenic pressure. Indeed, a lower variability of flow and an increase of drought periods contributed to provide optimal conditions for the vegetation growth, contributing to stabilize the existing bars and to trap suspended sediment.

Within the same collaboration, several data were acquired regarding a tributary of the Po River, the Secchia River. In this case, our work is towards the development of a rating curve between the concentration of suspended sediments and the backscatter signal coming from a horizontal Acoustic Doppler Current Profiler. Most of the work is already done, but a comparison with similar data of the Albanian river Devoll will be done in the next months.

Thanks to the several data available for both rivers, aside from these studies some numerical simulations will be performed, aiming to provide future scenarios in response to changing hydrology (climate change) or possible management strategies. These simulations will be made using freeware codes like Hec-Ras and iRIC, as well as commercial models like CCHE2D, depending on the aims, which are still under evaluation.

MODELLING OF TRANSPORT PROCESSES

Impact of initial conditions on the prediction of the spread of thermal pollution in rivers

Thermal pollution is a result of any unnatural process that changes ambient water temperature. It is often caused by discharged heated water used for cooling purposes. Since the increase of water temperature may be dangerous for the environment, the prediction of possible increase of water temperature caused by an artificial heat source is of crucial importance. Such predictions are usually made using numerical models where the choice of initial conditions for which the prediction is made constitutes a key problem. In principle, such predictive computations should be performed for the most severe situations from the environmental point of view. But the choice of such conditions usually requires an in-depth analysis of the historical data for a particular case.

The influence of initial conditions on the prediction of the increase of river temperature below the point of release of heated water for a designed power plant has been analysed in this

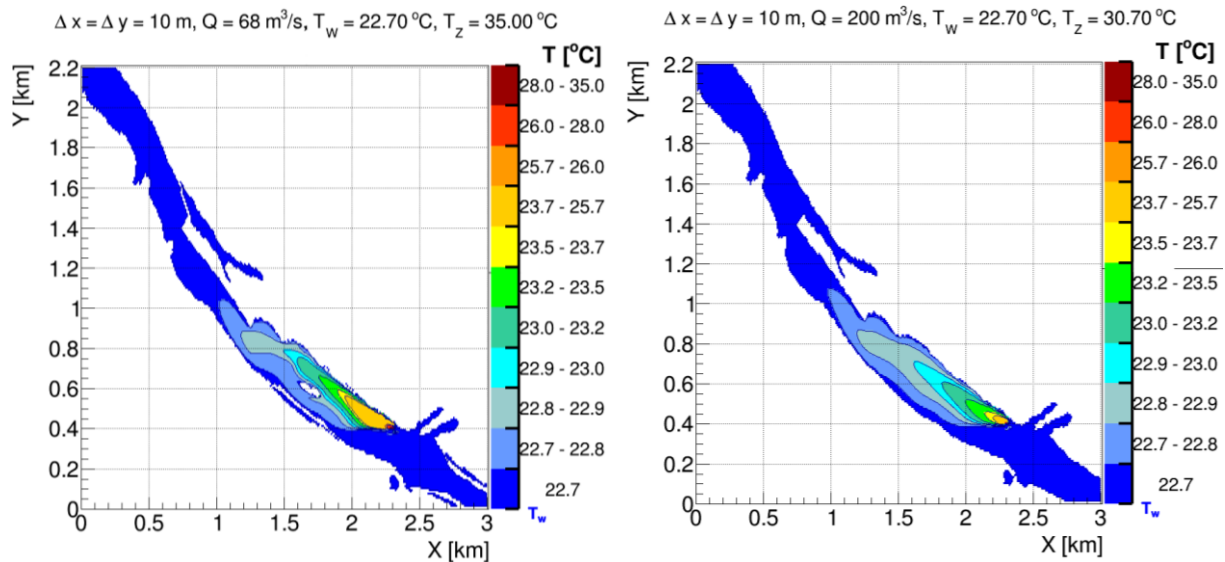


Fig. 1. Predicted 2D temperature distributions within the considered river reach for the selected case – the worst (left) and the best (right) scenarios (after Kalinowska et al. 2018).

study. The results for different assumed values of river flow and different temperatures of the discharged heated water have been presented. The two-dimensional in-house RivMix model has been used to simulate the temperature distribution whereas the two-dimensional depth-averaged turbulent open channel flow model CCHE2D has been used to simulate the velocity fields and the water depths for the selected flows of the river.

We fully realize that the influence of initial conditions on final results in boundary value problems dissipates and the temperatures of water tend to the same values no matter what initial conditions we set. However, the speed at which this influence dissipates reflects different patterns of the transport of the heated water plume. This pattern is crucial since we are extremely interested in determining in which area the temperature of heated water may pose a threat to the biological life in the stream. The study is related to a designed hydro-engineering construction in a lowland river. The focus of this study was on the choice of initial conditions, such as river flow and temperatures of ambient and released water. Those conditions influence the detailed velocity field, water depths, bed shear stresses and, consequently, the dispersion coefficients which in turn influence the solutions of heat transfer equations and thus the temperature distributions (Fig. 1).

MODELLING OF TRANSPORT PROCESSES

Effect of water-air heat transfer on the spread of thermal pollution in rivers

While working on practical problems related to the spread of thermal pollution in rivers, we face difficulties related to the collection of necessary data. However, we would like to predict the increase in water temperature at the best accuracy to forecast possible threats to the environment.

In most cases in the mid-field zone, omission of all terms related to heat exchange with the environment including the heat exchange with the atmosphere is recommended. Not perfect input data may in some cases introduce a much larger error to the final results than just simple omitting of the heat fluxes terms (Fig. 1). The problem is especially important in practical cases when we deal with limited and not ideal data. We of course fully realize that in some applications it is necessary to include the heat exchange with the atmosphere and/or other heat fluxes. The situation very much depends on the considered case and time and space scale, to

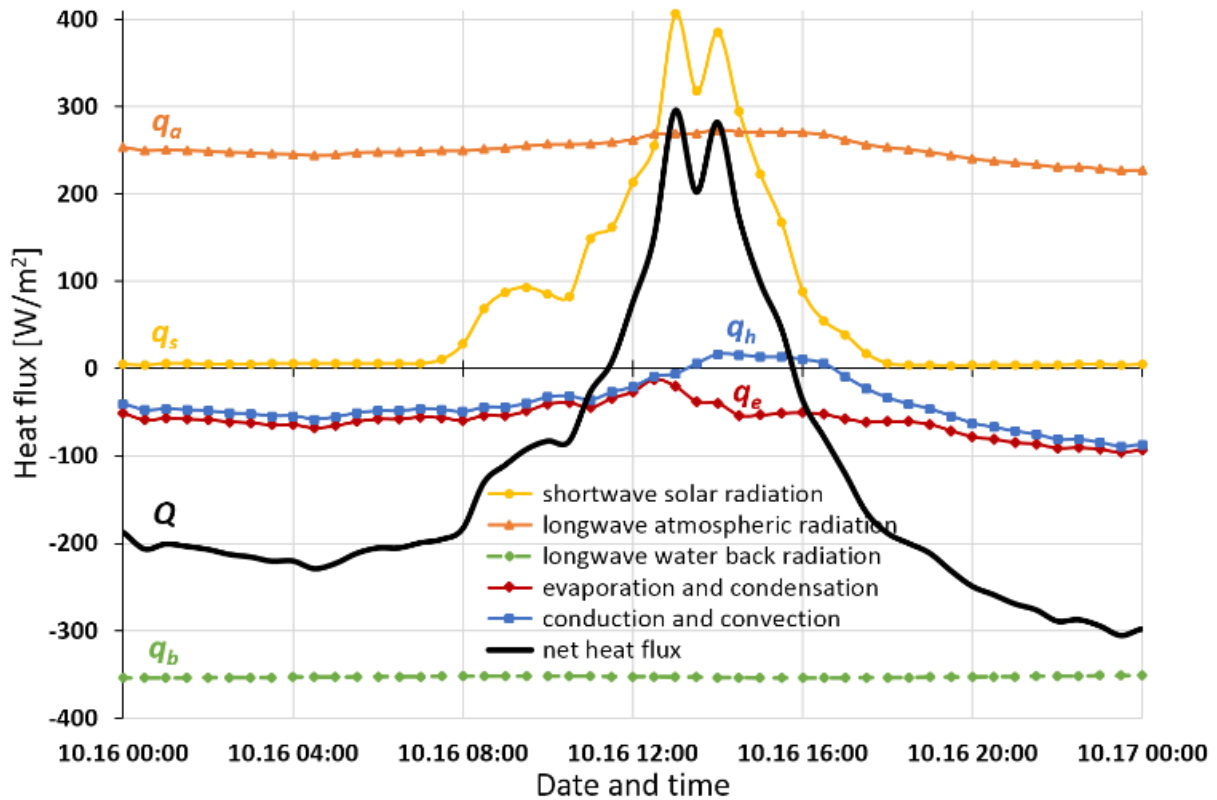


Fig. 1. Heat fluxes exemplary values calculated for a selected case over the day (Narew River, Poland, 16 October 2013) (after Kalinowska 2019).

decide whether 1, 2 or 3D approach is appropriate and which additional heat exchange processes should be taken into account.

First, the expected outcome together with the appropriate time and space scale should be defined. Next all affecting processes should be analysed subject to their significance and the availability of necessary input data, but also taking into account all other errors that may be committed during the calculations.

In the cases where the heat exchange with the atmosphere estimation is necessary, it is important to bear in mind that its estimation is based on empirical formulae that depend on many uncertain parameters. To be precise it will be necessary to measure many parameters directly on the site taking into account their space and time dependence to adjust the applied empirical formula to the current conditions.

In most cases for various reasons, there is not enough data to perform all the necessary calculations and prediction must be done based on existing historical, often limited and incomplete, sometimes also inaccurate data, as has been shown using two case studies presented in the paper. Therefore, in practical applications, heat exchange with the atmosphere estimation is full of judgements and extremely subjective. The most problematic to estimate is the wind speed function and atmospheric emissivity formulae. The most fragile to local conditions are measured shortwave solar radiation and wind speed value.

References

Kalinowska, M.B. (2019), Effect of water–air heat transfer on the spread of thermal pollution in rivers, *Acta Geophys.* **67**, 597–619, DOI: 10.1007/s11600-019-00252-y.

MODELLING OF TRANSPORT PROCESSES

Flow-biota-sediment interactions

The investigation of the hydrodynamics of water flow-vegetation interactions depends on three groups of plant characteristics: (1) plant morphology characteristics, (2) plant material characteristics, and (3) flow-plant interaction characteristics (Fig. 1a). These interplays result from the interaction of three groups of forces that control the hydrological regime, i.e., flow-induced forces (e.g., drag forces), plant-induced forces (e.g. buoyancy forces) and plant-reaction forces (e.g., bending forces) (Fig. 1b). The study of these features and their connections was the aim of the study of research group (Anna Łoboda, PhD, and Łukasz Przyborowski, MSc) from the Department of Hydrology and Hydrodynamics. Measurements were conducted on different rivers, e.g., the Wilga River and the Świder River (Fig. 2).

Based on a series of biomechanical measurements of three freshwater plants, i.e., *Potamogeton pectinatus* L., *Potamogeton crispus* L., and *Elodea canadensis* Michx., the analysis of biomechanical properties and their seasonal variability of aquatic plants rooted in flowing

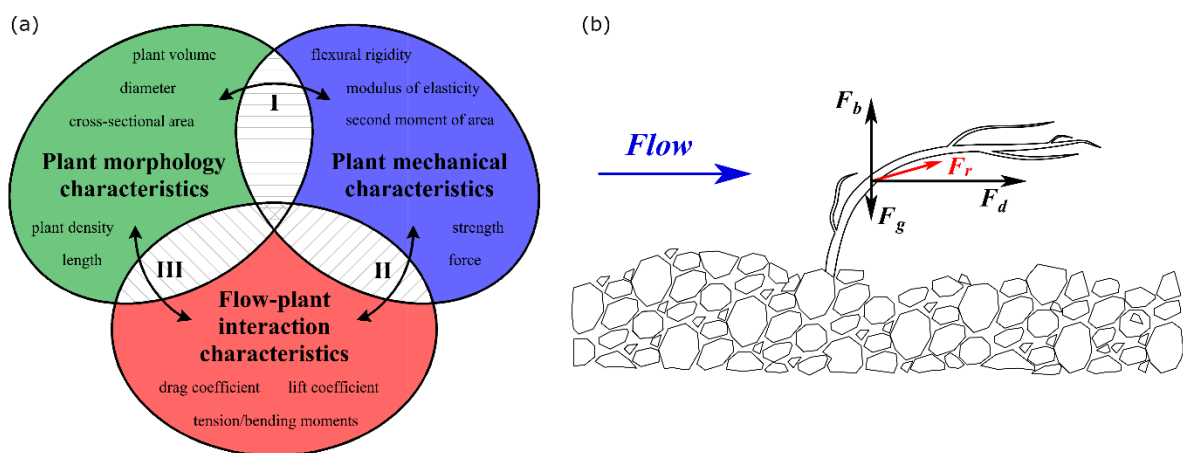


Fig. 1. A schematic of the divisions of plant characteristics (a) and the main forces acting upon a plant stem: the drag force F_d , the buoyancy force F_b , the gravity force F_g , and the resultant force of these loads F_r (b) (after Łoboda et al. 2018b).

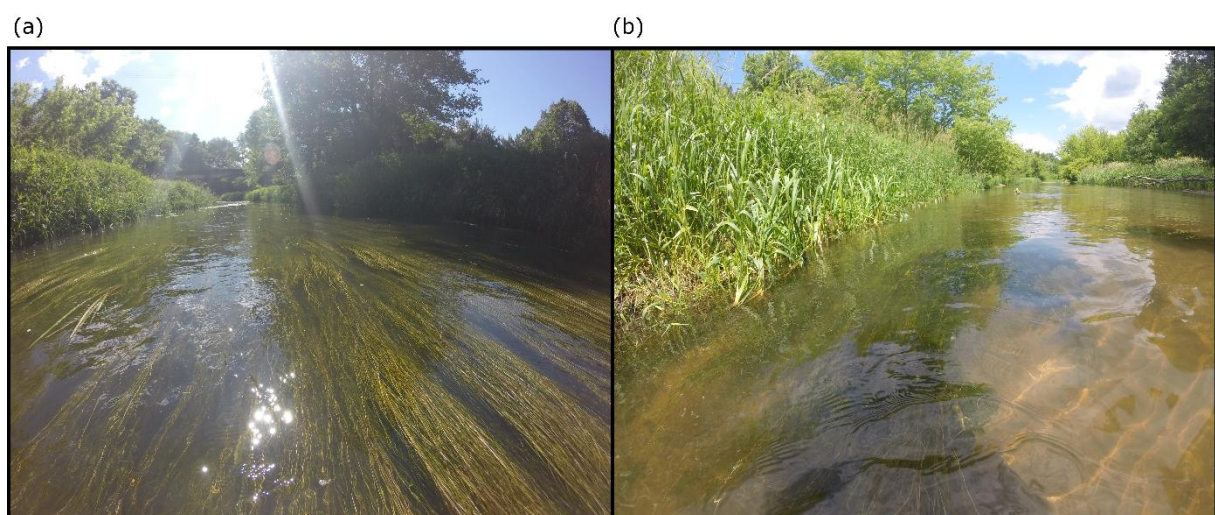


Fig. 2. The channel of the Wilga River (a) and the Świder River (b) during vegetative growth at the sampling sites (Fig. 2a after Łoboda et al. 2019).

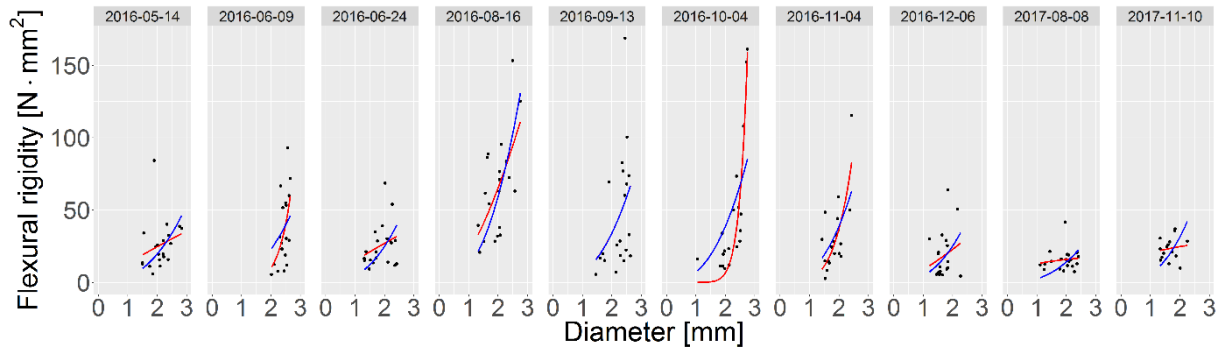


Fig. 3. Model matching for *P. crispus*. The red line represents case 1 (detailed approach), and the blue line represents case 2 (general approach) (after Łoboda et al. 2018b).

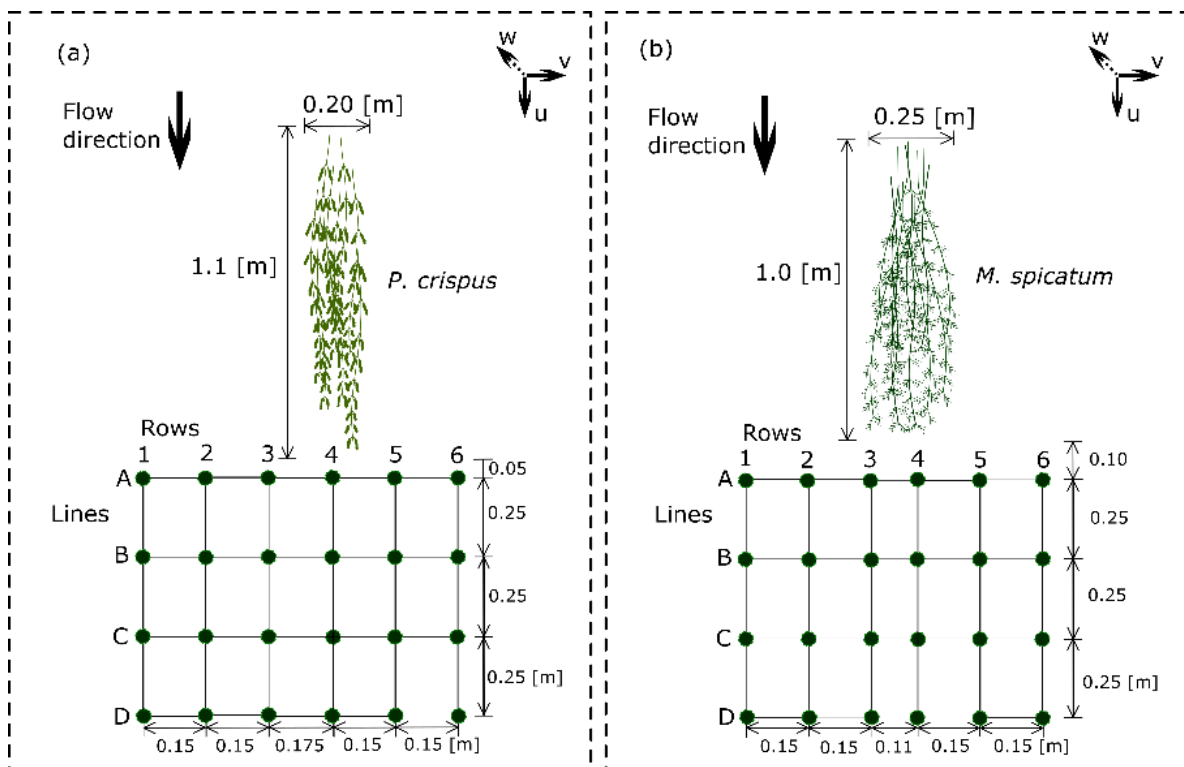


Fig. 4. Scheme of vertical profiles of velocity measurements downstream two aquatic plants in July and August 2017 (after Przyborowski et al. 2019).

waters was carried out to develop a model that shows the correlation between the diameter of the stem and its flexural rigidity, i.e., $EI = a \times db$, where EI is the flexural rigidity, d represents the diameter of the stem, and a and b represent the model coefficients determined using nonlinear regression. The flexural rigidity has a meaningful impact on drag forces, as it modifies the adaptive mechanisms of the plant and the flow patterns, where a flexible plant generates much lower resistance than vegetation with rigid stems, producing eddies. The EI values can be determined using a detailed approach that includes the effect of seasonality on the flexural modulus and plant morphology, or a general approach, in which changes in the diameter of stems play a smaller role (Fig. 3). The model is the response to one of the interdisciplinary problems of aquatic ecosystems, namely, the lack of biomechanical models of river plants. The proposed formula would allow for the estimation of the flexural rigidity based on the stem morphology, which is necessary to determine the drag generated by hydrophytes in rivers.

The second part of the studies was the search for the interactions between turbulent flow and representative flexible submerged vegetation. It was conducted by a series of field experiments from 2017 in the Świder and Jeziorka Rivers, which are the lowland, sandy-bed rivers. In the experiments, acoustic Doppler velocimeters were used as well as a special platform to maintain their position in the river current. A few cases were investigated, where patches of different aquatic plant species were found, i.e., *Myriophyllum spicatum* L., *M. alterniflorum* L., *P. pectinatus*, and *P. crispus*. Detailed flow field measurements (e.g., Fig. 4) were used to determine which patch characteristics could alter the flow and which turbulent structures could be associated. Biomechanical tests were used to give additional information about plant reconfiguration capabilities.

Results showed that both morphological and biomechanical traits may cause certain flow disturbances, e.g., the generation of a mixing layer or “dead zone”, where water velocity and turbulence were diminished. More rigid plants as well as patches of sufficient density and bed coverage are deemed to have a much stronger influence on flow than the smaller and weaker ones. This proved that plant biomechanics is an important factor in flow-biota interactions. All measurements and the analysis of obtained results were presented in detail in six scientific papers in 2018.

References

- Łoboda, A.M., R.J. Bialik, M. Karpiński, and Ł. Przyborowski (2019), Two simultaneously occurring Potamogeton species: similarities and differences in seasonal changes of biomechanical properties, *Pol. J. Environ. Stud.* **28**, 1, 1–16, DOI: 10.15244/pjoes/85202.
- Przyborowski, Ł., A.M. Łoboda, R.J. Bialik, and K. Västälä (2019), Flow field downstream of individual aquatic plants—Experiments in a natural river with *Potamogeton crispus* L. and *Myriophyllum spicatum* L., *Hydrol. Process.* **33**, 9, 1324–1337, DOI: 10.1002/hyp.13403.

MODELLING OF TRANSPORT PROCESSES

Experimental studies on (1) gravity currents and (2) sedimentation of particles in complex ambient conditions carried out in Hydrodynamic Models Laboratory

A methodology for experimental study of gravity currents and measurements methodology using image analysis methods have been developed and tested. An experimental setup was prepared (Fig. 1) and a series of experiments were conducted. A volume of denser fluid (aqueous NaCl solution) was released from a lock into a rectangular tank filled with less dense ambient fluid (water). There was a small difference between the density of a current and ambient fluid ρ (1%) to ensure validity of Boussinesq condition.

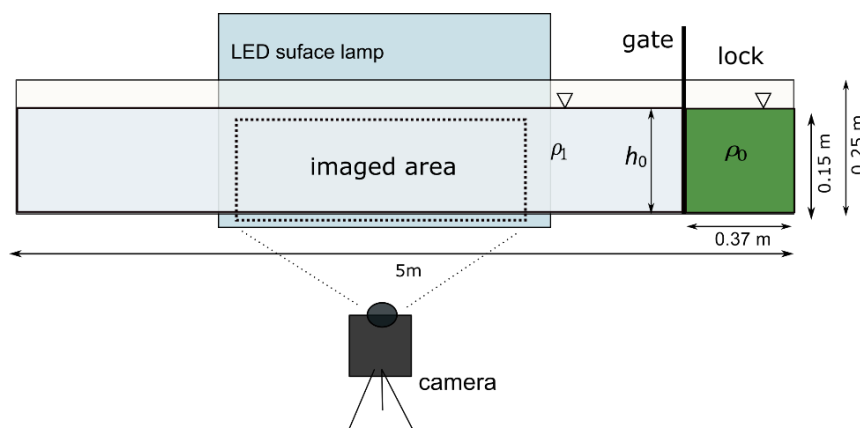


Fig. 1. Scheme of the experimental setup.

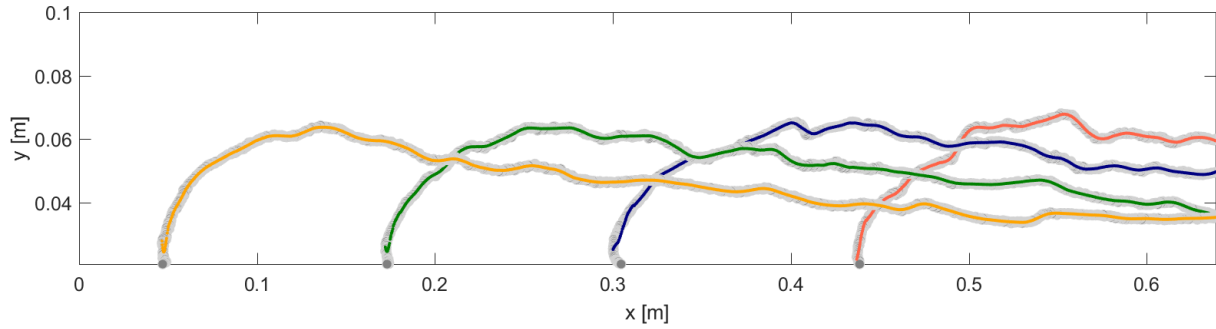


Fig. 2. Evolution of gravity current (four images of gravity current with 4 s time step). Contours of gravity current (grey) with fitted curves (colour).

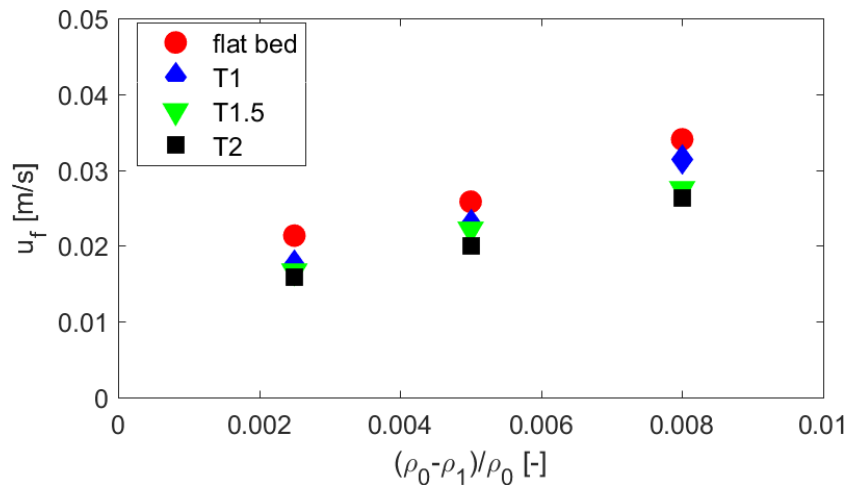


Fig. 3. Gravity current front velocity for various bed configurations and density conditions.

The aim of the study was to assess the impact of bed roughness on the propagation of gravity current. Gravity currents were released over four bed configurations – a smooth bed and three types of triangular macro-roughness elements. Image analysis methods have been applied to evaluate basic parameters describing the propagation of gravity current – front velocity and contours of the current (Fig. 2). The results have demonstrated a linear relationship between a current front and time (constant front velocity) indicating that the current was in a slumping phase. Moreover, a decrease in the front velocity with the increase in the height of roughness elements has been observed (Fig. 3). Simultaneously, a numerical model has been under development within the cooperation with an external group (IG PAS plus the University of Warsaw).

The dynamics of particle settling in non-Newtonian solutions was studied experimentally. Settling experiments in a low Reynolds number regime were carried out using spherical and non-spherical particles and solutions of natural polymers. The impact of polymer content on settling velocity, drag, and orientation of settling particle was studied. This study was performed in cooperation with Warsaw University of Technology. The results were analysed along with rheological properties of solutions, i.e., viscoelastic and flow properties.

It has been shown that rheological properties of non-Newtonian fluids modify settling behaviour of particles compared to Newtonian fluid. The drag coefficient increased with polymer content as a result of the increase in viscosity. A negative wake was identified using the Particle Tracking Velocimetry method developed in the laboratory (Fig. 4). Settling velocity fluctuations were observed, which is the effect of rheological properties of a fluid. Non-spherical particles settled with the longest axis vertical, as a result of normal stresses.

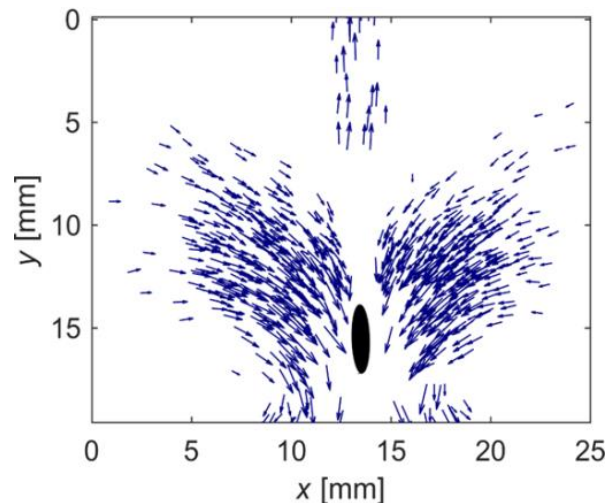


Fig. 4. Negative wake behind settling particle (after Mrokowska and Krztoń-Maziopa 2019).

References

- Mrokowska, M.M., and A. Krztoń-Maziopa (2019), Viscoelastic and shear-thinning effects of aqueous exopolymer solution on disk and sphere settling, *Sci. Rep.* **9**, 7897, DOI: 10.1038/s41598-019-44233-z.

MODELLING OF HYDROLOGICAL PROCESSES

Testing of innovative metaheuristics and their application to the calibration of hydrological processes models

Particle Swarm Optimization (PSO) has been successfully used in versatile scientific fields, ranging from humanities, engineering, chemistry, medicine, to advanced physics. Since its introduction in 1995, the method has been widely researched, which led to the development of hundreds of PSO versions and to numerous theoretical and empirical findings on their convergence and parameterization. However, so far there is no wide-scale study on the proper choice of PSO swarm size that affects the performance of metaheuristics. In most applications, authors restrict the population size to 20–50 particles. In this study, we relate the performance of eight PSO variants with swarm sizes that range from 3 up to 1000 particles. Tests are performed on sixty 10- to 100-dimensional scalable benchmarks and twenty two 1- to 216-dimensional real-world problems. Although results differ for the specific PSO variants, for the majority of considered PSO algorithms the best performance is obtained with swarms composed of 70–500 particles, indicating that the classical choice is often too small. Larger swarms frequently improve the effectiveness of the method for practical applications.

Numerous Differential Evolution algorithms (DE) have been proposed during last twenty years for numerical optimization problems. Recently a number of successful history-based adaptive DE variants with linear population size reduction (L-SHADE) have been considered among the most efficient Evolutionary Algorithms. In this study, we show that the performance of L-SHADE variants may be improved by adding a population-wide inertia term (PWI) to the mutation strategies. The PWI term represents an averaged direction and size of moves that were successful in the previous generation. The PWI term is implemented into four L-SHADE variants proposed during 2014–2018 period. Empirical tests are performed on 60 artificial benchmark problems from IEEE CEC'2014 and IEEE CEC'2017 test sets, and on 22 real-world problems from IEEE CEC'2011. For each considered test set every L-SHADE variant performs better with PWI term than without it.

Among the plentiful DE versions proposed so far, those that are based on mutation strategies and control parameter adaptation methods introduced within JADE and SHADE variants show especially encouraging performance. In this study, in-deep insight into the performance of twenty two JADE/SHADE-based variants on a large sets of artificial benchmarks and real-world problems is presented. The impact of the pre-assumed maximum number of function calls and the algorithm population size on the results is verified and discussed. The main aim of the study is to point out these among recently introduced JADE or SHADE-based operators that turn out to be especially successful and to determine conditions under which they either achieve desired results or fail.

MODELLING OF HYDROLOGICAL PROCESSES

Relationship between calibration time and final performance of conceptual rainfall-runoff models

This paper aims at studying the impact of the assumed number of function calls to be used during calibration of the lumped conceptual rainfall-runoff model on the final performance. Tests with different numbers of function calls (1000, 3000, 10 000, and 30 000) are performed

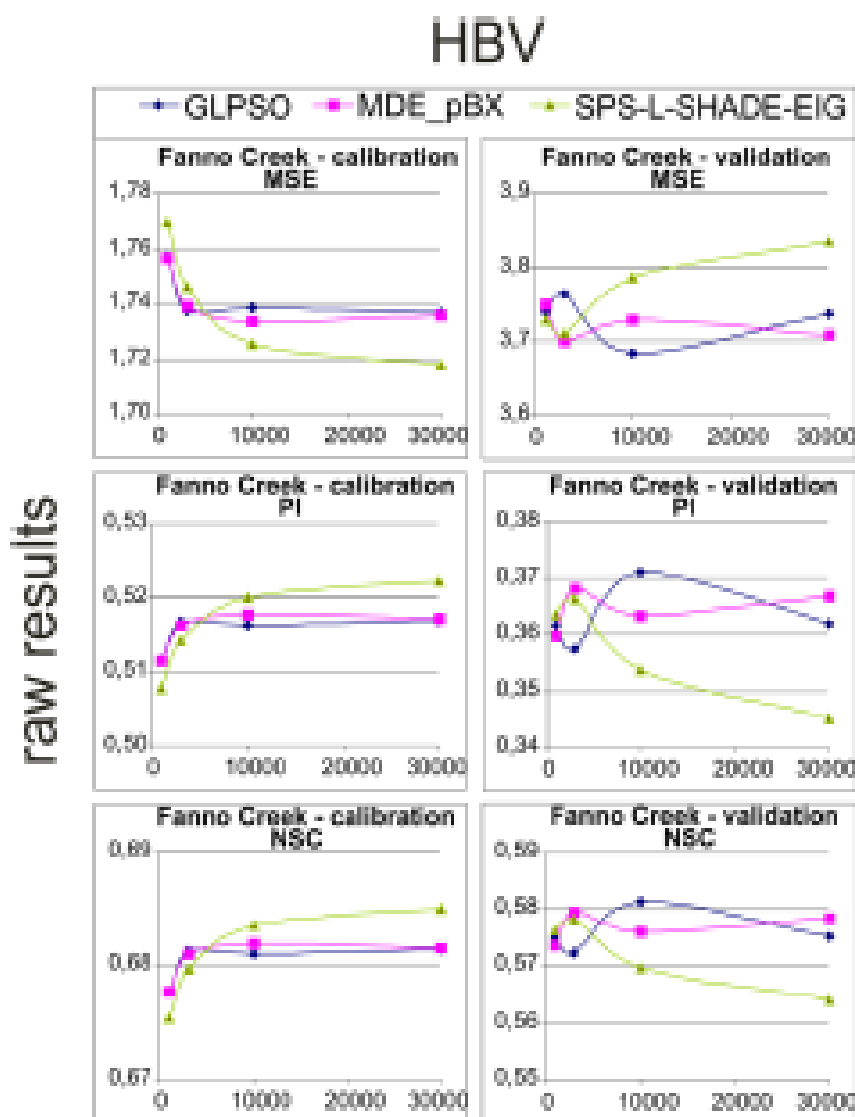


Fig. 1. Relation between the performance of HBV model without error correction procedure for Fanno Creek (after Piotrowski et al. 2019).

independently; hence, a longer calibration does not necessarily imply better results. Two models are tested (HBV and GR4J), each applied with or without an error correction procedure, and with three calibration procedures (GLPSO, MDE_pBX, and SPS-LSHADE-EIG) at five catchments (the mountainous Biała Tarnowska, Poland, and Cedar River, WA, USA; the hilly Fanno Creek, OR, USA; the lowland Irondequoit Creek, NY, USA; and Supraśl, Poland) located in temperate climatic conditions. Research is based on 14–39 years long daily data that are divided into calibration and validation parts.

At the calibration stage, when more than 10 000 function calls is used, only marginal improvement in model performance has been found, irrespective of the catchment or calibration algorithm. For validation data, the relation between the number of function calls and model performance is even weaker, in some cases the longer calibration, the poorer modelling performance. It is also shown that the opinion on the model performance based on different popular hydrological criteria, like the Nash-Sutcliffe (NSC) coefficient or the Persistence Index (PI), may be misleading. This is because very similar, largely positive values of Nash-Sutcliffe coefficient obtained on different catchments may be accompanied by contradictory values of the Persistence Index. The exemplar result of the relation between the number of function calls and the model performance is presented in Fig. 1 for the Fanno Creek.

References

Piotrowski, A.P., J.J. Napiorkowski, and M. Osuch (2019), Relationship between calibration time and final performance of conceptual rainfall-runoff models, *Water Resour. Manage.* **33**, 19–37, DOI: 10.1007/s11269-018-2085-3.

MODELLING OF HYDROLOGICAL PROCESSES

Performance of the air2stream model that relates air and stream water temperatures depends on the calibration method

A number of physical or data-driven models have been proposed to evaluate stream water temperatures based on hydrological and meteorological observations. Physical models require a large amount of information that is frequently unavailable, while data-based models ignore the physical processes. Recently the air2stream model has been proposed as an intermediate alternative that is based on physical heat budget processes, but it is so simplified that the model may be applied like data-driven ones.

In this study, 12 optimization algorithms were tested for the calibration of the air2stream model with eight parameters, for hydro-meteorological daily data from six streams located in the temperate climatic conditions of northern USA, Poland, and Switzerland. Each optimization algorithm was run 30 times to calibrate the air2stream model for every stream. It was shown that the performance of the air2stream model largely depends on the selected calibration procedure. The best and most robust results for each stream are obtained with the CoBiDE and GA-MPC methods. A number of other optimization procedures lead to less reliable results, and two out of the 12 optimization algorithms tested turned out to be inappropriate for the air2stream calibration. The wrong choice of calibration method may lead to misleading simulation of stream water temperatures. The exemplar results for the Biała Tarnowska catchment, obtained for selected 500 day periods, from the validation set when the air2stream model is calibrated by Rcr-JADE are illustrated in Fig. 1.

Although the values of the Nash-Sutcliffe criterion for the air2stream model, calibrated with the best optimization procedures, range between 0.93 and 0.98 for the validation data, depending on the catchment, the forecasting skills of the model are limited, as per the

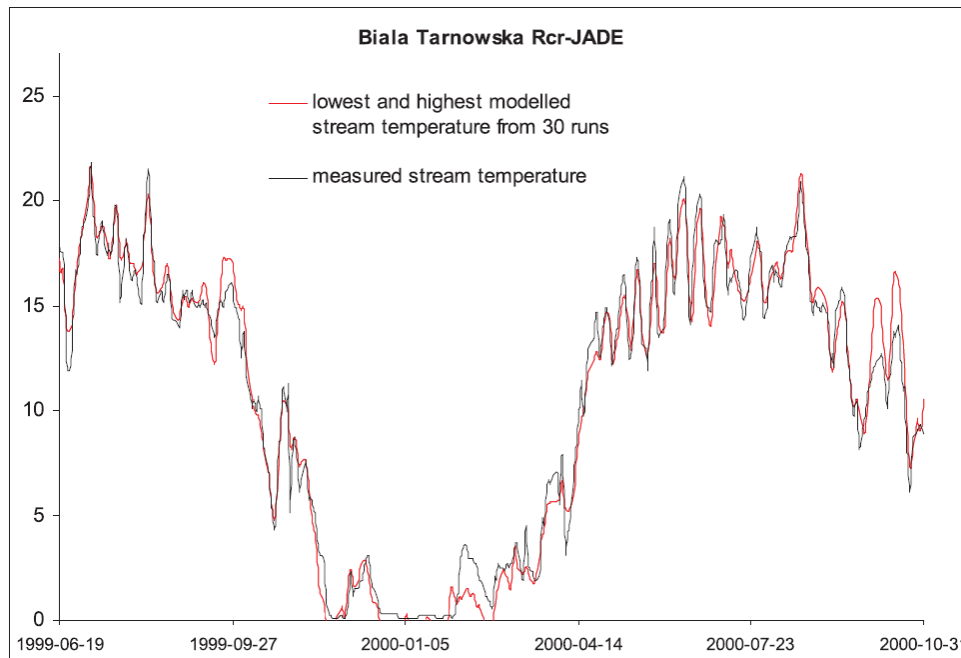


Fig. 1. Biala Tarnowska River. Highest and lowest air2stream model simulations from 30 calibrations by the Rcr-JADE and cNrGA algorithms (after Piotrowski and Napiórkowski 2018a).

Persistence Index criterion, which is often negative and never higher than 0.3. This is because the air2stream model does not have a bias correction module.

The air2stream model, calibrated by well-selected optimization procedures, clearly outperforms data-based stream water temperature models that are widely used in the recent literature.

MODELLING OF HYDROLOGICAL PROCESSES

Simple modification of nonlinear regression stream temperature model for daily data

Among various stream temperature models those based on nonlinear regression frequently attract attention due to their simplicity and small number of required variables. Among such approaches, the Mohseni logistic regression model developed twenty years ago for weekly data is still widely used in various scientific studies that require quick and simple calculation of stream-water temperature. The model has been modified a number of times in recent years to capture the relationship between daily stream water temperatures, air temperatures and flow. In this study, we propose further modifications of the logistic regression model that do not require any additional variables that may be hard to measure. The proposed models capture the relationship between the stream temperature and the declination of the Sun, the air temperature and the flow from a number of recent observations. The proposed approaches are tested on six rivers located in diverse orographic conditions of temperate climate zones of Europe and USA. Although the proposed models remain very simple, their performances are competitive against the performances of more advanced semi-physical or data-driven models

MODELLING OF HYDROLOGICAL PROCESSES

Hydrodynamic derivation of parameters of the Muskingum model

To describe the unsteady flow in rivers by means of the methods of mathematical physics, it is necessary to know with sufficient accuracy the geometrical and hydraulic characteristics of the channel reach as well as the initial and boundary conditions. The difficulties of meeting these

requirements led to the development in the hydrology of lumped conceptual models, in particular the Muskingum model.

There exists a direct possibility of deriving the Muskingum equations from St. Venant equations. One approach is the lumping of the hydrodynamic model under the assumption of linear changes of water level along the river reach and then linearizing it around the steady state. The second approach uses the method of inverse order. First, a state trajectory variation method is applied to the complete St. Venant equations and then the resulting equations are lumped. In both approaches the resulting equations are equivalent to the linear form of the Muskingum model. Hence the relationships between the hydraulic parameters of the St. Venant equation and the lumped parameters of the Muskingum model are derived.

MODELLING OF HYDROLOGICAL PROCESSES

The hydrology of a small Arctic permafrost catchment

The overall aim of the present study is to examine the relationships between temporal changes of active layer depth and hydrological model parameters, together with variation in the catchment response. The analysis was carried out for the small unglaciated catchment Fuglebekken, located in the vicinity of the Polish Polar Station Hornsund on Spitsbergen.

For hydrological modelling, the conceptual rainfall-runoff HBV model was used (Fig. 1). The model was calibrated and validated on runoff within subperiods. A moving window approach (3 weeks long) was applied to derive temporal variation of parameters. Model calibration, together with an estimation of parametric uncertainty, was carried out using the Shuffled Complex Evolution Metropolis algorithm. This allowed the dependence of HBV model parameters on ALT to be analysed. Also, we tested the influence of model simplification, correction of precipitation, and initial conditions on the modelling results.

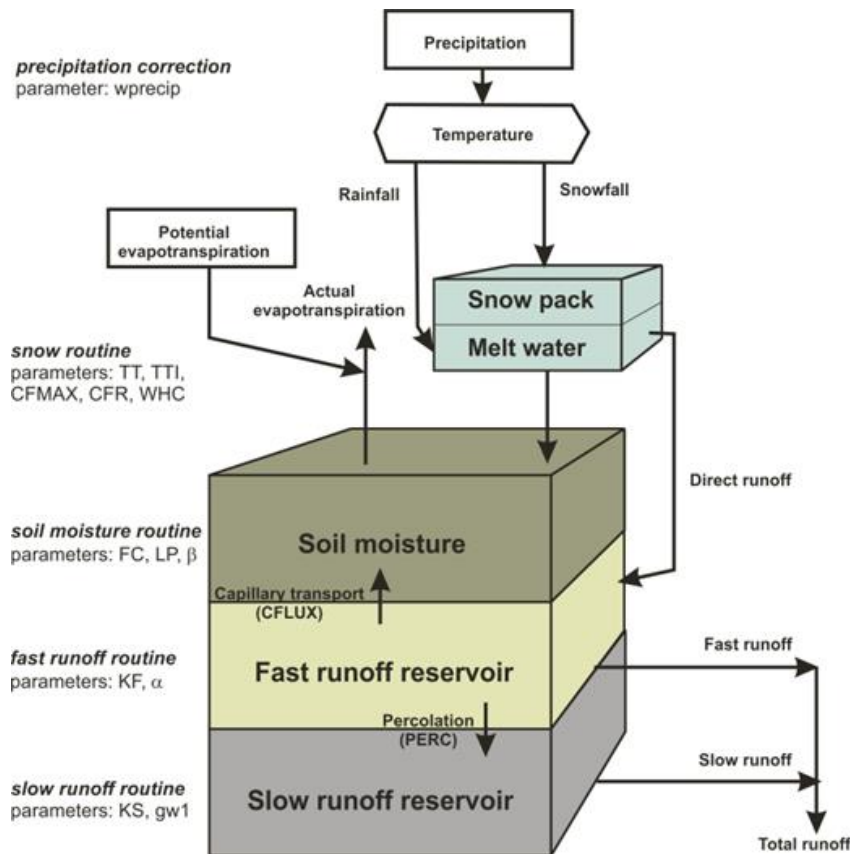


Fig. 1. HBV catchment runoff model (after Wawrzyniak et al. 2017).

The nonstationarity of the parameters of the catchment runoff model has been tested in the case of a catchment with varying geophysical conditions (changes in the thickness of the active layer). To this end, the model has been successfully calibrated in successive time windows, enabling the estimation of model parameters and their variability depending on the thickness of the active layer and other hydro-climatic indices.

References

Wawrzyniak, T., M. Osuch, A. Nawrot, and J.J. Napiórkowski (2017), Run-off modelling in an Arctic unglaciated catchment (Fuglebekken, Spitsbergen), *Ann. Glaciol.* **58**, 75, 36–46, DOI: 10.1017/aog.2017.8.

6.6 Seminars and teaching

Seminars and lecture outside of the IG PAS:

- R. Romanowicz, Climate change impact on hydrological processes at a catchment scale, University Twente, Twente, Netherlands, Seminar;
- R. Romanowicz, Climate change impact assessment – a hydrological perspective, EcoPol, Poznań, Poland, Invited lecture;
- P. Rowiński, Polish Academia towards Climate Change Studies. Safeguarding Our Climate, Advancing Our Society event accompanying UN Climate Summit COP24, Pontifical Academy of Science, Casina Pio IV, Vatican City, Invited lecture;
- P. Rowiński, Silny uniwersytet badawczy – czy jest to możliwe w warunkach polskich?, ASSECO, Warszawa, Poland, Invited lecture;
- P. Rowiński, Uczelnie badawcze, czyli jakie?, Fundacja Rozwoju Systemu Edukacji, Warszawa, Poland; Invited lecture;
- M. Nones, Modelling process in hydroengineering projects, BTU Cottbus-Senftenberg, Cottbus, Germany; 30 hour course.

6.7 Completed PhD thesis defense

- A. Łoboda, The influence of the seasonal variability of biomechanical properties of selected plant species rooted in flowing waters on flow resistance, Supervisor: R. Bialik;
- E. Karamuz, Wpływ zmian klimatu oraz użytkowania terenu na przepływ środkowej Wisły, Supervisor: R. Romanowicz;
- H.K. Meresa, Modelling of hydrological extremes under the influence of future climate change, Supervisor: R. Romanowicz;
- S.E. Debele, Frequency analysis of extreme river flows: selected methods and their application, Supervisor: R. Romanowicz.

6.8 Visiting scientists

- J. Juha, Aalto University, Aalto, Finland, 25–28.11.2018,
- J. Aberle, Technical University Braunschweig, Braunschweig, Germany, 24–27.11.2018,
- V. Kaisa, Aalto University, Aalto, Finland, 1–15.01.2018, 26–29.11.2018.

6.9 Meetings, workshops, conferences, and symposia

Presentations of the Department's members:

International Conference on Fluvial Hydraulics, River Flow 2018, Lyon-Villeurbanne, France, 5–8 September 2018

- M. Kalinowska, P. Rowiński, Impact of initial conditions on the prediction of the spread of thermal pollution in rivers, Oral;

5th IAHR Europe Congress, Trento, Italy, 12–14 June 2018

- M. Kalinowska, Heat and mass transport under complex natural conditions – introduction to the special session, Oral;
- Ł. Przyborowski, A. Łoboda, Effect of Myriophyllum Species on Downstream Turbulence in a Natural River. In New Challenges in Hydraulic Research and Engineering, Oral;
- P. Rowiński, M. Kalinowska, Heat and mass transport under complex natural conditions – review, Oral.

OSH2018 – Ogólnopolska Szkoła hydrauliki, Gdańsk, Poland, 15–18 May 2018

- M. Kalinowska, P. Rowiński, Modelowanie prędkości w kanale prostokątnym częściowo pokrytym roślinnością z użyciem modelu CCHE2D, Oral.

XXXVII Sympozjum Polarne "Polar Change – Global Change", Poznań, Poland, 7–10 June 2018

- M. Osuch, Snow cover development on Spitsbergen coastal tundra environment –present state and predictions for the end of xxi century, Oral.

Konferencja Naukowo-Techniczna, Warszawa, Poland, 14 June 2018

- K. Kochanek, Informacja historyczna w analizie częstości występowania powodzi, Oral;
- I. Markiewicz, Wielo-modelowe podejście do estymacji kwantyli powodziowych, Oral.

III Krajowy Kongres Hydrologiczny, Warszawa, Poland

- K. Kochanek, E. Bogdanowicz, I. Markiewicz, Accuracy of the coefficient of skewness and flood quantiles estimated by weight function for Pearson type 3 distribution, Oral;
- K. Kochanek, E. Bogdanowicz, I. Markiewicz, Error of the estimation of the flood quantiles calculated by means of the data series of the historical information only, Oral;
- I. Markiewicz, E. Bogdanowicz, K. Kochanek, Two ways of a multimodel approach to the estimation of seasonal and annual maxima flow distributions, Oral;
- R. Romanowicz, The application of cumulants to flow routing, Oral;
- E. Bogdanowicz, K. Kochanek, I. Markiewicz, Asymptotic standard error of annual maximum flow quantile estimated by seasonal approach, Oral.

Budapest, Hungary, 30–31 October 2018

- M. Osuch, Modelling snow water equivalent in the coastal tundra of Hornsund fiord. Towards a better harmonization of snow observations, modeling and data assimilation in Europe, Oral.

9th International Plant Biomechanics Conference, Montreal, Canada, 9–14 August 2018

- A. Łoboda, To what we endeavour in the biomechanics of aquatic plants?, Poster.

SIOS, Svalbard, 13–16 March 2018

- M. Osuch, Permafrost monitoring in Hornsund area, SW Spitsbergen. Permafrost thermal state in Svalbard 2016–2017 (PermaSval), Oral.

Nordic Water 2018, Bergen, Norway, 13–15 August 2018

- M. Osuch, Water temperature modelling of small high Arctic stream (Fuglebekken, SW Spitsbergen), Oral.

8th Global Freshwater Conference, Beijing, China, 6–9 November 2018

- M. Osuch, Projections of hydro-climatic conditions in small arctic unglaciated catchment Fuglebekken (SW Spitsbergen), Oral;
- M. Osuch, The influence of permafrost degradation on runoff generation in small arctic unglaciated catchment (Fuglebekken, Spitsbergen), Oral.

Warszawski Festiwal Nauki 2018, Warszawa, Poland, 20 September 2018

- R. Romanowicz, Wpływ zmian klimatu na ekstremalne zjawiska hydrologiczne. Globalne ocieplenie – różne perspektywy, Oral.

Rozwiązania bliskie naturze dla poprawy zasobów wodnych, Warszawa, Poland, 22 March 2018

- P. Rowiński, Rozwiązania bliskie naturze dla poprawy zasobów wodnych – wprowadzenie, Oral.

LAHTI LAKES 2018 – Restoration of Eutrophic Lakes: Current Practices and Future Challenges, Lahti, Finland, 4–6 June 2018

- P. Rowiński, M. Kalinowska, Environmental two-stage channels: potential for catchment-scale reductions in nutrient transport?, Oral.

6.10 Publications

ARTICLES

- Bialik, R.J.**, and **M. Karpiński** (2018), On the effect of the window size on the assessment of particle diffusion, *J. Hydraul. Res.* **56**, 4, 560–566, DOI: 10.1080/00221686.2017.1397780.
- Doroszkiewicz, J.**, **R.J. Romanowicz**, and A. Kiczko (2018), The influence of flow projection errors on flood hazard estimates in future climate conditions, *Water* **11**, 1, 49, DOI: 10.3390/w11010049.
- Kalinowska, M.B.**, **P.M. Rowiński**, and A. **Magnuszewski** (2018), Impact of initial conditions on the prediction of the spread of thermal pollution in rivers, *E3S Web Conf.* **40**, 05048, DOI: 10.1051/e3sconf/20184005048.
- Kochanek, K.** (2018), ‘New insight into statistical hydrology’ preface to the special issue, *Acta Geophys.* **66**, 4, 739–740, DOI: 10.1007/s11600-018-0151-0.
- Bogdanowicz, E., **K. Kochanek**, and **W.G. Strupczewski** (2018), The weighted function method: A handy tool for flood frequency analysis or just a curiosity?, *J. Hydrol.* **559**, 209–221, DOI: 10.1016/j.jhydrol.2018.02.020.
- Giang, N.V., **K. Kochanek**, et al. (2018), Landfill leachate assessment by hydrological and geophysical data: case study NamSon, Hanoi, Vietnam, *J. Mater. Cycles Waste Manage.* **20**, 3, 1648–1662, DOI: 10.1007/s10163-018-0732-7.
- Manfreda, S., et al., **K. Kochanek** (2018), The impact of climate on hydrological extremes, *Water* **10**, 6, 802, DOI: 10.3390/w10060802.
- Łoboda, A.M.**, **Ł. Przyborowski**, **M. Karpiński**, **R.J. Bialik**, and V.I. Nikora (2018a), Bio-mechanical properties of aquatic plants: The effect of test conditions, *Limnol. Oceanogr. – Meth.* **16**, 4, 222–236, DOI: 10.1002/lom3.10239.

- Łoboda, A.M., M. Karpiński, and R.J. Bialik** (2018b), On the relationship between aquatic plant stem characteristics and drag force: is a modeling application possible? *Water* **10**, 5, 540, DOI: 10.3390/w10050540.
- Łoboda, A.M., R.J. Bialik, M. Karpiński, and Ł. Przyborowski** (2018c), Seasonal changes in the biomechanical properties of *Elodea canadensis* Michx, *Aquat. Bot.* **147**, 43–51, DOI: 10.1016/j.aquabot.2018.03.006.
- Markiewicz, I., E. Bogdanowicz, and K. Kochanek** (2018), Two ways of a multi-model approach to the estimation of seasonal and annual maxima flow distributions [Dwa sposoby wielomodelowego podejścia do estymacji rozkładów maksymalnych przepływów sezonowych i rocznych], *Monografie Komitetu Gospodarki Wodnej Polskiej Akademii Nauk* **41**, 47–62, Wydawnictwa KGW PAN, Warszawa (in Polish).
- Mrokowska, M.M.** (2018), Stratification-induced reorientation of disk settling through ambient density transition, *Sci. Rep.* **8**, 1, 412, DOI: 10.1038/s41598-017-18654-7.
- Mrokowska, M.M., P.M. Rowiński, et al.** (2018), Laboratory studies on bedload transport under unsteady flow conditions, *J. Hydrol. Hydromech.* **66**, 1, 23–31, DOI: 10.1515/johh-2017-0032.
- Osuch, M., R.J. Romanowicz, and W.K. Wong** (2018), Analysis of low flow indices under varying climatic conditions in Poland, *Hydrol. Res.* **49**, 2, 373–389, DOI: 10.2166/nh.2017.021.
- Helmert, J., **M. Osuch, et al.** (2018), 1st Snow Data Assimilation Workshop in the framework of COST HarmoSnow ESSEM 1404, *Meteorol. Z.* **27**, 4, 325–333, DOI: 10.1127/metz/2018/0906.
- Piotrowski, A.P.** (2018), Across Neighborhood Search algorithm: A comprehensive analysis, *Inform. Sci.* **435**, 334–381, DOI: 10.1016/j.ins.2018.01.004.
- Piotrowski, A.P.** (2018), L-SHADE optimization algorithms with population-wide inertia, *Inform. Sci.* **468**, 117–141, DOI: 10.1016/j.ins.2018.08.030.
- Piotrowski, A.P., and J.J. Napiórkowski** (2018a), Performance of the air2stream model that relates air and stream water temperatures depends on the calibration method, *J. Hydrol.* **561**, 395–412, DOI: 10.1016/j.jhydrol.2018.04.016.
- Piotrowski, A.P., and J.J. Napiórkowski** (2018b), Step-by-step improvement of JADE and SHADE-based algorithms: Success or failure?, *Swarm Evol. Comput.* **43**, 88–108, DOI: 10.1016/j.swevo.2018.03.007.
- Piotrowski, A.P., and J.J. Napiórkowski** (2018c), Some metaheuristics should be simplified. *Inform. Sci.* **427**, 32–62, DOI: 10.1016/j.ins.2017.10.039.
- Przyborowski, Ł., A.M. Łoboda, and R.J. Bialik** (2018), Experimental investigations of interactions between sand wave movements, flow structure, and individual aquatic plants in natural rivers: A case study of *Potamogeton Pectinatus* L., *Water* **10**, 9, 1166, DOI: 10.3390/w10091166.
- Kiczko, A., et al., **R.J. Romanowicz** (2018), Optimal capacity of a stormwater reservoir for flood peak reduction, *J. Hydrol. Eng.* **23**, 4, 04018008-1, DOI: 10.1061/(ASCE)HE.1943-5584.0001636.
- Rowiński, P.M., et al., M.B. Kalinowska** (2018), How vegetation can aid in coping with river management challenges: A brief review, *Ecohydrol. Hydrobiol.* **18**, 4, 345–354, DOI: 10.1016/j.ecohyd.2018.07.003.

Najafabadi, E.F., H. Afzalimehr, and **P.M. Rowiński** (2018), Flow structure through a fluvial pool-riffle sequence – case study, *J. Hydro-environ. Res.* **19**, 1–15, DOI: 10.1016/j.jher.2018.01.001.

Strupczewski, W.G., E. Bogdanowicz, K. Kochanek, and I. Markiewicz (2018), Asymptotic standard error of annual maximum flow quantile estimated by seasonal approach [Asymptotyczny błąd oceny kwantyli maksymalnych przepływów rocznych w ujęciu sezonowym], *Monografie Komitetu Gospodarki Wodnej Polskiej Akademii Nauk* **41**, 91–102, Wydawnictwa KGW PAN, Warszawa (in Polish).

7. DEPARTMENT OF MAGNETISM

Waldemar Jóźwiak

7.1 About the Department

The main research directions in the Department of Magnetism include studies of the lithosphere structures using electromagnetic methods, research in the field of magnetohydrodynamics with applications to the dynamics of the Earth's interior, paleomagnetism and research in the field of environmental magnetism.

Paleomagnetic team in 2018 took part in a wide range of activities. The environmental magnetism group working on the NM1 task, continued the application of combined magnetic and non-magnetic methods to study the anthropogenic pollution in various settings such as road and air dust, water bank deposits, and soil pollution. The collaborate efforts with other teams allowed for a multidisciplinary approach to resolve the questions concerning sources of pollution. These methods were also tested in polar areas at Svalbard. The group directed active efforts towards integration of the environmental studies community in Poland with organization of a workshop in Warsaw. The service of continued monitoring of the PM dust with magnetic methods was also expanded.

The research work conducted within the NM2 task focused mostly on the problems of paleographic reconstructions. The research concerned palaeogeographic positions of both large lithospheric plates as well as smaller units, such as terranes, individual tectonic blocks or nappes. The processes of collision of lithospheric plates and the associated formation of mountain belts together with rock deformations were also investigated. The works were carried out in the Carpathians (Slovakia and Poland), Africa (eastern Zimbabwe), and also in the Svalbard area. In addition, research was conducted on Silurian gas-bearing shales (northern Poland) where magnetic methods were applied for determination of the degree of their tectonic deformation and direction of sediment transport in the sedimentation basin.

The magnetic dynamo team within the NM3 has conducted research on the role of diffusive effects in stability of magnetohydrodynamic flows and large-scale field generation. The results involve determination of spatial scales of evolution for magnetically buoyant parcels and novel nonlinear mechanisms of generation of natural large-scale magnetic fields.

The research within the NM3 task involved development of a final 3D model of the conductivity distribution for the Fore-Sudetic Monocline and efforts were undertaken in order to identify the structure of the crust and the upper mantle in Poland. The data from several profiles crossing the TESZ zone in Poland was reinterpreted. Some methodological work was carried out on a 3D inversion algorithm, with particular emphasis on the influence of regularization parameters and the selection of the transition function on the inversion results. The relationship between the seismic activity in nearby areas and the observed changes of magnetotelluric transition functions was investigated. Seasonal changes in the transfer functions were analyzed and the way to obtain the correct estimation was determined. A combined quantitative interpretation of GCM and DC-R methods was also performed.

The research group for geomagnetic observations has conducted absolute measurements and continuous recording of the Earth's magnetic field in Belsk, Hel, and Hornsund (Spitsbergen) observatories. All three observatories are members of the global INTERMAGNET network. A continuous recording of geomagnetic field changes with real-time data access has been carried out in the permanent stations Birzai (Northern Lithuania), Suwałki, Poleski Park Narodowy, and Zagórze near Cracow. Moreover, Schumann Resonance observations have been continued in Polish Polar Station Hornsund and Suwałki in 2018. Also the group was strongly engaged in EPOS project.

In addition, the Department of Magnetism is responsible for the Task 3 and Task 4 of the EPOS-PL project. In 2018 the palaeomagnetic laboratory was refurbished and equipped with a new set of palaeomagnetic and rock magnetic devices (total of 1.5 M PLN). The works on the paleomagnetic and magnetotelluric database were also continued.

The paleomagnetic team co-organized the international conference the 16th Castle Meeting “New Trends on Paleo, Rock and Environmental Magnetism” in Chęciny in June 2018 acting as LOC, and the short course for students preceding the meeting – sponsored by IAGA.

7.2 Personnel

Head of the Department

Waldemar Józwiak
Associate Professor

Tomasz Werner
Head of Paleomagnetism Research Team

Professors

Magdalena Kądziałko-Hofmokl
Marek Lewandowski
Maria Teisseyre-Jeleńska

Associate Professors

Tomasz Ernst
Beata Górka-Kostrubiec
Rafał Junosza-Szaniawski
Krzysztof Mizerski
Krzysztof Nowożyński
Vladimir Semenov

Assistant Professors

Katarzyna Dudzisz
Sylwia Dytłow
Ashley Gumsley
Krzysztof Michalski

Research Assistant

Szymon Oryński
Iga Szczepaniak-Wnuk

Laboratory Technician

Grzegorz Karasiński

Technicians

Paweł Czubak
Krzysztof Kucharski
Mariusz Neska
Anna Wójcik
Stanisław Wójcik

Head of Belsk Observatory

Jan Reda

PhD Students

Marek Grądzki, Poland; Krzysztof Mizerski – PhD supervisor
 Katarzyna Dudzisz, Poland; Rafał Szaniawski – PhD supervisor
 Magdalena Gwizdała, Poland; Maria Teisseyre-Jeleńska – PhD supervisor
 Mariusz Burzyński, Poland; Marek Lewandowski – PhD supervisor
 Iga Szczepaniak-Wnuk, Poland; Beata Górka-Kostrubiec – PhD supervisor
 Dominika Niezabitowska, Poland; Rafał Szaniawski – PhD supervisor
 Agata Bury, Poland; Anne Neska – PhD supervisor

7.3 Main research projects

- Diversity of technogenic magnetic particles in the soil environment depending on the emission sources and their role in transport of potentially toxic elements, B. Górka-Kostrubiec, National Science Center, 2017–2020;
- Magnetic properties of sediments applied for assessment of pollution level of heavy metals of Vistula River water within Warsaw, I. Szczepaniak-Wnuk, National Science Center, 2018–2020;
- EPOS – PL European Plate Observing System; Task 4 – CIBAL – Centre of Research Infrastructure of Analytical Laboratories, T. Werner, POIR, 2017–2022;
- EPOS – PL European Plate Observing System; B. Górka-Kostrubiec, POIR, 2017–2022;
- Paleomagnetic studies of Lower Triassic sandstones from the autochthonous cover of Central West Carpathian targeted to further define the degree of rotation of this unit with respect to the European platform, R. Junosza-Szaniawski, National Science Center, 2015–2018;
- Fire, and then the ice: calibrating southern Africa’s position within the Neoproterozoic supercontinent Rodinia, A. Gumsley, National Science Center, 2018–2019;
- On the edge of an Old continent: the search for the eastern margin of the European Variscan orogen, A. Gumsley, National Geographic Society, USA, 2018–2019;
- Changeability of the Earth’s resistivity and its relation to seismicity around the Trans-European Suture Zone, V. Semenov, National Science Center, 2015–2018;
- Buoyancy driven magnetic dynamo, K. Mizerski, National Science Center, 2018–2021;
- The role of lithospheric memory in the spatial and temporal localization of the intraplate deformation – investigating a deep structure of the Grójec Fault Zone based on potential field anomalies and seismic data, W. Józwiak, National Science Center, 2018–2021;
- EPOS – PL European Plate Observing System; Task 3, W. Józwiak, POIR, 2017–2022.

7.4 Instruments and facilities

Equipment

- Equipment for magnetic susceptibility measurements in the field:
 - MS2 susceptibility meter (Bartington, UK) with sensor,
 - MS3 susceptibility meter (Bartington, UK) with sensors.
- Equipment for PM dust collection (environmental magnetism studies):
 - PNS15C/ PM dust samplers (Atmoservice, Poland) – 3 units,
 - PNS18T/ PM dust samplers (Atmoservice, Poland and Comde Derenda) – 3 units.
- Equipment for magnetotelluric survey and magnetic observations:
 - 2 Magnetotelluric broad-band stations Phoenix,
 - 7 Magnetotelluric low-frequency stations Geomag,
 - 7 Low-frequency magnetometers LEMI,

- 6 PMP proton magnetometers,
- 5 Low-frequency PSM magnetometers,
- 5 DIFLUX magnetometers for absolute measurements,
- 19 NDL digital recorders,
- 18 LB-480 digital recorders.

Laboratory

Laboratory for paleomagnetism and environmental studies – list of the laboratory equipment:

- Equipment for measurements of magnetic remanence with step-wise AF/TH demagnetization:
 - 755–1.65 2G Enterprises cryogenic magnetometer DC SQUID with AF degausser, JR6a automated dual speed spinner magnetometer (Agico, Czech republic),
 - MMTDSC - Nonmagnetic furnace for thermal demagnetization Magnetic Measurements, Great Britain,
 - MMTD-80 Nonmagnetic furnace for thermal demagnetization by Magnetic Measurements, Great Britain,
 - MMTD1 Nonmagnetic furnace for thermal demagnetization by Magnetic Measurements, Great Britain.
- Equipment for acquisition of magnetic remanence:
 - LDA5/PAM1 Alternating Field Demagnetizer/ Anhysteretic and Pulse Magnetizer, Agico Czech Republic,
 - LDA3a/AMU1a, Alternating Field Demagnetizer/ Anhysteretic Magnetizer, Agico Czech Republic,
 - Two MMPM10 pulse magnetisers, Magnetic Measurements, Great Britain,
 - SI6 – Pulse magnetizer, Sapphire Instruments, Canada,
 - Two MMLFC low field cages, Magnetic Measurements, Great Britain.
- Equipment for magnetic susceptibility measurements:
 - KLY-5A/CS-4/CS-L Susceptibility bridge Agico, Czech Rep.,
 - MFK1-FA - Susceptibility bridge, Agico, Czech Rep.,
 - KLY-3/CS-3/CS-L - Susceptibility bridge, Agico, Czech Rep.,
 - KLY2 Susceptibility bridge, Geofyzika Brno, Czechoslovakia,
 - MS2 susceptibility meter (Bartington, UK),
 - MS3 susceptibility meter (Bartington, UK).
- Equipment for studies of magnetic hysteresis and Curie temperatures:
 - Micromag AGFM 2900-02 Alternating gradient force magnetometer, Princeton Measurements Corp., USA,
 - AVFTB (Advanced Variable Field Translation Balance) Petersen Instruments, Magnetic Measurements, Great Britain),
 - VSM Nuvo Vibrating Sample Magnetometer, Molspin Ltd, Gr. Britain.

7.5 Research activity and results

Brief description/abstracts/summaries of some of the achievements of the Department's staff:

IDENTIFICATION OF METALLIC IRON IN AN URBAN DUST USING MAGNETOMETRY, MICROSCOPIC OBSERVATIONS AND MÖSSBAUER SPECTROSCOPY

B. Górka-Kostrubiec, T. Werner, S. Dytlow, I. Szczepaniak-Wnuk, M. Teisseyre-Jeleńska

The work presents a thermomagnetic study of fresh, unheated indoor dust, outdoor dust, street dust and dust from the cabin air filters of cars. Detailed analysis of thermomagnetic curves

clearly indicated the presence of two magnetic transitions: the first identified at the Curie temperature $T_C \sim 585^\circ\text{C}$ for magnetite; the second T_C detected at about $\sim 765^\circ\text{C}$, indicating the presence of metallic iron and/or iron-based alloys. The “tail”, i.e., the substantial decreasing of κ visible on the heating curves of $\kappa(T)$ between 600°C and 700°C , was attributed to the metallic iron or iron-based alloys (see Fig. 1). The presence of a high-temperature Fe-phase is not dependent on the types of urban dust or the sampling method, as variable amounts of metallic iron were detected in material collected from different environments: both indoor and outdoor dust, and dust gathered by sweeping indoor floor surfaces as well as dust collected with a vacuum cleaner.

The presence of metallic iron in different types of dust was confirmed by non-magnetic methods. Electron microscopic observations with energy-dispersive X-ray spectroscopy revealed elongated shaving-like particles comprised of metallic iron (see Fig. 1). A component with a magnetic hyperfine field of $B_{\text{hf}} \sim 33^\circ\text{T}$ and an almost zero value for isomeric shift as well as zero quadrupole splitting typical of metallic $\alpha\text{-Fe}$ at micrometer size or Fe-based alloys was recognized in all the Mössbauer spectra.

Additional measurements of hysteresis properties at high temperatures (up to 750°C) and after step-wise annealing indicated the process of oxidation of iron to magnetite. This has a strong effect on the run of $\kappa(T)$ and $M(T)$ curves during heating and cooling that M and κ are strongly dependent on the apparent concentration of both ferromagnetic phases (magnetite and metallic iron).

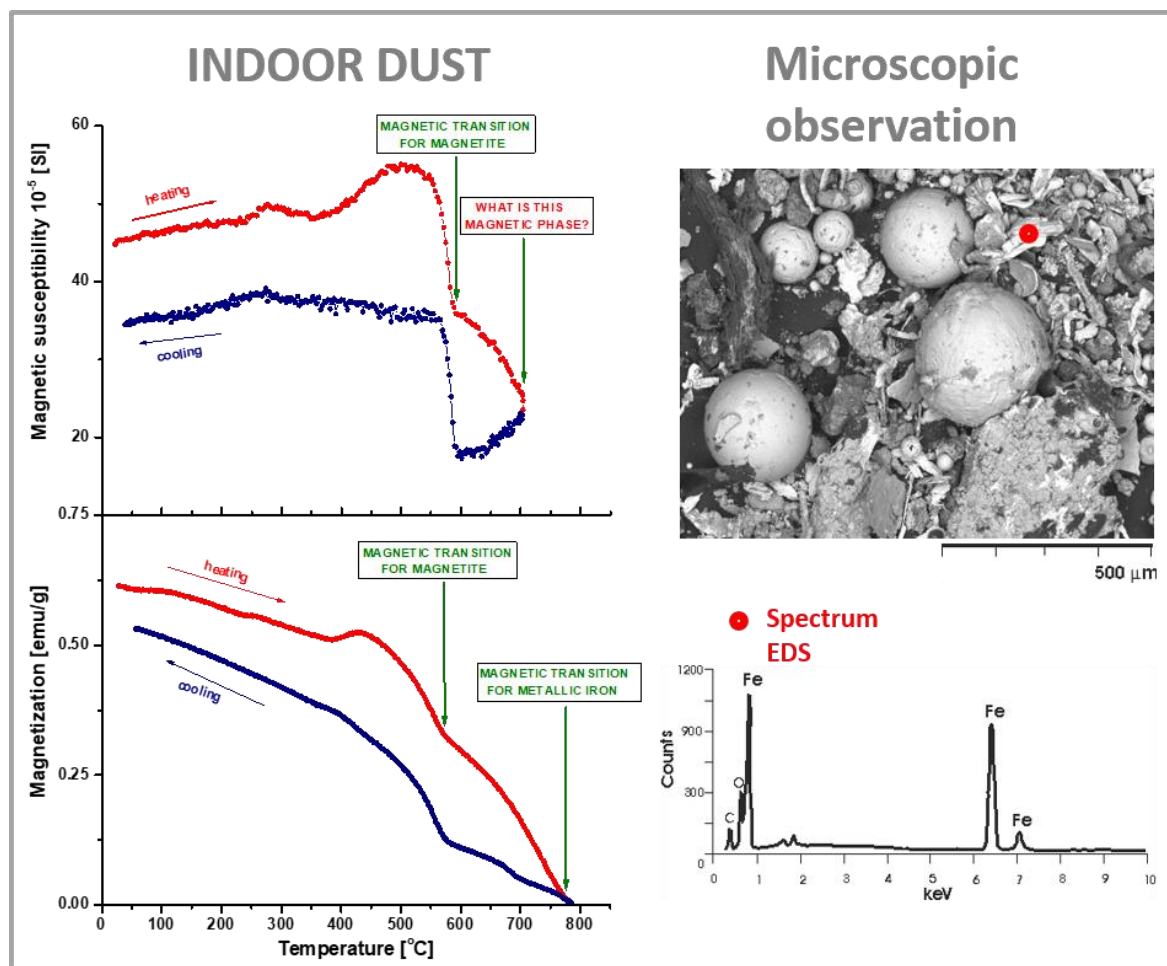


Fig. 1. The curves of $\kappa(T)$ and $M(T)$ for the same sample of indoor dust. Images of SEM with the spectra of EDS for the magnetic extract of dust from cabin air filters of car (after Górká-Kostrubiec et al. 2019).

References

Górka-Kostrubiec, B., T. Werner, S. Dytłow, I. Szczepaniak-Wnuk, M. Jeleńska, and A. Hanc-Kuczkowska (2019), Detection of metallic iron in urban dust by using high-temperature measurements supplemented with microscopic observations and Mössbauer spectra, *J. Appl. Geophys.* **166**, 89–102, DOI: 10.1016/j.jappgeo.2019.04.022.

EFFECTIVE AND UNIVERSAL TOOL FOR EVALUATING HEAVY METALS—PASSIVE DUST SAMPLERS

S. Dytłow, B. Górka-Kostrubiec

The study presents designating, accomplishing, optimizing, and validating a new tool – “passive sampler” (PS) that can be effectively used as a proxy to assess the level of traffic-related pollution. To construct the PS, a drainage pipe filled with a mixture of coarse sand and peat in a volume ratio of 1:1 was used; this was previously verified to exhibit high ability to accumulate pollutants (see Fig. 1). Magnetic methods supplemented with chemical method evaluating heavy metal content and electron microscopic observations were used to detect the effectiveness of the PS. The PS was validated in Warsaw, Poland, by observing the capacity and trends in the accumulation of traffic-related heavy metals as well as magnetic particles and by comparison of the properties of magnetic fraction of PS filling and street dust collected from the surface of road. A depth decreasing trend in distributions of magnetic susceptibility related to the concentration of magnetic particles and the content of heavy metals confirmed a very strong accumulation of pollution in the surface layer of samplers and their depth-migration. Magnetic fraction of PS filling and street dust revealed similarities in terms of magnetic mineralogy, grain size, domain state, morphology, and chemical composition. The good correlation of concentration of magnetic particles with traffic-related heavy metals indicates their similar transport pathway from road to sampler (see Fig. 1). Passive sampler is a compact, mobile, low-cost tool that does not require electricity for installation and can be effectively used for the identification of traffic-derived pollution. Moreover, the PS can overcome disadvantages of street dust arising from different geological backgrounds, cleaning of the road surface, runoff of deposited dust, etc., which cause the underestimation of pollution level.

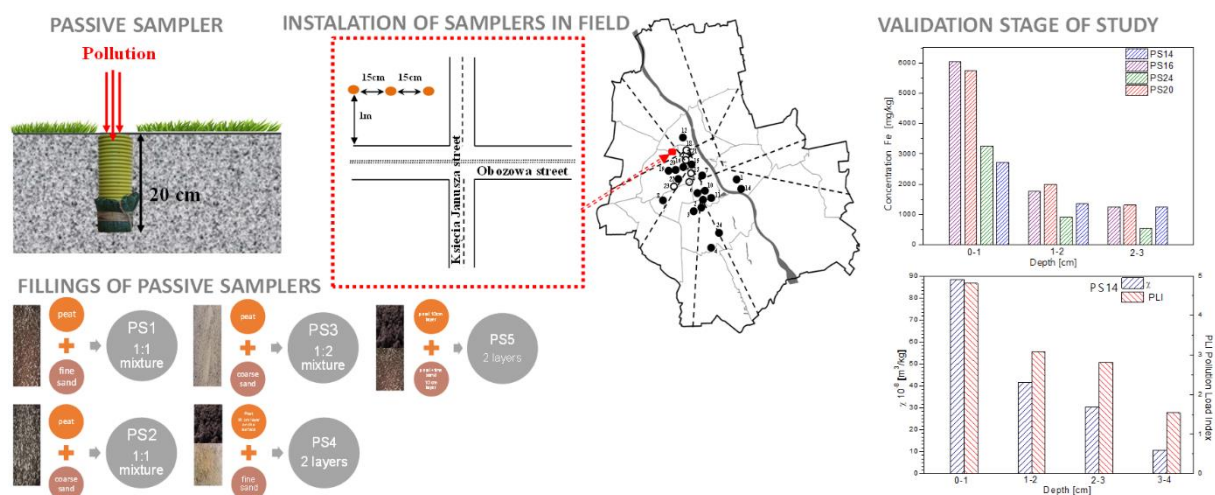


Fig. 1. The figure shows the construction of passive sampler and its implementation in field, the types of fillings of sampler, the locations of installation of samplers in Warsaw and the results of depth distribution of iron in four samplers, Pollution Load Index and magnetic susceptibility in sampler PS14 (after Dytłow and Górka-Kostrubiec 2019).

References

Dytłow, S., and B. Górka-Kostrubiec (2019), Effective and universal tool for evaluating heavy metals—passive dust samplers, *Environ. Pollut.* **247**, 188–194, DOI: 10.1016/j.envpol.2019.01.030.

MAGNETIC PROPERTIES OF DIFFERENT GRANULOMETRIC FRACTIONS OF STREET DUST FROM WARSAW

S. Dytłow, B. Górka-Kostrubiec

The study presents variations in the magnetic properties and heavy metal concentrations of five granulometric fractions, i.e., 500 μm , 250 μm , 100 μm , 71 μm , and less than 71 μm , for street dust collected at two locations in Warsaw (see Fig. 1). Combination of grain-size determination, magnetometry, electron microscope observation, mineral composition and chemical analyses was applied as an effective and multidisciplinary approach for the complete characterization of individual fractions of street dust. The magnetic properties of street dust were influenced by their grain size; concentration-dependent magnetic parameters, e.g., the magnetic susceptibility, saturation magnetization, saturation remanence and anhysteretic remanent magnetization of the finest fraction ($d < 0.071$ mm) were about three times higher than that of the coarsest fraction ($d > 0.5$ mm). For all fractions the main magnetic mineral was near stoichiometric magnetite. The fractions with grain size less than 250 μm additionally contain a phase with a Curie point $\sim 770^\circ\text{C}$, ascribable to metallic iron. The distribution of mass fractions showed that the smallest contribution to the total mass is from the finest size fractions, which simultaneously contain the highest concentrations of the traffic-related heavy metals. The differences in traffic intensity and type of vehicles movement (fluent driving, repeated braking, and accelerating) between both studied sites were well reflected by the concentration of anthropogenic magnetic particles strongly associated with traffic-related heavy metals (see Fig. 1). Magnetic extract of finest fraction dust contains a mixture of spherical magnetic particles and irregular angular par-

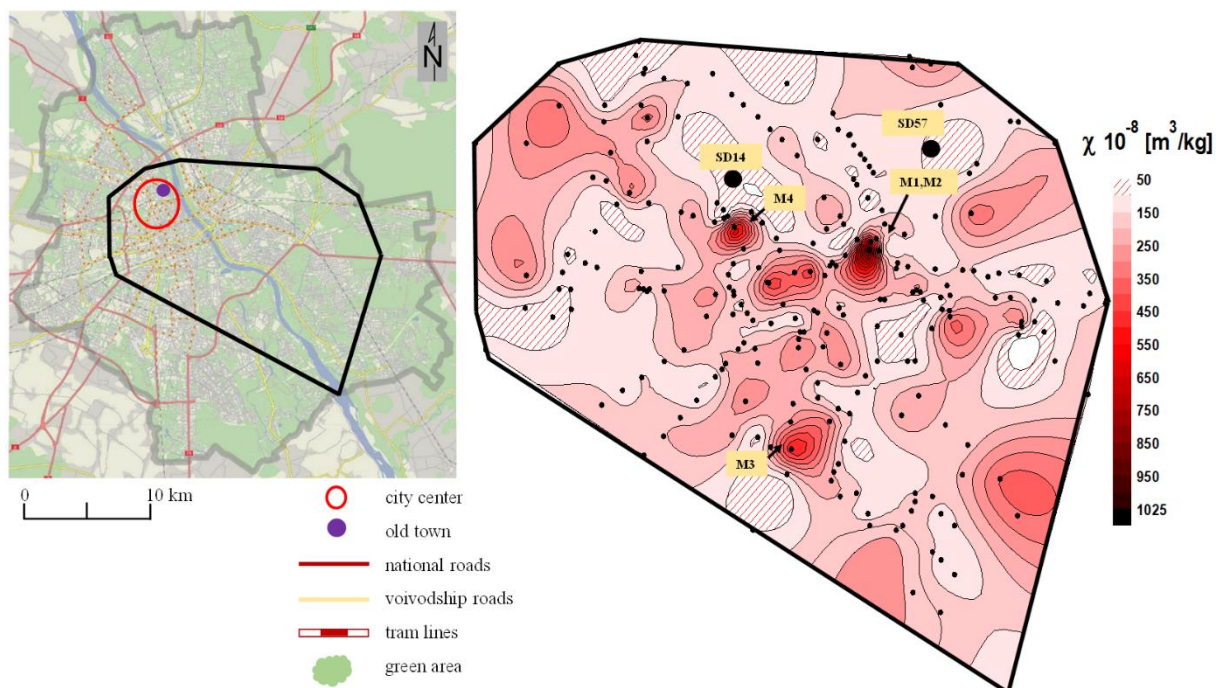


Fig. 1. Spatial distribution of magnetic mass susceptibility (χ) of street dust in Warsaw (Poland) (after Dytłow et al. 2019).

ticles containing iron-oxides with Mg, Al, Na, Ca, K, and Si. The study of the granulometric fractions of street dust can significantly contribute to their complete characterization, with interesting implications on the definition of their impact on environment and human health.

References

Dytłow, S., A.Winkler, B. Górka-Kostrubiec, and L. Sagnotti (2019), Magnetic, geochemical and granulometric properties of street dust from Warsaw (Poland), *J. Appl. Geophys.* **169**, 58–73, DOI: 10.1016/j.jappgeo.2019.06.016.

COMPARISON OF TRAFFIC-RELATED POLLUTION LEVEL USING STREET DUST AND PASSIVE DUST SAMPLE

S. Dytłow, B. Górka-Kostrubiec

The magnetic susceptibility and concentrations of traffic-related heavy metals were used to compare the pollution level for 24 locations in Warsaw (Poland) estimated for street dust and passive dust samplers collected for the same sampling sites (see Fig. 1). The spatial distribution of magnetic susceptibility showed diversity ranging from $\sim 36 \times 10^{-8} \text{ m}^3/\text{kg}$ to $\sim 406 \times 10^{-8} \text{ m}^3/\text{kg}$ for passive samplers $-\chi_{\text{PDS}}$ and $\sim 49 \times 10^{-8} \text{ m}^3/\text{kg}$ to $\sim 520 \times 10^{-8} \text{ m}^3/\text{kg}$ for street dust $-\chi_{\text{SD}}$. Although the χ_{SD} and χ_{PDS} values of individual sampling sites significantly differ, they follow the same trend in case of traffic intensity (see Fig. 1). The values of χ_{SD} and χ_{PDS} were higher mainly at the crossroads of multilane roads with high-intensity traffic. For example, $\chi_{\text{PDS}2} \sim 400 \times 10^{-8} \text{ m}^3/\text{kg}$ and $\chi_{\text{SD}2} \sim 520 \times 10^{-8} \text{ m}^3/\text{kg}$ were obtained from one of the biggest and busiest crossroads in the city center with almost 70 000 cars and trams crossing through per day. In places of traffic restricted to privileged vehicles and public transport, relatively low values of $\chi_{\text{PDS}18} \sim 61 \times 10^{-8} \text{ m}^3/\text{kg}$ and $\chi_{\text{SD}18} \sim 104 \times 10^{-8} \text{ m}^3/\text{kg}$ were noted (see Fig. 1). The lowest values of $\chi_{\text{PDS}21} \sim 49 \times 10^{-8} \text{ m}^3/\text{kg}$ and $\chi_{\text{SD}21} \sim 36 \times 10^{-8} \text{ m}^3/\text{kg}$ were observed in one of the biggest park in the center of Warsaw (see Fig. 1). Although the park is surrounded by streets with heavy traffic, it is sepa-

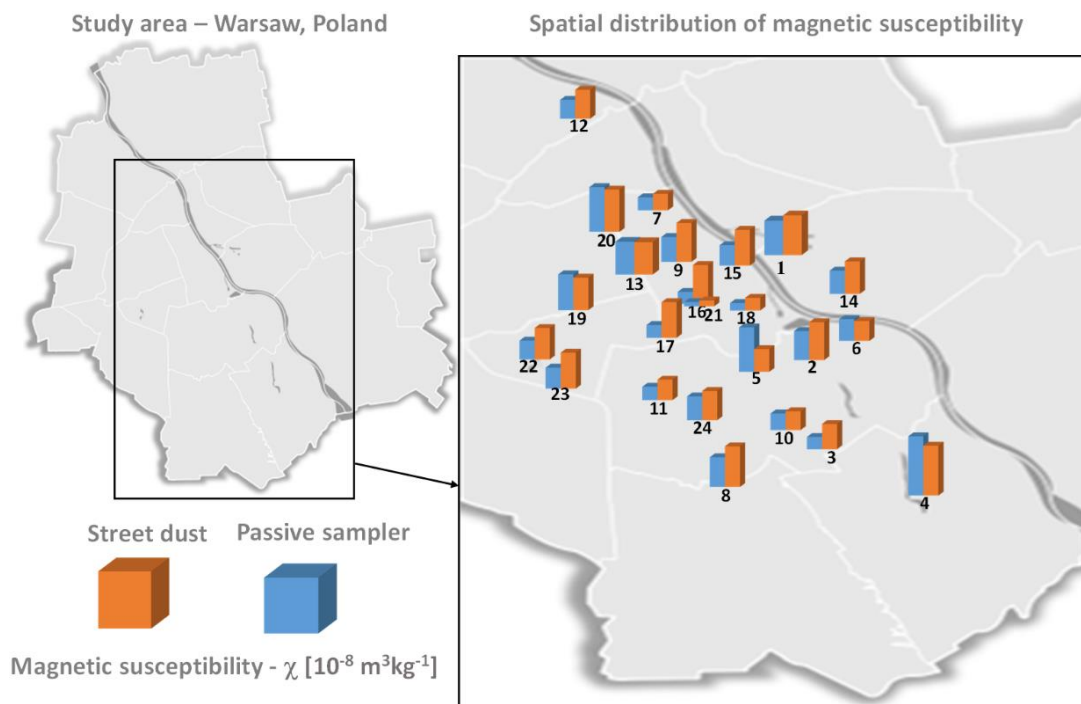


Fig. 1. Spatial distribution of mass magnetic susceptibility (χ) of passive dust samplers and street dust in Warsaw (Poland) (after Dytłow and Górka-Kostrubiec 2018).

rated from the roads by tree lines. Thus, it proves that green walls and effectively reduce traffic-related pollution.

A general trend between traffic intensity and χ values cannot be observed in all sampling sites because of several local factors, e.g., different concepts of space management (density, height of buildings, distance of buildings from road edge) and surface runoff (often rainfall, cleaning streets) that disturb the spread of street dust particles. For example, the high value of $\chi_{\text{PDS5}} \sim 366 \times 10^{-8} \text{ m}^3/\text{kg}$ obtained from the sampler installed at a multilane crossroad (sampling site number 5) reflects the impact of high traffic intensity with $\sim 73\,000$ cars crossing per day. However, the relatively low value of $\chi_{\text{SD5}} \sim 187 \times 10^{-8} \text{ m}^3/\text{kg}$ obtained from another crossroad suggests the influence of several factors on the distribution and amount of street dust particles. The crossroad is characterized as unusual by the Warsaw land development due to the absence of buildings and the presence of ample open area providing good ventilation and, thus, facilitating the particles being blown away and lowering the χ than that of passive sampler. However, this effect was not observed for PDS5, which is able to accumulate and preserve the pollution particles by transporting them inside the sampler. All these observations proved that the properties of street dust could rather be used for preliminary tests or as a supporting measurement than for detailed studies.

ASSESSMENT OF HEAVY METAL POLLUTION OF VISTULA RIVER SEDIMENTS USING MAGNETIC METHODS

I. Szczepaniak-Wnuk, B. Górka-Kostrubiec, S. Dytłow

The aim of the study was to evaluate the level of heavy metal pollution of Vistula River, within high urbanized area. The river surface sediments that accumulate pollutant particles and reflect the level of water contamination was investigated. The study was conducted in Warsaw agglomeration, which is the largest emitter of urban pollution in the central part of Poland. Measurements were performed for fine fractions ($71 \mu\text{m}$ and less than $71 \mu\text{m}$) of sediments taken from the surface layer of river bank. An interdisciplinary approach including magnetic methods (e.g. mass magnetic susceptibility χ , temperature dependence magnetic susceptibility and hysteresis loop parameters), microscopic and chemical analyses was undertaken to assess the level of heavy metal pollution.

The results showed local impact of Warsaw's activity on the level of heavy metals pollution. This was indicated by the maximum values of magnetic susceptibility and the maximum concentrations of heavy metals in the city center (see Fig. 1). The anthropogenic origin of pollution was confirmed by magnetic mineralogy of finest granulometric fraction (less than $0.071 \mu\text{m}$), dominating by magnetite and large amount of spherical magnetic particles. The dominant sources of sediments pollution were discriminated by analysis the relationship between magnetic parameters dependent on the domain structure of magnetic particles and the concentrations of individual heavy metals (see Fig. 1). It was found that the source of cadmium, zinc, and copper were mainly vehicle emissions and the motion process of vehicles such as abrasion of road surfaces, brake discs, brake pads, etc. These chemical components are associated with irregularly-shaped particles. Nickel, aluminum, titanium, and chromium were connected with spherical shaped particles originated from high temperature combustion processes. Results suggested that the source of large amount spherical particles in sediments observed in the city center was the storage of ashes from coal power plant, located at the south of Warsaw. This was demonstrated by the similarity in mineralogy and morphology of magnetic particles observed in sediments and street dust collected from the road at the vicinity of the waste disposal site.

The study demonstrated that magnetic method have a useful and practical application for detecting and mapping heavy metal pollution of river systems.

The project is financed by the National Science Centre (NCN) Preludium 13 programme.

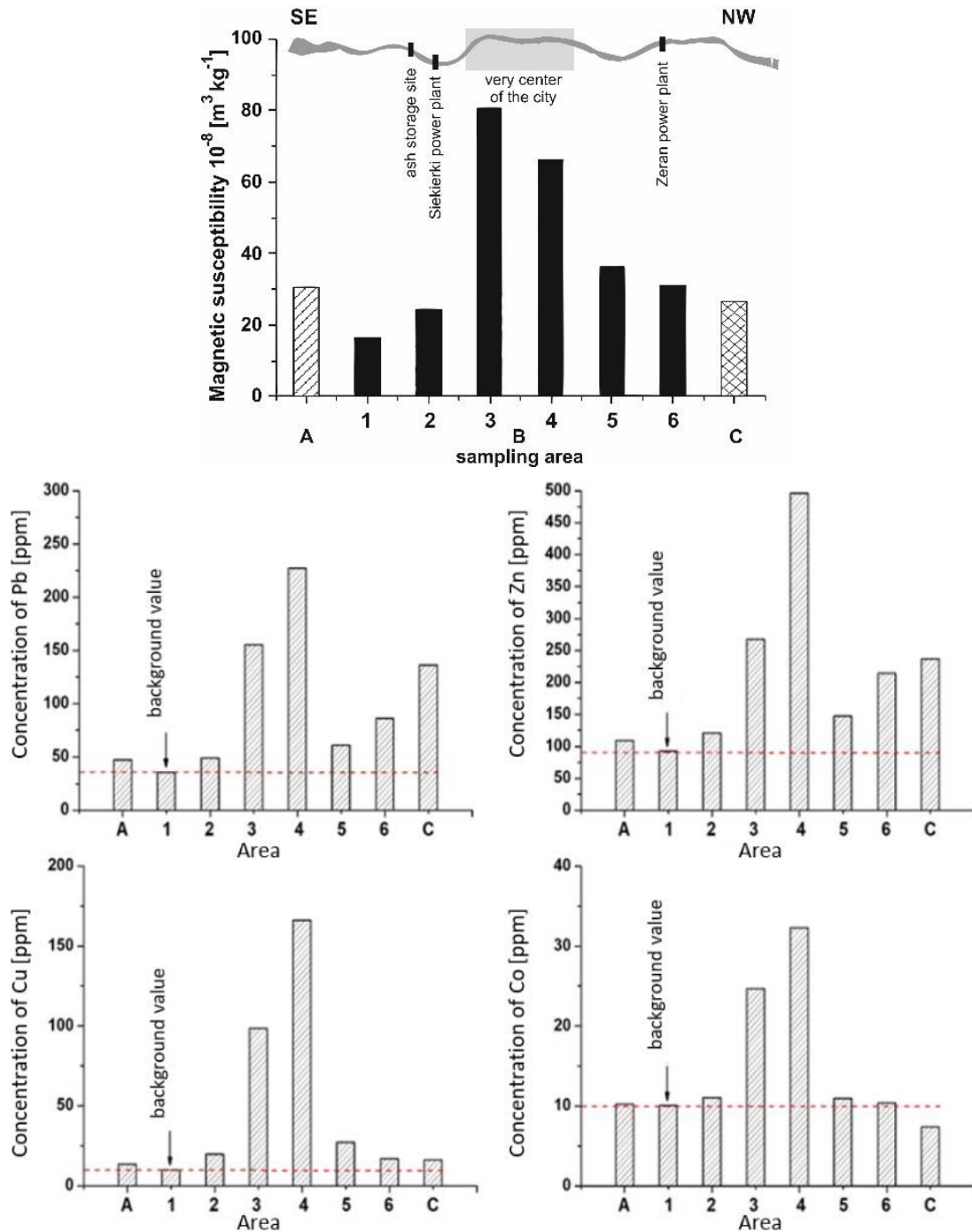


Fig. 1. Distribution of average magnetic susceptibility (χ_{av}) of surface Vistula River sediments for area A (stripes pattern column), for area B with corresponding subareas 1–6 (black columns), and for area C (column with grid pattern). Concentrations of selected heavy metals for “<0.071” fraction of sediments from area A and subareas (1–6) of area B and area C (after Szczepaniak-Wnuk et al. 2020).

References

- Szczepaniak-Wnuk, I., B. Górka-Kostrubiec, S. Dytłow, P. Szwarczewski, P. Kwapuliński, and J. Karasiński (2020), Assessment of heavy metal pollution in Vistula river (Poland) sediments by using magnetic methods, *Environ. Sci. Pollut. Res.* **27**, 24129–24144, DOI: 10.1007/s11356-020-08608-4.

THE MAGNETIC METHOD AS A TOOL TO INVESTIGATE THE WERENSKIOLDBREEN ENVIRONMENT (SOUTH-WEST SPITSBERGEN, ARCTIC NORWAY)

M. Gwizdała, M. Teisseyre-Jeleńska, L. Łęczyński

We used a novel approach of applying magnetic analyses to investigate the material released from the receding glacier Werenskioldbreen on Spitsbergen, Svalbard, Arctic Norway (Fig. 1). Surface sediments were taken from the bay Nottinghambukta and the Werenskioldbreen foreland, along two main proglacial streams. Magnetic analyses, namely the low-field mass magnetic susceptibility (Fig. 2), anhysteretic susceptibility mass normalized and hysteresis parameters, served to determine magnetic properties and identify the magnetic composition of the study material. We selected two distinct types of sediments. The first group, consisting of

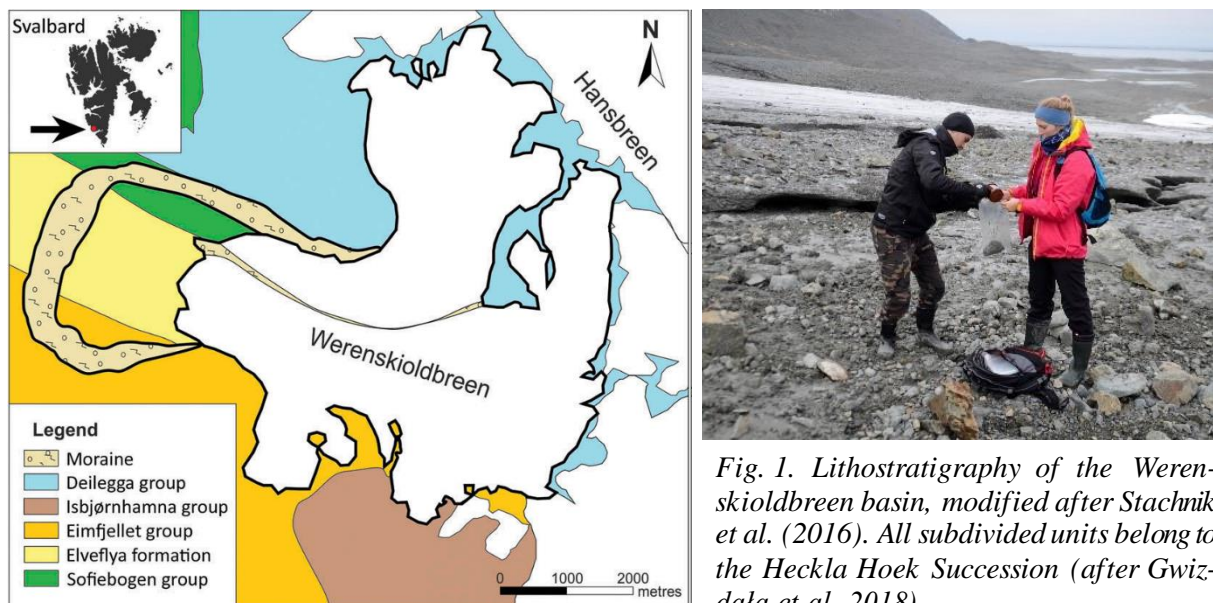


Fig. 1. Lithostratigraphy of the Werenskioldbreen basin, modified after Stachnik et al. (2016). All subdivided units belong to the Heckla Hoek Succession (after Gwizdała et al. 2018).

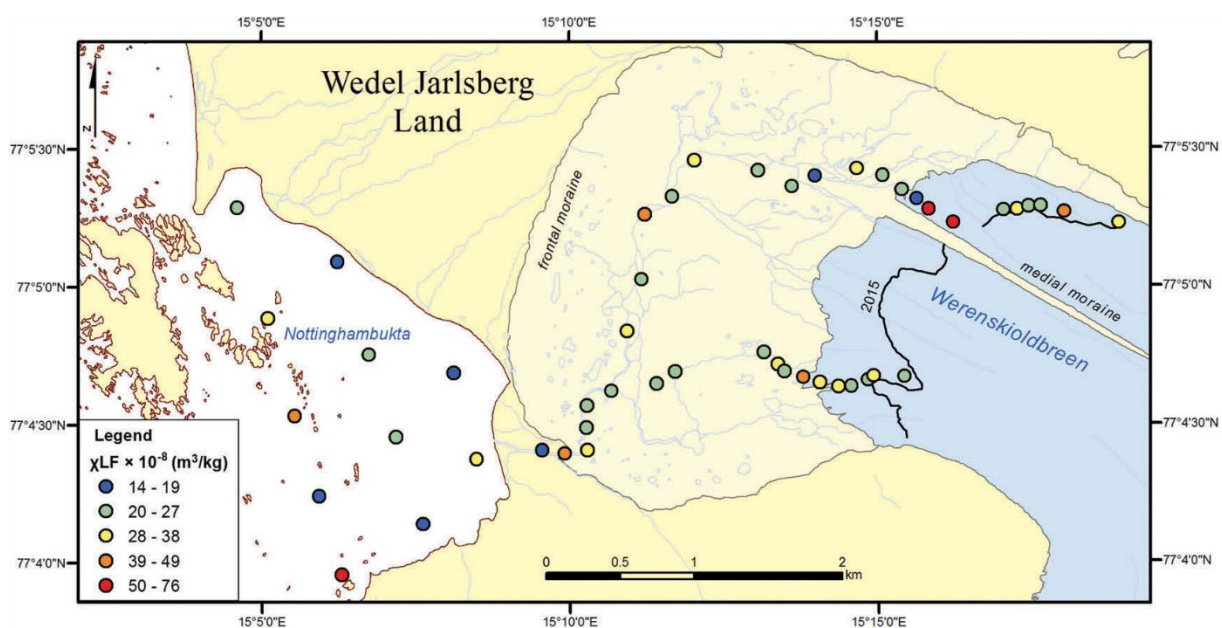


Fig. 2. Distribution of magnetic susceptibility in the investigated area (based on Norwegian Polar Institute maps at <http://toposvalbard.npolar.no/>) (after Gwizdała et al. 2018).

magnetite and pyrrhotite, has more single-domain grains in comparison to the second one, containing only magnetite. In the second group, multi-domain particles dominate. Deposits from the north stream, glacier river and an area close to the estuary of Nottinghambukta include magnetite and pyrrhotite. Magnetite was found in the south stream and in the outside part of the bay. Magnetic composition reflects different source rocks of sediments. This study demonstrates the utility of the magnetic method in analysing the current state of glacier environments.

Details at: Gwizdała, M., M. Jeleńska, and L. Łęczyński (2018), The magnetic method as a tool to investigate the Werenskioldbreen environment (south-west Spitsbergen, Arctic Norway), *Polar Res.* **37**, 1, 1436846, DOI: 10.1080/17518369.2018.1436846.

This work was partially financed by funds from the Leading National Research Centre, received by the Centre for Polar Studies for the period 2014–2018.

MAGNETIC PROPERTIES OF CHROMITE ORES: FE-CR MIXED BINARY SPINELS AS ACCESSORY MAGNETIC MINERALS IN THE SUDETIC OPHIOLITIC ROCKS

M. Kaździałko-Hofmoki, T. Werner

The project is carried out within statutory activities since 2010. In the project effects of substantial structure changes of the chromitites on their magnetic properties were studied in the Sudetic ophiolite.

Sudetic ophiolite is formed of three serpentinite massives situated around the Sowie Góry Mts Block: Jordanów-Gogołów Massif (JGSM), Braszowice-Brzeźnica Massif (BBSM), and Szklary Massif (SZM). Chromite Fe-Cr spinels occur in chromium ore (chromitites) in JGSM and BBSM (ore fragments on waste heaps) and as scattered grains in ultramafic rocks (Fig. 1).

The Fe-Cr chromite series have a general formula of $(\text{Fe}^{2+}_{1-x}\text{Fe}^{3+}_x)[\text{Fe}^{2+}_{1-x}\text{Fe}^{3+}_{2-2y-x}\text{Cr}^{3+}_{2y}]_2\text{O}_4$ is built of mixed spinels with end members: primary chromite (Fe^{2+})[Cr_3^{+2}] O_4 ($y = 1$)

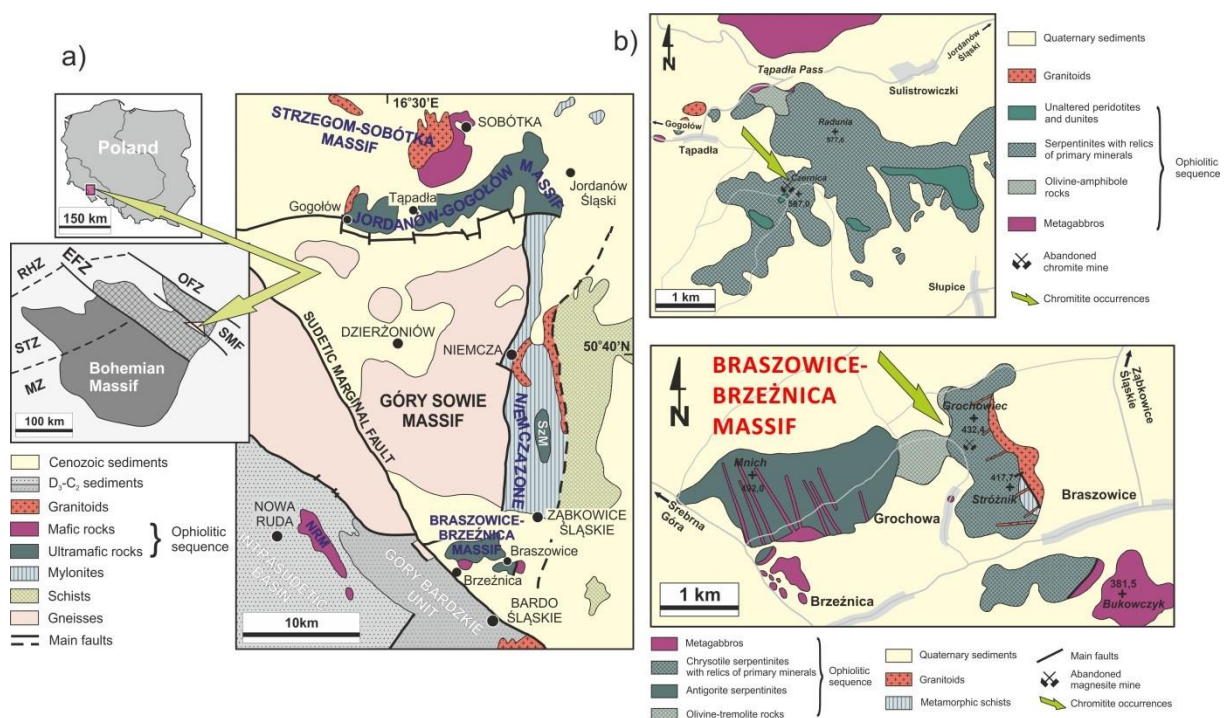


Fig. 1. Chromite occurrences: a) scattered within serpentinites, dunites, harzburgites, peridotites, eclogites of Sudetic ophiolite (Jordanów-Gogołów Massif (JGSM), Braszowice-Brzeźnica Massif (BBSM), Nowa Ruda gabbro (NR), Szklary massif (SZM); b) chromite ore (chromitite) – at Tapadla pass at JGSM and Grochowa at BBSM (modified after K. Delura, personal communication).

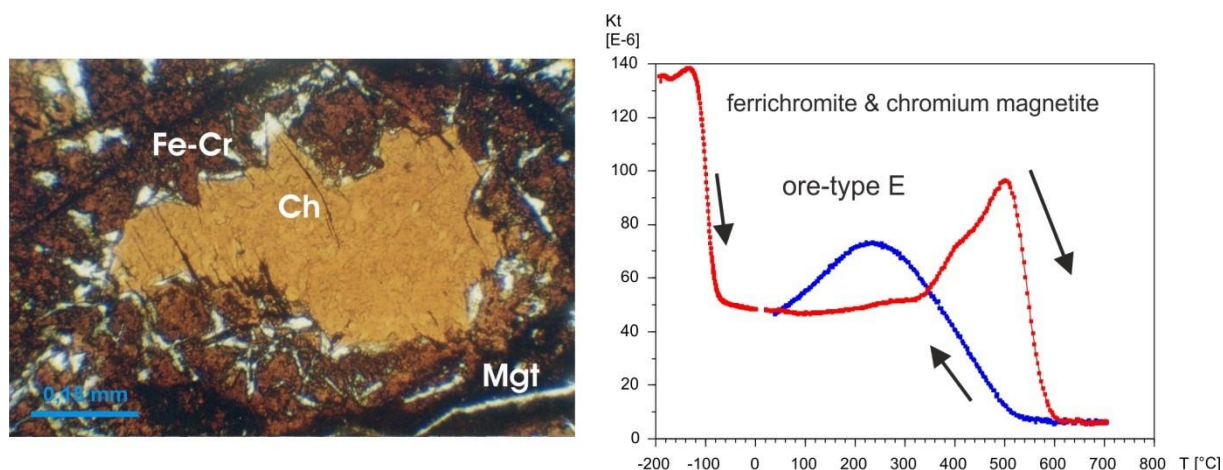


Fig. 2. SEM maps for chromite grains from chromite ore (JGSM, Tapadla), $K(T)$ curves for chromite ore (chromitite) – at Tapadla pass (modified after K. Delura, personal communication).

with normal ordered spinel structure ($x = 0$) and magnetite (Fe^{3+})[$\text{Fe}^{2+}\text{Fe}^{3+}\text{O}_4$] ($y = 0$) with inverted ordered spinel structure ($x = 1$). The composition affects substantially Curie temperatures: T_C of primary chromite is -202°C , T_C above r.t. for ferrichromites up to T_C of 585°C for magnetite. The primary chromites crystallize from mafic melt in upper mantle-lower crust environments. They are very stable against metamorphism and retain primary composition of their cores long during later metamorphism. Under cooling below ca 600°C chromite begin to alter: magnetite starts to replace chromite, with subsolidus exsolutions and oxidations processes. The core of the grain retains its primary composition with typical T_C of -180° up -120°C , around it ring 1 composed of Fe-Cr solution grains of ferrichromite and ring 2 of Cr-magnetite formed during metamorphism were observed.

Apart of changes in composition additional alterations, namely order-disorder transformation takes place (e.g. described by Harrison and Putnis (1998)). Such transformation is caused by electron hopping between tetrahedral and octahedral sublattices with help of oxygen ions (x in the above formula presents a fraction of 3+ cations in tetrahedral sublattice).

Chromites from Sudetic ophiolite and Lutynia chromite rich olivine were studied with magnetic methods as determinations of the magnetic susceptibility upon temperature curves ($km-T$; Fig. 2) at the range -190°C up to 700°C for fresh and previously heated samples as well as with hysteresis properties studies. The $km-T$ experiments for fresh samples showed a wide spectrum of $km(T)$ curves depending on the composition. Changes in composition influence changes in T_C observed on the heating branch of $km-T$ curve, changes in ordering impart changes in T_C observed on the cooling branch. Therefore $k-T_c$ curves are irreversible and T_C of samples observed in Cr-magnetites during heating is higher by $10-20^\circ\text{C}$ than observed during cooling. During next heating-cooling cycles both branches become reversible. The observed thermal hysteresis during heating-cooling cycle is due to kinetic lag in cation ordering during cooling (Harrison and Putnis 1996). The coercivity usually increases due to heating suggesting subsolidus exsolutions.

In 2018 results were presented at the 16th Castle Meeting “New Trends on Paleo, Rock and Environmental Magnetism” in Chęciny, Poland.

References

- Harrison, R.J., and A. Putnis (1996), Magnetic properties of the magnetite-spinel solid solution: Curie temperatures, magnetic susceptibilities, and cation ordering, *Am. Mineral.* **81**, 375–384, DOI: 10.2138/am-1996-3-412.

Harrison, R.J., and A. Putnis (1998), The magnetic properties and crystal chemistry of oxide spinel solid solutions, *Surv. Geophys.* **19**, 6, 461–520, DOI: 10.1023/A:1006535023784.

EPOS – PL EUROPEAN PLATE OBSERVING SYSTEM; TASK 4: CIBAL – CENTRE OF RESEARCH INFRASTRUCTURE OF ANALYTICAL LABORATORIES

T. Werner, B. Górka Kostrubiec, G. Karasiński, S. Dytłow, R. Szaniawski, K. Michalski, M. Kądziałko-Hofmokl, M. Teisseyre-Jeleńska, K. Dudzisz



The Task 4 – CIBAL – Centre of Research Infrastructure of Analytical laboratories is a part of the Polish activities (EPOS-PL) within the European Plate Observing System (EPOS) Infrastructure project. In general, European Plate Observing System (EPOS) Infrastructure is an interdisciplinary and interoperable research infrastructure which gathers data from measurement networks scattered all around the Europe. Processed, standardized and integrated data is stored in databases connected with web portals, where the data can be visualized and analyzed with the use of dedicated applications and visualizations.

CIBAL will belong to the first layer of Research Infrastructure in Poland built by so-called Research Infrastructure Centers (RICs). It will provide a complete dataset concerning palaeomagnetic and environmental magnetism data with basic data storage and basic computing resources. CIBAL resources will be connected to the EPOS Thematic core service (TCS) of the MultiScale Laboratories.

Within activities to build CIBAL the enhancement of the research potential of the IG PAS palaeomagnetic laboratory was performed in 2018 supported by funds of EPOS-PL. The motion to establish ties with EPOS-EU MSL group was initiated to collaborate with other EPOS EU laboratories in following years. The third activity is connected to the task to shear the data and results in the building of the database system for data and metadata created and stored according to rules of EPOS WP16 Multiscale Laboratories.

Palaeomagnetic Laboratory hosts a set of the complementary equipment for palaeomagnetic and rockmagnetic studies, that was set up in years 1990–2013. The new set of equipment was added for measurements of magnetic properties and laboratory experiments (magnetometer, magnetic susceptibility bridge, amagnetic furnace, low field magnetic cage, equipment for magnetizing samples in the laboratory) (Fig. 1). The additional units for sampling and analyzing of magnetic properties of environmental pollution (dust samplers, magnetic susceptibility meters) were also acquired.

Planned data bases:

- of palaeomagnetic results,
- of rock-magnetic properties,
- of results of environmental magnetism.

Experimental data from years 1990–2016 stored locally outside the database system are being processed and prepared for access according to procedures of WP 16 EPOS including standardization of data and metadata. The software to access the CIBAL databases, to process measurement data: collect, store, standardize, support the generating of metadata is under development.

After the successful application to Transnational access to MSL Laboratory scheme implementation of rules to admit other researchers for short-term visits according to rules set in „Transnational access WP 16 EPOS” will be set. In 2018 the laboratory were undergoing some preparation these visits (procedures, training of the staff, laboratory space refitting).



Fig. 1. Paleomagnetic team in a refitted lab space with some new acquired equipment financed by the EPOS-PL (low-field cage, JR6 spinner magnetometer, demagnetizer).

The EPOS-PL project is financed by the Operational Programme Smart Growth 2014–2020; Priority IV: Increasing the Research Potential, Action 4.2: Development of Modern Research Infrastructure of the Science Sector, Co-financing from European Regional Development Fund.



Republic
of Poland

European Union
European Regional
Development Fund



NEW PALEOMAGNETIC AND MAGNETIC FABRIC RESULTS FROM HEMATITE-BEARING LOWER TRIASSIC REDBEDS OF THE CENTRAL WESTERN CARPATHIANS

Rafał Szaniawski

The progressive collision of the Alcapa and Tisza-Dacia microplates with the European Platform resulted in the formation of the Carpathian orogeny (Fig. 1). With the objective of better constraining the regional paleogeographic evolution, we carried out paleomagnetic studies within the Central Western Carpathians, representing a fragment of the Alcapa microplate. Our investigations were focused on Lower Triassic red sandstones from the autochthonous cover overlying the crystalline basement. This study is a continuation of our earlier works performed in the Tatra Mts. Here we present results from the nearby mountain massifs of Low Tatra, Velka

Fatra, and Strazovske Vrchy. Petromagnetic studies reveal that the dominant ferromagnetic carrier in the studied red sandstones is hematite, whereas magnetic susceptibility and magnetic fabric are mostly governed by paramagnetic minerals (phyllosilicates). AMS studies document the occurrence of a distinct magnetic foliation compatible with the bedding plane, and of a magnetic lineation of tectonic origin (Fig. 2). Such a lineation lies in the bedding plane, but it is not exactly parallel to the strike of the bedding. The orientation of the lineation most probably reflects the multi-stage character of the deformation – folding and thrusting were followed by uplift and/or block faulting which affected the present day bedding attitude.

The hematite carrier records a characteristic component characterized by maximum unblocking temperatures of 680°C. This component displays both normal (dominant) and reversed polarity, as well as shallow to moderate inclinations, i.e. similar to those expected from reference paleomagnetic data from the European Platform. Declination values are rather uniform for all four studied mountain massifs and indicate moderate counterclockwise rotations of the Central Western Carpathians.

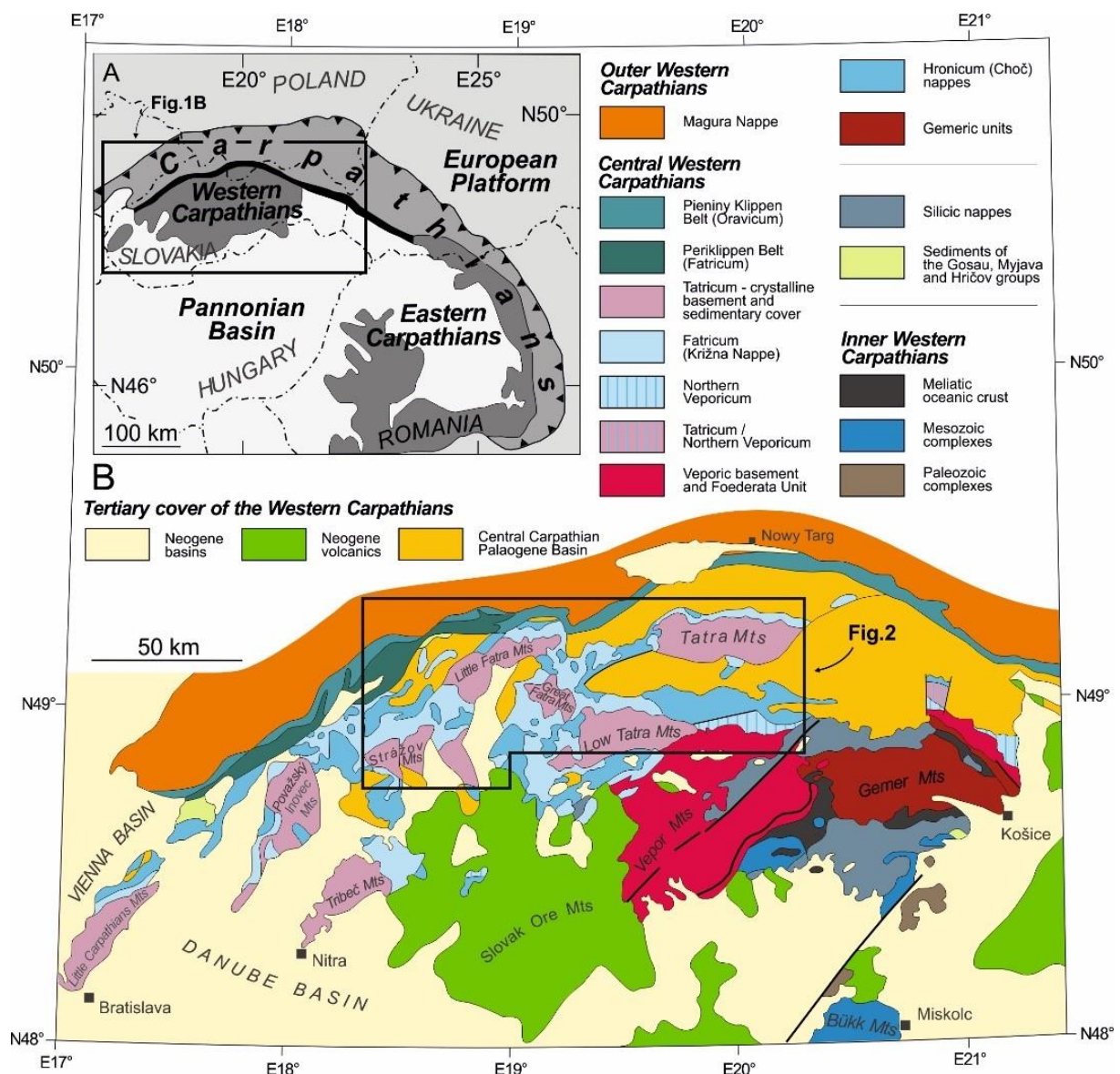


Fig. 1. Schematic tectonic map of the Western Carpathians with marked location of study area (compiled after Bezák et al. 2004; Lexa et al. 2000; Plašienka 2003) (after Szaniawski et al. 2020).

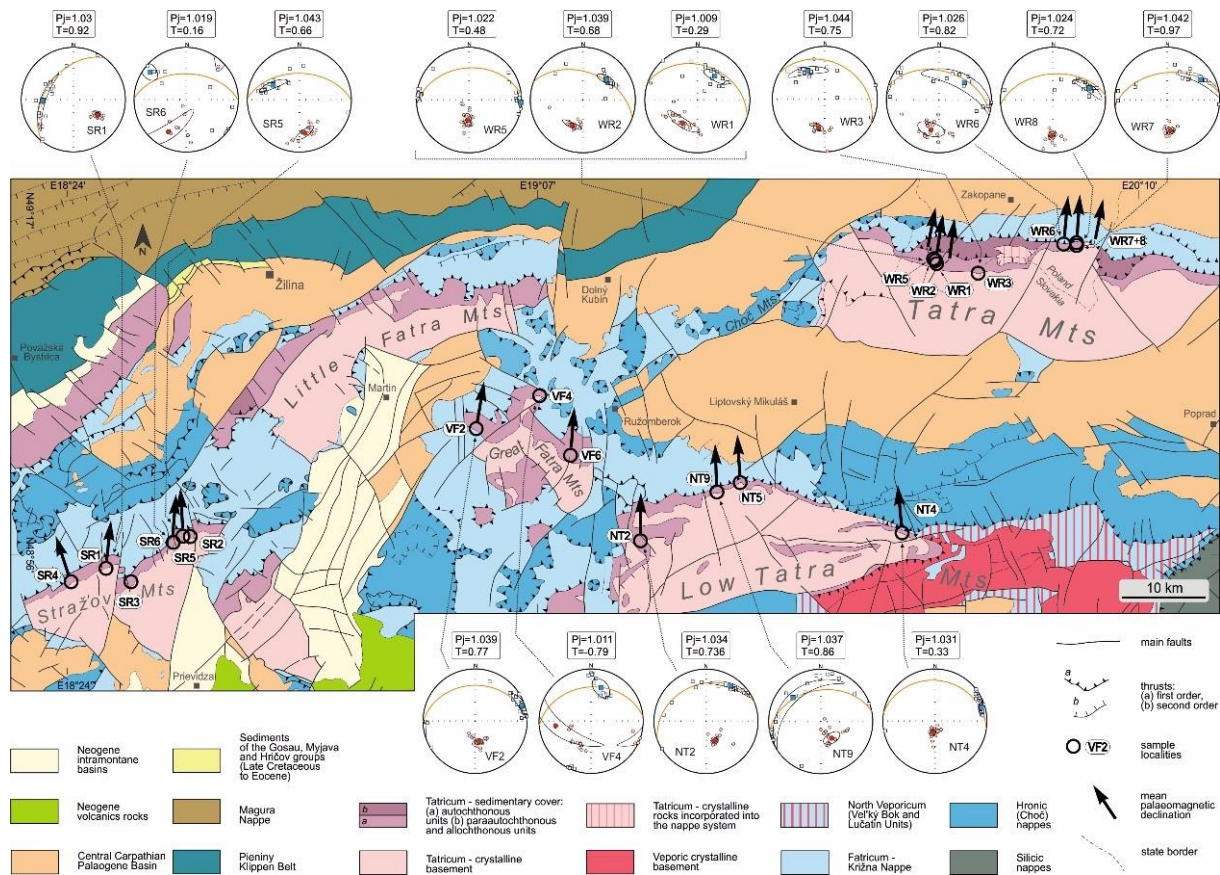


Fig. 2. Simplified geological map of the study area with marked location of sampling sites (compiled after Biely et al. 1992; Mahel' et al. 1982; Polák et al. 1997; Nemčok et al. 1994). Stereographic diagrams show AMS results (only for samples in which the susceptibility is higher than 30×10^{-6} SI volume), AMS principal axes are marked as red circles (K_{min}) and blue squares (K_{max}). Larger symbols representing site mean principal axes shown with their 95% confidence ellipses. Orange circle is mean bedding. T – shape parameter, P_j – corrected anisotropy degree (both parameters after Jelínek 1981) (after Szaniawski et al. 2020).

References

- Bezák, V., I. Broska, J. Ivanička, P. Reichwalder, J. Vozár, et al. (2004), Tectonic map of Slovak Republic, Ministerstvo Životného Prostredia Slovenskej Republiky, ŠGÚDŠ, Bratislava, scale 1:50,000, 2 sheets.
- Biely, A., P. Beňuška, et al. (1992), Geological map of the Nízke Tatry Mountains, Slovenský Geologický Úrad, ŠGÚDŠ, Bratislava.
- Jelínek, V. (1981), Characterization of the magnetic fabric of rocks, *Tectonophysics* **79**, 3–4, 63–67, DOI: 10.1016/0040-1951(81)90110-4.
- Lexa, J., V. Bezák, M. Elečko, J. Mello, M. Polák, M. Potfaj, et al. (2000), Geological map of Western Carpathians and adjacent areas 1:500,000, Issued by Ministry of the Environment of Slovak Republic, Geological Survey of Slovak Republic, Bratislava.
- Mahel', M., S. Kahan, P. Gross, I. Vaškovský, and J. Salaj (1982), Geologická mapa Strážovských vrchov, Slovenský Geologický Úrad, ŠGÚDŠ, Bratislava.
- Nemčok, J., V. Bezák, et al. (1994), Geological map of the Tatra Mountains, Ministerstvo Životného Prostredia Slovenskej Republiky, ŠGÚDŠ, Ministerstvo Ochrany Šrodo-

wiska, Zasobów Naturalnych i Leśnictwa, Państwowy Instytut Geologiczny, scale 1:50,000, 1 sheet.

Plašienka, D. (2003), Development of basement-involved fold and thrust structures exemplified by the Tatric-Fatric-Veporic nappe system of the Western Carpathians (Slovakia), *Geodin. Acta* **16**, 1, 21–38, DOI: 10.1016/S0985-3111(02)00003-7.

Polák, M., A. Bujnovský, et al. (1997), Geological map of the Veľká Fatra Mts., Ministerstvo Životného Prostredia Slovenskej Republiky, Geologická Služba Slovenskej Republiky, Bratislava, scale 1:50,000, 1 sheet.

Szaniawski, R., M. Ludwiniak, S. Mazzoli, J. Szczygieł, and L. Jankowski (2020), Paleomagnetic and magnetic fabric data from Lower Triassic redbeds of the Central Western Carpathians: new constraints on the paleogeographic and tectonic evolution of the Carpathian region, *J. Geol. Soc.* **177**, 509-522, DOI: 10.1144/jgs2018-232.

MAGNETIC ANISOTROPY IN SILURIAN GAS-BEARING SHALE ROCKS FROM THE POMERANIA REGION (NORTHERN POLAND)

D. Niezabitowska, R. Szaniawski

Analysis of anisotropy of magnetic susceptibility (AMS) and anhysteretic remanent magnetization (AARM) was conducted on unconventional gas-bearing Silurian shales from northern Poland. Samples of these rocks were collected from depths greater than 3 500 m from two exploration drill cores (Fig. 1). The main aim was to investigate magnetic fabrics to verify current

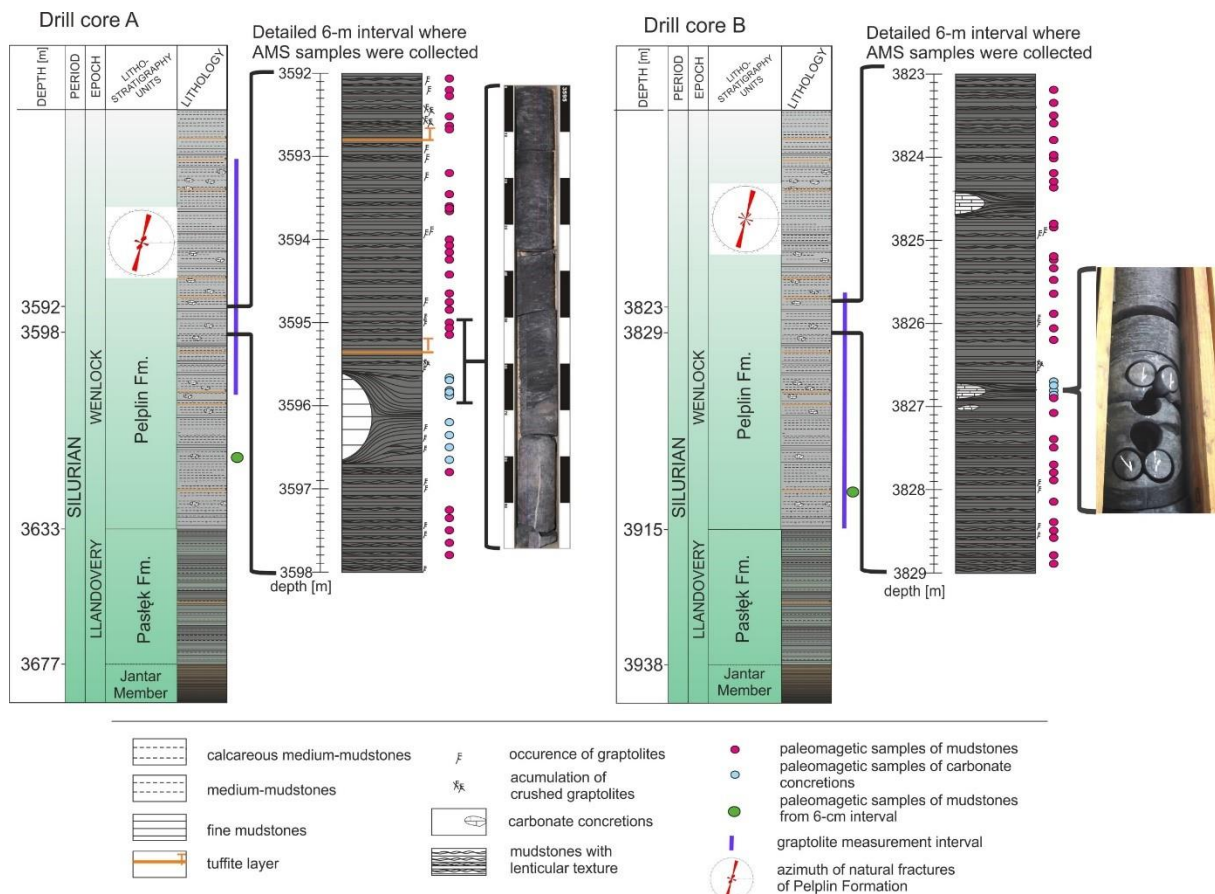


Fig. 1. Lithostratigraphic profiles of Wenlockian rocks from the Pomerania region with marked locations of the drilled samples, intervals of graptolite measurements and orientations of natural fractures in the Pelplin Formation (after Kinga Bobek – unpublished materials of the ShaleMech project).

models of depositional conditions, current direction, and/or tectonic evolution. To obtain an in-depth interpretation, rock magnetic studies, microscopic analyses, and graptolite orientation measurements were performed.

The results of AMS and AARM indicate that the magnetic susceptibility is mainly governed by paramagnetic minerals (phyllosilicates) with a small contribution of ferromagnetic minerals, mostly magnetite. Typically, the studied mudstones and carbonate concretions are characterized by bedding-parallel foliation, resulting mostly from compaction. The foliation is much weaker in the associated early-diagenetic concretions, indicating that cementation occurred during the early stage of diagenesis. This phenomenon resulted in preservation of the early diagenetic fabric from the initial stages of the compaction process. In other words, in the concretions, the orientations of the phyllosilicates (AMS results) and other rock-forming minerals (SEM-BSE results) show some small/weak incipient arrangement in the horizontal plane and have been frozen in time by the early calcite crystallization and formation of rigid concretions. The mudstone rocks surrounding the concretions were subjected to further compaction, which resulted in a much better horizontal alignment of minerals and thus a much stronger magnetic foliation.

A weak magnetic lineation with an orientation of NNW-SSE is preserved in the early-diagenetic, rigid concretions, and the same trend also prevails in the preferred orientation of graptolites. This observation suggests that the observed alignment was produced by bottom currents. We interpret these bottom currents along the Baltica margin as longshore currents. The observed directions show that during the Wenlock (Silurian) in the studied part of the Baltic Basin, the dominant currents had an orientation of circa NNW-SSE along the margin of Baltica. The results suggest that there is no clear evidence for significant CDF accretionary prism activity, such as turbidity currents, influencing the sediment transport process in this part of basin during the early Wenlock (Silurian) epoch. Moreover, our results confirm that even in such fine-grained sediments, in which there are no other unequivocal directional sedimentary indicators, paleocurrent directions can be determined by applying AMS and AARM methodology.

FIRE, AND THEN THE ICE: CALIBRATING SOUTHERN AFRICA'S POSITION WITHIN THE NEOPROTEROZOIC SUPERCONTINENT RODINIA

A. Gumsley, M. Lewandowski, B. Luks

In this year, we conducted a field trip to eastern Zimbabwe to obtain geochronological and paleomagnetic samples from the supposed 0.72 Ga NNE-trending Mutare Dyke Swarm. This dyke swarm has some unpublished ages on it, which indicated an age of approximately ca. 0.72 Ga. During the field trip, we took samples from a total of 9 sites for paleomagnetic analysis, and 31 samples in total for U-Pb geochronological and geochemical investigations, which are complimentary to the paleomagnetic results. In the meantime, we also procured samples from 7 dykes which are linked to the same dyke swarm in eastern Antarctica (Dronning Maud Land), the Fingeren Dyke Swarm. These were sampled on a South African National Antarctic Programme (SANAP) expedition during the southern hemisphere summer of 2017/2018. These samples were collected for geochronological and paleomagnetic investigations. In the paleomagnetic investigations, a portable hand drill was used in Zimbabwe (Fig. 1) for sampling oriented cores, whereas oriented samples were taken in Antarctica.

The samples from Antarctica have been prepared for geochemistry, geochronology, and paleomagnetic investigations. Petrographic and geochemical studies have also been completed using light and scanning microscopy (to identify alteration and the presence of baddeleyite for geochronology), together with electron microprobe analysis, to determine the minerals present, and the degree of alteration (Fig. 2). The results reveal a similar geochemistry of the dykes, indicative of it being from same swarm, and age determinations indicate that the swarm



Fig. 1. Sampling in the eastern highlands of Zimbabwe, with the Nyanga mountains visible on the horizon. Photo by M. Lewandowski.

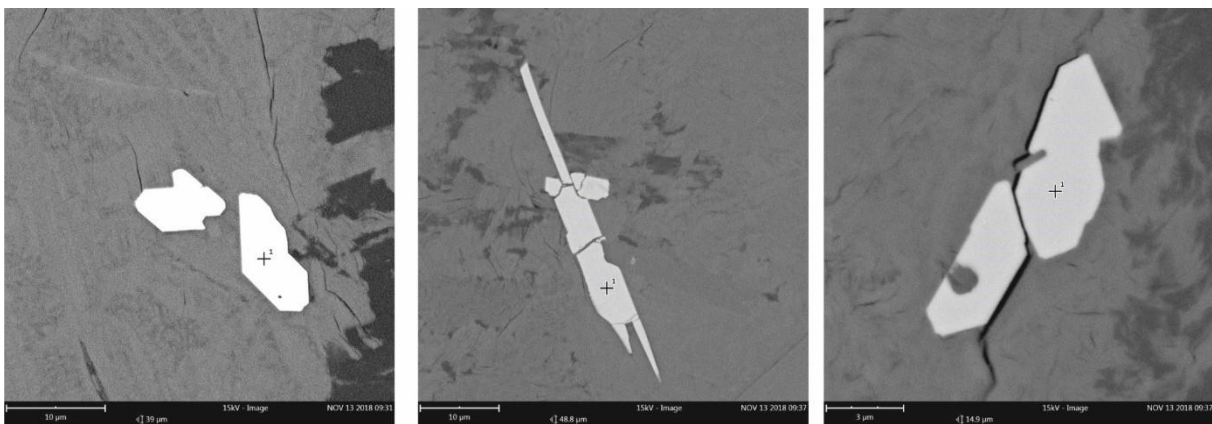


Fig. 2. Baddeleyite (ZrO_2) present in dykes from Antarctica, found using scanning electron microscopy. Each grain is approximately $10\ \mu m$ in size.

is ca. 0.72 Ga. Further age dating, using both U-Pb on baddeleyite and apatite will help to reveal better crystallisation ages of the swarm, as well as its metamorphic history, which appears to be lower greenschist facies, according to the petrography. Some samples from Zimbabwe have been processed in a similar manner, although many more samples are expected to arrive in January 2019. Preliminary data from Zimbabwe indicates lower to upper greenschist facies in many of the dykes, depending on the region. However, U-Pb crystallisation ages appear identical to those in Antarctica at ca. 0.72 Ga. Further U-Pb crystallisation and cooling ages by baddeleyite and apatite will be sought in 2019, combined with further petrographic and geochemical studies. Paleomagnetic sample analysis of the dykes from Antarctica will begin in January 2019, and samples from Zimbabwe in February 2019.

IDENTIFICATION OF STAGES OF REMAGNETIZATION WITHIN MESOZOIC COVER OF WESTERN SPITSBERGEN. ORIGIN OF THE WEST SPITSBERGEN FOLD AND THRUST BELT BASED ON ANISOTROPY OF MAGNETIC SUSCEPTIBILITY RESULTS

K. Michalski, K. Dudzisz, R. Szaniawski

A. Palaeomagnetic, rock-magnetic and mineralogical investigations of the Lower Triassic Vardebukta Formation from the southern part of the West Spitsbergen Fold and Thrust Belt. Magnetic, petrological and mineralogical data from 13 sites (99 independently oriented samples) of the Lower Triassic rocks located in the SW segment of the West Spitsbergen Fold and Thrust Belt (WSFTB) are presented in order to identify the ferrimagnetic carriers and establish the origin of the natural remanent magnetization (NRM). Volcanic lithoclasts and other detrital resistive grains in which the primary magnetization might endure are present in some samples. On the other hand, petrological studies indicate that sulphide remineralization could have had an important influence on the remagnetization of these rocks. The dominant ferrimagnetic car-

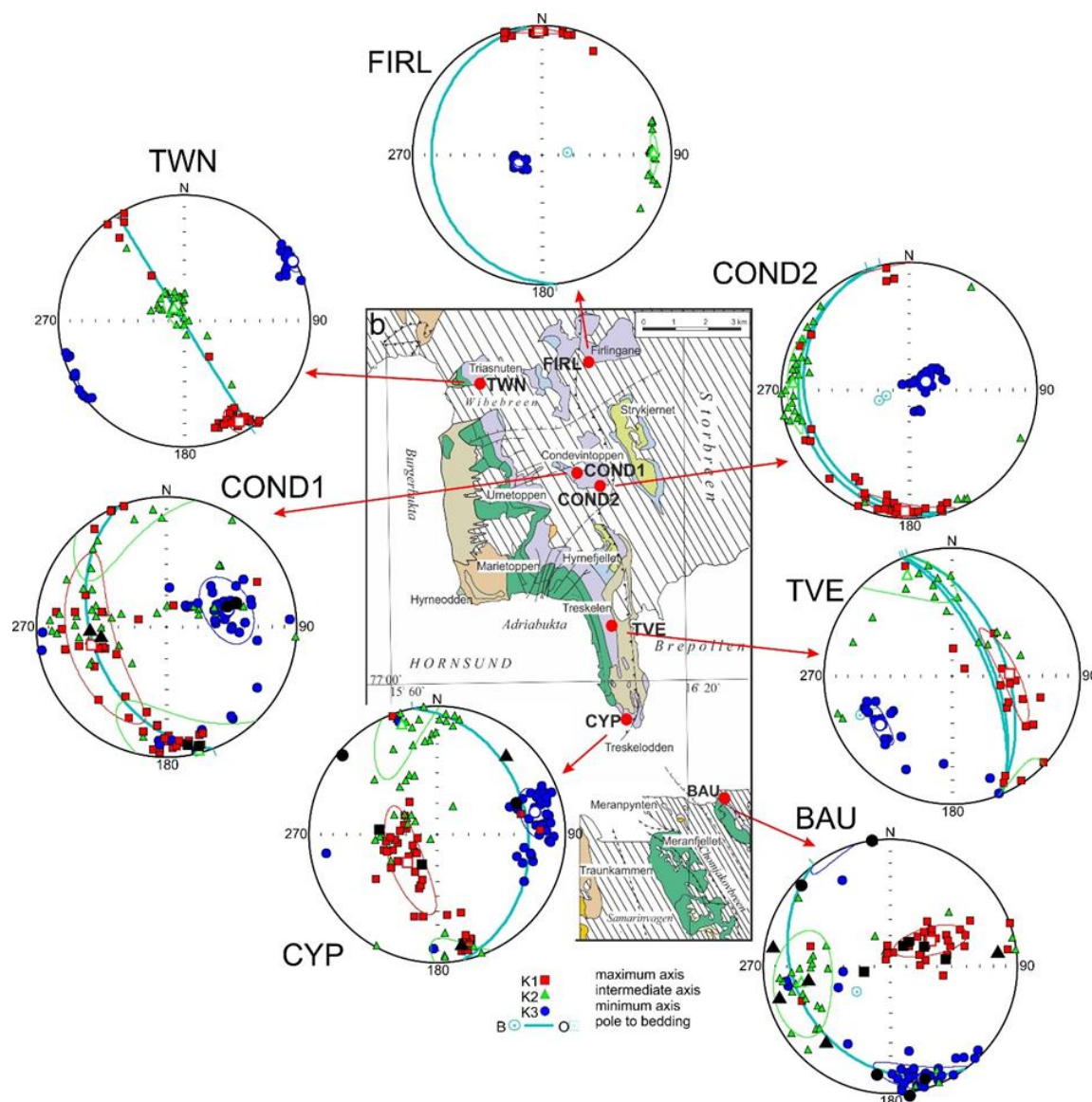


Fig. 1. The low-field and high-field AMS (black symbols) results of sites located along the WSFTB at Hornsund. Equal-area lower-hemisphere projections show results in the geographic coordinate system (after Dudzisz et al. 2018b).

riers are titanomagnetite and magnetite. While the titanomagnetite may preserve the primary magnetization, the magnetite is a more likely potential carrier of secondary overprints. The complex NRM patterns found in most of the samples may be explained by the coexistence and partial overlapping of components representing different stages of magnetization. Components of both polarities were identified in the investigated material. The reversal test performed on the most stable components that demagnetized above 300°C proved to be negative at the 95% confidence level at any stage of unfolding. They are better grouped, however, after 100% tectonic corrections and the most stable components are clustered in high inclinations (c. 70–80°). This suggests that at least part of the measured palaeomagnetic vectors represent a secondary prefolding magnetic overprint that originated in post-Jurassic time before the WSFTB event. Vitritite reflectance studies show these rocks have not been subjected to any strong heating (<200°C).

B. Rock magnetism and magnetic fabric of the Triassic rocks from the West Spitsbergen Fold-and-Thrust Belt and its foreland

Magnetic fabric and magnetomineralogy of the Early Triassic sedimentary rocks, collected along the length of the West Spitsbergen Fold-and-Thrust Belt and from subhorizontal beds on its foreland, is presented with the aim to compare magnetic mineralogy of these areas, determine the carriers of magnetic fabric and identify tectonic deformation reflected in the magnetic fabric. Magnetic mineralogy varies and only in part depends on the lithology. The magnetic fabric at all sampling sites is controlled by paramagnetic minerals (phyllosilicates and Fe-carbonates). In the fold belt, it reflects the low degree of deformation in a compressional setting with magnetic lineation parallel to fold axis NW-SE (Fig. 1). This is consistent with pure orthogonal compression model of the WSFTB formation, but it also agrees with decoupling model. Inverse fabric, observed in few sites, is carried by Fe-rich carbonates. In the WSFTB foreland, magnetic lineation reflects the Triassic paleocurrent direction (NE-SW). The alternation between normal and inverse magnetic fabric within the stratigraphic profile could be related to sedimentary cycles.

IDENTIFICATION OF LATE, POST – CALEDONIAN TECTONIC ROTATIONS WITHIN METAMORPHIC BASEMENT OF CENTRAL WESTERN SPITSBERGEN

K. Michalski, M. Burzyński

A. Mineralogical, rock-magnetic and palaeomagnetic properties of metadolerites from central western Svalbard.

A combination of mineralogical, rock-magnetic, and palaeomagnetic methods were employed in an attempt to shed a new light on the tectonism and paleogeography of Central Western Svalbard. The focus is on six metadolerite sites from the metamorphic Proterozoic–Lower Palaeozoic complex of south-western Oscar II Land (Western Spitsbergen). The primary mineral compositions of the metadolerites were strongly remineralized during Caledonian (*sensu lato*) greenschist-facies metamorphism although some younger tectonothermal modification is also apparent from the rock-magnetic studies. Rock-magnetic experiments supported by thin-section mineral identification and separation of Fe-containing fractions indicate that the main ferromagnetic carriers of the Natural Remanent Magnetization are represented by low-coercivity pyrrhotite and magnetite/maghemite. The investigated metadolerites are characterized by complex pattern of magnetization. The low-temperature palaeomagnetic components which demagnetized up to 250°C, are characterized by high inclinations (~70–80°) potentially representing Mesozoic–Cenozoic remagnetization. The most stable middle-high temperature directions

which demagnetized from 250°C, were obtained from only two of six sites. Two Virtual Geomagnetic Poles calculated from two of the middle-high temperature site means do not correlate with the Laurussia reference path for syn to post-Caledonian time. Two possible explanations of observed inconsistency are discussed. These are a modification of the Oscar II Land Caledonian basement geometry by listric faulting and/or tectonic rotations related to Daudmannsdalen–Protectorbreen high-strain (shear) zone. The results presented here suggest that post-Caledonian tectonic modification of the palaeomagnetic directions may be more a widespread feature of Western Svalbard.

B. Palaeomagnetism of metacarbonates and fracture fills of Kongsfjorden islands (western Spitsbergen).

A total number of 156 palaeomagnetic specimens of metacarbonates from 9 sites in Blomstrandhalvøya and Lovénøyane (Kongsfjorden, western Spitsbergen) and an additional 77 spec-

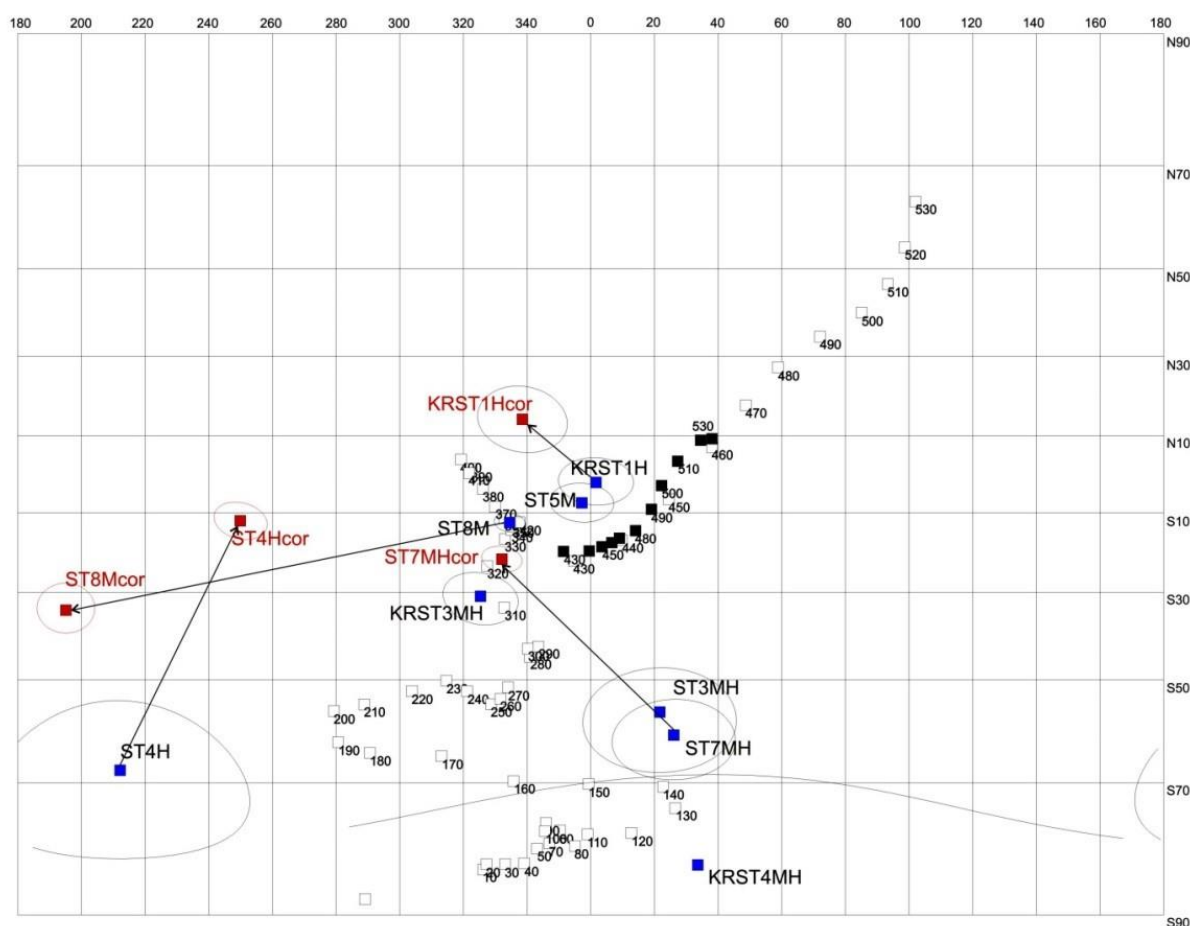


Fig. 1. Palaeopoles calculated for middle- to high-temperature components (M, H, MH) identified in Kongsfjord (this study) with their ellipses of the confidence limit α_{95} against reference path of Laurussia (open squares, palaeopoles 0–430 Ma), Baltica (open squares, palaeopoles 440–530 Ma), and Laurentia (filled squares, palaeopoles 440–530 Ma); reference palaeopoles were taken from Torsvik et al. (2012). Ages of particular palaeopoles are given; blue filled squares represent position of in situ palaeopoles before tectonic; in the case of metacarbonates red filled squares represent positions of VGP's after tectonic corrections according to F2 deformations; as ST5 was characterized by horizontal schistosity in that site tectonic correction was not applied; in the case of KRST1 site red filled square indicates position of VGP after correction according to identified weakly developed AMS foliation; Galls projection (after Michalski 2018).

iments of unmetamorphosed sediments infilling fractures (4 sites) within the Caledonian metamorphic basement of Blomstrandhalvøya were demagnetized. No relicts of pre-metamorphic magnetization were identified. The Natural Remanent Magnetization (NRM) pattern of meta-carbonates is dominated by Caledonian (*sensu lato*) – Svalbardian and Late Mesozoic/ Cenozoic secondary magnetic overprints carried by the pyrrhotite and magnetite/maghemite phases, respectively. The NRM of unmetamorphosed sediments infilling the karstic/tectonic fractures is dominated by hematite carrier. It revealed three stages of magnetization: Caledonian *sensu lato*, Carboniferous and Late Mesozoic/Cenozoic, which can be related to their initial fracturing, karstification and sedimentation or reactivation. As the majority of the palaeopoles calculated for the Kongsfjorden sites fit the 430–0 Ma sector of Laurussia reference path in an *in situ* orientation these results support the hypothesis that Blomstrandhalvøya and Lovénøyane escaped main Eureka deformations (Fig. 1). The potential rotation of the Kongsfjorden basement by any west dipping listric fault activity rotating the succession accompanying the opening of North Atlantic Ocean was not documented by obtained the palaeomagnetic data.

References

Torsvik, T.H., R. Van Der Voo, U. Preeden, C. Mac Niocail, B. Steinberger, P.V. Doubrovine, D.J.J. Van Hinsbergen, M. Domeier, C. Gaina, E. Tohver, J.G. Meert, P.J.A. McCausland, and L.R.M. Cocks (2012), Phanerozoic polar wander, paleogeography and dynamics, *Earth-Sci. Rev.* **114**, 3–4, 325–368, DOI: 10.1016/j.earsci-rev.2012.06.007.

DEEP LITHOSPHERIC STRUCTURE BENEATH DOLSK AND ODRA FAULT ZONES AS A RESULT OF INTEGRATED MAGNETOTELLURIC 1-D, 2-D, AND 3-D DATA INTERPRETATION

S. Oryński, W. Józwiak, K. Nowożyński

The scientific aim of the project is detailed identification of the crust and upper mantle structure around a part of the Fore-Sudetic Monocline. The data obtained from the measurements and the data from the Pomerania studies and also from our previous research from eastern part of Fore-Sudetic Monocline, will be used to a better establishment of the boundaries of lithospheric blocks (terrane) as well as to recognise their origin. The magnetotelluric (MT) soundings were carried out to achieve this goal. The collected data allow to construct 3-D models of the conductivity distribution. The area where the investigation is going to be done involves the region of the Dolsk fault and the Odra fault. These zones are important geologic borders of a regional nature and they pull apart the crust blocks which have different origins. The character of this geological structure is currently almost unknown. We hope that our investigation could shed additional light on the problems connected with the geology and geotectonic of this area. The Variscan basement between these two faults is not well-known as well, that is why it attracts interest a strong group of researchers. The previous geophysical results, mainly seismic, show that it is highly likely that the Dolsk fault zone mark out the polish, northern border of the Variscan crust. It is worth to admit that the Odra fault is a natural continuation of the Elbe fault in the eastern Germany.

Magnetotelluric deep soundings, respectively, differ significantly from most other methods in the way, they use natural sources. The methods have a great practical importance, especially in environmental research. Variations of the external magnetic field induce electric currents in the Earth, direction and intensity of which depend on the electrical conductivity distribution in geological structures. In the case of local horizontal heterogeneities presence, the induced cur-

rents generate also a vertical component of the Earth's magnetic field. The relationships between corresponding components of the electric and magnetic fields define so-called transfer functions. These functions depend on the location and on frequency and base on them we are able to derive numerical models of distribution of electrical conductivity in the Earth. Collected data is a subject to the numerical processing.

There were conducted 51 soundings on five parallel profiles. That allow to construct a regular mesh in the area of the Fore-Sudetic Monocline. Processing and preliminary data interpretation were conducted according to the progress of field work. There were created 1-D and 2-D models by using the inverse algorithms. The models were prepared for each profile separately. There were apply a parallel (ModEM) 3-D inversion codes. ModEM is an inversion code which employs MPI and which, besides impedances, includes tippers and magnetic tensor (Fig. 1).

The research area is characterized by remarkably complex geological structure and unclear history of tectonic evolution. Geotectonic processes that occurred in this region are currently unknown. The area was covered with a relatively dense network of deep seismic profiles but the doubts about the fault zones are not settled. Taking into account the previous local logging and geological studies, the need for a thorough and large-scale magnetotelluric basic research, seems to be natural. The study allows a relevant supplement of foregoing knowledge, thereby to obtain more delighted recognition of the Dolsk and Odra fault zones. Sub-vertical orientation of the Dolsk fault that is suggested by the seismic and geological data, implicate a strike-slip character of this dislocation. Even though the direction of them is still unidentified. The other problem is the origin of the basement block between these two faults. This research project substantially permits for better reconstruction of the tectonic evolution of Baltika foredeep (Fig. 1).

The complexity of the geological structure of the Fore-Sudetic Monocline, is manifested by occurrence numerous dislocations and tectonic zones. The boundaries between the particular

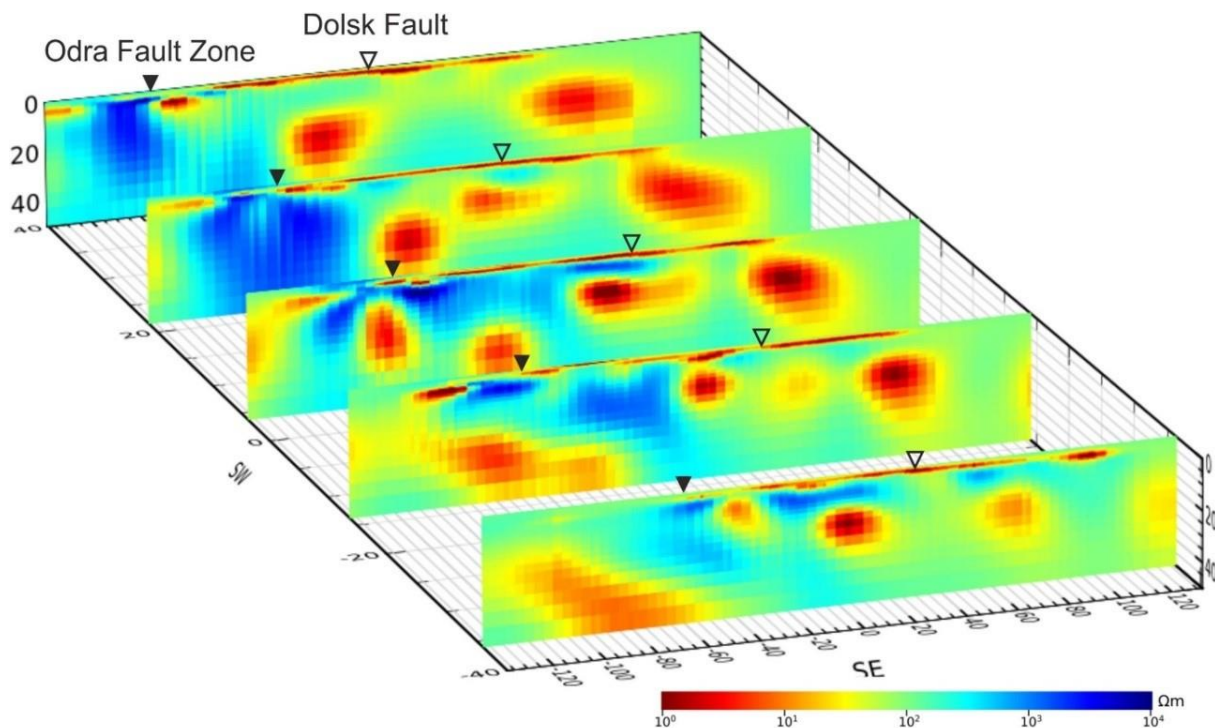


Fig. 1. The results of 3-D NLCG in ModEM, presented as a section on every profile (from 0 to IV).

basement units are most probably near-vertical sutures representing trans current zones, mostly accompanied by Permo-Carboniferous well-conducting deposits. The zone equivalent to the central-German crystalline zone (MGCR), which separates the Saxo-Thuringian Zone and Rheno-Herzynian Zone, is probably not located below the middle Odra fault zone as was postulated. The results of the study indicate that it is located more to the north (about 40 km), in the Lower Silesian Basin between the Bielawa-Trzebnica High and Wolsztyn-Leszno High. 3-D approach is a major advance and give a more reliable image of geoelectrical structure than was possible with a 2-D approach. Moreover the 3-D structures are better specified on 3-D inversion results.

DEEP LITHOSPHERIC STRUCTURE BENEATH THE POLISH PART OF THE EAST EUROPEAN CRATON AS A RESULT OF MAGNETOTELLURIC SURVEYS

S. Oryński, A. Neska

The scientific aim of this project is the investigation of deep crust and upper mantle structure in north-eastern Poland. For this purpose, all profiles which were carried out in this region were collected. The majority of them is crossing Poland from the South-West to the North-East. Two of these profiles were made in the last three years, by Institute of Geophysics, Polish Academy of Sciences, using Geomag Apparatus. For the common interpretation the magnetotelluric profile II (it is a part of a bigger profile named Zgorzelec-Wizajny), which was made by PBG Geophysical Exploration Company Ltd in 2006 was also used. The data was processed and then a database in the WinGLink Software was constructed (Fig. 1). The one-dimensional Occams

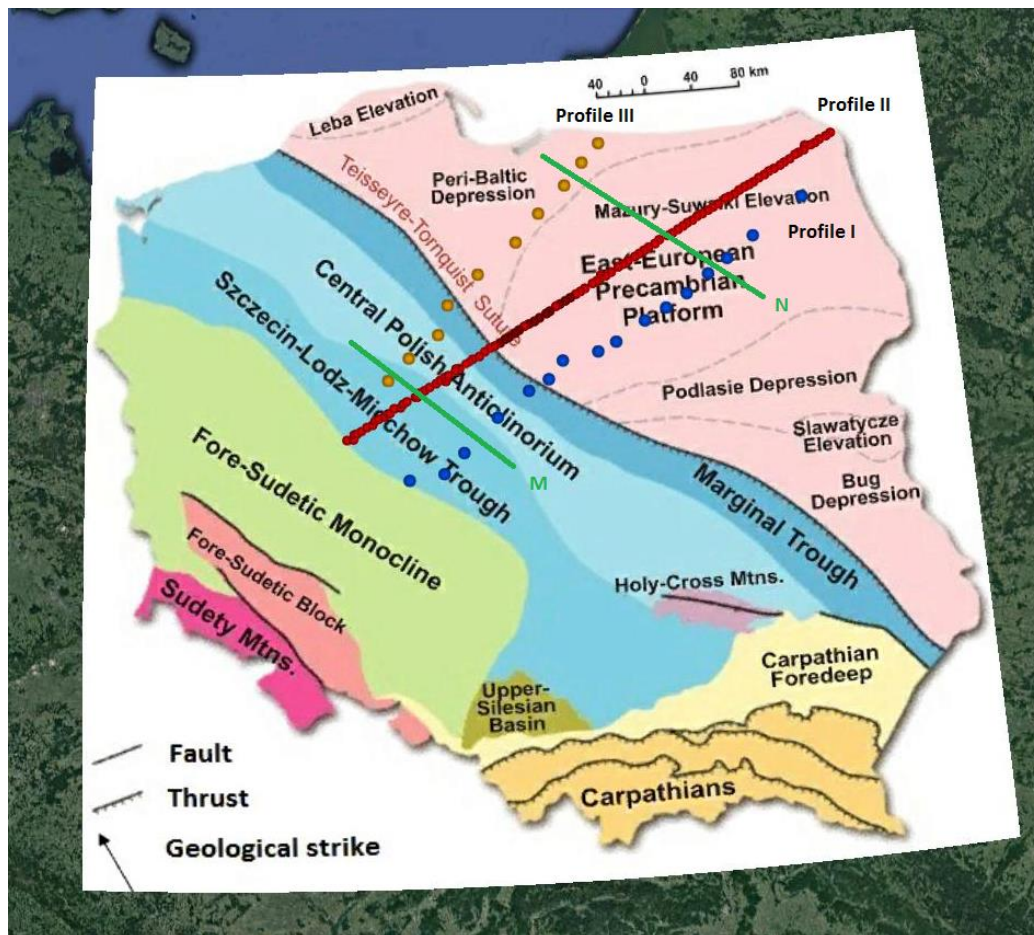


Fig. 1. Tectonic map of the survey area with profiles. Source: Google Earth. Red dots mark Profile II (Zgorzelec-Wizajny), orange ones Profile III, and blue ones Profile I.

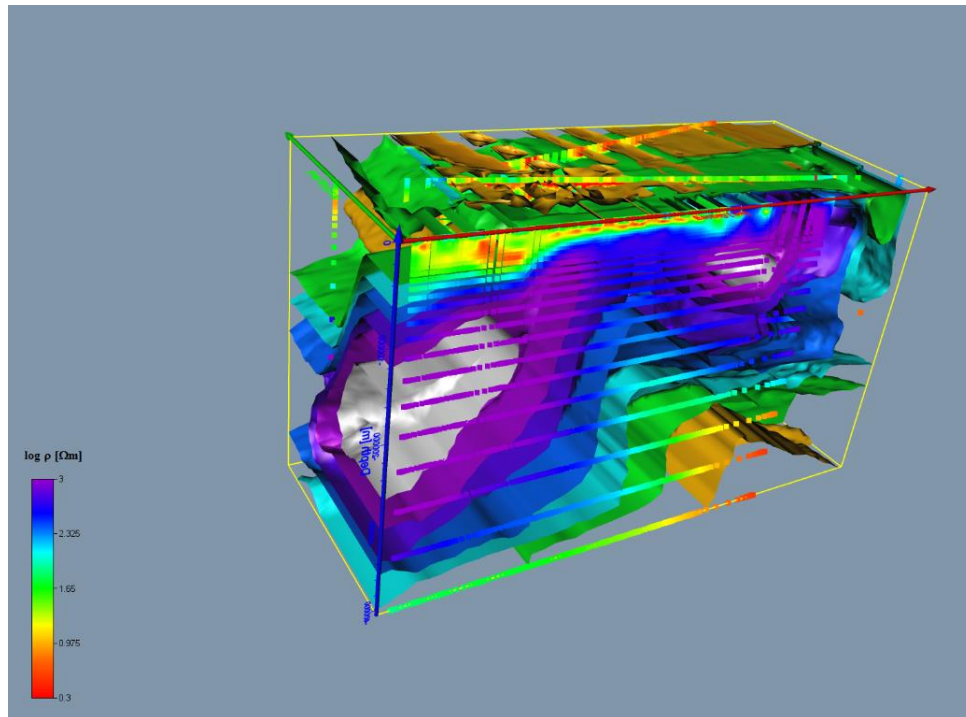


Fig. 2. 3-D visualization of the results of 2-D inversion of all the profiles presented in GS Voxler as a scatter plot combined with isosurfaces.

inversion and the two-dimensional NLCG inversion, using this software, were carried out. The results of these two types of inversion were presented as sections of the apparent resistivity distribution, and then compared and contrasted. The analysis of polar diagrams revealed that for the most of research area, two-dimensional structures were observed. The fitting to the known geological model was much better for 2D inversion than for 1D. The final results were presented as a 3D cube, which was made from the interpolation between sections.

In the present work, we jointly interpreted 1D and 2D resistivity models obtained by the inversion of 420 magnetotelluric sites. Structural dimensionality of the dataset was analysed by polar diagrams and this analysis showed clearly that underlying resistivity structure is not one dimensional. Only for several higher frequencies it is possible to accept a layered model. Good results are obtained only for depths up to 20 km, what has been confirmed by a skew analysis and polar diagrams. Two-dimensional inversions give satisfactory results. There are clearly visible the Trans European Suture Zone in form of a good conductor in mid-crustal depth on every profile and especially in the 3-D visualization (Fig. 2). The shape of this structure agrees very well to the previous research from the Polish Pomerania region (Ernst et al. 2008; Slezak et al. 2016). The most interesting result seems to be deep regions of lower resistivity within the East European Craton. These structures occur consistently on each profile and it is highly probable that there are two of them. This is visible at the most densely sampled Profile II. This effect is very pronounced in the case of a three-dimensional visualization. A possible interpretation of these structures is that the platform hosts numerous ancient rifts or aulacogens. Some of them were possibly caused by a cluster of mantle plumes.

Some structures do not continue consistently from profile to profile. This indicates a certain three-dimensionality of the deep structure, which is not unexpected, e.g., in context of intrusions. Hence there is a need to carry out a three-dimensional inversion using all available data from this region. It would help to come to a final geologic interpretation of the data which have been analysed in this work.

References

- Ernst, T., H. Brasse, V. Červ, N. Hoffmann, J. Jankowski, W. Jozwiak, A. Kreutzmann, A. Neska, N. Palshin, L.B. Pedersen, M. Smirnov, E. Sokolova, and I.M. Varentsov (2008), Electromagnetic images of the deep structure of the Trans-European Suture Zone beneath Polish Pomerania, *Geophys. Res. Lett.* **35**, 15, L15307, DOI: 10.1029/2008GL034610.
- Ślęzak, K., W. Józwiak, K. Nowożyński, and H. Brasse (2016), 3-D inversion of MT data for imaging deformation fronts in NW Poland, *Pure Appl. Geophys.* **173**, 2423–2434, DOI: 10.1007/s00024-016-1275-2.

COMBINED QUANTITATIVE INTERPRETATION OF GCM AND DC SOUNDING DATA FROM SELECTED AREA IN CRACOW, POLAND

S. Oryński

Apparent conductivity is a value that is measured with the use of Ground Conductivity Meters (GCM). The apparent conductivity, σ_a [mS/m], is a geoelectric parameter, which characterizes heterogeneous medium that is in the field of view of the measurement array. The apparent conductivity can be treated as some resultant conductivity of a heterogeneous medium, in which the spatial distribution of “true” conductivity is imposed by the geological built-up. Apparent conductivity is measured using the horizontal (HD) and vertical (VD) magnetic dipole at a several levels of depth (using different spacing). The area around the transmitting coil in which (for given frequency and conductivity) measurement is done is called near zone or induction zone.

Ground conductivity meters: CMD-MiniExplorer and CMD-Explorer, produced by the GF Instruments, s.r.o., are designed for induction profiling. The equipment employs the HD and VD configurations and measures apparent conductivity, and owing a six different options for spacing ($s = 0.32, 0.71, 1.18$ for MiniExplorer and $1.48, 2.82, 4.49$ for Explorer). There are two types of configuration available. It allows to regulate the depth of penetration.

The GCM measurements were made along two profiles with a one meter measurement step in two different areas of Cracow (Poland). For the purposes of the geoelectrical identification of the medium, there were carried out a benchmark DC-resistivity soundings, with a measuring step of 5 meters along the same profiles. Measurement were carried out with the Schlumberger 4-electrode system.

The results of quantitative interpretation of DC-resistivity and GCM soundings were linked to the lithology of the studied medium. There were used two different interpretation algorithms for both methods: Occam and Levenberg-Marquardt (LMA). In the LMA method there is obtained a model with a clear contrast between the successive layers as a result of the interpretation. The result of the Occam interpretation is a model with smoothed resistivity distribution and diffuse boundaries between layers.

The research was carried out in two different areas in Cracow, first one in the Błonia area (right side of the Vistula river) and second one in the Ruczaj district (left side of the Vistula river). The distribution of the interpreted resistivity was compared with the literature data about lithology and resistivity occurring in this area. In the second case, the first interpreted layer is soil with a subsoil (conductivity approx. 20 mS/m) and a volume of several dozen centimetres. Below them, there are clays (conductivity approx. 55–60 mS/m) and a thickness of about 3 m. Below the layer of clays there is a gypsum complex with conductivity about 14 mS/m and a thickness of about 12 m. The conductivity of this complex determined as a result of the interpretation of GCM data is greater – it is about 30 mS/m. This is due to much greater sensitivity

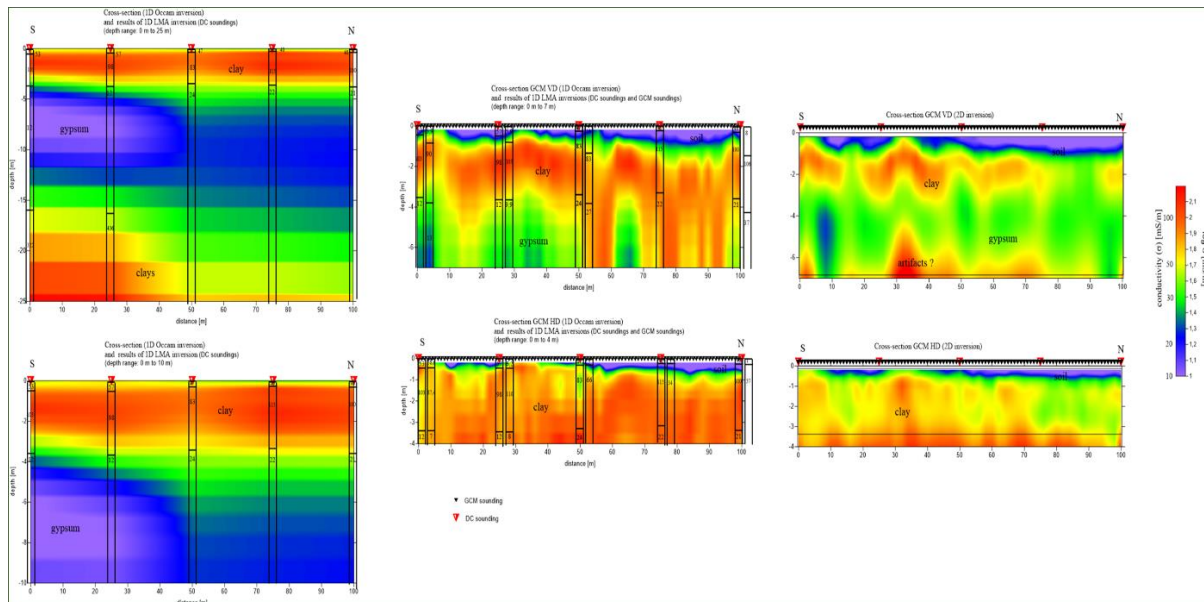


Fig. 1. Comparison of cross-sections: DC – 1D Occam, GCM – 1D Occam, GCM – 2D, for two different depth ranges (Klityński et al. 2019).

of the GCM method to the occurrence of small, dispersed conductive zones in the gypsum (e.g., loams, wet karst voids). These gypsums are part of the evaporative works that have been created as a result of Tortonian sea regression. The Miocene aquifer is associated with the layer of skeletal gypsum. The last recognized layer is the low-resistive loam of the Wieliczka layers. This layer is too deep to be recognized by the GCM method. The resistivity of clays obtained as a result of the interpretation of DC-R soundings is about $3 \Omega\text{m}$ (conductivity approx. 300 mS/m).

Carrying out GCM measurements for six different depth ranges (levels) allowed to perform a two-dimensional GCM data inversion using the Res2Dinv software. The inversion results in the form of cross-cut conductivities are smoothed (i.e. the conductivity at the boundaries between different mediums changes gradually) and are a certain averaging of the conductivity distribution in the studied medium (Fig. 1).

The GCM method proved to be effective in recognizing shallow geological layers in the Cracow area. Due to the specific geological structure, the range of conductivity of geological layers (from a dozen to several dozen mS/m) allowed to qualify the condition of the near-field zone for the GCM method and the clear geoelectric contrasts allowed to separate the most important layers.

References

Klityński, W., S. Oryński, and N.D. Chau (2019), Application of the conductive method in the engineering geology: Ruczaj district in Kraków, Poland, as a case study, *Acta Geophys.* **67**, 3, 1791–1798, DOI: 10.1007/s11600-019-00335-w.

CHANGEABILITY OF THE EARTH'S GEOELECTRIC PARAMETERS AND ITS RELATION TO SEISMICITY AROUND THE TRANS-EUROPEAN SUTURE ZONE

V. Semenov, W. Jóźwiak, K. Nowożyński, M. Neska

Investigation of the Earth's geoelectric structure and of possible temporal changes in its parameters requires both reliable observation data and an appropriate data processing method. The

Earth's interior based on measurements of electromagnetic field variations. An advantage of this method is that it is non-invasive for the environment, whereas a drawback is the complexity of the measured signals which come from different sources.

A new methodology of performing induction soundings have been finished as a part of ongoing work and a software package for analysis and interpretation of long-term magnetotelluric and magnetovariational data has been created.

Geomagnetic observatories at mid-latitudes of Eurasia ($50^{\circ} \pm 10^{\circ}$ of the northern hemisphere) operating at least in the years 1957–2010 have been chosen for deep induction soundings along a profile going from Europe through Asia up to the Pacific Ocean.

Good correlations between apparent resistivity and change in the number of earthquakes taken from NEIC PDE catalog within a 700 km radius around the center of sounding were established in the first zone (Fig. 1a, Europe). Sample earthquakes with magnitudes over 3 were taken from the catalog NEIC PDE. The second zone has been fixed in Siberia (Fig. 1b) where deep soundings have been made for group of stations AAA, IRT, and NVS, because exactly there a good earthquake statistics (ten and more events per year) was observed in the years 1973–2010. Such a statistics of earthquakes is absent in Western Siberia. The third zone includes part of the Pacific Ocean shore (Fig. 1c), that stands in the way of correct deep soundings.

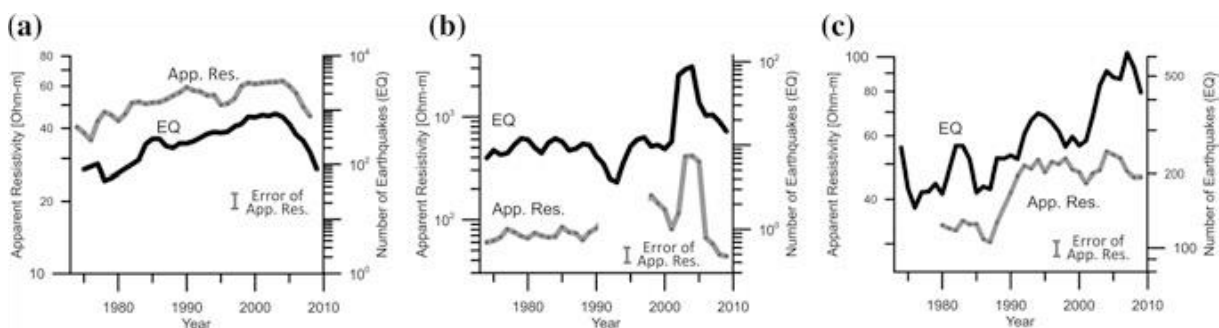


Fig. 1. Correlations of secular apparent resistivities ($T = 9$ h) and number Earthquakes (EQ) in 1973–2010 in: (a) Europe: FUR-HRB-BEL; (b) Asia: AAA-IRT-NVS; and (c) Pacific coast: KAK-MMB-VLA (the names of the geomagnetic observatories used are marked with international codes) (after Semenov and Petrishchev 2018a).

The application of the new methodology enabled a documentation of temporal changes in the Earth's resistivity for both long- and short-period geomagnetic field variations. In Poland it is most visible in the region of the TT Zone (Fig. 2). These changes are clearly correlated with the level of seismic activity in the Mediterranean Region. Also it has been shown that earthquakes in this region are preceded by anomalous electromagnetic signals that are clearly visible in both magnetic and telluric spectra. Similar analyses for data of Asian observatories have shown that there exist analogous zones to the TESZ in which clear resistivity changes are observed that are correlated to seismic activity as well. Furthermore there has been shown that the length and direction of induction arrows change with time. They are very probably connected with conductivity changes in the lower mantle. Possibly this is the reason for the magnetic jerks that are observed at the Earth's surface.

The changes in the electromagnetic field of the Earth and consequently, the changes of geoelectric parameters are extremely interesting. The nature of the phenomena taking place in the Earth's interior that are the source of the observed signals has not been finally understood and hence further research is necessary.

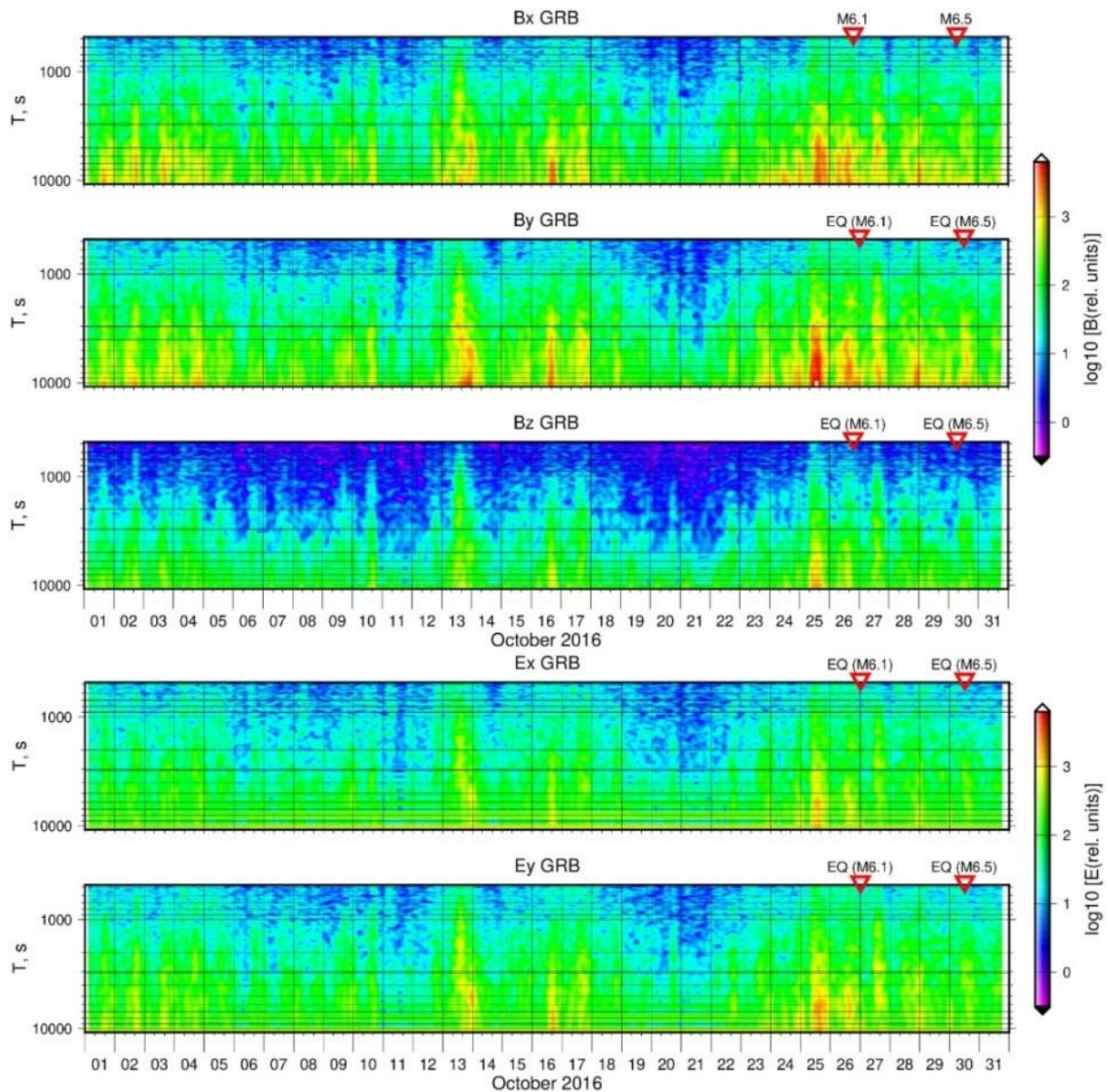


Fig. 2. Variability of EM spectra with time at point GRB in October 2016. Red triangles mark the earthquakes in Italy mentioned in text.

3-D STUDIES OF MT DATA IN THE CENTRAL POLISH BASIN: INFLUENCE OF INVERSION PARAMETERS, MODEL SPACE AND TRANSFER FUNCTION SELECTION

W. Józwiak, K. Nowożyński, S. Oryński

3-D inversion of geophysical data has become a practical, commonly used tool in the interpretation of magnetotelluric (MT) data. However, 3-D inversion is a nonlinear and ambiguous task and requires adopting additional assumptions. The influence of the selection of parameters on the solution can be investigated on the basis of synthetic models for which it is easy to verify the correctness of the results and therefore the adopted assumptions. In contrast, we analyze the influence of selection of inversion parameters in the case of previously published, real model for Pomerania region (Poland). This area is a fragment of the Trans European Suture Zone. This zone is a regional scale 2-D structure, which locally becomes 3-D. The analyzed model was accomplished by inversion of full impedance and tippers from 31 long-period MT stations with

the period range from 10 s to 10 000 s. A number of tests were performed employing an implementation of the freely available ModEM code. These included the choice of an appropriate initial model and an evaluation of model covariances as a means to control smoothness between adjoining model areas. Additionally, we compared the models calculated from all transfer functions (impedances and tippers) and from subsets (only tippers and off-diagonal components of the impedance tensor and tippers). Moreover, the tests with the rotation of the model's coordinate system were performed.

Inverse algorithms base on minimizing the misfit between data and model response (the RMS parameter). It happens, however, that we get relatively small and/or similar RMS values for models with a significantly different structure of conductivity distribution. Moreover, the model with the lowest RMS value does not always fit to the well-known geophysical or geological data, if available. Therefore, including such independent data allows to better select the inversion parameters. The RMS is defined using measurement data errors. These data are often a subject of a preliminary modification (by adopting an error floor or fixed error values for tippers). This affects the obtained RMS values and therefore we should not treat these values as an objective benchmark of choosing the best model (Fig. 1).

Our analysis has shown that initial model and the selection of the transfer function for inversion can significantly change the model. The coefficient values of the covariance matrix also have a significant impact on the results (Fig. 2). The selection of a too small value allows large contrasts between neighboring cells and then the model trends to set conductive areas shallower, only in a few first layers. On the other hand, the selection of a too big value leads to the "blurring" of conductive zones in the model while the conductivity values for these structures decrease (preserving their conductance). The optimal selection of covariance values requires preliminary test calculations, and of course, in this case, any independent geological and geophysical information is very useful. The selection of the coordinate system does not have a crucial influence on the inversion result; however, for a 3-D modeling of local-scale structures, it is advisable to orient the model (the model grid) obliquely to the global strike direction of the structure. Such an approach will not allow strengthening the dominant global 2-D character and it can make local 3-D areas more visible. Our tests have also confirmed that models based on tippers are less detailed and not sensitive to layered structures than the models based on telluric

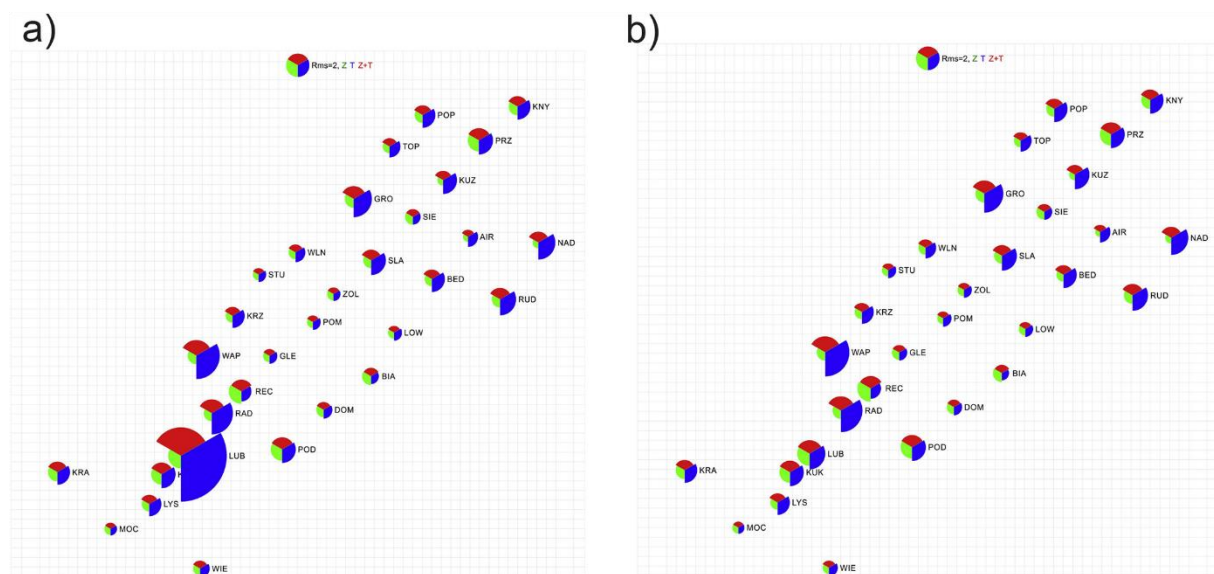


Fig. 1. On the left (a): the RMS values for individual points in case of inversion of all input data; on the right (b): the same values after removing one unrealistic vector for a period of 10 s for site Lub (the global RMS decreased from 1.9 to 1.7) (after Ślęzak et al. 2019).

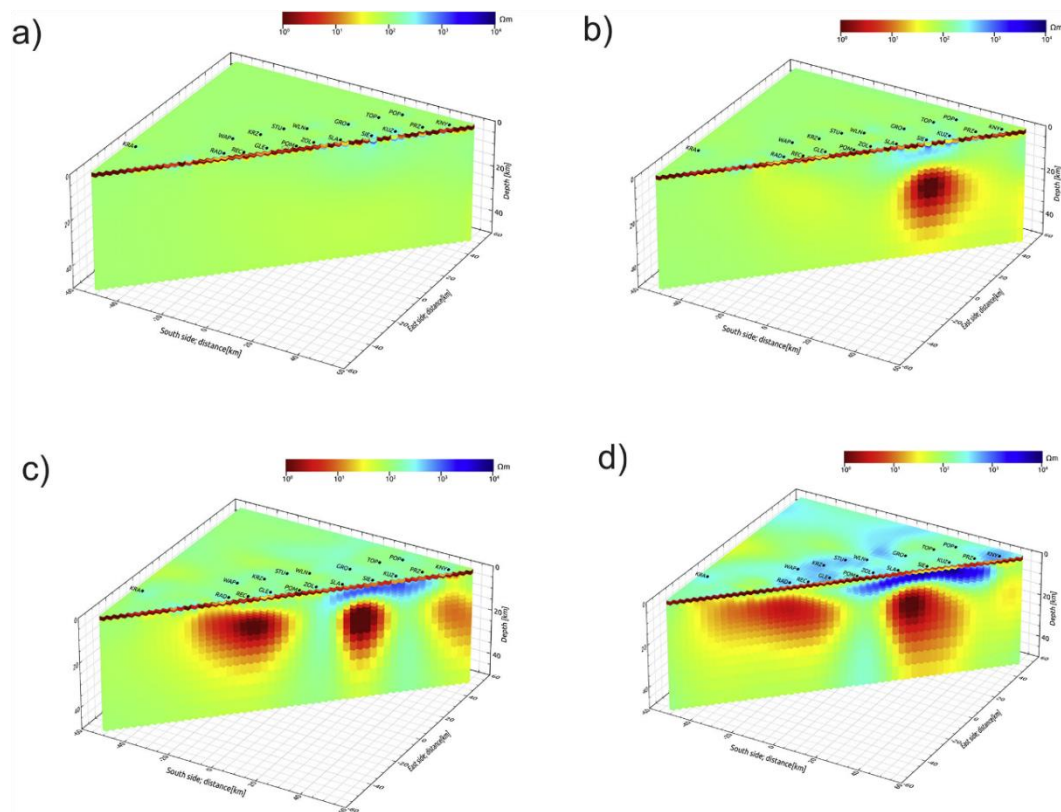


Fig. 2. 3-D models along the LT-7 profile for different covariances: 0.3 model covariance (a), 0.4 model covariance (b), 0.5 model covariance (c), and 0.7 model covariance (d). A homogeneous half-space of the initial model (background resistivity) of $100 \Omega\text{m}$ was used for each model and the RMS values were 2.017, 1.982, 1.824, and 2.005, respectively (after Ślęzak et al. 2019).

data (only impedances) and they provide complementary information on structure. Models based only on impedances may illustrate well smaller, local structures but they are potentially more sensitive to static shift. The addition of magnetic data that are not sensitive to static shift weakens these effects and leads to a more realistic model. Our tests indicate that 3-D algorithms are a great tool for modeling the conductivity distribution. However, their use requires a careful and appropriate selection of inversion parameters, in particular while modeling deep structures. Only then, we can expect that the inversion provides a reasonable model, which is close to the true geological structure. The criterion based only on the minimization of RMS does not guarantee this.

References

Ślęzak, K., W. Józwiak, K. Nowożyński, S. Oryński, and H. Brasse (2019), 3-D studies of MT data in the Central Polish Basin: Influence of inversion parameters, model space and transfer function selection, *J. Appl. Geophys.* **161**, 26–36, DOI: 10.1016/j.jappgeo.2018.11.008.

TEMPORAL CHANGES OF GEOMAGNETIC INDUCTION ARROWS IN NON-SEISMIC REGIONS – REALITY OR ESTIMATION ERRORS?

T. Ernst, K. Nowożyński, W. Józwiak

Various scientific articles report that induction arrows estimated in the same place are changing over the time, which should not happen in seismically non-active regions. The induction arrows

in geomagnetic sounding are strictly related to local deep conductivity distribution (geological structure). In general, the geological structure is stable in non-seismic areas. So, in our opinion, the temporal changes of induction arrows signaled in the literature are related to the estimation errors produced in calculation process by the presence of the external part of vertical field, appearing as noise in the data set. And additionally, what is very important, this noise is correlated with input signals.

To confirm our thesis, we estimated induction arrows at different time periods (seasons), analyzing carefully their variability. For calculations we used one-minute recordings of geomagnetic variations from some magnetic observatories and selected permanent sites in Poland and Lithuania registered between 2002 and 2015. The periods longer than three hours was filtered out. We used symmetric optimal filterers calculated by the algorithm of Parks&McClellan (1972) (see Fig. 1). In data processing we used our original algorithm based on the method of least squares in the time domain and Egbert's EMTF package (1986). Our task is a typical problem of studying a linear system (black box) of two input signals (horizontal components of geomagnetic field) and one output signal (induction part of the vertical field). Unfortunately, the assumption that external sources are spatially uniform is often not satisfying, and the external part of the vertical field usually exists, and sometimes is much bigger than the internal part.

In our opinion, the observed seasonal changes in the transfer function values (Fig. 2) are the result of incorrect estimation. The only way to receive a reliable estimation of induction vectors is the initial and subtle selection of the data. The data selection in our calculation process is based on an analysis of the external part of vertical geomagnetic field variation. The results we obtained show that induction arrows calculated in such way are stable over time.

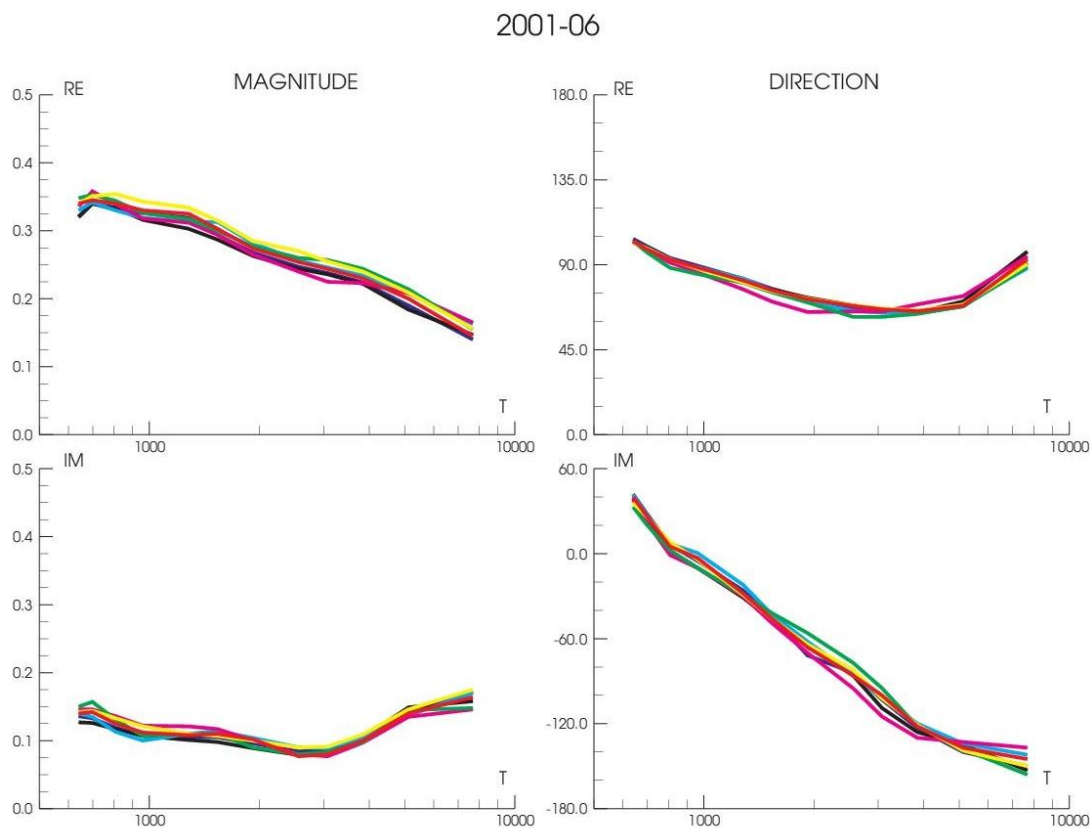


Fig. 1. The results of induction arrows estimation for Belsk (our original code working in time domain was used). The input data contained 50 selected 8-hour time series ($Z_e/Z < 0.2$). Colour curves shows the results for the data recorded between 2001 and 2006. Black curve for 2015. All curves are practically identical.

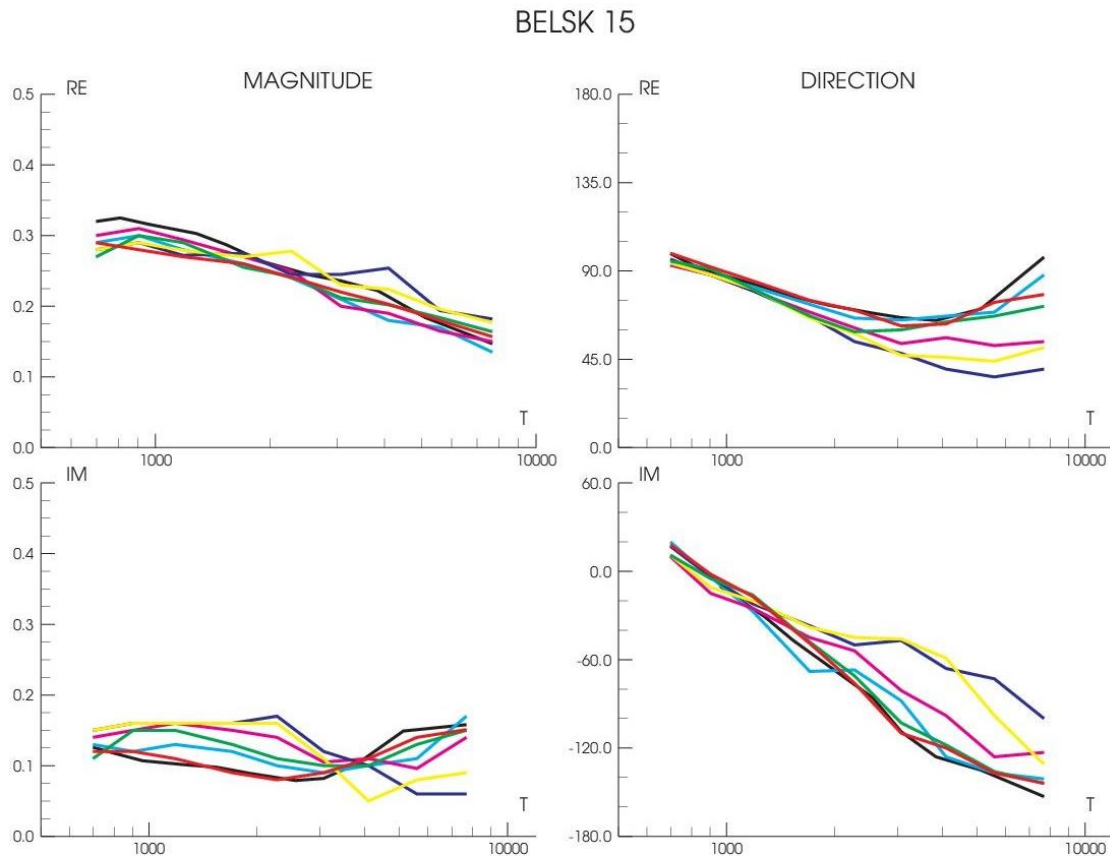


Fig. 2. The results of induction arrows estimation for site Belsk (BEL) in Poland. One-year data registered in 2015 were used. The annual data has been divided into six parts containing two consecutive months. The color curves show the results obtained for the six different input data sets containing different pairs of months. Initial data selection has not been made. The Egbert EMTF package was used for the calculated. One can see the large dispersion of estimated values for long periods. The obtained results using our own code for pre-selected data shows the black curve.

References

- Parks, T., and J. McClellan (1972), Chebyshev approximation for nonrecursive digital filters with linear phase, *IEEE Trans. Circuit Theory* **19**, 2, 189–194, DOI: 10.1109/TCT.1972.1083419.
- Egbert, G.D., and J.R. Booker (1986), Robust estimation of geomagnetic transfer functions, *Geophys. J. Int.* **87**, 1, 173–194, DOI: 10.1111/j.1365-246X.1986.tb04552.x.

INVESTIGATIONS OF DIFFUSIVE EFFECTS IN HYDROMAGNETIC DYNAMO THEORY

K. Mizerski, M. Grądzki

The dynamo team has concentrated efforts on two important topics from the hydro-magnetic dynamo theory about generation of large-scale magnetic fields by perfectly conducting (or more realistically extremely highly conducting) fluids and about buoyancy driven magnetohydrodynamic instabilities. In general terms the question which are at stake here can be formulated shortly:

Can the large-scale fast hydro-magnetic dynamos operate in real low-resistivity systems? How effective are the buoyancy effects in generating of natural magnetic fields?

The typical situation for dynamo action to occur, is when the flow field exhibits chirality (lack of reflexional symmetry), and this requires some mechanism (e.g. gravity g in conjunction with mean rotation Ω as in Moffatt (2008), or boundary forcing) that breaks the “up-down” symmetry of the field. An electromotive force $\varepsilon(\langle \mathbf{B} \rangle)$ (EMF) is then generated, which depends nonlinearly on the mean magnetic field $\langle \mathbf{B} \rangle$, and this leads to amplification of magnetic energy until the growing Lorentz force reacts back upon the flow field, leading to a saturated state.

It is frequently found that in the weak seed field limit the mean EMF is linear in the seed field $\varepsilon_i = \alpha_{ij} \langle B_j \rangle$, and that the trace $\alpha = \alpha_{ii} \rightarrow 0$ as the magnetic diffusivity $\eta \rightarrow 0$, thus excluding dynamo action at very high conductivities; the dynamo is then termed “slow”. If, on the other hand, $\alpha \rightarrow \text{const.} \neq 0$ as $\eta \rightarrow 0$ (leading also to a non-zero growth rate in this limit), then the dynamo is described as “fast”; this possibility has been intensively studied with a vast majority of investigations done in the simplest kinematic regime, with the fluid flow given beforehand, uninfluenced by the effect of the Lorentz force. In this case, it is generally found that fast-dynamo eigenmodes have a pathological structure, non-differentiable wherever they are non-zero; the applicability of fast-dynamo theory to real physical systems is then questionable.

New fast-dynamo mechanisms have been obtained and described by the team members at IGS PAS, for which the growing magnetic field remains smooth during the whole dynamo process. This results from a random superposition of waves, perturbed by the magnetic field through the action of the Lorentz force and nonlinear interactions between kinetic and magnetic components of distinct waves.

It is well known that a field of random inertial waves in a fluid of non-zero resistivity η is capable of exciting a large-scale magnetic field through the α -effect mechanism, pronounced in the induction equation

$$\partial_t \langle \mathbf{B} \rangle = \nabla \times \varepsilon + \nabla \times [\langle u \rangle \times \langle \mathbf{B} \rangle] + \eta \nabla^2 \langle \mathbf{B} \rangle, \quad (1)$$

where $\varepsilon = \langle u' \times B' \rangle = \alpha \cdot \langle \mathbf{B} \rangle$ is the large-scale electromotive force induced by the kinetic and magnetic components of small-scale wave field. In the fully dynamical situation, when the effect of the Lorentz force is taken into account, the α tensor is nonlinear in the mean field $\langle \mathbf{B} \rangle$, which is of great significance, since even if the mean EMF lacks ability to induce an exponential growth of the weak seed magnetic field in the linear regime, there still remains a possibility for nonlinear amplification, even faster than exponential. Such an effect has been obtained numerically in the recent paper published in the *SIAM J. Appl. Math.* Indeed it was shown, that in an idealized setting (half-space and no boundary conditions at infinite depth) initial period of mean field decay was followed by strong nonlinear amplification, faster than exponential. This was achieved by consideration of interactions of linear waves generated by a vertically oscillating top boundary (vertical direction was associated with the direction of background rotation). These were the well-known Lehnert waves and in the absence of fluid’s resistivity the large-scale EMF was generated by interactions of two waves with distinct frequencies. Such an EMF has an oscillatory time structure, however, due to nonlinear dependence on the mean magnetic field its time average is non-zero and it turns out to be capable of fast mean field amplification.

A similar study involved the effect of beats (named by analogy with the acoustic effect of “beat”), published in *J. Plasma Phys.* – that is interactions between distinct forced MHD waves with close frequencies, which led to a more standard dynamo picture with exponential amplification of a weak seed field, in perfectly conducting fluids, in the limit of weak wave amplitudes, that is weak MHD turbulence. No geometric constraints resulting from presence of

boundaries were included in the study and a weak forcing of very general structure, in the form of two Fourier modes was applied. Furthermore, two other mechanisms of large-scale EMF generation were proposed; the first one in the recent joint study with Professor Keith Moffatt, published in *Geophys. Astrophys. Fluid Dyn.* on large-scale dynamos by decaying Lehnert waves, were the mean EMF which was due to viscous decay was induced only temporarily, but lead to large-scale field amplification in a perfectly conducting medium. The last mechanism is based on dynamo driving by instabilities.

The second topic involved determination of the influence of weak thermal and magnetic diffusion on the so-called magnetic buoyancy instability. It is often conjectured in the literature, that the magnetic buoyancy instability has a profound influence on the dynamics of the Solar magnetic field. The PhD thesis of Marek Grądzki, published in the form of a scientific article in the *Astrophys. J. Suppl. Series*, has been concerned with the issue of establishing a scaling law for the spatial length scales of variation of perturbations in the Solar tachocline and determination of the dynamical regime in that region. It has been shown, that the joint effect of the ohmic resistivity and thermal diffusion is very non-trivial, involving situation unallowed when only one of the effects is considered.

Finally some analysis of the geomagnetic data has also been performed with the aim to identify perturbations in the Earth's core via the time-series analysis. Based on the data from the World Data Centre maps of the magnetic field evolution during the last 70 years at the Core-Mantle Boundary have been prepared.

References

Moffatt, H.K. (2008), Magnetostrophic turbulence and the geodynamo. **In:** Y. Kaneda (ed.), *IUTAM Symposium on Computational Physics and New Perspectives in Turbulence*, IUTAM Bookseries, Vol. 4, Springer, Dordrecht, 339–346, DOI: 10.1007/978-1-4020-6472-2_51.

CONDUCTING CONTINUOUS OBSERVATIONS OF GEOMAGNETIC FIELDS IN BELSK, HEL, AND POLISH POLAR STATION HORNSUND. MODERNIZATION OF APPARATUS AND DEVELOPMENT OF MEASUREMENT METHODS

J. Reda, M. Neska, P. Czubak, S. Wójcik, A. Wójcik

The main purpose of the research was a continuation of observations of geomagnetic field in three observatories of the Institute of Geophysics, Polish Academy of Sciences: Central Geophysical Observatory at Belsk, Polish Polar Station at Hornsund, and Geophysical Observatory at Hel (Fig. 1). All three observatories are members of IAGA (International Association of Geomagnetism and Aeronomy).

The main activity of geomagnetic observatories comprehends recording changes of the geomagnetic field with full absolute control and publishing the observation results.

All three Polish geomagnetic observatories continued their work in INTERMAGNET (International Real-time Magnetic Observatory Network) in 2018. Data of geomagnetic field elements XYZF have been sent to the INTERMAGNET centre in real time so they are publicly available on the internet. At the beginning of 2018 we carried out the final data processing of the whole year observations of 2017. The final data (status Definitive) were provided for INTERMAGNET. Definitive Data are published on INTERMAGNET websites and also on a DVD containing data from all participating observatories for the given year. The final compilation of such DVDs is carried out in Belsk, what is an additional contribution of IG PAS to the INTERMAGNET program. The final geomagnetic data of IG PAS are provided to WDC Centers for Geomagnetism as well.

The network of geomagnetic observatories/permanent stations IG PAS in 2018

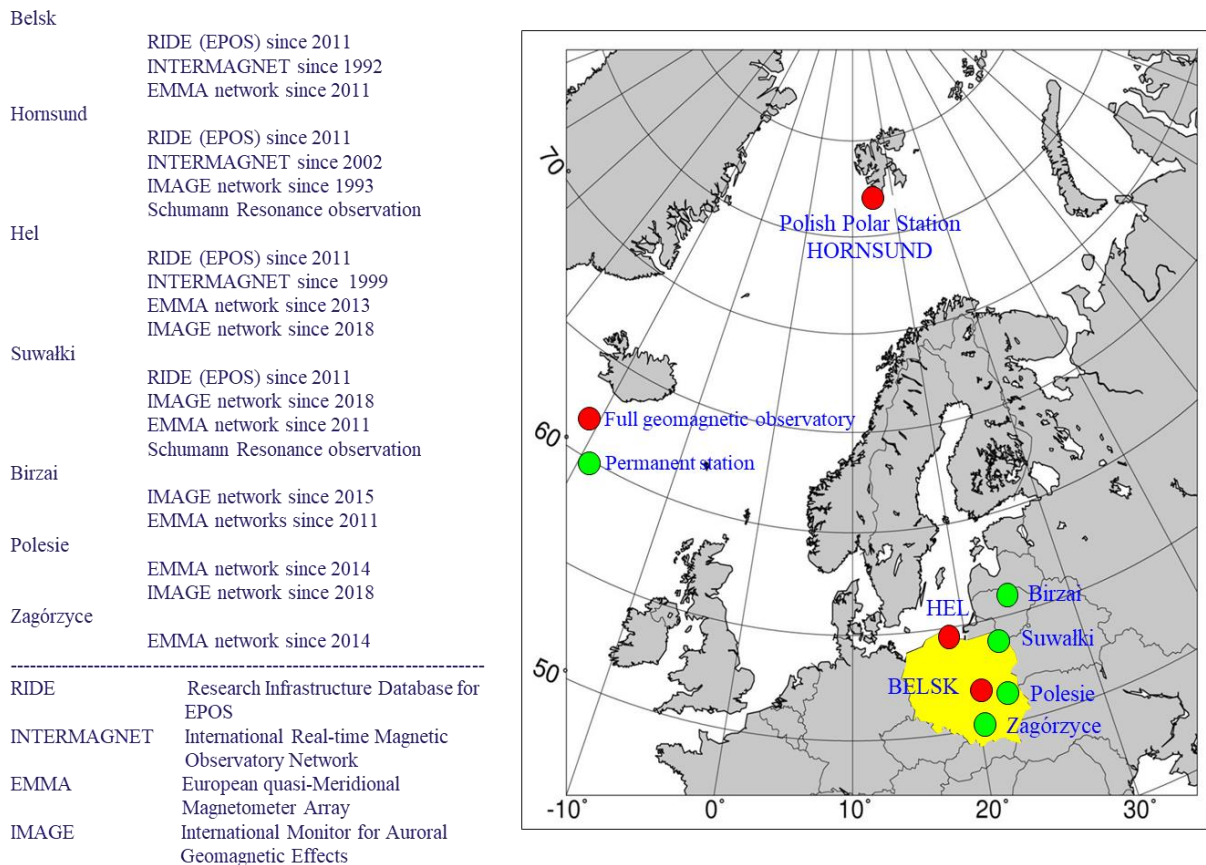


Fig. 1. Map of IG PAS observatories and permanent stations performing continuous observations of the Earth's magnetic field in 2018.

In 2018 there were prepared and provided for INTERMAGNET Quasi-Definitive Data every month. A quality of Quasi-Definitive is similar to Definitive-Data, but provided much earlier. These data are very important for the scientific world particularly in the context of the current SWARM satellite mission.

The Polish Polar Station Hornsund, Hel Observatory and the permanent stations in Birzai, Suwałki and Polesie (Fig. 1) have worked for the IMAGE program during the whole year (2018). The station Polesie and observatory Hel joined to IMAGE in 2018. The primary objectives of IMAGE is to study auroral electrojets and moving two-dimensional current systems. All five stations sent their real-time data to the IMAGE centre in Helsinki.

The recording and providing of real-time data series to EMMA network (European quasi-Meridional Magnetometer Array) has been continued. These data are exploited for investigation of the plasmasphere. From our side it involves Birzai, Suwałki, Hel, Belsk, Polesie, and Zagórzycze stations.

Furthermore in the permanent station Suwałki and in Polish Polar Station Hornsund the Schumann Resonance monitoring has been continued in 2018. It consists of measuring two horizontal magnetic components with a sampling frequency of 100 Hz. This recording was initiated by IG PAS in 2004.

An important element of our work in 2018 was training the members of the 41st Polar Expedition in the field of geomagnetic observations. Moreover, Belsk and Hel observatories provided assistance to institutions interested in geomagnetic observations such as the Institute

of Geodesy and Cartography (IGiK) and the Space Research Centre of PAS (CBK PAN). In case of IGiK the cooperation concerned the Polish repeat station network conducted by IGiK. Belsk and Hel observatories are references for this network. CBK PAN was the recipient of real-time data from Belsk observatory, also there were provided K indices of geomagnetic activity every day except non-working days.

EPOS – PL EUROPEAN PLATE OBSERVING SYSTEM; TASK 3: CIBOGM - CENTRE OF RESEARCH INFRASTRUCTURE OF GEOMAGNETIC AND MAGNETOTELLURIC OBSERVATIONS

W. Jóźwiak, A. Neska, J. Reda, K. Nowożyński, M. Neska, S. Oryński, P. Czubak

The aim of the European Plate Observing System (EPOS) project is creating an infrastructure for access to as well as exchange and integration of European geophysical data and metadata. The main task of EPOS-PL in the field of earth magnetism is an integration and dissemination of results obtained in geomagnetic observatories. First of all, time-series data measured in Polish observatories (Belsk, Hel, and Hornsund/Spitsbergen) and permanent variometer stations (Biržai/Lithuania, Suwałki, Polesie, Zagórze) will be provided to EPOS along with their meta-data in an xml format that facilitates integration with magnetotelluric time-series data. The appropriate software, e.g. for format conversion, is developed. Moreover, archival analog geomagnetic recordings from the mentioned and historical (i.e., Świder and Arctowski/Antarctica) observatories are scanned and arranged in proper order.

Thanks to EPOS, also the infrastructure for both magnetotelluric and observatory measurements (instrument pool) is modernized. A DI-flux theodolite, four Overhauser and two fluxgate magnetometers, 17 data loggers, two sets of induction coils for Schumann resonance monitoring, and two broadband magnetotelluric instruments have been or are planned to be purchased in this framework.

Its MT part or rather Thematic Core Service (TCS) is called EMTDAMO (European Magnetotelluric Data and Models). The project is on the first stage of its implementation and it will last for another few years. Whereas the focus on electric resistivity models is still a task for the future, some work on MT time series and transfer functions has been done already.

Metadata play a decisive role in both documentation and checking availability of certain types of data in an automated way. For these reasons EPOS attaches special importance to them. Metadata of MT time series in EPOS comprehend (but are not limited to) precise information on site location, measurement time and sampling interval, measured channels/EM field components, instrumentation including system responses, underlying projects, and the institutions behind the data. Currently, we have an xml time series metadata format for internal purposes, and discussions with the international European community have led to an agreement on a json format for exchange of both time series and transfer function data along with their metadata. A format standard for exchanging resistivity models shall follow.

Currently the archival data sets prepared for EPOS comprehends 254 long period MT and GDS sites (Fig. 1), some of which were occupied by an instrument not only once. The oldest data have been measured 20 years ago. The sites were situated in six countries (mainly in Poland and Germany) and on the Baltic Sea. The measurements were conducted by the Institute of Geophysics PAS in Warsaw, the Free University of Berlin, and the GEOMAR Helmholtz Centre for Ocean Research in Kiel. The distribution of sites over space and time MT and GDS sites prepared for EPOS. Those referred to later on the poster are marked is displayed on the map.

The main aim of EMTDAMO is making results of magnetotellurics, i.e., models of electric resistivity distribution in the solid earth, easier accessible to practitioners of other branches of earth sciences and comparable with their results. However, transfer functions and time series

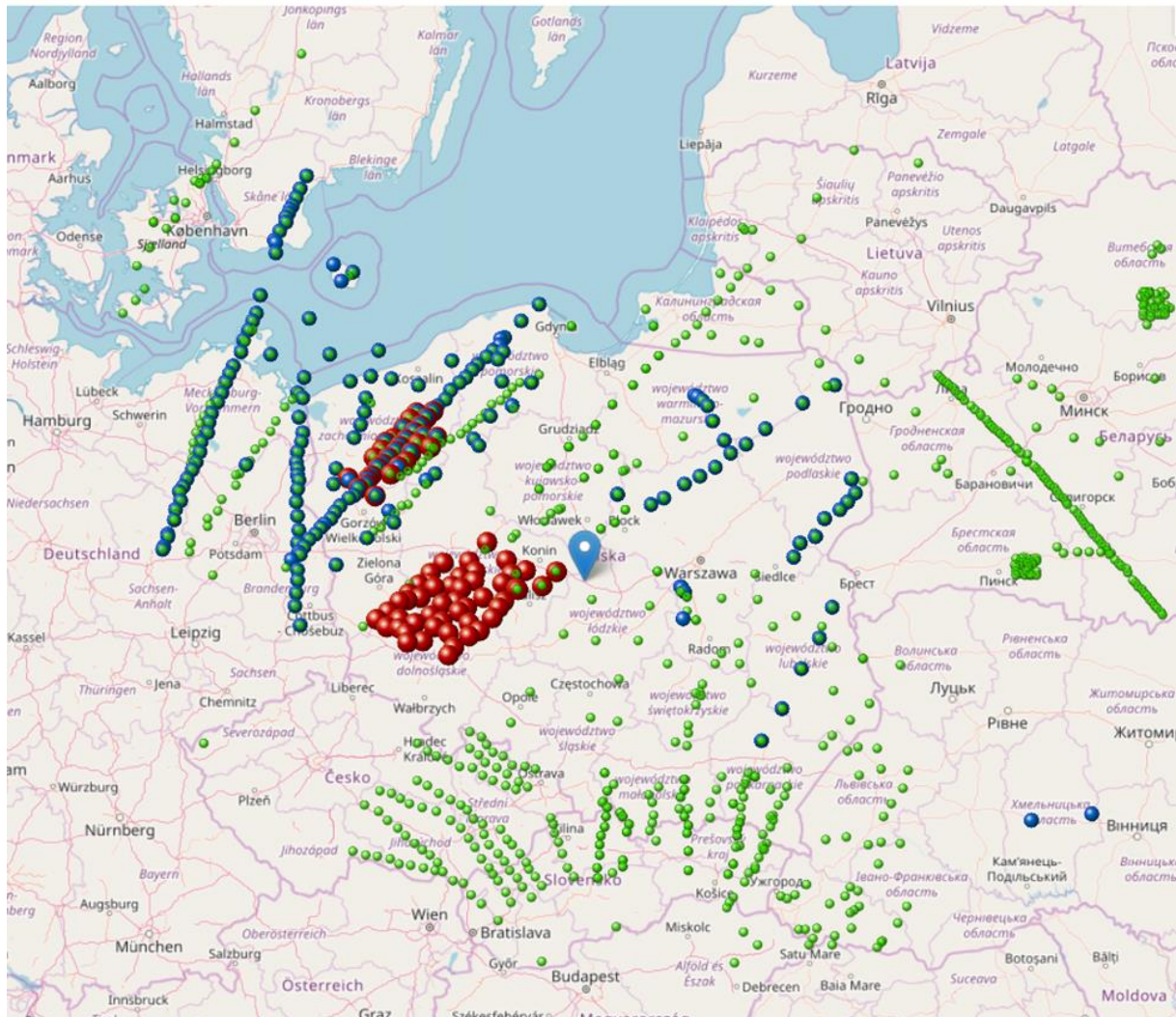


Fig. 1. MT and GDS sites prepared for EPOS.

are included not only for reasons of model reproducibility but they can have their own scientific value. The latter are, e.g., potentially compatible with observatory and satellite data or they can be newly combined for sounding purposes when provided and documented in the way intended by EPOS.

The EPOS-PL project is financed by the Operational Programme Smart Growth 2014–2020; Priority IV: Increasing The Research Potential, Action 4.2: Development of Modern Research Infrastructure of the Science Sector, Co-financing from European Regional Development Fund.



**European
Funds**
Smart Growth



**Republic
of Poland**

European Union
European Regional
Development Fund



7.6 Seminars and teaching

Seminars and lecture outside of the IG PAS:

- A. Gumsley, The hunt for Earth's first supercontinent, University of Johannesburg, Johannesburg, South Africa, Invited lecture;

- A. Gumsley, Supercontinents, large igneous provinces and environmental change: applying U-Pb geochronology to stratigraphy at the beginning of the Proterozoic, University of Silesia, Sosnowiec, Poland, Invited lecture;
- K. Mizerski, Równania hydrodynamiki a turbulencja, University of Warsaw, Warsaw, Poland, Lecture;
- K. Mizerski, Podstawy teorii ziemskiego dynama magnetycznego, Institute of Fundamental Technological Research Polish Academy of Sciences, Warsaw, Poland, Seminar;
- M. Grądzki, Influence of diffusion on magnetic buoyancy instability, Institute of Fundamental Technological Research Polish Academy of Sciences, Warsaw, Poland, Seminar;
- M. Grądzki, Wpływ dyfuzji na niestabilność wyporności magnetycznej, University of Warsaw, Warsaw, Poland, Seminar;
- A. Bury, Analiza zaburzeń pola magnetycznego Ziemi widocznych w danych pomiarowych, University of Warsaw, Warsaw, Poland, Seminar.

7.7 Teaching thesis

- D. Staneczek, Rekonstrukcja paleonaprężeń w rejonie Gór Choczańskich na podstawie analizy anizotropii podatności magnetycznej i mezostrukturalnej, Supervisor: R. Szaniawski;
- E. Gaitán, U-Pb geochronological and chemical constraints on the ca. 2170 Ma magmatic event of the Kaapvaal Craton: implications for continental reconstructions, Supervisor: U. Söderlund (primary), A. Gumsley (co-supervisor);
- K. Rzepka, Przestrzenna analiza wyników interpretacji 1Di 2D krzywych sondowań magnetotellurycznych dla wybranych danych z rejonu polskiej części platform wschodnioeuropejskiej, Supervisor: W. Jóźwiak.

7.8 Completed PhD thesis defense

- M. Grądzki, Wpływ oporności elektrycznej i przewodnictwa cieplnego na krótkofalową niestabilność wyporności magnetycznej, Supervisor: K. Mizerski;
- M. Gwizdała, Zastosowanie własności magnetycznych osadów glacialno-morskich do jakościowej analizy egzaracji lodowca Werenskiolda (SW część Ziem Wedela Jarlsberga, Spitsbergen), Supervisor: M. Teisseyre-Jeleńska;
- K. Dudzisz, Paleomagnetic and rock magnetic investigations of the Triassic rocks from Svalbard Archipelago, Supervisor: R. Szaniawski;
- M. Burzyński, Paleomagnetyzm, własności magnetyczne oraz petrografia skał meta-magmowych Zachodniego Spitsbergenu, Supervisor: M. Lewandowski.

7.9 Visiting scientists

- Mark Dekkers, Utrecht University, Earth Sciences Department, Utrecht, the Netherlands, 7–18.06.2018;
- Bernard Henry, Institut de Physique du Globe, Paris, France, 10–19.06.2018;
- Ann Hirt, Institute of Geophysics, ETH Zurich, Zurich, Switzerland, 7–18.06.2018;
- Aldo Winkler, Istituto Nazionale di Geofisica e Vulcanologia, Roma 2 Section, Rome, Italy, 14–20.11.2018;
- Hana Grison, Institute of Geophysics, Academy of Sciences of the Czech Republic, Prague, Czech Republic, 10–16.06.2018;

- Frantisek Hrouda, AGICO Ltd., Brno, Czech Republic; Charles University, Faculty of Sciences, Prague, Czech Republic, 7–16.06.2018;
- Prof. David W. Hughes, Department of Applied Mathematics, University of Leeds, Leeds, United Kingdom, 18–21.11.2018;
- Dr Grace Cox, Dublin Institute for Advanced Studies, Dublin, Ireland, 28.10–16.11.2018.

7.10 Meetings, workshops, conferences, and symposia

Presentations of the Department's members:

16th Castle Meeting "New Trends on Paleo, Rock and Environmental Magnetism", Chęciny, Poland, 10–16 June 2018

- S. Dytłow, B. Górka-Kostrubiec, Passive dust samplers as more effective study material than street dust for characteristic of traffic derived pollution, Oral;
- T. Gonet, B. Górka-Kostrubiec, B. Łuczak-Wilamowska, Assessment of topsoil contamination near the Stanisław Siedlecki Polish Polar Station in Hornsund, Svalbard, using magnetic methods, Poster;
- B. Górka-Kostrubiec, T. Werner, S. Dytłow, I. Szczepaniak-Wnuk, M. Jeleńska, A. Hanc-Kuczkowska, Identification of metallic iron in an urban dust using magnetometry, microscopic observations and Mössbauer spectroscopy, Poster;
- M. Gwizdała, M. Jeleńska, L. Łęczyński, Environmental conditions in the Werenskiöld Glacier basin (Spitsbergen, Arctic): magnetic study, Poster;
- M. Jeleńska, Magnetometry used for comparison of heavy metals air pollution inside and outside home; case study from Warsaw, Poster;
- M. Kądziałko-Hofmokl, T. Werner, Fe-Cr mixed binary spinels as accessory magnetic minerals in the Sudetic ophiolitic rocks, Poster;
- J. Muraszko, P. Ziółkowski, R. Blukis, T. Werner, Cosmic dust as a carrier of natural remanent magnetisation? A Case study from the Jurassic stromatolites from the Zalas quarry, Krakow Upland, Poland, Poster;
- I. Szczepaniak-Wnuk, B. Górka-Kostrubiec, Assessment of heavy metal pollution of Vistula River sediments using magnetic method, Poster;
- K. Dudzisz, A. Hanc-Kuczkowska, A detailed study on the magnetic mineralogy of the Lower Triassic sedimentary rocks from Spitsbergen, Oral;
- D. Niezabitowska, R. Szaniawski, M. Jackson, Magnetic mineral composition as a potential indicator of depositional conditions in gas-bearing silurian shale rocks from Northern Poland, Poster;
- M. Burzyński, K. Michalski, K. Nejbart, G. Manby, J. Domańska-Siuda, Meta-igneous rocks from South-Western Oscar II Land (Western Spitsbergen) and their usefulness in palaeomagnetic investigations, Oral;
- K. Michalski, Palaeomagnetism in the High Arctic. Palaeomagnetic investigations of Svalbard Archipelago conducted by the Institute of Geophysics, Polish Academy of Sciences from 1999 to 2018, Invited oral;
- M. Lewandowski, T. Werner, G. Karasiński, D. Matesič, M. Paszkowski, Palaeomagnetic inclination error in the red-beds deposits: A contribution from the ediacaran sedimentary rocks of the western part of the East European Platform, Oral;
- A. Gumsley, D. Evans, W. Bleeker, K. Chamberlain, M. de Kock, U. Söderlund, The geological and paleomagnetic evidence for a late Neoproterozoic to early Paleoproterozoic supercontinent, Poster;

3rd International Conference on Atmospheric Dust – DUST2018, Bari, Italy, 29–31 May 2018

- S. Dytłow, B. Górka-Kostrubiec, Passive dust samplers – effective tool to assess traffic related pollution level, Oral;
- B. Górka-Kostrubiec, T. Gonet, B. Łuczak-Wilamowska, Topsoil pollution level near the Stanisław Siedlecki Polish polar station in Hornsund, Svalbard, evaluated by distribution of magnetic susceptibility and microscopic observation, Poster;
- B. Górka-Kostrubiec, T. Werner, S. Dytłow, I. Szczepaniak-Wnuk, M. Jeleńska, A. Hanc-Kuczkowska, Presence of metallic iron in an urban dust detected by magnetic methods, microscopic observations and Mössbauer spectra, Poster;

II Scientific Meeting in the Environmental Magnetism, Warsaw, Poland, 29 November 2018

- I. Szczepaniak-Wnuk, B. Górka-Kostrubiec, S. Dytłow, Badania zanieczyszczenia metalami ciężkimi osadów rzeki Wisły na wybranych jej odcinkach z zastosowaniem metod magnetycznych (Polish), Oral;
- B. Górka-Kostrubiec, D. Olszewska, Integracja infrastruktury badawczej w ramach projektu EPOS-PL, Oral;
- T. Werner, Udostępnianie infrastruktury badawczej laboratorium paleomagnetycznego dla polskiego środowiska naukowego w ramach projektu EPOS-PL (Polish), Oral;

EGU General Assembly 2018, Vienna, Austria, 8-13 April 2018

- K. Dudzisz, R. Szaniawski, K. Michalski, M. Chadima, Rock magnetism of the Lower Triassic sedimentary rocks from Spitsbergen, Poster;
- R. Szaniawski, L. Jankowski, M. Ludwiniak, S. Mazzoli, J. Szczygieł, New paleomagnetic and magnetic fabric results from hematite-bearing Lower Triassic redbeds from the Central Western Carpathians, Poster;
- A. Bury, K. Mizerski, Investigation of the fundamental types of the Earth's core perturbations in the oscillations of the geomagnetic field, Oral;

AAPG ICE 2018, Capetown, South Africa, 4–7 November 2018

- D. Niezabitowska, R. Szaniawski, M. Jackson, Magnetic mineral composition as a potential indicator of depositional conditions in gas-bearing silurian shale rocks from Northern Poland, Poster;

Geocongress, Johannesburg, South Africa, 18–20 July 2018

- A. Gumsley, Direct Mesoproterozoic connection of Congo and Kalahari cratons in proto-Africa, Oral;
- A. Gumsley, The 2789–2782 Ma Klipriviersberg large igneous province: implications for the chrono-stratigraphy of the Ventersdorp Supergroup and the timing of Witwatersrand gold deposition, Oral;
- A. Gumsley, A controversy resolved: a precise U-Pb baddeleyite age for the Ongeluk Large Igneous Province, Oral;
- A. Gumsley, The Molopo Farms Complex's age and country rock provenance: implications for Transvaal Supergroup correlations in southern Africa, Oral.

33rd Nordic Geological Winter Meeting, Copenhagen, Denmark, 10–12 January 2018

- K. Michalski, G. Manby, K. Nejbort, J. Domańska-Siuda, M. Burzyński, Integration of palaeomagnetic, isotopic and structural data to understand Svalbard Caledonian Terranes assemblage, Oral.

11th Geosymposium of Young Researchers, Istebna, Poland, 12–14 September 2018

- A. Gumsley, The late Neoproterozoic: the crossroad between the modern and ancient Earth, Oral;
- A. Gumsley, Kenorland: Earth's first supercontinent?, Oral.

Ny-Ålesund Atmosphere Flagship open workshop, Potsdam, Germany, 15–19 October 2018

- G. Karasiński, Preliminary results of the analysis of the inflow of air masses to the area of Hornsund fjord for the years 2005–2017, Oral.

Workshop on Changes of the Polar Ecosystem, Czech Republic, Mala Skala, 7–10 November 2018

- G. Karasiński, First view on air masses inflow in the surroundings of Polish Polar Station at Hornsund by analysis of backward trajectories, Oral.

The 24th EM Induction Workshop, Helsingør Denmark, 13–20 August 2018

- T. Ernst, W. Józwiak, Temporal changes of geomagnetic induction arrows in non-seismic regions: fiction or reality?, Poster;
- S. Oryński, W. Józwiak, K. Nowożyński, Deep lithospheric structure beneath Dolsk and Odra fault zones as a result of integrated Magnetotelluric 1-D, 2-D, and 3-D data interpretation, Poster;
- W. Klityński, S. Oryński, Combined quantitative interpretation of GCM and DC sounding data from selected area in Cracow, Poland, Poster;
- A. Neska, H. Brasse, Magnetotelluric data and models within the EPOS project the Polish contribution to EMTDAMO, Poster.

World Congress on Plasma Science & Technology, Stockholm, Sweden, 4–7 November 2018

- K. Mizerski, K. Moffatt, Magnetic field relaxation in the configuration of a sheet pinch in a low- β plasma, Oral.

MHD Days and GdRI Dynamo Meeting, Dresden, Germany, 26–28 December 2018

- K. Mizerski, Mean field dynamo mechanisms in highly conducting fluids, Oral;
- M. Grądzki, K. Mizerski, The effect of weak magnetic and thermal diffusion on magnetic buoyancy instability, Oral.

The XVIIIth IAGA Workshop on Geomagnetic Observatory Instruments, Data Acquisition and Processing, Conrad Observatory, Austria, 24–29 June 2018

- A. Neska, How the K index of geomagnetic activity helps to assess the data amount for magnetotelluric soundings, Oral;
- J. Reda, R. Koźlakiewicz, M. Neska, P. Czubak, Scanning historical magnetograms kept in the archives of Institute of Geophysics, Polish Ac. of Sc., Oral.

ICAE 2018, 16th International Conference on Atmospheric Electricity, Nara, Japan, 17–22 June 2018

- E. Williams, A. Guha, Y. Liu, R. Boldi, E. Pracser, R. Said, G. Satori, T. Bozoki, J. Bor, M. Atkinson, C. Beggan, S. Cummer, F. Lyu, B. Fain, Y. Hobara, A. Koloskov, A. Kulak, R. McCraty, J. Mlynarczyk, J. Montanya, R. Moore, M. Neska, P. Ortega, C. Price, R. Rawat, M. Sato, A. Sinha, Y. Yampolski, The ranking of Africa in daily global lightning activity, Poster.

INTERMAGNET Meeting 2018, Vienna, Austria, 2–4 July 2018

- J. Reda, The collection of one-minute 2015 definitive data, Oral.

7.11 Publications

ARTICLES

- Burzyński, M.T., K. Michalski**, et al. (2018), Mineralogical, rock-magnetic and palaeomagnetic properties of metadolerites from Central Western Svalbard, *Minerals* **8**, 7, 279, DOI: 10.3390/min8070279.
- Dudzisz, K., K. Michalski, R. Szaniawski**, et al. (2018a), Palaeomagnetic, rock-magnetic and mineralogical investigations of the Lower Triassic Vardebukta Formation from the southern part of the West Spitsbergen Fold and Thrust Belt, *Geol. Mag.* **156**, 4, 620–638, DOI: 10.1017/S0016756817001145.
- Dudzisz, K., R. Szaniawski, K. Michalski**, et al. (2018b), Rock magnetism and magnetic fabric of the Triassic rocks from the West Spitsbergen Fold-and-Thrust Belt and its foreland, *Tectonophysics* **728–729**, 104–118, DOI: 10.1016/j.tecto.2018.02.007.
- Dytłow, S.**, and **B. Górka-Kostrubiec** (2018), Comparison of traffic-related pollution level using street dust and passive dust samplers, *ProScience* **5**, 31–36, DOI: 10.14644/dust.2018.006.
- Stanica, D.A., **T. Ernst, W. Jóźwiak**, et al. (2018), Pre-seismic geomagnetic and ionosphere signatures related to the Mw5.7 earthquake occurred in Vrancea zone on September 24, 2016, *Acta Geophys.* **66**, 167–177, DOI: 10.1007/s11600-018-0115-4.
- Górka-Kostrubiec, B., T. Werner, S. Dytłow, I. Szczepaniak-Wnuk, M. Jeleńska**, and A. Hanc-Kuczkowska (2018), Detection of metallic iron in urban dust by magnetic methods and microscopic observations, *Proscience* **5**, 46–51, DOI: 10.14644/dust.2018.008.
- Gonet T., **B. Górka-Kostrubiec**, and B. Łuczak-Wilamowska (2018), Assessment of topsoil contamination near the Stanisław Siedlecki Polish Polar Station in Hornsund, Svalbard, using magnetic methods, *Polar Sci.* **15**, 75–86, DOI: 10.1016/j.polar.2017.12.006.
- Salminen, J., **A. Gumsley**, et al. (2018), Direct Mesoproterozoic connection of the Congo and Kalahari cratons in proto-Africa: Strange attractors across supercontinental cycles, *Geology* **46**, 11, 1011–1014, DOI: 10.1130/G45294.1.
- Gwizdała, M., M. Jeleńska**, et al. (2018), The magnetic method as a tool to investigate the Werenskioldbreen environment (south-west Spitsbergen, Arctic Norway), *Polar Res.* **37**, 1, 1436846, DOI: 10.1080/17518369.2018.1436846.
- Schito, A., **R. Junosza-Szaniawski**, et al. (2018), Burial and exhumation of the western border of the Ukrainian Shield (Podolia): a multi-disciplinary approach, *Basin Res.* **30**, S1, 532–549, DOI: 10.1111/bre.12235.
- Mazur, S., M. Malinowski, **M. Lewandowski**, et al. (2018), On the nature of the Teisseyre-Tornquist Zone, *Geol. Geophys. Environ.* **44**, 1, 17–30, DOI: 10.7494/geol.2018.44.1.17.
- Michalski, K.** (2018), Palaeomagnetism of metacarbonates and fracture fills of Kongsfjorden islands (western Spitsbergen): Towards a better understanding of late- to post-Caledonian tectonic rotations, *Pol. Polar Res.* **39**, 1, 51–75, DOI: 10.24425/118738.
- Mizerski, K.A.** (2018a), Large-scale dynamo action driven by forced beating waves in a highly conducting plasma, *J. Plasma Phys.* **84**, 4, 735840405. DOI: 10.1017/S0022377818000764.

- Mizerski, K.A.** (2018b), Large-scale hydromagnetic dynamo by Lehnert waves in nonresistive plasma, *SIAM J. Appl. Math.* **78**, 3, 1402–1421, DOI: 10.1137/17M1133336.
- Mizerski, K.A.**, and H.K. Moffatt (2018), Dynamo generation of a magnetic field by decaying Lehnert waves in a highly conducting plasma, *Geophys. Astrophys. Fluid Dynam.* **112**, 2, 165–174, DOI: 10.1080/03091929.2018.1425407.
- Błęcki, J.S., and **K.A. Mizerski** (2018), Subtle structure of streamers under conditions resembling those of Transient Luminous Events, *Arch. Mech.* **70**, 6, 535–550, DOI: 10.24423/aom.3009.
- Grądzki, M.J., and **K.A. Mizerski** (2018), The effect of weak resistivity and weak thermal diffusion on short-wavelength magnetic buoyancy instability, *Astrophys. J. Suppl. Ser.* **235**, 1, 13, DOI: 10.3847/1538-4365/aaa408.
- Neska, A., J.T. Reda, M.L. Neska**, et al. (2018), On the relevance of source effects in geomagnetic pulsations for induction soundings, *Ann. Geophys.* **36**, 2, 337–347, DOI: 10.5194/angeo-36-337-2018.
- Niezabitowska, D., R. Junosza-Szaniawski**, et al. (2018), Magnetic anisotropy in Silurian gas-bearing shale rocks from the Pomerania region (Northern Poland), *J. Geophys. Res. Solid Earth* **124**, 1, 5–25, DOI: 10.1029/2018JB016374.
- Del Corpo, A., **J. Reda**, et al. (2018), Observing the cold plasma in the Earth’s magnetosphere with the EMMA network, *Ann. Geophys.* **62**, 4, GM447, DOI: 10.4401/ag-7751.
- Szaniawski, R.**, et al. (2018), New paleomagnetic and magnetic fabric results from hematite-bearing Lower Triassic redbeds of the Central Western Carpathians. **In:** *Proc. Conf. 20th EGU General Assembly, EGU2018, 4–13 April 2018, Vienna, Austria*, 19563.
- Szczepaniak-Wnuk, I.**, and **B. Górka-Kostrubiec** (2018), Magnetic study of sediments from the Vistula River in Warsaw—preliminary results. **In:** M. Jeleńska, L. Łęczyński, and T. Ossowski (eds.), *Magnetometry in Environmental Sciences*, GeoPlanet: Earth and Planetary Sciences, Springer, Cham, 23–35, DOI: 10.1007/978-3-319-60213-4_2.
- Teisseyre-Jeleńska, M., B. Górka-Kostrubiec**, and **S. Dytłow** (2018), Magnetic vertical structure of soil as a result of transformation of iron oxides during pedogenesis. The case study of soil profiles from Slovakia and Ukraine. **In:** M. Jeleńska, L. Łęczyński, and T. Ossowski (eds.), *Magnetometry in Environmental Sciences*, GeoPlanet: Earth and Planetary Sciences, Springer, Cham, 103–125, DOI: 10.1007/978-3-319-60213-4_8.
- Nawrocki, J., **T. Werner**, et al. (2018a), The Hilina Pali palaeomagnetic excursion and possible self-reversal in the loess from western Ukraine, *Boreas* **47**, 3, 954–966, DOI: 10.1111/bor.12305.
- Nawrocki, J., **T. Werner**, et al. (2018b), ‘Is the Hilina Pali “palaeomagnetic excursion” becoming another example of the reinforcement syndrome? A comment inspired by Nawrocki et al. (2018)’: Reply to comments, *Boreas* **47**, 3, 969–970, DOI: 10.1111/bor.12329.

CHAPTERS

- Król, E.**, and P. Szwarczewski (2018), Magnetic susceptibility of sediments as an indicator of the dynamics of geomorphological processes. **In:** M. Jeleńska, L. Łęczyński, and T. Ossowski (eds.), *Magnetometry in Environmental Sciences*, GeoPlanet: Earth and Planetary Sciences, Springer, Cham, 79–89, DOI: 10.1007/978-3-319-60213-4_6.
- Semenov, V.**, and M. Petrishchev (2018a), Electromagnetic monitoring. **In:** *Induction Soundings of the Earth’s Mantle*, Geo-Planet: Earth and Planetary Sciences, Springer, Cham, 79–100, DOI: 10.1007/978-3-319-53795-5_5.

Semenov, V., and M. Petrishchev (2018b), Impedances, sources and environments. **In:** *Induction Soundings of the Earth's Mantle*, Geo-Planet: Earth and Planetary Sciences, Springer, Cham, 1–24, DOI: 10.1007/978-3-319-53795-5_1.

Semenov, V., and M. Petrishchev (2018c), Modeling of deep soundings. **In:** *Induction Soundings of the Earth's Mantle*, Geo-Planet: Earth and Planetary Sciences, Springer, Cham, 45–56, DOI: 10.1007/978-3-319-53795-5_3.

Semenov, V., and M. Petrishchev (2018d), Results of deep soundings in Europe. **In:** *Induction Soundings of the Earth's Mantle*, Geo-Planet: Earth and Planetary Sciences, Springer, Cham, 57–78, DOI: 10.1007/978-3-319-53795-5_4.

Semenov, V., and M. Petrishchev (2018e), Several impedances from one equation. **In:** *Induction Soundings of the Earth's Mantle*, Geo-Planet: Earth and Planetary Sciences, Springer, Cham, 25–44, DOI: 10.1007/978-3-319-53795-5_2.

BOOKS

Jeleńska, M., L. Łęczyński, and T. Ossowski (eds.), *Magnetometry in Environmental Sciences*, GeoPlanet: Earth and Planetary Sciences, Springer, Cham, DOI: 10.1007/978-3-319-60213-4.

Semenov, V., and M. Petrishchev (2018f), *Induction Soundings of the Earth's Mantle*, Geo-Planet: Earth and Planetary Sciences, Springer, Cham, 100 pp., DOI: 10.1007/978-3-319-53795-5.

8. DEPARTMENT OF GEOPHYSICAL IMAGING

Michał Malinowski

8.1 About the Department

Department activities in 2018 were traditionally split between the two groups. The first one was focused on the geophysical imaging of geological structures in various scales; the second on the mathematical analysis of complex system in geophysics. The scale of applications ranged from near-surface to the deep crust. We have been working towards solving some fundamental research questions like the structure of the crust in NE Poland from reprocessing of the Poland-SPAN regional profiles or structure of the crust within the Nankai Trough seismogenic zone in Japan, employing innovative methods like full-waveform inversion (FWI). We finalized seismic/borehole measurements in Hornsund (Sptisbergen) in a project devoted to studying the temporal changes of the permafrost layer. In another Arctic-related project, we successfully collected passive seismic data from the temporary seismic network operating on the Hans glacier (Hornsund). Near-surface seismic field measurement were also performed for solving geological problems at various locations (mostly in the Holy Cross Mts.), validating our methodology. Another area is related to more applied research within the broader scope of sustaining the raw material supply for Europe by supporting mineral exploration. This year we finished the COGITO-MIN project, in which together with partners from Finland, we have been developing active/passive seismic methods for mineral exploration using the data acquired in the Kylylahti area (Outukumpu mineral belt, Finland). This topic is further being developed in the framework of the EU-funded H2020 Research and Innovation Action project called “Smart Exploration”, in which we aim to improve seismic imaging by the use of FWI. We also keep working on the methodology for characterization of the unconventional reservoirs (shale gas bearing), both using the active source seismic, as well as microseismic data. This year, a special section of the SEG “Interpretation” journal was published devoted to “Characterization of potential Lower Paleozoic shale resource play in Poland”, in which we contributed with 4 papers. The “theoretical” group was working towards the construction of a universal model in the form of a stochastic cellular automaton integrating fundamental empirical laws describing statistical properties of earthquakes and enabling the study of the relationship between these laws. The biggest organizational achievement this year was the 18th edition of the biennial International Symposium on Deep Seismic Profiling of the Continents and their Margins (SEISMIX 2018), which was held in Kraków between 17–22 June.

8.2 Personnel

Head of the Department

Michał Malinowski
Associate Professor

Associate Professors

Mariusz Białecki
Mariusz Majdański

Assistant Professor

Andrzej Górszczyk

Research Assistants

Marta Cyz
Brij Singh
Jacek Trojanowski

PhD Students

Arpan Bagchi, India; Mariusz Białeccki – PhD supervisor
 Michał Chamarczuk, Poland; Michał Malinowski – PhD supervisor
 Wojciech Gajek, Poland; Michał Malinowski – PhD supervisor
 Silvana Magni, Italy; Mariusz Białeccki – PhD supervisor
 Artur Marciniak, Poland; Mariusz Majdański – PhD supervisor
 Miłosz Mężyk, Poland; Michał Malinowski – PhD supervisor
 Quang Nguyen, Vietnam; Michał Malinowski – PhD supervisor
 Bartosz Owoc, Poland; Mariusz Majdański – PhD supervisor
 Rishabh Sharma, India; Mariusz Białeccki – PhD supervisor
 Brij Singh, India; Michał Malinowski – PhD supervisor

8.3 Main research projects

- Linking deep and shallow geological processes in the transition from Precambrian to Palaeozoic platform in the southern Baltic Sea using new geophysical data, M. Malinowski, National Science Centre, 2018–2021;
- Crustal structure of the East European Craton margin in northern Poland based on the new geophysical data, M. Malinowski, National Science Centre, 2016–2019;
- Three dimensional model of the lithosphere in Poland with verification of seismic parameters of the wave field, M. Majdański, National Science Center, 2016–2019;
- Relationship of permafrost with geomorphology, geology and cryospheric components based on geophysical research of the Hans glacier forefield and its surroundings. Hornsund, Spitsbergen, M. Majdański, National Science Centre, 2017–2020;
- Mechanistic explanation of a generation of (and deviations from) the universal curve of the Earthquake Recurrence Time Distribution by means of constructions of solvable stochastic cellular automata and their analytical description, M. Białeccki, National Science Centre, 2018–2021;
- COst-effective Geophysical Imaging Techniques for supporting ongoing MINeral exploration in Europe (COGITO-MIN), M. Malinowski, National Science Centre, 2016–2018;
- Sustainable mineral resources by utilizing new Exploration technologies (SMART EXPLORATION), M. Malinowski, National Science Centre, 2017–2020;
- Determining structure and physical properties of the crust in the Nankai Trough area (Japan) using multiparameter full-waveform inversion, A. Górszczyk, National Science Centre, 2016–2018.

8.4 instruments and facilities

Equipment

- 40 × DATA-CUBE seismic recorders with 1C 4.5 Hz geophones;
- 20 × DATA-CUBE seismic recorders with 3C 4.5 Hz geophones;
- Seismic source PEG-40 with carriage and timing system.

Laboratory

- Facilities for seismic data processing, imaging, modelling and interpretation including local InfiniBand cluster, GPU Workstation and NAS data storage systems; Industry state-of-the-art software, such as ProMAX, Reveal, Globe Claritas, TSUNAMI, VISTA, OMNI3D, Petrel, Kingdom Suite, GOCAD, Hampson Russell + in-house and academic software.

8.5 Research activity and results

Brief description/abstracts/summaries of some of the achievements of the Department's staff:

IMAGING EAST EUROPEAN CRATON MARGIN IN NORTHERN POLAND USING EXTENDED-CORRELATION PROCESSING APPLIED TO REGIONAL REFLECTION SEISMIC PROFILES

M. Malinowski, M. Mężyk

In NE Poland, the Eastern European Craton (EEC) crust of the Fennoscandian affinity is concealed under a Phanerozoic platform cover and penetrated by the sparse deep research wells. Most of the inferences regarding its structure rely on geophysical data. Until recently, this area was covered only by the refraction/wide-angle reflection (WARR) profiles, which show a relatively simple crustal structure with a typical cratonic 3-layer crust. ION Geophysical Poland-SPAN™ regional seismic program, acquired over the marginal part of the EEC in Poland, offered a unique opportunity to derive a detailed image of the deeper crust. Here, we apply extended correlation processing to a subset (~950 km) of the PolandSPAN™ dataset located in NE Poland (Fig. 1), which enabled us to extend the nominal record length of the acquired data from 12 to 22 s (~60 km depth). Our new processing (Fig. 2) revealed reflectivity patterns, that we primarily associate with the Paleoproterozoic crust formation during the Svekofennian (Svekobaltic) orogeny and which are similar to what was observed along the BABEL and FIRE profiles in the Baltic Sea and Finland, respectively. We propose a mid- to lower-crustal lateral flow model to explain the occurrence of two sets of structures that can be collectively interpreted as kilometre-scale S-C' shear zones. The structures define a penetrative deformation fabric pointing out to ductile extension of hot orogenic crust. Subsequent, localized reactivation

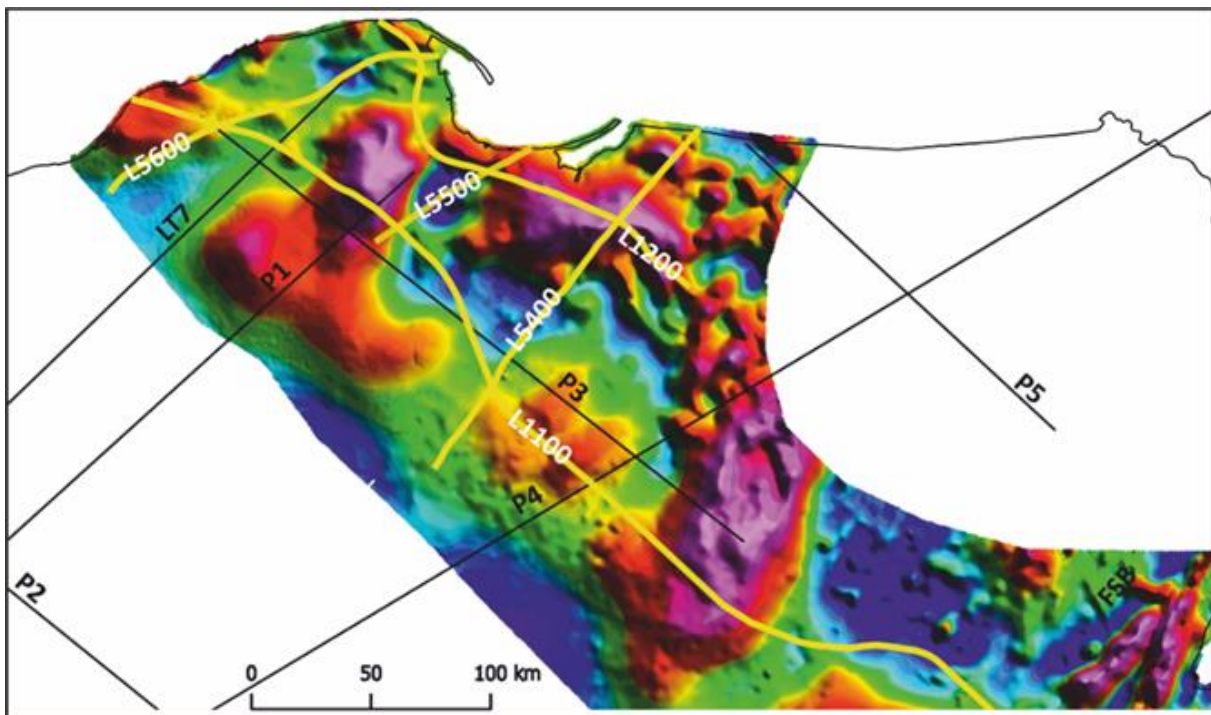


Fig. 1. Location of the PolandSPAN™ seismic profiles on the background of a total magnetic field anomaly map of NE Poland (reduced to pole) (data compilation of S. Mazur) (after Mężyk et al. 2019).

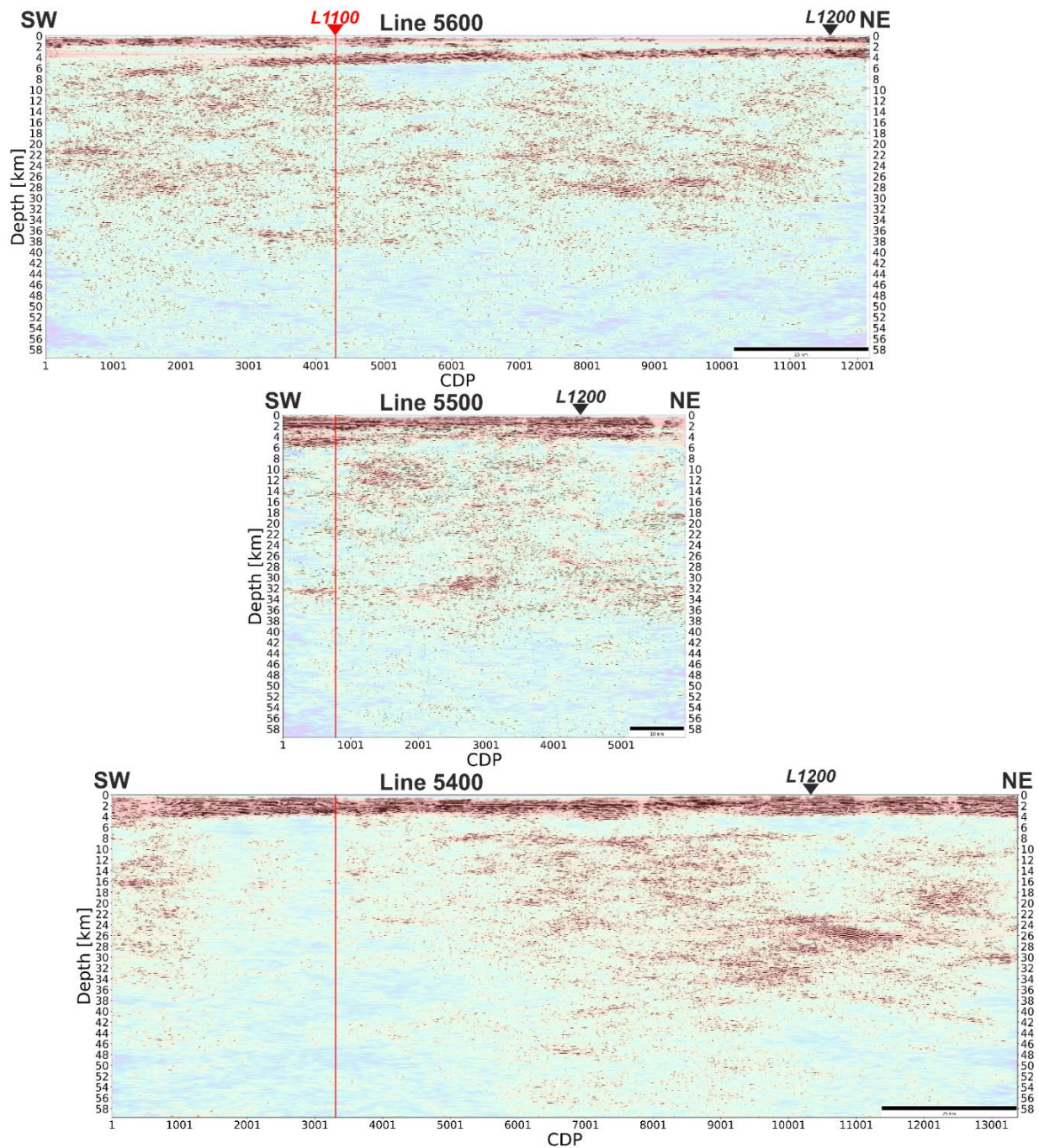


Fig. 2. Final migrated depth-converted section along PolandSPANTM profiles 5600, 5500, and 5400 (envelope and amplitude combined plot). Profiles are centered at the intersection with line 1100 (vertical red line) (after Mężyk et al. 2019).

of these structures provided conduits for subsequent emplacement of gabbroic magma that produced a Mesoproterozoic anorthosite-mangerite-charnockite-granite (AMCG) suite in NE Poland. Delamination of overthickened orogenic lithosphere may have accounted for magmatic underplating and fractionation into the AMCG plutons. We also found sub-Moho dipping mantle reflectivity, which we tentatively explain as a signature of the crustal accretion during the Svekofennian orogeny. Later tectonic phases (e.g. Ediacaran rifting, Caledonian orogeny) did not leave a clear signature in the deeper crust, however, some of the subhorizontal reflectors

below the basement, observed in the vicinity of the AMCG Mazury complex, can be alternatively linked with lower Carboniferous magmatism.

References

Mężyk, M., M. Malinowski, and S. Mazur (2019), Imaging the East European Craton margin in northern Poland using extended correlation processing of regional seismic reflection profiles, *Solid Earth* **10**, 3, 683–696, DOI: 10.5194/se-10-683-2019.

DERIVING COST-EFFECTIVE GEOPHYSICAL IMAGING TECHNIQUES FOR SUPPORTING ONGOING MINERAL EXPLORATION IN EUROPE (COGITO-MIN)

M. Malinowski, M. Chamarczuk, B. Singh

In 2016, the COGITO-MIN project acquired new types of active and passive seismic data at the Kylylahti sulphide mine site in Eastern Finland (Fig. 1). Kylylahti is situated within the historical Outokumpu ore district that hosts polymetallic Cu Co Zn Ni Ag Au semimassive-to-massive sulphide deposits. Overall, the new experiments consisted of a 2D seismic survey, sparse active-source and passive 3D seismic surveys, as well a VSP survey partly utilizing novel fibre-optic Distributed Acoustic Sensing (DAS) technology. The experiments were designed with different stages of the exploration workflow in mind; from mapping of the ore host rocks at larger scale to high-resolution resource delineation.

The COGITO-MIN 3D experiments (Fig. 1) included a passive seismic survey in which 1000 one-component wireless receivers recorded ambient noise for a month. The receivers were deployed in a 3.5×3 km grid, with 200 m line spacing and 50 m inline receiver interval. The

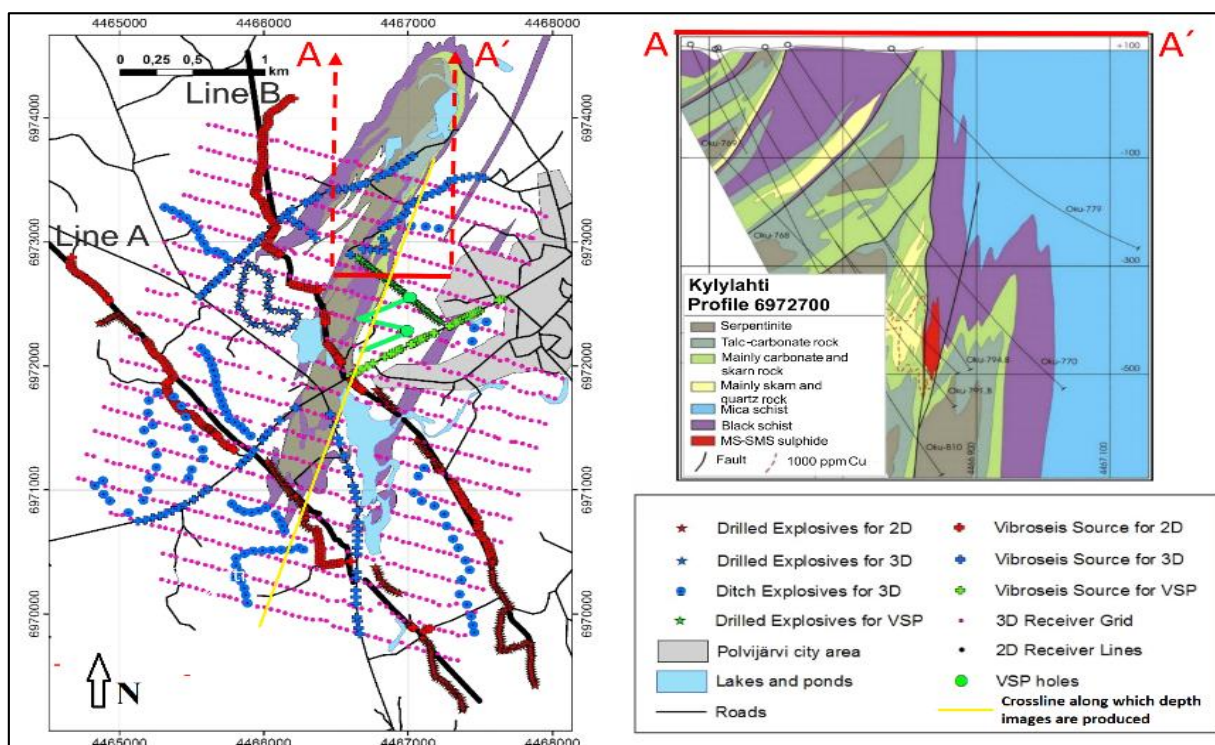


Fig. 1. Acquisition geometry of the COGITO-MIN 3D seismic survey (left). A-A' is cross-section through the Kylylahti deposit (right) (after Chamarczuk et al. 2018). Yellow line marks the crossline position intersecting the ore zone, shown in Fig. 3.

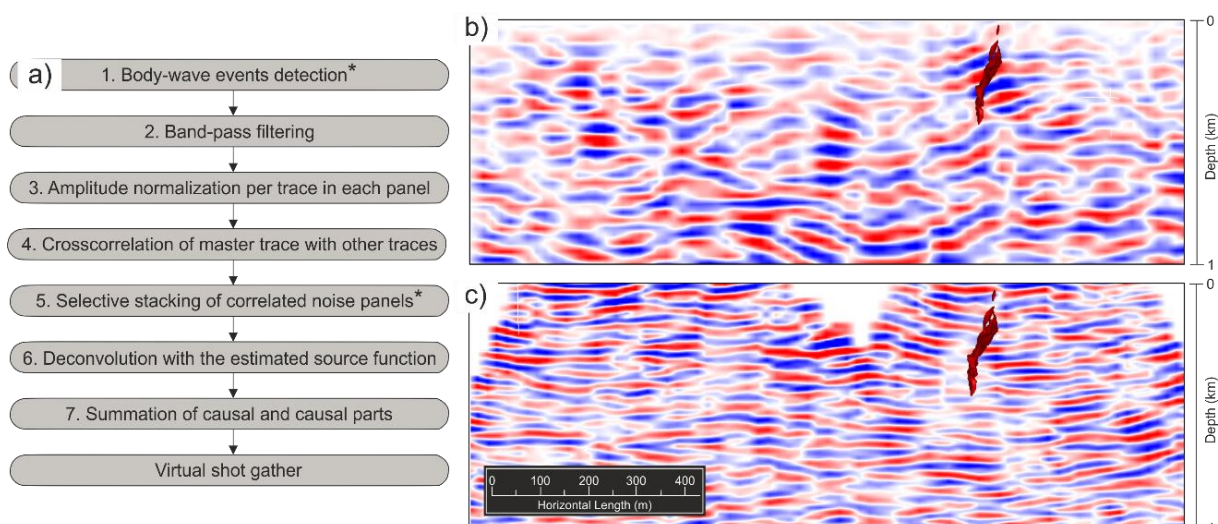


Fig. 2: (a) The MESI processing workflow; (b) Example of an inline migrated seismic section obtained from the MESI-processed data compared to (c) the migrated co-located inline section from the active data. Projection of the massive sulphide ore lens is shown as a red shape (after Chamarczuk et al. 2018).

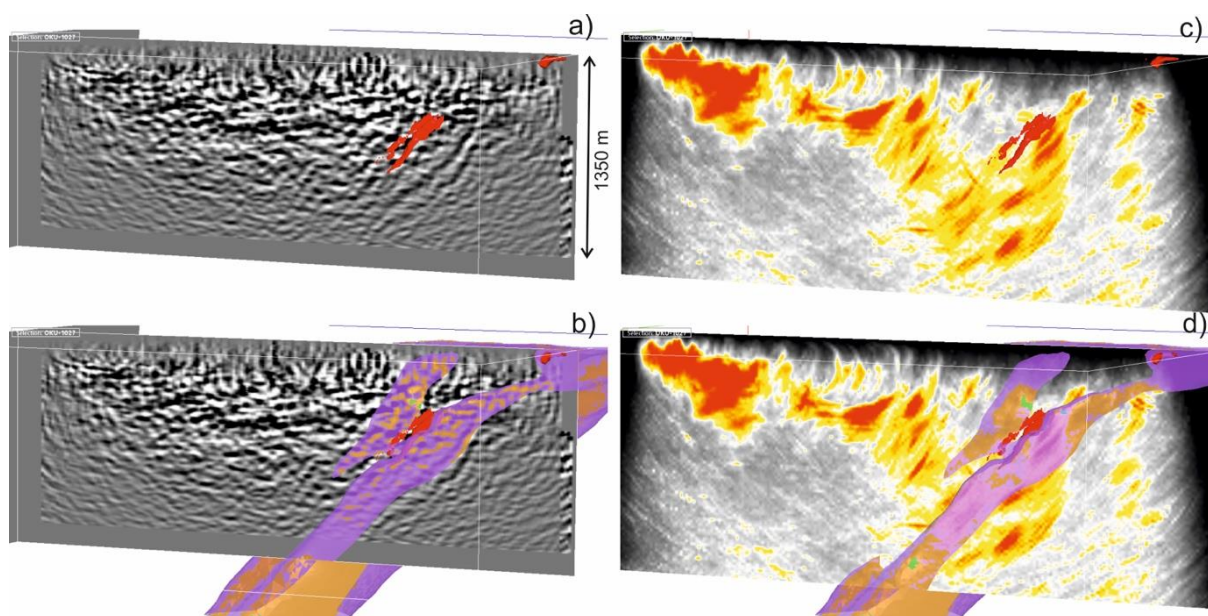


Fig. 3. Comparison of standard Kirchhoff PreSDM (a, b) and CBFVM (c, d) along a crossline through the ore zone, which is marked by a red surface. The base of the Outokumpu assemblage is identical with the base of the Kylylahti formation, which is shown as a purple surface in (b) and (d).

aim was to test and develop a cost-effective method for mapping the continuity of the ore host rocks through the application of body-wave seismic interferometry (SI). In the COGITO-MIN project, Chamarczuk et al. (2017, 2018) have developed a new workflow (called MESI) for processing such data acquired in the crystalline rock terrain. This workflow involves detection of body-wave events, evaluating their locations, and selective stacking over stationary-phase areas for creating virtual shot gathers (Fig. 2). The 3D grid was also used for a sparse 3D active-source survey with an irregular distribution of Vibroseis and explosive sources. However, even with the sparse source distribution, the 3D survey has provided new details about the architecture of the Kylylahti area, in particular about the spatial extent of the Outokumpu assemblage

rocks (Fig. 3). Both time and depth imaging was performed for 3D data, however time imaging failed to provide a clear image of the main structure of the steeply dipping Kylylahti formation, showing only sparse, discontinuous reflectors. Motivated by the earlier successful application of Kirchhoff pre-stack depth migration (PreSDM) to the COGITO-MIN 2D data (Heinonen et al. 2018), we decided to apply it also to the 3D data. Apart of the Kirchhoff PreSDM, we also used the coherency-based Fresnel Volume Migration (CBFVM) approach developed a TU Freiberg. It is well suited for sparse acquisition geometries because it reduces migration artefacts caused by insufficient coverage of the survey area.

References

Chamarczuk, M., M. Malinowski, E. Koivisto, S. Heinonen, S. Juurela, and COGITO-MIN Working Group (2017), Passive seismic interferometry for subsurface imaging in an active mine environment: case study from the Kylylahti Cu-Au-Zn mine, Finland. **In:** G. Bellefleur and B. Milkereit (eds.), *Proceedings of Exploration '17: Seismic Methods & Exploration Workshop, 21–25 October 2017, Toronto, Canada*, 51–56, Decennial Mineral Exploration Conferences.

FACING THE 3D CRUSTAL-SCALE IMAGING VIA FULL-WAVEFORM INVERSION OF THE OCEAN-BOTTOM SEISMOMETER DATA – PHASE I: BUILDING A 3D SYNTHETIC MODEL OF A SUBDUCTION ZONE AND WAVEFIELD MODELLING

A. Górszczyk

The current paradigm on how onshore, crustal-scale velocity models based on long-offset stationary-receiver surveys are built relies on 2D ray-based methods such as first-arrival traveltime tomography (FAT). This is mainly because such methods offer acceptable resolution for delineating the main crustal units while remaining affordable in terms of data acquisition and processing. As an alternative approach, full-waveform inversion (FWI) allows one to develop subsurface models at wavelength-scale resolution and has the potential to be utilized for multiparameter reconstructions. Moreover, it does not require the identification and picking of individual phases, since the ultimate goal of FWI is to automatically account for all types of arrivals.

On the other hand, our imaging relies on the 2D assumption which implies some important limitations: structures are imaged along vertical section with possible artifacts resulting from limited fold and illumination, 3D propagation effects, empirical 3D-to-2D amplitude and phase corrections etc. This raises the issue of designing next generation of 3D sea-bottom acquisitions for deep crustal investigations. In order to move towards high resolution 3D imaging of the whole crust and to broaden our knowledge about the structural factors that govern active geodynamical processes in various environments, we must first define the specifications of new-generation OBS surveys that are amenable to FWI at crustal scale. Among others, different key points are related to the acquisition geometry and logistic in particular in terms of sampling and spread, the computer implementation of FWI for large-scale optimization problems (parallelism, time versus frequency domain modeling engines, compressive sensing), the development of optimization strategies to mitigate the nonlinearity and ill-posedness of the inverse problem etc.

To mitigate the mentioned issues we start with building of a realistic 3D marine crustal-scale model amenable to evaluate different acquisition geometries and processing techniques suitable for deep crustal imaging. The model has been inspired by the geologically complex structure of the Nankai subduction zone combined with the previous results of geophysical

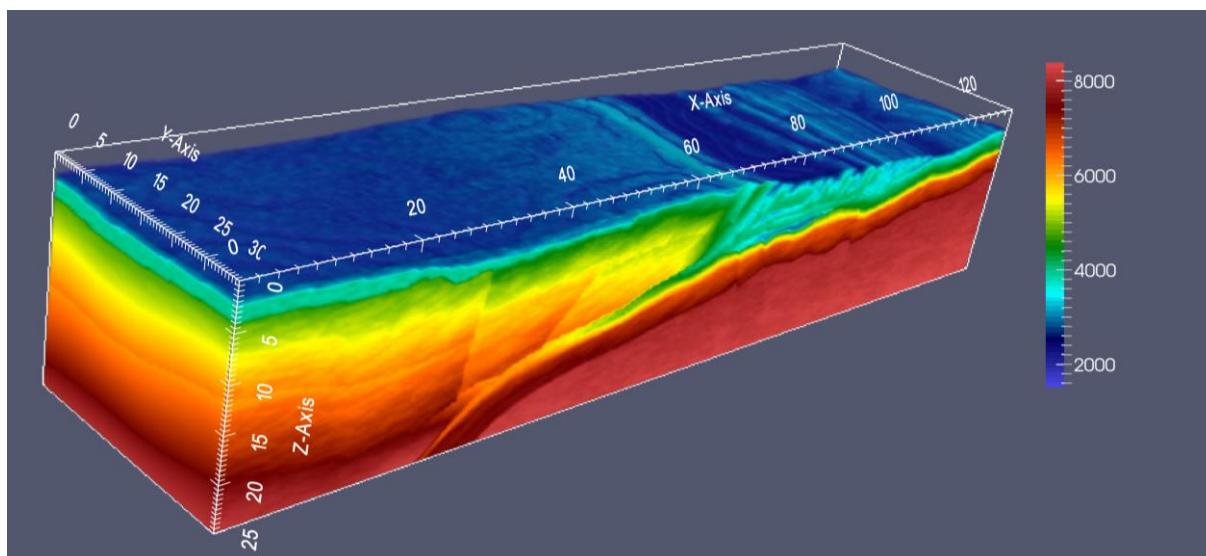


Fig. 1. Perspective view on the part of 3D P -wave velocity model.

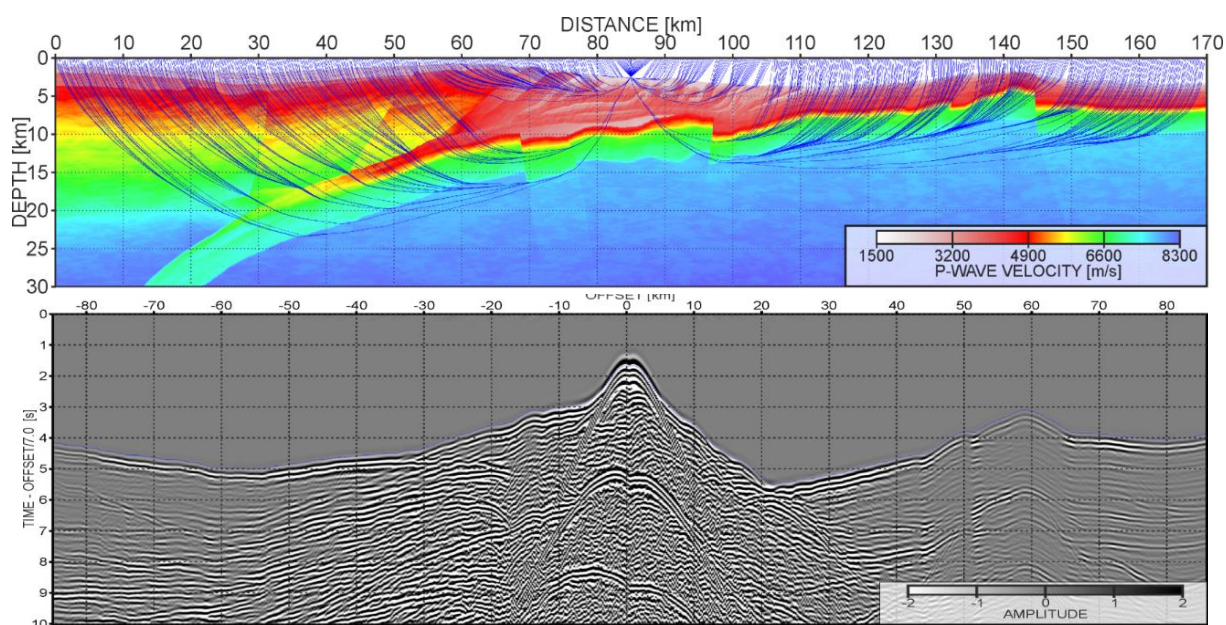


Fig. 2. Ray-tracing (upper panel) and P -wave modeling (lower panel) performed along one of the inlines extracted from 3D cube. Note the complexity of the wavefield reflecting the rich structural information incorporated into the synthetic model.

investigations of this area. It contains wide range of realistic features like strong bathymetry variations, oceanic ridges, subducted topography highs, low-velocity zones, velocity gradients, complex accretionary prism, large faults and thrusts with local damage-zones as well as shallow sedimentary basins. Additionally we incorporate different stochastic components to mimic more realistic wave propagation. We further obtain S -wave velocity and density models using polynomial functions derived from empirical relations between P -wave velocity and other physical parameters. These elastic models are consequently modified according to our assumptions about local heterogeneities in the model.

The model is cast in 3D cube which dimension is $30 \times 170 \times 105$ km with 25 m grid interval. Subpart of the full model is presented in Fig. 1. Such parameterization of the model

leads to more than 34 billion degrees of freedom imposing challenge from the point of view of computational resources and the high performance computing implementations. Examples of the first-arrival raypaths and the corresponding OBS gather simulated along the single 2D inline of the model are presented in Fig. 2.

We believe that through the development of this synthetic model and the following visco-elastic dataset we have chance to better understand the determinants of the crustal-scale imaging via FWI of the OBS data and stimulate its popularization in the communities aiming on regional data acquisition and imaging.

CRUSTAL-SCALE DEPTH IMAGING VIA JOINT FWI OF OBS DATA AND PSDM OF MCS DATA

A. Górszczyk

Pre-Stack Depth Migration (PSDM) imaging from Multi-Channel Seismic (MCS) reflection data at the scale of the whole crust is inherently difficult. This mainly results because the depth

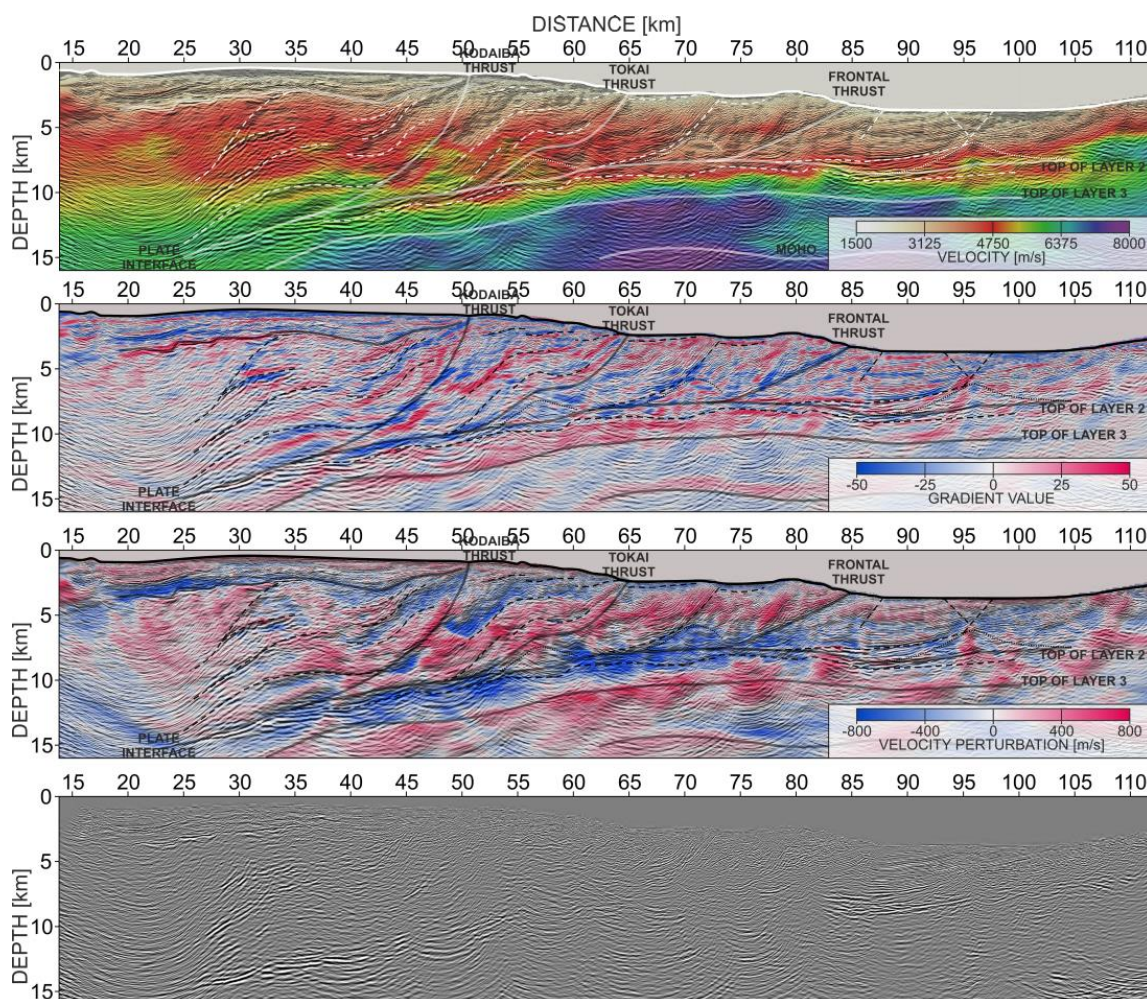


Fig. 1. Results of crustal scale imaging derived from joint FWI of OBS data and PSDM of MCS data. From top to bottom panels present: (i) PSDM section superimposed on the absolute FWI velocity model; (ii) PSDM section superimposed on the gradient of FWI velocity model; (iii) PSDM section superimposed on the FWI velocity model after removing polynomial velocity trend; and (iv) PSDM section. Note the detailed geological information coming from the velocity models which support the interpretation of the PSDM section.

penetration of the seismic wavefield is controlled, firstly (i) by the acquisition design, like streamer length and air-gun source configuration, and secondly (ii) by the complexity of the crustal structure. Moreover, the limited length of the streamer makes the estimation of velocities from deep targets challenging due to the velocity-depth ambiguity. The problem is even more pronounced when processing 2D seismic data, due to the lack of multi-azimuthal coverage. Therefore, in order to broaden our knowledge about the deep crust from seismic methods, one can target the development of specific imaging workflow combining (i) first-arrival traveltime tomography and full-waveform inversion (FWI) of wide-angle/long-offset data collected by Ocean Bottom Seismometers (OBS) for velocity model building and (ii) pre-stack depth migration of short-spread multichannel reflection data for reflectivity imaging, using the former velocity model as background model. We present an application of such workflow on seismic data collected by Japan Agency for Marine-Earth Science and Technology (JAMSTEC) and Institut Français de recherche pour l'exploitation de la mer (IFREMER) in the eastern Nankai Trough (Tokai area) during the 2000/2001 SFJ experiment. We show that the FWI model, although derived from OBS data, provides yet an acceptable background velocity field for the PSDM of the MCS data. Furthermore, from the initial PSDM, we first refine the FWI background velocity model by minimizing the residual moveouts (RMO) picked in the pre-stack migrated volume through slope tomography (ST), from which we generate a better focused migrated image. Such integration of different seismic data sets and imaging techniques led to optimal imaging results at different resolution levels (see Fig. 1). That is, the large-to-intermediate scale crustal units identified in the high-resolution FWI velocity model complement the short-scale reflectivity inferred from the MCS data to better constrain the structural factors controlling the geodynamics of the Nankai trough area.

APPLICATION OF THE STOCHASTIC INVERSION FOR SHALE RESERVOIR CHARACTERIZATION

M. Cyz, M. Malinowski

Seismic inversion is an important tool for subsurface modelling and characterization. It allows to obtain the spatial distribution of the elastic properties (e.g. density (ρ), P -wave (V_p), and S -wave (V_s) velocities) based on existing seismic reflection and well data. Seismic inversion methods can be divided into two categories: deterministic and geostatistical. Deterministic inversion is based on low frequency models and has limited bandwidth and result in smooth inverted models with low-resolution, but they manifest the general trends within the considered property. Geostatistical inversion simulates possible property models based on well data and a model describing the expected spatial continuity pattern of the property of interest. This allows to retrieve high-resolution inverted models and assess uncertainty of the predictions. However, these methods are computationally expensive, requires good quality data and proper well-to-seismic ties. Obtaining high-resolution models is especially important while dealing with the characterization of thin beds, what is mostly the case in the shale reservoirs.

Here, we apply geostatistical seismic Amplitude-versus-Angle (AVA) inversion (Azevedo et al. 2018) to characterize the unconventional Lower Palaeozoic shale reservoir from Baltic Basin, Northern Poland where the most interesting targets are of small thickness (up to 25 m) and deeply buried (ca. 3 km depth). This inversion method allows inverting pre-stack angle-domain seismic gathers simultaneously for elastic properties (ρ , V_p , V_s). The procedure uses direct stochastic simulation and co-simulation (DSS) as the model perturbation technique and a genetic algorithm as a global optimiser to ensure the convergence of the iterative procedure. The elastic properties are simulated and co-simulated sequentially from available well-log following a pre-defined spatial continuity pattern as expressed by a variogram model. The resulting models exhibit high-resolution and allow assessing uncertainty on the predictions.

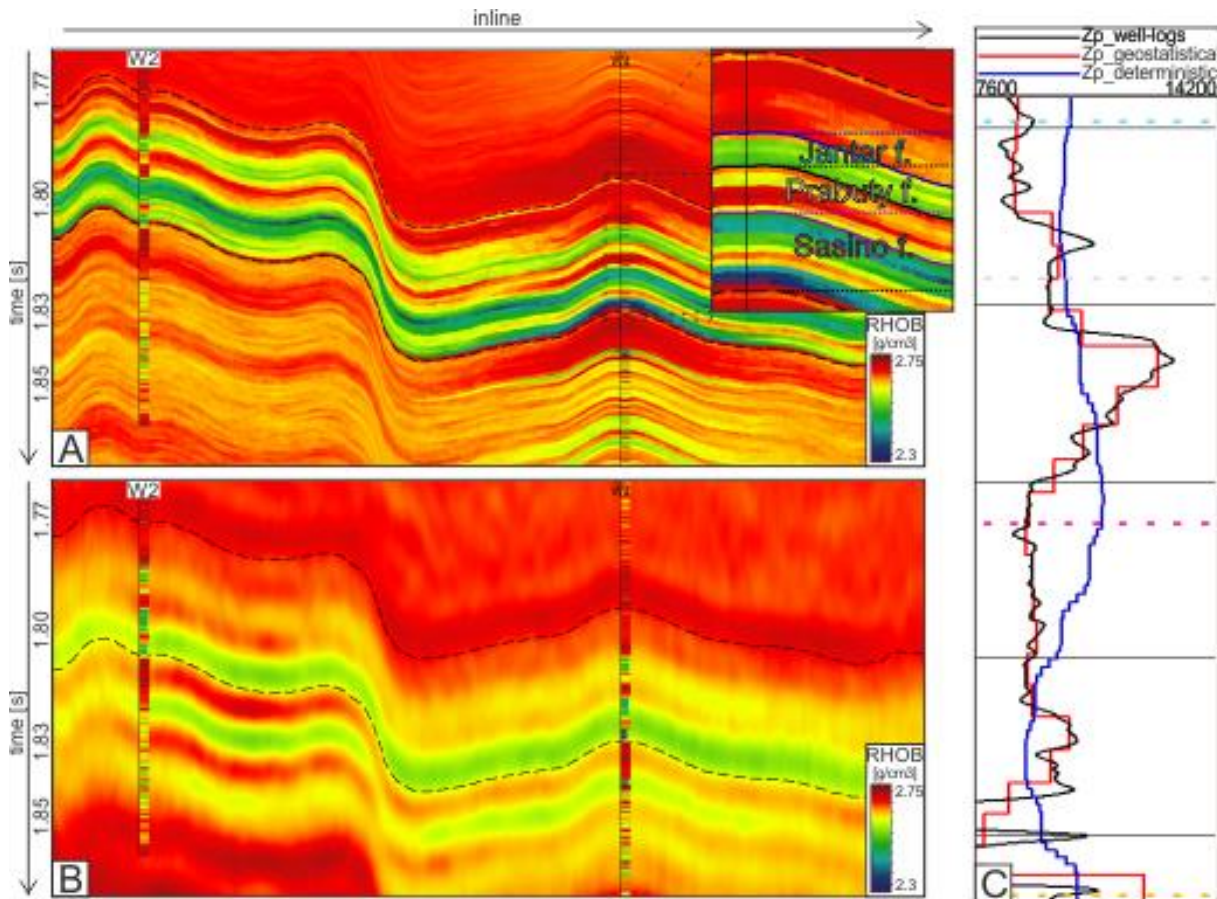


Fig. 1. Vertical well sections through density model resulting from (A) geostatistical and (B) deterministic inversion. The dashed, black horizons mark the area of the main interest. Solid lines at a zoomed section marks the top horizons of a key formations. Models are overlaid with the actual well-log properties. (C) P-wave impedance (Z_p) calculated from the results of the geostatistical inversion (red line) and deterministic inversion (blue line) versus actual well log Z_p (black line) (after Cyz et al. 2019).

Elastic properties obtained from the geostatistical inversion are compared with the results of the more standard, deterministic simultaneous Amplitude-versus-Offset (AVO) inversion.

The application of a geostatistical inversion was successful and allowed for obtaining the high resolution results and delineation of the thin target formations (Fig. 1A), what was not possible to reach with the deterministic inversion application (Fig. 1B). The geostatistical inversion also properly reproduce the well-log data while with the deterministic inversion only the general trend over a bigger interval is observed (Fig. 1C).

References

- Azevedo, L., R. Nunes, A. Soares, G.S. Neto, and T.S. Martins (2018), Geostatistical seismic amplitude-versus-angle inversion, *Geophys. Prospect.* **66**, S1, 116–131, DOI: 10.1111/1365-2478.12589.
- Cyz, M., L. Azevedo, and M. Malinowski (2019), Application of geostatistical seismic AVA inversion for shale reservoir characterization and brittleness prediction with machine learning. **In:** *Proc. 81st EAGE Conference and Exhibition 2019*, Vol. 2019, No. 1, pp. 1–5, European Association of Geoscientists and Engineers, DOI: 10.3997/2214-4609.201900691.

HANS GLACIER SEISMIC MONITORING USING A DEDICATED LOCAL NETWORK

W. Gajek

We have deployed a pilot 3-season long-term seismic network to monitor the dynamic activity of Hans glacier in Hornsund, Svalbard (Fig. 1). The network was continuously gathering seismic data from September 2017 to April 2018, hence from the late summer throughout whole winter until the spring season. It consisted of 11 recorders commonly used in controlled-source seismology (DATA CUBES) equipped with 4.5 Hz three-component geophones and powered by battery packages. The stations were placed either directly on ice (2 stations) or rocky base-ment in the close vicinity of Hans glacier terminus, with some of them only a couple hundreds of meters from it.

Recorded data is rich and complex – it consist of more than half a year multi-station records at arctic environment. Recorded wave field consists of events of different characteristics. We can observe short-lasting events present in a broad range of high frequencies (above 20 Hz), short-lasting spiky events, and monochromatic low-frequency events. A phenomenon of repeating events with same mechanisms displaying high correlation of the waveforms have been found. Some of the events are strong enough to be registered on all of the stations. Recorded events display expected seasonal distribution based on the observations from permanent seismological station HSPB only, but much more data is now available. Next step will be to work towards locating the registered events and to study the correlation between their location and character.

We established collaboration with geophysicists from glaciology group at ETH Zurich working in alpine glacier environment.

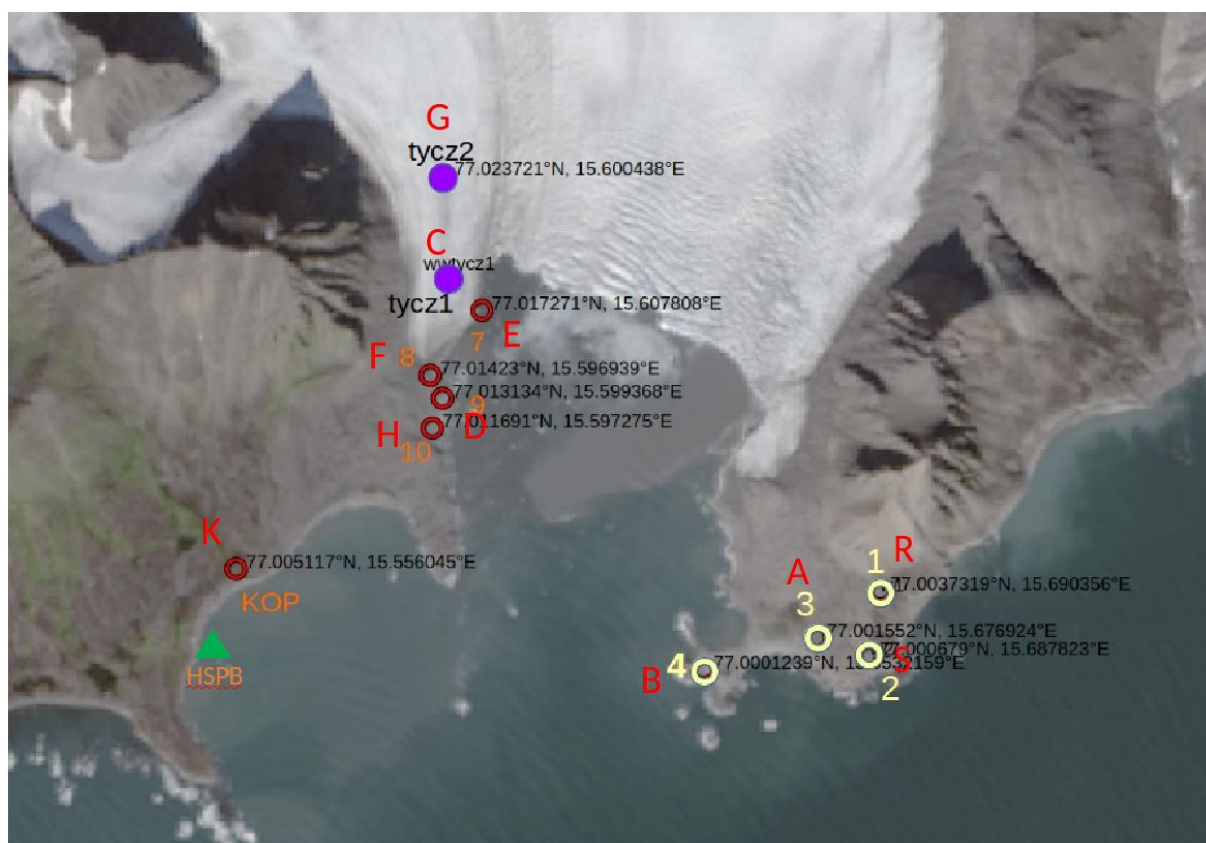


Fig. 1. Locations of 11 temporarily deployed seismic stations and a HSPB permanent seismological station in the Hornsund fjord, Svalbard.

THEORY OF THE DETECTION FUNCTION FOR MIGRATION-BASED METHODS FOR THE DETECTION OF MICROSEISMIC EVENTS AND OPTIMIZED DETECTION SCHEME

J. Trojanowski

A theoretical study was performed to describe a detection function which is used during the migration-based detection of microseismic events. A potential event is detected when a detection function exceeds some specified threshold value. However, the value of this threshold is usually selected manually; therefore, the detection process is subjective and lacks constraints on the probability of exceeding the threshold. In practice, any change in the detection algorithm results in a change in the distribution of the detection-function values. Consequently, the threshold value must be adjusted to have the same probability of exceedance as before. A general probabilistic theory of the detection-function was developed that is valid for any migration-based detection method. For the sake of transparency and the inter-changeability of the results, it is recommended to use the definition of a threshold in terms of the exceedance probability. To do so, it is necessary to define a probability distribution of the detection-function. There is also developed a general method for assessing the detectability of a given stacking method for the purpose of comparing different migration-based methods.

The optimization of the detection scheme was performed using real microseismic data provided by MicroSeismic Inc. The data were acquired by a surface array during one stage of hydraulic stimulation of shale rocks. Different ways of data conditioning were tested. It turned out that it was crucial for the performance of detection to reduce the influence of noisy traces on stacking process by, e.g., balancing or trace selection. Application of the two developed denoising methods further improves the detectability of microseismic events recorded with low signal-to-noise ratio. The number of detected microseismic events highly varied with changes to the processing sequence. The best achieved result was 210 (Fig. 1) detected events and the worst was 0. It shows that a careful and conscious choice of the processing steps is crucial to achieve a high detectability of microseismic events. It is particularly important for the surface microseismic monitoring which is often criticized for providing a low number of detected microseismic events comparing to the borehole monitoring.

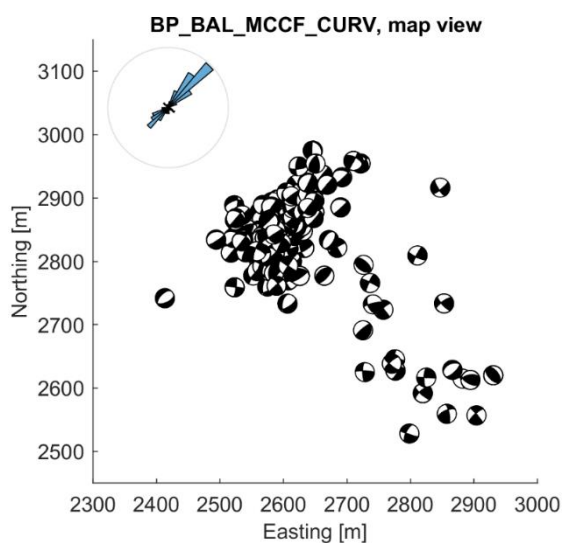


Fig. 1. Horizontal locations and source mechanisms for 210 detected microseismic events. Symbols representing a double-couple part of the source mechanism solution are plotted at locations of respective events. The inset in the top plot is a rose diagram plot of strike azimuths for all events and the solution with the highest dip angle (more vertical plane) (after Trojanowski 2019).

References

- Trojanowski, J. (2019), *Advanced Migration and Filtration Techniques for Microseismic Data*, PhD Thesis, Institute of Geophysics, Polish Academy of Sciences, Warsaw.

RECOGNITION OF THE VARYING PERMAFROST CONDITIONS IN THE SW SVALBARD BY MULTIPLE GEOPHYSICAL METHODS

A. Marciniak, B. Owoc, M. Majdański

In the presented work, we applied multiple geophysical methods and tools, to recognize horizontal and vertical distribution as well as ongoing changes in the seasonally and perennially frozen ground. The study site, located near the Polish Polar Station in the Hornsund (Svalbard), is unique due to its location between sea-shore and mountainous ridges and close presence of the retreating Hans Glacier. Such an environment allows for conducting research encompassing various dynamical cryospheric, geological and other environmental processes. The monitoring of the ground temperature variations in the several boreholes, with detailed ERT, GPR and MASW modeling, allow for recognition and analyses of the active layer spatial variability and the permafrost changes in this area. The seismic recognition, based on the dense 2D seismic reflection and refraction methods (Fig. 1), allows for the direct comparisons between observations conducted during the summer and winter seasons. Results obtained by those methods are directly targeted to visualize not only the active layer thickness but also the permafrost which until today is unknown in the area of Southern Spitsbergen. Additionally, the comparison of the data-set quality between two seasons allowed to select the best conditions for future data acquisition. The recognition of vertical and horizontal changes of the permafrost as well as the active layer depth provided unique information about the thermal ground conditions.

Obtained results, gives us the opportunity for explanation of seasonal changes which were observed, measured, and modeled. This information allows for better understanding of the geophysical processes responsible for the cryospheric and geological processes occurring in the study site, and further better estimation of the climate change impacts on the environment SW Spitsbergen.



Fig. 1. Active seismic team during the field works in Hornsund in April 2018; seismic line composed by DATA-CUBE stations (left), and seismic source PEG-40 mounted on sledges (right). Photos by A. Marciniak.

NEAR-SURFACE STRUCTURE OF THE CARPATHIAN FOREDEEP MARGINAL ZONE IN THE ROZTOCZE HILLS AREA

M. Majdański, B. Owoc

Shallow seismic survey was made along 1280 m profile in the marginal zone of the Carpathian Foredeep. Measurements performed with standalone wireless stations and especially designed accelerated weight drop system (Fig. 1) resulted in high fold (up to 60), long offset seismic data. The acquisition has been designed to gather both high-resolution reflection and wide angle



Fig. 1. Seismic source PEG-40 adapted to new carriage system, that can be operated without a car. This system can operate in rough terrain like steep hills and dense forest. Photo by M. Majdański.

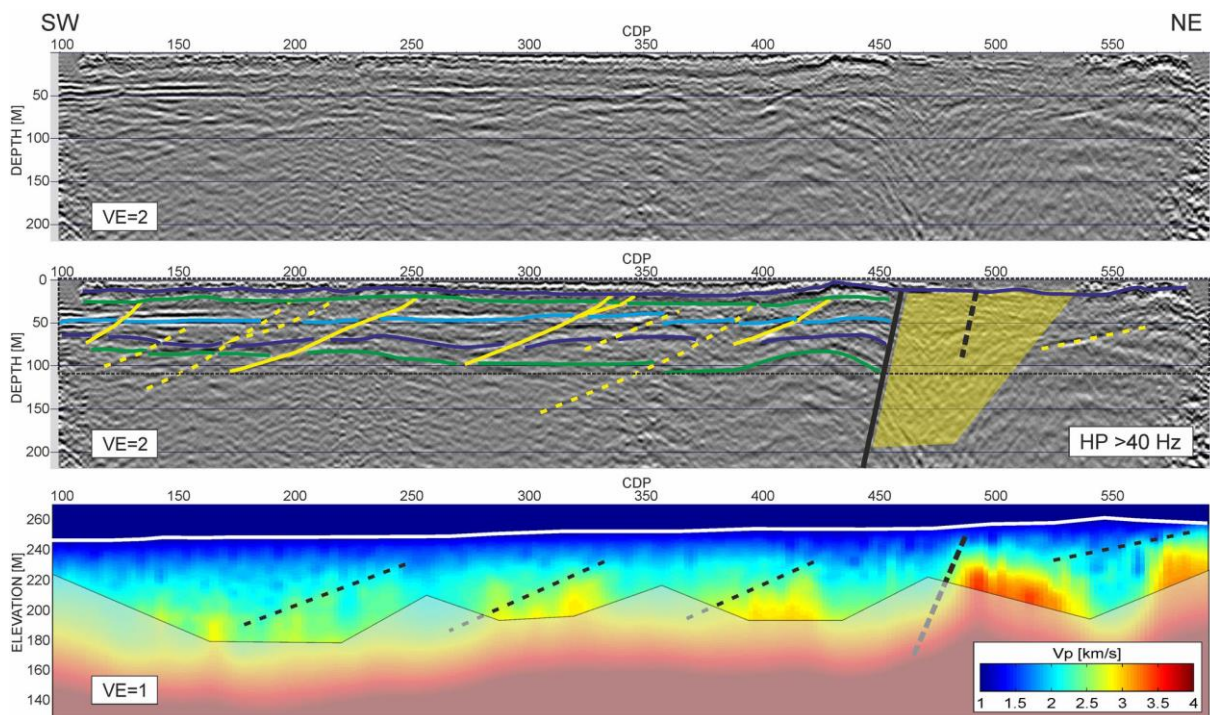


Fig. 2. Shallow structure in the depth domain obtained with shallow reflections enhanced processing (top). The bottom panel shows several discontinuities in the flat reflections (marked with colour solid lines) that do not reach the surface. Those marked with solid yellow lines are confirmed with tomography. Yellow polygon marks the area of the low reflectivity that differs from surrounding structures, and corresponds to a zone of the strong velocity gradient in tomography (after Owoc et al. 2019).

refraction data at long offsets. Seismic processing has been realised separately in two paths with focus on the shallow and deep structures. Data processing for the shallow part combines the travel time tomography and the wide angle reflection imaging. This difficult analysis shows that a careful manual front mute combined with correct statics leads to detailed recognition of structures between 30 and 200 m. For those depths, we recognised several SW dipping tectonic displacements and a main fault zone that probably is the main fault limiting the Roztocze Hills

area, and at the same time constitutes the border of the Carpathian Forebulge. The deep interpretation clearly shows a NE dipping evaporate layer at a depth of about 500–700 m. We also show limitations of our survey that leads to unclear recognition of the first 30 m, concluding with the need of joint interpretation with other geophysical methods.

Shallow seismic investigations yielded detailed images of the Carpathian Foredeep marginal zone (Fig. 2). A large offset survey combined with modified accelerated weight drop source was specially designed to allow both high resolution reflection image and refraction tomography. Four strokes of the source give enough energy to observe refractions at all offsets up to 350 m, but also to recognize a deep structure down to 700 m. Two processing paths were used to enhance both shallow and deep structures, resulting in detailed image of the near-surface faults, but also a sharp deep reflection. The 5-m spacing used for both shots and receivers was not dense enough to clearly recognize the first 30 m. Additional information like ERT experiment or different seismic processing, e.g., MASW, and finally joint interpretation might be used to further verify this part of the structure. Still, a clear image of a main fault in the area was presented. This weight drop seismic profile was performed to recognize near-surface structures, that is why it was surprising to observe clear reflection at 700 m. For surveys of this type with limited number of stations we suggest to use different spacing for shots and receivers. For example deploying stations with 8 m spacing and shooting with 2 m spacing will result in similar fold, but would limit number of deployments, limiting number of repeated shots. Thanks to dense shooting it would be possible to recover shallower structures, but wider deployments would give important long offset refracted arrivals. In the end acquisition time should be similar with higher resolution results. To make it optimal it would be beneficial to perform test shooting and recognize the maximum offset of clear observations, and design the survey for specific environment.

References

- Owoc, B., A. Marciniak, J. Dzierżek, S. Kowalczyk, and M. Majdański (2019), Seismic imaging of the Mesozoic bedrock relief and geological structure under quaternary sediment cover: The Bolmin Syncline (SW Holy Cross Mountains, Poland), *Geosciences* **9**, 10, 447, DOI: 10.3390/geosciences9100447.

GEO-ENGINEERING FIELDWORK SUMMER SCHOOL IN CHEŹCINY WITH IMAGING OF THE QUATERNARY FLUVIAL SYSTEM

M. Majdański, A. Marciniak, B. Owoc, M. Malinowski

In June 2018 a week-long fieldwork summer school has been organized in the cooperation with Department of Geology, University of Warsaw. The school covers both theoretical lectures about reflection imaging, tomographic methods and surface wave method (MASW), and practical computer classes presenting Globe Claritas, Geopsy and JIVE3D software. Moreover, during an outdoor training, several geophysical measurements have been collected along three profiles. The most important one called Mosty 1 covers a quaternary sediment basin. Along the 800 metres profile, high-resolution reflection profiling has been shot using enhanced PEG-40 accelerated weight drop and 60 DATA-CUBE 1C 4.5 Hz stations (Fig. 1). This measurement has been supported with georadar profile and precise geodetical measurements.

All obtained data will be interpreted together. In 2018 an initial reflection image (Fig. 2) has been prepared. Separately MASW analysis and a travel time tomography using JIVE3D and new Tomo3D codes has been conducted and will be finished in 2019.



Fig. 1. Outdoor training at the profile Mosty 1. Assembling of enhanced PEG-40 seismic source. Photo by M. Majdański.

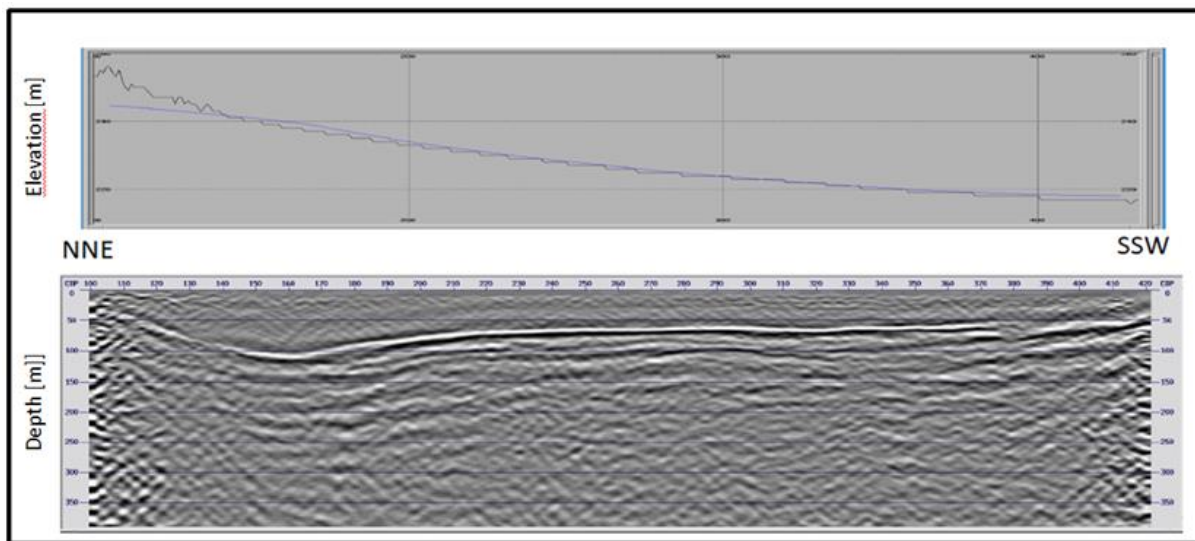


Fig. 2 Precise elevation along profile (top); Initial reflection imaging after the depth conversion (bottom).

DEEP NEURAL NETWORK AND MULTI-PATTERN BASED ALGORITHM FOR PICKING FIRST-ARRIVAL TRAVELTIMES

M. Mężyk, M. Malinowski

Static corrections are amongst the most important steps in processing land seismic data. First-order statics solution is conventionally obtained by application of refraction statics based on first-arrival traveltimes and the quality of such static solution is directly connected with the ability to pick reliable first-breaks. Picking can be difficult, especially with the low signal-to-noise Vibroseis data and very laborious (e.g. picking millions of seismic traces in large surveys). Modern seismic processing systems employ several methods of automatic first-break picking, based e.g. on STA/LTA method or artificial neural networks (ANN). There is however no universal method that will work on every dataset and still several passes of QC by an interpreter are required. In order to improve picking accuracy and reduce this QC time, we proposed an ANN-based approach whose core mechanism relies on pattern recognition techniques and

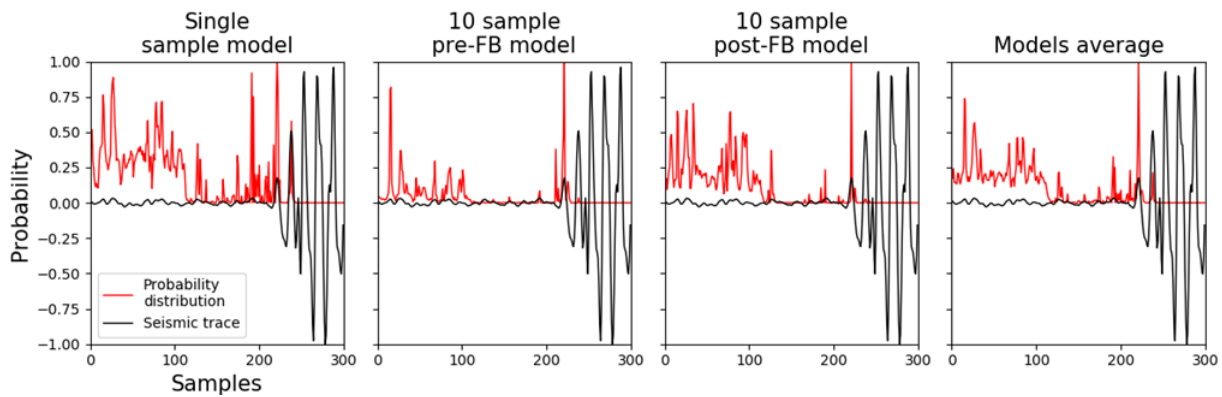


Fig. 1. Arbitrary seismic trace juxtaposed with the various model predictions (after Mężyk and Malinowski 2019).

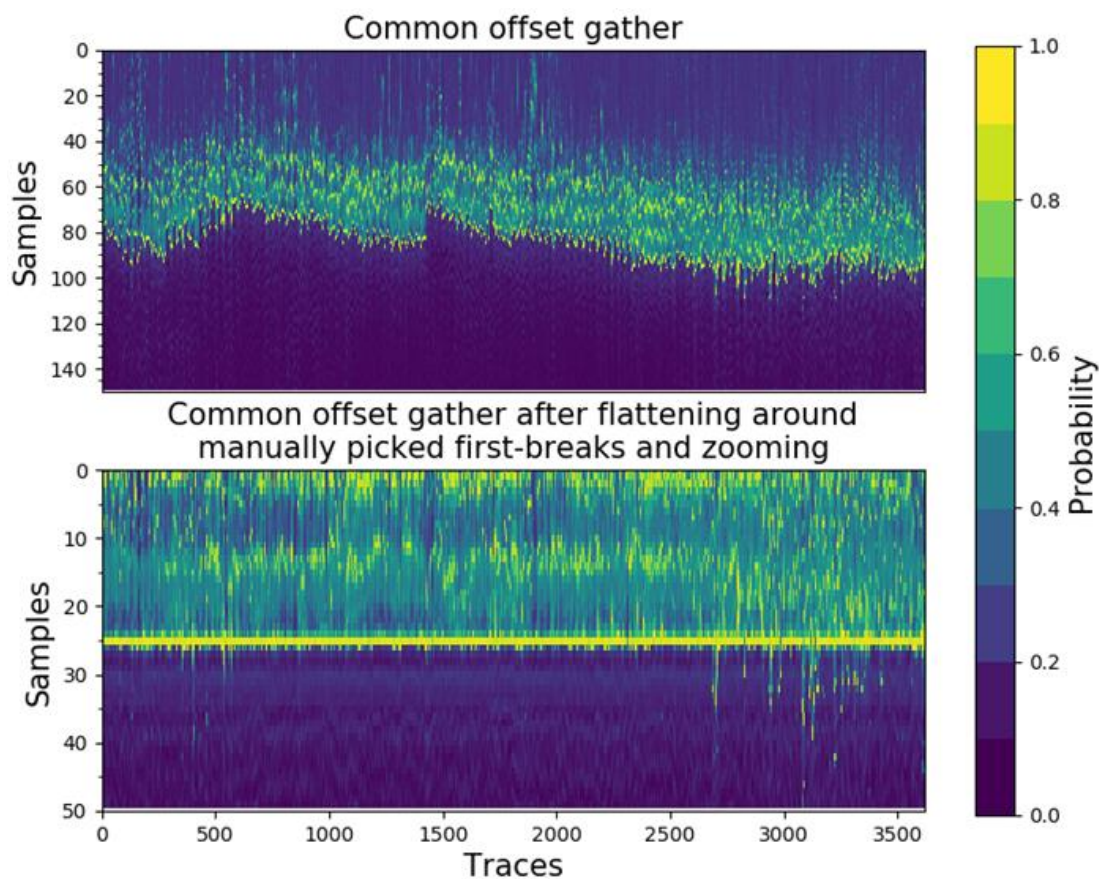


Fig. 2. Common offset gather after first-break prediction (top) and the same gather flattened around manually-picked first-break times (bottom) (after Mężyk and Malinowski 2019).

signal-based methods of generating these patterns. The first-break picking is treated here as a binary classification problem that requires a model to differentiate first-break sample from all others samples. In order to provide a sufficient training dataset a STA/LTA method, an entropy-based method, and a variogram fractal-dimension method have been used (Fig. 1). The approach appears robust and flexible in a way of adding new pattern generators that might contribute to even better performance.

In our study case, we exploited the high quality 2D Vibroseis data, that has already undergone the manual picking during the conventional seismic processing. These manually

derived picks were retrieved and properly conditioned to serve as learning patterns. The model building process involved not only collecting the data, but also finding and understanding the relations between the most important features in the data to answer the questioned we asked.

Pattern-recognition algorithms, after being properly set up once, turns out to be useful method that tremendously reduce the need for human interaction in tedious processing steps as picking first-break times and their QC. It appears robust and flexible in a way of adding new pattern generators that might contribute to even better performance. The core of the method is based on straightforward idea provide a training data, create a model and predict an answer by linking first-break representations across different domains to output single probability value of positive event at analyzed sample (Fig. 2). That means that the binary classification algorithm might be easily adapted to address different kind of problems, e.g., a noisy trace editing. Moreover, already trained models can be saved and reproduced for another dataset collected with similar acquisition parameters (e.g., in multi-line surveys) or on totally new seismic survey.

References

Mężyk, M., and M. Malinowski (2019), Multi-pattern algorithm for first-break picking employing open-source machine learning libraries, *J. Appl. Geophys.* **170**, 103848, DOI: 10.1016/j.jappgeo.2019.103848.

CHARACTERIZATION OF POTENTIAL LOWER PALEOZOIC SHALE RESOURCE PLAY IN POLAND

M. Malinowski, M. Cyz, W. Gajek, J. Trojanowski

The August 2018 issue of SEG “Interpretation” journal features a special section on the “Characterization of potential Lower Paleozoic shale resource play in Poland”, in which our group published 4 papers summarizing the results of the NCBR-funded SHALEMECH project. M. Malinowski served as the Assistant Editor of this special section.

The Lower Paleozoic shale play in Poland comprises Ordovician to Silurian shales that were deposited within a vast sedimentary basin located above the southwestern edge of the East European Craton, which was later tectonically divided into three sub-basins: the Baltic, the Podlasie, and the Lublin Basins. The recent shale gas exploration boom in Poland resulted in acquisition of a large amount of new, good-quality data, but did not lead to a commercial production. While the current oil price plays a role, the original assumptions that Polish shales would be similar to North American shales proved to be untrue, with Polish shales being both deeper (below 2500 m) and older (Ordovician and Silurian rather than Carboniferous and Cretaceous). For this reason, the goal of this special section is to capture our learnings and knowledge about the geological setting and reservoir properties of the Lower Paleozoic shales to better understand the key factors that can lead to not only the reopening of the exploration possibilities in this play, but to provide broader understanding of shale plays in general. The papers in this special section focus on the Baltic Basin in Northern Poland (nine papers), with only one case study covering the Lublin Basin.

Cyz and Malinowski (2018) present an application of Amplitude versus Azimuth analysis (AVAz) for quantifying weak anisotropy (1–2%) in the thin-layers case of the Lower Paleozoic shales from the Baltic Basin. Obtained results match well available calibration data, e.g. XRFMI image logs, cross-dipole sonic logs or microseismic shear-wave splitting inversion results.

Cyz et al. (2018) present a case study of brittleness prediction by integrating well and 3D seismic data using machine learning technique for the Lower Paleozoic shales in Baltic Basin.

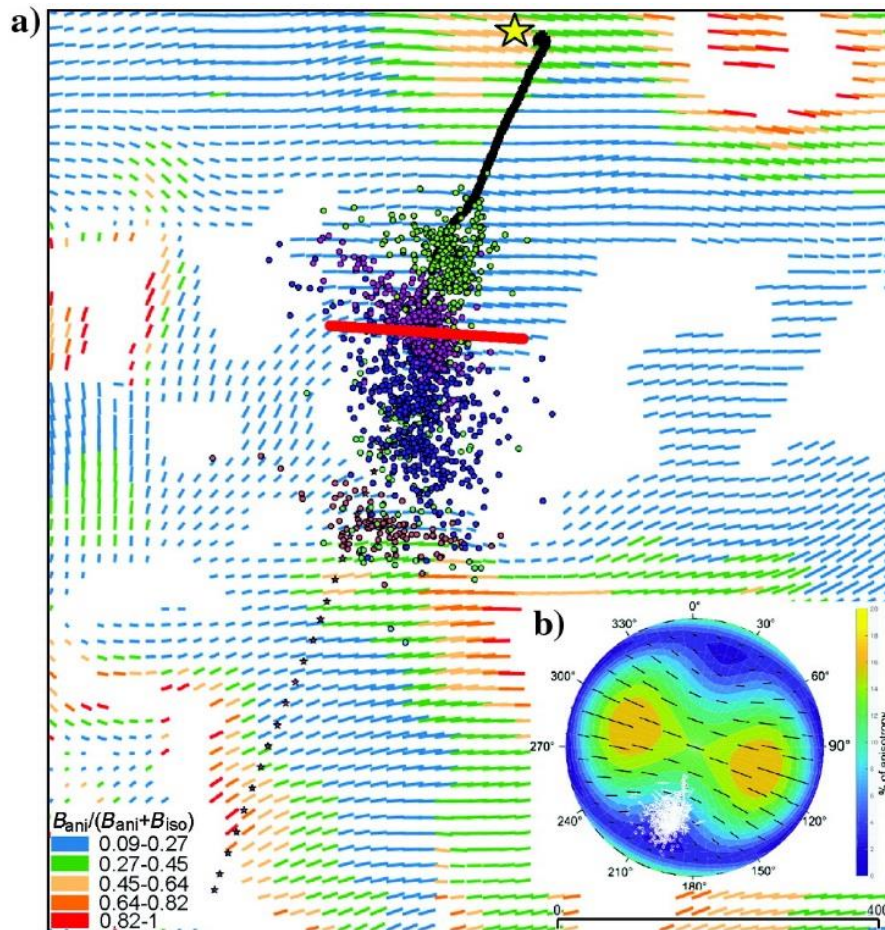


Fig. 1. (a) Map of the AVAZ-derived azimuthal anisotropy orientation and magnitude for the stimulated Sasino Formation close to the horizontal well overlaid with microseismic event locations (after Gajek et al. 2018a). The yellow star points out an observation well location. The red line marks the average anisotropy azimuth around the horizontal well (approximately 95°). (b) Fracture strike as determined from the SWS analysis (approximately 108°) (after Gajek et al. 2018b).

Prediction was successful and allowed for differentiation of ductile and brittle zones within thin shale formations with improved resolution while compared with original input seismic data. The important part of the success was the appropriate definition of the mineralogical brittleness index tailored to the local geological conditions.

Gajek et al. (2018a) present results from borehole microseismic monitoring of a pilot hydraulic stimulation job in Poland. This case study elaborates on challenging anisotropic velocity model building and evaluates the stimulation effectiveness in the geomechanical context.

Gajek et al. (2018b) utilize shear-wave splitting measurements derived from the borehole microseismic data to invert for anisotropic rock-physics model unrevealing strike and density of pre-existing fractures in the stimulated shale gas reservoir (Fig. 1).

RECONSTRUCTING UNIVERSAL STATISTICAL PROPERTIES OF EARTHQUAKES BY SIMPLE STOCHASTIC CELLULAR AUTOMATA

M. Bialecki, A. Bagchi

The subject of the research topic is investigation of constructions of a simple models in the form of a stochastic cellular automaton, that capture universal mechanisms for generating earthquakes and reconstruct fundamental empirical laws describing their statistical properties. Such

models are constructed in order to study these laws and a relationship between them. In particular we work on reconstruction of inter-event time between occurrence of successive earthquakes. It is known, after Alvaro Corral's discovery in 2004, that the probability of waiting time for the next earthquake can be described by one universal distribution, as long as the time is expressed in units corresponding to the average seismicity of the region. The existence of such a universal formula, which does not depend neither on local geological and tectonic conditions, nor on how much the area is seismically active, strongly indicates the universal nature of the mechanism for a generation of the distribution of waiting times for earthquakes.

Investigated models are extensions of studied for almost ten years Random Domino Automaton, describing the slow accumulation of energy and its abrupt releases, controlled by specific probabilistic rules. For the construction and analysis of Random Domino Automaton models we use advanced physical concepts and mathematical methods, including: stochastic processes, graph theory, analytical combinatorics, difference equations, Markov processes as well as elements of theory of complex systems and statistical physics.

A novel version of Random Domino Automaton was defined on Bethe Lattice and respective set of equations describing statistically stationary state in mean-field like approximation was derived. In particular, this model was able to produce truncated inverse power distributions (see Fig. 1). For these distributions, the range of independent variables, for which power law holds, is limited without introducing artificially any "ad hoc" value. These and other new findings extend our ability to model fundamental properties of earthquakes and other natural phenomena.

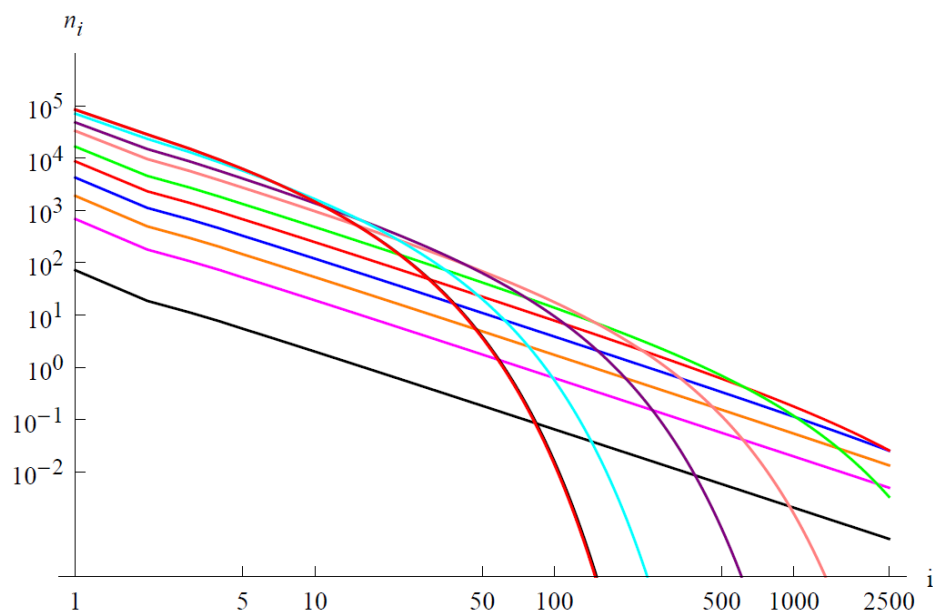


Fig. 1. Distribution of avalanches calculated from equations of Random Domino Automaton on Bethe Lattice (with coordination number 3) for various parameters ranging from exponential limit (curved red line), through piece-wise inverse power distributions with exponential tail, up to inverse power distribution – the limit related to Self-Organized Criticality.

8.6 Seminars and teaching

Seminars and lecture outside of the IG PAS:

- A. Bagchi, Various undergrad courses, Santipur College, Kalyani University, Santipur, India, Lecture;
- M. Malinowski, Geophysical methods in mineral exploration, International Center for Geological Education, Chęciny, Poland, Invited lecture;

- M. Malinowski, Introduction to seismic processing/imaging, International Center for Geological Education, Chęciny, Poland, Invited lecture;
- M. Majdański, Seismika szerokokątowa we współczesnej geofizyce, International Center for Geological Education, Chęciny, Poland, Invited lecture.

8.7 Completed PhD thesis defense

- A. Adamczyk, Application of full-waveform inversion to land datasets: how much does the acquisition matter?, Supervisor: M. Malinowski.

8.8 Visiting scientists

Satish Singh, IPGP, Paris, France (1 day),

Ian Jones, ION Geophysical, London, UK (1 day),

Olaf Hellwig, TU Freiberg, Freiberg, Germany (1 week).

8.9 Meetings, workshops, conferences, and symposia

Presentations of the Department's members:

CHAOS2018 Conference, Rome, Italy, 5–8 June 2018

- A. Bagchi, Solvable probabilistic cellular automaton on Bethe lattice with smooth transition between inverse-power and exponential distributions of avalanches, Oral.

32nd IUGG Conference on Mathematical Geophysics, Nizhny Novgorod, Russia, 23–28 June 2018

- M. Białecki, A universal solvable model of slow accumulation of energy and its abrupt releases with smooth transitions from exponential to inverse-power distributions, Oral.

Symmetries and Integrability of Difference Equations SIDE 13, Fukuoka, Japan, 11–17 November 2018

- M. Białecki, Random Domino Automaton on Bethe lattice, Poster.

International Symposium on Deep Earth Exploration and practices DEEP-2018, Beijing, China, 24–26 October 2018

- M. Malinowski, Imaging East European Craton margin in Northern Poland using extended-correlation processing applied to regional seismic profiles, Oral;
- M. Malinowski, Application of full-waveform inversion to crustal-scale velocity model building in complex subduction zone setting: Eastern Nankai Trough, Japan, Oral.

EGU General Assembly, Vienna, Austria, 8–13 April 2018

- M. Mężyk, Imaging East European Craton margin in Northern Poland using extended-correlation processing applied to regional seismic profiles, Poster;
- B. Owoc, The uncertainty in seismic traveltime tomography, Poster;
- M. Majdański, Seismic image of the Carpathian Foredeep Marginal Zone, Poster;
- A. Marciniak, Seismic tomography and MASW analysis of the results of Spitsbergen seismic experiment – case study, Poster;
- A. Górszczyk, Feasibility of crustal-scale imaging from 3D OBS data by Full Waveform Inversion. Phase I: building a 3D synthetic model of a subduction zone and wavefield modelling, Oral;

- M. Chamarczuk, Towards adapting seismic interferometry to retrieve body-wave reflections for mineral exploration: the passive seismic experiment in the Kylylahti Cu-Au-Zn mine area, Finland, Oral.

18th International Symposium on Deep Seismic Profiling of the Continents and their Margins (SEISMIX 2018), Kraków, Poland, 17–22 June 2018

- M. Mężyk, Imaging East European Craton margin in Northern Poland using extended-correlation processing applied to regional seismic profiles, Poster;
- B. Owoc, Estimation of the uncertainty in seismic tomography, Poster;
- M. Majdański, Near-surface structure of the Carpathian Foredeep marginal zone in the Roztocze Hills area, Poster;
- A. Górszczyk, Synthetic study on the crustal-scale imaging via FWI of the 3D OBS data building a realistic benchmark model of a subduction zone, Oral;
- M. Chamarczuk, Using large N arrays in mineral exploration: the passive seismic experiment in the Kylylahti Cu-Au-Zn mine area, Finland, Oral;
- M. Cyz, Characterization of the lower paleozoic shales in Northern Poland from the analysis of wide azimuth seismic data, Poster.

LXXXVI Zjazd Naukowy Polskiego Towarzystwa Geologicznego, Łuków, Poland, 5–7 September 2018

- M. Mężyk, Imaging East European Craton margin in Northern Poland using extended-correlation processing applied to regional seismic profiles, Poster.

80th EAGE Conference & Exhibition, Copenhagen, Denmark, 11–14 June 2018

- M. Mężyk, Deep neural network and multi-pattern based algorithm for picking first-arrival traveltimes, Oral.

13th SEGJ International Symposium, Tokyo, Japan, 12–14 November 2018

A. Górszczyk, Crustal-scale depth imaging via joint FWI of OBS data and PSDM of MCS data – the eastern Nankai Trough seen in high resolution, Oral (invited).

Near Surface Geoscience Conference & Exhibition 2018, Porto, Portugal, 9–12 September 2018

- B. Owoc, The discussion of the uncertainty in the traveltimes seismic tomography, Poster;
- A. Marciniak, Uncertainty based multi-step seismic analysis for the near surface imaging, Poster.

EAGE 2nd Conference on Geophysics for Mineral Exploration and Mining, Porto, Portugal, 9–12 September 2018

- M. Chamarczuk, Seismic interferometry for mineral exploration: passive seismic experiment over Kylylahti mine area, Oral.

Workshop: Worldwide Mineral Exploration Challenges and Cost-Effective Geophysical Methods, Porto, Portugal, 9 September 2018

- M. Chamarczuk, Seismic interferometry reflection imaging for mineral exploration using ambient noise recorded with large-N geophone array, Oral.

XXXVII Sympozjum Polarne „Polar Change - Global Change”, Poznań, Poland, 7–10 June 2018

- A. Marciniak, Seismic tomography and MASW analysis of the results of Spitsbergen seismic permafrost study, Oral;
- W. Gajek, Latest results of seismic monitoring of Hans glacier, Svalbard, Oral.

7th EAGE Workshop on Passive Seismic, Kraków, Poland, 26–29 March 2018

- W. Gajek, Downhole microseismic monitoring at a pilot hydraulic fracturing site in Poland, Poster.

ESC General Assembly, Valetta, Malta, 2–7 September 2018

- W. Gajek, Feasibility of 3-season long glacier monitoring by temporal seismic networks at Hans glacier, Svalbard, Oral;
- A. Górszczyk, Facing the 3D crustal-scale imaging via full-waveform inversion of the ocean-bottom seismometer data, Oral.

8.10 Publications

ARTICLES

- Bagchi, A.** (2018), Notion of Random Domino Automaton revisited, *J. Phys.: Conf. Ser.* **965**, 012007, DOI: 10.1088/1742-6596/965/1/012007.
- Cyz, M., M. Malinowski**, et al. (2018), Brittleness prediction for the Lower Paleozoic shales in northern Poland, *Interpretation* **6**, 3, SH13–SH23, DOI: 10.1190/INT-2017-0203.1.
- Cyz, M.**, and **M. Malinowski** (2018), Seismic azimuthal anisotropy study of the Lower Paleozoic shale play in northern Poland, *Interpretation* **6**, 3, SH1–SH12, DOI: 10.1190/INT-2017-0200.1.
- Gajek, W., J. Trojanowski, M. Malinowski**, et al. (2018a), Results of downhole microseismic monitoring at a pilot hydraulic fracturing site in Poland — Part 1: Event location and stimulation performance, *Interpretation* **6**, 3, SH39–SH48, DOI: 10.1190/INT-2017-0205.1.
- Gajek, W., M. Malinowski**, and J.P. Verdon (2018b), Results of downhole microseismic monitoring at a pilot hydraulic fracturing site in Poland — Part 2: S-wave splitting analysis, *Interpretation* **6**, 3, SH49–SH58, DOI: 10.1190/INT-2017-0207.1.
- Majdański, M., J. Grzyb, B. Owoc**, et al. (2018), Near-surface structure of the Carpathian Foredeep marginal zone in the Roztocze Hills area, *Acta Geophys.* **66**, 179–189, DOI: 10.1007/s11600-018-0131-4.
- Krzywiec, P., et al., **M. Malinowski** (2018), Deeply concealed half-graben at the SW margin of the East European Craton (SE Poland) — Evidence for Neoproterozoic rifting prior to the break-up of Rodinia, *J. Palaeogr.* **7**, 1, 88–97, DOI: 10.1016/j.jop.2017.11.003.
- Mazur, S., **M. Malinowski, M. Lewandowski**, et al. (2018), On the nature of the Teisseyre-Tornquist Zone, *Geol. Geophys. Environ.* **44**, 1, 17–30, DOI: 10.7494/geol.2018.44.1.17.
- Riedel, M., et al., **M. Malinowski** (2018), Underground vertical seismic profiling with conventional and fiber-optic systems for exploration in the Kylylahti polymetallic mine, eastern Finland, *Minerals* **8**, 11, 538, DOI: 10.3390/min8110538.

Trojanowski, J. (2018), Theory of the detection function for migration-based methods for the detection of microseismic events, *Geophysics* **83**, 6, A87–A91, DOI: 10.1190/geo2018-0237.1.

CHAPTERS

Konon, A., et al., **M. Malinowski** (2018), Późnosylursko-wczesnodewońskie deformacje tektoniczne na przedpolu pomorskiego odcinka orogenu kaledońskiego. **In:** *LXXXVI Zjazd Naukowy Polskiego Towarzystwa Geologicznego, Łuków, 2–5 września 2018 r. Na Krawędzi Platformy*, 10-15.

EXTENDED ABSTRACTS

Chamarczuk, M., M. Malinowski, et al., and the COGITO-MIN Working Group (2018), Seismic interferometry for mineral exploration: passive seismic experiment over Kylylahti mine area, Finland. **In:** *Proc. EAGE 2nd Conference on Geophysics for Mineral Exploration and Mining, 9–12 September 2018, Porto, Portugal*, 5 pp., DOI: 10.3997/2214-4609.201802703.

Väkevä, S., et al., **M. Chamarczuk**, and **M. Malinowski** (2018), 3C seismic interferometry at the polymetallic Kylylahti deposit, Outokumpu district, Finland. **In:** *Lithosphere 2018 Tenth Symposium on Structure, Composition and Evolution of the Lithosphere, 14–16 November 2018, Oulu, Finland*, 125–126.

Väkevä, S., **M. Chamarczuk**, **M. Malinowski**, et al., and the COGITO-MIN Working Group (2018), Passive seismic three-component interferometry experiment at the Kylylahti mine site, Eastern Finland. **In:** *Proc. EAGE 2nd Conference on Geophysics for Mineral Exploration and Mining, 9–12 September 2018, Porto, Portugal*, 5 pp., DOI: 10.3997/2214-4609.201802715.

Gajek, W., J. Trojanowski, and **M. Malinowski** (2018), Downhole microseismic monitoring at a pilot hydraulic fracturing site in Poland. **In:** *Proc. 7th EAGE Workshop on Passive Seismic, Kraków, Poland, 26–29 March 2018*, 6 pp., DOI: 10.3997/2214-4609.201800059.

Górszczyk, A., et al. (2018), Crustal-scale depth imaging via joint FWI of the OBS data and PSDM of MCS data – the eastern Nankai Trough seen in high resolution. **In:** *Proc. 13th SEGJ International Symposium, 12–14 November 2018, Tokyo, Japan*, 70–73, DOI: 10.1190/SEGJ2018-019.1.

Heinonen, S., **M. Malinowski**, et al. (2018), COGITO-MIN seismic reflection profiling for mineral exploration in Polvijärvi, Finland. **In:** *Lithosphere 2018 Tenth Symposium on Structure, Composition and Evolution of the Lithosphere, 14–16 November 2018, Oulu, Finland*, 17–20.

Heinonen, S., **M. Malinowski**, et al., and The COGITO-MIN Working Group (2018), Seismic exploration in the Kylylahti Cu-Au-Zn mining area: comparison of time and depth imaging approaches. **In:** *Proc. EAGE 2nd Conference on Geophysics for Mineral Exploration and Mining, 9–12 September 2018, Porto, Portugal*, 5 pp., DOI: 10.3997/2214-4609.201802713.

Koivisto, E., **M. Malinowski**, **M. Chamarczuk**, et al., and the COGITO-MIN Working Group (2018), From regional seismics to high-resolution resource delineation: Example from the Outokumpu ore district, Eastern Finland. **In:** *Proc. EAGE 2nd Conference on Geophysics for Mineral Exploration and Mining, 9–12 September 2018, Porto, Portugal*, 5 pp., DOI: 10.3997/2214-4609.201802716.

- Koivisto, E., **M. Malinowski**, **M. Chamarczuk**, et al., and the COGITO-MIN Working Group (2018), Testing of seismic mineral exploration methods at different scales at the Kylylahti polymetallic mine site, Eastern Finland. **In:** *Lithosphere 2018 Tenth Symposium on Structure, Composition and Evolution of the Lithosphere, 14–16 November 2018, Oulu, Finland*, 49–52.
- Riedel, M., et al., **M. Malinowski** (2018), Distributed Acoustic Sensing versus conventional VSP imaging of the Kylylahti polymetallic deposit. **In:** *Proc. EAGE 2nd Conference on Geophysics for Mineral Exploration and Mining, 9–12 September 2018, Porto, Portugal*, 5 pp., DOI: 10.3997/2214-4609.201802744.
- Marciniak, A.**, et al., and **M. Majdański** (2018), Uncertainty based multi-step seismic analysis for the near surface imaging. **In:** *24th European Meeting of Environmental and Engineering Geophysics, 9–12 September 2018, Porto, Portugal*, 1 pp., DOI: 10.3997/2214-4609.201802562.
- Mężyk, M.**, and **M. Malinowski** (2018), Deep neural network and multi-pattern based algorithm for picking first-arrival traveltimes. **In:** *Proc. 80th EAGE Conference and Exhibition, 11–14 June 2018, Copenhagen, Denmark*, 5 pp., DOI: 10.3997/2214-4609.201801109.
- Owoc, B.**, **A. Górszczyk**, and **M. Majdański** (2018), The discussion of the uncertainty in the travelttime seismic tomography. **In:** *Proc. 24th European Meeting of Environmental and Engineering Geophysics, 9–12 September 2018, Porto, Portugal*, 5 pp., DOI: 10.3997/2214-4609.201802559.

9. DEPARTMENT OF POLAR AND MARINE RESEARCH

Marek Lewandowski

9.1 About the Department

I. Variability of snow cover parameters in polar and mountainous areas

Dust in the snowpack and firn

Aeolian dust in glaciers of Spitsbergen: an environmental messenger and a player in global change processes. Multilateral (geochemistry, mineralogy, remote sensing) approach to identification of dust components deposited in glaciers of Spitsbergen, with applications to glaciostratigraphy, glaciotectonics, and back trajectory analysis of atmospheric circulation.

Snow cover in Sudety Mountains

A preliminary study of the snow cover accumulation patterns and its impact on vegetation (and vice versa) in the chosen areas of the Karkonoski National Park. The first step was done in September 2018: terrestrial laser scanning.

Modelling of snow water equivalent in the coastal tundra of Hornsund fiord

Methodology for estimation of snow water equivalent in Hornsund coastal zone using daily snow depth observations was developed. Set of regression models was optimized and calibrated for consecutive stages of snowpack accumulation and ablation. The proposed approach for estimation of snow water equivalent gave very promising results, with the coefficient of determination higher than 0.9 for both calibration and validation therefore it's assumed that method could be extended to other Arctic sites where snow water equivalent measurements are rare.

II. Glaciated catchment components modelling

Calving ice front investigated with LiDAR scanning

Using LiDAR and video data from 2013, from Greenwich Island, South Shetland Island, it was possible to determine how does reflectivity of an ice wall changes with time elapsed since calving event. Discovered brightening of the surface was interpreted as development of layer of weathered ice. A scientific article was published with the results.

Study of mass balance of a Chilean glacier with use of digital elevation models

Four digital models of surface relief (ASTER, SRTM, TanDEM-X DEM and an aerial laser scanning based one) were used to measure change of Universidad glacier in central Chile. In addition, performance of TanDEM-X DEM in glaciological work was assessed.

III. Hydrological and hydrochemical characteristics of glaciated and unglaciated catchments (AN, TW)

Diagnosis of the hydrology of a small Arctic permafrost catchment using HBV conceptual rainfall-runoff model

The relationships between temporal changes of active layer depth and hydrological HBV model parameters, together with variation in the catchment response. The influence of model simplification, correction of precipitation, and initial conditions on the modelling results was tested.

Aluminum export from Werenskiöldbreen, Svalbard, shows association with glacier-derived nutrients (SiO₂, Fe)

The study aims to determine the relationship between the processes sourcing labile Al and glacier-derived labile nutrients (particularly Fe and Si) in glacierised basins.

Weather breakdown influence removal of invertebrates from cryoconite holes on an Arctic valley glacier (Longyearbreen, Svalbard)

The main goal of this research was to investigate any links between changes in weather conditions and short temporal changes in invertebrate densities on glaciers.

Spatial variations in air temperature and humidity over Hornsund fjord Spitsbergen)

This study deals with variations in air temperature and humidity in the region of the Hornsund fjord for the period from 1 July 2014 to 30 June 2015. Based on measurements at 11 sites, it was established that significant topoclimatic differences were dependent on height above sea level, substrate type, distance from the sea, exposition, atmospheric circulation and the ice conditions. The thermal and humidity conditions of individual sites are presented in relation to the weather conditions at the Polish Polar Station in Hornsund.

Factors controlling tidewater glacier front fluctuations in Svalbard-Hansbreen as an example

This research investigated seasonal and interannual fluctuations of the Hansbreen terminus in 23 years period. The data is mainly obtained from digitization of remote satellite imagery from a variety of sources. Then attempt to link the derived terminus fluctuations to various potential drivers (atmospheric and oceanographic) through correlation investigations. PDD+ and SST are used as proxies for surface melt (= subglacial discharge) and for fjord water temperature, respectively.

Climate changes related to SST trends in the North Atlantic, and long-term analysis of meteorological conditions in two fjords – Porsanger and Hornsund

Changes in the multiyear SAT (the air temperature 2 m above the ground), SST (sea surface temperature) and WS (wind speed) were studied on the basis of monthly Era-Interim reanalyses, as well as analyses of local differences between the two high-latitude fjords, based on data from three meteorological stations: Lakselv (L), Honningsvåg (Ho), and Hornsund (Hr).

IV. Geophysical methods in marine environment studies in polar and analogue areas

- The development of methods for analyzing data from multibeam sonar and sediment profiler to determine the differences in the morphology of the bottom sediments and identification of bodies of young periglacial,
- The use of passive acoustic monitoring of marine for determining the processes occurring in the icy Arctic fjords.

V. Attempt to prediction of environmental change after Barents sea-Greenland sea ice-barrier breakup

We have studied changes of the coastal area in southern Svalbard with the glacier bridge between Torell Land and Sørkapp Land since the beginning of the 20th century. The results confirm the existence of a continuous subglacial depression below sea level (c. 40 m deep) between Hornsund and the Barents Sea. If the retreat continues at the 2000–2015 average rate, the ice bridge between Hornsund and Hambergbukta will be broken sometime between 2055 and 2065 and the Hornsund strait will separate Sørkapp Land from the Spitsbergen Island. The work was completed and published in journal of the JCR list.

9.2 Personnel

Head of the Department

Marek Lewandowski
Professor

Professor

Piotr Głowacki

Adjunct

Bartłomiej Luks
Mateusz Moskalik
Adam Nawrot
Tomasz Wawrzyniak

Project Coordinator

Agata Goździk
Wojciech Piotrowski

Educator

Dagmara Bożek-Andryszczak
Jerzy Giżejowski
Julian Podgórski

Methodological adviser

Piotr Stankiewicz

PhD Students

Daniel Kępski, Poland; Bartłomiej Luks – supporting PhD supervisor
Joanna Cwiąkała, Poland; Mateusz Moskalik – supporting PhD supervisor
Joanna Szilo, Poland; Robert Bialik – PhD supervisor
Kacper Wojtysiak, Poland; Robert Bialik – PhD supervisor
Julian Podgórski, Poland; Piotr Głowacki, Michał Pętliski – PhD supervisors

9.3 Main research projects

- EDUARCTIC, Goździk A., H2020, 2016–2019;
- ERIS, Goździk A., Erasmus+, 2016–2018;
- ODYSSEY, Goździk A., Erasmus+, 2018–2021;
- BRITEC, Goździk A., Erasmus+, 2018–2021;
- INTERACT, Piotrowski W., H2020, 2017–2019;
- SIOS (Svalbard Integrated Arctic Earth Observing System), Głowacki P., MNiSW, 2018–2023;
- EU Polarnet, Głowacki P., H2020, 2015–2020;
- INTAROS, Głowacki P., H2020, 2016–2021;
- Snow Observation in Svalbard – SOS, Luks B., SIOS/SIOS pilot project, 2018–2018;
- Hindcasting and projections of hydro-climatic conditions of Southern Spitsbergen, Wawrzyniak T., National Science Centre, 2018–2021;
- Spatial distributions of black carbon and mineral dust in air and snow surface layers upon Svalbard glaciers: BC-3D, Nawrot A., Research Council of Norway SSF Svalbard Strategic Grant, 2018–2020;
- The impact of the sea ice conditions in the nearshore zone and shore ice on the wave propagation and coastal morphodynamics in polar regions on the example of south-western Spitsbergen – the analysis of processes, modeling, and prediction, Moskalik M., National Science Centre, 2014–2018;

- Small-scale dynamics of Arctic coastal sediments: Isbjornhamna, Svalbard, Wojtysiak K., Research Council of Norway, Svalbard Science Forum (SSF), Arctic Field Grant (AFG), 2018–2018;
- Measuring the melt rate of glacier ice with underwater noise, Głowacki O., Internal research project, 2017–2019;
- Measuring the melt rate of glacier ice with underwater noise, Głowacki O., National Science Foundation (NSF) Early-concept Grants for Exploratory Research (EAGER), 2018–2020;
- Relationship of permafrost with geomorphology, geology and cryospheric components based on geophysical research of the Hans glacier forefield and its surroundings. Hornsund, Spitsbergen, Wawrzyniak T., National Science Centre, 2017–2020.

9.4 Instruments and facilities

Equipment

- Rain gauges, Hanna multiparametric measurer, Water level, electrolytic conductivity and temperature automatic sensors; Autosampler; 2 Meteorological automatic stations Vaisala; Snow-bars; Harbortronics cameras; differential GPS; Valeport miniCTD; Niskin bootle; Sediment trapps; Muffle furnace; Transducer magnetometer GEOMAG i LEMI; Proton magnetometers; DI-fluxgate magnetometer; Induction magnetometer; Ionosonde; GPS signal scintillation monitor GSV4004; Seismometer STS-2; Logger MK-6; Atmospheric electricity sensors; 2 RBR wave sensors; Side Scan Sonar Wesmar 700; Orectech 3010 sediment profiler; CODA DA 100; 4 hydrophons with 2 Tascam registrator, RDI ADCP Sientiel 20;
- Air sampling station AZA-1000; Total radiation measurer and UV measurer: CMP11, CMP21, UV S-E-T;
- Insolation measurer CSD3; 4-component net radiometer CNR4; Cimel photometer; Ceilometer CHM-15k; Sky camera Fuji-Campbell, dGPS station (referencial); Terrestrial Laser Scanner, DJI Phantom 4 Pro drones (3pcs), DJI Mavic Air drone .

Laboratory

The Hornsund Polish Polar Station (Spitsbergen) is year-round laboratory for research in the following fields:

Meteorology. Data for forecasting and climatological purposes is collected at the Station. The Hornsund weather station works as part of the Norwegian station network and is registered by the WMO (World Meteorological Organisation) as number 01003. Basic meteorological parameters are measured and observed here systematically, 24 hours a day, pursuant WMO standards.

Seismology. The seismology station in Hornsund belongs to the international network of seismological observatories. It is the only station constituting part of the Polish seismological network but located outside Polish territory. The main purpose of the seismology lab in Hornsund is to continuously record local earth tremors caused by plate tectonics and glaciers.

Earth magnetism. Changes in elements of the Earth's natural magnetic field are continuously recorded at the Station. Due to its geographic location, the Hornsund observatory records some of the greatest changes in the Earth's magnetic field. They are approximately five times greater than those observed in Poland, for instance, so the results of this research are significant for scientists the world over. Since 2002, the Hornsund magnetic observatory has been part of the INTERMAGNET global research network.

Ionospheric research. The Station carries out long-term research on the structure of the ionosphere. This is aimed at determining the impact of particles and plasma originating from Solar flares on our planet.

Glaciology. The nearby Hans Glacier forms the object of glaciological research in the Hornsund region. Measurements are taken here to determine the mass balance and glacier change dynamics and, in addition, the depth of the snow cover is observed. This data is sent to the World Glacier Monitoring Service.

Atmospheric physics and optics. Observations of atmospheric phenomena include changes in the Earth's electric field, UV radiation and aerosol. This data is sent to the international AERONET network and to NASA.

Environmental research. The Station's chemical laboratory analyses the chemical composition of surface and precipitation waters. The purpose of this is to determine the biogeochemical processes occurring in them, as well as the quantities of pollutants reaching this region and depositing here, also of anthropogenic origin.

Apart from the research conducted as part of the Station's year-round research plan, in the spring and summer various groups of scientists pursuing their own scientific projects, conduct research—including in the fields of biology, geology, geodesy, geomorphology, glaciology and oceanology—in the Hornsund region. They then use the logistical and scientific facilities of the Station. The Polish Polar Station in Hornsund also participates in numerous scientific projects, both Polish and international.

Unique Polar Laboratory PolarPOL

PolarPOL was appointed by the Minister of Science and Higher Education on February 26, 2011. It functions as a National Research Center in the framework of the Polish Road Map of Research Infrastructures and, at the same time, as a separate infrastructural unit of the Institute of Geophysics PAS.

The aim of the Laboratory is to develop technical facilities, as well as to expand the organizational possibilities of conducting multilateral scientific research in the Arctic. The laboratory strengthens Polish participation in the global network of research and monitoring of land and sea polar zones. It also consolidates the current scientific potential of Polish polar explorers. PolarPOL secures Poland's participation in international polar research, which is of fundamental importance to Poland's position in the sphere of foreign policy of the state. The task of PolarPOL is to use the results of basic research for application needs, among others in the field of submarine resources of raw materials, the use of marine biological resources and new shipping opportunities that are opening up, as well as tourist activities.

9.5 Research activity and results

Brief description/abstracts/summaries of some of the achievements of the Department's staff:

VARIABILITY OF SNOW COVER PARAMETERS IN POLAR AND MOUNTAINOUS AREAS

M. Lewandowski, A. Nawrot, B. Luks

Dust in glaciers: project objectives, methodology and first results (accepted as a keynote presentation at IASC workshop)

Our knowledge on ice caps and ice sheets history, structure and physiochemical record increased significantly during the last decades due to research on ice cores, particularly in the framework of EPICA (European Project for Ice Coring in Antarctica) and GRIP (Greenland Ice Core Project) projects. However, paucity still exists about nature of solid phases impurities in

snow, firn and ice. Ice caps and glaciers of Svalbard were frequently analyzed in terms of water-soluble ion chemistry record, but natural and artificial, micrometer-sized solid mineral (and amorphous) phases of aeolian origin, as well as organic particles transported by wind from distant sources, were not studied extensively so far. These particulates may be of different origin, potentially carrying important information about an impact of distant events and processes on the High Arctic environment.

The goal of this proposal is to describe an inventory of mineral (and amorphous) phases and biotic components of both natural and anthropogenic origin, residing in four glaciers of Spitsbergen. The pattern of impurities assemblages, recently deposited in snow and firn, will be traced stratigraphically, aiming at identification and correlation of coeval horizons. In general, the proposal is focused on potential usefulness of identified material for stratigraphic and environmental interpretations. Taking into account interdisciplinary research scope of this proposal, it is a first at such scale ever undertaken on Svalbard. Analysis of biogenic particulates, with the focus on cryoconite and glacial micro-fauna will also be performed in search of viable organisms of the glacial environment.

Research methodology

Selected glaciers will be cored to depths of 2–3 m (shallow) and 9–10 m (deep), yielding 16 cores of total length about 50 m, providing 200 samples of c. 1.5 kG each. Each sample will be weighed, melted and filtrated using membranes with 0.45 μm pore size. Dried residuum will be packed and distributed among cooperating laboratories, in order to identify mineral or amorphous phases and biogenic components. Analytical methods cover a wide spectrum of geochemical analyses, employing scanning microscopes (ASEM), mass spectrometry including of Nd, Hf, Sr, X-ray diffractometry and tomography, and noble gas spectrometry. Results of geochemical isotope analyses on volcanic ash particles of Nd, Hf, and $^{87}\text{Sr}/^{86}\text{Sr}$, along with the K-Ar ages, will point to dust source area. Analyses of REE are also planned. Magnetic phases will be identified using a unique Micromag AGFM 2900-02 Alternating Gradient Force Magnetometer for measurements of magnetic hysteresis of very fine samples (up to 50 μg) in room temperature.

Expected impact on the development of science

- a) Dust distribution over the area under study for a last 8–10 years (for longer cores) and 2–4 years (for shorter cores) years, as well as quantitative concentration (ng/g) of water-insoluble light-absorbing particulates in the snow cover and firn will contribute to better understanding of recent albedo variation;
- b) Identified assemblages of particles will be traced horizontally (for the first time on Spitsbergen), attempting to establish horizons of reference, to trace differences in a pace of the glacier seasonal firn increments, validating existing models and giving a way to infer on internal glaciers dynamics, if compared to results similar studies in future;
- c) Relative concentration of dusts from season to season may be considered a proxy in the source area environment (humid/warm vs. arid/cold);
- d) A role of the black carbon particles, whatever origin, as a climate forcing agent over Svalbard will be estimated based on their concentration;
- e) Concentration of anthropogenic phases will be estimated as well;
- f) Back trajectory analysis of atmospheric circulation as well as isotope geochemistry methods will point to the dust components source area.

Results obtained in 2018

First results of chemical analyses are promising for this project. Detrital residuals were obtained from five cores of c. 1 m long, acquired from different glaciers, Residuals show a wide spec-

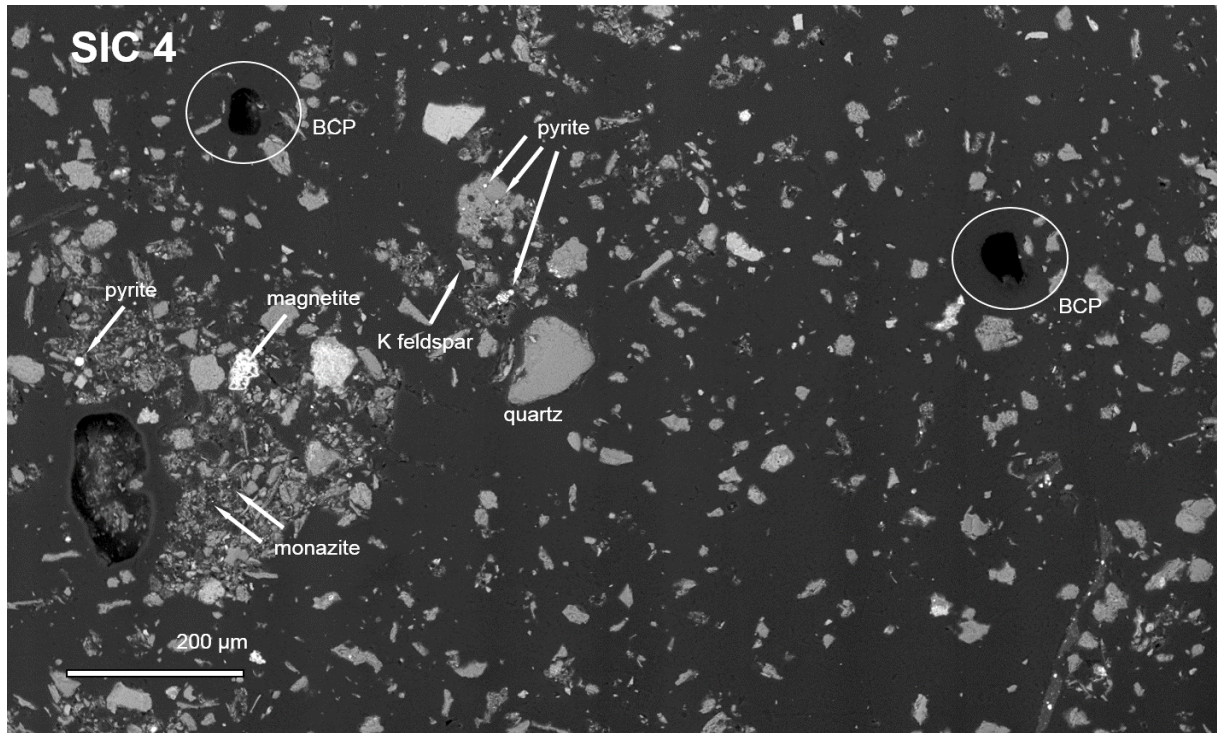


Fig. 1. Secondary electron image of uncoated dust sample SIC 4 from Storbreen. SEM; BCPs are shown circled. Courtesy Dr. Monika Kusiak (after Lewandowski et al. 2020).

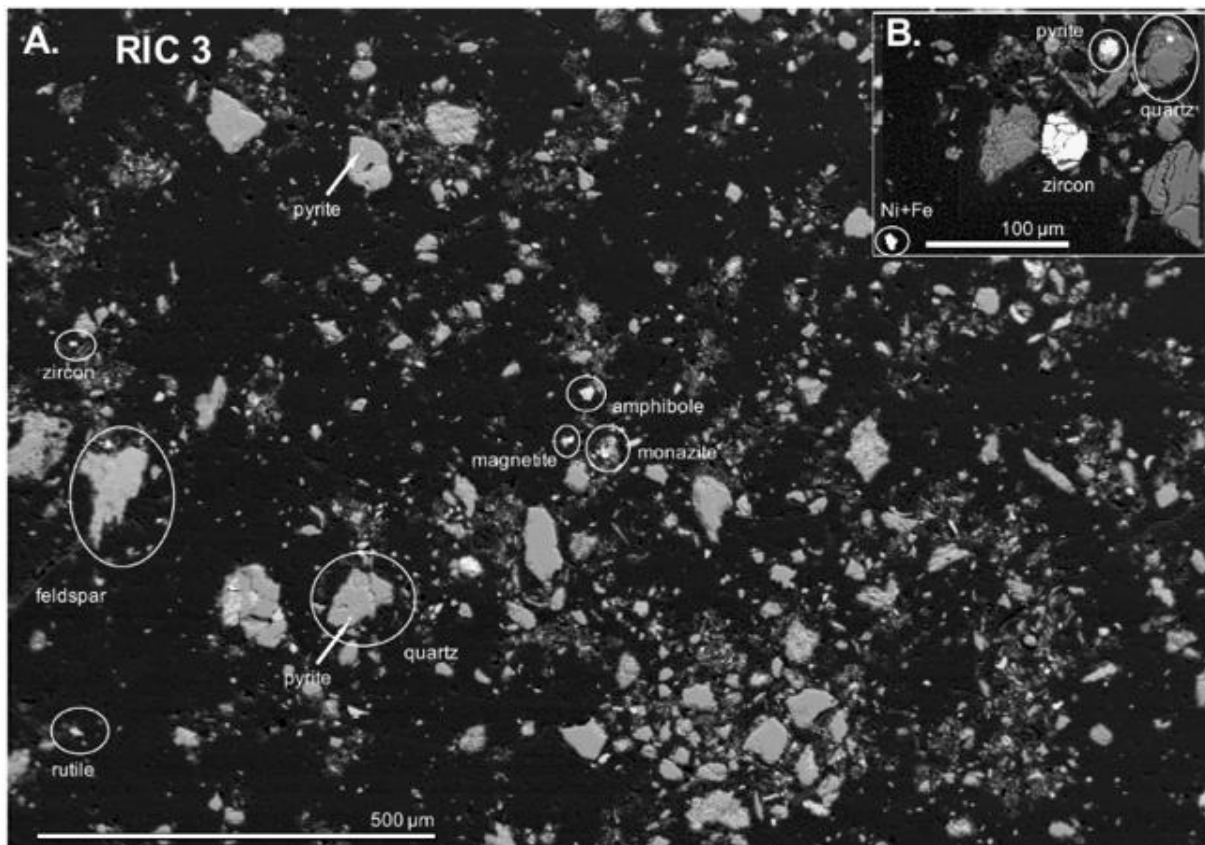


Fig. 2. Back scattered electron (BSE) image of the dust sample from Recherchebreen. Micrometeorite (?) and a zircon grain are seen in the sector B. Courtesy Dr. Monika Kusiak (after Lewandowski et al. 2020).

trum of mineral phases with a strong potential to the environmental interpretation (Figs. 1 and 2). Within a frame of a pilot study, two samples were selected to recognize mineral phases of the dust present in different glaciers. Quartz and K feldspar are predominating the mineral inventory of each sample (ca. 70% of the dust material). Phases of zircon, monazite and rutile are present in both of them. Sample SIC4 (Fig. 1) is characterized by the presence of BCP. These particles will be of the great importance to recognize historic record of anthropogenic activities in the area. Sample RIC3 (Fig. 2) from the Recherchebreen glacier contains significant amount of Fe oxide, pyrite and most probably micrometeorite.

References

Lewandowski, M., M.A. Kusiak, T. Werner, A. Nawrot, B. Barzycka, M. Laska, and B. Luks (2020), Seeking the sources of dust: geochemical and magnetic studies on “Cryodust” in glacial cores from Southern Spitsbergen (Svalbard, Norway), *Atmosphere* **11**, 12, 1325, DOI: 10.3390/atmos11121325.

GLACIATED CATCHMENT COMPONENTS MODELLING

J. Podgórski, P. Głowacki

The work in the task involves processing of digital observational data – sourced from field measurements with laser scanner, satellite imagery and global digital elevation models. Computer programming in Matlab and Python languages allows to draw meaningful results and conclusions from large volumes of data. The objective of the task is to investigate dynamics of components of glaciated catchments, particularly changes of glacial cover. This is to give new insight into processes occurring in these environments.

The work is conducted in cooperation with two foreign institutions: Centro de Estudios Científicos, Valdivia, Chile, and Université du Québec à Trois-Rivières, Trois-Rivières, Canada. Michał Pełlicki and Christophe Kinnard, from the two places respectively, are strongly involved in scientific work on the task.

In the year 2018 one scientific article was published in a peer-reviewed journal listed on the A list of the Ministry of Science and Higher Education of Poland: Cold Regions Science and Technology (Impact factor: 1.92) (Podgórski et al. 2018). The paper describes an empirical model linking changes in reflectivity of a front of a tidewater glacier with time elapsed since a calving event happened. The work based on field data obtained by Michał Pełlicki on Greenwich Island, South Shetland Islands, Antarctica in 2013. The reflectivity has been measured with use of a terrestrial laser scanner, while calving events were registered with use of a video camera. These observational data were processed with help of Matlab programming language to arrive at an exponential form of the relationship (Fig. 1).

Brightening of glacial ice with time since a calving event revealed it to the elements was found, an unexpected result. It was proposed, that formation of a layer of weathered ice on the ice cliff surface is responsible for the phenomenon. Description of the process of ice cliff weathering in quantitative terms is a scientific innovation brought by the paper.

Most of the work during the year was dedicated to investigation of geodetic mass balance of Universidad glacier, located in central Chile. TanDEM-X DEM digital elevation model, obtained from the German Space Agency in 2017 in a call for proposals, was the centerpoint of these efforts. This project had two objectives: one was to determine mass balance of the glacier in question in the 21st century, while the other was to ascertain how useful the new TanDEM-X DEM is for glaciological work. Three other elevation models were used in the study: SRTM and ASTER DEM are global datasets showing surface relief in 2000 and 2003, respectively. In

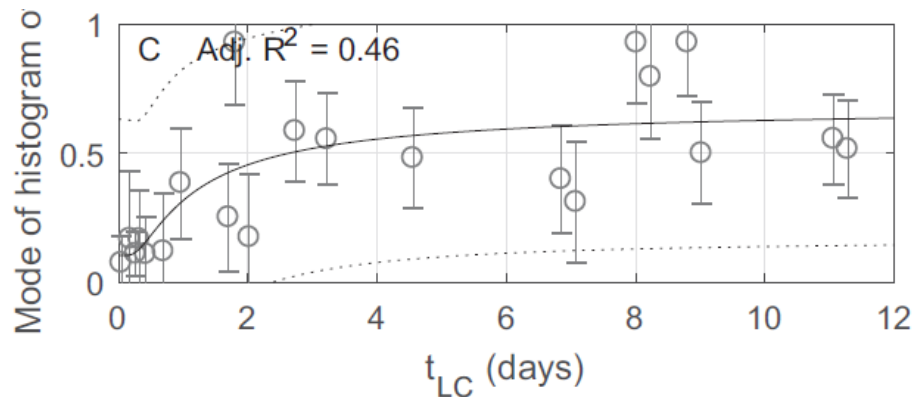


Fig. 1. Exponential function fitted to the dataset of mode of reflection intensity histogram (vertical axis) and time since the last calving event (t_{LC} , horizontal axis). Increase of the values indicates brightening of the ice surface (after Podgórski et al. 2018).

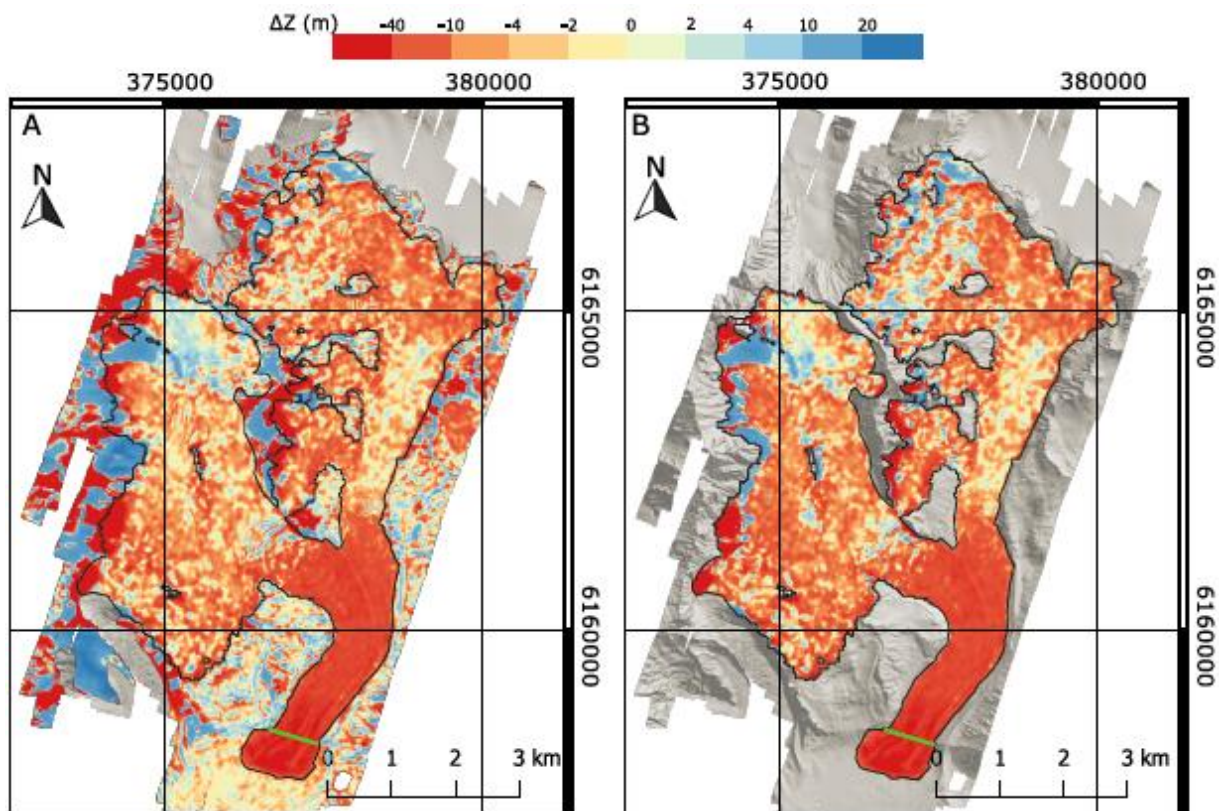


Fig. 2. Maps of difference of surface elevation between 2000 (SRTM DEM) and 2013 (ALS DEM on Panel A and TanDEM-X DEM on Panel B). Red colour indicates strong lowering of surface and thus ice loss. Blue colour indicates thickening – result of ice accumulation or vertical movement of ice (after Podgórski et al. 2019).

addition an aerial laser scanning (ALS) based elevation model served as ground reference and accurate representation of surface elevation in 2013. The four models were compared to each another and measures of TanDEM-X DEM quality and Universidad glacier change were computed.

Both goals have been achieved. TanDEM-X DEM was shown as a high-quality dataset, well suited for glaciological change detection study. Its accuracy relative to the ALS-based DEM is 0.02 ± 3.48 m in the study area, a score better, than that of the older ASTER and SRTM.

Discontinuities and noise was found in TanDEM-X DEM on steep slopes surrounding the glacier, but these had little to no impact on the mass balance results.

Universidad glacier has been shown to lose mass in nearly all its parts, with exception of limited accumulation in the highest parts of its accumulation zone. Particularly strong ablation was noted in the tongue of the glacier, where bands of debris are thick enough to hinder ablation and led to formation of troughs and ridges (Fig. 2). Overall the glacier has been losing 0.44+/-0.08 m of water equivalent per year between 2000 and 2013.

A manuscript of a scientific article summarizing the results of this part of the task was written and prepared for publication. It was accepted for publication in *Remote Sensing*, a peer-reviewed journal (Impact Factor 3.4). Revised version of the manuscript has been submitted close to the end of the year and the final decision on publication is pending now.

References

- Podgórski, J., M. Pęćlicki, and C. Kinnard (2018), Revealing recent calving activity of a tide-water glacier with terrestrial LiDAR reflection intensity, *Cold Reg. Sci. Technol.* **151**, 288–301, DOI: 10.1016/j.coldregions.2018.03.003.
- Podgórski, J., C. Kinnard, M. Pęćlicki, and R. Urrutia (2019), Performance assessment of TanDEM-X DEM for mountain glacier elevation change detection, *Remote Sens.* **11**, 2, 187, DOI: 10.3390/rs11020187.

HYDROLOGICAL AND HYDROCHEMICAL CHARACTERISTICS OF GLACIATED AND UNGLACIATED CATCHMENTS

M. Osuch, T. Wawrzyniak, A. Nawrot (published in: Diagnosis of the hydrology of a small Arctic permafrost catchment using HBV conceptual rainfall-runoff model, *Hydrol. Res.* (2019), **50**, 2, 459–478, DOI: 10.2166/nh.2019.031)

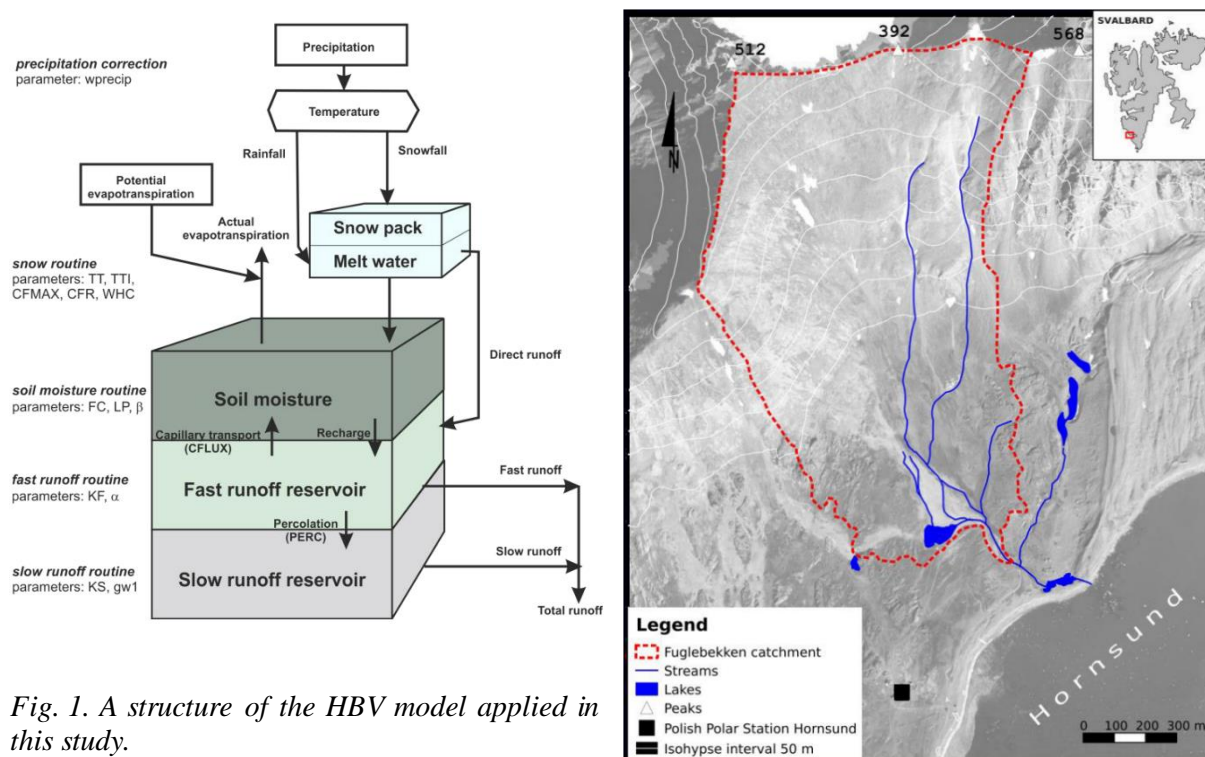


Fig. 1. A structure of the HBV model applied in this study.

General warming is observed across Svalbard Archipelago and corresponds to increases in ground temperatures. Changes in active layer thickness over Arctic and permafrost regions have an important impact on rainfall-runoff transformation. General warming is observed across Svalbard Archipelago and corresponds to increases in ground temperatures. Permafrost thaw and changes in active layer thickness due to climate warming alter how water is routed and stored in catchments, and thus impact both surface and subsurface processes. The overall aim of the present study is to examine the relationships between temporal changes of active layer depth and hydrological model parameters, together with variation in the catchment response. The analysis was carried out for the small unglaciated catchment Fuglebekken, located in the vicinity of the Polish Polar Station Hornsund on Spitsbergen. For hydrological modelling, the conceptual rainfall-runoff HBV model was used (Fig. 1). The model was calibrated and validated on runoff within subperiods. A moving window approach (3 weeks long) was applied to derive temporal variation of parameters. Model calibration, together with an estimation of parametric uncertainty, was carried out using the Shuffled Complex Evolution Metropolis algorithm. This allowed the dependence of HBV model parameters on active layer thickness to be analysed. Also, we tested the influence of model simplification, correction of precipitation, and initial conditions on the modelling results.

HYDROLOGICAL AND HYDROCHEMICAL CHARACTERISTICS OF GLACIATED AND UNGLACIATED CATCHMENTS

A. Arażny, R. Przybylak, P. Wyszynski, **T. Wawrzyniak**, **A. Nawrot**, T. Budzik (published in: Spatial variations in air temperature and humidity over Hornsund fjord (Spitsbergen) from 1 July 2014 to 30 June 2015, *Geogr. Ann. A* (2018), **100**, 1, 27–43, DOI: 10.1080/04353676.2017.1368832)

Based on measurements at 11 sites in the region of the Hornsund fjord (Fig. 1), it was established that significant topoclimatic differences were dependent on height above sea level, substrate type, distance from the sea, exposition, atmospheric circulation and the ice conditions.

The thermal and humidity conditions of individual sites are presented in relation to the weather conditions at the Polish Polar Station in Hornsund (HOR). In the study period, the warmest annual mean air temperature occurred at Hyttevika (HYT), and the coldest on the summit of Fugleberget (FUG), respectively, +1.1 degrees C and –3.7 degrees C relative to HOR. Meanwhile, relative humidity differs from HOR values most strongly on Fugleberget, where it is greater by an average of 14%. Atmospheric circulation and ice cover were shown to

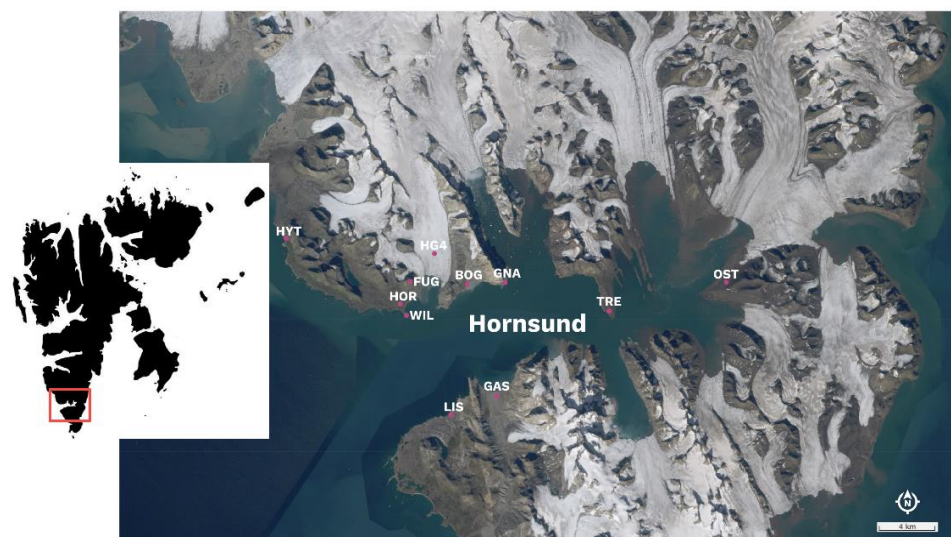


Fig. 1. Spatial distribution of meteorological stations across Hornsundfjord (base layer source: topo-svalbard.npolar.no).

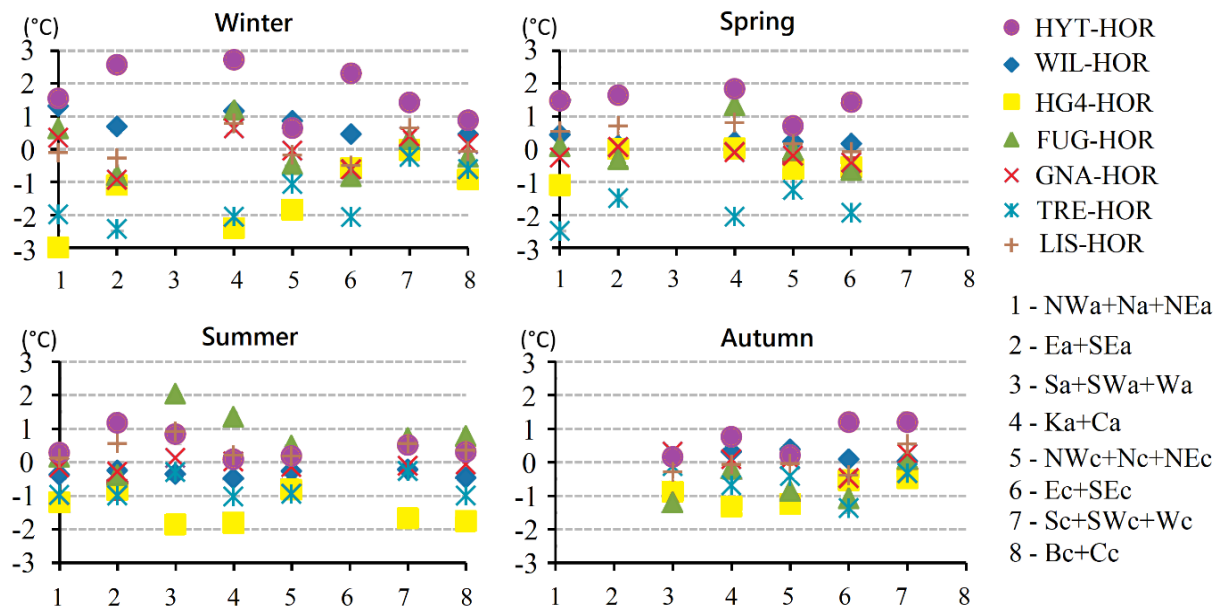


Fig. 2. Variation of air temperature at multiple locations in comparison with meteorological site at the Hornsund station for different atmospheric circulation types (modified after Arażny et al. 2018).

have a significant impact on thermal and humidity conditions. The greatest spatial variations in air temperature (3.0 degrees C) in Hornsund region (between HOR and FUG) occurred in winter during anticyclonic advection from the northern sector. The greatest difference in relative air humidity (20%) relative to HOR occurred in FUG in autumn during cyclonic advection from the eastern sector. The east-west thermal and humidity gradients along the fjord are more pronounced when sea ice is present. Differences in air temperature and relative humidity between the sites located in the inner (TRE) and outer parts of the fjord (HG4 and HYT) rose by about 2.0–2.5 degrees C and 7–9%, respectively (Fig. 2).

SUBMARINE GEOMORPHOLOGY AT THE FRONT OF THE RETREATING TIDEWATER GLACIERS (HANSBREEN, RECHERCHEBREEN)

J. Ćwiakała, M. Moskalik, M. Forwick, K. Wojtysiak, J. Gizejewski, W. Szczuciński (published in: Submarine geomorphology at the front of the retreating Hansbreen tidewater glacier, Hornsund fjord, southwest Spitsbergen, *J. Maps* (2018), **14**, 2, 123–124, DOI: 10.1080/17445647.2018.1441757)

A 1:10 000 scale bathymetric map as well as 1:20 000 scale backscattering and geomorphological maps of two bays Isbjørnhamna and Hansbukta in the Hornsund fjord (Spitsbergen) present the submarine relief that was primarily formed during and after the retreat of the Hansbreen tidewater glacier. Geomorphological mapping was performed using multibeam bathymetric data and seismoacoustic profiling. The identified landforms include two types of transverse ridges interpreted as terminal and annual moraines, flat areas that are depressions filled with glaciomarine sediments, iceberg-generated pits and ploughmarks, pockmarks and fields of megaripples. Most of the identified landforms are genetically related to the retreat of Hansbreen since the termination of the Little Ice Age at the beginning of the twentieth century. Although Hansbreen has been speculated to be a surge-type glacier, no evidence of surging was identified in the submarine landform assemblage, which is in accordance with the absence of historically documented surges for that period (Fig. 1).

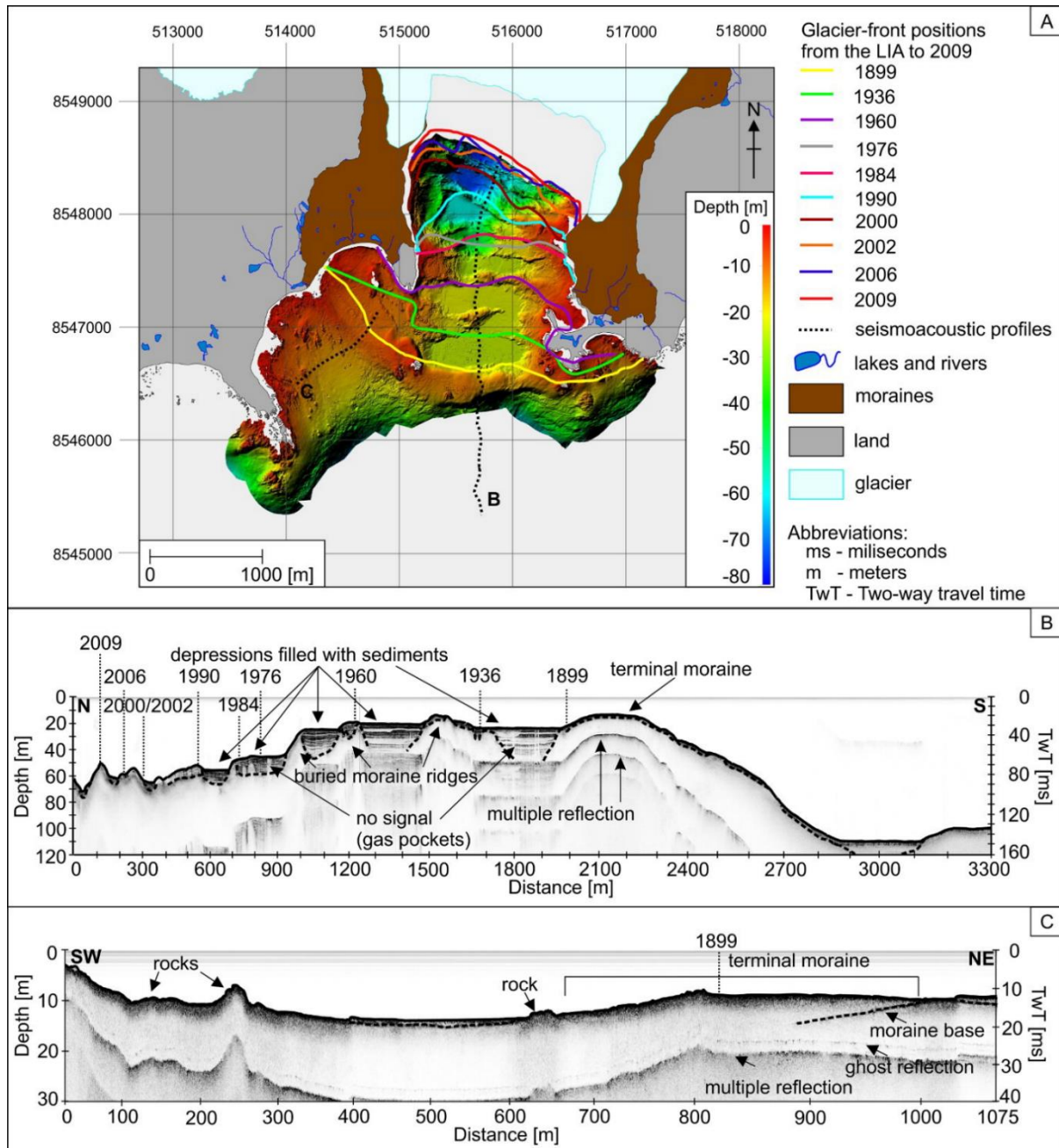


Fig. 1: (A) Bathymetric map of Isbjørnhamna and Hansbukta with marked glacier-front positions for selected years and the locations of the seismoacoustic profiles; (B) Seismoacoustic profile with interpretation in Hansbukta; (C) Seismoacoustic profile with interpretation in Isbjørnhamna. The numbers (years) provided in (B, C) refer to glacier-front positions. The distance scales on (B, C) differ.

SUBMARINE GEOMORPHOLOGY AT THE FRONT OF THE RETREATING TIDEWATER GLACIERS (HANSBREEN, RECHERCHEBREEN)

M. Moskali, P. Zagórski, L. Łęczyński, **J. Cwiakała**, P. Demczuk (published in: Morphological characterization of Recherchefjorden (Bellsund, Svalbard) using marine geomorphometry, *Pol. Polar Res.* (2018), **39**, 1, 99–125, DOI: 10.24425/118740)

Geomorphological research based on geomorphological mapping seeks to identify the origins and age of forms as well as to describe the process that created or transformed a particular form. One of the most important aspects of this study is the morphometry and morphology of the

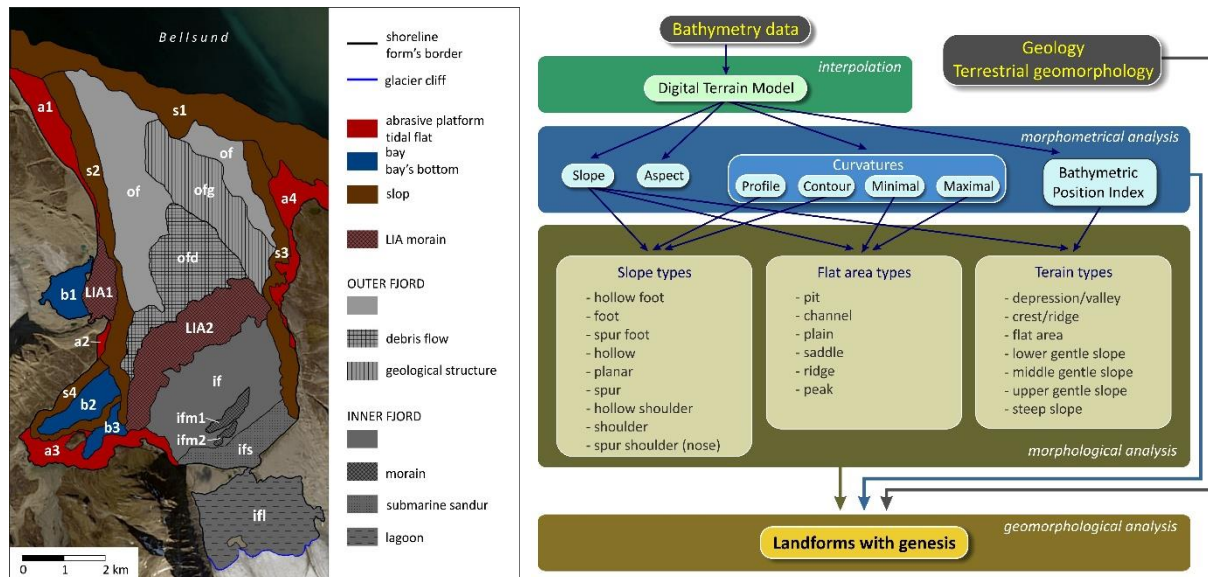


Fig. 1. Sets of landforms obtained through morphometric study and diagram of the steps of data processing and measurement results.

landscape. This also applies to the submarine areas, and issues related to marine geomorphometry. Bathymetric data used in this study were obtained from the measurements of the Norwegian Hydrographic Service and measurements conducted by the authors. Its main goal was: to determine the bathymetry of the Recherchefjorden (Bellsund, Svalbard), establish morphometric parameters for the analysis of the morphology of the bottom. The boundaries of zones, related to the specific character of bottom geomorphology linked with geological structure, tectonics and, in particular, the impact of glacial system, was delineated. The sets of landforms (areas) were distinguished based on the morphometric analysis resulting from the determined parameters: slopes, its aspects, curvatures and Bathymetric Position Index. Basically, these areas are concentrated in two zones: the main Recherchefjorden and its surroundings. The delimitation also takes into account the origins and location of them in relation to the glacial systems. On this basis, moraine areas were distinguished. They are linked with the Holocene advances of two glaciers, Renardbeen and Recherchebreen, mainly during the Little Ice Age. They constitute boundary zones between areas with different morphometric parameters: outer fjord and inner fjord. Moreover, taking into account geology and terrestrial geomorphology it was possible to describe paraglacial processes in this area (Fig. 1).

AMBIENT NOISE ACOUSTIC IN FJORDS

O. Głowacki, G.B. Deane, **M. Moskalik** (published in: The intensity, directionality, and statistics of underwater noise from melting icebergs, *Geophys. Res. Lett.* (2018), **45**, 9, 4105–4113, DOI: 10.1029/2018GL077632)

Freshwater fluxes from melting icebergs and glaciers are important contributors to both sea level rise and anomalies of seawater salinity in polar regions. However, the hazards encountered close to icebergs and glaciers make it difficult to quantify their melt rates directly, motivating the development of cryoacoustics as a remote sensing technique. Recent studies have shown a qualitative link between ice melting and the accompanying underwater noise, but the properties of this signal remain poorly understood. Here we examine the intensity, directionality, and temporal statistics of the underwater noise radiated by melting icebergs in Hornsund Fjord, Svalbard, using a three-element acoustic array. We present the first estimate of noise energy

per unit area associated with iceberg melt and demonstrate its qualitative dependence on exposure to surface current. Finally, we show that the analysis of noise directionality and statistics makes it possible to distinguish iceberg melt from the glacier terminus melt. Recent studies have demonstrated that impulsive underwater noise produced by tiny air bubbles released from melting glacier ice is a spectacular signal of the changing planet. A direct link between the melt rate and related noise would provide a first tool to study subsurface melting in a direct way. However, to make it possible, at first we need to better understand the properties of these sounds. To address this issue, we investigate intensity, directionality, and statistics of the melt noise. The results prove that icebergs can be automatically detected and tracked using several acoustic receivers immersed in water. Moreover, we provide the first estimate of acoustic energy produced by melting icebergs (Fig. 1).

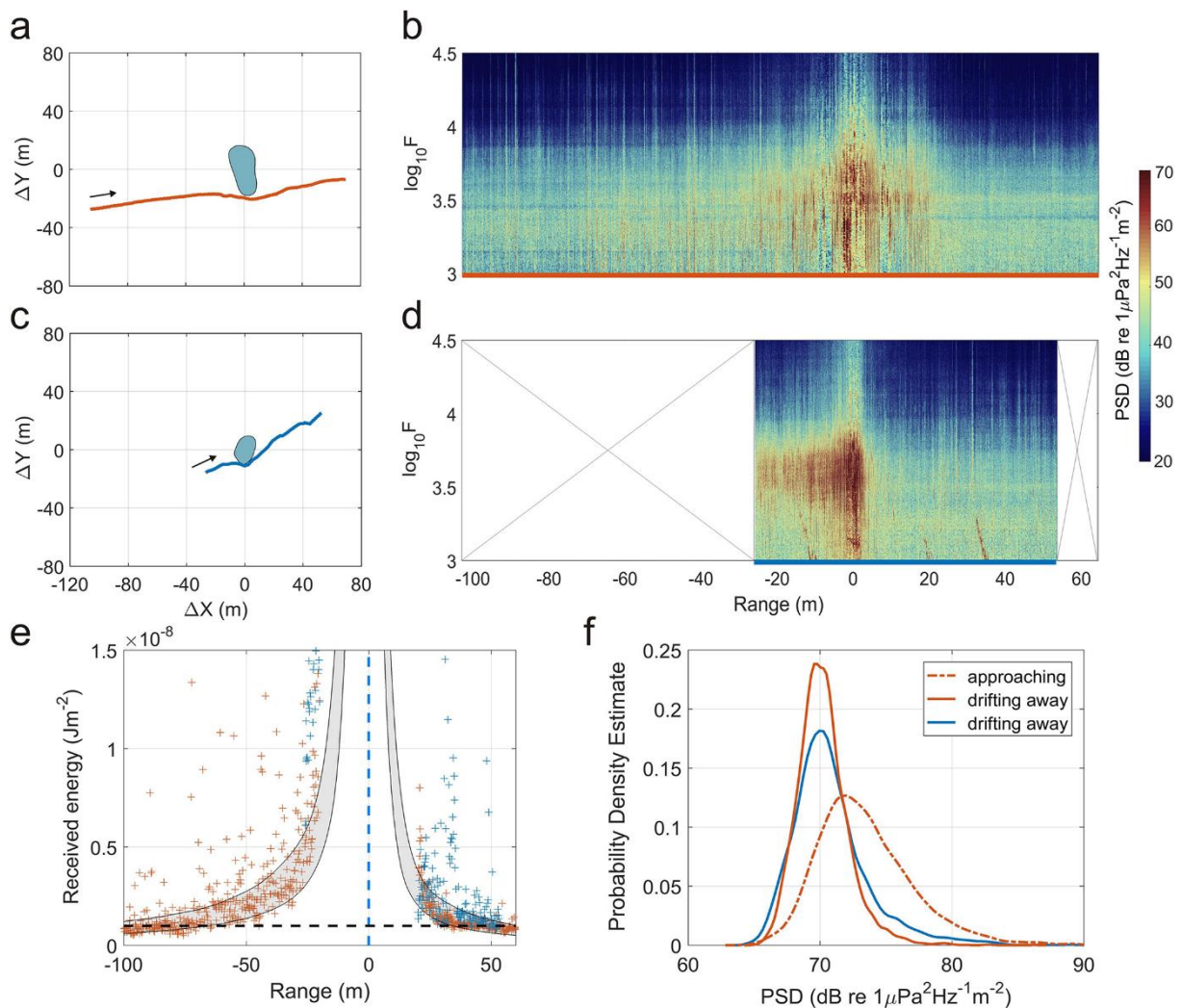


Fig. 1. Comparison between acoustic emission of icebergs 1 and 5, tracked during deployments 20150606/1 (red) and 20150606/4 (blue), respectively. Upper panels show geometry of the experiments (a, c) and frequency dependence of power spectral density estimates per square meter of submerged ice area in relation to the distance between the boat and icebergs (b, d). Lower panels present received energy per square meter versus range (e), and probability density estimates of power spectral density estimates per square meter, scaled to 1 m from the melting ice (f). Gray shaded area denotes transmission loss computed using Bellhop model for source frequency changing from 1 to 10 kHz and depths of 1 to 6 m. The data segment contaminated with a bearded seal call, visible between 32 and 36 m at plot (d), was removed before determining the probability density estimates of noise power.

FIORD SEDIMENTOLOGY

M. Moskalik, J. Ćwiakała, W. Szczuciński, A. Dominiczak, O. Głowacki, K. Wojtysiak, P. Zagórski (published in: Spatiotemporal changes in the concentration and composition of suspended particulate matter in front of Hansbreen, a tidewater glacier in Svalbard, *Oceanologia* (2018), **60**, 4, 446–463, DOI: 10.1016/j.oceano.2018.03.001)

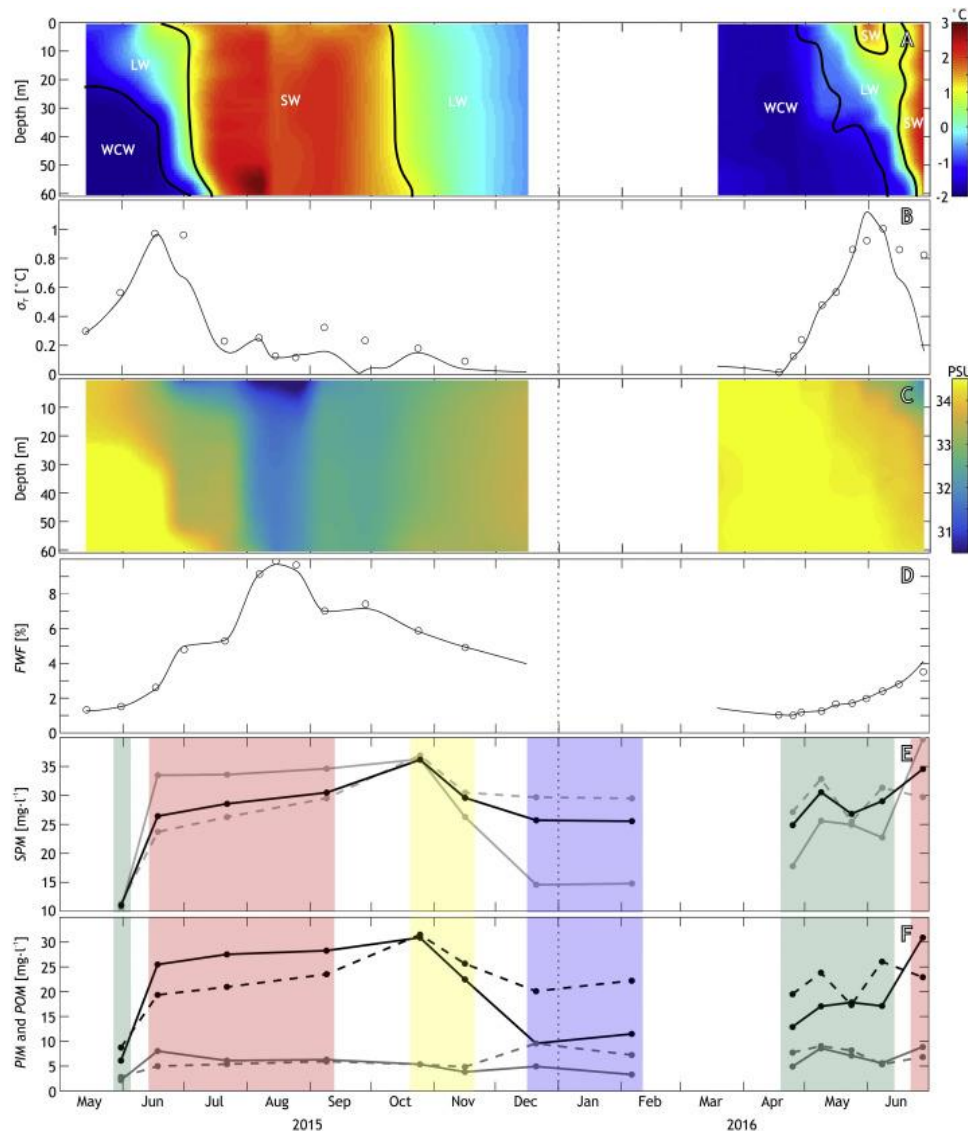


Fig. 1. Annual changes in the oceanographic conditions and mean interpolated suspended particle matter (SPM) concentration and composition data. (A) Interpolated water temperature depth profile changes over time. The abbreviations refer to water mass types. WCW – winter-cooled water, LW – local water, and SW – surface water (see text for details); (B) standard deviations of water temperature (σT) from interpolated (black line) and measured (black circles) values; (C) interpolated water salinity depth profile changes over time; (D) the freshwater fraction (FWF) calculated from interpolated (black line) and measured (black circles) values; (E) the mean concentration of SPM from interpolated data over the total water column (black line), its surface concentration (grey line) and deeper subsurface concentration (dashed grey line). The surface part of the water column refers to the layer from the surface to a depth of 10 m, and deep water refers to the layer from 20 to 50 m below surface; (F) average concentrations of the interpolated particulate inorganic matter (PIM – black lines) and particulate organic matter (POM – grey lines) within the surface (solid lines) and deeper subsurface (dashed lines) parts of water. The time intervals coloured on (E) and (F) represent measurements assigned to the spring (green), summer (red), autumn (yellow), and winter (blue) seasons.

Tidewater glaciers supply large amounts of suspended particulate matter (SPM) and freshwater to fjords and affect oceanographic, sedimentological, and biological processes. Our understanding of these processes, is usually limited to the short summer season. Here, we present the results of a one-year-long monitoring of the spatial variability in SPM characteristics in a context of oceanographic and meteorological conditions of a glacial bay next to Hansbreen, a tidewater glacier in Hornsund (southern Spitsbergen). The observed range of SPM concentrations was similar to ranges measured in other sub-polar glaciated fjords, especially in Svalbard. The major source of SPM is the meltwater discharge from the glacier. The maximum water column-averaged SPM concentrations did not correlate with peaks in freshwater discharge and were observed at the beginning of the autumn season, when the fjord water transitioned from stratified to fully mixed. The observed spatiotemporal variations in the total SPM, particulate organic matter (POM), and particulate inorganic matter (PIM) are likely controlled by a combination of factors including freshwater supply, water stratification and circulation, bathymetry, the presence of sea ice, biological productivity, and sediment resuspension. During the ablation season, the SPM maximum concentrations were located within the upper water layer, whereas during the winter and spring, the greatest amounts of SPM were concentrated in deeper part. Thus, typical remote sensing-based studies that focus on SPM distributions may not reflect the real SPM levels. POM and PIM concentrations were correlated with each other, during most of the time suggesting that they may have a common source (Fig. 1).

WAVE CLIMATE ON SVALBARD

K. Wojtysiak, A. Herman, **M. Moskalik** (published in: Wind wave climate of west Spitsbergen: seasonal variability and extreme events, *Oceanologia* (2018), **60**, 3, 331–343, DOI: 10.1016/j.oceano.2018.01.002)

Waves are the key phenomenon directly influencing coastal morphodynamics. Facing insufficient observations, wind wave climate of the west coast of Spitsbergen can be characterized on the basis of the modelled data. Here we have used the results of spectral wave models: Wave Watch III (WW3) hindcast and WAM in ERA-interim (ERAi) reanalysis. We have observed the presence of seasonal cycle with difference of up to 1 m between significant wave heights in summer and winter. In wave-direction analysis we have noticed the southwestern swell component of remarkably narrow width, thus we expect unidirectional swell impact on the coastline. Extreme events analysis revealed that storms occur mainly in winter, but the most energetic ones (significant wave height of up to 9.5 m) occur in spring and autumn. We have identified positive trends in storms' frequency (2 storms per decade) and storms' total duration (4 days per decade) on the south of the study area. More storms can result in the increase of erosion rate on the south-western coasts of Spitsbergen, but this change may be highly dependent on the sea ice characteristics. Wave heights of wind sea and swell are correlated with the relevant atmospheric circulation indices, especially the North Atlantic Oscillation. In the recent decade, the correlation is stronger with WW3 than with ERAi data, at some locations explaining over 50% (over 30%) of the total variance of wind sea (swell) wave heights. In ERAi data, the relationship with circulation indices seems sensitive to the length of the analysis period (Fig. 1).

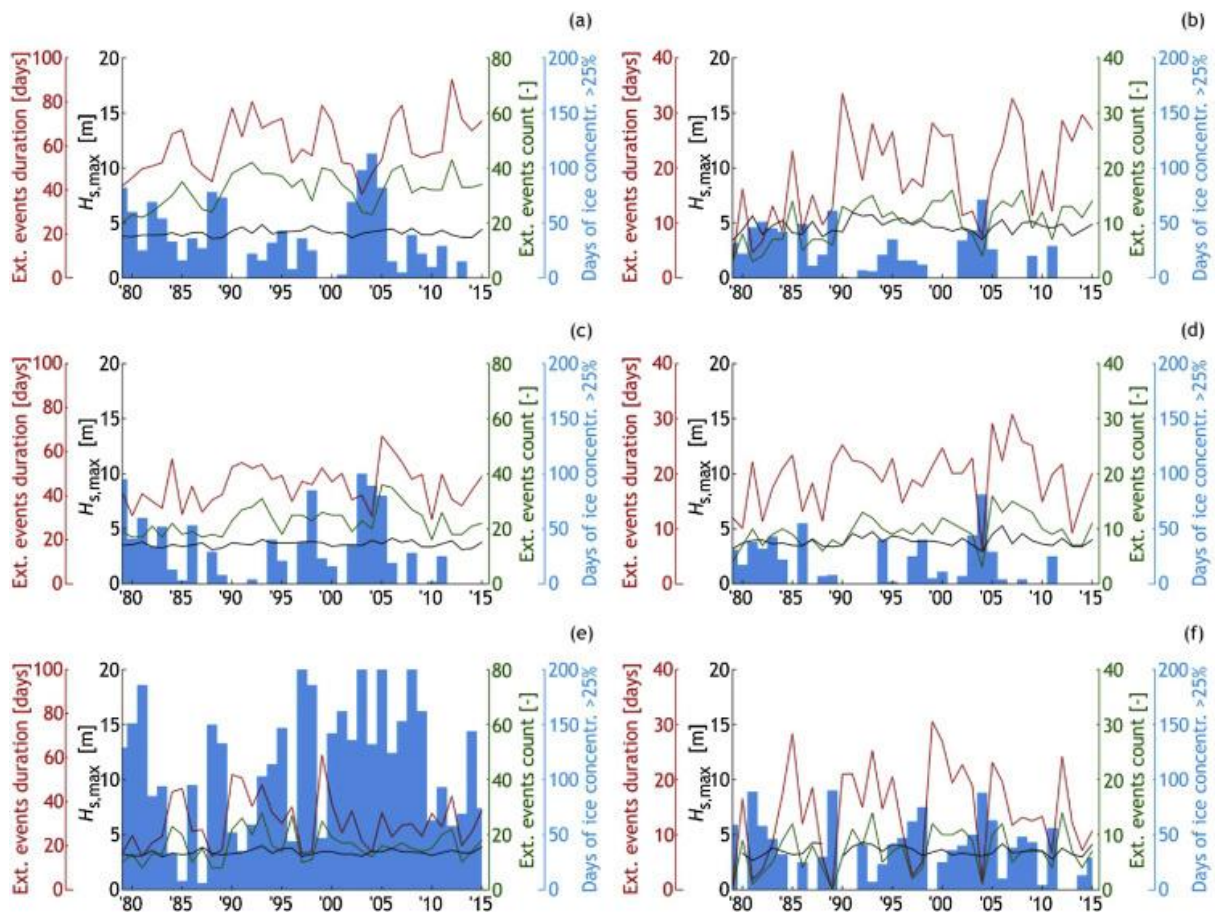


Fig. 1. Extreme event parameters calculated from ERAi dataset for annual (a, c, e) and winter (DJF) (b, d, f) for points on south (a, b), centre (c, d), and north (e, f) part of Spitsbergen. Individual variables have separate y-axes to enable easy absolute value readout. Please note that the scales differ between annual and winter charts.

ATTEMPT TO PREDICTION OF ENVIRONMENTAL CHANGE AFTER BARENTS SEA-GREENLAND SEA ICE-BARRIER BREAKUP

M. Grabcic, D. Ignatiuk, J.A. Jania, **M. Moskalik**, **P. Głowacki**, M. Błaszczuk, T. Budzik, W. Walczowski (published in: Coast formation in an Arctic area due to glacier surge and retreat: The Hornbreen–Hambergreen case from Spistbergen, *Earth Surf. Proc. Land.* (2018), **43**, 2, 387–400, DOI: 10.1002/esp.4251)

Glaciated coasts undergo faster geomorphic processes than unglaciated ones. We have studied changes of the coastal area in southern Svalbard with the glacier bridge between Torell Land and Sørkapp Land since the beginning of the 20th century. The existence of a continuous subglacial depression beneath the Hornbreen–Hambergreen glacier system has been debated since the 1960s, with inconclusive results. In this study we assess both the subglacial topography and the bathymetry of Hornsund Fjord and Hambergbukta bay. This included ~40 km of radar surveys over the glacial system and sea depth sounding. The extent of the glaciers from maps and satellite images together with digital terrain models and surface elevation data based on GPS profiling were used to analyse geometry changes of the glacier surfaces. The results confirm the existence of a continuous subglacial depression below sea level (c. 40 m deep) between Hornsund and the Barents Sea (Fig. 2). The Hornbreen-Hambergreen system has changed in

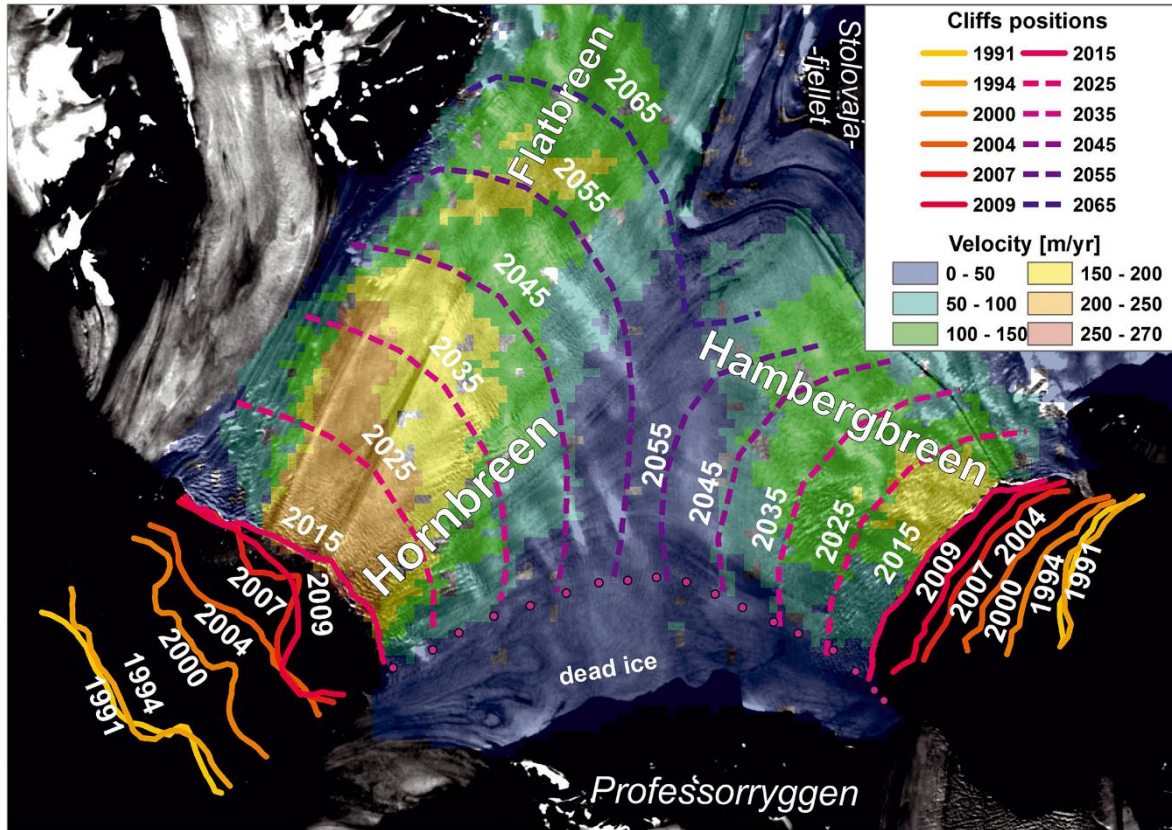


Fig. 1. The extent of Hornbreen and Hambergbreen in the period 1991–2015 (continuous lines) and the retreat scenario for 2025–2065 (dashed lines). Background image Landsat 8 (2015–09-17) with clearly visible foliation indicating the direction of ice movement. Ice surface velocity map for the period 1–13 October 2015 from Sentinel-1.

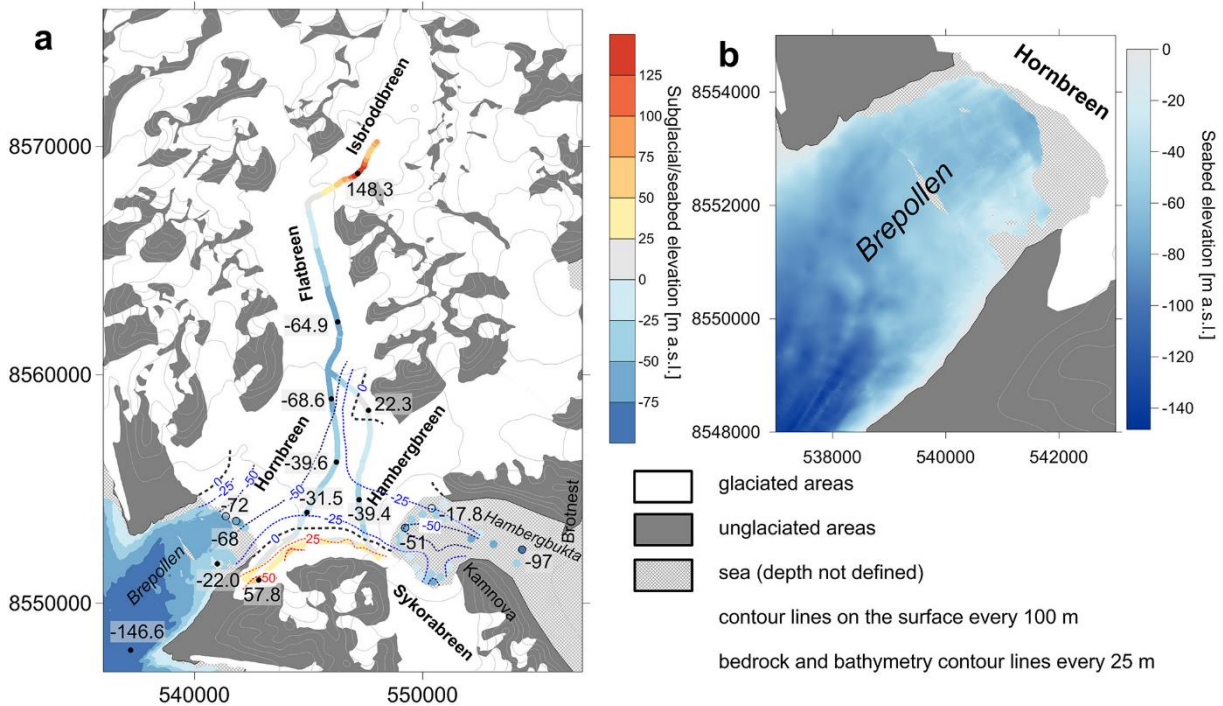


Fig. 2. Glacial bed along the GPR profiles from 2013 and 2014, depth of Hambergbukta (a) and inner Brepollen bathymetry (b). Selected depths and points marked. The dashed line represents probable contours of the subglacial topography and isobaths in Hambergbukta.

shape over the past century, reflecting its dynamic origin and activity, also exemplified by the sequential surges identified since 1899. There was a pre-surge build-up event of Flatbreen causing a surge and subsequent lowering of the Hornbreen-Hambergbreen frontal parts by the 1960s. After, the entire surface lowered, albeit with a delay in the Hornbreen terminal zone. Since the year 2000, Hornbreen terminus has retreated at an average rate of 106 m a^{-1} ; ~50% faster than that of Hambergbreen. If the retreat continues at the 2000–2015 average rate, the ice bridge between Hornsund and Hambergbukta will be broken sometime between 2055 and 2065 and the Hornsund strait will separate Sørkapp Land from the Spitsbergen island (Fig. 1). The processes and events described in this study, particularly the effects of the glacier surge, may provide a model for changes likely to occur in other coastal glaciated regions experiencing rapid change (Copyright © 2017 John Wiley & Sons, Ltd.).

SCIENCE COMMUNICATION AND EDUCATION

A. Goździk (published in: Research and education cooperation example: educational packages of ERIS project. **In:** *Electronic Proc. ESERA 2017 Conference “Research, Practice and Collaboration in Science Education”*, Dublin, Ireland, 21–25 August 2017, (2018), Part 5, 734–744.

One very promising model of learning designs is the model of Research and Education Cooperation activities. ERIS project proposes exploitation of research results in school practice. ERIS is EU funded project (ERASMUS+) aiming to increase the interest of pupils in lower and upper secondary schools in science, and the choice of a scientific career. Thanks to the development, pilot implementation and dissemination of educational packages and methodological materials, research results will be exploited in the education systems of at least 3 European countries: Poland, Romania, and France.

ERIS packages are dedicated to various topics, e.g.: glaciers, earthquakes, geomagnetism, meteorology in the Arctic, UV radiation, etc. They use freely available research databases or results published online, which may be analyzed by pupils with the help of instructions prepared by scientists. The packages include materials for teachers to work with pupils during classes or extracurricular activities. They contain worksheets for pupils and guidance for teachers. 30 packages were tested in schools in Poland, Romania, and France. The results of evaluation studies are presented and discussed. Teachers found packages interesting and useful for school practice. They found the tasks for pupils rather difficult, as it was a challenge for pupils to apply a new approach, which wasn't taught at schools before. Pupils could not solve tasks in a schematic ways, which they often use when solving typical school exercises, and it might have caused difficulties. However, challenging tasks are developing interest and engagement. ERIS packages and proposed teaching approach may be considered as an efficient way of increasing pupils' interest in science and scientific topics.

National packages were tested in lower and upper secondary schools in partners' countries. Subsequently, English versions of packages were prepared and freely proposed to European secondary schools (not only in partners' countries). Each package was tested by at least 5 groups of students.

For each package online lessons were conducted by scientists, who prepared educational materials for packages. After lessons teachers and pupils were encouraged to work additionally with worksheets prepared for each package. Subsequently, they could have filled in the survey dedicated to the materials in the package. This survey contained some statistical questions (type of school, age of pupils, subject taught by a teacher, who participated in testing), four content questions (about importance of the topic, transparency of materials, sufficient explanations and level of difficulty), and two fields for suggestions. The results are based on 32 surveys obtained

from teachers from secondary schools in Poland, who tested ERIS packages in Polish. Teachers declared that packages contain important educational materials (definitely yes: 81%, rather yes: 19%). They assessed the materials included in the packages as clear and transparent (definitely clear: 59%, rather clear: 41%). They also found explanations and instructions for the tasks sufficient (definitely sufficient: 59%, rather sufficient: 41%). Teachers assessed materials included in the packages as generally difficult (very difficult: 3%, rather difficult: 56%, rather easy: 41%).

The second step of the evaluation was dedicated to the assessment of the general impact of proposed materials and methods on pupils' skills and interests. This survey was conducted by each partner institution after finishing of testing packages in national languages in Poland, Romania and France. Teachers were requested to assess how many students developed the ability to apply research methods in solving problems in the field of mathematics and natural sciences, and number of students, who developed skills of analytical and synthetic thinking. Moreover, they were also assessing the number of students, whose interest in scientific topics increased.

The results are based on 44 surveys obtained from teachers from secondary schools in Poland (18 surveys), Romania (23 surveys), and France (3 surveys), who tested ERIS packages in national languages. Teachers worked with 44 groups of students. Total number of students, who tested the packages was 1054 (356 students from Poland, 631 students from Romania, and 67 students from France).

The results from the surveys show that the impact of the project on students skills and interest in scientific topics is significant. Teachers declared that for 70% of their students, who tested the packages, they observed increase of the ability to apply research methods in solving problems in the field of mathematics and natural sciences. They assessed that 70% of their students developed skills of analytical and synthetic thinking, with a slight difference between upper and lower secondary schools (result for lower secondary schools students is 71%, for upper secondary schools students – 69%). Moreover, teachers observed significant increase of students' interest in scientific topics. They declared that for 72% of their students interest increased. Some differences between younger and older students were observed. Students from lower secondary schools got more interested than those from upper secondary schools (73% compared to 70%).

9.6 Seminars and teaching

Seminars and lecture outside of the IG PAS:

- T. Wawrzyniak, How can Arctic and Antarctic research engage students to STEM education?, Federal University of Minas Gerais, Belo Horizonte, Brasil, Invited lecture;
- A. Goździk et al., High schools all over the world, Webinars, Invited lecture.

9.7 Teaching thesis

- T. Wawrzyniak, Introduction to geology and physical geography, Warsaw School of Information Technology.

9.8 Completed PhD thesis defense

- D. Kępski, Wpływ rzeźby i pokrycia terenu na rozkład przestrzenny i dynamikę zmian pokrywy śnieżnej na tundrze w okolicy Polskiej Stacji Polarnej na Spitsbergenie, Supervisor: K. Mięgała, Supporting supervisor: B. Luks;

- J. Cwiąkała, Zapis recesji uchodzącego do morza lodowca Hansa w świetle badań geofizycznych, geomorfologicznych i sedymentologicznych w zatokach Isbjørnhamna i Hansbukta, Hornsund, południowy Spitsbergen, Supervisor: W. Szczuciński, Supporting supervisor: M. Moskalik;
- J. Szilo, Wpływ recesji lodowców na rzeźbę obszaru i warunki hydrologiczne zachodniego wybrzeża Zatoki Admiralicji (Wyspa Króla Jerzego), Supervisor: R. Bialik.

9.9 Visiting scientists

Arko Olesk, Tallin University, Baltic Film, Media, Arts and Communication School, Tallin, Estonia, 21–25.05.2018,

Michał Pętlicki, Centro de Estudios Científicos, Valdivia, Chile, 7.07–13.08.2018,

Flavio Justino, Universidade Federal de Viçosa, Viçosa, Brazil, 15–20.10.2018.

9.10 Meetings, workshops, conferences, and symposia

Presentations of the Department's members:

XXVIII Seminarium Meteorologii i Klimatologii Polarnej, Sosnowiec, Poland, 11–12 May 2018

- P. Głowacki, CLIMEV – nowe narzędzie badawcze dla badań atmosfery w rejonach polarnych, Oral;

FARO Annual Meeting 2018, Davos, Switzerland, 12 June 2018

- P. Głowacki, History of FARO, Oral;

International Conference POLAR 2018, Davos, Switzerland, 20 June 2018

- P. Głowacki, W. Sielski, The Hornsund Polish Polar Station, Spitsbergen, Svalbard – Access and infrastructure, Oral;
- L. Leppänen, J.I. López Moreno, A. Nadir Arslan, P. Dagsson Waldhauserova, C. Fierz, D. Finger, L. Holko, B. Luks, C. Marty, G. Picard, R. Pirazzini, A. Sensoy Sorman, A. Arda Sorman, Results from COST ES1404 Action for Harmonization of Snow Measurements in Europe, Poster;
- C. Larose, E. Barbaro, M. Björkman, J.-C. Gallet, J. Kohler, K. Koziol, B. Luks, T. Martma, T.V. Schuler, A. Spolaor, C. Zdanowicz, Lessons learned from interdisciplinary snow research in Svalbard, Poster.

Svalbard Science Forum Meeting, Longyearbyen, Norway, 25 April 2018

- Piotr Głowacki, Polish research activity plan in 2018 at Svalbard, Oral.

INTAROS Annual Meeting 2018, Helsinki, Finland, January 2018

- P. Głowacki, WP7 – Dissemination and outreach (Update of the first 12 months of activity and plan for the future proposals), Oral;
- T. Wawrzyniak, Unique long time meteorological data series collected at the Polish Polar Station Hornsund on Spitsbergen, Oral.

W cieniu COP24 – w Centrum Studiów Polarnych, Sosnowiec, Poland, 6 December 2018

- P. Głowacki, Polarna szkoła doktorska a szkoła życia, Oral;
- A. Goździk, EDU-ARCTIC – atrakcyjne nauczanie bez granic, Oral.

SnowHydro – International Conference on Snow Hydrology, Heidelberg, Germany, 14 February 2018

- D. Kępski, B. Luks, K. Migala, A. Uszczyk, S. Westermann, T. Budzik, Evolution of snow cover stratigraphy during ablation period in High Arctic tundra environment (SW Spitsbergen), Oral.

IGS Cryosphere and Biosphere, Kyoto, Japan, 16 March 2018

- D. Kępski, B. Luks, M. Osuch, A. Dobler, K. Migala, S. Westermann, T. Budzik, T. Wawrzyniak, Snow cover development in a High-Arctic coastal tundra environment: present state and predictions for the future, Oral.

Towards a better harmonization of snow observations, modeling and data assimilation in Europe, Budapest, Hungary, 30 October 2018

- J.I. Lopez-Moreno, L. Leppänen, B. Luks, L. Holko, A. Sanmiguel-Vallelado, E. Alonso-González, D.C. Finger, G. Picard, K.A. Gillemot, R.S. Azzoni, C. Marty, A. Soncini, P. Dagsson-Waldhauserova, A.S. Sensoy, A. Sorman, A. Nadir Arslan, Differences on snow density and snow water equivalent estimation using different snow tubes: instrumental bias, variability induced by observers and influence of snow and terrain conditions, Oral;
- B. Luks, M. Osuch, Modelling snow water equivalent in the coastal zone of Hornsund fiord, Poster.

Konferencja MATLAB 2018, Warsaw, Poland, 17 April 2018

- J. Podgórski, Badanie odbiciowości lodu lodowcowego przy pomocy LiDARu, Oral.

EGU General Assembly, Vienna, Austria, 8–13 April 2018

- W. Szczuciński, A. Dominiczak, M. Forwick, K. Apolinarska, T. Goslar, M. Moskalik, M. Woszczyk, Warming-controlled glaciers retreat and enhanced carbon burial – is there a negative feedback effect? – summary of multidisciplinary study in fjords of Svalbard, Poster.

The International Symposium on The Cryosphere in a Changing Climate, 5th Symposium APECS-Brazil, Belo Horizonte, Brazil, 15–18 May 2018

- T. Wawrzyniak, A. Goździk, P. Głowacki, How can Arctic and Antarctic Research engage students in STEM education?, Oral.

Harmosnow Workshop on Snow Chemistry Monitoring, Kolm Saigum, Sonnblick, Austria, 26 February – 2 March 2018

- A. Nawrot, B. Luks, K. Koziół, Ł. Stachnik, Snow monitoring led by Polish Polar Station Hornsund, Workshop.

Nordic Water 2018, Bergen, Norway, 13–15 August 2018

- M. Osuch, A. Nawrot, T. Wawrzyniak, A.P. Piotrowski, Water temperature modelling of small high arctic stream (Fuglebekken, SW Spitsbergen).

Symposium Polarne, Poznań, Poland, 7–10 June 2018

- M. Lewandowski, A. Nawrot, Polish Polar Station Dobrowolski – past, present and future, Oral.

The 8th Global Freshwater Conference, Beijing, China, 6–9 November 2018

- T. Wawrzyniak, M. Osuch, A. Nawrot, The influence of permafrost degradation on runoff generation in small arctic unglaciated catchment (Fuglebekken, Spitsbergen);

- M. Osuch, T. Wawrzyniak, Projections of hydro-climatic conditions in small arctic unglaciated catchment Fuglebekken (SW Spitsbergen).

Permafrost thermal state in Svalbard 2016–2017 (PermaSval) SIOS, The University Centre in Svalbard (UNIS), 13–16 March 2018

- M. Osuch, T. Wawrzyniak, State of permafrost in Hornsund area, SW Spitsbergen.

Krajowe Warsztaty Scientix, IG PAS, Warsaw, Poland, 25 April 2018

- A. Goździk, Co project Scientix oferuje polskim nauczycielom, Oral.

Druga Krajowa Konferencja Scientix, IG PAS, Warsaw, Poland, 23–24 November 2018

- A. Goździk, Scientix w pigułce, Oral.

Światowe Forum Wody – Konferencja PAN, Polish Academy of Sciences, Warsaw, Poland, 22 March 2018

- A. Goździk, Wybrane inicjatywy z zakresu edukacji środowiskowej i wodnej, Oral.

9th International Conference “Education, Research & Development”, Elenite, Bulgaria, 23–27 August 2018

- A. Goździk, EDU-ARCTIC competitions as an effective way to increase interest in STEM, Oral.

Societal Relevance of Polar Research, Institute of Oceanology PAS, Sopot, Poland, 27–28 November 2018

- A. Goździk, What do youngsters know about the Arctic – results of the EDU-ARCTIC survey, Oral.

Dzień Informacyjny Programu SWAFS Horyzont 2020, Krajowy Punkt Kontaktowy Programów Badawczych, Warsaw, Poland, 11 December 2018

- A. Goździk, EDU-ARCTIC – doświadczenia koordynatora projektu, Oral.

9.11 Publications

ARTICLES

- Ćwiąkała, J., M. Moskalik, K. Wojtysiak, J. Giżejowski**, et al. (2018), Submarine geomorphology at the front of the retreating Hansbreen tidewater glacier, Hornsund fjord, southwest Spitsbergen, *J. Maps* **14**, 2, 123–134, DOI: 10.1080/17445647.2018.1441757.
- Głowacki, O.**, G.B. Deane, and **M. Moskalik** (2018), The intensity, directionality, and statistics of underwater noise from melting icebergs, *Geophys. Res. Lett.* **45**, 9, 4105–4113, DOI: 10.1029/2018GL077632.
- Kosek, K., **K. Koziol**, et al. (2018), The interaction between bacterial abundance and selected pollutants concentration levels in an arctic catchment (southwest Spitsbergen, Svalbard), *Sci. Total Environ.* **622–623**, 913–923, DOI: 10.1016/j.scitotenv.2017.11.342.
- Lewandowski, M.**, and **K. Birkenmajer** (2018), In Memoriam. Professor Krzysztof Paweł Krajewski (1955–2017) geologist, polar explorer, mountaineer and a good fellow, *Pol. Polar Res.* **39**, 1, 175–176, DOI: 10.24425/118744.
- Opala-Owczarek, M., **B. Luks, D.D. Kępski**, et al. (2018), The influence of abiotic factors on the growth of two vascular plant species (*Saxifraga oppositifolia* and *Salix polaris*) in the High Arctic, *Catena* **163**, 219–232, DOI: 10.1016/j.catena.2017.12.018.

- Mazur, S., **M. Malinowski**, **M. Lewandowski**, et al. (2018), On the nature of the Teisseyre–Tornquist Zone, *Geol. Geophys. Environ.* **44**, 1, 17–30, DOI: 10.7494/geol.2018.44.1.17.
- Moskalik, M.**, et al., **J. Ćwiąkała** (2018), Morphological characterization of the Recherchefjorden (Bellsund, Svalbard) using marine geomorphometry, *Pol. Polar Res.* **39**, 1, 99–125, DOI: 10.24425/118740.
- Moskalik, M.**, **J. Ćwiąkała**, **O. Głowacki**, **K. Wojtysiak**, et al. (2018), Spatiotemporal changes in the concentration and composition of suspended particulate matter in front of Hansbreen, a tidewater glacier in Svalbard, *Oceanologia* **60**, 4, 446–463, DOI: 10.1016/j.oceano.2018.03.001.
- Grabiec, M., D. Ignatiuk, J.A. Jania, **M. Moskalik**, **P. Głowacki**, et al. (2018), Coast formation in an Arctic area due to glacier surge and retreat: The Hornbreen–Hambergreen case from Spistbergen, *Earth Surf. Proc. Land.* **43**, 2, 387–400, DOI: 10.1002/esp.4251.
- Pętlicki, M.** (2018), Subglacial topography of an icefall inferred from repeated terrestrial laser scanning, *IEEE Geosci. Remote Sens. Lett.* **15**, 9, 1461–1465, DOI: 10.1109/LGRS.2018.2845342.
- Podgórski, J.**, et al. (2018), Revealing recent calving activity of a tidewater glacier with terrestrial LiDAR reflection intensity, *Cold Reg. Sci. Technol.* **151**, 288–301, DOI: 10.1016/j.coldregions.2018.03.003.
- Szilo, J.**, and R.J. Bialik (2018), Grain size distribution of bedload transport in a glaciated catchment (Baranowski Glacier, King George Island, W Antarctica), *Water* **10**, 4, 360, DOI: 10.3390/w10040360.
- Szilo, J.**, and R.J. Bialik (2018), Recession and ice surface elevation changes of Baranowski Glacier and its impact on proglacial relief (King George Island, West Antarctica), *Geosciences* **8**, 10, 355, DOI: 10.3390/geosciences8100355.
- Arażny, A., **T. Wawrzyniak**, **A. Nawrot**, et al. (2018), Spatial variations in air temperature and humidity over Hornsund fjord (Spitsbergen) from 1 July 2014 to 30 June 2015, *Geogr. Ann. A* **100**, 1, 27–43, DOI: 10.1080/04353676.2017.1368832.
- Wojtysiak, K.**, A. Herman, and **M. Moskalik** (2018), Wind wave climate of west Spitsbergen: seasonal variability and extreme events, *Oceanologia* **60**, 3, 331–343, DOI: 10.1016/j.oceano.2018.01.002.

CHAPTERS

- Kinnard, C., **M. Pętlicki**, et al. (2018), Mass balance and meteorological conditions at Unversidad Glacier, Central Chile. **In:** D.A. Rivera, A. Godoy-Faundez, and M. Lillo-Saavedra (eds.), *Andean Hydrology*, CRC Press, Boca Raton.

"Publications of the Institute of Geophysics, Polish Academy of Sciences: Geophysical Data Bases, Processing and Instrumentation" appears in the following series:

A – Physics of the Earth's Interior

B – Seismology

C – Geomagnetism

D – Physics of the Atmosphere

E – Hydrology (formerly Water Resources)

P – Polar Research

M – Miscellanea

Every volume has two numbers: the first one is the consecutive number of the journal and the second one (in brackets) is the current number in the series.

